Univerzitet u Novom Sadu
FAKULTET TEHNIČKIH NAUKA
DEPARTMAN ZA PROIZVODNO MAŠINSTVO
Novi Sad, Srbija

14. MEĐUNARODNA NAUČNA KONFERENCIJA

14th INTERNATIONAL SCIENTIFIC CONFERENCE

ETIKUM 2023

ZBORNIK RADOVA
PROCEEDINGS

NOVI SAD DECEMBAR/DECEMBER 2023

University of Novi Sad
Faculty of Technical Sciences
Department of Production Engineering

ETIKUM 2023

PROCEEDINGS

Novi Sad, 07-09th December 2023

PROCEEDINGS OF THE INTERNATIONAL SCIENTIFIC CONFERENCE
ETIKUM 2023
Novi Sad 2023

Publisher: **UNIVERSITY OF NOVI SAD, FACULTY OF TECHNICAL SCIENCES**
DEPARTMENT OF PRODUCTION ENGINEERING
CHAIR OF METROLOGY, QUALITY, FIXTURES, TOOLS AND ECOLOGICAL ENGINEERING ASPECTS
21000 NOVI SAD, Trg Dositeja Obradovica 6, SERBIA

Organization of this Conference was approved by Educational-scientific Council of Faculty of Technical Sciences in Novi Sad

Technical treatment and design: Boris AGARSKI,
Mario ŠOKAC,
Aleksandar MILOŠEVIĆ.

CIP classification:

CIP - Каталогизација у публикацији
Библиотеке Матице српске, Нови Сад

62:006.91(082)(0.034.2)
62:502(082)(0.034.2)

INTERNATIONAL Scientific Conference ETIKUM (14 ; 2023 ; Novi Sad)
Proceedings [Elektronski izvor] / [14th International Scientific Conference] ETIKUM 2023, Novi Sad, 7-9th December 2023. - Novi Sad : Faculty of Technical Sciences, Department of Production Engineering, 2023
Način pristupa (URL): http://etikum.ftn.uns.ac.rs/. - Nasl. sa naslovnog ekrana. - Opis zasnovan na stanju na dan 28.11.2023. - Radovi na srp i engl. jeziku. - Elektronska publikacija u formatu pdf opsega 269 str. - Bibliografija uz svaki rad.

ISBN 978-86-6022-617-6

а) Инжењерство -- Метрологија -- Зборници
б) Инжењерство -- Животна средина --Зборници
COBISS.SR-ID 131426825

Financing of the Proceedings was sponsored by the Provincial Secretariat for Science and Technological Development of AP Vojvodina.

ETIKUM 2023

INTERNATIONAL SCIENTIFIC CONFERENCE
NOVI SAD, SERBIA, DECEMBER 07-09, 2023

CONFERENCE ORGANIZER

University of Novi Sad, Faculty of Technical Sciences, Department of Production Engineering
Chair of Metrology, Quality, Fixtures, Tools and Ecological Engineering Aspects

PROGRAMME COMMITTEE

ORGANIZING COMMITTEE

ACKNOWLEDGEMENT

Organization of International Scientific Conference ETIKUM 2023 was made possible with understanding and financial help of the following sponsors:

- **PROVINCIAL SECRETARIAT FOR HIGHER EDUCATION AND SCIENTIFIC RESEARCH OF AP VOJVODINA** – Novi Sad, SERBIA
- **FACULTY OF TECHNICAL SCIENCES -** Novi Sad, SERBIA
- **DEPARTMENT FOR PRODUCTION ENGINEERING AT THE FACULTY OF TECHNICAL SCIENCES -** Novi Sad, SERBIA
- **TOPOMATIKA D.O.O. –** Sveta Nedelja, CROATIA

Predgovor

Međunarodna naučno stručna konferencija ETIKUM 2023 se održava tradicionalno već četrnaesti put. U vreme kada je koncipirana, 2006. godine, konferencija je osmišljena kao informativno-edukativna i naučno-stručna. Informativno-edukativna dimenzija se oslikava kroz učešće predavača iz redova stručnih predstavnika eminentnih proizvođača opreme koja se koristi u edukativnim i istraživačkim procesima na našem Fakultetu. Pri tome je akcenat na diseminaciji informacija i edukaciji u vezi sa tehnološkim novitetima u oblasti hardverskih i softverskih komponenti. Naučno-stručna dimenzija konferencije se ostvaruje kroz predstavljanje naučnih i stručnih rezultata, pre svega, iz oblasti koje obuhvata Katedra za metrologiju, kvalitet, pribore, alate i ekološko inženjerske aspekte. Pored toga, zahvaljujući razvoju interdisciplinarne saradnje, konferencija je i ove godine obuhvatila i srodne naučno stručne oblasti, u okviru kojih članovi Katedre realizuju naučno-istraživačke i stručne projekte.

Od 2016. godine, uvedena je nagrada za najbolji rad mladog istraživača u znak sećanja na Prof. dr Janka Hodoliča. Programski odbor ETIKUM konferencije je i 2023. godine nagradio najbolji rad mladog istraživača ETIKUM konferencije sa Prof. dr Janko Hodolič nagradom.

Konferencija ETIKUM 2021 je strukturirana u tri tematske celine:

1. *Metrologija i kontrola kvaliteta u proizvodnom inženjerstvu;*
2. *Metrologija i kontrola kvaliteta u biomedicinskom inženjerstvu;*
3. *Metrologija i kvalitet u zaštiti životne sredine i zaštiti na radu;*

Prva tematska oblast je, pored klasičnih aspekata metrologije i kvaliteta u oblasti proizvodnog mašinstva, obuhvatila i precizno inženjerstvo, odnosno nano metrologiju i srodne tehnologije.

U okviru druge tematske oblasti su predstavljeni rezultati aktivnosti u oblasti biomedicinskog inženjerstva od strane istrazivača i sa drugih departmana FTN-a.

Treća tematska oblast privukla je istraživače iz različitih oblasti zaštite životne i radne sredine. U okviru treće tematske oblasti predstavljena su istraživanja vezana za merenja i analize zagađujućih materija emitovanih u vazduh, vodu, zemljište, merenje i monitoring fizičkih aspekata životne sredine kao što su buka, zračenje i vibracije, kao i ocenjivanje životnog ciklusa proizvoda i procesa.

Na konferenciji ETIKUM 2023 je prezentovano ukupno 64 naučnih i stručnih radova, dok je u radu konferencije učestvovalo preko 80 predavača i slušalaca iz akademskih institucija i privrede iz više evropskih zemalja. Prethodno pomenute činjenice predstavljaju, sa jedne strane, potvrdu koncepcije konferencije, a sa druge strane, garanciju da će konferencija ETIKUM i narednih godina predstavljati značajan informativno-edukativni i naučno-stručni događaj na ovim geografskim prostorima.

Novi Sad, Decembar 2023 *PROGRAMSKI I ORGANIZACIONI* ODBOR

Foreword

International Scientific-Expert Conference ETIKUM 2023 will be held for the fourteenth time and it has become a tradition. When established in 2006, the conference is designed as informative-educational and scientific-expert. Informative and educational dimension is reflected through the participation of lecturers from among expert representatives of the eminent manufacturers of equipment connected to educational and research processes at the Faculty. Moreover, the emphasis are on the dissemination of information as well as on education in relation to technological innovations related to both - hardware and software components. Scientific and expert, i.e., professional dimensions of conference are achieved through the presentation of scientific and expert results, primarily from the field of the Chair of metrology, quality, fixtures, tools and ecological-engineering aspects. In addition, thanks to the development of interdisciplinary cooperation, the conference this year included the related scientific and technical fields, in which Chair members implement research and professional projects.

From 2016, in memoriam of Prof. dr Janko Hodolic, an award for the best paper of the young researcher was introduced. The best paper of the young researcher from ETIKUM 2023 conference was rewarded with the "Prof dr Janko Hodolic" award on behalf of the ETIKUM conference Programme committee.

In the context of this conception, the conference was divided into three thematic sections:

1. Metrology and quality control in the production engineering;
2. Metrology and quality control in the biomedical engineering;
3. Metrology and quality in the field of environmental protection and occupational safety.

The first thematic area, in addition to the classical aspects of metrology and quality in the field of production engineering, included subjects related to precision engineering and nano metrology and related technologies.

The second thematic area presented the results of activities in the field of biomedical engineering conducted by researchers from various departments of the Faculty of Technical Sciences (FTN).

The third thematic area this year attracted researchers from various areas of environmental protection and occupational safety. Research in field of measurement and analysis of pollutants to air, water, and soil, measurement and monitoring of physical aspects of environment such as noise, radiation and vibrations, as well as life cycle assessment of products and processes is presented in third thematic area.

At ETIKUM 2023 conference 64 scientific-expert papers were presented, while the conference was attended by over 80 speakers and listeners from academia and business from several European countries. The previously mentioned facts are, on the one hand, the confirmation of the conference's concept, and on the other hand, a guarantee that the ETIKUM conference will be considered as important informative and educational, scientific and professional event in these regions.

Novi Sad, December 2023

PROGRAMME AND ORGANIZING COMMITTEE

ETIKUM 2023

INTERNATIONAL SCIENTIFIC CONFERENCE
NOVI SAD, SERBIA, DECEMBER 07-09, 2023

CONTENTS

SESSION 1: METROLOGY AND QUALITY CONTROL IN THE PRODUCTION ENGINEERING

SESSION 2: METROLOGY AND QUALITY CONTROL IN THE BIOMEDICAL ENGINEERING

SESSION 3: METROLOGY AND QUALITY IN THE FIELD OF ENVIRONMENTAL PROTECTION AND OCCUPATIONAL SAFETY

INTERNATIONAL SCIENTIFIC CONFERENCE - ETIKUM 2023

PROCEEDINGS

Session 1:

METROLOGY AND QUALITY CONTROL IN THE PRODUCTION ENGINEERING

Novi Sad, 07 – 09th December 2023

ETIKUM 2023 **INTERNATIONAL SCIENTIFIC CONFERENCE NOVI SAD, SERBIA, DECEMBER 7-9, 2023**

Božić, D., Milošević, M., Lukić, D., Santoši, Ž.

PRIMENA VIZUELNOG PRETRAŽIVAČA 3D CAD MODELA KOD REDIZAJNIRANJA PROIZVODA

Rezime: *Prilikom projektovanja proizvoda odabir standardnih delova predstavlja vrlo izazovan zadatak. Kako bi se olakšao ovaj proces, u ovom radu prikazana je primena platforme za vizuelno pretraživanje 3D Findit, koja omogućava efikasnu identifikaciju standardnih i već gotovih komponenti različitih proizvođača iz različitih oblasti industrije. Akcenat je dat na praktičan odabir jednog odgovarajućeg zamenskog dela na osnovu 3D modela, pružajući tako brzu i preciznu pretragu zahvaljujući kompletnim geometrijskim podacima sadržanim u 3D modelu. U slučaju nedostatka 3D modela dela, sistem nudi najbližu zamenu dostupnu na tržištu, omogućavajući dizajneru da prilagodi konstrukciju proizvoda prema raspoloživom standardnom delu pre nego što se započne proces njegove proizvodnje.*
Ključne reči: *CAD model, vizuelni pretraživač, dizajn proizvoda, ležaj*

1. UVOD

U eri industrije 4.0 digitalne transformacije i napretka tehnoloških dostignuća, oblasti poput inženjeringa, dizajna i proizvodnje doživljavaju duboke promene [1]. Centralno mesto u ovom evolucijskom procesu zauzimaju CAD (Computer-Aided Design) modeli, koji predstavljaju osnovu za razvoj i proizvodnju kompleksnih inženjerskih proizvoda. Sa porastom dostupnosti digitalnih alata i softvera za modeliranje, broj i kompleksnost CAD modela kontinuirano raste, postavljajući izazove u efikasnom upravljanju ovim resursima. U ovom kontekstu, vizuelni pretraživači CAD modela postaju ključni instrument za olakšavanje pristupa, pretragu, i analizu ovih digitalnih entiteta.

Vizuelni pretraživači CAD modela predstavljaju inovativni pristup u optimizaciji procesa pronalaženja, analize i korišćenja CAD podataka [2–5]. Ovi alati omogućavaju inženjerima, dizajnerima i drugim profesionalcima u oblasti inženjeringa da brže i efikasnije identifikuju relevantne CAD modele, istraže njihove karakteristike i primene, te tako ubrzaju razvoj i proizvodnju proizvoda.

Baze podataka trodimenzionalnih modela koje se koriste širom interneta postaju sve veće, stoga je potreban razvoj sistema za brzo i intuitivno pronalaženje takvih 3D modela u bazama podataka [6].

U okviru narednih poglavlja ovog rada, predstavljene su osnovne komponente vizuelnih pretraživača 3D CAD modela, primer njihove upotrebe u realnim scenarijima, kao i izazovi za buduća istraživanja na ovom polju.

2. PLATFORMA ZA VIZUELNU PRETRAGU 3D CAD MODELA - 3D FIND IT

Jedna od ključnih karakteristika platforme za vizuelnu pretragu je dostupnost preko 5000 kataloga CAD modela proizvođača komponenata, standardnih delova, sklopova i sl. (Slika 1). Ovi katalozi su dragoceni resursi za profesionalce u dizajnu i inženjeringu, jer sadrže veliki obim 3D CAD, CAE (računarski podržani inženjering) i BIM (modeliranje informacija o zgradi) modela i podataka vezanih za komponente i delove od pouzdanih dobavljača [7]. Ovo omogućava korisnicima da lako pristupe i integrišu ove komponente u svoje projekte, pojednostavljujući tako procese dizajna i inženjeringa [8].

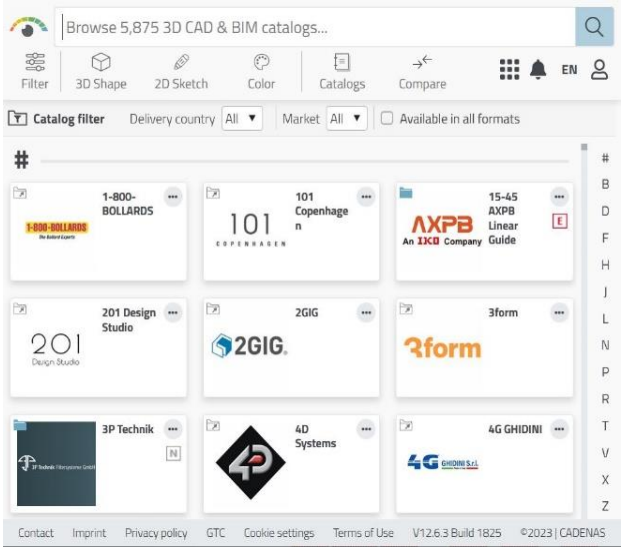

Sl. 1. 3D Findit platforma za vizuelnu pretragu 3D CAD, CAE i BIM modela.

Korisnik ima više mogućnosti za pretragu poput teksta, boje, 2D skice i/ili 3D modela. Na slici 2 prikazan je osnovni algoritam primene platforme 3D Findit za vizuelnu pretragu potrebnog modela iz baze kataloga 3D modela, na osnovu raspoloživog ulaznog 3D modela.

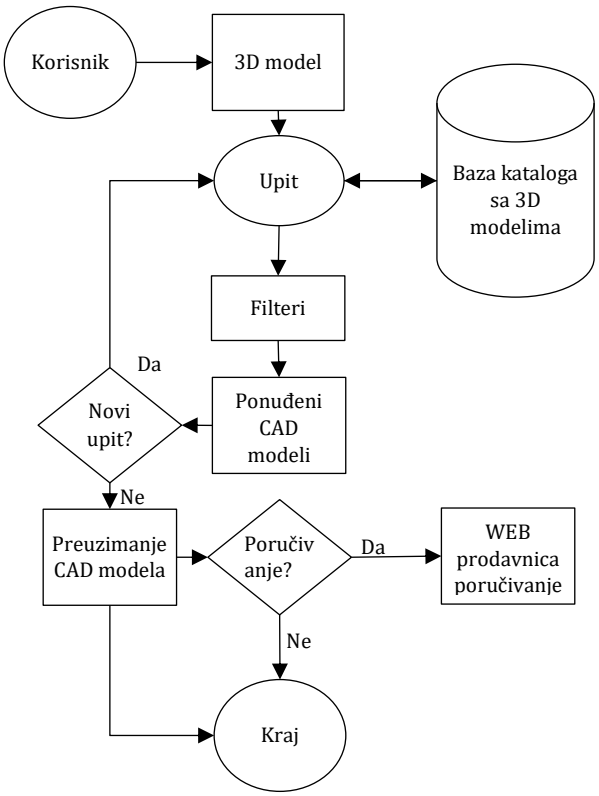

Sl. 2. Osnovi algoritam izbora odgovarajućeg 3D modela primenom 3D modela kao ulazne informacije

Korisnik učitava postojeći 3D model na platformu u jednom od podržanih formata. Sistem analizira učitan 3D model preuzimajući dostupne informacije o obliku i dimenzijama. Nakon toga moguće je primeniti veliki broj filtera kako bi se što tačnije i preciznije definisao odgovarajući zamenski deo. Kao rezultat platforma pruža spisak sa ponuđenim 3D modelima odgovarajućih delova.

3. STUDIJA SLUČAJA - IZBOR STANDARDNOG ZAMENSKOG LEŽAJA U SKLOPU

Poznato je da 3D modeli u bilo kom softveru za modeliranje mogu biti raznih oblika, veličina, sastavljeni od standardnih i/ili specijalizovanih delova. Za potrebe ovog istraživanja izabran je sklop električne tračne brusilice – sklop ETB (Slika 3). Sklop ETB je preuzet sa GrabCAD online zajednice, koja predstavlja najveću onlajn zajednicu profesionalnih inženjera, dizajnera, proizvođača i STEM studenata na planeti [9]. U okviru GrabCAD-a postoji baza sa preko 5900000 različitih modela i sklopova koji su dostupni za besplatno preuzimanje.

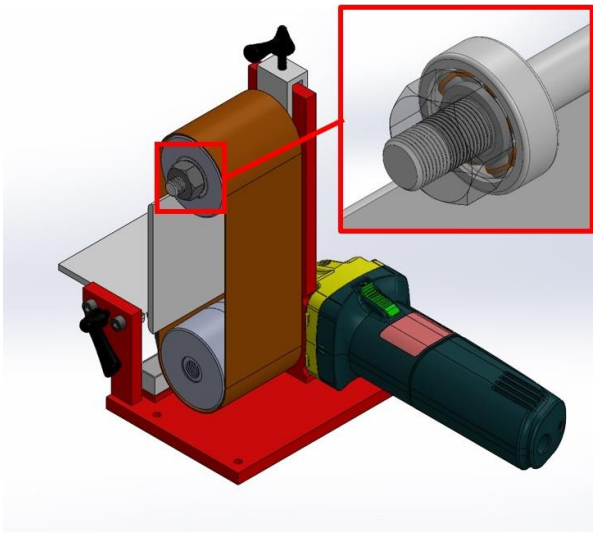

Sl. 3. 3D model električne tračne brusilice

U posmatranom sklopu EBT pronađen je ležaj koji je 3D modeliran na klasičan način i nije generisan pomoću baze podataka u samom softveru ili povučen iz eksterne biblioteke. Jedan od problema prilikom proizvodnje ovog proizvoda, kada se posmatra kao celina, predstavlja to što sam ležaj nema oznaku koja bi uputila na određeni ležaj nekoga od proizvođača širom sveta. Određivanje tačne oznake ležaja i upućivanje na određenog proizvođača, koji ima u ponudi upravo takav ležaj koji odgovara sklopu ETB drastično bi ubrzao vreme nabavke pred samu fazu montaže komponenti sklopa ETB.

Nakon izrade nestandardizovanih delova dolazi se do momenta kada se razmišlja o nabavci što pristupačnijih standardnih delova koji treba da zadovolje kako geometrijske, tako i ekonomske zahteve. Ležaj, kao standardni deo koji se vrlo često nalazi u sklopovima različitih namena spada upravo u tu grupu, ali mora biti definisan kako bi se tačno odredilo koji ležaj je potrebno poručiti prilikom nabavke delova, koji će kasnije u montaži biti ugrađen u sklop.

3.1 Primena platforme 3D Findit za pretraživanje 3D CAD modela

Prvi korak u pretraživanju baze podataka predstavlja učitavanje raspoloživog 3D modela sa njegovim geometrijskim karakteristikama na samu platformu 3D findit. Ova platforma podržava uvoz 3D modela u više različitih formata poput: .stl, .stp, .step, .sat, .x_t, .x_b, .lwo, .lws, .ase, .3ds, .fbx, .dae, .ply, .obj i .jt. Na slici 4 je prikazan prozor u

kome se nalazi učitan 3D model ležaja u .step formatu za koji je potrebno pronaći odgovarajućeg proizvođača.

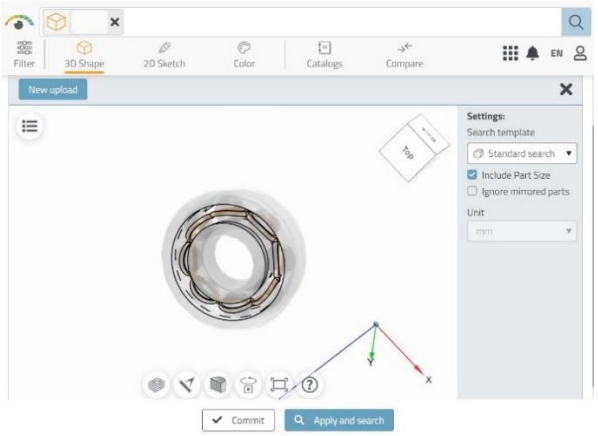

Sl. 4. Prikaz učitanog 3D modela ležaja

Nakon toga pristupa se pretraživanju na Apply and search. Kao rezultat pretrage dobija se prikaz najsličnijih delova iz raspoložive baze podataka koji se tu nalaze. Na slici 5 prikazan je rezultat pretrage sa najsličnijim 3D modelima određenih proizvođača i one koji se podudaraju po izabranim karakteristikama u procentima sličnosti.

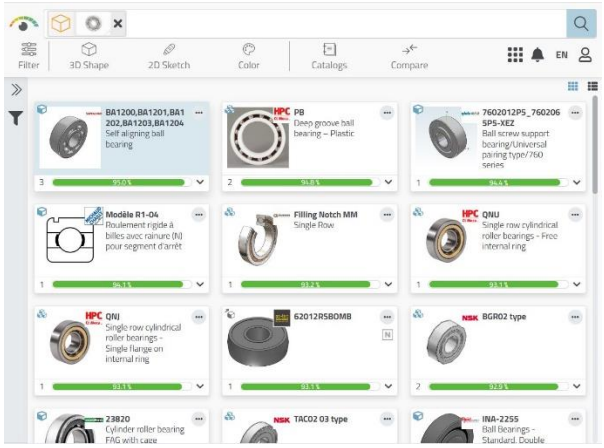

Sl. 5. Rezultat pretrage najsličnijih delova iz baze podataka

Rezultat pretrage 3D modela moguće je filtrirati na razne načine koji su dostupni u samom prozoru 3D Shape search.

U sledećem koraku potrebno je suziti veliki izbor sličnih delova koji je ponuđen od strane platforme. Izbor se može vršiti prema procentu sličnosti, proizvođaču (ako postoje problemi sa nabavkom delova od određenog proizvođača ili postoji već ostvarena saradnja sa određenim proizvođačem), funkcionalnosti, vrsti dostupnog CAD formata, standardu i sl. Kao glavni kriterijum za filtriranje izabran je kriterijum prema procentu sličnosti. Na taj način se dobijaju ležajevi koji dolaze od različitih proizvođača i distributera ležaja širom sveta. Neki od njih su: NSK, SKF, MICHAUD CHAILY itd. Izabrani model ležaja predstavlja ležaj prema kompaniji MICHAUD CHAILY. (Slika 6). Prikaz 3D modela i detalji o tehničkoj specifikaciji na platformi se mogu vršiti na više načina, kao tehnički prikaz dela, 2D prikaz dela sa jasnim dimenzijama ili kao 3D model. U izabranom prikazu pomoću 3D modela postoje razni alati koji služe za bolje sagledavanje, odnosno kao dodatna provera da li izabrani ležaj odgovara potrebama ili ne. Neki od alata su: mreža koja nam služi kao pomoć u dobijanju projekcija i tačnih dimenzija dela, zatim lenjir uz pomoć koga se može proveriti svaka kota na 3D modelu, presek dela u proizvoljno definisanoj ravni ili kao 3D animacija dela.

Izabrani model se može preuzeti kao 3D model u nekom neutralnom formatu ili se može sačuvati u formatu softvera koji je korišćen za 3D modeliranje i dizajn početnog sklopa, kako bi posedovali izvorni format za korekcije ukoliko se jave potrebe za izmene. U okviru ovog prozora prikazuje se tabela sa svim tehničkim podacima o samom delu, u ovom slučaju ležaju. Ukoliko u bazi podataka postoji veći broj različitih konfiguracija samoga modela, moguće je izabrati tačno određeni, na osnovu nekih od bitnih karakteristika. Sa desne strane prethodno pomenute tabele postoji i direktan link na sajt sa kog možemo direktno poručiti izabrani ležaj, što predstavlja najveću prednost ove platforme, jer se može dobiti informacija o ceni i zalihama od strane proizvođača.

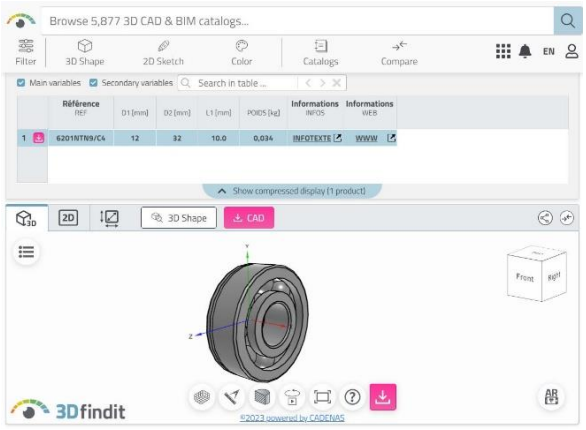

Sl. 6. Prikaz izabranog modela ležaja

Vrlo bitan momenat u postupku provere valjanosti ležaja koji je prvobitno izabran jeste mogućnost preuzimanja modela u formatu koji nam najviše odgovara. Dodavanje istog u sam sklop može se proveriti vizuelno i geometrijski da li je ležaj odgovarajući, a nakon potvrde, odnosno konačnog izbora ležaja, vratiti na 3D findit platformu i poručiti upravo taj ležaj direktno od proizvođača.

Platforma nudi i direktno poređenje modela u slučaju da postoji nedoumica u izboru dela, za čega se koristi funkcija Compare. Ova funkcija daje mogućnost samostalnog izbora najzanimljivijih delova koji se upoređuju direktno, nakon toga se dobija novi prozor u kome su prikazana oba izabrana modela, a u gornjem delu se prikazuju paralelno sve karakteristike koje oni poseduju (Slika 7).

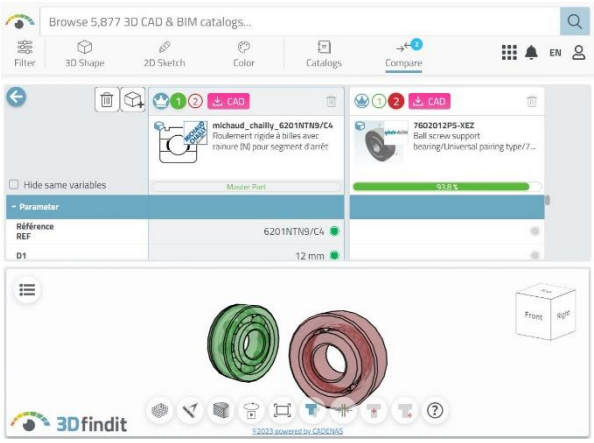

Sl.7. Prikaz prozora Compare funkcije za poređenje izabranih delova

Nakon ove analize otklanja se dilema koji deo će se uzeti kao konačan i postaviti u sklop, a uz to dobija se i uvid u konačne cene u zavisnosti od potrebne količine samih delova u sklopu.

4. ZAKLJUČAK

Prilikom dizajniranja proizvoda izbor standardnih delova može da predstavlja veoma zahtevan posao. Iz tog razloga platforme za vizuelno pretraživanje poput 3D Findit omogućavaju veoma brzu i laku pretragu standardnih, ali i već gotovih proizvoda određenih proizvođača iz raznih oblasti industrija. U ovom radu predstavljen je način izbora odgovarajućeg zamenskog dela na osnovu njegovog 3D modela.

Pretraga pomoću 3D modela predstavlja veoma brzu i pouzdanu pretragu upravo zbog činjenice da se u samom 3D modelu nalaze svi potrebni geometrijski podaci i na taj način je moguće pronaći odgovarajući deo. Ukoliko to ipak nije slučaj, sistem će ponuditi najsličniji deo koji postoji na tržištu i na taj način omogućiti dizajneru da pre puštanja u proizvodnju izmeni i prilagodi dizajn prema standardnom delu.

Pravci budućih istraživanja bi imali za cilj upoređivanje različitih platformi za pretragu 3D modela sa aspekta brzine pretrage, ponuđenih filtera i veličine same baze 3D modela.

5. ZAHVALNICA

Ovaj rad je podržan od strane Ministarstva nauke, tehnološkog razvoja i inovacija kroz projekat broj 451-03-47/2023-01/200156 „Inovativna naučna i umetnička istraživanja iz domena delatnosti FTN-a“.

6. REFERENCE

[1] H. Matyi, P. Veres, T. Banyai, V. Demin, and P. Tamas, “*Digitalization in Industry 4.0: the Role of Mobile Devices*,” Journal of Production Engineering, vol. 23, no. 1, pp. 75–78, 2020.

[2] T. Funkhouser *et al.*, “*A search engine for 3D models*,” ACM Transactions on Graphics, vol. 22, no. 1, pp. 83–105, 2003.

[3] J. Wang, H. Cai, and Y. He, “*A Method for Content-Based Searching of 3D Model Databases*,” Data Science Journal, vol. 7, no. April, pp. 46–53, 2008.

[4] D. Chen, X. Tian, Y. Shen, and M. Ouhyoung, “*On Visual Similarity Based 3D Model Retrieval*,” Computer Graphics Forum, vol. 22, no. 3, pp. 223–232, Sep. 2003.

[5] P. Min, J. A. Halderman, M. Kazhdan, and T. A. Funkhouser, “*Early experiences with a 3D model search engine*,” Web3D Symposium Proceedings, 2003.

[6] E. A. Lmaati, A. El Oirrak, and M. N. Kaddioui, “*A 3D search engine based on 3D curve analysis*,” Signal, Image and Video Processing, vol. 4, no. 1, pp. 89–98, 2010.

[7] “Download 3D CAD Models for free.” https://www.3dfindit.com/en/ (accessed Nov. 03, 2023).

[8] Y. Shen, D. Chen, X. Tian, and M. Ouhyoung, “*3D Model Search Engine Based on Lightfield Descriptors*,” Forum American Bar Association, pp. 23–30, 2003.

[9] “GrabCAD Making Additive Manufacturing at Scale Possible.” https://grabcad.com/ (accessed Nov. 10, 2023).

Autori: **MSc. Dejan Božić, prof. dr Mijodrag Milošević, prof. dr Dejan Lukić, doc. dr Željko Santoši,** Univerzitet Novi Sad, Fakultet Tehničkih Nauka, Trg Dositeja Obradovica 6, 21000 Novi Sad, Serbia, Tel: +381 21 485 2350, Fax: +381 21 454-495.

E-mail: bozic997dejan@uns.ac.rs
mido@uns.ac.rs
lukicd@uns.ac.rs
zeljkos@uns.ac.rs

ETIKUM 2023 **INTERNATIONAL SCIENTIFIC CONFERENCE**
NOVI SAD, SERBIA, DECEMBER 7-9, 2023

Erić Obućina J., Pravdić P., Obućina V.

NOISE AND VIBRATIONS IN HYDRAULIC CONTROL SYSTEMS OF MOTORS VEHICLES

Abstract: *In hydraulic power steering systems of motor vehicles, often unintended acoustic phenomena can result from certain driving situations. The acoustic phenomenon known as "rattling" is generated by impacts on the steering cylinder, if the car rides over bumps, kerb stones or imilar obstacles. In special friction conditions between tyre and road surface during parking, a phenomenon called "shuddering" occurs and leads to strong vibrations. These are audible by the driver as noise, and sensory through shaky steering wheel torque. In this paper are presenting noise and vibration in hydraulic power steering systems of motor vehicles.*
Key words: *hydraulic, steering systems, noise, vibration*

1. INTRODUCTION

In motor vehicles of the upper class are hydraulic systems due to their power density, low power to weight ratio and good controllability used. The noise reduction of hydraulic systems in motor vehicles is therefore given much attention. Loud noises from the driver as felt uncomfortable and annoying and are a key feature in the assessment the value of a motor vehicle. The extremely fluid sound that occur in hydraulic systems by local fluctuations of pressure and flow of power-transmitting fluid. These pulsations able by a hydraulic line system easily transported over long distances body and are adjacent to excite vibrations. [2] Referred to as structure-borne sound haptic perceptible vibration from the driver. The emergence of the purely acoustic perceptible air by the vibration of sound is done in conjunction with the air standing body. Both air-borne noise and suggestions must be small, not to be evaluated from the rider's comfort-reducing. The noise-causing pulsations in hydraulic steering systems for their manifestations categorized. As transient pulsation, all fluid a changes denotes that occur only temporary, while expected from a normal state of the system vary. That caused by collisions and as a "rattling" sound familiar phenomenon in power steering is an example of transient pulsations.

Use hydraulic servo steering gear we first began to heavy vehicles and buses, then on medium-heavy, with tendency applications and easier to economic vehicles. [1] This is especially and mainly applies to vehicles that are driving in the city traffic. Effectively, it can be said that the broadest application with the cars have hydraulic servo steering gear. Do not create a big noise, are relatively small in size, but also amortization strikes that encourage activities of times on the control wheel. The time required to activate hydraulic servo steering gear (0.05 s) is considerably less than the time at pneumatic (0.3 to 0.4), which is also important.

2. HYDRAULIC STEERING SYSTEMS

Two problems in road traffic contributed to the start of serial production of hydraulic steering:

- Increased traffic density and high vehicle speeds require increased safety in road traffic. To this end, it is not enough to construct a single vehicle, which, based on its stability, meets all requirements, but on the contrary, care must be taken to relieve the driver as much as possible, so that he can devote his attention to the traffic on the road. This is also significant because the driver's power to control and engage the gearbox is reduced to the smallest possible extent. Thus, there is only one way to facilitate steering: using hydraulics as an auxiliary force. [4]
- The agility of the vehicle, which primarily depends on the transmission ratio of the steering wheel, had to be preserved and, if possible, even increased. If the transmission ratio of the steering wheel does not increase with high axle loads, without increasing the steering forces, then this condition can only be met here if the hydraulic auxiliary force is applied.

Servo steering gear with a servo-mechanical feedback. In the picture shown is a block diagram of work hydraulic servo steering gear. Driver wrap around controller cars for the corner (ψ) to arm hydraulic servo steering gear rotation for a certain angle (φ). Therefore, admission to the servo system is angle (ψ),output is angle(φ). [2]

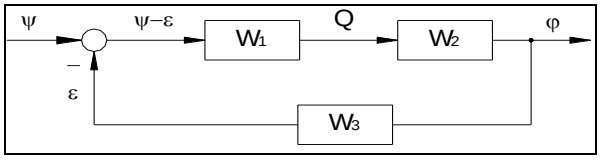

Fig. 1. Block diagram of work servo steering gear [2]

With the progress of technology, and in order to facilitate human work in all domains, it led to the application of an additional auxiliary force for management - the application of hydraulic steering. With heavier trucks and buses, this application has long since become a reality for serial production. [1]

Until recently, for medium-duty vehicles, the installation of power steering was considered a special optional equipment, as well as for larger passenger vehicles. However, now even in these categories of vehicles, hydraulic controls are installed as standard. This especially and mainly applies to vehicles that are driven in city traffic.

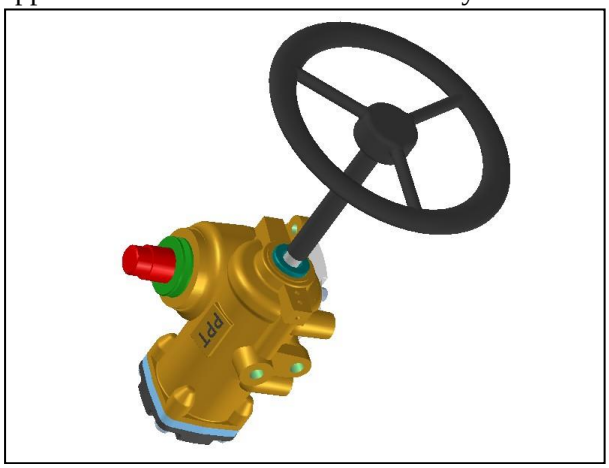

Fig. 2. Hydraulic servo steering gear PPT Trstenik [1]

Similar to the field of hydraulic brakes, practice has led to the fact that even in the production of hydraulic steering, a strong orientation towards one manufacturer can be observed, which is applied to several vehicle manufacturers. This is a great relief for vehicle users and workshops, as they are regularly informed by only one steering manufacturer.

The task of steering is possible in an unambiguous assignment of the steering wheel rotation and the change in direction of the vehicle. [4] To fulfill this task, a position control have prevailed in two models, which differ by the type of steering gear. For one, the ball-nut power steering should be mentioned, especially in the heavy vehicles will be built (see Figure 3).

Due to the high weight and high however, this design costs will disappear more and more of the market.

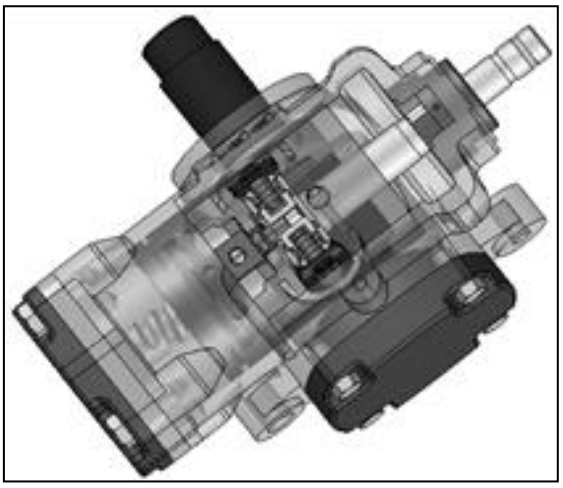
Fig. 3. Mechanical recirculating ball steering [3]

Very affordable and lighter hydraulic steering rack, which in recent years enforced, even with heavy vehicles have (see Figure 4).


Fig. 4. Mechanical rack and pinion steering

The application of hydraulic steering in domestic motor vehicles began first on heavy goods vehicles and buses, then on medium-heavy ones, with a tendency to use them on lighter commercial vehicles as well. [3]

Although the most necessary instructions on power steering are given along with the maintenance instructions for the complete vehicle, for a more comprehensive introduction to power steering and better maintenance, a special and more extensive familiarization with this very important and vital device for vehicle safety in traffic is necessary.

The increasing demand for comfort to the steering system of a modern car and the rising environmental awareness among the population in parallel with the development of motor vehicles also for the continuous further development of steering systems performed. This increasing demands on a steering system can be developed over the years to additional functions that extend the purely mechanical steering system to reflect and allow the example of the rack and pinion steering system of a systematic classification.

3. NOISE AND VIBRATIONS IN HYDRAULIC STEERING SYSTEMS

The known noise phenomena in hydraulic steering systems fall into two groups divided. The first group includes those who are detached from the overall vehicle inherently can also be caused in the steering system itself. These include one the pump pulsation, caused by the irregular operation of the pump delivery will flow and the other sounds on the steering valve, on the chosen by the manufacturer control edge geometry, beam delivery and the manufacturing process are returned to lead. [1] The second group can be assigned to all noise phenomena that occur only when certain dynamic driving conditions prevail and the cause of the noise generation the interaction of the entire vehicle and steering system originates. Foremost among these are one hand, shocks that go beyond the tie rods to the steering cylinder and thus the hydraulic system and affect other undamped vibrations in the steering of the steering cylinder in the state to adverse road surfaces.

3.1 Pump pulsation

The main cause of pulsations in the hydraulic steering system is the hydrostatic displacement unit. [1] Typical designs used in steering systems are the external gear pump and vane pump. The results from the pump pulsation discontinuous operation, many of hydrostatic pumps. They can be after the formation mechanisms subdivided into:

- Kinematic pulsation

These are the geometric factors related to the displacement unit flow pulsations, since the is continuous displacement of the rotation angle work.

- Compression-related pulsation

The compression-induced pulsation arises from the compression work of the displacement space enclosed oil volume in the transition from low pressure to high-pressure chamber and vice versa.

- Kinetic pulsation

In valve-controlled displacement units, the compression is largely due to pulsation away, as the displacer can be switched under pressure control. However, comes it in between the mechanical components of the valves and connecting channels of the oil column to vibration effects, which in turn lead to pulsations.

- Leakage induced pulsation

If the load pressure of a pump varies over the angular position of the shaft, this leads to a changing internal leakage flow, the total volume flow from subtracted.

A fluctuating pump flow caused depending on the connected hydraulic system to dynamic pressure pulses, which generate noise. State of the art in the damping of the pulsations of power steering pump is the use of tubular stretch.

3.2 Flow noise at the steering valve

By over the years achieved marked reduction of sound radiation from combustion engines are noises of ancillary units, e.g. power steering, in the passenger perceptible. Steering valves of automotive power steering systems in operation, it can cause flow noise. Familiar sounds on the steering valve flow pipes are valve or hiss.

Since in the motor vehicle has a mechanical connection between the steering valve and steering wheel is, the flow of body noises and sound radiation in air reach the passenger compartment and up to the driver's ear penetrate. [3]

The steering valve caused noise is predominantly at the valve control edges, which cause overflow of pressure and density fluctuations in the fluid. Responsible for them in addition to transient fluid dynamics and cavitations. Especially on the closing control edges can lead to high flow velocities and low static pressures, the cavitations nuclei favor.

Also, the beam line has an influence on the noise excitation. It leads to unsteady flow phenomena, such as turbulence, jet separation and turbulence. Although the edges of a steering control valve are created equal, it can still differences give the sharp edges of the control edges, the manufacturing process used to is due.

In modern hydraulic steering systems, flow noise by a suitable choice of the control edge geometry and manufacturing process is largely avoided.

A another way to avoid high flow rates is that insertion of ridges in the grooves of the valve spool. This is an intermediate pressure in the valve slide chambers generated, which reduces cavitation and vortex motion.

A disadvantage of this measure is the higher energy consumption of the steering system due to the intermediate pressure, of a higher percentage of fuel demand generated steering.

3.3 Shocks to the steering cylinder

A In certain driving situations can impact on the roadway via the tie rods in the steering system can be initiated. Although the hydraulic steering system is inherently attenuated, to shocks to the steering cylinder by the axle kinematics - especially when the articulated wheels - are amplified and cause unwanted noise.

One example is the driving over curbs or parking garage lowered thresholds mentioned. Performs impact excitation of the track rods to a

noise stimulus, not as a single event imperceptible, but by the impact excitation still swings over several periods, people talk about "rattling". It is necessary to distinguish whether the clatter of a lift-off the rack from the pinion can be recycled, or whether the cause of the rattling search elsewhere in the system. The former can be a major bias of the pressure element, which is a push away the rack from the pinion to be avoided to prevent. This measure is not effective, further studies necessary to identify the causes of the rattling.

3.4 Self-excited vibration of the steering cylinder

In the series production of steering gears but finds a 100% inspection of the hydraulic work more, yet small tolerance variations in the steering valve can, in certain working points of the position of the steering control loop lead to instability. [1]

The definition of valve characteristic is usually done by the automobile manufacturers themselves use the valve characteristic is the vehicle-specific steering feel determined.

4. FINAL REMARKS

This work deals with the development of intelligent secondary measures control of noise phenomena in hydraulic power steering systems, which in certain driving conditions occur.

Referred to as hydraulic rattle noise phenomenon in power steering is caused by collisions, which when driving over bumps, lowered curbs or similar barriers affect the steering cylinder. When the parking occurring chatter, which is also referred to as "Shudder" is known suggests that the steering system for certain friction between tire and road surface conditions to strong vibrations on. These will be the one perceived by the driver acoustically as noise, secondly, they are also tactile fluctuating due to a steering wheel torque perceptible. Both noise phenomena are so far in the vote in the steering driving test empirically tackled using passive secondary measures.

The best known secondary measure to prevent rattling and chattering is to change the direction of votes steering system. On the one hand, this is done by increasing the proportion in the hose line systems, other hand, stops in the hydraulic lines of the steering system integrated in order to change the transmission characteristics.

Both measures are secondary however, in a conflict. Is optimized to rattle down a line, reinforced the chatter in the steering system and vice versa.

5. REFERENCES

[1] Erić, J.: *Master work*, Faculty of Mechanical Engineering in Kraljevo, Serbia, 2007.Erić

[2] Erić J.: *Final work*, Faculty of Mechanical Engineering in Kraljevo, Serbia, 2004.,

[3] Obućina V.: *Final work*, Faculty of Mechanical Engineering in Kraljevo, Serbia, 2005.,

[4] Erić Obućina, J, Obućina V., *Noise And Vibrations In Hydraulic Steering Systems On Motors Vehicles*, 11th International Conference Research and Development in Mechanical Industry RaDMI 2011, 15 - 18. September 2011, Sokobanja, Serbia

[5] Baum, H., Hofmann, M.: *A New Method for Power Steering Hose Assembly Design and Acoustic Optimisation by means of Time Domain Hydraulic Line Simulation Models*, Centre for Power Transmission and Motion Control (PTMC), University of Bath, 2007

[6] Rösth M., Palmberg J.-O.: Robust Design of a Power Steering System with Emphasis on Chattering Phenomena, Scandinavian International Conference on Fluid Power, 10th SICFP, Finnland, 2007

[7] Erić Obućina, J., Obućina, V., Mihajlović, G., Mijatović M.: *Integrated Product Design And Technology Of Hydraulic Truck Power Steering*, METALURGIA INTERNATI-ONAL, (2012), vol. 17 br. 9, str. 58-64

[8] Babić A.: *Technology of assembly*, Faculty of Mechanical Engineering in Kraljevo, Serbia, 2005.,

[9] Rajamani, R.: *Vehicle Dynamics and Control*, University of Minnesota, USA, 2005.

Authors: **mr Jelena Erić Obućina,** Academy of Professional Studies Šumadija (ASSŠ) – Department Trstenik**, dr Predrag Pravdić** Academy of Professional Studies, Department in Kruševac, **Vladan Obućina,** Army of Serbia.

E-mail: jobucina@asss.edu.rs
thepera81@gmail.com
obucina_vladan@yahoo.com

ETIKUM 2023 **INTERNATIONAL SCIENTIFIC CONFERENCE NOVI SAD, SERBIA, DECEMBER 7-9, 2023**

Goluža B., Zovko O.

OPTIMIRANJE KONSTRUKCIJE ALATA ZA ISTISKIVANJE, KORIŠTENJEM FEM SIMULACIJE, ALUMINIJSKOG PROFILA KOMPLEKSNOG OBLIKA

Rezime: *Kvaliteta istisnutih profila ovisi o mogućnosti učinkovite kontrole protoka materijala trupca kroz alat za istiskivanje. Interakcija alata za istiskivanje i aluminijskog trupca može uzrokovati neuravnotežen protok metala i deformaciju oblika profila. Konstruktori alata kontrolu protoka metala postižu korištenjem empirijskih pravila ili jednostavno konstruiraju alat za istiskivanje metodom pokušaja i pogrešaka. Simulacija procesa istiskivanja, metodom konačnih elemenata, omogućava predviđanje rezultata istiskivanja, pomaže smanjiti mogućnost pogreške pri konstruiranju alata naročito kod kompleksnih oblika profila. U radu će biti prikazan praktičan primjer poboljšanja konstrukcije alata korištenjem simulacije metodom konačnih elemenata i izbjegavanje skupe i dugotrajne metode pokušaja i pogrešaka.*

Ključne riječi: *optimiranje konstrukcije alata, istiskivanje aluminija , FEM analiza*

1. UVOD

Veoma čvrsti dijelovi male težine i kontinuiranog presjeka se najčešće dobivaju procesom istiskivanja. Legure serije 6000 (Al-Mg-Si serije) imaju najveću zastupljenost na tržištu aluminija. Više od 80 % proizvoda od aluminijskih legura na svijetu su upravo proizvodi iz legura serije 6000 [1]. Razlog zašto se uzima ova grupa legura su dobre osobine za proizvodnju i primjenu. Legure serije 6000 imaju srednju čvrstoću, toplinski su obradive, imaju dobru mogućnost obrade i zavarljivosti.

2. FEM ANALIZA

Trenutno najčešće korištena metoda za modeliranje procesa istiskivanja aluminija je metoda konačnih elemenata (FEM).

Ova numerička tehnika može predstavljati složenu geometriju kao konačni broj elemenata spojenih čvorovima. Sile i granični uvjeti mogu se primijeniti na čvorove pri simuliranju sile i ograničenja koja djeluju na geometriju.

FEM simulacija može imati više namjena u analizi procesa istiskivanja i optimiranju konstrukcije alata. Ona može zamijeniti ili nadopuniti eksperimente na stvarnom istiskivanju kada dolazi do ispitivanja odnosa između parametara i ispitivanja prirode tečenja unutar recipijenta i alata. Simulacije nude dvije važne prednosti u odnosu na stvarne eksperimente. Prvo, neke je parametre mnogo lakše izmjeriti nego u eksperimentima na prešama za istiskivanje. Na primjer, mrtve zone vizualiziraju se relativno lako. Ovo pruža vrijedan uvid u ono što inače često ostaje nepoznanica. Ove informacije mogu pomoći u pružanju fizikalnih objašnjenja odnosa između parametara koji mogu biti otkriveni u simulaciji. Deformaciju alata također je vrlo teško izmjeriti prilikom eksperimenata. U FEM simulaciji prilično je jednostavno odrediti naprezanja i deformacije kritičnih područja u alatu do detalja. Druga važna prednost proučavanja parametara pomoću FEM-a je da se utjecaj pojedinih parametara u istraživanju može izolirati uklanjanjem utjecaja nad kojima istraživač obično ima ograničenu ili nikakvu kontrolu.

Na primjer, ako se ispituje veza između duljine radne površine i izlazne brzine, alat se može modelirati tako da se utjecaji deformacije (plastične) alata ostanu kao u matematičkim proračunima. Ovo je nemoguće prilikom eksperimenata u stvarnom procesu istiskivanja, gdje će se uvijek dogoditi neka deformacija s nepoznatim posljedicama za parametar koji se mjeri. Varijacije procesa poput fluktuacije temperature također se ne javljaju u numeričkim simulacijama. Međutim, treba napomenuti da se svako istraživanje može baviti samo vrlo malim dijelovima matrice zavisnosti istovremeno, a FEM simulacije nisu iznimka od toga. Pravila dizajna koja proizlaze iz ovog istraživanja još uvijek nisu često

prenosiva između tvrtki, jer je uključeno premalo parametara.

FEM se također može koristiti kao alat za provjeru konstrukcije novih alata ili kao sredstvo za ispitivanje alata koji su iz nepoznatih razloga pokazali razočaravajuće proizvodne rezultate. Ovim putem izvedba alata se može predvidjeti ili se mogu pronaći uzroci loših proizvodnih rezultata. Međutim, za simulacije složenih alata i profila koji se danas koriste u proizvodnji još uvijek uzima puno vremena [2-4].

3. TOK MATERIJALA PRILIKOM ISTISKIVANJA PROFILA

Tijekom procesa istiskivanja profila tečenje materijala je važno jer se prepoznaje oblik i odabiru parametri prešanja. Obično je istiskivanje aluminijskih profila vrlo složen proces tečenja metala koji uglavnom ovisi o dizajnu samog alata. Ako je brzina tečenja u poprečnom presjeku izlaza alata neujednačena greške poput uvijanja, valovitosti, pucanja i savijanja su izražene i često sam alat upropaste. Trenutni dizajn strukture alata za istiskivanje se temelji na metodi pokušaja i pogrešaka. Učinkovitost alata je u velikoj mjeri određena po iskustvu samog konstruktora alata. Ovakvim dizajnom je nemoguće zajamčiti kvalitetu proizvoda i produktivnost kada je struktura profila složenija i stvarna proizvodnja se mora zaustaviti ili odgoditi. Sa sve većom primjenom računalnih tehnika u posljednjem desetljeću veliki broj studija numeričke simulacije procesa istiskivanja se provodi kako bi se poboljšala kvaliteta proizvoda i učinkovitost proizvodnje. Numerički modeli se koriste za predviđanje naprezanja alata, raspodjelu temperature, gradijente napona i naprezanja prilikom istiskivanja, brzine tečenja, pritiske istiskivanja, dimenzije, deformacije,… koje je teško izmjeriti standardnim metodama. Osim toga utjecaj dizajna alata i parametara procesa istiskivanja na ovim varijablama mogu lako i učinkovito pretpostaviti kako optimizirati dizajn alata i parametre procesa.

Softverski paket uključuje nekoliko programa koji su dizajnirani za različite vrste industrije. Za simulaciju protoka materijala pri istiskivanju aluminijskih legura koriste se tri različita alata: HyperMesh, HyperXtrude i HyperView [5,6].

Razni znanstvenici su već radili na uvođenju numeričkih simulacija u proces konstruiranja alata za istiskivanje – predstavljen je postupak modeliranja komponenti koje su potrebne za simulaciju [7,8], optimizaciju alata na temelju rezultata simulacije [8] i simulaciju rezultata dobivenih u procesu istiskivanja [7-10].

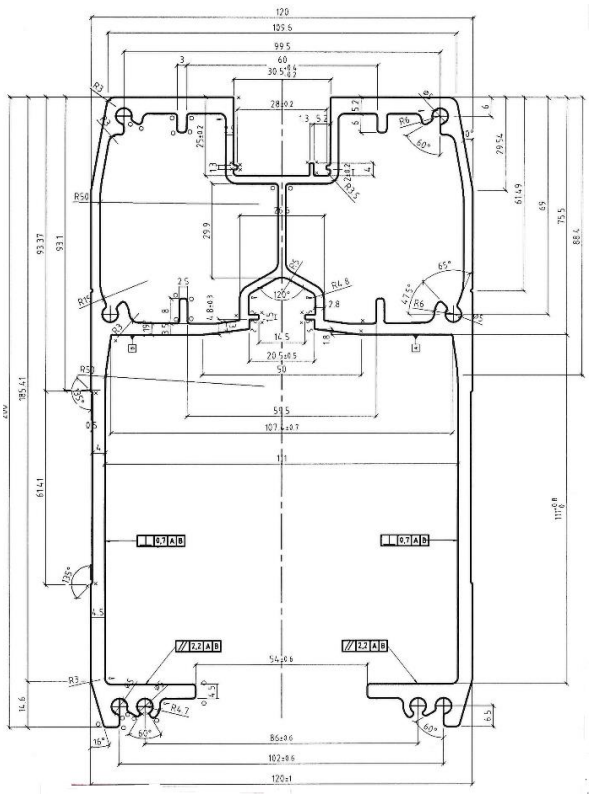

Sl. 1. Prikaz dimenzija i geometrije profila

4. PROTOK MATERIJALA KROZ ALAT

U procesu istiskivanja temperatura iz otvorenog dijela alata uglavnom utječe na prenošenje topline trenja i topline plastične deformacije.

Na istisnutom modelu se može vidjeti da se temperatura materijala najprije spušta, a zatim ide u smjeru ekstrudiranja. Razlog za to je što se toplina konstantno prenosi sa trupca na alat s nižom temperaturom.

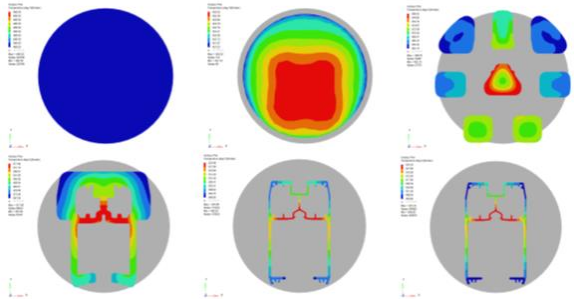

Sl. 2. Prikaz tečenja materijala u različitim fazama

Na početku procesa istiskivanja temperatura trupca pomalo se spušta. Zatim se trupac dijeli na više dijelova u zavisnosti od mjesta gdje se nalazi. Od ovog trenutka plastična deformacija je očito veća od one u ranoj fazi procesa istiskivanja, pa temperatura lagano raste, međutim temperatura materijala u ovom trenutku je još uvijek unutar početne temperature trupca. Kada materijal dođe na mjesta zavarivanja plastična deformacija postaje sve veća i veća, kao rezultat toga temperatura trupca neprekidno raste uzduž smjera istiskivanja. Pri dolasku materijala na radne površine alata događa se maksimalna deformacija i temperatura je najveća na ovom dijelu. Iz svega navedenog se može zaključiti da je porast temperature istisnutog materijala uglavnom uzrokovan oslobađanjem topline plastične deformacije tijekom procesa istiskivanja.

S numeričkim rješenjem proizvodi se alat i izvodi se praktično istiskivanje profila. Procesni parametri koji se koriste u simulacijama konačnih elemenata i u stvarnoj proizvodnji su isti. Teško je dobiti dobru eksperimentalnu provjeru numeričkih rezultata. Međutim, gruba usporedba sa stvarnim izlazom brzina se može postići ako se pogleda početak istiskivanja profila [11], koji se često koristi za podešavanje konstrukcije alata.

Na temelju tih rezultata, prilagodba konstrukcije matrice, kao što su geometrija i veličina dotoka, duljina radnih površina alata itd. može se izraditi radi kompenzacije za ovu brzinsku razliku.

Osim gore navedenih usporedbi, urađena je i dimenzionalna usporedba zahtjevanog i dobivenog profila nakon izrade alata. Dobiveni rezultati odgovaraju traženim po crtežu.

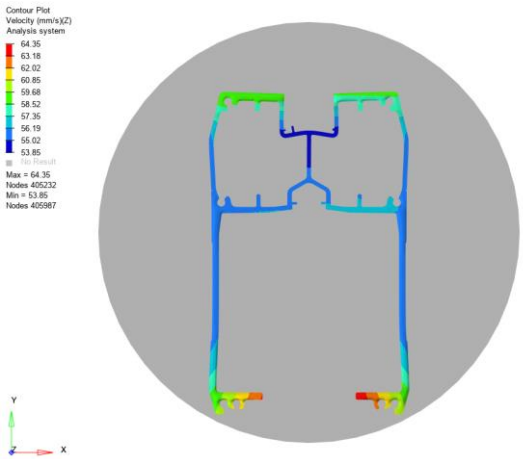

Sl. 3. Prikaz brzina tečenja materijala

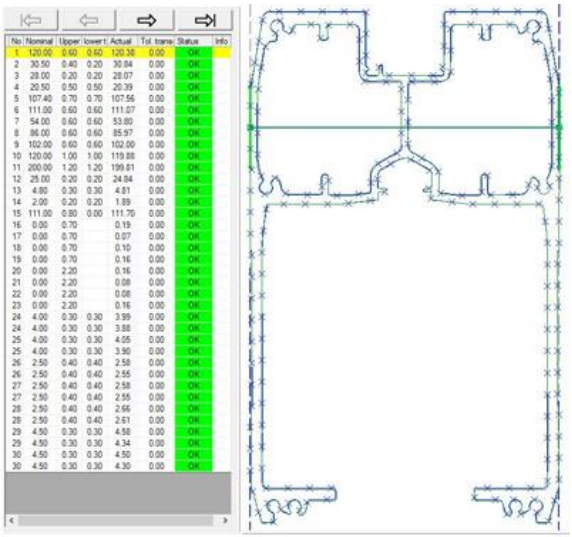

Sl. 4. Prikaz dimenzionalne uporedbe CAD modela i istisnutog profila

Iz svega se može zaključiti da numerički model može pružiti razumne rezultate i biti korisna smjernica za praktičnu proizvodnju.

5. ZAKLJUČAK

U ovom radu je prikazana simulacija istiskivanja profila kompleksnog poprečnog presjeka, koji se koristite u industriji. Simulacijom se može učinkovito uravnotežiti protok materijala tijekom procesa istiskivanja i ova bi studija mogla pružiti smjernice za praktičnu proizvodnju. Numerička simulacija se može učinkovito koristiti za smanjenje broja proba.

Protok materijala tijekom istiskivanja složenih oblika je simuliran kroz program HyperXtrude. Stoga bi se mogao istražiti utjecaj varijacija dizajna alata.

Opterećenje predviđeno simulacijom profila korištenih u eksperimentima bilo je unutar traženih eksperimentalnih rezultata. Utjecaj varijacije parametara istiskivanja kao i geometrije presjeka o temperaturi i opterećenju bilo je u danim granicama ispitivane geometrije. Predviđanje temperature istiskivanja je bilo blizu predviđenih i unutar simuliranih vrijednosti. Geometrija i omjer istiskivanja utjecali su na temperaturu i opterećenje prilikom istiskivanja.

Protok materijala tijekom cijelog procesa istiskivanja dobro je predviđen primjenom programa HyperXtrude. Sve razlike u protoku metala za različite oblike mogle bi biti zadovoljavajuće modelirane pomoću programa.

6. REFERENCE

[1] Al-Marahleh G.: *Effect of heat Treatment Parameters on distribution and Volume Fraction of Mg2Si in the Structural Al6063 Alloy*, American Journal of Applied Sciences, Vol. 3, No. 5, pp. 1819-1823, 2006.

[2] Lof, J.: *Developments in Finite Element Simulations of Aluminium Extrusion*. Ph.D. dissertation, University of Twente, 2000.

[3] Donati, L., et al. *Extrusion Benchmark 2007—Benchmark Experiments: Study on Material Flow Extrusion*, in Proceedings: Ninth International Aluminum Extrusion Technology Seminar, 2008.

[4] Fang, G., Zhou, J., Duszczyck, J.: *FEM Simulation of Aluminium Extrusion Through Two-Hole Multi-Step Pocket Dies*. Journal of Materials Processing Technology, Vol. 209, No. 4, pp. 1891-1900, 2009.

[5] Altair Engineering Inc., Hyper Works, Online:http://www.altairhyperworks.co.uk/,accessed on Feb. 13, 2013.

[6] Altair, HyperWorks 10.0., Help, 2009.

[7] Andredi, T.: *Extrusion simulations: a new approach in die-design process*, International Conference on Extrusion and Benchmark, Dortmund, 2009.

[8] Kumar, S., Vijay, P.: *Die design and experiments for shaped extrusion under cold and hot condition*, Journal of Materials Processing Technology, Vol. 190, No. 1-3, pp. 375-381, 2007.

[9] Krähenbühl, Y., Bourqui, B.: *Simulation aided extrusion in the design practice*, International Conference on Extrusion and Benchmark, Dortmund, 2009.

[10] Li, G., Yang, J., Oh, J. Y., Foster, M., Wu, W., Tsai, P., Chang, W.: *Advances of Extrusion Simulation in DEFORM-3D*, International Conference on Extrusion and Benchmark, Dortmund, 2009.

[11] Lof, J., Blokhuis, Y.: FEM simulations of the extrusion of complex thin-walled aluminium sections, Journal of Materials Processing Technology, Vol. 122, No. 2-3, pp. 344–354, 2002.

Autori: **Božo Goluža, mag. ing. stroj., Oliver Zovko, dipl. ing. stroj,** Fakultet strojarstva računarstva i elektrotehnike, Sveučilište u Mostaru, Matice hrvatske b.b, 88000 Mostar, BiH, Tel: +387 36 337 033, Fax: +387 36 337 033.

E-mail: bozo.goluza90@gmail.com
oliverzovko@gmail.com

ETIKUM 2023 **INTERNATIONAL SCIENTIFIC CONFERENCE**
NOVI SAD, SERBIA, DECEMBER 7-9, 2023

Havrlišan, S., Wang, H., Klarić, Š.

ISTRAŽIVANJE UTJECAJA PARAMETARA 3D PRINTANJA NA VLAČNU ČVRSTOĆU

Apstrakt: *Cilj rada je primenom planiranih pokusa istražiti utjecaj parametara (debljina sloja i gustoća ispune) 3D printanja na vlačnu čvrstoću te dobivanje regresijskog model za predviđanje vlačne čvrstoće. Primenjen je faktorski plan pokusa na dve razine s tri ponavljanja. Ulazni parametri menjani na dve razine su: debljina sloja (0,1 i 0,3 mm) i gustoća ispune (20 i 50%), dok je izlazni parametar vlačna čvrstoća. Statističkom analizom eksperimentalih podataka zaključeno je da na vlačnu čvrstoću utječu oba parametra (debljina sloja i gustoća ispune), dok interakcija ta dva parametra nema utjecaja. Dobiven je regresijski model za predviđanje vlačne čvrstoće s visokim koeficijentom determinacije* R^2.
Ključne reči: *3D printanje, planirani pokusi, regresijski model*

1. UVOD

3D printanje danas je prilično često te ima široku primenu u različitim područjima. Ta područja uključuju proizvodnu industriju, medicinu, arhitekturu, građevinu, automobilsku industriju, zrakoplovnu i svemirsku industriju, modu, umjetnost, znanost, edukaciju i dr. Primenjuju se različite tehnologije 3D printanja. Najčešće korištene tehnologije su: modeliranje fuzijskim taloženjem (eng. fused deposition modelling - FDM), stereolitografija (eng. stereolithography - SLA), selektivno lasersko sinteriranje (eng. selective laser sintering - SLS), i dr. [1-9]. Ovisno o nameni i specifičnim karakteristikama isprintanog dela primenjuju se različiti materijali: PLA, PLA+, ABS, ABS+, PETG, TPE, polikarbonati, najlon, metali, smole, keramika, biomaterijali, i dr [1-9].

Kako bi se poboljšala svojstva isprintanih delova istraživanja su često usmerena ka novim materijalima, novim tehnologijama printanja kao i ispitivanju mehaničkih svojstava 3D printanih delova [3-12].

Na mehanička svojstva 3D printanih delova utječe velik broj parametara. Najčešće istraživani parametri su: brzina ispisa, gustoća ispune, uzorak ispune, debljina sloja, temperatura filamenta, temperatura radnog stola, orijentacija filamenta, i dr. [1, 3-12].

U radu je primenjen faktorski plan pokusa na dve razine s tri ponavljanja kombinacije razina parametara. Cilj rada je istražiti utjecaj parametara 3D printanja (debljina sloja i gustoća ispune) na vlačnu čvrstoću te dobivanje regresijskog modela za predviđanje vlačne čvrstoće u ovisnosti o debljini sloja i gustoći ispune.

2. PROVEDBA EKSPERIMENTA

Prema ISO 527-2-2012 [13], određen je geometrijski model uzoraka koji je prikazan slici 1.

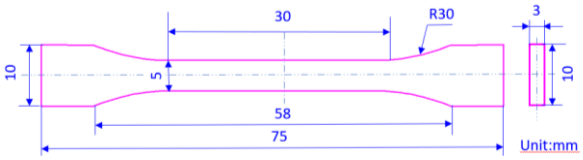

Sl. 1. Dimenzije 3D uzorka

Primenjen je faktorski plan pokusa na dvije razine. Ulazni parametri su debljina sloja (0,1 i 0,3 mm) i gustoća ispune (20 i 30 %). Izlazni parametar je vlačna čvrstoća. Prema planu pokusa i redosledu izvođenja pokusa prikazanom u tabeli 1, provedeno je printanje 12 ispitnih uzoraka od materijala PLA na 3D Flashforge Adventure 3 printeru (slika 2).

Tabela 1. Plan pokusa i redosled izvođenja pokusa

Kon. raspored	Broj pokusa	Debljina sloja / mm	Gustoća ispune / %
1	6	0,3	20
2	9	0,1	50
3	12	0,3	50
4	4	0,3	20
5	10	0,3	50
6	11	0,3	50
7	7	0,1	50
8	1	0,1	20
9	3	0,1	20
10	2	0,1	20
11	8	0,1	50
12	5	0,3	20

Nakon printanja uzoraka na 3D Flashforge Adventure 3 printeru, na elektroničkom tenzometru PC - 2000 provedeno je ispitivanje vlačne čvrstoće na 12 ispitnih uzoraka.

Sl. 2. 3D Flashforge Adventure 3 printer

Na slici 3 prikazani su isprintani uzorci prije provedbe ispitivanja, dok su na slici 4 prikazani uzorci nakon provedbe ispitivanja.

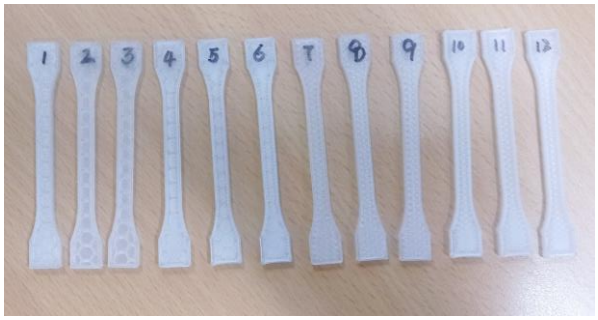

Sl. 3. Uzorci prije ispitivanja vlačne čvrstoće

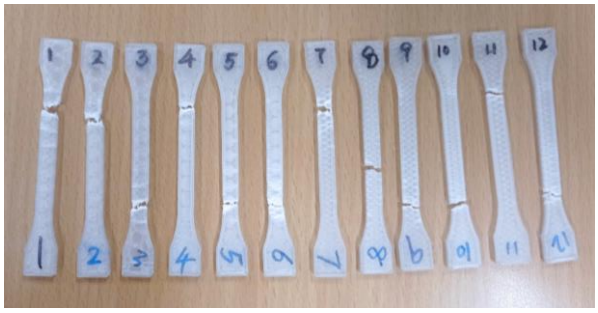

Sl. 4. Uzorci nakon ispitivanja vlačne čvrstoće

3. STATISTIČKA ANALIZA PODATAKA

Za statističku analizu eksperimentalnih podataka kao i za redosled izvođenja pokusa primenjen je licencirani statistički softver Design Expert [14].

U tabeli 2 prikazani su rezultati vlačne čvrstoće za 12 ispitnih uzoraka.

Podaci iz tabele 2 statistički su analizirani s ciljem određivanja utjecaja debljine sloja i gustoće ispune na vlačnu čvrstoću kao i s ciljem dobivanja regresijskog modela za predviđanje vlačne čvrstoće u ovisnosti o debljini sloja i gustoći ispune.

Tabela 2. Rezultati vlačne čvrstoće

Kon. raspored	Broj pokusa	Debljina sloja / mm	Gustoća ispune / %	Vlačna čvrstoća / MPa
1	6	0,3	20	34,32
2	9	0,1	50	30,22
3	12	0,3	50	38,05
4	4	0,3	20	36,93
5	10	0,3	50	38,42
6	11	0,3	50	37,68
7	7	0,1	50	30,96
8	1	0,1	20	29,47
9	3	0,1	20	27,98
10	2	0,1	20	28,35
11	8	0,1	50	31,71
12	5	0,3	20	35,05

Nakon analize podataka u tabeli 3 su prikazani neki od statističkih parametra za 12 ispitnih uzoraka (minimalna i maksimalna vrednost vlačne čvrstoće, prosečna vrednost te standardna devijacija).

Tabela 3 Statistički parametri - vlačna čvrstoća

Minimalna vrednost	Maksimalna vrednost	Prosečna vrednost	Standardna devijacija
27,98 MPa	38,42 MPa	33,26 MPa	3,93 MPa

Kako bi se istražio utjecaj parametara 3D printanja na vlačnu čvrstoću provedena je analiza varijanse. Rezultati analize varijanse vlačne čvrstoće prikazani su u tabeli 4.

Iz tabele 4 su vidljivi sledeći podaci:

Suma kvadrata odstupanja za parametar A - debljina sloja iznosi 145,32, broj stupnjeva slobode je 1, a srednje kvadratno odstupanje iznosi 145,32.

Suma kvadrata odstupanja za parametar B - gustoća ispune je 18,60, broj stupnjeva slobode je 1, a srednje kvadratno odstupanje iznosi 18,60.

Suma kvadrata odstupanja za interakciju parametara A i B (debljina sloja i gustoća ispune) iznosi 0,0481. Broj stupnjeva slobode je 1, a srednje kvadratno odstupanje za interakciju je 0,0481.

Tabela 4. Analiza varijanse vlačne čvrstoće

Izvor varijabilnosti	Suma kvadrata odstupanja	Stupnjevi slobode	Srednje kvadratno odstupanje	F_0	Verojatnost za F_0
A - debljina sloja	145,32	1	145,32	187,09	< 0,0001
B - gustoća ispune	18,60	1	18,60	23,95	0,0012
AB	0,0481	1	0,0481	0,0620	0,8097
Pogreška	6,26	9	0,6958		
Ukupno	170,19	11			

Verojatnost za izračunatu vrednost F_0 za parametar A - debljina sloja (187,09) je manja od 0,05 (verojatnost pogreške prve vrste α) što ukazuje da je parametar A značajan, tj. debljina sloja značajno utječe na vlačnu čvrstoću.

Verojatnost za izračunatu vrednost F_0 za parametar B - gustoća ispune (23,95) je manja od 0,05 (verojatnost pogreške prve vrste α) što ukazuje da je parametar B značajan, tj. gustoća ispune značajno utječe na vlačnu čvrstoću.

Verojatnost za izračunatu vrednost F_0 za interakciju parametara A i B - debljina sloja i gustoća ispune (0,0620) je veća od 0,05 (verojatnost pogreške prve vrste α) što ukazuje da interakcija parametara A i B nije značajna, tj. interakcija debljine sloja i gustoće ispune ne utječe na vlačnu čvrstoću.

U nastavku je provedeno i regresijsko modeliranje s ciljem dobivanja regresijskog modela s kojim će se moći predviditi vlačna čvrstoća u ovisnosti o debljini sloja i gustoći ispune.

Statističkom analizom podataka (tabela 2) primenom metode najmanjih kvadrata, procenjeni su regresijski koeficijenti u modelu, koji su prikazani izrazom 1.

$$\textit{Vlačna čvrstoća} = 23,397 + 34,8 \cdot \textit{debljina sloja} + \\ +0,083 \cdot \textit{gustoća ispune} \quad (1)$$

Izveštaj iz statističkog softvera Design Expert za analizu varijanse modela prikazan je u tabeli 5.

Tabela 5. Analiza varijanse modela

Izvor varijabilnosti	Suma kvadrata odstupanja	Stupnjevi slobode	Srednje kvadratno odstupanje	F_0	Verojatnost za F_0
Model	163,93	2	81,96	117,79	< 0,0001
Pogreška	6,26	9	0,6958		
Ukupno	170,19	11			

Iz tabele 5 je vidljivo da je ukupna suma kvadrata tj. suma kvadrata odstupanja svakog podatka u pokusu od aritmetičke sredine 170,19. Broj stupnjeva slobode je 11.

Pogreška tj. suma kvadrata odstupanja svakog podatka u pokusu od vrednosti dobivene modelom je 0,6958 (6,26/9 = 0,6958).

Suma kvadrata odstupanja modela tj. suma kvadrata odstupanja vrednosti dobivene modelom od aritmetičke sredine iznosi 163,93. Broj stupnjeva slobode za model je 2, jer su u modelu tri člana (3 – 1 = 2). Srednje kvadratno odstupanje za model iznosi 81,96 (163,93/2 = 81,96).

Verojatnost za izračunatu vrijednost F_0 za model (81,96/0,6958 = 117,79) je manja od 0,05 (verojatnost pogreške prve vrste α) što ukazuje da je model značajan.

Koeficijent determinacije R^2 iznosi 0,9632. Standardna devijacija iznosi 0,8342.

U tabeli 6 su prikazi rezultati pogreške tj. koliko vrednosti dobivene eksperimentalnim istraživanjem odstupaju od vrednosti dobivenih regresijskim modelom (predviđene/procenjene vrednosti).

Tabela 6. Odstupanje eksperimentalnih vrednosti od vrednosti dobivenih modelom (pogreška)

Rbr.	Experimentalna vrednost	Predviđena vrednost	Pogreška
1	34,32	35,50	–1,18
2	30,22	31,03	–0,8067
3	38,05	37,99	0,0633
4	36,93	35,50	1,43
5	38,42	37,99	0,4333
6	37,68	37,99	–0,3067
7	30,96	31,03	–0,0667
8	29,47	28,54	0,9333
9	27,98	28,54	–0,5567
10	28,35	28,54	–0,1867
11	31,71	31,03	0,6833
12	35,05	35,50	–0,4467

4. ZAKLJUČAK

U radu je istraživan utjecaj parametara 3D printanja, debljine sloja i gustoće ispune na vlačnu čvrstoću. Kako bi se istražio utjecaj navedenih parametara na vlačnu čvrstoću primenjen je faktorski plan pokusa na dve razine s tri ponavljanja. 12 ispitnih uzoraka isprintano je na je 3D Flashforge Adventure 3 printeru, nakon čega su uzorci podvrgnuti ispitivanju vlačne čvrstoće na elektroničkom tenzometru PC - 2000.

Dobiveni eksperimentalni podaci su statistički analizirani s ciljem istraživanja utjecaja na vlačnu čvrstoću. Iz provedene statističke analize eksperimentalnih podataka može se zaključiti kako ulazni parametri debljina sloja i gustoća ispune značajno utječu na vlačnu čvrstoću. Verojatnost za izračunatu vrednost F_0 za oba parametra (debljina sloja (F_0 = 187,09) i gustoća ispune (F_0 = 23,95)) je manja od 0,05 (verojatnost pogreške prve vrste α) što ukazuje da su oba parametra značajna. Interakcija debljine sloja i gustoće ispune nije značajna.

Eksperimentalni podaci su također dodatno analizirani s ciljem dobivanja regresijskog modela za predviđanje vlačne čvrstoće. Dobiven je značajan regresijski model s visokim koeficijentom determinacije (R^2 = 0,9632) s kojim će se uspešno predviditi vlačna čvrstoća u ovisnosti o debljini sloja i gustoći ispune.

5. REFERENCE

[1] Ngo, T. D., et al.: *Additive manufacturing (3D printing): A review of materials, methods, applications and challenges*, Composites Part B-Engineering, 143, 172-196, 2018.

[2] Liu, Z. G., et al.: *A critical review of fused deposition modeling 3D printing technology in manufacturing polylactic acid parts*, International Journal of Advanced Manufacturing Technology, 102, 2877-2889, 2019.

[3] Bahnini, I. et al.: *Accuracy Investigation of Fused Deposition Modelling (FDM) Processed ABS and ULTRAT Parts*, International Journal of Manufacturing, Materials, and Mechanical Engineering, 12, 1-19, 2022.

[4] Dixita, N. K., Srivastavab, R., Narainc, R.: *Comparison of Two Different Rapid Prototyping System based on Dimensional Performance using Grey Relational Grade Method*, Procedia Technology, 25, 908-915, 2016.

[5] Vasilescu, M. D., Fleser, T.: *Influence of Technological Parameters on the Dimension of GEAR Parts Generated with PLA Material by FDM 3D Printing*, Materiale Plastice, 55, 247-251, 2018.

[6] Chamil, A., et al..: *Optimization of fused deposition modeling parameters for improved PLA and ABS 3D printed structures*, International Journal of Lightweight Materials and Manufacture, 3, 284-297, 2020.

[7] Abas, M. et al.: Parametric Investigation and *Optimization to Study the Effect of Process Parameters on the Dimensional Deviation of Fused Deposition Modeling of 3D Printed Parts*, Polymers, 14, 1-22, 2022.

[8] Xu, J., et al. *The Effect of 3D Printing Process Parameters on the Mechanical Properties of PLA Parts*, Journal of Physics: Conference Series, 2133, 1-9, 2021.

[9] Cappellini, C. et al.: *The effect of process parameters on geometric deviations in 3D printing with fused deposition modelling*, The International Journal of Advanced Manufacturing Technology, 122, 1763-1803, 2022.

[10] Liu, Z. G., et al.: *A critical review of fused deposition modeling 3D printing technology in manufacturing polylactic acid parts*, International Journal of Advanced Manufacturing Technology, 102, 2877-2889, 2019.

[11] Mohamed, O. A., Masood, S. H., Bhowmik, J. L.: *Optimization of fused deposition modeling process parameters: a review of current research and future prospects*, Advances in Manufacturing, 3, 42-53, 2015.

[12] Ambati, S. S., Ambatipudi, R.: *Effect of infill density and infill pattern on the mechanical properties of 3D printed PLA parts*, Materials Today-Proceedings, 64, 804807, 2022.

[13] Cwikla, G., et al.: *The influence of printing parameters on selected mechanical properties of FDM/FFF 3D-printed parts*, IOP Conference Series: Materials Science and Engineering, 227, 012033, 2017.

[14] *Design Expert*, version 22.0.8, Stat-Ease, 2023.

Autori: **doc. dr. sc. Sara Havrlišan,** Sveučilište u Slavonskom Brodu, Strojarski fakultet u Slavonskom Brodu, Trg I. B. Mažuranić 2, 35000 Slavonski Brod, Hrvatska, Tel.: +385 35 493 439, Fax: +385 35 446 446.
E-mail: shavrlisan@unisb.hr

Huifeng Wang, izv. prof. dr. sc. Štefanija Klarić, Charles Darwin University, Faculty of Science and Technology, Darwin, Australia
E-mail: huifeng.wang@students.cdu.edu.au
stefanija.klaric@cdu.edu.au

ETIKUM 2023 **INTERNATIONAL SCIENTIFIC CONFERENCE**
NOVI SAD, SERBIA, DECEMBER 7-9, 2023

Ilić, V., Blesić, A., Nedović, Lj., Čomić, L., Ralević, N.M.

PRIMENA DESKRIPTORA OBLIKA U ZADACIMA PREPOZNAVANJA LICA

Rezime: *U ovom radu predstavićemo jedan novi pristup u zadacima prepoznavanja lica zasnovanog na analizi oblika. Brzi razvoj tehnologija za akviziciju slika kao što su kamere, mobilni telefoni i slično, doveo je do sve veće potrebe da se sam sadržaj na slikama analizira, prepozna u razume njegov kontekst unutar same slike. Jedan od otvorenih zadataka jeste i prepoznavanje lica na slici koja se dalje mogu upoređivati, klasifikovati, itd. Pristup koji ćemo ovde predstaviti je matematički prilično jednostavan, intuitivno jasan i kao takav u skladu sa ljudskom percepcijom. Nekoliko primera slika lica uzetih iz jedne od najčešće korišćenih javno dostupnih baza takođe su predstavljeni u radu.*
Ključne reči: *Oblik, Deskriptor oblika, Prepoznavanje lica*

1. UVOD

U ovom radu posebnu pažnju ćemo usmeriti na karakterizaciju lica koja se zasniva na analizi njegovog oblika. Pristup zasnovan na analizi oblika postao je veoma popularan u različitim zadacima obrade slike i kompjuterske vizije [3,4]. Razlog tome leži u činjenici da oblik kao jedan od osnovnih svojstava objekta, zajedno sa teksturom i bojom, poseduje različite atribute koji se mogu numerički evaluirati, odnosno karakterizovati. U ovom radu predstavićemo jedan drugačiji relativno novi pristup prepoznavanju lica koji u poslednje vreme zaslužuje posebnu pažnju [1]. Sam akcenat istraživanja nije usmeren na postizanju najboljeg mogućeg rezultata analize I prepoznavanja lica već predstavljanju jednog drugačijeg pristupa koristeći deskriptore oblika lica i njima pridružene mere. Evaluacija predloženog pristupa izvršena je na nekoliko ilustrativnih primera slika lica preuzetih iz odgovarajuće baze slika [2].

Rad je organizovan na sledeći način. Motivacija i osnovni pojmovi koji se koriste u radu opisani su u narednom poglavlju. U Poglavlju 3 uvedeni su odgovarajući deskriptori oblika lica. Eksperimentalni rezultati primene uvedenih deskriptora u zadacima prepoznavanja lica predstavljeni su u Poglavlju 4. Zaključne napomene date su u poslednjem poglavlju.

2. MOTIVACIJA I OSNOVNI POJMOVI

Kao što smo već pomenuli, oblik kao jedan od osnovnih karakteristika objekta može se numerički opisati na nekoliko različitih načina u skladu sa ciljevima koji su postavljeni na početku istraživanja. Jedan od uobičajenih načina, ali ne i jedini, jeste proučavanje određene karakteristike samog oblika, pogodnog za numeričku evaluaciju, *deskriptor oblika,* a zatim dizajniranje metode za evaluaciju u kojoj meri posmatrani oblik zadovoljava posmatranu karakteristiku, *mera oblika*. Kao rezultat toga, ponašanje dizajnirane mere se u određenim zadacima može prilično lako razumeti, ali i predvideti unapred. Uobičajeni pristup u takvim zadacima zasniva se na primeni nekoliko mera oblika koje se zatim mogu koristiti kao komponente odgovarajućeg vektora karakteristika pridruženih razmatranom objektu. Takav pristup omogućava da se odgovarajuća analiza, poređenje ili klasifikacija objekata može vršiti u vektorskom prostoru karakteristika umesto u prostoru objekata, što je od posebno važnosti u zadacima koji se izvršavaju na računaru.

Prirodno je očekivati da veća dimenzija vektora karakterstika, odnosno veći broj deskriptora oblika, treba da obezbedi veći stepen razlikovanja između objekata koji su predmet analize. Otuda i raste potreba za definisanjem novih deskriptora oblika i njima pridruženih mera, ali i novih mera već postojećih deskriptora oblika. Pored toga, zbog sve veće raznovrsnosti zadataka analize slike prirodno je očekivati da ne postoji mera koja će biti efikasna u svim zadacima analize objekata. Ovo poslednje sledi iz činjenice da mera koja se pokazala efikasnom u zadacima jedne klase problema ili baza slika, u opštem slučaju ne mora nužno davati rezultate u skladu sa našim očekivanjima u nekim drugim zadacima analize objekata. Brojni su primeri deskriptora oblika koji su od interesa u različitim zadacima analize objekata, obradi slike i kompjuterske vizije. Neki od njih imaju prilično jasno geometrijsko ili topološko značenje koje se može relativno lako unapred razumeti i predvideti njihovo ponašanje, i koji se kao takvi mogu prilično jednostavno numerički evaluirati. Neki od njih su: izduženost

[3], šestougaonost [3], kvadratnost [4], orijentabilnost [3,4] i slično. U ovom radu predstavićemo nekoliko novih deskriptora oblika lica i pokazati kako se njihovim kombinovanjem mogu dobiti prlično dobri rezultati u zadacima analize oblika i prepoznavanja lica.

3. DESKRIPTORI OBLIKA LICA

U ovom poglavlju predstavljamo deskriptore oblika koje smo izabrali u cilju ilustracije efikasnosti opisanog pristupa u zadacima prepoznavanja lica. Baza slika koju smo razmatrali sastoji se od ukupno 5000 slika ženskih slavnih ličnosti raspoređenih u 5 klasa prema obliku njihovog lica: *srcoidni, izduženi, ovalni, zaobljeni i kvadratni*. Svaka klasa sadrži po 1000 slika na slučajan način podeljenih na dve podgrupe: jedna koja ima 800 slika za obučavanje neuralne mreže (*engl. Training Set*), a druga koja ima 200 slika za testiranje tako obučene neuralne mreže (*engl. Testing Set*).

S obzirom da akcentat rada nije na dizajniranju novih deskriptora oblika već predstavljanju novog pristupa u zadacima prepoznavanja lica, u samom radu fokusiramo se samo na poslednje četiri klase oblika lica, imajući u vidu da prema dosadašnjem iskustvu i znanju autora sam deskriptor srcoidnosti nije do sada dizajniran. U tom smislu, dizajniranje jednog takvog deskriptora ostaje kao jedan od budućih zadataka autora koji zaslužuje posebnu pažnju. Shodno samoj raspodeli slika pomenuta četiri tipa lica (izduženi, ovalni, zaobljeni i kvadratni), mogu se uočiti određene pravilnosti i osobine kojima se međusobno odlikuju. Tako, na primer, ovalni tip lica (Slika 1. (a)) odlikuje se širokim obrazima, dok se deo lica ka čelu i bradi blago sužava. Sa druge strane, izduženi tip lica (Slika 1. (b)) je sličan ovalnom, dok je njegova dužina nešto veća od širine kod ovalnog tipa. Kod ovog tipa lica jagodice su visoke, čelo je široko a brada se naglo sužava, tzv. oštra brada. Što se tiče osoba koje pripadaju zaobljenom tipu lica (Slika 1. (c)), imamo da su dužina i širina lica približno jednake, zaobljenih linija lica, bez naglih i oštrih promena oblika. Kvadratni tip odlikuje se jednakom širinom obraza, jagodica i čela, a za razliku od predstavnika izduženog tipa lica brada se ne sužava naglo (Slika 1. (d)).

Shodno opisanim svojstvima i klasifikaciji tipova lica u posmatranoj bazi, od posebnog interesa su deskriptori definisani na sledeći način:

$$D_1(S) = \frac{Površina(FR(S) \setminus FE(S))}{Površina(FR(S))}, \quad (1)$$

$$D_2(S) = \frac{VelikaOsa(FE(S))}{MalaOsa(FE(S))}, \quad (2)$$

gde *FR(S)* (*engl. Fitted Rectangle of S)* i *FE(S)* (engl. *Fitted Ellipse of S*) označavaju "najbolji uklopljeni pravougaonik", odnosno "najbolju uklopljenu elipsu" u odnosu na razmatrani oblik *S*, dok sam termin "najbolji uklopljeni" proizilazi iz karakteristika lica koje smo prethodno opisali. Kako kod prva tri tipa lica od posebnog interesa su njegova širina i dužina, odnosno rastojanje od linije kose do dna brade, odgovarajući *FR(S)* je upravo određen širinom i dužinom lica. Što se tiče *FE(S)*, njene odgovarajuće ose određene su širinom i dužinom *FR(S)* (Slika 1. (a), (b) i (c)). Kod kvadratnog tipa lica, odgovarajući pravougaonik *FR(S)* i posledično elipsa *FE(S)* određeni su obrazima, jagodicama i čelom, ali ne i visinom lica shodno karakterizaciji opisanoj od strane autora baze slika (Slika 1. (d)).

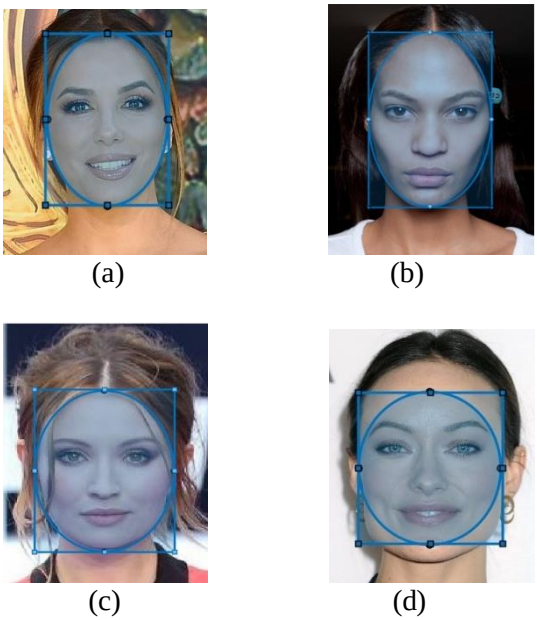

(a) (b) (c) (d)

Sl. 1. Primeri oblika lica: (a) ovalni, (b) izduženi, (c) zaobljeni i (d) kvadratni.

4. EKSPERIMENTALNI REZULTATI

U ovom poglavlju ilustrovaćemo kako se definisani deskriptori oblika lica $D_1(S)$ i $D_2(S)$ mogu primeniti u zadacima analize I prepoznavanja lica. U Tabeli 1. predstavljene su izmerene vrednosti ovih deskriptora za lica prikazana na Slici 1. Kao što se može videti, izmerene vrednosti deskriptora odgovaraju našoj percepciji ponašanja posmatranih deskriptora, i u skladu su sa našim očekivanjima. Zaista, ako posmatrane slike poređamo prema rastućim vrednostima $D_2(S)$ deskriptora, dobijamo poredak (b), (a), (c), (d). Možemo primetiti da je takav poredak u saglasju sa našom percepcijom, s obzirom da, kao što se i moglo očekivati, najveća

izmerena vrednost pridružena je izduženom obliku lica (Slika 1. (b)), koji ujedno predstavlja i najizduženiji tip među svim predstavljenim na Slici 1. Takođe, prirodno je očekivati da veća vrednost deskriptora $D_2(S)$ bude pridružena ovalnom obliku lica (Slika 1. (a)) pre nego zaobljenom (Slika 1. (c)), dok je najmanja vrednost $D_2(S)$ pridružena kvadratnom obliku lica (Slika 1. (d)). Dodatno, dobijena vrednost $D_2(S)$ deskriptora pridružena kvadratnom obliku lica 1.0699 (približno jednaka vrednosti 1) u skladu je sa našim očekivanjima, s obzirom da tri komponente lica koje su od interesa za ovaj tip lica (obrazi, jagodice i čelo) zajedno približno određuju oblik kvadrata. Ovo poslednje dodatno ide u prilog činjenici da je deskriptor $D_2(S)$ dobro osmišljen i dizajniran radi boljeg razlikovanja i klasifikovanja posmatanih tipova lica.

Što se tiče dobijenih vrednosti deskriptora $D_1(S)$, možemo primetiti da je najmanja vrednost 0.2113 pridružena ovalnom tipu lica koji se odlikuje blagim sužavanjem od obraza ka čelu i bradi, dok je najveća vrednost 0.2296 pridružena zaobljenom tipu lica bez naglih i oštrih linija lica. U skladu sa tim, dobijene vrednosti odgovaraju našoj percepciji, s obzirom da zaobljeni tip lica obuhvata najveći udeo pravougaonika $FR(S)$ koji nije sadržan u $FE(S)$ od svih posmatranih tipova lica na Slici 1. Sa druge strane, kod ovalnog tipa lica razlika između odgovarajućeg pravougaonika $FR(S)$ i elipse $FE(S)$ je najmanja pa je samim tim i njena površina najmanja među svim posmatranim licima. Za preostala dva tipa lica, izduženi i kvadratni, izmerene vrednosti odgovaraju našem razumevanju deskriptora $D_1(S)$. Zaista, kod kvadratnog oblika lica veći je relativni udeo $FE(S)$ unutar $FR(S)$ (brojilac $D_1(S)$) nego kod izduženog oblika, dok je površina $FR(S)$ (imenilac $D_1(S)$) veća kod izduženog nego kod kvadratnog tipa lica.

Tabela 1. Izračunate vrednosti deskriptora $D_1(S)$ i $D_2(S)$ za oblike lica predstavljenih na Slici 1. Podebljane su maksimalna i minimalna vrednost odgovarajućih deskriptora.

Tabela 1. Izračunate vrednosti deskriptora

	(a)	(b)	(c)	(d)
$D_1(S)$	**0.2113**	0.2172	**0.2296**	0.2199
$D_2(S)$	1.4130	**1.5561**	1.2584	**1.0699**

Da bismo ilustrovali kako se opisane mere deskriptora $D_1(S)$ i $D_2(S)$ mogu međusobno kombinovati i efikasno primeniti u zadacima prepoznavanja, odnosno klasifikacije posmatranih slika lica, na Slici 2. predstavljen je grafikon rasipanja (*engl. Scatter Diagram)* vektora karakteristika pridruženih svakom od tipova lica prikazanih na Slici 1. Kao što se može primetiti, predstavljeni deskriptori obezbeđuju prilično efikasno razdvajanje odgovarajućih tipova lica. Otuda, možemo zaključiti da su posmatrani deskriptori lica međusobno kompatibilni koji u svom razmatranju uključuju uglavnom nezavisne informacije o obliku lica, obezbeđujući na taj način relativno dobre razultate u zadacima prepoznavanja tipova lica. S tim u vezi, predložene deskriptore oblika možemo smatrati dobrom početnom osnovom za daljim razmatranjem novih deskriptora oblika lica, ali i dizajniranjem novih metoda za njihovu evaluaciju u različitim zadacima analize i prepoznavanja lica.

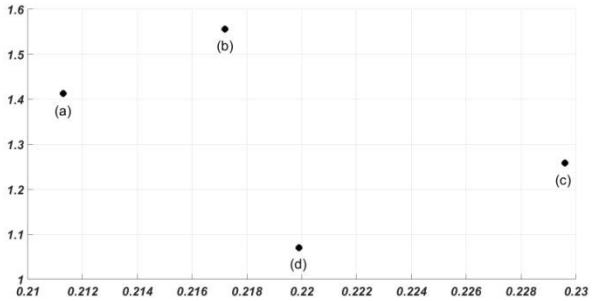

Sl. 2. Grafikon rasipanja (*engl. Scatter Diagram)* u dvodimenzionalnom vektorskom prostoru karakteristika $\mathbf{R}^2$ (*engl. Feature Vector Space*) odgovarajućih vektora karakteristika (*engl. Feature Vectors*) pridruženih slikama lica predstavljenih na Slici 1. primetimo relativno visok stepen razdvajanja vektora karakteristika pridruženih različitim tipovima lica.

5. ZAKLJUČAK

U ovom radu smo predstavili jedan relativno novi pristup u zadacima prepoznavanja lica osoba čije slike smo preuzeli iz javno dostupne baze [2]. Pristup predstavljen u ovom radu zasniva se na analizi oblika lica, s obzirom da oblik kao jedan od osnovnih elemenata objekta sadrži brojne intuitivno jasne karakteristike koje se mogu numerički jasno kvantifikovati. Sama motivacija istraživanja nije usmerena na postizanju najboljeg mogućeg rezultata u zadacima prepoznavanja lica već na predstavljanju jednog drugačijeg pristupa koji bi bio od interesa u zadacima ovog tipa. Poređenja radi sličan pristup je predstavljen od strane autora u radu [1], koji se zasnivao na primeni funkcija agregacije u kombinaciji sa analizom oblika. Radi ilustrovanja korisnosti predstavljenog pristupa, u radu smo predstavili dva nova deskriptora oblika kao i njima

pridružene mere $D_1(S)$ i $D_2(S)$. Dobijeni rezultati odgovaraju našim očekivanjima u zadacima analize i prepoznavanja lica kako pojedinačno tako i njihovim kombinovanjem. Razlog tome sledi direktno iz činjenice da dva deskriptora oblika lica uključuju nezavisne i međusobno komplementarne informacije o samom obliku lica. Pored toga, treba napomenuti da smo prilikom samog istraživanja iz razmatranja isključili slike lica koje pripadaju srcoidnom tipu lica, s obzirom da prema dosadašnjem iskustvu i poznavanju oblasti autora takav deskriptor oblika nije još definisan kao i njemu pridružena mera oblika. Otuda, dizajniranje jednog takvog deskriptora ostaje kao jedan od interesantnih zadataka u daljem naučno-istraživačkom radu samih autora. Dizajniranje jedne takve mere predstavljao bi jedan od veoma važnih koraka u procesu dizajniranja jednog novog efikasnijeg modela primenljivog u različitim složenijim zadacima prepoznavanja lica nezavisno od veličine posmatrane baze, stepena sličnosti lica istog tipa, odnosno nivoa različitosti lica različitog tipa, itd.

6. ZAHVALNICA

Autori su podržani od strane Pokrajinskog sekretarijata za visoko obrazovanje i naučnoistraživačku delatnost (AP Vojvodina, Republika Srbija), Projekat broj 142-451-3188/2023-01.

7. REFERENCE

[1] Ralević, N.M., Blesić, A., Ilić, V., Paunović, M., Čomić, L.: Aggregation Operators for Face Recognition, Intelligent and Fuzzy Systems. INFUS 2023, LNNS, Vol. 758, Springer, Cham.

[2] Face Shape Dataset. https://www.kaggle.com/datasets/niten19/face-shape-dataset/data

[3] Ilić, V., Ralević, N.M.: Hexagonality as a New Shape-Based Descriptor of Object. Journal of Mathematical Imaging and Vision, Vol. 62, 1136-1158, 2020.

[4] Rosin, P.L., Žunić, J.: Measuring Squareness and Orientation of Shapes. Journal of Mathematical Imaging and Vision, Vol. 39, 13-27, 2011.

Autori: **Doc. dr Vladimir Ilić, Asistent MSc Andrija Blesić, Vanr. Prof. dr Ljubo Nedović, Vanr. Prof. dr Lidija Čomić, Red. Prof. dr Nebojša M. Ralević,** Univerzitet Novi Sad, Fakultet Tehničkih Nauka, Trg Dositeja Obradovića 6, 21000 Novi Sad, Srbija

E-mail: vlada.mzsvi@uns.ac.rs
andrija.blesic@gmail.com
nljubo@uns.ac.rs
comic@uns.ac.rs
nralevic@uns.ac.rs

ETIKUM 2023 **INTERNATIONAL SCIENTIFIC CONFERENCE**
NOVI SAD, SERBIA, DECEMBER 7-9, 2023

Janković, P. Baralić, J., Petković, D.

ENHANCING PRODUCTION EFFICIENCY THROUGH MODELING

Abstract: *In the contemporary industrial landscape, the significance of modeling as a tool for enhancing production processes cannot be overstated. Modeling serves as a bridge between theoretical planning and practical application, allowing businesses to anticipate challenges and streamline operations. By creating detailed simulations of production processes, companies can visualize the entire lifecycle of their products, from initial design to final output. The paper aims to demonstrate the efficacy of modeling techniques in optimizing production process. Also, this paper presents some of the so far proposed processing model of abrasive water jet cutting. Through experiments and method of mathematical modeling the abrasive water jet front profile model has been developed.*
Key words: *Modeling, Mathematical modeling, Production process, Abrasive water jet cutting*

1. INTRODUCTION

In the dynamic field of manufacturing, the art and science of modeling emerge as cornerstones, harmonizing theoretical designs with practical execution. Modeling, essentially the craft of creating a virtual representation of real-world processes, stands at the forefront of manufacturing innovation. It serves as a bridge, translating intricate designs and theories into tangible, optimized production strategies.

At its core, modeling in manufacturing is a catalyst for transformation. It empowers manufacturers to foresee and refine the interplay of materials, processes, and technologies, leading to enhanced product quality and efficiency. By simulating complex manufacturing scenarios, it provides a sandbox for experimentation and problem-solving, reducing the risks and costs associated with physical trials. This virtual playground is not just a testbed for efficiency but also a platform for embracing customization, allowing manufacturers to swiftly adapt to market trends and consumer demands.

Modeling, in its broadest sense, refers to the creation of a representation of a real-world process or system. This representation, often mathematical or computational, serves to analyze, predict, and optimize various aspects of the system it mirrors. In the context of manufacturing, modeling becomes a pivotal tool, bridging the gap between theoretical designs and practical applications.

The role of modeling in enhancing manufacturing processes includes:

Predictive Analysis and Design Optimization: At the heart of manufacturing lies the challenge of transforming raw materials into finished products efficiently and cost-effectively. Modeling plays a crucial role here, allowing for predictive analysis of how materials and processes behave under different conditions.

Process Simulation and Troubleshooting: Manufacturing processes often involve complex interactions of various components and conditions. Through simulation models, manufacturers can replicate these processes in a virtual environment. This simulation enables them to make informed decisions without the cost and risk associated with trial-and-error in a physical setting.

Customization and Flexibility: In an era where customization is key to meeting diverse consumer demands, modeling provides the flexibility needed in manufacturing processes. By adjusting models, manufacturers can easily adapt to changes in product design, material selection, or production methods, thus enabling a more agile response to market trends.

Integration of Emerging Technologies: The integration of advanced technologies like AI, IoT, and robotics into manufacturing is revolutionizing the industry. Modeling serves as the foundation for these technologies, facilitating their seamless integration into existing processes.

Cost Reduction and Time Efficiency: By predicting outcomes and optimizing processes, modeling significantly reduces the time and cost involved in bringing a product to market.

In recent years, the industrial sector has seen a surge in the use of modern materials with enhanced properties [1]. The machining of these advanced materials often necessitates the use of various non-traditional machining techniques, including laser cutting, abrasive water jet (AWJ), electrical discharge machining (EDM), plasma cutting, and more [2]. Notably, the advancement in AWJ technology has elevated this method to a cutting-

edge status, offering high efficiency and the capability to cut a diverse range of materials, even those with complex profiles. A significant benefit of AWJ technology is its ability to machine without causing substantial temperature increases in the area being worked on, coupled with the minimal cutting forces involved [3].

The implementation of AWJ cutting technology in manufacturing firms is often suboptimal due to the absence of a tailored technological framework suited to specific production environments [4, 5]. The effect of process parameters in AWJ machining is investigated in a series of papers [6,7] but our knowledge about the many aspects of this technology is still limited. This paper presents some of the so far proposed processing model of abrasive water jet cutting. Through experiments and method of mathematical modeling the abrasive water jet front profile model has been developed.

2. IMPORTANCE OF MODELING

Scientific understanding is a multifaceted construct, intricately woven from the threads of theory, experiments, and modeling. Each element plays a distinct yet interconnected role in the pursuit of knowledge and the advancement of science.

Theories are the bedrock of scientific understanding. They offer predictions about how systems should behave and set the stage for both modeling and experimentation.

Experiments are the empirical backbone of science. They involve the direct manipulation and observation of the world to test the predictions made by theories. Through experimentation, theories are rigorously tested, validated, or refuted. This process is fundamental to the scientific method. Experiments provide concrete data and evidence that either support or challenge theoretical frameworks.

Modeling serves as a critical intermediary, bridging the gap between abstract theory and tangible experimentation. Models are simplified representations of reality, often expressed mathematically or through simulations. They allow scientists to explore the implications of theories and predict the outcomes of experiments before they are conducted. In many cases, modeling makes it possible to investigate phenomena that are too large, small, complex, or dangerous to study through direct experimentation.

The interplay between theory, experiments, and modeling is a dynamic and iterative process. Theories guide the creation of models and the direction of experimental inquiry. Models predict outcomes and help interpret experimental data. Experiments validate or challenge both models and theories. This synergy accelerates the pace of scientific discovery and deepens our understanding.

The relationship between theory, experiments, and modeling is not static; it is a continuous cycle of refinement and evolution (Fig. 1). As new experimental data is gathered, theories are adjusted, and models are refined. This process leads to a progressively deeper and more accurate understanding of the natural world. It's a testament to the dynamic nature of scientific inquiry, where understanding is always evolving, driven by the iterative and collaborative efforts of theory, experimentation, and modeling.

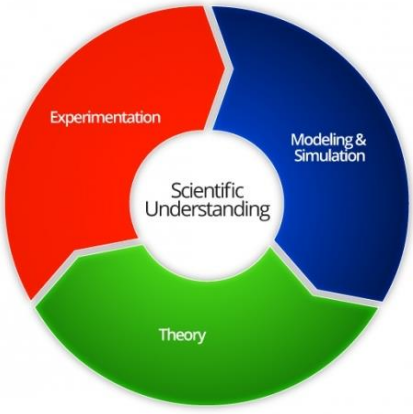

Fig. 1. Dynamic cycle of scientific understanding

In essence, the scientific understanding is a tapestry woven from the threads of theory, experiments, and modeling. Each element enriches and informs the others, creating a dynamic process that drives the advancement of knowledge and understanding in the world of science.

2.1. Forms and functions of model

There are limits to the human ability to understand complexity. Through modeling, we narrow the problem we are studying by focusing on only one aspect at a time.

At its core, a model is a simplified abstraction of reality. This simplification makes it possible to analyze, understand, and predict aspects of the real world without getting overwhelmed by its intricacies.

Models come in various forms (Fig. 2), ranging from physical models (like a scale model of a building) to mathematical formulas and computer simulations.

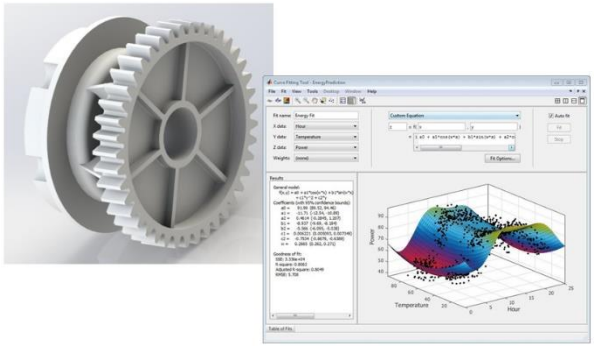

Fig. 2. Types of models

Models come in various types, each serving different purposes and suited to different fields of study or application. Here's an overview of some of the primary types of models:

- Physical Models
- Mathematical Models
- Statistical Models:
- Computer Models and Simulations

Each type serves the same fundamental purpose: to represent some aspect of reality in a way that is easier to manipulate and study. For instance, a climate model might use mathematical equations to simulate weather patterns, while a financial model could use statistical tools to predict market trends. It's important to recognize that models are not perfect replicas of reality. They are based on assumptions and simplifications that can limit their accuracy. The validity of a model depends on how well its assumptions match the real-world conditions it aims to represent.

2.2. Steps in modeling process

The modeling process typically involves several key steps, regardless of the type of model being developed. These steps are designed to ensure that the model is as accurate and useful as possible for its intended purpose. Here's an overview of the general steps involved in the modeling process:

- Problem Definition
- Research and Data Collection
- Conceptualization
- Choosing the Type of Model
- Model Formulation
- Model Testing and Validation
- Model Analysis

3. CASE STUDY – MODELING OF AWJ FRONT PROFILE

For a better understanding of the effect of certain processing parameters on the result of AWJ, such as the quality of cutting, it is necessary to understand the principles of AWJ material machining. Through experiments and method of mathematical modeling the abrasive water jet front profile has been developed.

In abrasive water jet cutting, the water jet primarily functions as a medium for transmitting energy, accelerating the abrasive material particles. The faster these solid particles strike the material being cut, the greater the rate of material removal. The primary challenge in abrasive water jet machining lies in the inconsistency of the machined surface quality. This variation is evident in several aspects: differences in surface roughness, deviations of the machined surfaces from the vertical plane (known as the taper of the cut), and the formation of curved lines on the machined surface, referred to as jet lag. These issues can be attributed to the loss of energy by the jet during the cutting process. The energy loss of the jet not only alters the quality of the machined surface but also causes deviations in the abrasive water jet's path, denoted as Y_{dev}, as shown in Fig. 3.

Fig. 3. Jet deviation shape and size

To define the shape of the abrasive water jet front profile (bending of the abrasive water jet), it was necessary to measure the deviation of the abrasive water jet, from the ideal front of the cut - vertical lines. The deviation is measured at ten points through the depth of the cut.

Based on a series of measurements [8] and the procedure carried out, a mathematical model of the front line of the water jet was defined. A mathematical model is a representation of a system, process, or phenomenon using mathematical concepts and language. The purpose of a mathematical model is to analyze, describe, and predict the behavior of the real-world system it represents.

Such a models are powerful tools in science, engineering, economics, and many other fields. They help to understand complex systems and to predict their behavior under various conditions. However, the reliability of a model's predictions is always contingent on its assumptions and the data it's based on.

By analyzing the results of measurements of

deviation of the cut front from ideal, depending on further influencing factors of the process, such as the abrasive flow rate and speed of the abrasive cutting head, it can be concluded that the geometry of the cut front line, could be expressed, depending on the processing parameters and depth of cut, as:

$$Y_{dev} = 132.3607 \cdot h^{1.687} \cdot p^{-1.4297} \cdot m_a^{-0.691} \cdot v_c^{0.9274} \quad (1)$$

The resulting analytical dependence can also be represented graphically, Fig. 4.

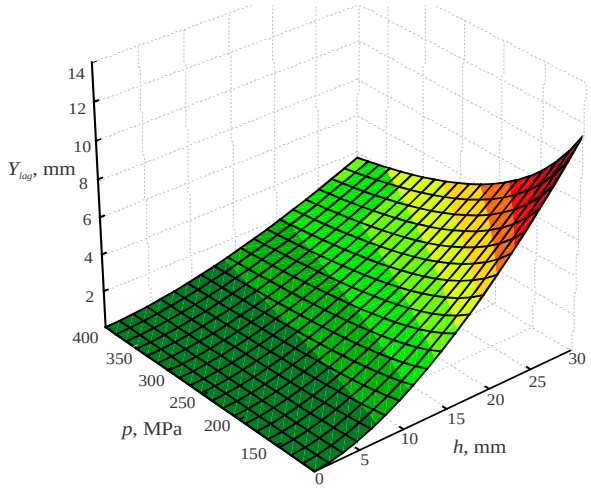

Fig. 4. shape of the front of the cut depending on the work pressure and depth of cut [9]

Based on the obtained mathematical model - the analytical dependence of the process parameter and the processing result, in this case the size of the water jet deflection, numerous conclusions can be drawn that characterize the actual processing process.

For example, based on Fig. 4, it can be concluded that with increasing depth of cut increases and the deviation of the cut front lines from ideal. However, the increase in the value of the operating pressure leads to a reduction in deviation of the cut front lines.

4. ACKNOWLEDGMENT

This research was financially supported by the Ministry of Science, Technological Development, and Innovation of the Republic of Serbia (Contract No. 451-03-47/2023-01/ 200109)

5. REFERENCES

[1] Madić, M., Kovačević, M., Radovanović, M., Blagojević, M.: *Software Tool for the Laser Cutting Process Control – Solving Real Industrial Case Studies*, Facta Universitatis, Series: Mechanical Engineering, 14, pp. 135-145, 2016.

[2] Chatterjee, P., Mondal, S., Boral, S., Banerjee, A., Chakraborty, S.: *A Novel Hybrid Method for Non-Traditional Machining Process Selection Using Factor Relationship and Multi-Attributive Border Approximation Method*, *Facta* Universitatis, Series: Mechanical Engineering, 15, pp. 439-456, 2017.

[3] Janković P., Radovanović M., Baralić J., Nedić B.: *Topography of surface machined by abrasive water jet cutting*, Proceedings of The 3rd International Conference MASING 2015, Niš, University of Niš, pp. 383-386, 2015.

[4] Trifunović, M, Janković, P, Vitković, N,: *Optimization of cutting parameters for minimizing part production costs in multi-pass rough turning of EN-GJL-250 grey cast iron*, Proceedings of the 5th international conference "Mechanical engineering in XXI century", University of Niš, pp. 255 - 258, 2020.

[5] Janković, P., Madić, M., Radovanović, M., Petković, D., Mladenović, S.: *Optimization of Surface Roughness from Different Aspects in High-Power CO_2 Laser Cutting of AA5754 Aluminum Alloy*, Arabian Journal for Science and Engineering 44 (12), 10245-10256, 2019.

[6] Janković, P., Radovanović, M., Dodun, O., Madić, M., Petković, D.: *Aspects of machining parameter effect on cut quality in abrasive water jet cutting*, Applied Mechanics and Materials, Part 1, pp. 201-206, 2015.

[7] Janković, P., Madić, M., Petković, D., Radovanović, M.: *Analysis and modeling of the effects of process parameters on specific cutting energy in abrasive water jet cutting*, Thermal Science, pp. S1459-S1470, 2018.

[8] Baralić, J., Janković, P., Popović, M.: *The influence of cutting speed and depth of cut on the geometry of the cutting front line during machining with an abrasive water jet*, Journal IMK-14, pp: 27-30, 2019.

[9] Marušić, V., Baralić, J., Nedić, B., Rosandić, Ž.: *Effect of machining parameters on jet lagging in abrasive water jet cutting*, Tehnički vjesnik, No 20, Vol. 4, pp 677-682, 2013.

Authors: **Full. prof. dr Predrag Janković, Assis. prof. dr Dušan Petković,** University of Niš, Faculty of Mechanical Engineering, A. Medvedeva 14, 18000 Niš, **Assoc. prof. dr Jelena Baralić,** University of Kragujevac, Faculty of Technical Sciences Čačak,

E-mail: predrag.jankovic@masfak.ni.ac.rs
jelena.baralic@ftn.kg.ac.rs
dusan.petkovic@masfka.ni.ac.rs

ETIKUM 2023 **INTERNATIONAL SCIENTIFIC CONFERENCE NOVI SAD, SERBIA, DECEMBER 7-9, 2023**

Jovanović Pešić, Ž., Džunić, D., Pešić, M., Milenković, S., Kostić, S., Kočović, V.

UTICAJ BRZINE ALATA NA KARAKTERISTIKE MATERIJALA KOD POVRŠINSKE OBRADE TRENJEM - PREGLED

Rezime: *Površinska obrada trenjem (eng. Friction Stir Processing - FSP) je jedna od vodećih tehnika za proizvodnju površinskih kompozita. FSP se koristi za poboljšanje mehaničkih, triboloških, korozionih i drugih svojstava materijala kao što su aluminijum, magnezijum, bakar, čelik, itd. U ovom preglednom radu analiziran je uticaj brzine alata (rotacione brzine i transverzalne brzine) na mikrotvrdoću kompozitnih materijala dobijenih postupkom površinske obrade trenjem.*
Ključne reči: *površinska obrada trenjem, brzina alata, kompozitni materijali*

1. UVOD

Površinska obrada trenjem, kao varijacija frikcionog zavarivanja mešanjem (eng. Friction Stir Welding -FSW) razvijena je 1999. godine [1]. Značajan broj istraživača analizira i ispituje formiranje površinskih kompozita procesom površinske obrade trenjem. U prvoj deceniji dvadeset prvog veka broj radova iz ove oblasti bio je manji od 50 radova po godini, dok je u poslednjih pet godina taj broj veći od 350 rada po godini (slika 1.).

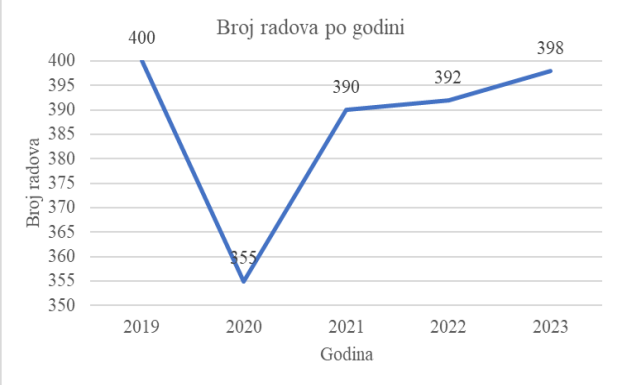

Sl. 1. Broj publikovanih radova na temu površinske obrade trenjem

Prednost površinske obrade trenjem se ogleda u tome što je temperatura obrade niža od temperature topljenja osnovnog materijala [2, 3]. FSP se primenjuje za poboljšanje mehaničkih, triboloških, korozionih i drugih svojstava materijala poput aluminijuma, magnezijuma, bakra i drugih [4]. Površinska obrada trenjem koristi se i za uklanjanje površinskih defekata, poput pukotina i pora [5]. Sa druge strane, karakteristike prevlaka dobijenih FSP postupkom zavise od vrste i svojstava ojačavača, kao i od samih parametara procesa.

2. FSP PRINCIP RADA

FSP radi na osnovnom principu FSW [6]. Na radnom komadu koji se obrađuje površinskom obradom trenjem razlikujemo istosmernu i suprotnosmernu stranu [7, 8]. Kod FSP postupka koriste se dve vrste alata: alat sa pin-om i alat bez pin-a. Alat koji vrši rotaciono kretanje, prodire u radni komad dok čelo alata i radni komad ne ostvare kontakt. Kao posledica kontakta čela alata i radnog komada dolazi do trenja između alata i radnog komada usled čega dolazi do lokalnog zagrevanja [7-9]. Kada se dostigne odgovarajuća temperatura, alat započinje transverzalno kretanje u željenom pravcu. Rotaciono i transverzalno kretanje alata omogućava mešanje ojačavača i osnovnog materijala, na taj način formirajući površinski kompozit. Na slici 2 prikazan je princip rada FSP postupka.

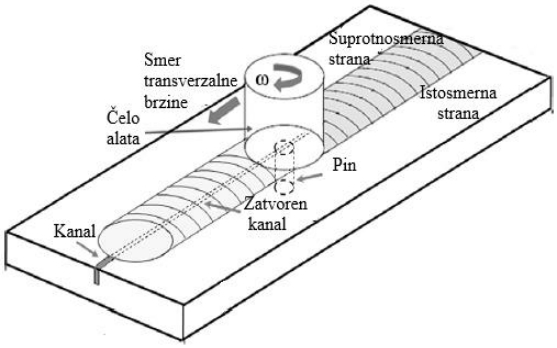

Sl. 2. FSP postupak – princip rada

3. FSP PARAMETRI PROCESA

Kod površinske obrade trenjem, različiti parametri utiču na kvalitet finalnog kompozita. FSP parametre procesa možemo podeliti u četiri celine: parametre mašine, parametre alata, materijala i ostale parametre. Asadi i ostali [10] u svom radu su proučavali uticaj različitih

parametara procesa kao što su menjanje broja prolaza i smera rotacije alata i utvrdili su da promena smera rotacije alata dovodi do smanjenja veličine zrna kompozita kod kog je ojačavač AZ91. Isti autori su otkrili da promena parametara procesa dovodi do povećanja tvrdoće materijala sa 63 HV na 98 HV. Arora i ostali [11] su proučavali kako brzina rotacije i broj prolaza tokom površinske obrade trenjem utiču na svojstva materijala. Kod legure AE42 (legura na bazi magnezijuma) promena parametara procesa dovela je do povećanja tvrdoće. Slika 3 prikazuje različite parametre FSP procesa.

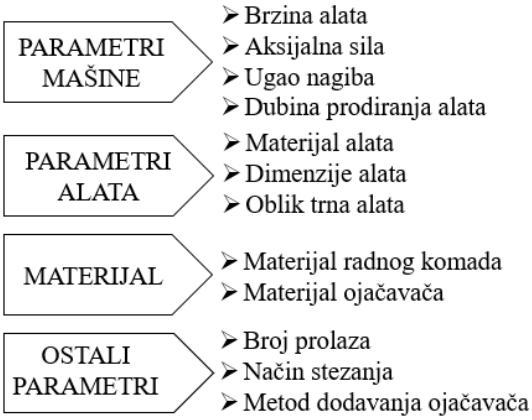

Sl. 3. Uticajni parametri FSP procesa

4. BRZINA ALATA

Postoje dve vrste brzina koje se mogu menjati tokom postupka površinske obrade trenjem: brzina rotacije alata i transverzalna brzina [12]. Brzina rotacije je brzina kojom alat rotira oko svoje ose, dok transverzalna brzina sluzi za kretanje alata duž ose radnog komada. Rotacija ili brzina rotacije mogu biti u smeru kazaljke na satu ili suprotno smeru kazaljke na satu. Kod FSP postupka, pravilan izbor brzine rotacije alata i transverzalne brzine je veoma bitan. Povećanjem brzine rotacije i smanjenjem transverzalne brzine, stvara se više toplote u zoni obrade što može dovesti do rasta zrna i daljeg omekšavanja materijala [13]. S druge strane, smanjena brzina rotacije alata i povećana transverzalna brzina uzrokovaće nedovoljnu količinu generisane toplote. Dakle, obe brzine treba izabrati u odgovarajućim granicama da bi se proizvela dovoljna količina toplote, a da pritom ne dođe do prevelikog omekšavanja materijala. Uticaj različite kombinacije brzine rotacije i transverzalne brzine na svojstva materijala biće razmatrani dalje u radu.

4.1 Uticaj brzine na tvrdoću

U radu [14] autori su površinskom obradom trenjem obrađivali ploču koja je dobijena livenjem legure A319. Prilikom obrade varirali su vrednosti za tri translatorne i pet rotacionih brzina alata. Vrednosti translatornih brzina bile su: 22.2 mm/min, 40.2 mm/min i 75 mm/min. Dok su vrednosti brzina rotacije bile u opsegu od 800 do 1600 o/min (slika 4.).

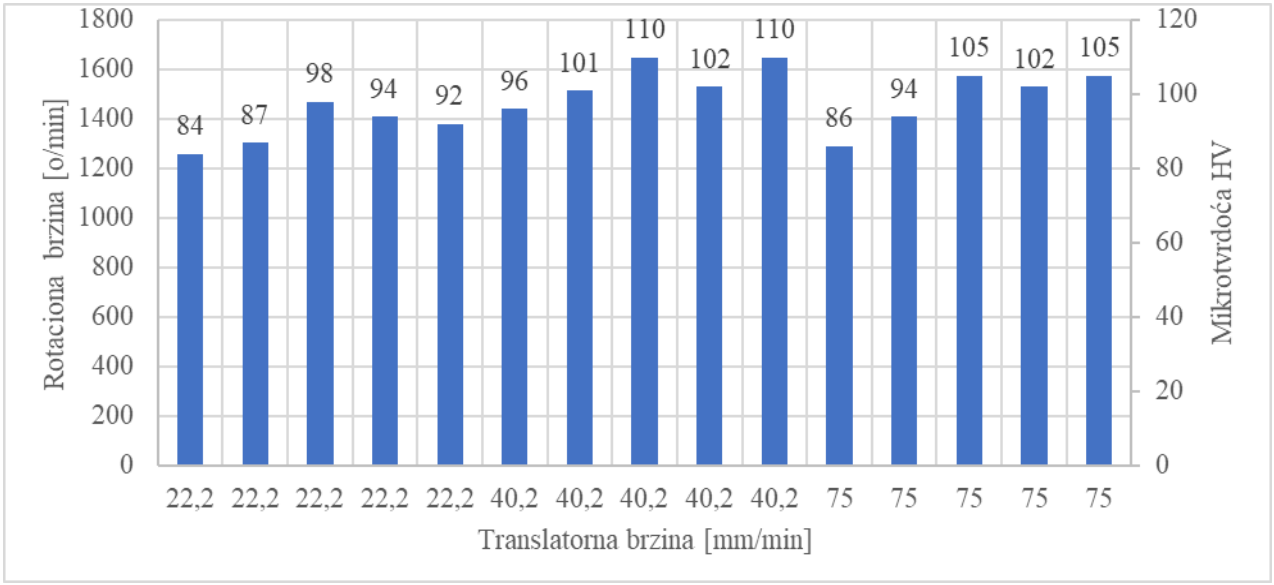

Sl. 4. Prikaz vrednosti mikrotvrdoće u zavisnosti od brzine

Kao što se može videti sa slike 4, kada je translatorna brzina 22.2 mm/min, najveća vrednost mikrotvrdoće je pri rotacionoj brzini od 1200 o/min. Ta zakonitost se može uočiti i kod druga dva slučaja promene translatorne brzine. Sa aspekta produktivnosti najbolja kombinacija translatorne brzine i rotacione brzine je 75 mm/min i 1200 o/min, pri tome da vrednost

mikrotvrdoće iznosi 105 kg/mm^2.

Kwon i ostali su dokazali da smanjenje brzine rotacije alata sa 1840 o/min, preko 1350 o/min i 980 o/min do 560 o/min, uz konstantnu vrednost translatorne brzine (155 mm/min) dovodi do povećanja tvrdoće od 40% [15].

Kod legure aluminijuma A1050 koja je ojačana SiC, uz optimalne vrednosti brzina dolazi do povećanja tvrdoće četiri puta u odnosu na tvrdoću osnovnog materijala. Autori su u radu [16] varirali 3 vrednosti translatorne brzine (15, 20 i 30 mm/min), kao i tri brzine rotacije (500, 700 i 1000 o/min). Najbolje vrednosti tvrdoće dobijene su pri brzinama od 15 mm/min i 1000 o/min. Vrednost tvrdoće je sa 37 HV (legura A1050), porasla na 150 HV (legura A1050 ojačana SiC i tretirana postupkom površinske obrade trenjem.

Parametri procesa su jedan od glavnih faktora koji utiču na proces obrade. Uticaj parametara procesa pri proizvodnji AZ91/SiO_2 kompozita ispitivan je u radu [17]. Brzina rotacije je konstantna i iznosi 1250 o/min uz variranje tri translatorne brzine (20, 40, 63 mm/min). Debljina ploče od legure magnezijuma je 8 mm. Rezultati pokazuju da je povećanjem translatorne brzine, veličina zrna značajno smanjena i tvrdoća porasla. Maksimalna tvrdoća postignuta u ovom eksperimentu bila je 124 HV i minimalna veličina zrna od 8 mm.

Površinska obrada trenjem legure AZ31, povećaće tvrdoću obrađenog materijala 2 puta u odnosu na osnovni materijal [18].

Obrada trenjem sa mešanjem je korišćena za proizvodnju AZ31/Al_2O_3 nanokompozita [19]. Povećanjem brzine rotacije, kao rezultat većeg unosa toplote, povećana je veličina zrna osnovne legure uz bolju distribuciju nanočestica. Prosečna veličina zrna matrice kompozita bila je u rasponu od 1–5 μm, a njihova mikrotvrdoća je bila 85–92 HV.

Fuleren je uspešno deponovan u A5083 obradom trenjem sa mešanjem [20]. Tvrdoća je značajno povećana. Parametri obrade: brzina rotacije 500-2000 o/min i translatorna brzina 50 mm/min.

5. ZAKLJUČAK

Izbor parametara brzine povećava tvrdoću kompozitnih materijala dobijenih površinskom obradom trenjem. Optimalnim izborom brzine rotacije i translatorne brzine može se i do 20%, povećati vrednost mikrotvrdoće kod legura poput A319.

Smanjenjem brzine rotacije 3 puta dovodi do povećanja tvrdoće za 40%.

U radu je pokazano da pored uticaja na tvrdoću i mikrotvrdoću brzina rotacije i translatorna brzina utiču na veličinu zrna i na pravilnu distribuciju čestica ojačavača u osnovni materijal.

6. LITERATURA

[1] Mishra, R.S., Mahoney, M.W., McFadden, S.X., Mara, N.A., Mukherjee, A.K.: *High strain rate superplasticity in a friction stir processed 7075 Al alloy*. Scripta Materialia, Volume 42, p.p. 163–168, 1999.

[2] Zykova, A.P., Tarasov, S.Yu., Chumaevskiy, A.V., Kolubaev, E.A.: *A Review of Friction Stir Processing of Structural Metallic Materials: Process, Properties, and Methods*. Metals, Volume 10, p.p. 772, 2020.

[3] Mishra, R.S., De, P.S., Kumar, N.: *Friction Stir Welding and Processing: Science and Engineering*. Springer International Publishing, Cham, 2014.

[4] Rathee, S., Maheshwari, S., Siddiquee, A.N.: *Issues and strategies in composite fabrication via friction stir processing: A review*. Materials and Manufacturing Processes, Volume 33, p.p. 239–261, 2018.

[5] Bharti, S., Ghetiya, N.D., Patel, K.M.: *A review on manufacturing the surface composites by friction stir processing*. Materials and Manufacturing Processes, Volume 36, p.p. 135–170, 2021.

[6] Węglowski, M.S.: *Friction stir processing – State of the art*. Archives of Civil and Mechanical Engineering, Volume 18, p.p. 114–129, 2018.

[7] Rathee, S., Maheshwari, S., Siddiquee, A.N.: *Issues and strategies in composite fabrication via friction stir processing: A review*. Materials and Manufacturing Processes, Volume 33, p.p. 239–261, 2018.

[8] Heydarian, A., Dehghani, K., Slamkish, T.: *Optimizing Powder Distribution in Production of Surface Nano-Composite via Friction Stir Processing*. Metall Mater Trans B, Volume 45, p.p. 821–826, 2014.

[9] Nelaturu, P., Jana, S., Mishra, R.S., Grant, G., Carlson, B.E.: *Influence of friction stir processing on the room temperature fatigue cracking mechanisms of A356 aluminum alloy*. Materials Science and Engineering: A, Volume 716, p.p. 165–178, 2018.

[10] Asadi, P., Givi, M.K.B., Parvin, N., Araei, A., Taherishargh, M., Tutunchilar, S.: *On the role of cooling and tool rotational direction on microstructure and mechanical properties of friction stir processed AZ91*. The International Journal of Advanced Manufacturing Technology, Volume 63, p.p.

987–997, 2012.
[11] Arora, H.S., Singh, H., Dhindaw, B.K.: *Parametric Study of Friction Stir Processing of Magnesium-Based AE42 Alloy*. Journal of Materials Engineering and Performance, Volume 21, p.p. 2328–2339, 2012.
[12] Mishra, R.S., De, P.S., Kumar, N.: *Fundamental Physical Metallurgy Background for FSW/P, in: Friction Stir Welding and Processing*. Springer International Publishing, Cham, p.p. 59–93, 2014.
[13] Sathiskumar, R., Murugan, N., Dinaharan, I., Vijay, S.J.: *Effect of Traverse Speed on Microstructure and Microhardness of Cu/B4C Surface Composite Produced by Friction Stir Processing*. Transactions of the Indian Institute of Metals, Volume 66, p.p. 333–337, 2013.
[14] Karthikeyan, L., Senthilkumar, V.S., Padmanabhan, K.A.: *On the role of process variables in the friction stir processing of cast aluminum A319 alloy*. Materials & Design, Volume 31, p.p. 761–771, 2010.
[15] Kwon, Y.: *Mechanical properties of fine-grained aluminum alloy produced by friction stir process*. Scripta Materialia, Volume 49, p.p. 785–789, 2003.
[16] Kurt, A., Uygur, I., Cete, E.: *Surface modification of aluminium by friction stir processing*. Journal of Materials Processing Technology, Volume 211, p.p. 313–317, 2011.
[17] Khayyamin, D., Mostafapour, A., Keshmiri, R.: *The effect of process parameters on microstructural characteristics of AZ91/SiO2 composite fabricated by FSP*. Materials Science and Engineering: A, Volume 559, p.p. 217-221, 2013.
[18] Chang, C.I., Du, X.H., Huang, J.C., 2007. *Achieving ultrafine grain size in Mg–Al–Zn alloy by friction stir processing*. Scripta Materialia, Volume 57, p.p. 209–212, 2007.
[19] Azizieh, M., Kokabi, A.H., Abachi, P.: *Effect of rotational speed and probe profile on microstructure and hardness of AZ31/Al2O3 nanocomposites fabricated by friction stir processing*. Materials & Design, Volume 32, p.p. 2034–2041, 2011.
[20] Morisada, Y., Fujii, H., Nagaoka, T., Nogi, K., Fukusumi, M.: *Fullerene/A5083 composites fabricated by material flow during friction stir processing. Composites Part A*: Applied Science and Manufacturing, Volume 38, p.p. 2097–2101, 2007.

Autori: **Istr. sar. Živana Jovanović Pešić[1], Vanr. Prof. Dr Dragan Džunić[1], Istr. sar. Miloš Pešić[2], Istr. sar. Strahinja Milenković[1], Prof. strukovnih studija dr Sonja Kostić[3], Doc. dr Vladimir Kočović[1]**

[1]Univerzitet u Kragujevcu, Fakultet inženjerskih nauka, Sestre Janjic 6, 34000 Kragujevac, Srbija, Telefon: +381 34 335 990, Fax: +381 34 333 192;
[2]Univerzitet u Kragujevcu, Institut za informacione tehnologije, Jovana Cvijića bb, 34000 Kragujevac, Srbija, Telefon: +381 34 6100195;
[3]Akademija strukovnih studija Šumadija, Kosovska 8, 34000 Kragujevac, Telefon: +381 34 381418.

E-mail: zixi90@gmail.com
dzuna@kg.ac.rs
milospesic@uni.kg.ac.rs
strahinja.milenkovic@fink.rs
skostic@asss.edu.rs
vladimir.kocovic@kg.ac.rs

ETIKUM 2023 **INTERNATIONAL SCIENTIFIC CONFERENCE**
NOVI SAD, SERBIA, DECEMBER 7-9, 2023

Jovicic, G., Kanovic, Z., Sokac, M., Santosi, Z., Mitrovic, S., Simunovic, G., Vukelic, D.

MODELLING OF SURFACE ROUGHNESS AND TOOL WEAR DURING THE TURNING OF INCONEL 601 ALLOY USING ARTIFICIAL NEURAL NETWORKS

Abstract: *In this paper, the turning process of Inconel 601 is modeled. Turning process was performed with various cutting speeds, feeds, insert shapes, corner radius, rake angles and approach angles. After turning, the arithmetic mean surface roughness and flank wear were measured. For the measured values, the process is modeled using artificial neural networks. The generation of models with different architectures of artificial neural networks, was carried out through three training algorithms in order to determine the most adequate one. Validation of the model was performed through additional confirmation experiments. Prediction and measurement results were compared using percentage and absolute errors. The obtained data indicate that it is best to use the Levenberg-Marquardt algorithm for modeling the turning process using artificial neural networks.*
Key words: *Turning, surface roughness, tool wear*

1. INTRODUCTION

The turning of Inconel alloy has been investigated from different perspectives and on different bases through numerous theoretical, simulation and experimental studies [1-5]. Various methodologies have been developed for the analysis of the turning process. The most numerous are experimental studies [2]. In most of these studies, the effects of the cutting parameters (cutting speed, feed and depth of cut) on the output characteristics of the turning process were considered. Some of the research also took into account the geometry of the cutting tool, energy consumption, material removal rate, coolant and lubricant effects, etc. The most common output characteristics of the process that were studied were the surface roughness, machining time, etc. [2,3]. The disadvantage of experimental research, especially in the conditions of a large number of experiments, is that it is expensive and time-consuming. Further, a major drawback of experimental research is that the obtained results can only be applied to the conditions in which the experiments were conducted [4,5].

As a response to the previous problem, there are studies in which appropriate models have been developed. The model establishes a dependency that links input and output parameters. Empirical modeling methods are based on experimental data, and on the establishment of functional dependence between input and output parameters of the turning process. The Taguchi method, artificial neural networks (ANN), regression modeling (RM) and support vector machines (SVM) are most often used to model the turning process [4,5]. These methods are tolerant of imprecision, uncertainty and approximation. It is essential that the errors occurring between the predicted and experimental values are within acceptable limits. If the turning process is correctly modeled and acceptable errors are achieved, the costs and time of experimental research are reduced. At the same time, the technologist's subjective influence on the obtained results is reduced [5]. Also, the universality is greater, and therefore the possibility of practical application, since the models can be applied in the range of input variables, and not only for experimental results. The main problem is to choose which method and when to apply, given that each of them has its own advantages and disadvantages. Regardless of some guidelines that exist, it is still impossible to define an algorithm by which the selection of an adequate modeling method will be made. Therefore, the essential issue is to choose an adequate method and formulate a sufficiently accurate model that will represent a sufficiently accurate approximation of the turning process.

The main goal of this research is to evaluate the influence of six input parameters of the turning process and to generate and compare prediction models of arithmetic mean surface roughness and flank wear.

2. MATERIALS AND METHODS

The research was carried out on workpieces with dimensions Ø 40x400 mm made of Inconel 601 alloy. The turning operation was carried out on a CNC lathe without the use of coolant and lubricant with the depth of cut a_p=1,5 mm. Coated

PVD cutting inserts were used in the experiments. The research was conducted according to the full factorial design of the experiment. During the experimental research, six input parameters were varied. The levels of the input parameters are shown in Table 1.

Table 1. Input parameter levels

Parameter	Min.	Mean	Max.
Feed f (mm/rev)	0.15	-	0.25
Cutting speed v_c (mm/min)	40	-	60
Insert shape IS	triangular	-	square
Corner radius r (mm)	0.4	0.8	1.2
Rake angle γ (°)	3	6	9
Approach angle κ (°)	60	75	90

The measurement of arithmetic mean surface roughness (Ra) was carried out on a Talisurf measuring device. A Gaussian filter was used. The measurement was carried out with a sampling length of 0.8 mm at an evaluation length of 4 mm. Measurement of flank wear (VB) was performed on a Leitz Orthoplan microscope.

The experimental research was conducted in accordance with the randomized full factorial experiment. A total of 216 experiments were performed. A small part of measurement results is shown in Table 2.

Table 2. Small part of the measurement results [6]

No.	*f* (mm/rev)	v_c (mm/min)	*IS*	*r* (mm)	*γ* (°)	*κ* (°)	*Ra* (μm)	*VB* (mm)
1	0.15	60	T	1.2	3	90	1.230	0.257
2	0.25	40	T	0.4	9	75	4.646	0.247
3	0.25	60	T	0.8	3	60	3.680	0.279
4	0.25	60	T	1.2	6	75	2.541	0.277
5	0.15	40	T	0.8	6	60	1.832	0.184
...	...	...	...	...	...	...	...	...
214	0.15	60	T	0.8	9	60	1.789	0.279
215	0.15	60	S	0.4	6	90	2.434	0.278
216	0.15	60	T	1.2	6	90	0.887	0.267

3. RESULTS

After the measurements, the process was modeled using ANN. The developed prediction model is based on feed-forward neural networks with back propagation training algorithm. The three-layer architecture of the ANN model, Fig. 1, consists of 6 input parameters (f, v_c, IS, r, γ, κ) and two output parameters (Ra, VB). Input parameters are in 6×216 format, while output parameters are in 2×216 format.

The training data set consists of 216 samples that are randomly divided into three groups with a proportion of 70:15:15. The first group consists of 152 samples which were used as the training dataset, the second group of 32 samples was used as the validation dataset, while the third group of 32 samples was used as the testing dataset. For all three groups of data sets, mean squared error (MSE) values are calculated as performance measures.

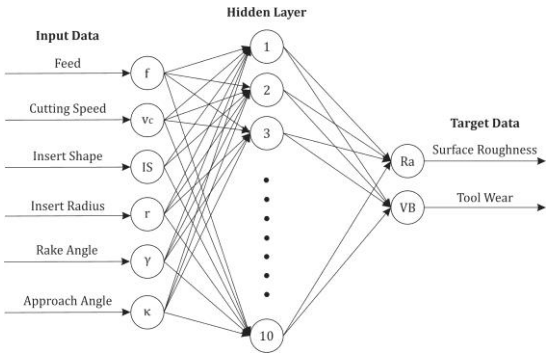

Fig. 1. ANN model architecture [6]

For ANN models training Levenberg-Marquardt, Bayesian regularization and Scaled Conjugate Gradient Backpropagation algorithm were used. The model training is an iterative process performed using an input and output data set which were obtained experimentally. Performance and regression plots, for all three models, are shown in Fig. 2-4.

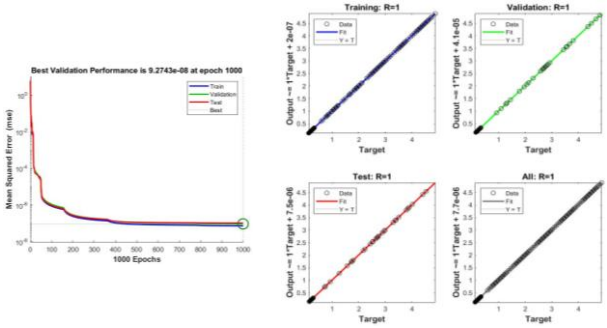

a) b)

Fig. 2. Training results applying Levenberg-Marquardt algorithm, a) performance, b) regression

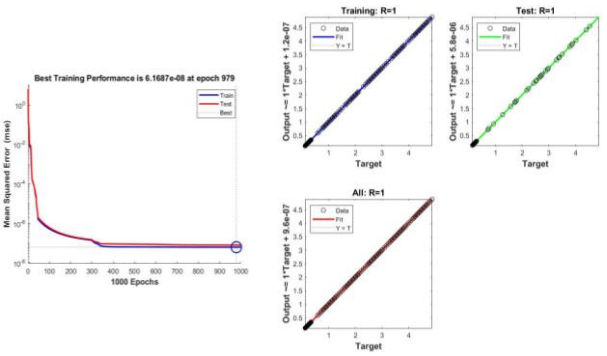

a) b)

Fig. 3. Training results applying Bayesian Regularization algorithm, a) performance, b) regression

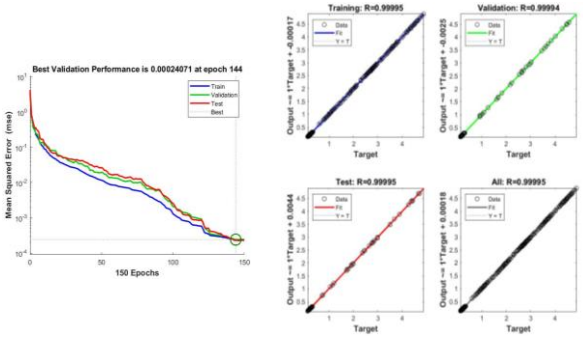

a) b)

Fig. 4. Presentation of training results applying Scaled Conjugate Gradient Backpropagation algorithm, a) performance, b) regression

Based on the graphical results, it can be concluded that an excellent correlation was achieved between the target data and the output data from the network. Based on a comprehensive analysis of the training results for all three algorithms, it can be concluded that the Levenberg-Marquardt algorithm provides the best solution of the ANN model.

3.1. Prediction with developed ANN models

Modeling performance for all three training algorithms was evaluated by calculating percentage (PE) and absolute errors (AE) for each experiment. The graphical interpretation of the obtained minimum, maximum and mean arithmetic values of PE and AE for Ra and VB, for all three algorithms are shown in Fig. 5.

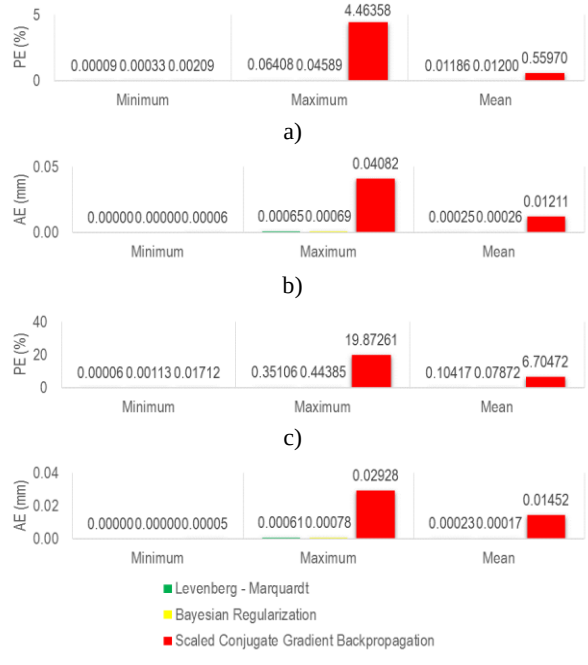

Fig. 5. Errors for different algorithms during training, validation and testing
a) PE for Ra, b) AE for Ra, c) PE for VB, d) AE for VB

It can be seen from figures that the least minimum, maximum and mean arithmetic values for percentage and absolute errors are obtained for the Levenberg - Marquardt algorithm, slightly higher for the Bayesian Regularization algorithm and significantly higher for the Scaled Conjugate Gradient Backpropagation algorithm.

3.2. Confirmation of ANN models

Confirmation of the obtained models for all three training algorithms was performed through eighteen additional experiments. Confirmation experiments were performed with combinations of input parameters different from those used for training, testing and validation of neural networks, in order to check the generalization ability of the formed models. The obtained results are shown in Table 3.

Table 3. Measured values of Ra and VB for confirmation experiments

No.	f (mm/rev)	v_c (mm/min)	*IS*	r (mm)	γ (°)	κ (°)	*Ra* (μm)	*VB* (mm)
1	0.2	50	T	1.2	3	60	2.269	0.174
2	0.2	50	S	1.2	3	60	2.099	0.139
3	0.2	50	T	1.2	6	60	1.938	0.183
4	0.2	50	S	1.2	6	60	1.766	0.148
5	0.2	50	T	1.2	9	60	2.099	0.194
6	0.2	50	S	1.2	9	60	1.933	0.160
7	0.2	50	T	1.2	3	75	2.351	0.184
8	0.2	50	S	1.2	3	75	2.173	0.149
9	0.2	50	T	1.2	6	75	2.051	0.193
10	0.2	50	S	1.2	6	75	1.842	0.159
11	0.2	50	T	1.2	9	75	2.194	0.204
12	0.2	50	S	1.2	9	75	2.001	0.169
13	0.2	50	T	1.2	3	90	2.413	0.193
14	0.2	50	S	1.2	3	90	2.249	0.159
15	0.2	50	T	1.2	6	90	2.061	0.203
16	0.2	50	S	1.2	6	90	1.911	0.169
17	0.2	50	T	1.2	9	90	2.261	0.214
18	0.2	50	S	1.2	9	90	2.072	0.178

The graphical interpretation of the obtained minimum, maximum and mean arithmetic values of percentage and absolute errors for Ra and VB, for all three algorithms, is shown in Fig. 6. It is noticeable from the figures that the least minimum, maximum and mean arithmetic values for PE and AE are obtained for the Levenberg - Marquardt algorithm and the highest values for the Scaled Conjugate Gradient Backpropagation algorithm. The obtained results indicate that the Levenberg - Marquardt algorithm gives the best prediction results.

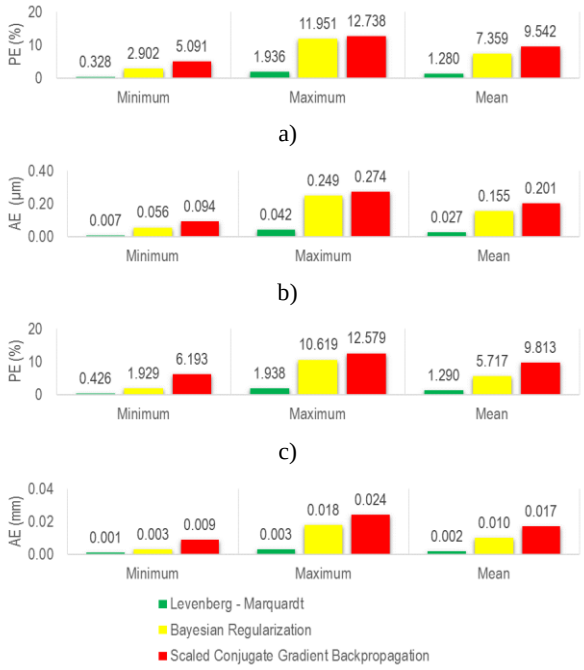

Fig. 6. Errors for different algorithms during confirmation
a) PE for Ra, b) AE for Ra, c) PE for VB, d) AE for VB

4. CONCLUSION

In this research, the parameters and geometry of the cutting inserts were modeled from the point of view of the quality of the processed surface (arithmetic mean surface roughness) and the stability of the cutting tool (flank wear). Based on the established dependence and the development of an adequate model, it is possible to predict the outputs of the turning process depending on the inputs. The results indicate that the Levenberg-Marquardt algorithm outperforms the other two algorithms used for training of artificial neural networks models of the turning process.

Future research will be focused on modeling a larger number of variables, i.e. the inclusion of a larger number of input and output parameters in the model, as well as the examination of the possibility of modeling the process with other methods and techniques.

5. REFERENCES

[1] Buddaraju, K.M., Ravi Kiran Sastry, G., Kosaraju, S.: *A review on turning of Inconel alloys*, Materials Today: Proceedings, Vol. 44, pp. 2645-2652, 2021.

[2] Chandrasekaran, M., Muralidhar, M., Krishna, C. M., Dixit, U.S.: *Application of soft computing techniques in machining performance prediction and optimization: a literature review*. International Journal of Advanced Manufacturing Technology, Vol. 46, pp. 445–464, 2010.

[3] Dogra, M., Sharma, V.S., Dureja J.: *Effect of tool geometry variation on finish turning – A Review*, Journal of Engineering Science and Technology Review, Vol. 4, pp. 1-13, 2011.

[4] Dureja, J.S., Gupta, V.K., Sharma, V.S., Dogra, M., Bhatti, M.S.: *A review of empirical modeling techniques to optimize machining parameters for hard turning applications*, Proceedings of the Institution of Mechanical Engineers, Part B: Journal of Engineering Manufacture, Vol. 230, pp. 389-404, 2016.

[5] Garg, A., Bhalerao, Y., Tai, K.: *Review of empirical modelling techniques for modelling of turning process*, International Journal of Modelling Identification and Control, Vol. 20, No. 2, pp. 121-129, 2013.

[6] Jovicic, G., Milosevic, A., Kanovic, Z., Sokac, M., Simunovic, G., Savkovic, B., Vukelic, D.: *Optimization of Dry Turning of Inconel 601 Alloy Based on Surface Roughness, Tool Wear, and Material Removal Rate*, Metals, Vol. 13, No. 6, Article Number: 1068, 2023.

Authors:

MSc Goran Jovicic, PhD Zeljko Kanovic, PhD Mario Sokac, PhD Zeljko Santosi, PhD Djordje Vukelic, University of Novi Sad, Faculty of Technical Sciences, Trg Dositeja Obradovica 6, 21000 Novi Sad, Serbia.
E-mail: goran.ns@hotmail.com
kanovic@uns.ac.rs
marios@uns.ac.rs
zeljkos@uns.ac.rs
vukelic@uns.ac.rs

PhD Slobodan Mitrovic, University of Kragujevac, Faculty of Engineering, Sestre Janjic 6, 34000 Kragujevac, Serbia.
E-mail: boban@kg.ac.rs

PhD Goran Simunovic, University of Slavonski Brod, Mechanical Engineering Faculty, Trg Ivane Brlic Mazuranic 2, 35000 Slavonski Brod, Croatia
E-mail: gsimunovic@unisb.hr

ETIKUM 2023 **INTERNATIONAL SCIENTIFIC CONFERENCE**
NOVI SAD, SERBIA, DECEMBER 7-9, 2023

Karabegović, I., Husak, E., Karabegović, E., Mahmić, M.

COMPARATIVE ANALYSIS OF THE IMPLEMENTATION OF ROBOT TECHNOLOGY AS THE BASIC TECHNOLOGY OF INDUSTRY 4.0 IN AMERICA (USA) AND CHINA

Abstract: *We are aware that major changes are taking place thanks to the application of Industry 4.0 technologies in recent years. The concept itself is not represented enough in production processes in the industry, but changes are still taking place, reshaping production systems, consumption, delivery, logistics, as well as in all segments of production processes. Thanks to innovations in Industry 4.0 technologies, changes are taking place in the basic technologies, and some of them are: Robotics, Smart Sensors, Flexible Automation, Internet of Things (IoT), 3D Printing, Big Data, Cloud Computing, Radio Frequency Identification (RFID), Virtual and Augmented Reality (AR), Artificial Intelligence (AI), etc. A comparative analysis of the global trend of international patent families (IPF) in the basic technologies of Industry 4.0 is analyzed. The paper itself provides an analysis of robotic technology as an Industry 4.0 technology, as well as a comparative analysis of the application of robots in the USA with the application of robots in China. The implementation of the basic technologies of Industry 4.0 in both countries is taking place rapidly, and the reason is the competitiveness of companies on the global world market. Among the listed technologies of Industry 4.0, robotic technology is in the first place, without which there is no automation of production processes*

Key words: *Robotics, Industry 4.0, Flexible Automation, Robot, Production Process*

1. INTRODUCTION

The world is currently implementing the fourth industrial revolution, which relies on digitization and networking. Industry 4.0 is the frontier of the fourth industrial revolution that initiates major changes both in production processes and in the values of creation and consumer behavior. Industry 4.0 transforms existing production processes into new generations of production processes that are digitized and based on a combination of cyber-physical systems (CPS) and digital technologies. Industry 4.0 provides intelligent production processes that are integrating the physical world with the digital and virtual world [1]. The concept of Industry 4.0 is based on the smart connection of devices in the production process, which contributes to the development of new technologies and business models, as well as new approaches to work and thinking. We are witnessing everyday development and implementation of new technologies that are included in the concept of Industry 4.0. Some of the basic technologies on which the concept of Industry 4.0 is based are the following: Cyber-Physical Systems (CPS), Digital Product Memory (DPM), Radio Frequency Identification (RFID), Near Field Communication (NFC), Smart Machining, Machine-to-Machine (M2M), Man-Machine Interaction (MMI), Assisted Operator, Robotics, Smart Sensors, Energy Efficiency Monitoring, Renewable Energy Integration, Smart/Mobile Maintenance, Condition Monitoring, Augmented Reality (AR), Virtual Reality (VR), Code (QR), Digital Twin, Digital Shadow, Reconfigurable Factory, Plug & Produce, Shop Food Management I4.0, Lean management, Batch Size 1, Pick By Light, Smart Devices, Horizontal & Vertical Integration, Industrial Cyber Security, Real-Time Communication, Manufacturing Execution Systems (MES), Enterprise Resource Planning (ERP), Intelligent Logistics, Supplier Relationship, Customer Relationship, Additive Manufacturing – AM, Internet of Things-IoT (Industrial Internet of Things-IioT), Cloud Computing (CC), Artificial Intelligence (AI), Big Data and analytics, and Smart Factory [2,3,4]. From the above listed basic technologies of Industry 4.0, we will single out the most important technologies that transform production processes and industrial production: Robotics, Smart Sensors, Internet of Things-IoT (Industrial Internet of Things-IioT), Horizontal & Vertical Integration, Cloud Computing (CC), Cyber Security, Additive Manufacturing-AM, Augmented Reality (AR), Big Data and analytics, Artificial Intelligence (AI), and others. The development of the mentioned technologies enables development based on technologies, automation and autonomy. Artificial Intelligence (AI) is increasingly being used in the automation of

production processes, and the largest share is provided by robotics, autonomous vehicles, autonomous service robots, smart sensors, and robots that work side by side with humans in jobs that are dangerous to human health, but robots can perform them much faster [5,6]. The development and research of technologies Industry 4.0 can be traced through the number of global innovations or approved patents in the world, which are growing dramatically. In order to get a real insight, we made an analysis of the global innovation trend from Industry 4.0.

2. THE TREND OF GLOBAL INNOVATIONS FROM INDUSTRY 4.0

The trend of global innovations in the listed technologies of Industry 4.0 has been growing rapidly during the last decade. An analysis of the global trend of the growth of IPFs in Industry 4.0 technologies in developed countries: the USA, Japan, Republic of Korea, China and Europe was conducted and shown in Figure 1 [7-9].

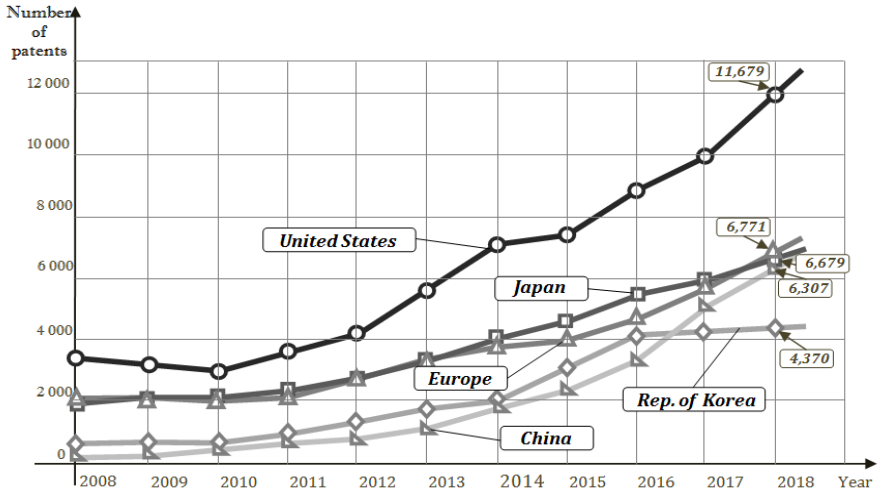

Source: European Patent Office

Fig. 1. Global growth trend of IPFs (International patent families) in Industry 4.0 technologies in the USA and China as well as in the European Union, Japan, and Republic of Korea in the period 2008-2018 [8]

The global growth trend of IPFs in Industry 4.0 technologies in the European Union, the USA, Japan, the Republic of Korea and China has been continuously growing since 2008. We have to single out the USA, which is in first place and stands out from the other observed countries, so that in 2018 it had 11.679 registered IPF patents. The second place is shared by Japan and the European Union (Sweden, Switzerland, United Kingdom, Finland, Germany, Spain, Italy, France, the Netherlands – developed EU countries) with the same application of IPF patents in 2018, i.e., 6.771 IPF patents were registered in the EU, and 6.679 IPF patents were registered in Japan. China holds the third place with 6.307 IPF patents registered in 2018, followed by the Republic of Korea with 4.370 registered IPF patents. This growth trend has continued until today, and it is expected in the coming years as well [11]. Based on Figure 2, we can see that the automotive industry is leading in terms of IPF patents, which is the industry that most widely uses Industry 4.0 technologies: robotics, cloud computing, sensors, radio frequency identification-RFID. We have created a comparative analysis of the implementation of industrial robots in production processes in the USA, Japan, the Republic of Korea, Germany with China, because these are the top countries in the application of innovations from Industry 4.0. It is interesting to notethe trend of IPF applications from Industry 4.0 technologies in different technological fields. The analysis was prepared for the period 2008-2018 and shown in Figure 2 [7-9, 10].

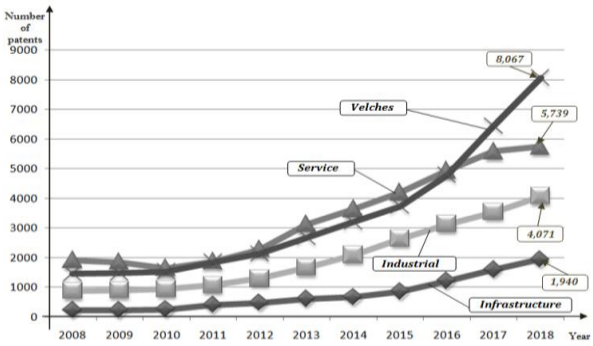

Source: European Patent Office

Fig. 2. Global growth trend of IPFs (International patent families) in the fields of industry, vehicles, services and infrastructure in the world for the period 2008-2018 [7]

Figure 2 shows the global growth trend of IPFs in Industry 4.0 technologies in the following technological areas: industry, vehicles, service and infrastructure. We come to the conclusion that since 2010, the global trend of IPF applications from Industry 4.0 technologies in all the mentioned technological fields has been growing intensively. The first place is held by the area of vehicles, where 8.065 IPF applications were registered in 2018, while in second place is the service area with 5.739 registered IPF patents. Furthermore, a growing trend in IPF patent applications was recorded from year to year, so that in 2018 there were 4.071 applications from industry and 1.904 from infrastructure. Such a trend is expected because the automotive industry is present in the global market and in order for companies to be world leaders,they must engage in the implementation of Industry 4.0 in order to make their production processes fully flexible and intelligent [12-14].

3. COMPARATIVE ANALYSIS OF THE TRENDS OF PATENTS AND IMPLEMENTATION OF ROBOTIC TECHNOLOGY IN PRODUCTION PROCESSES IN THE UNITED STATES OF AMERICA AND CHINA

To analyze the application of robotic technology, an analysis of the application of industrial robots in the world was made. The data on the number of robots was taken from the International Federation of Robotics (IFR), the UN Economic Commission for Europe (UNECE) and the Organization for Economic Cooperation and Development (OECD) [16]. Figure 3 shows the use of robots in the world on an annual basis in the period 2010-2020 [17-19].

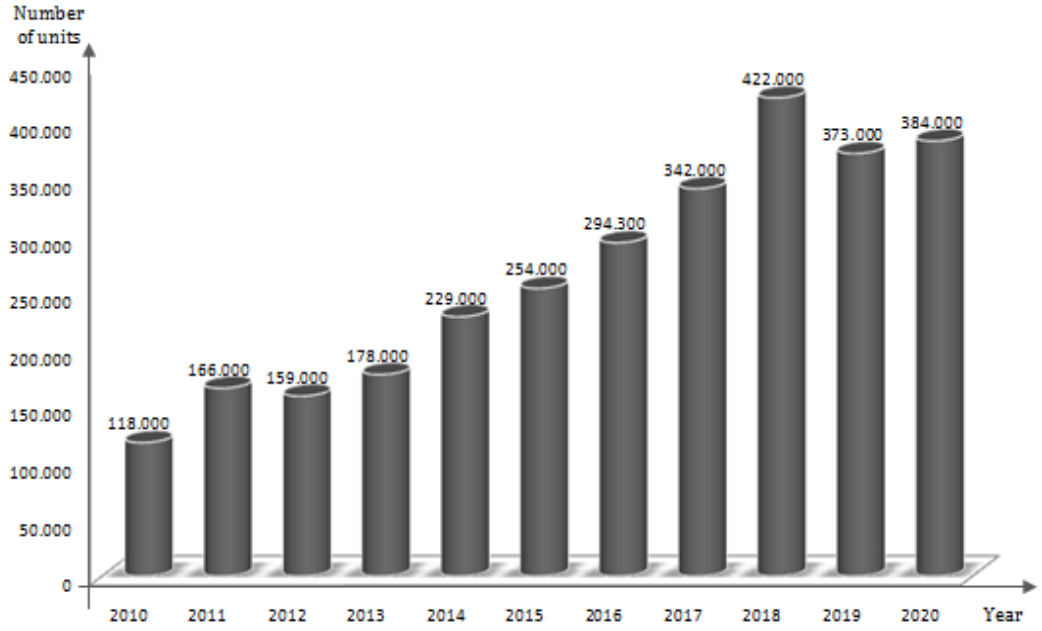

Fig. 3. The trend of the use of robots in the world on an annual basis in the period 2010-2020

The trend of the implementation of industrial robots had a growing character as of 2010 until 2018, as shown in Figure 5. The increase in the trend went from 118.000 units of industrial robots in 2010 to 422.000 robot units in 2020. In other words, in only eight years, the implementation has increased about 3.5 times. In 2019 and 2020, the implementation trend was reduced so that in 2020 it amounted to around 384.000 robot units. The reason that the trend of implementation of robots has decreased is due to the fact that the world has been affected by the pandemic of the COVID 19 virus.

It is expected that after the end of the pandemic in the world, there will be an increase in the trend of implementation of industrial robots in the world.

In the following years, the trend of implementation of industrial robots will increase rapidly due to the implementation of Industry 4.0, which is being implemented by all companies that are at the top of the global market. In order to get the real insight, Figure 4 provides the information which countries in the world implement the most industrial robots. [17]

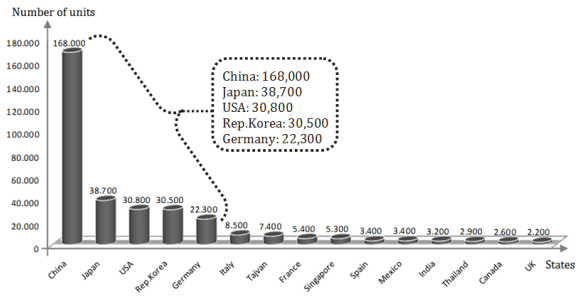

Fig. 4. Implementation of industrial robots in 2020 in fifteen top countries in the world with reference to the USA and China

The analysis of implementation of industrial robots in 2020 shown in Figure 4 provides us with the conclusion the first five top countries are: China, Japan, the USA, the Republic of Korea and Germany. The first place is held by China with around 168.000 units of implemented robots, and is far ahead of the top five countries in the world in terms of implementing robots as the base technology of Industry 4.0. The United States of America is in third place with the implementation of around 30.800 robot units, which is far less than China. In 2020, about 5.45 times more industrial robots were implemented in China than in other countries. The second place is held by Japan about 38.700 robot units, followed by the USA with about 30.800 implemented robot units, the Republic of Korea with about 30.500 robot units and lastly Germany with around 22.300 units of implemented robots. The other thirteen top countries in the world are: Japan, the Republic of Korea, Germany, Italy, Taiwan, Singapore, Spain, Mexico, India, Thailand, Canada and the United Kingdom, where the implementation of industrial robots varies depending on the country, as shown in Figure 4. Such a trend is expected in the last few years due to the fact that the first five countries have developed automotive and electro/electronic industry, which are the two industries where about 50% of all industrial robots in the world are implemented on an annual basis [23-25]. Another reason for this trend is that these countries are implementing Industry 4.0, which would not be possible without industrial robots, since robot technology is one of the basic technologies of Industry 4.0. The third reason for this trend is the fact that these countries invest in research and development in innovations of robotic technology and its implementation in production processes, which is demonstrated by the trend of approved robotics patents in the countries of China, Japan, Republic of Korea, USA, and Germany in 2019, as shown in Figure 5. [9].

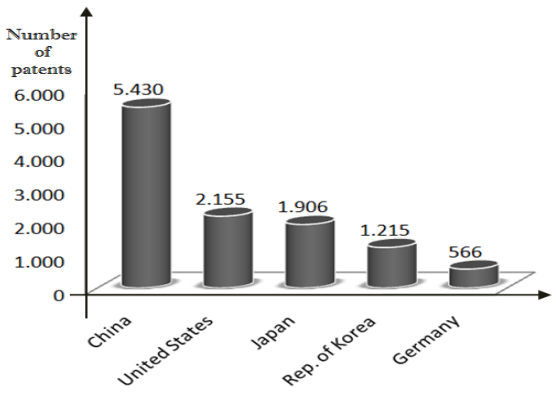

Fig. 5. The trend of approved robotics patents in the countries of China, Japan, Republic of Korea, USA and Germany in 2019, with a special focus on China and USA

The analysis of Figure 5, which shows the trend of approved patents in robotics in 2019, has provided us with the conclusion that China holds the first place with 5.430 approved patents in robotics, followed by the Unites States of America with 2.155 approved patents. China has implemented about 2.5 times more patents in the same year compared to the USA. The third place is held Japan with 1.906 approved robotics patents, followed by the Republic of Korea with 1.215 approved patents and Germany with 566 approved robotics patents. Hereby we prove the fact that these five countries rightfully represent the top countries in the world in terms of the implementation of industrial robots, because they invest in development and research in robotic technology. They also implement Industry 4.0 in order for their companies to be competitive on the global market [15,20-22]. After analyzing the approved patents in robotic technology, it is interesting to observe the trend of implementation of industrial robots in each of these four top countries: the USA, Japan, the Republic of Korea and Germany, and to make a comparison with the implementation of industrial robots in China. The trend of implementation of industrial robots in five top countries is shown in Figure 6 [5,17-19]. By analyzing the trend of the implementation of industrial robots in Germany, the Republic of Korea, the USA, Japan and China in the period 2010-2021, we conclude that in 2010 China was in the penultimate place with the implementation of about 15.000 robot units, which is slightly more compared to Germany that implemented about 14.000 robots.

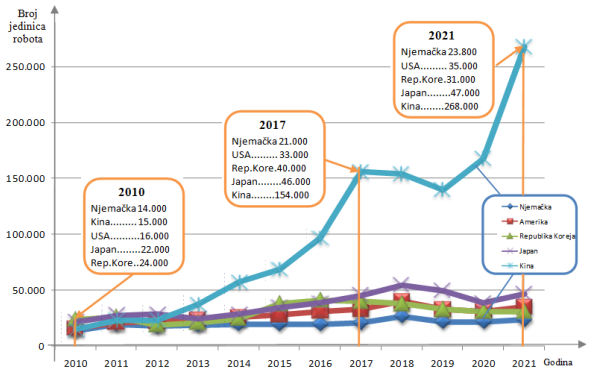

Fig. 6. The trend of implementation of industrial robots on an annual basis in Germany, the Republic of Korea, USA and Japan in relation to China in the period 2010-2021, with a special with reference to China and USA

In the following years, China was in first place in the world in terms of robot implementation. The USA was able to have a higher amount of implemented robots than China in 2010. The USA is implementing industrial robots and following the countries of Japan, the Republic of Korea and Germany, with somewhat less average than Japan and more than the Republic of Korea and Germany, depending on the year. As of 2012, China has become the leader in the implementation of industrial robots in the world, so that, for example, China implemented about 156.000 robot units in 2017. In this period, the growth trend of the implementation of industrial robots increased on annual basis according to an exponential function. The same trend continued until 2021. However, we noticed that in the period 2019-2020 there was a slight decrease in the implementation of industrial robots due to the CORONA virus pandemic. In 2021, there was an increase in the implementation of industrial robots, so that China held the first place with the implementation of about robot 268.000 units, which is far ahead of the robot implementation in the USA.

China is the leader in the use of robots in the world, and some of the reasons are [28]:

- China adopted the National Program for research, development and implementation of high technologies called "863 Program", whose goal is to transform China into a technologically developed country,
- China is developing the automotive industry as well as the electrical/electronic industry where robots are mostly used.
- China, like technologically developed countries in the world, implements Industry 4.0 technologies, robot technology is the basic technology of Industry 4.0.
- The price of labor in China is increasing, and the price of robot labor is decreasing, so companies are going to use robots in production processes.

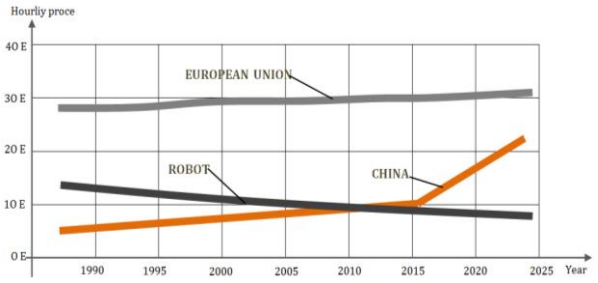

Fig. 7. The price of a robot working hour, the European Union and China

The price of a robot's working hour is continuously decreasing. The trend of the labor price in the European Union is slightly increasing every year, while the price of labor in China has been skyrocketing since 2015, which justifies the introduction of industrial robots into the production processes in China. This is not a sufficient parameter for us to have a true insight into the extent to which the implementation of robotic technology in the production processes of companies is represented in technologically developed countries [26,27]. In order to get a more complete picture of the representation of robotic technology in one country, an analysis of the density of robots per 10.000 employees in production processes must be conducted, which indicates the country with the largest number of implemented robots in production processes. An analysis of the density of robots per 10.000 employees in production processes in twenty top countries in the world by the implementation of industrial robots for the year 2020 was conducted and shown in Figure 8 [17-19]. Based on the analysis in Figure 7, we can conclude that the world average of robot density per 10.000 workers in production processes in 2019 was 126 robots.

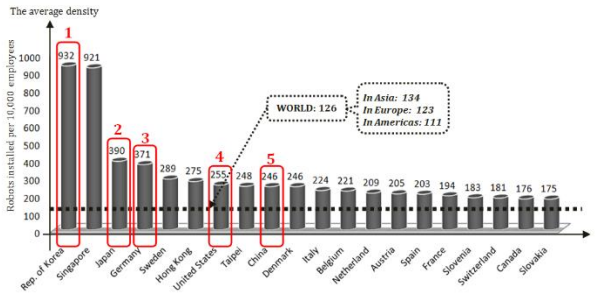

Fig. 8. Robot density per 10.000 employees in production processes in 2020 in the top twenty countries in the world with special reference to the USA and China

The average in Asia is 134 robots, which is higher than the world average, whereas Europe's average is 123 robots which is slightly less than the world average. The smallest average of robot density is recorded in America, i.e., 111 robots. The first place in the world in 2019 is occupied by the Republic of Korea with 932 robot units per 10.000 employees in production processes, followed by Singapore with 921 robot units per 10.000 employees in production processes.The Republic of Korea has had a leading role in the world for years and is in first place when it comes to robot density. The USA is in seventh place in the world with robot density of 255, whereas the seventh place among the analyzed countries is held by China with a density of 246 robots. We must note that the USA, China, as well as the other eighteen analyzed countries shown in Figure 7, are above the world average for the robot density per 10.000 employed workers. Even though China has been the leading country in the world in the implementation of industrial robots since 2013, it holds the last place in terms of density robots compared to other countries. We must note that in 2010, China had a robot density of only 18 robots per 10.000 employees [28], and in just ten years it progressed and reached a density of 246 robots, which no other country in the world has achieved. There are two reasons for China's progress in implementing industrial robots and increasing the density of robots per 10.000 employed workers. One reason is that the Chinese government has adopted a strategy called ''Made in China 2025'' which aims to position China as the most technologically developed country in the world, and has divided the strategy into stages until 2049. Another reason is that the labor cost of workers in China is increasing year by year, whereas the labor cost of industrial robots is decreasing, which is why companies are deciding to implement industrial robots.

We have to single out China, which holds the first place, compared to the USA and other analyzed countries that show an increase in the implementation of robotic technology as the basic technology of Industry 4.0 every year [28-29]. We believe that this trend of robotic technology implementation will continue in these countries in the years to follow. There are few reasons, among which are that all these countries have an Industry 4.0 implementation strategy and their companies want to be competitive on the global market, which can only be achieved by implementing as many basic technologies of Industry 4.0 as possible.

4. CONCLUSION

Companies throughout the world have implemented new technologies due to global competition on the market, which can only be achieved by automation of production processes and changing and improving the production methods. These processes would not be possible without the implementation of basic technologies of Industry 4.0, especially without the use of industrial robots. There are many technologies on which Industry 4.0 is based (according to some authors, over 40), but the fundamental are the following: robotics, automation, Internet of Things (IoT), Big Data, Cloud Computing, 3D printing, smart sensors, Radio Frequency Identification (RFID), Virtual and Augmented Reality (AR), Artificial Intelligence (AI), advanced security systems, Cyber-Physical Systems (CPS), etc. Basic technology of Industry 4.0 is robotic technology, and its application can be monitored through the implementation of robots in production processes. We have concluded that the global growth trend of IPFs (International patent families) in Industry 4.0 technologies is getting higher (Figure 1) every year. The first place in terms of growth trend in the world is held by the USA, followed by China, the Republic Korea, Japan, Germany and other countries. Similarly, the global trend of IPFs (International patent families) in the fields of industry, vehicles, services and infrastructure in the world has a growing trend as well (Figure 2), the first being the vehicle industry because it invests in the development and implementation of the latest technologies in production processes due to global competition. Likewise, the participation of robotic technology in production processes is increasing every year worldwide. The number of implemented industrial robots is increasing every year and in 2020 it amounted to 384.000 robot units in the world. We must single out China because it has been the leader ever since 2013, as shown by the parameter implementation of industrial robots and the number of approved patents in robotics technology. In addition, China is the leader in the implementation of robotics as the base technology of Industry 4.0 compared to the USA. This is not the case with the other base technologies of Industry 4.0 that we have listed in the introduction, such as Cloud Computing and 3D Printing, where America (USA) is the leader in terms of development, research and implementation compared to all other countries. We can conclude that robotic technology is one of the basic technologies of Industry 4.0, and the trend of its implementation will continue to grow in the coming years.

5. ACKNOWLEDGEMENT

The authors acknowledge the financial support from the Ministry of Science, Higher Education and Youth, Canton Sarajevo, Bosnia and Herzegovina, grant for cofinancing of scientific research/artistic research and research projects of special interest to Sarajevo Canton for 2022. (Number 27-02-35-37081-14/23, Sarajevo: 14.09.2023).

6. REFERENCES

[1] Karabegović, I., Kovačević, A., Banjanović Mehmedović, L., Dašić, P..: *Integrating Industry 4.0 in Busniess and Manufacturing*, IGI Global, Hershey, PA, USA, 2020.

[2] Schwab, K.: *The Fourth Industrial Revolution*, World Economic Forum, Geneva, Switzerland, 2016.

[3] Majsorović, V., Đuričić, D., Mitrović, R.: *Idustrija 4.0: Renesansa inženjerstva*, Univerzitet u Beogradu, Mašinski fakultet, Beograd, Srbija, 2022.

[4] Karabegović, I., Turmanidze, R., Dašić, P.: *Structural Network for the Implementation of "Industry 4.0" in Production Processes*, International Scientific Journal "Industry 4.0",Year VII, Issue 1, pp. 3-6, 2022.

[5] Karabegović, I., Karabegović, E., Mahmić, M., Husak, E.: *The Implementation of Industry 4.0 in the Function of Application of Industrial and Service Robots in Production Processes*, International Scientific Conference, Application of Industriy 4.0 on Opportunity for a New Step Forward in All Industrial Branches, Special Editons, Volume CCII, Department of Technical Sciences, Volume 20, ANU B&H, pp. 103-117, 2022.

[6] Esmaeilian, B., Behdad S., Wang, B.: *The evolution and future of manufacturing: a review*, Journal Manufacturing System, Vol. 39, pp. 79-100, 2016.

[7] UNCTAD: *Technology and innovation report*, United Nations conference on Trade and Development; based on data from Maddison Project Database, version 2018, 2021.

[8] European Patent Office, Munich, Germany, 2020, pp. 7-13, https://baa.no/en/services/ip-rights/

[9] *Trademarks and patents in China: The impact of non-market factors on filing trends and IP systems*. January 2021, https://www.uspto.gov/sites/default/files/documents/USPTOTrademarkPatentsInChina.

[10] Abdulla, S. M.: *China's Robotics Patent Landscape*, Center for Security and Emerging Technology-CSET, 2021.

[11] Karabegović, I., Turmanidže, R., Dašić, P.: *Analysis of Patent Trends from Industry 4.0 and the Implementation of Robot Technology in the Countries of China, USA, Japan, Republic of Korea and Germany*, 6th International Scientific Conference, Conference on Mechanical Engineering Technologies and Applications-COMET-a, 17th-19th November, East Sarajevo, pp. 273-286., RS, Bosnia and Herzegovina, 2022.

[12] Wang, K.: *Intelligent Predictive Maintenance (IPdM) system - Industry 4.0 scenario*, WIT Transactions on Engineering Sciences, Vol. 113, pp. 259–268. 2016.

[13] Muller, J. M., Buliga, O., Voigt, K. I.: *Fortune favors the prepared: How SMEs approach business model innovations in Industry 4.0*, Technological Forecasting and Social Change, Vol. 132, Iss. C, pp. 2–7, 2018.

[14] Karabegović, I., Karabegović, E., Mahmić, M., Husak E.: *The Implementation of Industry 4.0 by Using Industrial and Service Robots in the Production Processes*, Chapter 1. Handbook of Research on Integrating Industry 4.0 in Business and Manufacturing, IGI Global, USA, pp. 1-30, 2020.

[15] Chryssolouris, G., Mavrikios, D., Papakostas, N., Mourtzis, D., Michalos, G., Georgoulias, K.: *Digital manufacturing: History, perspectives, and outlook*, Proceedings of the Institution of Mechanical Engineers, Part B, Journal of Engineering Manufacture, pp. 451–462. 2009.

[16] Karabegovic E., Karabegovic I., Hadzalic E.: *Industrial Robot Application Trend in World's Metal Industry*, Inzinerine Ekonomika - Engineering Economics, Vol. 23, No. 4, pp. 368-378. 2012.

[17] International Federation of Robotics, "*World Robotics Report: 'All-Time High' with Half a Million Robots Installed in one Year*," IFR International Federation of Robotics. https://ifr.org/ifr-press-releases/news/wr-report-all-time-highwith- half-a-million-robots-installed, Accessed: Dec. 16, 2022.

[18] Bill, M., Müller, C., Kraus, W., Bieller, S.,: *World Robotics Report*, Available: https://ifr.org/downloads/press2018/2022_WR_extended_version.pdf, 2022.

[19] International Federation of Robotics, *Executive Summary World Robotics 2022 Industrial Robots*. Available: https://ifr.org/img/worldrobotics/Executive_Summary_WR_Industrial_Robots_2022.pdf, 2022.

[20] Hermann, M., Pentek, T., Otto, B.: *Design*

principles for industrie 4.0 scenarios, In Proceedings of the IEEE 2016, 49th Hawaii International Conference on System Sciences (HICSS), Koloa, HI, USA, pp. 3928–3937, 2016.
[21] Thoben, K.D.; Wiesner, S.; Wuest, T.: *Industrie 4.0 and smart manufacturing-a review of research issues and application examples*, International Journal Automation Technology, Vol. 11, pp. 4–16. 2017.
[22] Botlikov, M., Botlikov, J.: *Local Extemes of Selected Industry 4.0, Indicators in the Europen Space-Structure for Autonomous Systems*, Journal of Risik Managment, Vol.13/13. 2020.
[23] Karabegović. I., Karabegović, E., Mahmić, M., Husak, E.: *The application of service robots for logistics in manufacturing processes*, Advances in Production Engineering & Management, Vol. 10, No. 4, pp. 185-194, 2015.
[24] Thoben, K.D.; Wiesner, S.; Wuest, T. *Industrie 4.0 and smart manufacturing-a review of research issues and application examples*, International Journal Automation Technology, Vol. 11, pp. 4–16, 2017.
[25] Karabegović, I.: *The Role of Industrial and Service Robots in the Fourth Industrial Revolution*, ACTE Technica Corviniensis-Bulletin of Engineering, University Politehnica Timisoara, Vol. 11, No. 2, pp. 11-16. 2018.
[26] Mićič, V.: *Industry 4.0 Development Conditions in the Republic of Serbia*, Journal facta Universitatis, Economcs and Organization, Vol. 17, No 2., pp. 97-112, 2020.
[27] Karabegović, I., Karabegović, E., Mahmić, M., Husak, E.: *Implementation of Industry 4.0 and Industrial Robots in Production Processes* In: Isak Karabegović (eds) New Technologies,Development and Application II 2019. Lecture Notes in Networks and Systems. Springer Nature Switzerland AG 76, pp.96-102. 2020.
[28] Karabegović, I., Husak, E., Karabegović, E., Mahmić, M.: *How the Core Technologies of Industry 4.0 are Changing the Automotive Industry in the World, With a Focus on China*, IX International Congress Motor Vehicles and Motors (MVM 2022) IOP Conf. Series: Materials Science and Engineering, 1271 012017, pp.1-14, 2022.
[29] Oesterreich, T. D., Teuteberg, F.: *Understanding the Implications of Digitisation and Automation in the Context of Industry 4.0: A Triangulation Approach and Elements of a Research Agenda for the Construction Industry*, Computers in Industry, 83, 121-139, 2016.

Authors:

Prof. dr Isak Karabegović, Academy of Sciences ana Arts of Bosnia and Herzegovina, Bistrik 7., 71000 Sarajevo, Bosnia and Herzegovina.
E-mail: isak1910@hotmail.com

Assis. Prof. dr Ermin Husak, Prof. dr Edina Karabegović, Prof. dr. Mehmed Mahmić, University of Bihać, Faculty of Technical Bihać, Ul. Irfana Ljubijankića bb, 77000 Bihać, Bosnia and Herzegovina.
E-mail: erminhusak@yahoo.com
edina-karabeg@hotmail.com
mmahmić@gmail.com

ETIKUM 2023 **INTERNATIONAL SCIENTIFIC CONFERENCE NOVI SAD, SERBIA, DECEMBER 7-9, 2023**

Kos, J., Drvar, N., Hercigonja, T.

PREDNOSTI ROBOTIZIRANIH OPTIČKIH 3D SKENERA I CT MJERITELJSKIH SUSTAVA ZA MJERENJE I ANALIZU DEFEKATA U PROIZVODNJI

Rezime: *Za proizvođače i dobavljače u proizvodnim industrijama ključni zahtjev je skratiti vrijeme od razvoja do razine gotovosti proizvoda spremnog za prodaju. Jedan od načina za postizanje skraćenja vremena proizvodnog ciklusa je poboljšanje kontrole kvalitete u proizvodnji. U tu svrhu sve više tvrtki koristi robotizirane mjerne ćelije i mjeriteljske CT uređaje za brza i sveobuhvatna mjerenja alata, poluproizvoda i komponenata u svim fazama proizvodnog procesa, koje osim što skraćuju vrijeme mjerenja efektivno umanjuju i ljudske greške. Rad donosi pregled uspješnih robotiziranih industrijskih primjena ZEISS ScanBox mjernih ćelija i ZEISS METROTOM računalnog tomografskog sustava.*
Ključne reči: *nerazorno ispitivanje, CT skeniranje, robotizirano 3D skeniranje, ATOS, METROTOM*

1. UPRAVLJANJE KVALITETOM KROZ SVE PROIZVODNE PROCESE

Svakim danom raste potreba za sve kvalitetnijim i oblikom kompleksnijim proizvodima. Poseban naglasak stavlja se na sigurnost u proizvodnji i funkcionalnost gotovog proizvoda.

Kako bi poduzeća u suvremenoj proizvodnji ispunjavale visoke zahtjeve svojih kupaca, sve više usmjeravaju svoje upravljanje kvalitetom na kontrolu svih proizvodnih procesa umjesto na krajnji proizvod, kako je to inače bilo uobičajeno.

Kontrola procesa započinje već pri izradi i isprobavanju alata, što rezultira dosljedno visokom kvalitetom i malim količinama odbačenih djelova.

Kako bi uspjeli zadovoljiti visoke zahtjeve, u inspekciju proizvodnih procesa uvode 3D optičke robotizirane sustave i mjeriteljske CT sustave.
Prednosti koje nude ovi sustavi:

- efektivno umanjenje utjecaja operatera na rezultate mjerenja
- statističko praćenje i analiza rezultata
- ciljana optimizacija u proizvodnim procesima s manje ponavljanja
- minimalizirana upotreba mjernih instrumenata i kontrolnih naprava
- stalna dostupnost digitaliziranih podataka

2. GLAVNA OBILJEŽJA 3D SKENIRANJA I CT SKENIRANJA

Zajedničko obilježje digitalizacije optičkim 3D skeniranjem i CT skeneiranjem je digitalizacija kompletne površine proizvoda i evaluacija rezultata u istom programskom paketu ZEISS Inspect.

Glavna razlika u ova dva načina digitalizacije je u tome što 3D skeneri snimaju samo vanjsku oku vidljivu površinu, dok CT sustavi digitaliziraju odjednom vanjske površine i unutrašnje oku nevidljive te strukturu materijala.

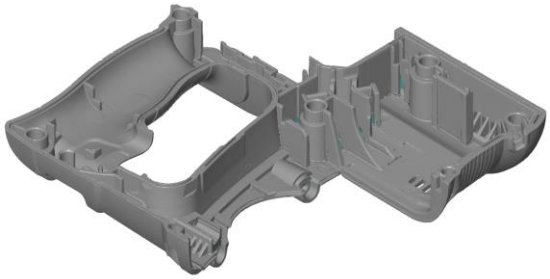

Sl. 1. Primjer rezultata 3D digitalizacije

Mjerenja i analize koje je moguće provesti na rezultatima kada je digitalizirana kompletna površina proizvoda:

- usporedba površina referentne i stvarne geometrije sa prikazom odstupanja u mapi boja,
- analizu sklopa više komponenti,
- analizu presjeka sklopa,
- dimenzijsku i GD&T analizu,
- analizu na presjecima proizvoda,
- analizu debljine stijenki,
- izradu mjernog izvještaja.

3. ROBOTIZIRANI 3D OPTIČKI MJERNI SUSTAVI

Momentalno na tržištu najinovativniji 3D optički mjerni sustav za robotizirana trokoordinatna mjerenja je ZEISS ScanBox - "*plug-and-play*" mjerna ćelija za neprestanu 3D kontrolu kvalitete.

ZEISS ScanBox povezuje optimizirane industrijske komponente, mobilnost i maksimalnu sigurnost u 3D standardizirani mjerni uređaj.

Ovakav koncept podržava zahtjeve suvremene proizvodnje i premještanje mjernih sustava iz laboratorija u proizvodne pogone.

Sl. 2. ZEISS ScanBox 5120

Glavne prednosti koje navode korisnici ovih sustava:

- uvođenjem automatizirane mjerne ćelije ZEISS ScanBox u proizvodnju, prije svega dobiveno je na vremenu izvođenja i kvaliteti obavljenih mjerenja
- jedan programski paket za upravljanje i evaluaciju rezultata ZEISS ScanBox sustavom omogućuje da se u vritualnoj mjernoj ćeliji kompletan mjerni protokol i simulacija mjerenja izvrši *offline* prije nego li je stvarni proizvod gotov
- *Smart Teach* funkcija pruža jednostavno programiranje robota bez potrebe za unošenjem koda, već se jednim klikom miša na temelju mjernog plana generiraju pozicije potrebne za digitalizaciju i mjerenje
- značajno smanjenje vremena mjerenja u odnosu na konvencionalne taktilne metode, čak do 60% brže
- jednostavno KIOSK korisničko sučelje za radnike u proizvodnji koji s lakoćom sami mjere u svim smjenama rada

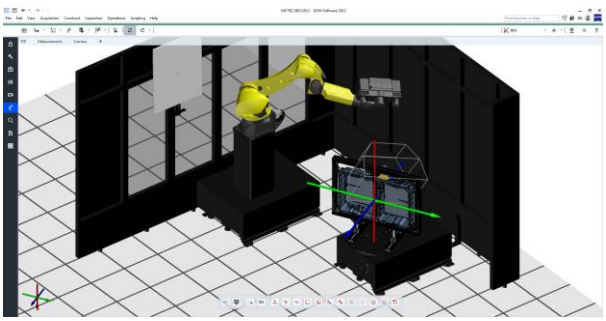

Sl. 3. Virtualna mjerna soba u programskom paketu ZEISS Inspect

Sl. 4. Primjer ScanBox ćelije instalirane u proizvodnom okruženju

Sl. 5. KIOSK sučelje za upravljanje u proizvodnji što omogućuje da svaki radnik bude mjeritelj

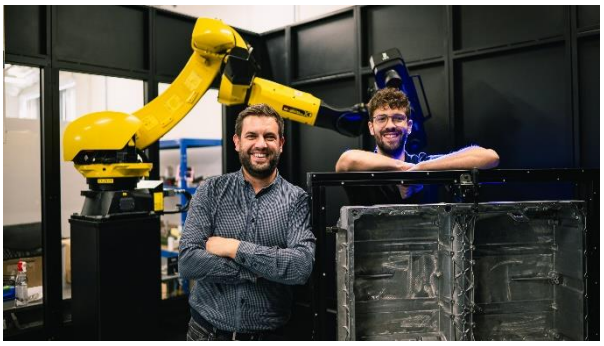

Sl. 6. Josip Kos i Luka Lukačić, inženjeri u poduzeću Topomatika d.o.o. zaduženi za ZEISS ScanBox sustave

4. MJERITELJSKI CT SUSTAVI

Posljednjih godina, u industrijskim aplikacijama sve više se za mjerenje i analizu materijala upotrebljavaju sustavi koji elektromagnetskim zračenjem prozračuju proizvod te na taj način pružaju mogućnost digitalizacije i pogleda u unutrašnjost zadanog proizvoda.

U odnosu na druge mjerne tehnologije, ovim sustavima moguće je analizirati i mjeriti oku nevidljivu unutrašnjost proizvoda, komponente u sklopu ili oku nevidljive vanjske površine proizvoda.

Kad govorimo o sustavima elektromagnestkog zračenja važno je odvojiti grupu uređaja koji se

koriste samo kako bi provjerili unutrašnjost proizvoda bez mogućnosti preciznih mjerenja i na sustave kojima možemo provjeriti unutrašnjost i mjeriti detekrtirane defekte i skrivene značajke proizvoda. Uređaji koji služe za mjerenje nazivaju se CT mjerni sustav te ćemo u nastavku dati primjere njihove upotrebe. Na slici pogledajte primjer CT uređaja iz ZEISS METROTOM familije – ZEISS METROTOM 6 scout.

Sl. 7. ZEISS METROTOM 6 scout

Sl. 8. Luka Kurtalj, aplikacijski inženjer u Topomatika d.o.o. laboratoriju

Glavna prednost CT skeniranja nad konvencionalnim metodama mjerenja je mogućnost nerazorne analize unutrašnjosti proizvoda.

Često se kod proizvodnog postupka lijevanja plastike ili metala u unutrašnjosti proizvoda pojave volumenski defekti koji negativno utječu na mehanička i vizualna svojstva proizvoda. Zbog toga je potrebno:

- provjeriti ukupni volumen defekata,
- njihovu raspodjelu u proizvodu,
- veličinu ili udaljenost do vanjske površine.

4.1 Ukupni volumen i raspodjela defekata

Ukupni volumen defekata jedna je od najbitnijih stavki volumenske analize, jer pokazuje koliko je proizvod ustvari nehomogen.

Ukoliko je ukupni volumen defekata van tolerancija, sva mehanička ispitivanja koja su vršena nad uzorcima materijala više ne vrijede, te se svojstva proizvoda ne mogu garantirati.

Primjerice, CT uređajem ZEISS Metrotom 6 Scout, mogu se detektirati defekti do 3 µm pri maksimalnoj rezoluciji, što garantira vrlo preciznu analizu ukupnog volumena defekata.

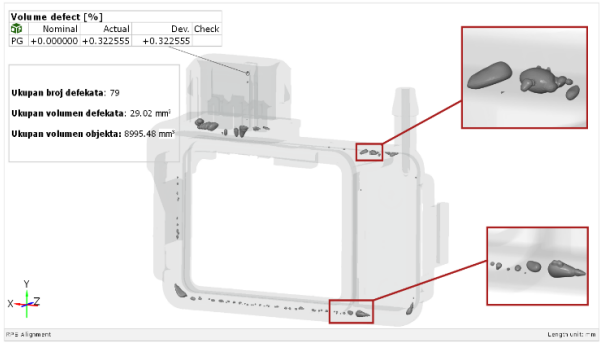

Sl. 9. Ukupan volumen i broj defekata

4.2 Veličine pojedinog defekta

Često nije dovoljno znati samo ukupni volumen defekata, već postoje i ograničenja dimenzija svakog pojedinog defekta.

Pomoću ZEISS Inspect programskog paketa na defektima se može izmjeriti volumen, maksimalna dijagonala, promjer, površina, te dimenzije u smjeru x, y i z osi.

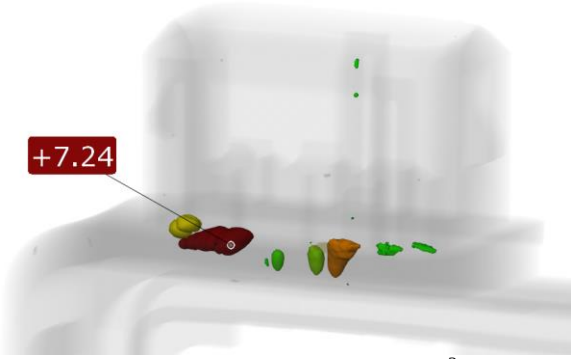

Sl. 10. Volumen defekta u mm^3

4.3 Udaljenost defekata do vanjske površine

Kada se radi o proizvodu koji je nosivi element u sklopu, tada je bitno da volumenski defekti nisu preblizu površine, kako ne bi došlo do pucanja stijenke i narušavanja integriteta sklopa. Pogledajte iduću sliku.

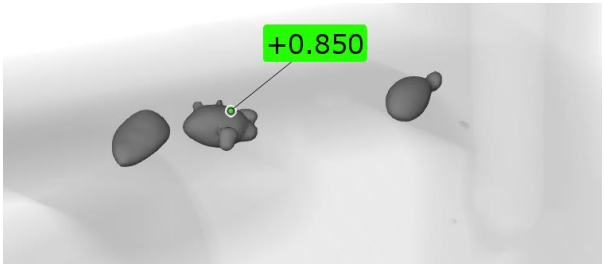

Sl. 11. Udaljenost defekta do najbliže površine u mm

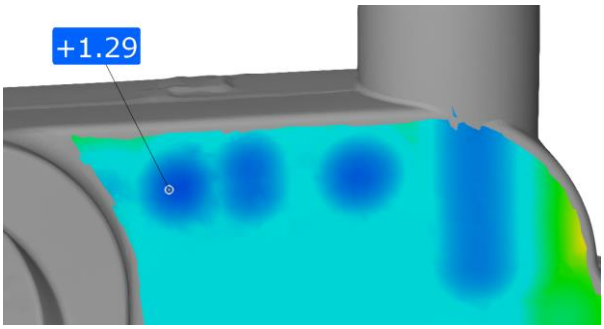

Sl. 12. Utjecaj defekata na debljinu stijenke plastičnog priozvoda (defekti umanjuju debljinu stijenke), vrijednost u mm

4.4 GD&T analiza

S obzirom na činjenicu da govorimo o mjeriteljskom CT uređaju, velika prednost ovakvog načina digitalizaije pruža mogućnost mjerenja skrivenih površina i provođenje GD&T analize i na oku nevidljivim površinama. Pogledajte iduću sliku.

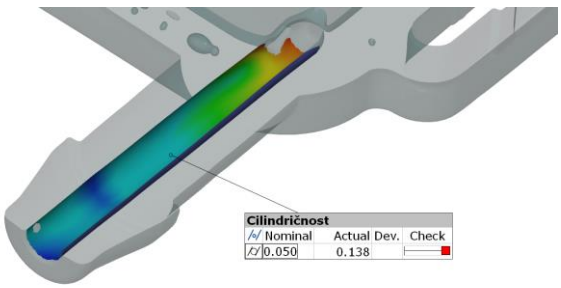

Sl. 13. Mjerenje cilindričnosti optički nedostupne površine dobivene CT skeniranjem

4.5 Ostale analize

Rezultati CT digitalizacije pružaju mogućnost analize na bilo kojem 2D presjeku digitalnog modela stvarnog proizvoda. Na idućoj slici crna boja prikazuje zrak, sivkasta osnovni materijal proizvoda, a bijela karbonska vlakna kojima je ojačan osnovni materijal. Crne točke unutar proizvoda su mjehurići (lunkeri) zarobljenog zraka.

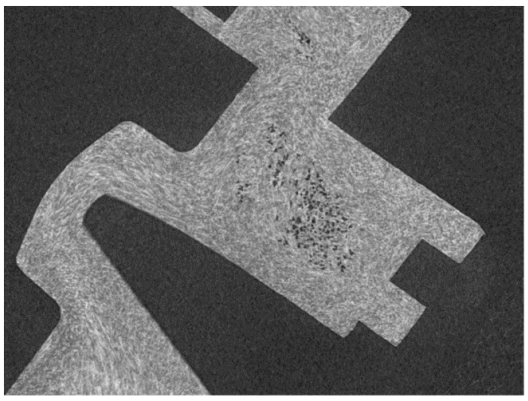

Sl. 14. Pogled u unutrašnjost proizvoda na jednom presjeku rezultata CT skeniranja

5. REFERENCE

[1] Kurtalj, L., Kos, J. Drvar, N. Hercigonja, T.: CT *skeniranje za mjerenje i analizu defekata plastičnih proizvoda*, INDUSTRIJSKI FORUM, Portorož, 2022.
[2] Kos, J. Drvar, N. Hercigonja, T.: *Praktični primjeri automatiziranog 3d optičkog mjeriteljstva u suvremenoj industrijskoj proizvodnji*, INDUSTRIJSKI FORUM, Portorož, 2017.
[3] www.topomatika.hr
[4] www.gom.com

Autori: Josip Kos, Dr.sc. Nenad Drvar, Tomislav Hercigonja, Topomatika d.o.o., Industrijska ulica 3, 10431 Novaki, Hrvatska, Tel: +385 91 3496 010,
E-mail: j.kos@topomatika.hr
n.drvar@topomatika.hr
t.hercigonja@topomatika.hr

ETIKUM 2023 **INTERNATIONAL SCIENTIFIC CONFERENCE NOVI SAD, SERBIA, DECEMBER 7-9, 2023**

Kosarac, A., Sekulic, M., Savkovic, B., Moljevic, S., Sikuljak, L., Anic, J., Aleksic, A.

SMALL DATASET CHALLENGES: ASSESSING THE PERFORMANCE OF NEURAL NETWORKS AND RANDOM FORESTS IN TI6AL4V ALLOY MACHINING OPTIMIZATION

Abstract: *This paper examines machine learning on a small dataset, focusing on optimizing the machining of Ti6Al4V alloy. Using 27 results from a Ti6Al4V alloy cutting experiment, this research shows how neural networks and random forests perform with limited dataset. The goal is to understand how random seed selection influences the partitioning of the datasets for training, testing, and validation. Comparing neural networks and random forests, this research shows their performance in small dataset scenarios. The findings not only show differences between the algorithms but also emphasize the impact of seed choice on the reliability of the models. Data analysis was performed using the Seaborn, Scikit-learn, NumPy, and Pandas machine learning libraries and Keras framework for Python.*
Key words: *machine learning, neural networks, random forest*

1. INTRODUCTION

The machining of Ti6Al4V alloy is very important, especially in industries like aerospace and medicine. Improving cutting conditions remains a constant challenge, prompting the need for advancements in machining techniques. This study specifically explores the application of machine learning to achieve the minimal values of average surface roughness, with a particular focus on addressing challenges associated with limited datasets. This research has focused on optimizing the cutting parameters during Ti6Al4V alloy milling using two very popular machine learning algorithms, neural networks and random forests.

The central question is how these algorithms perform when confronted with a limited dataset having 27 samples and what role the choice of random seed plays in their behavior.

The paper is structured to introduce the experimental setup, followed by a detailed exploration of the methodology. Subsequently, the presentation and discussion of experiment results lead to conclusions that provide insights into the implications for materials processing and the broader field of small dataset machine learning.

2. LITERATURE REVIEW

Different machine learning algorithms becoming a widely used tool for predicting surface roughness (Ra), sometimes using small datasets [1,2]. In addressing this challenge, some researchers select neural networks, a popular machine learning algorithm, to optimize cutting parameters [3-5]. Their choice reflects a strategic approach to extracting meaningful insights from a limited dataset, recognizing the inherent difficulties posed by the scarcity of experimental samples. In various studies, researchers have utilized neural networks to predict Ra values, enabling them to comprehend complex patterns in data. Multiple researchers used neural networks experimenting with the number of hidden layers to predict surface roughness [6-9]. These studies entail thorough experimentation, adjusting the number of hidden layers, varying the neurons within those layers, and deploying diverse training algorithms. The goal is to find the neural network configuration that achieves optimal performance in predicting surface roughness, underscoring the adaptability of neural networks across varying experimental conditions. On the other hand, other researchers explore the efficacy of different machine learning algorithms, such as random forests. Their research shows that these algorithms sometimes exhibit superior performances in the optimization of cutting regimes, even with a constrained dataset of 27 samples. Dubey et al. [10] conducted an investigation into surface roughness during the machining of AISI 304 Steel. The experiment encompassed 27 samples. Utilizing the experimental data, the researcher developed three machine-learning models—Linear Regression (LR), Random Forest (RF), and Support Vector Machine (SVM)—aimed at predicting surface roughness based on input parameters. The study findings unveiled that the Random Forest (RF) model outperformed the other two models, demonstrating superior accuracy in predicting surface roughness. Agrawal et al. [11] conducted an experiment with AISI 4340 steel, systematically altering the depth of cut,

feed rate, cutting speed, and measuring surface roughness. A dataset of 39 samples was collected. The authors developed three regression models: Multiple Regression, Random Forest, and Quantile Regression. The study's outcomes indicated that the Random Forest regression model exhibited superior performance compared to the other models in predicting surface roughness.

This paper offers a comparison of two popular ML algorithms, neural network and Random Forest to handle small datasets and regression issues. The findings highlight that the widely adopted machine learning algorithm, Random Forest, demonstrates exceptional proficiency in addressing regression problems.

3. EXPERIMENTAL SETUP

The study investigates the influence of four variables on surface roughness in milling titanium alloy Ti-6Al-4V: cutting speed (v), feed rate (f), axial depth of cut (a), and various types of coolants/lubricants, each at three distinct levels. Table 1 shows the experimental factors and their levels.

Table 1. Experimental factors and levels

Factors	**Levels**		
	Low level	**Middle level**	**High level**
	-1	**0**	**1**
Cutting speed (mm/min)	30	60	90
Feed rate per tooth (mm/tooth)	0,05	0,12	0,20
Axial depth of cut	0,3	0,6	0,8
Cooling/lubricating technique	Emulsion	Dray cutting	Vortex tube

The experiment was designed using the Taguchi methodology, encompassing a total of 27 experimental runs. All experimental runs were conducted under consistent machining conditions and on the Emco Concept Mill 250 milling center. The spindle milling cutter HF 16E2R030A16-SBN10-C, equipped with two BNGX 10T308SR-MM: M8345 inserts designed for superalloy cutting, was used in the experiments. Surface roughness (Ra) was measured using the Mitutoyo SJ-210 measuring device. Following the machining process, each workpiece underwent three measurements at different positions. The workpiece, with dimensions of 35 × 25 × 20, was clamped using a versatile milling vise. The machining operation covered both sides of the sample parts and utilized the climb milling method, selected to enhance the quality of the machined surface. Table 2 shows the orthogonal matrix consists of 27 rows corresponding to the number of conducted experimental runs.

Table 2. Experimental plan—L27 orthogonal array

No. of trials	Cutting speed (m/min)	Feed per tooth (mm/tooth)	Axial depth of cut (mm)	Cooling / lubricating technique	Ra1 (μm)	Ra2 (μm)	Ra3 (μm)	Ra (aver.)
1	30	0,05	0,3	Emulsion	0.287	0.344	0.307	0.312
2	30	0,05	0,6	Dray machining	0.311	0.285	0.229	0.275
3	30	0,05	0,8	Vortex tube	0.304	0.292	0.245	0.28
4	30	0,12	0,3	Dray machining	0.561	0.568	0.64	0.589
5	30	0,12	0,6	Vortex tube	0.344	0.377	0.332	0.351
6	30	0,12	0,8	Emulsion	0.597	0.635	0.527	0.586
7	30	0,2	0,3	Vortex tube	0.441	0.485	0.401	0.442
8	30	0,2	0,6	Emulsion	1.463	1.335	0.993	1.263
9	30	0,2	0,8	Dray machining	1.405	1.505	1.432	1.447
10	60	0,05	0,3	Emulsion	0.236	0.244	0.238	0.239
11	60	0,05	0,6	Dray machining	0.259	0.312	0.207	0.259
12	60	0,05	0,8	Vortex tube	0.232	0.267	0.288	0.262
13	60	0,12	0,3	Dray machining	0.588	0.414	0.461	0.487
14	60	0,12	0,6	Vortex tube	0.365	0.322	0.331	0.339
15	60	0,12	0,8	Emulsion	0.661	0.544	0.559	0.588
16	60	0,2	0,3	Vortex tube	0.421	0.419	0.411	0.417
17	60	0,2	0,6	Emulsion	1.306	1.006	1.121	1.144

18	60	0,2	0,8	Dray machining	1.03	1.136	1.091	1.085
19	90	0,05	0,3	Emulsion	0.31	0.228	0.285	0.274
20	90	0,05	0,6	Dray machining	0.312	0.294	0.232	0.279
21	90	0,05	0,8	Vortex tube	0.377	0.249	0.308	0.311
22	90	0,12	0,3	Emulsion	0.582	0.686	0.641	0.636
23	90	0,12	0,6	Dray machining	0.436	0.435	0.442	0.437
24	90	0,12	0,8	Vortex tube	0.979	1.001	0.891	0.957
25	90	0,2	0,3	Vortex tube	0.593	0.508	0.618	0.573
26	90	0,2	0,6	Emulsion	0.976	0.979	1.139	1.031
27	90	0,2	0,8	Dray machining	1.304	1.369	1.478	1.383

4. A MACHINE LEARNING APPROACH WITH NEURAL NETWORKS AND RANDOM FOREST ALGORITHMS FOR SURFACE ROUGHNESS PREDICTION

In machine learning, dealing with small datasets can be challenging. Most models need lots of data to learn well, but only a few can handle small amounts. The right dataset size for training depends on many things, like how complex the problem is and what the model needs. There's no fixed "perfect" dataset size, but there are some general rules for different machine learning methods. This study compares two algorithms, neural network, and Random Forest, to predict surface roughness in milling using regression techniques. Each of these algorithms has its pros and cons, making them good for different kinds of data and problems. When dealing with regression problems and small datasets, random forests can be advantageous due to their ensemble nature, which helps mitigate overfitting. Neural networks, on the other hand, might excel in capturing intricate patterns if the dataset is sufficiently large. The choice between the two depends on the specific characteristics of the data, and the problem complexity.

4.1 Neural Networks for surface roughness prediction

A neural network is a powerful machine-learning algorithm inspired by the structure and functioning of the human brain. It consists of interconnected nodes, or neurons, organized in layers. Neural networks are capable of learning complex patterns and relationships within data by adjusting the weights of connections during a training process. The input layer receives data, and information is progressively transformed through hidden layers, ultimately leading to an output layer that produces predictions or classifications. Neural networks excel at capturing intricate and nonlinear relationships in data, making them well-suited for tasks such as image recognition, natural language processing, and complex pattern recognition. The training process involves adjusting the network's parameters using optimization techniques, like gradient descent, to minimize the difference between predicted and actual outcomes. In Figure 1, a visual representation of the neural network configuration is provided, shedding light on the specific architectural topology it employs. The diagram showcases the interconnected layers of neurons, including the input layer responsible for receiving data, hidden layers where complex transformations occur, and the output layer producing the final predictions or classifications.

4.2 Random forest for surface roughness prediction

Random Forest is an ensemble machine learning algorithm that combines the predictions of multiple decision trees to enhance overall predictive accuracy and generalization. Each decision tree in the forest is built on a random subset of the dataset, and predictions are made by aggregating the results from individual trees. This method helps reduce over fitting and improves the model's robustness. Random Forest is widely used for both classification and regression tasks, known for its ability to handle complex relationships in data and provide insights into feature importance. The workflow of neural network algorithms involves a systematic process of learning and adaptation. Initially, the network is initialized with random weights and biases. As data is fed into the network, it undergoes a forward pass, traversing through the layers of interconnected neurons. During this phase, each neuron performs a weighted sum of its inputs, followed by the application of an activation function to introduce non-linearity. Subsequently, the algorithm compares the predicted output with the actual target values, calculating the error. The backpropagation phase follows, where the algorithm adjusts the weights and biases iteratively using optimization techniques such as gradient descent. This process is aimed at minimizing the error and optimizing the network's parameters. The training cycle repeats until the algorithm achieves satisfactory performance on

the training data. Once trained, the neural network can make predictions on new, unseen data by performing a forward pass through the learned weights and biases. This iterative learning process allows neural networks to adapt and uncover complex relationships within the data, making them versatile and powerful tools for various machine-learning tasks. Figure 2 shows a visual representation of the random forest algorithm. The diagram illustrates the collaborative decision-making process of multiple decision trees, each constructed on a random subset of the dataset.

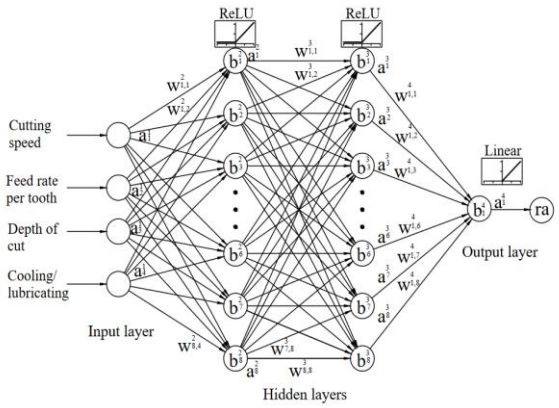

Fig. 1. Neural network topology [12]

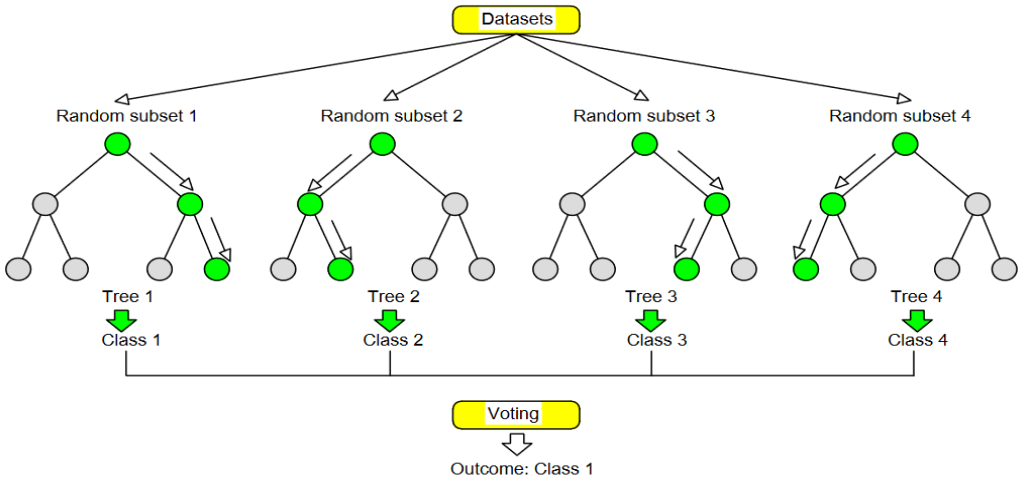

Fig. 2. Workflow of random forest algorithms

5. A COMPARATIVE ANALYSIS OF NEURAL NETWORK AND RANDOM FOREST ALGORITHMS

The dataset used for training and testing the neural network model comprises 27 samples generated from an experiment conducted using a Taguchi-designed experimental plan, as detailed in Table 2. During the training phase, 80% of these samples were employed, amounting to 21 instances for training and six samples designated for testing and validation. Notably, variations in training and testing sets arise from different random states, introducing a range of potential neural network performances. To mitigate this variability, a systematic approach involves testing multiple seeds through an iterative loop to identify the optimal network performance. Evaluation metrics, such as Mean Squared Error (MSE) and R-squared, contribute to this determination.

Figure 3 illustrates a scatter plot depicting actual versus predicted values generated through a random forest algorithm applied to the testing dataset. Each point on the graph corresponds to a specific data instance, with its placement indicating the proximity of the predicted value to the actual value. The optimal outcome would be a diagonal line (y = x), signifying perfect predictions where all points align with this line. In the context of Figure 3, the coefficient of determination (R-squared) is calculated to be 0.9703. This high R-squared value suggests that approximately 97.03% of the variability in the actual values can be explained by the predicted values from the random forest algorithm. The close alignment of the points to the ideal diagonal line signifies the model's effectiveness in capturing and predicting patterns within the dataset. The neural network architecture employed in this study follows a configuration of 4 input nodes, 12 nodes in the hidden layer, and a single output node, denoted as the 4-12-1 architecture. This specific architecture was identified as optimal in a prior study [12] that addressed a closely related problem. The training process utilizes the Adam optimization algorithm, a widely used optimization technique in neural network training. Additionally, a learning rate of 0.001 is applied as part of the training rule. These parameters were selected based on their successful implementation in the referenced study and contribute to the overall methodology for training the neural network in our investigation.

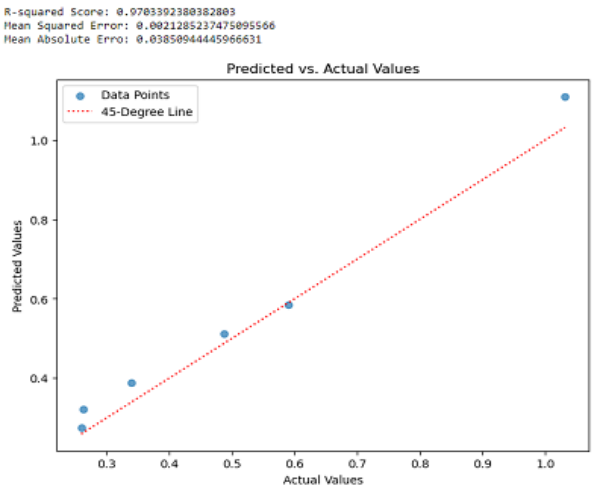

Fig. 3. Actual vs. predicted values for random forest algorithms

Figure 4 illustrates the trend of the validation loss over the training the deep neural network. The Mean Squared Error (MSE) computed for this model is 0.0077, representing the average deviation of predicted values from the actual values in the validation dataset. The validation loss curve, as depicted in Figure 4, extends from the initial stages of training up to 150 epochs. Although the total number of epochs set for training was 2000, the training process was prematurely terminated by an early stop function when the validation loss ceased to show significant improvement.

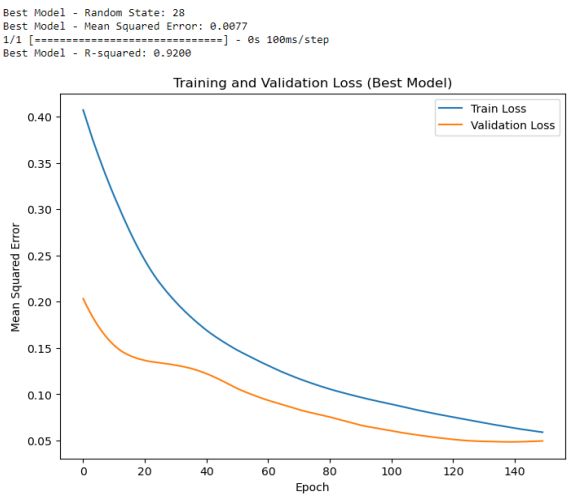

Fig. 4. Training and validation lost for neural network 4-12-1

In Figure 5, the performance of the deep neural network model on a previously unseen dataset is presented through a plot illustrating actual versus predicted values. An R-squared value of 0.92 indicates that the model's predictions elucidate approximately 92% of the variability in the actual values. This finding underscores the model's robust predictive capacity and its ability to generalize well to new and unseen data.

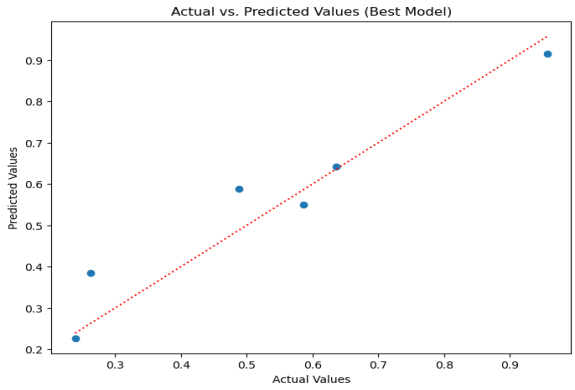

Fig. 5. Actual vs. predicted values for neural network 4-12-1

6. CONCLUSION

The dataset, comprising 27 sets, was utilized to train various neural networks, and a comprehensive comparative analysis was conducted to evaluate their performance.

The selection of the best models was determined through an iterative loop, wherein various random seeds were tested. This approach ensured a robust evaluation, capturing the variability in model performance and contributing to the overall reliability of the findings.

The Best Random Forest algorithm demonstrated outstanding performance, exhibiting a remarkably low Mean Squared Error (MSE) of 0.0021 and a notably high R-squared value of 0.97 when tested on the dataset. These results emphasize the robustness of Random Forests in effectively addressing challenges posed by small datasets.

In contrast, the Neural Network exhibited slightly lower performance, achieving an MSE of 0.0077 and an R-squared value of 0.92.

Considering these outcomes, the Random Forest algorithm emerges as a preferable choice, displaying more consistent and reliable performance. However, it is crucial to acknowledge that the selection of the optimal algorithm hinges on the specific problem context.

This underscores the importance of meticulous model selection and fine-tuning based on the inherent characteristics of the problem. In essence, this investigation highlights the versatility of a diverse range of regression techniques, providing valuable insights for decision-making in model selection and evaluation.

It's noteworthy that speed is a critical factor in real-world applications, and Random Forest, with its inherent parallelization capabilities and efficient computation, emerged as significantly faster compared to the Neural Network, further contributing to its practical appeal in scenarios

where computational efficiency is paramount.

In conclusion, for small datasets, the optimal solution emerges as Random Forest, showcasing superior performance in terms of accuracy, robustness, and computational efficiency when compared to alternative models, making it the preferred choice for such scenarios.

7. REFERENCES

[1] Beatrice, B.A.; Kirubakaran, E.; Thangaiah, P.R.J.; Wins, K.L.D.: *Surface roughness prediction using artificial neural network in hard turning of AISI H13 steel with minimal cutting fluid application.* Procedia Eng. 2014, 97, 205–211.

[2] Pal, S.K.; Chakraborty, D. : *Surface roughness prediction in turning using artificial neural network*., Neural Comput. Appl. 2005, 14, 319–324.

[3] Hossain, M.I.; Amin, A.N.; Patwari, A.U. *Development of an artificial neural network algorithm for predicting the surface roughness in end milling of Inconel 718 alloy*. In Proceedings of the 2008 International Conference on Computer and Communication, Engineering, Kuala Lumpur, Malaysia, 13–15 May 2008; pp. 1321–1324.

[4] Benardos, P.; Vosniakos, G.C.: *Prediction of surface roughness in CNC face milling using neural networks and Taguchi's design of experiments*. Robot, Comput.-Integr. Manuf. 2002, 18, 343–354.

[5] Eser, A.; Askar Ayyıldız, E.; Ayyıldız, M.; Kara, F. *Artificial intelligence-based surface roughness estimation modelling for milling of AA6061 alloy*. Adv. Mater. Sci. Eng. 2021, 2021, 5576600.

[6] Rajesh,A. S., Prabhuswamy, M. S., Rudra Naik, M.: *Machine Learning Approach: Prediction of Surface Roughness in Dry Turning Inconel 625.* Advances in Materials Science and Engineering, Special Issue Advanced Functional Graded Materials: Processing and Applications, 2022

[7] Zain, A.M.; Haron, H.; Sharif, S.: *Prediction of surface roughness in the end milling machining using Artificial Neural Networ*k. Expert Syst. Appl. 2010, 37, 1755–1768.

[8] Zhong, Z.; Khoo, L.; Han, S. *Prediction of surface roughness of turned surfaces using neural networks.* Int. J. Adv. Manuf. Technol. 2006, 28, 688–693.

[9] Vardhan, M.V.; Sankaraiah, G.; Yohan, M. *Prediction of surface roughness & material removal rate for machining of P20 steel in CNC milling using artificial neural networks*. Mater. Today Proc. 2018, 5, 18376–18382.

[10] Dubey, V., Sharma, A.,K., Pimenov,D.Y.: *Prediction of Surface Roughness Using Machine Learning Approach in MQL Turning of AISI 304 Steel by Varying Nanoparticle Size in the Cutting Fluid.* MDPI, Lubricants, 2022.

[11] Agrawal, A., Goel, S., Bin Rashid, W., Price, M.: *Prediction of surface roughness during hard turning of AISI 4340 steel (69 HRC).* Applied Soft Computing, Volume 30, May 2015, Pages 279-286

[12] Kosarac, A., Tabakovic,S., Mladjenovic,C., Zeljkovic,M., Orasanin,G.: *Next-gen Manufacturing: Machine Learning for Surface Roughness Prediction in Ti-6Al-4V Biocompatible alloy Machining.* Journal of Manufacturing and Materials Processing, MDPI, 2023

FUNDING

This paper presents a portion of the research results from the project „Advanced Processing Technologies of Modern Engineering Materials", No. 142-451-334/2023-01/2, which is being carried out as part of the "Financing of Joint Research Projects of Scientific Research Organizations" initiative, jointly funded by the Autonomous Province of Vojvodina and scientific research organizations from the Republic of Srpska in 2023.

Authors: **Assoc. prof. dr Aleksandar Kosarac[1], Prof. dr Milenko Sekulic[2], Assoc. prof. dr Borislav Savkovic[2], Prof. dr Slavisa Moljevic[1], Asisstant MSc Lana Sikuljak[1], Asisstant MSc Jelica Anic[1], Asisstant MSc Andjelko Aleksic[2],** [1]University of East Sarajevo, Faculty of Mechanical Engineering, 71126 Lukavica, East Sarajevo, Republic of Srpska, Bosnia and Herzegovina [2]University of Novi Sad, Faculty of Technical Sciences, Trg Dositeja Obradovica 6, 21000 Novi Sad, Serbia, Phone.: +381 21 485 2329, Fax: +381 21 454-495, [2]Comenius University in Bratislava, Faculty of Management, 820 05 Bratislava, Slovakia, [3]International Technology and Management Academy – MTMA, Novi Sad, Serbia

E-mail: aleksandar.kosarac@ues.rs.ba
milenkos@uns.ac.rs
savkovic@uns.ac.rs
slavisa.moljevic@ues.rs.ba
lana.sikuljak@ues.rs.ba
jelica.anic@ues.rs.ba
andjelkoa94@uns.ac.rs

ETIKUM 2023 **INTERNATIONAL SCIENTIFIC CONFERENCE NOVI SAD, SERBIA, DECEMBER 7-9, 2023**

Kosec, B., Bizjak, M., Gojić, M., Štrbac, B., Ivanić, I., Nagode, A., Karpe, B.

THERMAL PROPERTIES OF RAPIDLY SOLIDIFIED COPPER BASED Cu-Al-Ni-Mn SHAPE MEMORY ALLOY

Abstract: *Shape memory alloys (SMA) are relatively a new class of advanced functional materials which are able to memorize and recover its original shape after being significantly deformed from heating over the phase transformation temperature. The mechanical properties and microstructure of copper base shape memory alloys are relatively well known, while data on thermal properties (thermal conductivity, specific heat, and thermal diffusivity) are not available. In the frame of our investigation work thermal properties of rapidly solidified copper-based Cu-Al-Ni-Mn shape memory alloy were determined. As the first part of the work, a study and evaluation of the operation of the device for determining the thermal properties of Hot Disk TPS 2200, today one of the most modern and high-quality instruments for determining thermal properties, has been carried out. In the second part of the work, the measurements and analysis of thermal properties of rapidly solidified Cu-Al-Ni-Mn shape memory alloy in accordance with the standard ISO 22007-2 at ambient and elevated temperatures has been done.*
Key words: *Thermal properties; Cu base shape memory alloy; Rapid solidification; Measurement*

1. INTRODUCTION

Shape memory alloys (SMA) are relatively new class of advanced functional materials which are able to memorize and recover its original shape after being significantly deformed from heating over the phase transformation temperature [1].

The main advantage of copper based SMAs are their low price compared to other SMAs. Properties of Cu-Al-Ni alloys are superior to those of Cu-Zn-Al alloys due to their wide range of useful transformation temperature and small hysteresis. Although Cu-Al-Ni alloys have a better thermal and electrical stability and a higher operating temperatures, their practical applications are sometimes restricted by very small shape changes due to their poor workability and susceptibility to brittle intergranular cracks [2]. Their very high elastic anisotropy and large grain size cause brittle and poor mechanical properties owing to the high degree of order in the parent phase.

Typically, composition of Cu-Al-Ni SMA is in the range Cu-(13-15 m. %) Al-(3-4.5 m. %) Ni [3]. Adding some alloying elements such as Mn, Fe, Ti, Zr, B etc. to the alloys can significantly improve their ductility and other properties which modify their operating temperatures [4,5].

In the frame of our investigation we have investigated thermal properties of rapidly solidified Cu-Al-Ni-Mn shape memory alloy [6] produced by melt-spinning procedure (Figure 1). The chemical composition of the testing Cu-Al-Ni-Mn alloy is presented in Table 1.

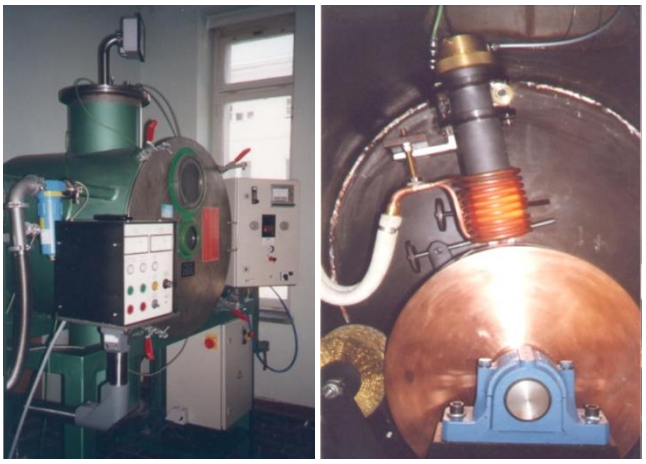

Fig. 1. Melt spinner at Faculty of Natural Sciences and Engineering University of Ljubljana.

Table 1. Chemical composition of the testing Cu-Al-Ni-Mn alloy

% Al	% Ni	%Mn	% Cu
12.7	4.2	2.4	rest

Single Roll Melt Spinning is the most commonly used process for the production of rapidly solidified thin metal foils or ribbons with amorphous, microcrystalline or even combined microstructure.

In this type of a process, a molten material is introduced onto a surface of the spinning wheel, where melt puddle is formed, and as final results a metal ribbons are formed (Figure 2).

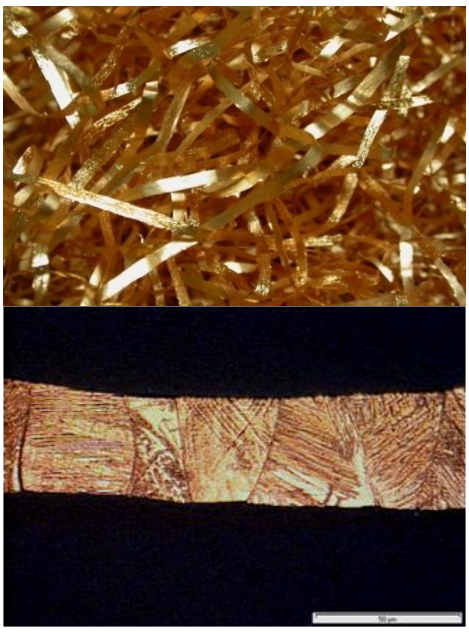

Fig. 2. Rapidly solidified Cu-Al-Ni-Mn shape memory alloy thin ribbons, microstructure.

The final products are in the form of thin and narrow ribbons, which could be in further production steps subjected to milling and molded into useful shapes by different methods of powder metallurgy. In our case we were made disks from ground and molded alloys (Figure 3). From them testing samples to perform measurements of thermal properties of dimensions Ø40 x 13 mm have been done.

Fig 3. Disks from ground and molded rapidly solidified Cu-Al-Ni-Mn shape memory alloy.

2. THERMAL PROPERTIES MEASUREMENT

In our research, we used one of the most advanced instruments for determining the thermal properties, Hot Disk TPS 2200, a product of Hot Disk AB company, Gothenburg, Sweden (Figure 4) [7].

Fig. 4. Instrument Hot Disk TPS 2200.

The instrument can be used for determining thermal properties of various materials including pure metals, alloys, minerals, ceramics, plastics, glasses, powders and viscous liquids with thermal conductivity in the range from 0.01 to 500 W/mK, thermal diffusivity from 0.01 to 300 mm^2/s and heat capacity up to 5 MJ/m^3K. Measurements can be perform in a temperature interval between 50 °C up to 750 °C [8].

Hot disk measuring method is a transient plane source technique (TPS). Based on the theory of TPS, instrument utilizes a sensor element in the shape of 10 μm thick double spiral, made by etching from pure nickel foil. Spiral is mechanically strengthen and electrically insulated on both sides by thin polyimide foil (Kapton ®Du Pont) for measurements up to 300 °C or mica foil for measurements up to 750 °C. Sensor acts both as a precise heat source and resistance thermometer for recording the time dependent temperature increase.

During measurement of solids, encapsulated Ni-sensor is sandwiched between two halves of the sample and constant precise pre-set heating power is released by the sensor, followed by 200 resistance recording in a pre-set measuring time, from which the relation between time and temperature change is established. Based on time dependent temperature increase of the sensor, thermal properties of the tested material are calculated.

2.1 Experimental Work

Measurements and analysis of thermal properties of testing samples from the testing rapidly solidified copper base shape memory alloy were performed in accordance with ISO 22007-2 standard [9] in the Laboratory for Thermotechnical Measurements, Faculty of Natural Sciences and Engineering, University of Ljubljana. In Figure 6 are presented complete results of thermal properties measurements.

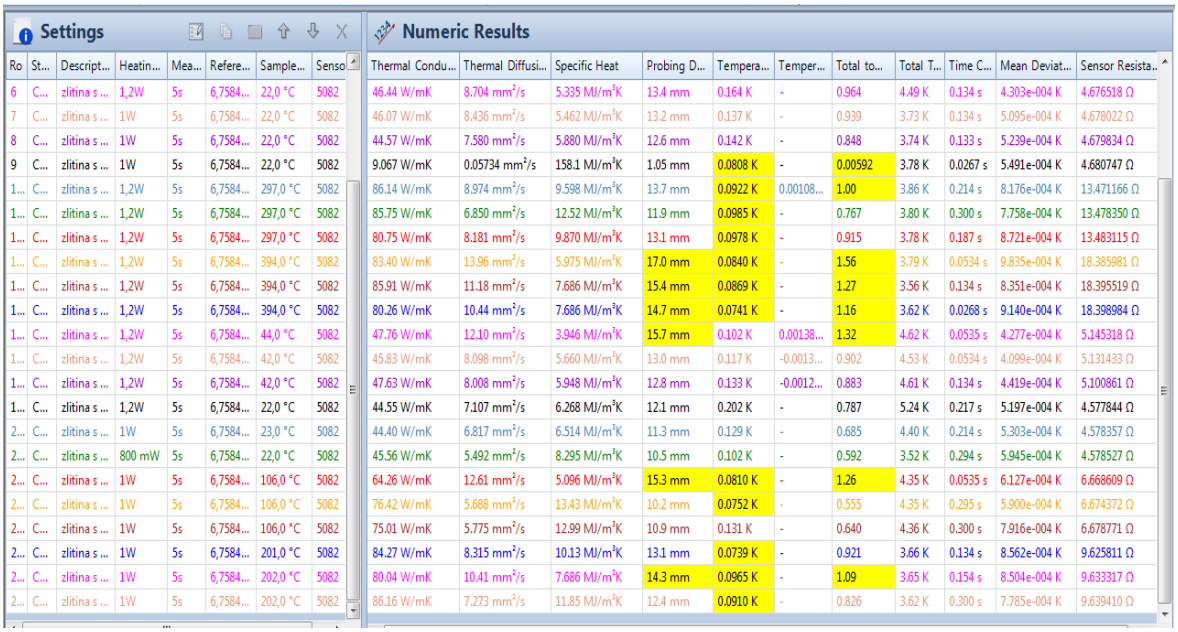

Settings

Ro	St...	Descript...	Heatin...	Mea...	Refere...	Sample...	Senso
6	C...	zlitina s ...	1,2W	5s	6,7584...	22,0 °C	5082
7	C...	zlitina s ...	1W	5s	6,7584...	22,0 °C	5082
8	C...	zlitina s ...	1W	5s	6,7584...	22,0 °C	5082
9	C...	zlitina s ...	1W	5s	6,7584...	22,0 °C	5082
1...	C...	zlitina s ...	1,2W	5s	6,7584...	297,0 °C	5082
1...	C...	zlitina s ...	1,2W	5s	6,7584...	297,0 °C	5082
1...	C...	zlitina s ...	1,2W	5s	6,7584...	297,0 °C	5082
1...	C...	zlitina s ...	1,2W	5s	6,7584...	394,0 °C	5082
1...	C...	zlitina s ...	1,2W	5s	6,7584...	394,0 °C	5082
1...	C...	zlitina s ...	1,2W	5s	6,7584...	394,0 °C	5082
1...	C...	zlitina s ...	1,2W	5s	6,7584...	44,0 °C	5082
1...	C...	zlitina s ...	1,2W	5s	6,7584...	42,0 °C	5082
1...	C...	zlitina s ...	1,2W	5s	6,7584...	42,0 °C	5082
1...	C...	zlitina s ...	1,2W	5s	6,7584...	22,0 °C	5082
2...	C...	zlitina s ...	1W	5s	6,7584...	23,0 °C	5082
2...	C...	zlitina s ...	800 mW	5s	6,7584...	22,0 °C	5082
2...	C...	zlitina s ...	1W	5s	6,7584...	106,0 °C	5082
2...	C...	zlitina s ...	1W	5s	6,7584...	106,0 °C	5082
2...	C...	zlitina s ...	1W	5s	6,7584...	106,0 °C	5082
2...	C...	zlitina s ...	1W	5s	6,7584...	201,0 °C	5082
2...	C...	zlitina s ...	1W	5s	6,7584...	202,0 °C	5082
2...	C...	zlitina s ...	1W	5s	6,7584...	202,0 °C	5082

Numeric Results

Thermal Condu...	Thermal Diffusi...	Specific Heat	Probing D...	Tempera...	Temper...	Total to...	Total T...	Time C...	Mean Deviat...	Sensor Resista...
46.44 W/mK	8.704 mm²/s	5.335 MJ/m³K	13.4 mm	0.164 K	-	0.964	4.49 K	0.134 s	4.303e-004 K	4.676518 Ω
46.07 W/mK	8.436 mm²/s	5.462 MJ/m³K	13.2 mm	0.137 K	-	0.939	3.73 K	0.134 s	5.095e-004 K	4.678022 Ω
44.57 W/mK	7.580 mm²/s	5.880 MJ/m³K	12.6 mm	0.142 K	-	0.848	3.74 K	0.133 s	5.239e-004 K	4.679834 Ω
9.067 W/mK	0.05734 mm²/s	158.1 MJ/m³K	1.05 mm	0.0808 K	-	0.00592	3.78 K	0.0267 s	5.491e-004 K	4.680747 Ω
86.14 W/mK	8.974 mm²/s	9.598 MJ/m³K	13.7 mm	0.0922 K	0.00108...	1.00	3.86 K	0.214 s	8.176e-004 K	13.471166 Ω
85.75 W/mK	6.850 mm²/s	12.52 MJ/m³K	11.9 mm	0.0985 K	-	0.767	3.80 K	0.300 s	7.758e-004 K	13.478350 Ω
80.75 W/mK	8.181 mm²/s	9.870 MJ/m³K	13.1 mm	0.0978 K	-	0.915	3.78 K	0.187 s	8.721e-004 K	13.483115 Ω
83.40 W/mK	13.96 mm²/s	5.975 MJ/m³K	17.0 mm	0.0840 K	-	1.56	3.79 K	0.0534 s	9.835e-004 K	18.385981 Ω
85.91 W/mK	11.18 mm²/s	7.686 MJ/m³K	15.4 mm	0.0869 K	-	1.27	3.56 K	0.134 s	8.351e-004 K	18.395519 Ω
80.26 W/mK	10.44 mm²/s	7.686 MJ/m³K	14.7 mm	0.0741 K	-	1.16	3.62 K	0.0268 s	9.140e-004 K	18.398984 Ω
47.76 W/mK	12.10 mm²/s	3.946 MJ/m³K	15.7 mm	0.102 K	0.00138...	1.32	4.62 K	0.0535 s	4.277e-004 K	5.145318 Ω
45.83 W/mK	8.098 mm²/s	5.660 MJ/m³K	13.0 mm	0.117 K	-0.0013...	0.902	4.53 K	0.0534 s	4.099e-004 K	5.131433 Ω
47.63 W/mK	8.008 mm²/s	5.948 MJ/m³K	12.8 mm	0.133 K	-0.0012...	0.883	4.61 K	0.134 s	4.419e-004 K	5.100861 Ω
44.55 W/mK	7.107 mm²/s	6.268 MJ/m³K	12.1 mm	0.202 K	-	0.787	5.24 K	0.217 s	5.197e-004 K	4.577844 Ω
44.40 W/mK	6.817 mm²/s	6.514 MJ/m³K	11.3 mm	0.129 K	-	0.685	4.40 K	0.214 s	5.303e-004 K	4.578357 Ω
45.56 W/mK	5.492 mm²/s	8.295 MJ/m³K	10.5 mm	0.102 K	-	0.592	3.52 K	0.294 s	5.945e-004 K	4.578527 Ω
64.26 W/mK	12.61 mm²/s	5.096 MJ/m³K	15.3 mm	0.0810 K	-	1.26	4.35 K	0.0535 s	6.127e-004 K	6.668609 Ω
76.42 W/mK	5.688 mm²/s	13.43 MJ/m³K	10.2 mm	0.0752 K	-	0.555	4.35 K	0.295 s	5.900e-004 K	6.674372 Ω
75.01 W/mK	5.775 mm²/s	12.99 MJ/m³K	10.9 mm	0.131 K	-	0.640	4.36 K	0.300 s	7.916e-004 K	6.678771 Ω
84.27 W/mK	8.315 mm²/s	10.13 MJ/m³K	13.1 mm	0.0739 K	-	0.921	3.66 K	0.134 s	8.562e-004 K	9.625811 Ω
80.04 W/mK	10.41 mm²/s	7.686 MJ/m³K	14.3 mm	0.0965 K	-	1.09	3.65 K	0.154 s	8.504e-004 K	9.633317 Ω
86.16 W/mK	7.273 mm²/s	11.85 MJ/m³K	12.4 mm	0.0910 K	-	0.826	3.62 K	0.300 s	7.785e-004 K	9.639410 Ω

Fig. 5. Results of TPS measurements.

In Table 2 are presented thermal properties (thermal conductivity, specific heat and temperature conductivity) of analysed rapidly solidified Cu-Al-Ni -Mn shape memory alloy at ambient temperature (approx. 22 °C).

Table 2. Thermal properties of analysed Cu-Al-Ni–Mn shape memory alloy at ambient temperature

	Cu-Al-Ni -Mn
Thermal conductivity	45.30 W/mK
Specific heat	6.29 MJ/m^{3}K
Temperature diffusivity	7.36 mm^2/s

In Figure 6 is thermal conductivity of analysed Cu-Al-Ni-Mn shape memory alloy on the temperature interval between ambient temperature and 400 °C.

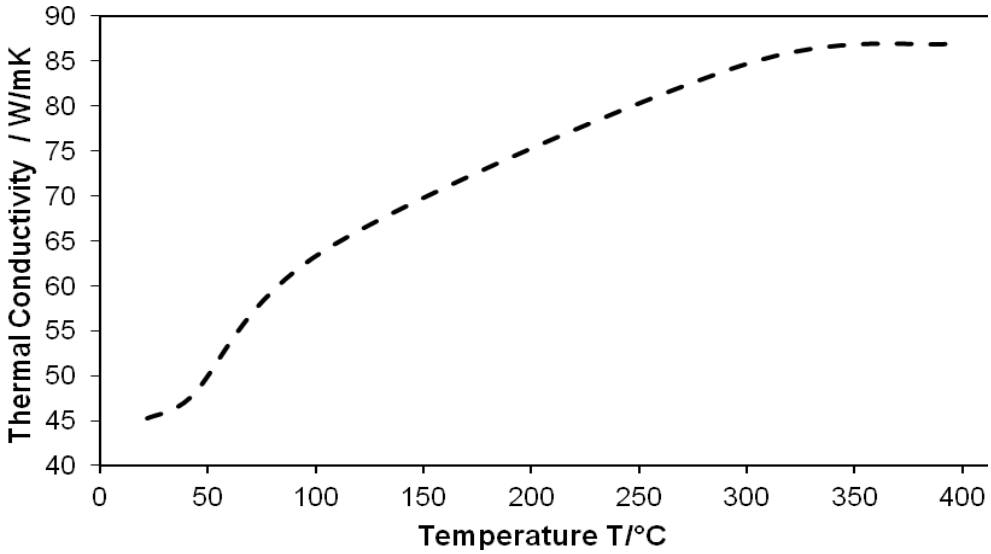

Fig. 6. Thermal conductivity at elevated temperatures.

3. CONCLUSIONS

In the frame of our investigation work thermal properties of rapidly solidified Cu-Al-Ni-Mn shape memory alloy were determined. The measurements and analysis of thermal properties of rapidly solidified Cu-Al-Ni-Mn shape memory alloy has been done.in accordance with the standard ISO 22007-2 at ambient and elevated temperatures.

The values of thermal properties of Cu-Al-Ni-Mn SMA at ambient temperature (approx 22 °C) are:

- thermal conductivity 45.30 W/mK,
- specific heat 6.29 MJ/m^{3}K, and
- temperature diffusivity 7.36 mm^2/s.

We found that investigated rapidly solidified Cu-Al-Ni-Mn shape memory alloy at ambient temperature has almost 100 % lower heat conductivity as at temperature 400 °C.

4. REFERENCES

[1] Libermann H.H., *Rapidly solidified alloys*, Marcel Dekker, London, 1993.

[2] Dobrzanski L.A., *Technical and Economical Issues of Materials Selection*, Silesian Technical University, Gliwice, 1997.

[3] Lojen G., Anžel I., Kneissl A.C., Unterweger E., Kosec B., Bizjak M., *Microstructure of rapidly solidified Cu-Al-Ni shape memory alloy ribbons*, Journal of Materials Processing Technology, 162/163 (2005), 220-229.

[4] Gojić M., Vrsalović L., Kožuh S., Kneissl A.C., Anžel I., Gudić S., Kosec B., Kliškić M., *Electrochemical and microstructural study of Cu-Al-Ni shape memory alloy*, Journal of Alloys and Compounds, 509 (2011) 41, 9782-9790

[5] Ivanić I., Kožuh S., Kosel F., Kosec B., Anžel I., Bizjak M., Gojić M., *The influence of heat treatment on fracture surface morphology of the CuAlNi shape memory alloy*, Engineering failure analysis. 77 (2017), 85-92

[6] Ivanić I., Gojić M., Kožuh S., Kosec B., *Microstructural analysis of CuAlNiMn shape-memory alloy before and after the tensile testing*, Materials and Technologies, 48 (2014) 5, 713-718.

[7] Kosec., B., Karpe, B., *Instrument for the thermal properties analysis Hot Disk TPS 2200*, IRT3000, 1 (2017), 67.

[8] Karpe B., Vodlan M., Kopač I., Budak I., Nagode A., Pavlič A., Puškar T., Kosec B., *Thermal properties of materials used in dental medicine*, Advanced technologies and materials, 43 (2018) 1, 7-10.

[9] International standard ISO 22007 (2009). *Plastics – Determination of thermal conductivity and thermal diffusivity – Part 1*: General principles. Reference: ISO 22007:2009(E).

Authors: **Full Prof. Dr. Borut Kosec,** University of Ljubljana, Faculty of Natural Sciences and Engineering, Askerceva 12, 1000, and University of Ljubljana, Faculty of Mechanical Engineering, Askerceva 6, 1000 Ljubljana, Slovenia, Tel: +386 1 200 04 10, Fax: +386 1 470 45 60.

Full Prof. Dr. Milan Bizjak , Full Prof. Dr. Aleš Nagode, Ass. Prof. Dr. Blaž Karpe, University of Ljubljana, Faculty of Natural Sciences and Engineering, Askerceva 12, 1000, Slovenia, Tel: +386 1 200 04 33, Fax: +386 1 470 45 60.

Full Prof. Dr. Mirko Gojić, University of Zagreb, Faculty of Metallurgy, Aleja narodnih heroja 3, 44103 Sisak, and University North, Trg dr. Žarka Dolinara 1, 48000 Koprivnica, Croatia, Tel: +385 44 533 378, Fax: +3851 44 533 380.

Assoc. Prof. Dr. Branko Štrbac, University of Novi Sad, Faculty Technical Sciences, Trg D. Obradovića 6, 21000 Novi Sad, Serbia, Phone.: +381 21 4852255, Fax: +381 21 4852313.

Ass. Prof. Dr. Ivana Ivanić, University of Zagreb, Faculty of Metallurgy, Aleja narodnih heroja 3, 44103 Sisak, Croatia, Tel: +385 44 533 378, Fax: +3851 44 533 380.

E-mail: borut.kosec@ntf.uni-lj.si
milan.bizjak@ntf.uni-lj.si
gojic@simet.hr
strbacb@uns.ac.rs
iivanic@simet.hr
ales.nagode@ntf.uni-lj.si
blaz.karpe@ntf.uni-lj.si

ETIKUM 2023 **INTERNATIONAL SCIENTIFIC CONFERENCE NOVI SAD, SERBIA, DECEMBER 7-9, 2023**

Kostić, S., Kočović, V., Vasiljević, S., Miletić, S., Jovanović Pešić, Ž., Džunić, D.

TENSILE TESTING OF ELECTROCHEMICALLY MACHINED SPECIMENS

Abstract: *The complexity of the procedure of specimens is primarily contained in the technological problems of making long thin samples with a circular cross section. Specimens for a small laboratory tensile testing device (SLTTD) are of non-standard shapes. Based on previous research, it was concluded that by reducing the cross-sectional area and increasing the original gauge length of specimen, the measurement accuracy increases. Such specimens cannot be made by conventional methods, but non-conventional one, such as electrochemical machining (ECM). Specimens made by ECM were tested on a SLTTD, and the obtained results were compared with test results available in the literature.*
Key words: *Tensile testing, Electrochemical machining, Small laboratory tensile testing device*

1. INTRODUCTION

In modern engineering practice, materials research and development play a key role in achieving high standards of safety, reliability and efficiency in various industries. One of the most important aspects of this research is related to the improvement of the mechanical properties of metals, since metals are often used for constructions subjected to significant mechanical loads.

ECM of metals is a complex discipline that connects the principles of chemistry and electrochemistry with materials engineering. This method allows controlled manipulation of the surface properties of metals, including hardness, strength, corrosion resistance and other mechanical properties, using ECM such as electrodeposition, electropolishing, anodic oxidation and the like. ECM has proven particularly useful in tensile testing, as it allows engineers and researchers to precisely adapt the properties of metals to meet the specific needs of different applications.

By using an electrode for the controlled introduction of electric current into the electrolyte solution of the metal, an electrode reaction is caused on the surface of the metal. After electrochemical treatment, the sample can be further prepared, for example, by grinding and polishing, in order to achieve the desired surface roughness and dimensional accuracy [1].

With the use of new materials of higher strength in the automotive, aerospace and manufacturing industries, difficulties arise with cutting by conventional machining processes, so the use of non-conventional machining processes is switched to. The work of Liu et al. (2023) provides a detailed overview of the influence of various process parameters on performance measures in the ECM [2].

In the work of Kumar et al. (2023) conclude that the unique feature of the toolless electrochemical jet machining is suitable for the finishing of additive manufacturing (AM) parts. Surface defects and irregularities on complex parts present challenges during processing with conventional processes [3].

Another review paper by Gautam et al. (2022) presents a study of electrical discharge machining, wire electrical discharge, and electrochemical machining. The paper provides optimal parameters for the above processes that can help increase production in various industries [4].

This scientific work aims to research and analyze the ECM of metal specimens with the intention of obtaining specimens with small cross-sections and relatively large original gauge lengths, which are difficult to obtain with conventional processing methods. The obtained samples were tested on a SLTTD [5], and the obtained results are comparative with the results presented in the literature. Through this analysis, this work contributes to a better understanding and control of the mechanical properties of metals, which has the potential to improve the performance and durability of metal structures in a wide range of engineering applications.

2. RESEARCH METHODOLOGY

The problems of obtaining the accurate values of the mechanical characteristics of the tensile devices arise due to a large number of factors.

Using a SLTTD for tensile testing of materials, and based on measuring the modulus of elasticity of the material as the most sensitive characteristic, Kostić et al. (2022) came to the conclusion that the specimens must be as small as possible in cross-section and as large as possible in original gauge length [5]. The described shape of the specimens guarantees satisfactory measurement accuracy without the use of an extensometer. This conclusion was reached by analyzing the errors of the measuring system, which are primarily the result of elastic deformation of the functional parts of the device structure due to the action of the tension force during the tensile testing, such as the clamping system. Non-standard specimens with a circular cross-section were made by ECM.

Faraday's law, which connects the amount of metal dissolved during electrolysis and the strength and time of current flow between two electrodes immersed in the electrolyte, represents the basis of electrochemical processing [6]. Controlled removal of material is performed by electrolysis, with the workpiece representing the anode (+) and the tool the cathode (-), Figure 1.

Fig. 1. ESM of a circular cross-section specimen with non-standard dimensions

The shape and geometric characteristics of the specimen, as well as a photo of the machined specimen, are given in Figure 2. The original gauge length of the specimen is 200 mm, and the diameter is 1.5 mm. The investigation was conducted on specimen made of non-alloy quality structural steel E360 whose chemical composition is: ≤ 0.045% P, ≤ 0.045% S, ≤0.012% N. The mechanical and physical characteristics of structural steel E360 are: Elastic modulus=190 GPa, hardness=210 HB, tensile strength=690-900 MPa, yield strength=350 MPa, Poisson ratio=0.29 and density=7.9 g/cm^3.

The specimen shown in Figure 2 is made of semi-finished products with a diameter of 2.5 mm. The thickening of the specimen was achieved by placing an insulating layer in those zones, in order to prevent the removal of material on the parts for receiving the specimen. The ECM process was carried out in a saline solution under the action of a DC voltage of 12V without relative movement of the electrodes. This voltage value was chosen after a preliminary test which showed that the specimens obtained under these conditions have the least dimensional and geometrical errors. The manufacturing process is slow but guarantees the required quality.

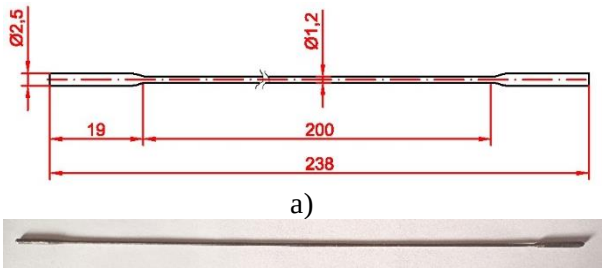

a)

b)

Fig. 2. Specimen a) shape and geometric characteristics and b) photograph

By increasing the voltage, the electrochemical process is accelerated, but dimensional and geometrical defects increase, Figure 3.

Fig. 3. Dimensional errors and surface defects of specimen made by ECM using 48V voltage

A high voltage value leads to a violent reaction, which is followed by a sudden decrease in diameter. The reduced diameter is intense and amounts to approximately 0.1 mm/min. The intensity of material removal in the first minute of processing is shown in Figure 4. The figure shows the process of making a brass specimen. Thus, the considered method provides the possibility of fine processing of all metal materials.

Depending on the processed material, the color of the electrolyte after processing will also differ, which is caused by the remains of the processed material, as shown in Figure 5.

The authors of this paper paid special attention to the clamping system of specimen, in order to minimize measurement errors. The specimen is freely supported in the clamping grips, and after that the bushing are pulled on and the receiving zone is tightened with a screw.

In this way, the alignment of the left and right clamping grips and the balance of forces in the directions normal to the tension axis are ensured, which eliminates the deformation of the specimen that occurs when the specimen is grounded without clamping, Figure 6.

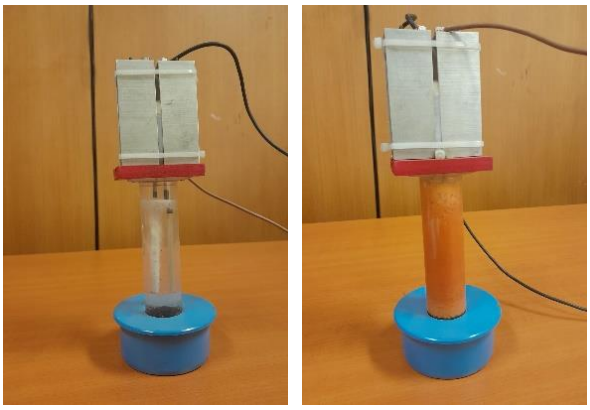

Fig. 4. Intensity of material removal in the first minute of processing by applying a voltage of 48V in the case of making a brass specimen

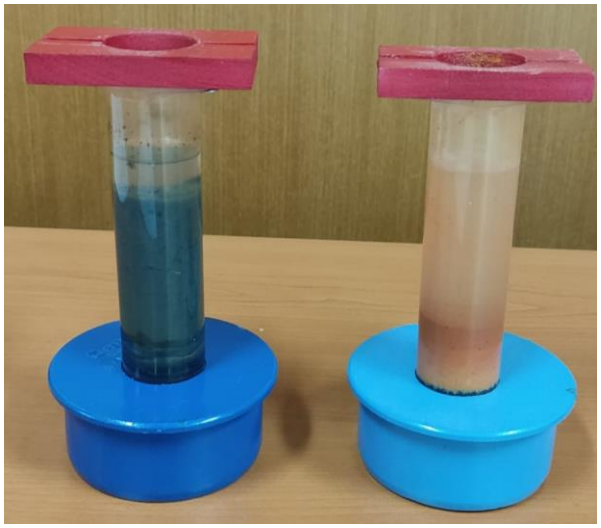

a) b)

Fig. 5. The appearance of the electrolyte after processing depends on the type of processed material a) steel; b) brass

The work is restricted to tests performed at ambient temperatures 23±2°C, with a digital acquisition of load and displacement. The tests are assumed to run continuously without interruptions on specimens that have uniform gauge lengths, and the procedure is restricted to tests performed under axial loading conditions. The experiments were conducted in controlled microclimatic conditions according to the standard EN ISO 6892-1:2019 [6].

SLTTD has load cell 2 kN nom. capacity, the elongation is measured by moving the clamping grip of the SLTTD. The diameter of specimen are measured with an accuracy of ±10 μm.

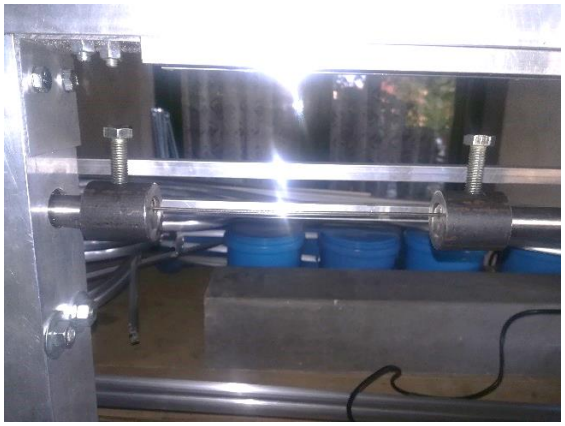

Fig. 6. Positioning specimen in clamping system on a SLTTD before starting the test

3. TEST RESULTS

The stress-strain diagram, which was obtained after tensile testing the E360 steel material on a SLTTD, is given in Figure 7.

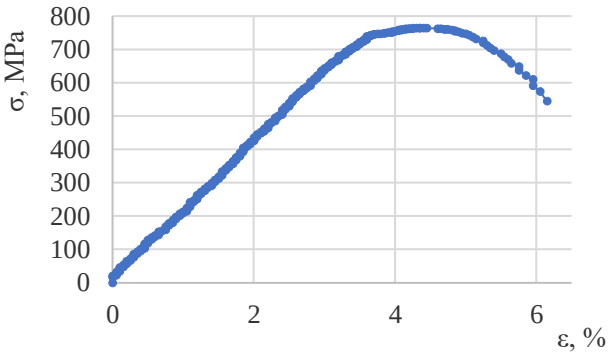

Fig. 7. Stress-strain diagram of the tested E360 steel material specimen

The diagram clearly shows the tensile strength value of 764.2 MPa, which represents a value that corresponds to the range of reference values given in the literature [8]. The fracture elongation is 6.15%, which also corresponds to the data available in the literature, Figure 7.

SLTTD is equipped with software, which performs automatic processing of collected data during testing [9]. In this way, diagrams of real stresses and deformations can be obtained immediately after the test, because during the test the cross-section changes, first by the appearance of uniform plastic deformations, and then by the formation of necks on specimen. After reaching the maximum force, uneven plastic deformations occur, which cause the formation of a narrowing of the cross-section at the point where the specimen will break. The diagram of the dependence of the real cross-sectional area of the specimen on the real stress during the test for the material steel E360 is

shown in Figure 8.

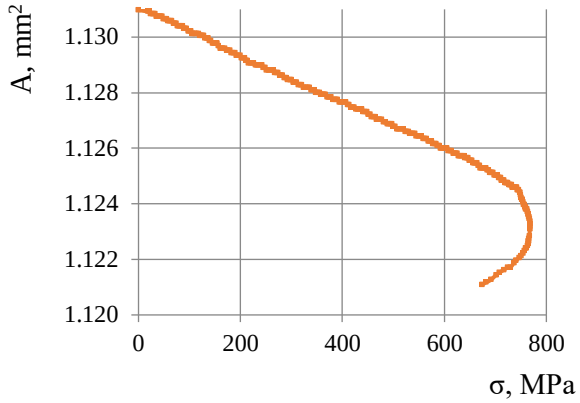

Fig. 8. Diagram real cross-sectional area of the specimen – real stress, of steel E360

The diagram in Figure 8 clearly shows the contraction of the cross section, which corresponds to the characteristics of the tested material. Small values of cross-section contraction, as well as deformation values shown in Figure 7, clearly indicate the properties of the tested steel.

4. CONCLUSION

Today's application of ECM most often focuses on the production of parts with complex shapes and materials that are difficult to process, and the precise shaping of material parts is a challenge for conventional processing methods. After the ECM treatment, there are no residual surface stresses, thus providing the material with better stability and reducing the risk of stress damage. This aspect makes ECM an attractive option in many industries that require a high degree of precision and control of the mechanical properties of materials.

Tensile testing specimens of non-standard shapes can be made by ECM. A comparison of tensile test results obtained on a SLTTD with test results available in the literature supports this claim.

Future research in this area will go in the direction of optimizing all parameters of the ECM of samples, such as electrolyte quality and properties, current strength, processing time, material, geometry and position of electrode, electrolyte flow. The precise setting of the parameters is crucial for achieving the desired characteristics of the material after electrochemical processing. Variations in these parameters can result in different properties of the machined material, including surface roughness, thickness of material removed, and other desired characteristics.

5. REFERENCES

[1] Fourdeux, A., Wronski, A., *New electrolytic method for cutting and shaping metal specimens*, British Journal of Applied Physics, 14, 4, pp. 218-220, 1963.

[2] Liu, S., Thangamani, G., Thangaraj, M., *Recent trends on electro chemical machining process of metallic materials: a review*, Archiv.Civ.Mech.Eng, 23, 158, 2023.

[3] Kumar, P., Dixit, P., Chaudhary, B., Jain, N.K., *Surface finishing of an additively manufactured part using electrochemical jet machining*, Materials Today Communications, 35, 105581, 2023.

[4] Gautam, N., Goyal, A., Sharma, S., Oza, A., Kumar, R., *Study of various optimization techniques for electric discharge machining and electrochemical machining processes*, Materials Today: Proceedings, 57, 2, pp 615-621, 2022.

[5] Kostić, S., Miljojković, J., Šimunović, G., Vukelić, Đ., Tadić, B., *Uncertainty in the determination of elastic modulus by tensile testing*, Engineering Science and Technology, an International Journal, 25, 100998, 2022.

[6] Lazić M.: *Nekonvencionalni postupci obrade*, Naučna knjiga, Beograd, 1990

[7] EN ISO 6892-1:2019: Metallic materials - Tensile testing - Part 1: Method of test at room temperature, Europian Committee for Standardization, 2019.

[8] ASM Atlas of Stress-Strain Curves, Second edition. ISBN:0-87170-739-X, 2002.

[9] Kostić, S., Košarac, A., Luković, V., Miljojković, J., *Theory Reviews - Hardware and Software Support for Testing Material on Specimens of the Small Cross Section*, Tribology in Industry, 41, pp. 109-114, 2019.

Authors: **Prof. of App. Studies. dr Sonja Kostić, Teaching Assis. Saša Vasiljević,** Academy of Professional Studies Šumadija, Department in Kragujevac, Kosovska 8, Kragujevac, Serbia**.**
E-mail: skostic@asss.edu.rs
svasiljevic@asss.edu.rs

Assis. prof. dr Vladimir Kočović, MEng. Stefan Miletić, MEng. Živana Jovanović Pešić, Assoc. prof. dr Dragan Džunić, University of Kragujevac, Faculty of Engineering, Sestre Janjić street, no. 6 - 34000 Kragujevac, Serbia.
E-mail: vladimir.kocovic@kg.ac.rs
stefan96miletic.finkg@gmail.com
zixi90@gmail.com
dzuna@kg.ac.rs

ETIKUM 2023 **INTERNATIONAL SCIENTIFIC CONFERENCE NOVI SAD, SERBIA, DECEMBER 7-9, 2023**

Kovač, P., Savković, B., Dudić, B., Ješić, D.

MODELLING OF SURFACE ROUGHNESS PARAMETERS USING THE DESIGN OF EXPERIMENTS PLANS OF THE FIRST ORDER AND ARTIFICIAL INTELLIGENCE METHOD DURING MACHINING

Abstract: *In the work, the parameters of the cutting mode were modelled during face milling of the Semi Solid Metal aluminium alloy. The input parameters in the modelling process were: cutting speed v, tooth displacement and cutting depth a, while the output characteristics of the process were the mean arithmetic roughness of the machined surface Ra and the maximum height of unevenness R_{max}. Modelling was done in two ways. The first model was created with the help of the mathematical statistical method of the factor plan of the DoE experiment, where a model without mutual influence of parameters was used. The second model was created on the basis of artificial intelligence, where an artificial neural network was used as the chosen tool.*

Key words: *face milling, machined surface roughness, factor plan, neural networks, modelling.*

1. INTRODUCTION

Rapid industrial progress, in parallel with the development of science, created the basis for the further development of the science of material stripping processes. Various techniques of artificial intelligence, from expert systems, artificial neural networks, fuzzy logic, genetic algorithms and genetic programming as well as other modelling techniques have found their application in this area. Through this work, we want to show the possibility of applying mathematical modelling based on the factor plan of the DoE experiment and artificial neural networks during milling, as one of the most common processing processes.

There is a need to improve processing processes by applying knowledge from advanced modelling techniques, i.e. simulations, which certainly includes modelling with the help of artificial intelligence methods. The models obtained in this way are used for analysis, management and selection of optimal process parameters. The resulting models can be used with sufficient accuracy in adaptive management and monitoring of processes and making solutions in real time, which is of great importance in the exploitation of intelligent production systems. It is also possible to optimize the input parameters of the process based on the set processing limits, with the aim of achieving one or more goal functions such as reducing the cutting resistance and/or minimizing the roughness of the processed surface, which from a technical point of view have the greatest practical value and meaning.

2. MODELLING OF THE PROCESS USING A MULTIFACTORIAL DESIGN OF THE EXPERIMENT - DOE

The model expresses the essential properties of an object, process or system. The mathematical model itself consists of a system of equations, states and algorithmic rules. When setting up a mathematical model, basic sources of information are used.

The most common multifactor models are experiments where the factors are varied in two levels (maximum and minimum value), whereby the mean value of the factor is not treated as a level of variation. These are experiments of the type:

$$N = 2^k + n_0 , \qquad (1)$$

where: k – number of factors (variables), n_0 – number of experiment variables.

Application of the design of the factorial design of the experiment (DoE) in the presentation ie. analysis of the results is very common. The field of application is wide, and this can be seen through literature sources [1-4] where different spheres of scientific research are represented.

3. APPLICATION OF ARTIFICIAL INTELLIGENCE IN PROCESSING PROCESSES

In terms of structure and management problems, the new production has few similarities from the 50s of the last centuries. The foundations on which today's production rests are the demands of the market, a new production philosophy based

on knowledge, advanced production and information technologies, new materials and modern processing and production systems. The biggest changes in technical-technological development in the history of mankind took place in the last fifty years thanks to the rapid development of technology and the appearance of computers. Artificial intelligence plays a special role in the automation and improvement of production processes.

3.1 Artificial neural networks

Artificial neural networks (ANNs) are nowadays used in almost all fields of science and technology, including mechanical engineering. Technological processing parameters are quantities that depend on a large number of factors. There are no exact patterns and procedures for determining some parameters, so in most cases empirical values are used, using various books, tables, graphs, etc. This is where neural networks can be of great use. Instead of a detailed calculation of processing parameters, a neural network is created that can, after a properly executed training process, predict unknown processing parameters.

More complex neural networks may have multiple hidden layers, feedback loops, and time-delay elements, which are designed to allow the most efficient separation of important features or patterns from the input layer. Today, multilayer neural networks are mostly studied and applied, which, in addition to the input and output layers, contain neurons on the middle (hidden) layers.

In order for ANN to be successfully applied to solve problems (modelling, simulation, optimization), which appear in processing processes, it is necessary to know their characteristics, concept and steps that should be carried out during their creation.

4. DESCRIPTION OF FACE MILLING EXPERIMENTS

Experimental tests were carried out on aluminium alloy 7075 (Al-Zn-Mg-Cu). The width and length of all workpieces was 100 mm, and the thickness was 15 mm. The machine on which the milling operations were performed is a vertical milling machine "PRVOMAJSKA" FSS-GVK-3. During the tests, the head for face milling "JUGOALAT" G.037 ϕ100 mm, with mechanically attached cutting plates, with the following characteristics was used: number of teeth z =5, attack angle κ=75°, chest angle γ = 0°. K20 quality hard metal turning plates were used as cutting tools. Modern surface roughness meters are used for quick measurement of unevenness on the object's surface. The devices show both the maximum height of unevenness R_{max} in μm.

4.1 Processing mode

The processing mode includes the following elements: cutting speed v, that is, the corresponding number of revolutions on the machine n; feed per tooth s1, i.e. the corresponding speed of movement of the milling table s, so that: $s=s_1 \cdot z \cdot n$ where the number of teeth during processing is z=1; cutting depth a.

The values of the processing mode elements were adopted based on recommendations from the literature and are shown in Table 1.

Table 1. Levels of experimental parameters for face milling

Levels	v, m/s	s_1, mm/t	a, mm	n, o/min
The bigest +1.41	5,864	0,223	2,6	1120
The big +1	4,712	0,177	1,72	900
The medium 0	3,717	0,141	1,14	710
The small -1	2,932	0,112	0,75	560
The smallest -1.41	2,356	0,089	0,5	450

When measuring the roughness of the treated surface, records of over 20 roughness parameters were obtained, of which the results for the maximum height of unevenness (R_{max}) were used in this research. An overview of the measured roughness of the treated surface is shown in summary Table 2.

Table 2. Summary experimental results required for the factorial design of experiments model

No.	v, m/s	s_1, mm/t	a, mm	R_{max}, μm
1	2,93	0,112	0,75	5,07
2	4,71	0,112	0,75	4,51
3	2,93	0,177	0,75	6,89
4	4,71	0,177	0,75	7,97
5	2,93	0,112	1,72	5,63
6	4,71	0,112	1,72	4,12
7	2,93	0,177	1,72	6,63
8	4,71	0,177	1,72	5,78
9	3,71	0,141	1,14	5,16
10	3,71	0,141	1,14	4,91
11	3,71	0,141	1,14	5,02
12	3,71	0,141	1,14	6,3

5. MODEL OF THE THREE-FACTOR DESIGN OF THE FACE MILLING PROCESS EXPERIMENT

Data processing according to the three-factor plan of the first-level experiment was performed for the maximum height of bumps R_{max}. The Microsoft Excel program package was used to create the model for simpler data processing. A model was developed without mutual influence of parameters. The general form of this type of model is shown by Eqs. Where by equation 2.

$$R = CF_1^{p_1} F_2^{p_2} F_3^{p_3} \quad (2)$$

In the given equation, R is the output characteristic of the machining process, while the parameters marked with F represent the following factors: F_1 - cutting speed a, mm

F_2 - feed per tooth s_1, mm/t

F_3 - cutting depth a, mm

The three-factor model of the first order for the maximum height of unevenness (3) during face milling depending on the cutting speed (v), feed per tooth (s_1) and cutting depth (a) has the following form:

$$R_{max} = Cv^{p_1} s_1^{p_2} a^{p_3} \quad (3)$$

Table 3 shows the measured and calculated values of the experiment for the first-order model, and

Table 3. Measured and calculated values

	The maximum height of unevenness	
No.	Measured values	Calculation values
1	5,07	4,66
2	4,51	4,00
3	6,89	7,37
4	7,97	6,32
5	5,63	4,75
6	4,12	4,08
7	6,63	7,52
8	5,78	6,45
9	5,16	5,49
10	4,91	5,49
11	5,02	5,49
12	6,3	5,49
13	5,76	6,37
14	4,3	4,74
15	3,34	3,47
16	7,77	8,69
17	5,31	5,38
18	6,83	5,60
19	6,11	6,37
20	4,63	4,74
21	3,45	3,47
22	7,47	8,69
23	5,66	5,38
24	6,3	5,60

6. REALIZATION OF THE NEURAL NETWORK

Neural Network Toolbox provides complete neural network engineering in the MATLAB environment starting from design through training to simulation of various neural network algorithms that are presented in MATLAB starting from the basic Perceptron model to the most complex so-called. self-organizing networks.

Training and testing are the most important features of a neural network because it is training and testing that determine its characteristics. During training, the first step is to enter questions to which we know the answer. The network answers the question, and the answer is compared to the correct answer. Then, the weight of connections between individual neurons is changes until the network gives the correct answer to the question. This procedure is repeated until the artificial neural network is adequately trained.

6.1 Creation of a neural network

Neural Network Toolbox was used to create and train a neural network in MatLab itself. Like other MATLAB packages, Neural Network Toolbox takes over much of the routine work so that the user can concentrate on the core problems. NNT provides more options for using the MATLAB package. Tools are available for creating, visualizing, realizing and simulating different networks.

Before the creation of the neural network, data is entered in the Command Window in the form of a matrix.

The input data are the cutting speed v (m/s), tooth displacement s_1 (mm/z), cutting depth a (mm). These input quantities are grouped into a unit called IN=(v, s_1, a). The output sizes Rmax are not grouped, but a new network is created for each individually. Accordingly, the models that were built were of the 3-1 type, three inputs - one output, Figure 1.

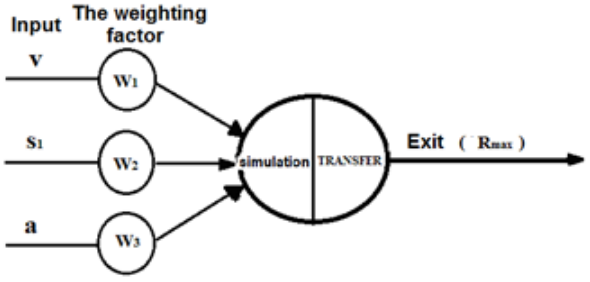

Fig. 1. Model of formed neural networks

Figure 2 shows the regression diagram in the neural network training process, where the goal is that the value of the regression coefficient should

be close to the number 1 (one), the regression lines should be at an angle of 45°, while most of the data with which the network is trained should be along the regression line itself.

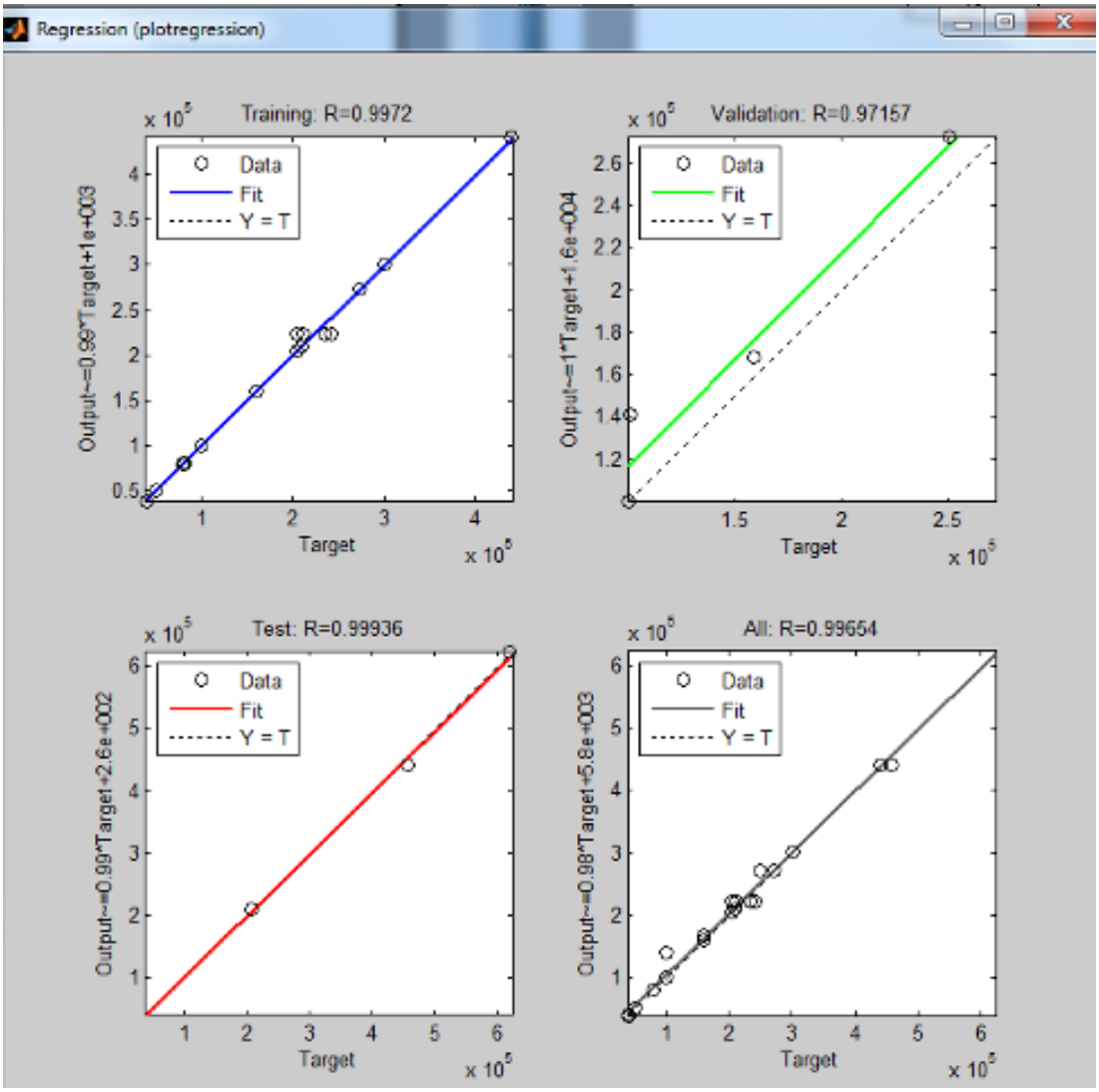

Fig. 2. The regression diagram in the neural network training process

Table 4 shows the results obtained through the neural network model (N.M.) with the percentage error E in relation to the experimental results for Rmax.

Figure 3 shows a graphic representation of the deviation of the value obtained through the neural network model (N.M.) in relation to the experimentally obtained quantities.

Table 4. Results obtained through neural network models (N.M.) with percentage error E for Rmax

No.	v, m/s	s_1, mm/t	a, mm	$R_{max\ Exp.}$, µm	$R_{max\ N.M.}$, µm	E, %
1.	2,93	0,112	0,75	5,07	5,33080	5,14
2.	4,71	0,112	0,75	4,51	4,19900	6,9
3.	2,93	0,177	0,75	6,89	7,63360	10,79
4.	4,71	0,177	0,75	7,97	7,11720	10,7
5.	2,93	0,112	1,72	5,63	5,70920	1,41
6.	4,71	0,112	1,72	4,12	4,17520	1,34
7.	2,93	0,177	1,72	6,63	5,93590	10,47
8.	4,71	0,177	1,72	5,78	6,38030	10,39
9.	3,71	0,141	1,14	5,61	5,54760	1,11
10.	2,35	0,141	1,14	5,935	7,12410	20,04

11.	5,86	0,141	1,14	4,465	4,81550	7,85
12.	3,71	0,089	1,14	3,395	2,37980	29,9
13.	3,71	0,223	1,14	7,62	7,85060	3,03
14.	3,71	0,141	0,5	5,485	6,30490	14,95
15.	3,71	0,141	2,6	6,565	6,48280	1,25
16.	2,35	0,089	0,5	5,9	6,01270	1,91
17.	2,35	0,223	2,6	7,91	7,65680	3,2
18.	3,71	0,223	0,5	8,78	7,88210	10,23
19.	5,86	0,089	2,6	5,6	5,58830	0,21
20.	5,86	0,141	0,5	7,48	4,63560	38,03
21.	5,86	0,223	1,14	8,47	7,84740	7,35
				Percentage error E ⇒		9,34

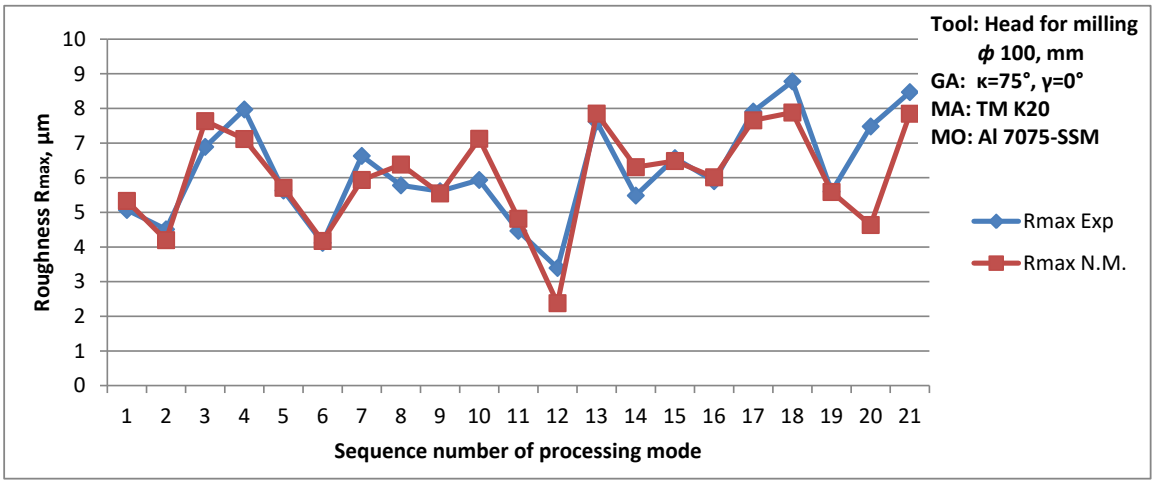

Fig. 3. Graphic representation of the obtained values for the maximum height of unevenness R_{max}

7. ANALYSIS OF RESULTS OBTAINED THROUGH DIFFERENT MODELS (DOE, ANN)

During the research, various models were developed for calculating the values of the output characteristics of the milling process (roughness of the machined surface). Different methods were used for this (DoE, ANN). Verification of the accuracy of those models was performed on the basis of 6 additional experiments, performed according to the plan given in Table 5. During the implementation of the previously mentioned models, the results obtained during these 6 experiments were not used. In the following, the model deviation analysis was performed and presented in the form of the mean error value.

For a clearer appearance of the diagram, the following abbreviations have been introduced for the models:

• N.M. - model formed on the basis of neural networks,

• F.P.1 - model obtained on the basis of factor plan, without mutual influence of factors.

Experimental values are shown with the abbreviation Exp.

Table 5. Additional summary experimental results required for model verification

No.	v, m/s	s_1, mm/t	a, mm	R_{max}, µm
1	3,71	0,141	0,75	7,6
2	3,71	0,141	1,72	5,07
3	3,71	0,112	1,14	4,63
4	3,71	0,177	1,14	5,5
5	2,93	0,141	1,14	7,33
6	4,71	0,141	1,14	3,97

Figure 4 shows the deviation diagram of the results obtained with the help of the appropriate model for the maximum height of unevenness Rmax. A histogram with the mean percentage error for each model is also shown for comparison.

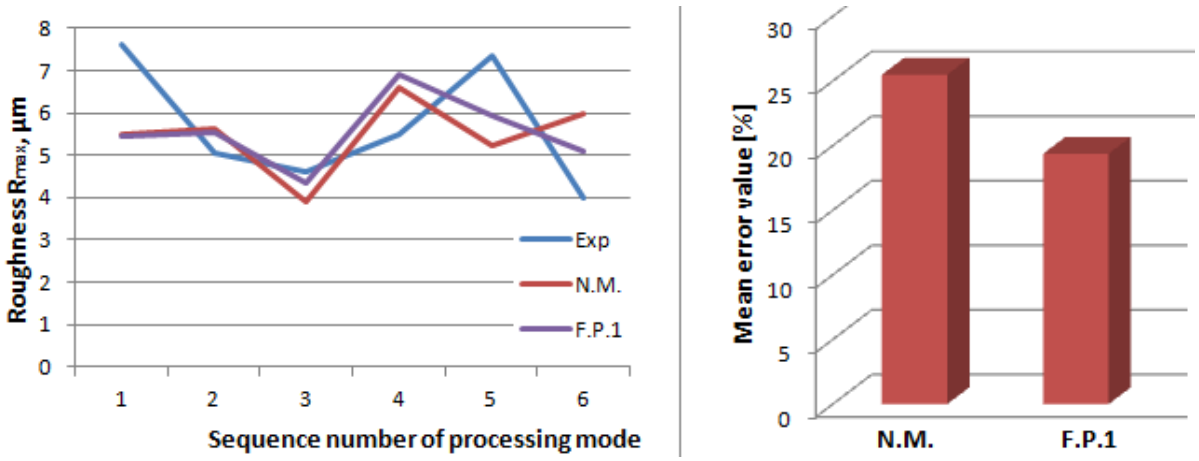

Fig. 4. Deviation diagram of the results obtained with the help of the appropriate model for R_{max}

8. CONCLUSION

By modeling the machinability functions of the milling process, i.e. the parameters of the processing mode and the output characteristics of the process state, the prerequisites for forecasting, management and optimization of the processing parameters were created. The modeling process was carried out with the help of mathematical models obtained on the basis of multi-factor regression analysis and with the help of methods based on artificial intelligence. The obtained models were comparatively analyzed and for each workability function it was proposed to adopt the most favorable model from the aspect of obtaining the smallest possible error of deviation from experimental values. Verification of the accuracy of the model was performed on the basis of additional experiments, which were not previously used in their implementation.

Separate theoretical and experimental research showed the applicability of new modeling methods to milling processes. Through modeling, management and optimization of process parameters, results were achieved that will enable predicting the impact of individual input parameters for given constraints and objective function. Also, the models developed with the help of artificial intelligence tools (neural networks) have practical application in industry, so the research results have their significance in this regard as well, i.e. they can be integrated into production systems that include machine tools with integrated memory for knowledge base. Such verified models obtained with the help of artificial intelligence, in addition to being able to be incorporated into production systems themselves, can also be infiltrated into computer systems based on finite element methods (FEM) in order to predict machinability functions (temperature, cutting resistance, machined roughness surface and chip shape).

9. REFERNCES

1. Kardara, P., Ebrahimia, M., Bastani, S., Jalili, M.: *Using mixture experimental design to study the effect of multifunctional acrylate monomers on UV cured epoxy acrylate resins*, Prog. Org. Coat., 64 (2009) 1, 74-80.
2. Yin, H.F., Chen., Z.G., Gu. Z.X., Han, Y.B.: *Optimization of natural fermentative medium for seleniumenriched yeast by D-optimal mixture design*, LWT. Food. Sci. Technol., 42 (2009) 1, 327-331.
3. Lin, S.S., Lin., J.C., Yang, Y.K.: *Optimization of mechanical characteristics of short glass fiber and polytetrafluoroethylene reinforced polycarbonate composites via D-optimal mixturedesign*, Polym. Plast. Technol. Eng., 49 (2010) 2, 195-203.
4. Chen, L.C., Huang, C.M., Hsiao, M.C., Tsai, F.R.: *Mixture design optimization of the composition of S, C, SnO_2-codoped TiO_2 for degradation of phenol under visible light*, Chem. Eng. J.: 165 (2010), 482-489.

Authors: **Prof. dr Pavel Kovač[1], Assoc. prof. dr Borislav Savković[1], Assis. prof. dr Branislav Dudić[2], dr. Dušan Ješić[3],** [1]University of Novi Sad, Faculty of Technical Sciences, Trg Dositeja Obradovica 6, 21000 Novi Sad, Serbia, Phone.: +381 21 485 2329, Fax: +381 21 454-495, [2]Comenius University Bratislava, Faculty of Management, 820 05 Bratislava, Slovakia, [3]International Technology and Management Academy – MTMA, Novi Sad, Serbia

E-mail: pkovac@uns.ac.rs
savkovic@uns.ac.rs
branislav.dudic@fm.uniba.sk
dusanjesic@hotmail.com

ETIKUM 2023 **INTERNATIONAL SCIENTIFIC CONFERENCE NOVI SAD, SERBIA, DECEMBER 7-9, 2023**

Maksimović N., Milutinović M., Labus Zlatanović D., Baloš S.

MIKROTVRDOĆA I MIKROSTRUKTURALNA ANALIZA FERITNOG NERĐAJUĆEG ČELIKA U DEFORMISANOM STANJU

Rezime: *U oblasti medicine i stomatologije poslednjih godina uvedene su mnogobrojne naučne i tehnološke inovacije. Primena kompjuterski zasnovanih inženjerskih tehnika omogućila je značajno poboljšanje u performansama i dizajnu biomedicinskih komponenti, uključujući implantate i proteze. Inkrementalno formiranje u jednoj tački (SPIF), omogućava ekonomičnu proizvodnju ovih komponenti „po meri". SPIF tehnologija se koristi za proizvodnju metalne bazne ploče (okvira) kompletne maksilarne (gornje) proteze za zamenu tradicionalne protetske procedure zasnovane na tehnici izgubljenog voska, koja je dugotrajna i zahteva mnogo ručnog rada. SPIF proces je u potpunosti dizajniran u digitalnom okruženju sa fokusom na postizanje visoke tačnosti i kvaliteta dela praćenog eksperimentalnom verifikacijom. Za validaciju, formirani deo je upoređen u pogledu geometrije i mehaničke čvrstoće sa referentnim delom proizvedenim tehnikom izgubljenog voska. Dobijeni rezultati su potvrdili visoku dimenzionalnu tačnost i dobru čvrstoću dela napravljenog od SPIF-a. Eksperimentalna istraživanja su uključivala i analizu stanjivanja lima, hrapavosti površine i mikrostrukture.*
Ključne reči: *proteze, deformisanje, deformaciono ojačavanje*

1. UVOD

Proteze su pokretne zubne nadoknade po meri koje se široko koriste. Polimetil metakrilat (PMMA), ima dobre estetske karakteristike, obradivost, biokompatibilnost i dovoljnu čvrstoću [1]. Njegova niska cena i laka popravka u slučaju oštećenja su dodatne prednosti proteza od PMMA. Međutim, PMMA proteze su sklone krtom lomu tokom rada zbog niskog zamora na savijanje i otpornosti PMMA na udar, kao i prisustva mikro-pukotina i drugih strukturnih oštećenja unutar materijala. Upravo zbog toga su napravljene različite strukturne modifikacije PMMA, kao i ojačanja različitim materijalima sa ciljem da se poboljšaju mehanička svojstva proteze. Jedan od najefikasnijih načina da se smanji rizik od preloma je ojačanje baze proteze metalnom pločom. Ovako projektovane proteze imaju centralno jezgro (okvir) koje se izrađuje po meri od metalnih legura, potom se dodaje akrilna smola koja zamenjuje potporna tkiva i veštački zubi. Proteze sa metalnim okvirom nude niz prednosti, uključujući povećanu krutost i otpornost na lom, dobar odnos zapremine i čvrstoce, dobru adaptaciju na potporna tkiva, visoku toplotnu provodljivost i pouzdanost u upotrebi. Za izradu livenih metalnih okvira konvencionalno se koristi tehnika livenja voštanih uzoraka, što je složena i dugotrajna procedura [2]. Stoga je neophodan prelazak sa postojeće procedure na nove, u kojima bi se ručni rad tehničara smanjio i zamenio automatizovanim procedurama. Tokom prethodnih godina, oblast dentalne medicine doživljava dinamične i značajne promene kao rezultat sveobuhvatnog tehnološkog razvoja. Promene se ne dešavaju samo u pogledu novih materijala, već i u pogledu načina na koji se stomatologija praktikuje. Danas se projektovanje zubnih nadoknada i procedure za njihovu izradu često izvode u digitalnom okruženju korišćenjem različitih kompjuterski podržanih (CAx) tehnika i uz pomoć tehnika medicinskog snimanja (kompjuterska tomografija (CT) i magnetna rezonanca (MRI)) [3]. Fleksibilne proizvodne tehnologije treba, stoga, da se koriste za postizanje isplative i efikasne proizvodnje ovih komponenti. U tom smislu, inkrementalno oblikovanja limova (ISF), kao što je inkrementalno deformisanje u jednoj tački (SPIF), su numerički kontrolisani, inovativni i veoma fleksibilni procesi, koji su prvenstveno razvijeni da zadovolje sve veće zahteve za izradu prototipa kao i proizvodnju malih serija u automobilskoj industriji [5].

Za razliku od konvencionalnih procesa oblikovanja limova, koji se izvode kao jednotaktni proces sa specijalizovanim alatima, SPIF je proces oblikovanja koji se vrsi bez kalupa u više prolaza u kojem univerzalni alat sa sferičnim vrhom deluje na malu površinu osnovne ploče od lima. CNC masina kontrolise put alata. Pošto se uzorak SPIF lima postepeno deformiše nizom lokalnih deformacija, ova metoda omogućava obradu materijala koji se teško deformišu, kao što su nerđajući čelik, titanijum i njegove legure. Dalje prednosti su kvalitet i manje sile oblikovanja,

habanje alata, kao i smanjenje buke i otpada materijala. Moguće je proizvesti različite biomedicinske komponente tankih zidova i od metala i od polimera. Međutim, glavni nedostatak SPIF-a u poređenju sa konvencionalnim dubokim izvlačenjem je relativno dugo vreme obrade i niža tačnost dimenzija.

U poređenju sa titanijumom i legurama titanijuma, nerđajući čelici pokazuju bolja mehanička svojstva, deformabilnost, stabilnost dimenzija, imaju izuzetno velika izduženja koja mogu dostići 50% i više, dok većina legura titanijuma ima izduženje pri kidanju manje od 15% i manje elastične deformacije [5]. Zbog toga, ploče proteza od nerđajućeg čelika pokazuju manje elastično opružanje nakon formiranja. Nasuprot tome, visok odnos granice tečenja i zatezne čvrstoće Rp/Rm, uglavnom preko 90%, čini legure titanijuma nepovoljnim za hladno oblikovanje. Danas su brojni medicinski instrumenti, uređaji, implantati i proteze napravljeni od nerđajućeg čelika. Ovi materijali su takođe pogodni za upotrebu u stomatologiji, na primer, za proizvodnju ortodontskih žica, baznih ploča za proteze i delimičnih kopči za proteze, itd, s obzirom da mogu da zadovolje sve kliničke zahteve za biomedicinske komponente [6].

Uzimajući u obzir prethodno navedeno, glavni cilj ovog rada je ispitivanje i karakterizacija mehaničkih svojstava i mikrostrukture osnovne ploče proteze za kompletnu maksilarnu protezu dobijenu SPIF tehnologijom. Izvršena je metalografska karakterizacija materijala nakon deformisanja, kao i analiza raspodele mikrotvrdoće.

2. EKSPERIMENTALNI DEO

Realizacija eksperimenta razvijenog SPIF procesa za izradu zubnih baznih ploča od čeličnog lima X6Cr17 izvedena je na 3-osnoj CNC vertikalnoj glodalici. Alat za oblikovanje sa poluloptastim vrhom i konstantnim poprečnim presekom izrađen je od alatnog čelika X165CrMoV12, tvrdoće 62 HRC, u fino brušenom i poliranom stanju. Stezni pribor je montiran na mašinski radni sto. Podloga je napravljena od šperploče, dok je meki čelik C60 korišćen za okvir, držač praznog dela i osnovnu ploču. I glava alata i površina obratka su podmazani konvencionalnim mineralnim uljem. Nakon formiranja, obradci su isečeni mašinom za lasersko sečenje da bi se dobila geometrija završnog dela.

Na SPIF gotovom uzorku izvršena je metalografska priprema. Uzorak je isečen prema šemi prikazanoj na slici 1, pri čemu su rezovi označeni brojevima od 1 do 7. Priprema uzorka se sastojala od sečenja, brušenja, poliranja i nagrizanja. Brušenje je obavljeno pomoću kompleta abrazivnog papira različite granulacije (P150, P240, P360, P500, P600, P800, P1000, P1500 i P2400, od najgrubljeg do najfinijeg). Poliranje je sprovedeno korišćenjem Buehler dijamantskih suspenzija, počevši od 6, zatim 3, 1 i ¼ mm. Na kraju, nagrizanje je urađeno Carskom vodom (17% HNO_3, 50% HCl u glicerinu). Metalografsko ispitivanje je izvršeno na svetlosnom mikroskopu Leitz Orthoplan. Transmisiona elektronska mikroskopija (TEM) je urađena na skenirajućem transmisionom elektronskom mikroskopu (STEM) JEOL JEM-2010F. Nakon metalografskog ispitivanja, izvršeno je merenje mikrotvrdoće po Vikersu.

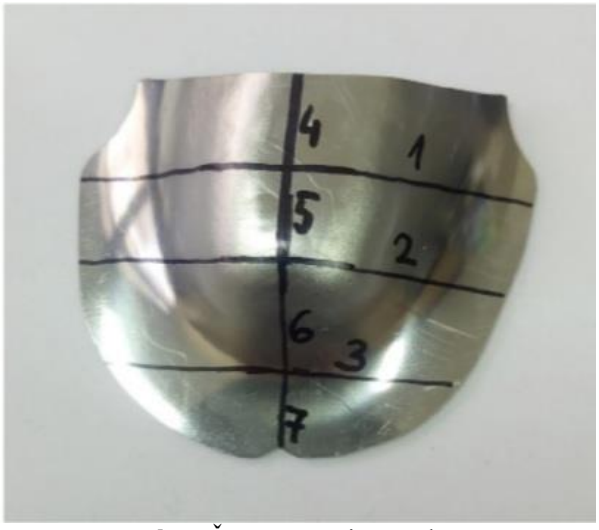

Sl. 1. Šema sečenja uzorka

3. REZULTATI I DISKUSIJA

3.1 Rezultati mikrotvrdoće po Vikersu

Rezultati ispitivanja mikrotvrdoće po Vikersu su prikazani na slici 2. Može se videti da postoje značajne razlike između preseka. Najveća vrednost mikrotvrdoće dobijena je u bočnom preseku 2, a zatim u presecima 4, 6 i 5, gde je postignut značajan stepen plastične deformacije. Najniža vrednost je dobijena u delu 7, gde je izvršena najmanja plastična deformacija. Ovo značajno povećanje mikrotvrdoće, koje se više nego udvostručilo između sekcija, može se pripisati deformacionom ojačavanju.

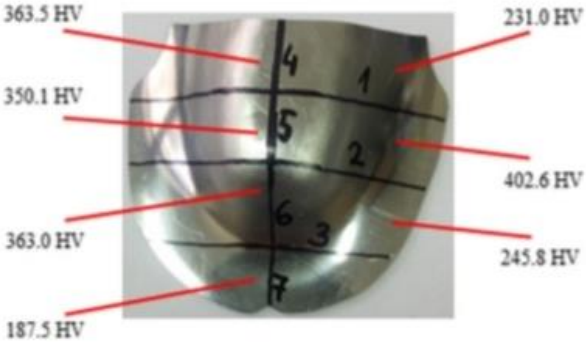

Sl. 2. Prosečne vrednosti mikrotvrdoće u različitim presecima uzorka

3.2 Rezultati ispitivanja svetlosnim mikroskopom

Rezultati mikrostrukturne analize preseka 1 i 2 prikazani su na slici 3. Iako su uzeti iz različitih preseka, ne mogu se uočiti značajne morfološke razlike: prisutna su poligonalna feritna zrna. Ipak, iako su uzorci uzeti iz dve susedne oblasti, u preseku 2 se mogu primetiti nešto sitnija feritna zrna (slika 3b u odnosu na a).

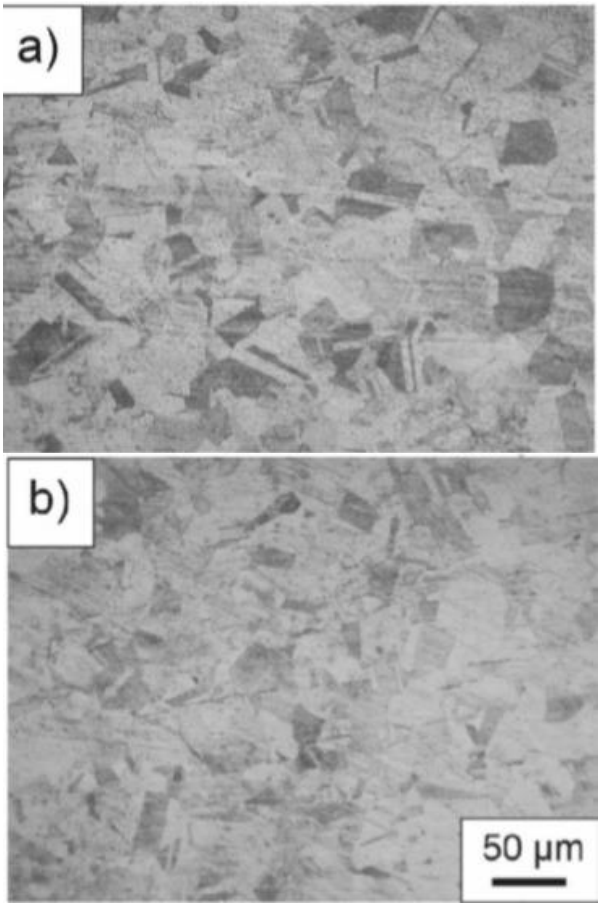

Sl. 3. Mikrostruktura materijala: a) preseka 1, b) preseka 2

Ako se ovi rezultati uporede sa rezultatima dobijenim ispitivanjem mikrotvrdoće, slika 2, pri čemu su u preseku 2 dobijene značajno veće vrednosti sasvim je jasno da je došlo do deformacionog ojačavanja. Međutim, sama morfologija mikrostrukture, odnosno krupnoća samih zrna ne ne sugeriše da je razlika u mikrotvrdoći gotovo dvostruka: 402,6 (presek 2) u odnosu na 231 HV (presek 1). Kako bi se dokazali uzroci značajnog porasta mikrotvrdoće, izvršena je analiza na STEM mikroskopu, što je dato u sledećem poglavlju.

3.3 Rezultati dobijeni na STEM

Rezultati STEM analize su prikazani na slici 4. Na oba uzorka se mogu uočiti dislokacione substrukture koje formiraju subzrna (slika 4b). Na slici 4a (presek 1), vidi se da su prisutne dislokacije u gornjem zrnu (do izlomljene linije – granica grna), čija gustina nije velika. Međutim, u donjem zrnu, ispod granice zrna, prisustvo dislokacija je ograničeno, što znači da je prenos napona iz gornjeg u donje zrno ograničen, što znači da je došlo do deformacije, ali da je ona relativno mala. S druge strane, na slici 4b se vidi značajno veći broj isprepletenih dislokacija, koje su rezultat znatno veće deformacije na uzorku 2. Oblik dislokacija na slici 4 je karakterističan za Frank-Readov izvor displokacija, što je u skladu sa rezultatima dobijenim od strane autora Shimokawa i Kitada [7]. Osim toga, na slici 4b se sa leve strane vidi tamnija linija koja verovatno predstavlja splet displokacija (velika gustina displokacija) koji formira granicu subzrna. Ove granice subzrna se ne vide na svetlosnom mikroskopu, jer se zahteva značajno veće uvećanje od prikazanog na slici 3 (200x). Upravo se u pojavi subzrna i značajno veće gustine displokacija treba tražiti uzrok značajno veće mikrotvrdoće kod uzorka 2 u odnosu na uzorak 1, čime se dokazuje značaj elektronske mikroskopije, naročito transmisione u karakterizaciji materijala, čak i pri relativno jednostavnim eksperimentima kao što je prikazan u ovom radu. Dakle, uzroke povećanja mikrotvrdoće treba tražiti u deformacionom ojačavanju i ojačavanju granicama zrna, odnosno subzrna.

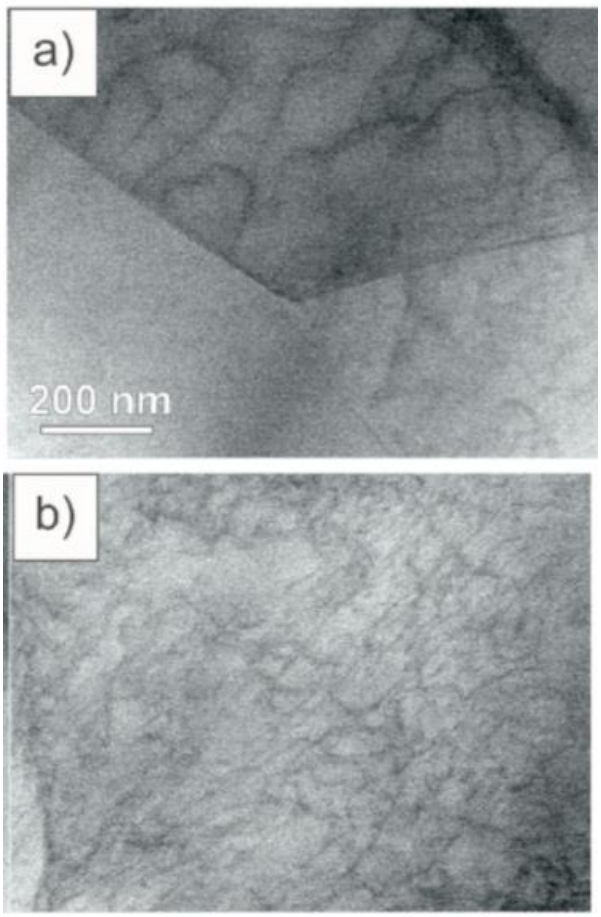

Sl. 4. Prikaz dislokacija na STEM: a) presek 1, b) presek 2

4. ZAKLJUČCI

Na osnovu dobijenih rezultata, može da se zaključi:

- SPIF postupak deformisanja pokazao se vrlo efikasnim u pogledu dobijanja oblika od nerđajućeg čelika
- Mikrotvrdoće značajno variraju, što zavisi od stepena deformisanja
- Svetlosna mikroskopija je pokazala manje razlike u morfologiji i krupnoći zrna
- STEM mikroskop se pokazao kao izuzetno značajna metoda karakterizacije, koja je pokazala da se značajno povećanje mikrostvrdoće može pripisati deformacionom ojačavanju i ojačavanju granicama zrna, odnosno subzrna.

5. ZAHVALNICA

Ovaj rad je rezultat rada autora u okviru projekta pod naslovom „Savremeni materijali, tehnologije spajanja i srodni postupci“ Laboratorije za ispitivanje materijala i Laboratorije za zavarivanje, Departmana za proizvodno mašinstvo, Fakulteta tehničkih nauka.

6. REFERENCE

[1] Balos S, Milutinovic M, Potran M, Vuletic J, Puskar T, Pepelnjak T. *The mechanical properties of moulded and thermoformed denture resins*. Strojniski Vestnik - Journal of Mechanical Engineering, 61, p.p. 138-145, 2015.

[2] Postic S. *Design of complete denture reinforced with metal base*. Serbian Dental Journal, 60, p.p.15-20, 2013.

[3] Gibson I. *Advanced manufacturing technology for medical applications*. Wiley ed.; 2005.

[4] Tanaka S, Nakamura T, Hayakawa K, Nakamura H, Motomura K. *Incremental sheet metal forming process for pure titanium denture plate*. In: Bariani P, editor. *Advanced technology of plasticity*. Proc. 8th ICTP, Verona, p.p. 135-136, 2005.

[5] Adamus J, Lacki P, Motyka M, Kubiak K. *Investigation of sheet-titanium drawability*. In: Zhou L, editor. Ti-2011: proceedings of the 12th world conference on titanium, June 2011, *China national convention center (CNCC)*. Beijing. Beijing: Science Press Beijing; 2012.

[6] Alla RK, Swam R, Vyas R, Konakanchi A. *Conventional and contemporary polymers for the fabrication of denture prosthesis: part I-overview, composition and properties*. International Journal of Applied Decision Sciences, 1 ,82-90, 2015.

[7] Tomotsugu Shimokawa, Soya Kitada, *Dislocation Multiplication from the FrankRead Source in Atomic Models*, Materials Transactions, 55, p.p. 58 – 63, 2014.

Autori:
Sar.u nas. Nikola Maksimović, red.prof. Mladomir Milutinović, doc. Dr Danka Labus Zlatanović, red. Prof. Sebastian Baloš, Univerzitet Novi Sad, Fakultet Tehničkih Nauka, Trg Dositeja Obradovica 6, 21000 Novi Sad, Serbia, Tel: +381 21 485 2320, Fax: +381 21 454-495.
E-mail: maksimovic2000nikola@gmail.com
mladomil@uns.ac.rs
danlabus@uns.ac.rs
sebab@uns.ac.rs

ETIKUM 2023 **INTERNATIONAL SCIENTIFIC CONFERENCE NOVI SAD, SERBIA, DECEMBER 7-9, 2023**

Marinković, D., Milošević, A., Knežev, M, Mlađenović, C.

PRORAČUN ELEMENATA I CAE ANALIZA MAŠINSKE STEGE

Rezime: *Mašinska stega je stezni pribor koji služi za stezanje i pozicioniranje obradaka na mašinama alatkama, te dovođenje alata i obratka u ispravan međusobni položaj. Kako bi se obezbedilo mirovanje radnog predmeta u toku obrade, mašinska stega treba da ostvari odgovarajuću silu stezanja. Sila stezanja je potrebna količina sile pri kojoj se radni predmet neće pomerati izvan dozvoljenih granica tolerancije u toku obrade. Do deformacija radnog predmeta ili elemenata stege dolazi usled njihovog prekomernog dinamičkog opterećenja, zbog čega se izvodi proračun mašinskih elemenata stege. Analiza dinamičkog ponašanja elemenata mašinke stege izvedena je pomoću računarske metode konačnih elemenata uz primenu odgovarajućeg softvera. Ova metoda se koristiti za izračunavanje naprezanja, deformacija, pomeranja itd. Cilj ovog rada bilo je pronalaženje rešenja za usavršavanje sistema stezanja mašinskim stegama, kao i načina ponašanja mašinske stege pri određenim opterećenjima.*
Ključne reči: *mašinska stega, pribori, dinamička analiza sistema*

1. UVOD

Kada je reč o obradi materijala jednu od veoma važnih uloga ima tehnika stezanja materijala. Još od davnina, kako bi se povećala snaga i stabilnost, u poređenju sa držanjem predmeta rukom, korišćena je baš ova tehnika uz pomoć klina i čekića. Vremenom je i tehnologija napredovala, tako je u srednjem veku došlo do početnih promena uvođenjem drvenih stega sa navojima. Alat koji se tada koristio imao je klizne čeljušti koje su se kretale horizontalno po podesivim prorezima. Kako je vreme prolazilo, uz razvoj industrije pojavila se i potreba za projektovanjem mašinski stega sa visokom tačnošću stezanja i pozicioniranja. Mašinska stega predstavlja jedan od najboljih mehaničkih alata koji se koristi za stezanje obradaka u gotovo svim radionicama. Tokom proizvodnih ili mašinskih operacija, držanje ili stezanje radnog komada je osnovni zadatak kako bi se sam proces obrade mogao ostvariti [1].

U procesima obrade rezanjem, naročito tankozidnih obradaka, najčešće se javljaju deformacije i pomeranja obradaka usled velikih vrednosti sila rezanja . Ova pojava ograničava preciznost i tačnost obrade i dovodi do moguće pojave škarta u proizvodnji. S druge strane, nedovoljna dinamička krutost sistema pri stezanju obradka često uzrokuje neželjene regenerativne vibracije, koje rezultiraju lošim kvalitetom površine, a takođe i one mogu čak i oštetiti ili uništiti obradke [2].

Bansal i saradnici [3] razvili su osnovni pristup za identifikaciju odgovarajućih konfiguracija stezanja i bio je zasnovan na analizi i klasifikaciji radnih predmeta i karakteristika obrade procesom rezanja. Kombinovan je metod za izdvajanje i grupisanje karakteristika obrade iz CAD modela sa razvijenim eskpertnim sistemom koji je uključivao operacije obrade, uslove okoline, alate i radne predmete kako bi klasifikovao i konfigurisao stezne elemente. Uz pomenuto, predstavili su i STEP baziranu razmenu podataka sa izvedenim komponentama i karakteristikama obrade, kao i sistem konfiguracije s obzirom na stabilnost, pristupačnost i tačnost koncepta stezanja.

Na tačnost i preciznost obrade direktno utiče dizajn steznih čeljusti, kao i samog sklopa stege, kako je u svom radu predstavio Nakajima [4]. Dizajn mašinskih stega nije uobičajen predmet rasprave u naučnim krugovima, delimično zbog autorskih prava na dizajn, što znači da kompanija koja se oslanja na dizajn svojih produkata da bi unapredila svoju proizvodnju obično drži u tajnosti znanje i stručnost postignutu višegodišnjom praksom.

2. PRORAČUN ELEMENATA MAŠINSKE STEGE

Mašinske stege se obično izrađuju od dva materijala. Čeljusti, klizači, telo stege pretežno se izrađuju od visoko kvalitetnog livenog gvožđa, dok su površine čeljusti, ručka i zavrtnji izrađeni od čelika. Liveno gvožđe je legura gvožđa koja ima grafitnu mikrosturkturu i sastoji se od 95% gvožđa, 3% silicijuma i 2% ugljenika. Liveno gvožđe ima visoku čvrstoću pod pritiskom, visoku otpornost na habanje i visok kapacitet prigušenja vibracija pa je veoma pogodan materijal za izradu

delova mašinske stege budući da oni zahtjevaju visoku pouzdanost i visok stepen prigušenja vibracija. Kaljeni čelik je veoma pogodan materijal za izradu ručke i zavrtnja mašinske stege jer ima visoku zateznu čvrstoću i dobru otpornost na koroziju. Pretežno se primjenjuju kaljeni čelici sa većim sadržajem ugljenika i hrom-karbida koji povećavaju otpornost na habanje.

Proračun mašinskih elementa obuhvata izbor: materijala, oblika i dimenzija mašinskih delova koji ulaze u sastav mašinskog elementa ili izbor standardnih delova iz odgovarajućih razvijenih familija. Proračun elemenata mašinske stege se odnosi na proračun osnovnih elemenata koji predstavljaju delove mašinske stege opterećene silom *F*.

2.1 Opterećenja elemenata mašinske stege

Radni predmet pozicioniran i stegnut između čeljusti mašinske stege u toku procesa obrade izložen je dinamičkim opterećenjima,a samim tim, dinamička opterećenja se prenose i na elemente stege. Popustljivosti veze između elemenata za stezanje i radnog predmeta, pri dejstvu sila rezanja, ima veliki uticaj na kvalitet obrade. Popustljivost veze između elemenata stege i radnog predmeta se javlja usljed deformacija radnog predmeta ili elemenata stege, pod dejstvom svih sila koje djeluju na radni predmet u toku obrade (sile rezanja, sile stezanja, reakcije oslonaca, gravitacione sile, sile zemljine teže, sile trenja). Do deformacija radnog predmeta ili elemenata stege dolazi usljed njihovog prekomijernog dinamičkog opterećenja. Sklop funkcionisanja mašinske stege prikazan je na slici 1.

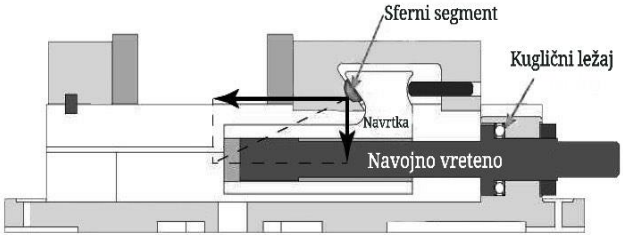

Sl. 1. Opterećenje elemenata mašinske stege

2.2Dimenzionisanje navonog vretena

Da bi se izvršilo dimenzionisanje navojnog vretena prvo je potrebno izvršiti prethodni proračun navojnog vretena po merodavnim kriterijumima i usvojiti potrebne dimenzije navojnog vretena. Nakon toga se radi završni proračun, kojim se potvrđuje da je usvojena dimenzija navojnog vretena dobra.

2.3 Prethodni proračun navojnog vretena

Dimenzionisanje navojnog vretena se vrši na osnovu sile i dužine. Zadati podaci: F = 10 000 N, l = 500mm i materijal čelik E295. Navojno vreteno se dimenzioniše sa obzirom na normalni napon usled zatezanja ili pritiskanja. Na osnovu čvrstoće navojnog vretena usvojen je trapezni navoj **Tr16x4** sa dimenzijama: d_2=14 mm; d_3=11,5 mm; A_3=104 mm^2; H_1=2 mm; P=4 mm. Na osnovu izvijanja navojnog vretena usvojen je trapezni navoj Tr20x4 sadimenzijama:d_2=18 mm; d_3=15,5 mm; A_3=189 mm2; H_1=2 mm; P=4 mm.

Na osnovu prethodnog proračuna, usvojen je trapezni navoj - **Tr*20*×4**, sa karakterističnim dimenzijama potrebnim za dalji proračun: d_2 = 18 mm, d_3 = 15,5 mm, A_3 = 189 mm^2, H_1 = 2 mm, P = 4 mm. Materijal navojnog vretena je čelik E295 i njegove karakteristike su: $\sigma_K = R_{eH}$ = 295 N/mm^2 za zatezanje, $\tau_K = \tau_T$ = 200 N/mm^2 za uvijanje, R_m= 500 N/mm^2, E = 2,1*10^5N/mm^2. Usvojena dužina navrtke - L_n=36 mm. Materijal navrtke sa karakteristikom -p_{doz} = 12 N/mm^2, za čelik.

2.4 Proračun zavrtnjeva

S obzirom da se mašinska stega koristi za stezanje radnog predmeta pri postupcima obrade bušenjem i glodanjem, pri kojima se javljaju različiti otpori rezanja, a samim tim i različita opterećenja zavrtnjeva pri stezanju, izvršen je proračun zavrtnjeva pri bušenju i pri glodanju.

Na osnovu prethodnog proračuna, odnosno sile prethodnog pritezanja, momenta savijanja i minimalnog efektivnog preseka zavrtnja, usvojen je metrički navoj M8 sa osnovnim karakteristikama: A_s = 36,6mm^2 ; P =1,25mm; d_2 = 7,188 mm; d_3 = 6,466mm; φ=3,17°; zavrtnji su izrađeni od čelika klase čvrstoće 8.8 sa karakteristikama R_{eH} = 640 N/mm^2; τ_t = 390 N/mm^2. Završnim proračunom, ustanovljeno je da metrički navoj M8 zadovoljava stepene sigurnosti na kraju pritezanja i stepen sigurnosti zavrtnja u radu.

2.5 Dimenzionisanje ručice

Dužina ručice proračunava se prema ukupnom obrtnom momentu T i ručnoj sili kojom se treba ostvariti taj moment. Ručna sila se uzima 150 - 250 N za duži rad, odnosno 300 – 400 N za kraći rad, u slučaju manjih visina dizanja. Stepen sigurnosti se usvaja S =3, u odnosu na zateznu čvrstoću, kada je dovoljno spriječiti lomljenje ručice.Na osnovu tih parametara usvojena je dužina ručice L=180 mm i prečnik ručice d_r=13mm.

3. RAČUNARSKA ANALIZA MAŠINSKE STEGE

Za računarsku analizu korišćen je CAD model mašinske stege prikazan na slici 2.

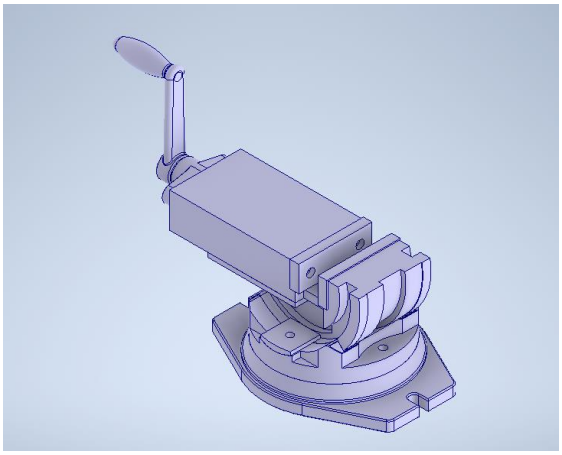

Sl. 2. CAD model projektovane mašinske stege

3.1. CAE analiza mašinske stege

Nakon definisanja modela potrebno je CAD model iz programskog sistema za modelovanje prebaciti u programski sistem za obradu metodom konačnih elemenata, pomoću neutralnog STEP formata. Nakon toga potrebno je izvršiti definisanje mreže konačnih elemenata, odnosno, diskretizaciju sistema. Diskretizacija je proces podjele domena na konačne elemente i predstavlja jedan od najvažnijih koraka u analizi metodom konačnih elemenata s obzirom da od veličine i vrste elemenata i načina diskretizacije direktno zavise rezultati analize. Cilj diskretizacije sistema je da što vernije definiše oblik i ponašanje realnog fizičkog sistema. U ovom slučaju diskretizacija je izvršena automatskim generisanjem mreže, kao što je prikazano na slici 3 [5].

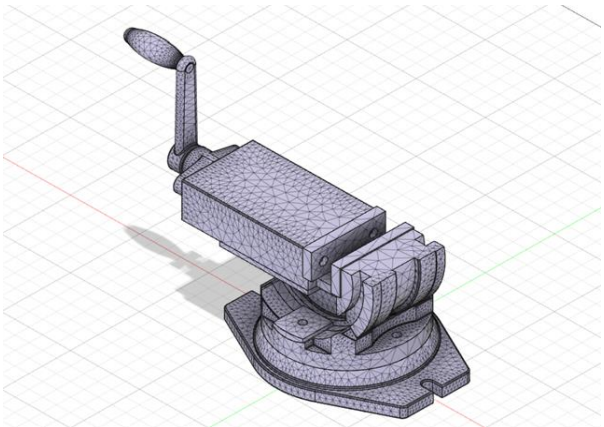

Sl. 3. Mrežni model mašinske stege

Bitnu ulogu pri analizi ima i definisanje mehaničkih osobina materijala. Programski sistemi za analizu metodom konačnih elemenata omogućavaju korišćenje različitih materijala. Da bi se izvršila analiza mašinske stege potrebno je uspostaviti vezu između svih njenih elemenata i definisati opterećenja i ograničenja elemenata. Postolju stege su oduzeti svi stepeni slobode kretanja odnosno ograničeno je translatorno pomeranje postolja u svim pravcima X, Y, Z osa, kao i sve rotacije postolja oko X, Y, Z osa. Na unutrašnjim stranama čeljusti u X pravcu je definisano opterećenje u vidu sile od 10 000 N, kao što se vidi na slici 4.

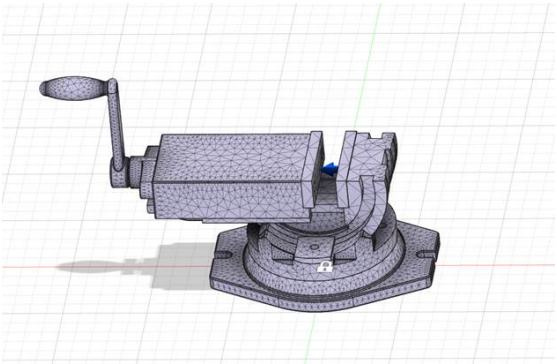

Sl. 4. Prikaz definisanih opterećenja i ograničenja elemenata mašinske stege

Nakon procesiranja (rešavanja postavljenog matematičkog modela) sledi prikupljanje dobijenih informacija i vizuelizacija dobijenih rezultata analize. Pri postprocesiranju podaci se mogu prikazati u dva oblika: numeričkom (rezultati su dati u vidu listinga) i grafičkom (rezultati se predstavljaju u formi grafičkog prikaza). Na slici 5 je dat grafički (konturni) prikaz rezultata analize pomeranja mašinske stege,koji omogućuje vizuelizaciju fizičke veličine na taj način što se određenim vrednostima dodjeljuju odgovarajuće boje. Dobijeni rezultati analize pokazuju da su pomijeranja kompletnog sklopa mašinske stege pri opterećenju horizontalnom silom intenziteta 10kN veoma mala, iznosit 0,02776 mm, i da je zadovoljen ukupan stepen sigurnosti.

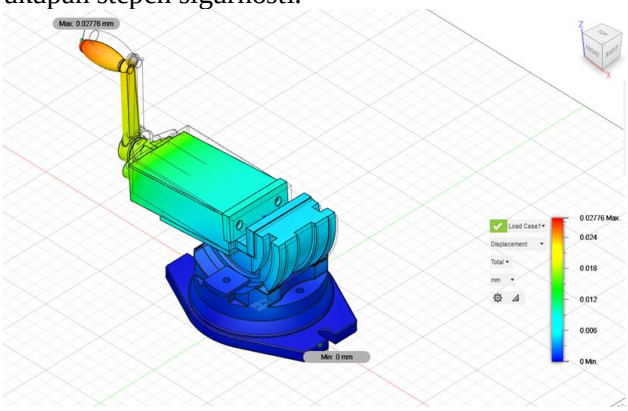

Sl. 5. Prikaz rezultata pomeranja pri deformaciji mašinske stege

Na osnovu dobijenih rezultata može se zaključiti da svi projektovani elementi sklopa mašinske stege zadovoljavaju funkcionalne kriterijume. Međutim, veliki broj složenih elemenata od kojih je stega izgrađena mogu uticati na pojavu vibracija u toku procesa obrade. Veza između elemenata mašinske stege i radnog predmeta direktno utiču na kvalitet obrade. Tako u slučaju prekomernih dinamičkih opterećenja koja se u toku procesa obrade prenose sa radnog predmeta na elemente mašinske stege može doći do deformacija ili prekomernih vibracija pojedinih elemenata. Budući da se mašinska stega sastoji od velikog broja složenih elemenata koji osim što utiču na mogućnost pojave vibracija u toku obrade utiču i na poskupljenje samog procesa izrade stege i otežavaju montažu.

4. ZAKLJUČAK

Držanje ili stezanje radnog predmeta u toku obrade predstavlja osnovu za ostvarenje samog procesa obrade. Mašinska stega predstavlja jedan od najznačajnijih mehaničkih alata koji se koristi za pozicioniranje i stezanje obradaka na mašinama alatkama u toku procesa obrade. Radni predmet je u toku procesa obrade izložen dinamičkim opterećenjima koja se prenose i na elemente stege pa je pri projektovanju mašinske stege neophodno izvršiti detaljan proračun svih elemenata koji su izloženi dinamičkim opterećenjima. S obzirom da se stezanje radnog predmeta ostvaruje pomeranjem pokretne čeljusti prema nepokretnoj pomoću navojnog vretena i navrtke izvršen je detaljan proračun navojnog vretena koje trpi najveća opterećenja, ali i detaljan proračun zavrtnjeva i ručice koji zajedno sa navojnim vretenom i navrtkom obezbeđuju zaključavanje čeljusti. Proračun mašinskih elemenata se odnosi na izbor materijala, oblika i dimenzija mašinskih delova. Proračunom elemenata mašinske stege usvojene su dimenzije svih njenih elemenata na osnovu kojih su definisana geometrijska obeležja stege. Na osnovu izmodeliranog sklopa izvršena je analiza kojom je utvrđeno da svi elementi sklopa zadovoljavaju odgovarajuće kriterijume u pogledu funkcionalnosti.

5. ZAHVALNICA

Ovo istraživanje je podržano od strane Ministarstva prosvete, nauke i tehnološkog razvoja kroz projekat broj 451-03-68/2022-14/ 200156 „Inovativna naučna i umetnička istraživanja iz domena delatnosti FTN-a“.

6. REFERENCE

[1] Milošević, A..: *Projektovanje elemenata mašinske stege primenom CAE tehnologije*, Diplomski rad, Fakultet tehničkih nauka Univerziteta u Novom Sadu, 2021.

[2] Feng, Q., Maier, W., Stehle, T., Mohring, H.: *Optimization of a clamping concept based on machine learining*, Production Engineering, p.p. 1-14, 2021.

[3] Bansal, S., Nagarajan, S., Reddy N.V.: *An integrated fixture planning system for minimum tolerances*, Int J Adv Manuf Technol p.p 501-513, 2008.

[4] Nakajima, T., Ohsaki, M., Fujiwara, J., Takeda, F.: *Configuration optimization of clamping memebers of frame-supported membrane structures*, Proceedings of the International Association for Shell and Spatial Structures (IASS) Symposium, 2010.

[5] Knežev, M., Živković, A., Mlađenović, C., Marinković, D., Ilić, V., Moravec, M.: *Finite element and experimental modal analysis of high speed spindle*, 16th International Conference on Accomplishments in Mechanical and Industrial Engineering, pp. 60-63, 2023.

Autori: **Ass. msr Dejan Marinković, Ass. msr Aleksandar Milošević, Ass. dr Miloš Knežev, Ass. Prof. dr Cvijetin Mlađenović**
Univerzitet Novi Sad, Fakultet Tehničkih Nauka, Trg Dositeja Obradovica 6, 21000 Novi Sad, Serbia, Tel: +381 21 485 2350, Fax: +381 21 454-495.
E-mail: dejan.marinkovic@uns.ac.rs
aleksandar.milosevic@uns.ac.rs
knezev@uns.ac.rs
mlađa@uns.ac.rs

ETIKUM 2023 **INTERNATIONAL SCIENTIFIC CONFERENCE**
NOVI SAD, SERBIA, DECEMBER 7-9, 2023

Matin, I., Štrbac, B., Hadžistević, M., Ranisavljev, M.

MOLD DESIGN OF MODULAR INJECTION MOLDS

Abstract: *The injection molding enables the production of complex shaped parts, thanks to the accurate narrow tolerances of the mold. This process is suitable for mass production, leading to reduced single part costs, but involves high initial investments. The life of a mold can be increased by exploiting variable cavity inserts. So, a design method has been conceived for modular injection molds by integrating CAD/CAE technique. From the early phases of design approach, the simulation models are configured with the different geometries as requested by design specifications. The mold components are designed with standard generic features in order to be fast exchanged. The modular mold should be reconfigurable as to manufacture two different but similar parts.*
Key words: *modular mold, CAD, injection molding, plastic*

1. INTRODUCTION

Injection Molding (IM) is a manufacturing technology suitable to produce cost effective and ready-to-use plastic parts without postprocessing. However, due to the high fixed costs of the injection molding system [1, 2], it is generally used for mass production series. In fact, the molds are conceived as integral systems specifically designed for each part, and geometry redesign are generally very expensive or even not possible [2, 3]. Due to the lack of flexibility of the molding system, IM is not suitable to address the current market demand of high product customization [3-5]. This limitation can be faced by conceiving modular molds, capable of producing different but similar parts, by reusing most mold inserts and customizing only a few ones. So, the cost of the mold can be spread over the production of more parts.

To address this challenge, a method for the design of modular molds with the integration of CAD/CAE techniques is presented. CAE became applicable technique for numerical simulation of IM process and mold design calculus [6, 7]. In industry, the IM simulation is mainly limited to cavity filling verification and design validation. However, preliminary simulations in the early design phases of the mold would lead to greater benefits in terms of efficiency and production quality [8-10].

The PTC Mold Design module has been occasionally used for modular mold design with reconfigurable cavity. [8, 11].

The research aims to evaluate the integration of CAD/CAE techniques in a design method for reconfigurable cavities i.e., modular molds [11-17]. As a case study, the design of a mold for the injected molding parts is presented. The mold should be reconfigurable as to produce two different sizes of the same part.

2. MATERIALS AND METHODS

The proposed design method for modular molds integrates consists of following phases:

- Product and process planning: Identification of constraints and requirements; Definition of the parts must be produced with the same mold; Definition of the design specifications of the parts and the appropriate modular mold.
- Parts design: Initial CAD models of the parts; Numerical simulation of the injection molding; Final CAD models and drawings of the parts; Final design of the related mold cavities; Definition of IM machine to be used; Iterative design and simulation review.
- Mold design: Provisional CAD modelling of the mold; Simulation of the mold as for filling, packing, cooling, and shrinkage analysis; Creating mold assembly; Definition of the modular mold layout; Design review and cost verification.
- Parts and mold detail design: Dimensional checks and verification; Final design review; Bill of Materials (BOM) of the mold.
- Mold optimization: Assessment of the modular mold using prototypes; Mold build; Mold testing and verification.

The following main contributions are fundamental in the method:

- Numerical simulation, which aims to detect and evaluate the effectiveness of the designed parts and appropriate mold. CAE enables to anticipate any modifications to the early design

phases, to design the cavity and its layout, and to make an early assessment of the models.

- Mold assembly design that leads to the definition of a layout that facilitates the mold assembly, its manufacturing as well as its modularity, resulting in customized product configuration strategies.

3. CASE STUDY AND RESULTS

The CAD model of the part is presented in Fig.1.

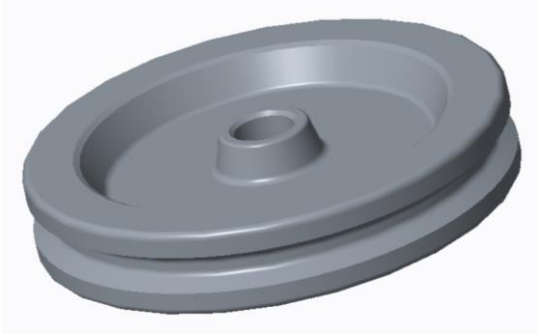

Fig. 1. CAD model of the part

The main issues in the mold design are related with the injection subsystem, cooling subsystem, and ejection subsystem. The reconfigurability goal of the mold is defined, identifying which parts can be produced with the same mold equipment (system). Finally, the mold design specifications are refined, especially for the tolerances of the various components of each mold layer.

The parts are classified in groups (types) in order to explicit common design requirements and constraints that will be addressed by the mold reconfigurability. The design includes generic design using Family Table option in PTC Creo Parametric software. The current design consists of complex part and two appropriate instances (types). In the preliminary analysis, the parts are grouped according to their overall dimensions such as diameter and width in order to properly size the mold cavities. The first type consists of part with a diameter of 180 mm and width of 32 mm. This size is the design constraint that defines the maximum size of the mold. The second type consists of parts with a 160 mm diameter and a 28 mm width. Therefore, the mold has to be modular as to produce both these two different sizes of the same part. The material of the parts is Acrylonitrile butadiene styrene (ABS 650) by Kumho company. This isotropic pure polymer has high impact strength and high mechanical properties in general. Melt Flow index of the selected material is MFI (220,10) = 5g/10min. The CAE critical numerical simulation parameters are presented in Table 1.

Table 1. CAE numerical simulation parameters

Parameters	Value
Maximal injection pressure (MPa)	220
Injection pressure (MPa)	200
Holding pressure (MPa)	200
Injection time (s)	9
Holding time (s)	12
Freeze temperature (°C)	115
Mold Temperature (°C)	55
Ejection time (s)	4
Mold opening time (s)	5
Cooling time (s)	45
Ejection temperature (°C)	109
Cooling medium temperature (°C) for H_2O+20%$C_2H_6O_2$	22
Poison`s ratio	0.39
Maximal melt temperature (°C)	260
Melt temperature (°C)	230

This simulation result is important because cooling time is the most significant role in the cycle time. The diameter of the cooling channel (waterline) is 8 mm. The specialized SAPA modular software is used for selecting all the remaining mold components such as, ejector pin, locating ring, guide pin bush, sprue bush, return pins, and screw. Thereafter the injection filling is simulated with the CAE software PTC Pro/Plastic Advisor in order to evaluate the parts suitability for injection molding (see Table 1). The final models of the parts as well as the design of the related mold cavities is delivered. The all phases start with the iteration of CAD modelling of the mold, CAE numerical simulation (filling, packing, cooling, warpage, shrinkage), designing mold assembly, creating of the modular mold layout as indicated in Fig. 2.

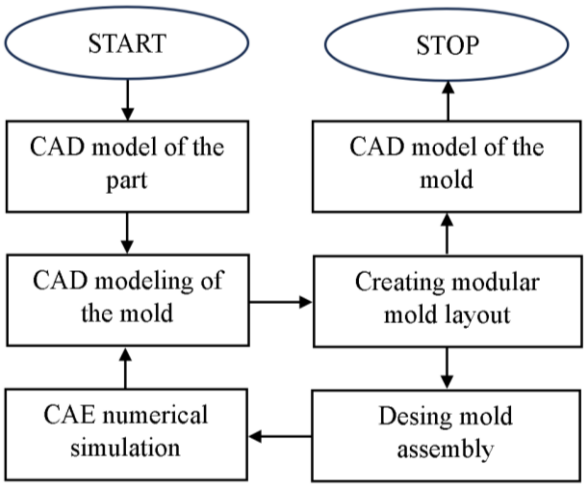

Fig. 2. Iterative cycle of the modular mold design

The CAD model of the modular mold is developed in PTC Creo Parametric and D-M-E mold base, which supports the reuse of standard components. The modelling starts with an initial two cavities mold, with support plates compliant with the current IM machine. The stationary and moveable support plates are both 156 mm height, as necessary to involve the cavities for the complex (generic) part, the cooling channels and the holes for the clamping screws. The CAD model of the stationary plate is shown in Fig. 3.

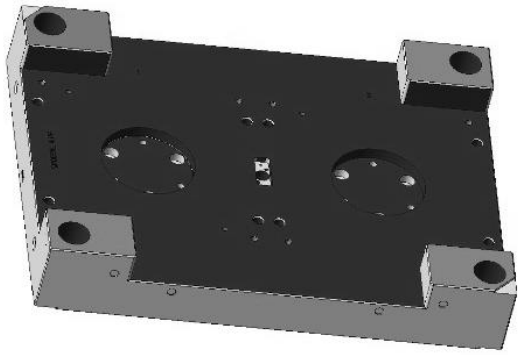

Fig. 3. Fixed plate of the mold

The one of the main components of the mold are the cavity inserts, to be mated together to compose the complete cavity for the molten plastic injection. In order to ensure the interchangeability of the cavity inserts, the same coupling between the various inserts is used. The two cavity inserts are mounting in to mold plate. The position of the insets is presented in mold fixed plate as indicated in Fig. 4.

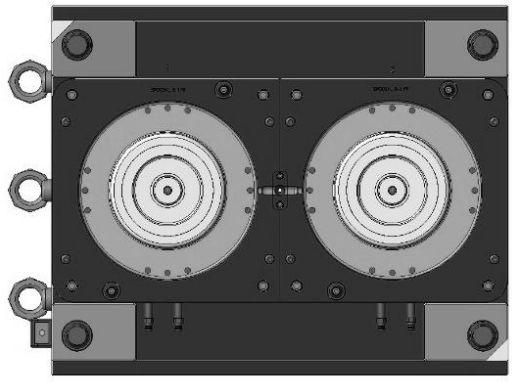

Fig. 4. The two cavity inserts assembled in the mold fixed plate

Based on the dimensions of the simulation model of the part and the type and size of the cooling system, the initial normal mold assembly is selected according to D-M-E standard using SAPA software. The assembly is composed of the following standard mold plates:

- top clamping plate N03,
- clamping plate N04,
- fixed plate N10A,
- movable plate N10B,
- support plate N20,
- risers N30,
- ejector retainer plate N40 and
- ejector plate N50.

The initial diameter of cooling channel is determinate using SAPA software, and the calculated value is verified by numerical simulation. A sprue with an initial nominal diameter of 8 mm is required from matching with the injection nozzle (diameter 5.5 mm). The runners continue horizontally with a diameter sized considering the injection speed and the density of the melt material, and slightly larger than the following gate, in order to avoid pressure drops in the gate area. This would ease the material flow and its separation, while reducing the shrinkage. Furthermore, to enable the cavity inserts interchangeability, all the ejectors in the moving plate. The optimization of the cooling system, thanks to recursive IM simulations, leads to the reduction of the shrinkage. Accordingly, the shrinkage allowance in the cavities is reduced.

4. DISCUSION AND CONCLUSIONS

This paper describes a design method of modular molds for the injection molding of similar plastic parts. A case study on the design of a mold for injection two different sizes the parts is presented. The integration of CAD/CAE techniques from the early design phases enables to conceive a modular mold and to optimize its features, such as the cooling channels, the geometries of the runners and the mold cavity. The determined IM parameters ensure regular and stable manufacture of the quality parts without postprocessing. The cycle time is assumed using numerical simulation. Furthermore, an increase of the expected productivity is achieved, thanks to the reduction of the cycle time.

As future works, other types and sizes of the similar parts are being designed with the same integrated method and will be validated through the same procedures.

5. REFERENCES

[1] Tan, C., Wang, D., Ma, W., Chend Shijin, Chen, Y., Chen, S., Yang, Y., Zhou, K.: *Design and additive manufacturing of novel conformal cooling molds*, Materials and Design, Vol. 196, p.p. 109-119, 2020.

[2] Wang, H., Zhou, X. H., Ruan. X.: *Research on Injection Mould Intelligent Cost Estimation System and Key Technologies*, The International Journal of Advanced Manufacturing Technology, Vol. 3, p.p. 215-222, 2003.
[3] Baldi-Boleda, T., Sadeghi, E., Colominas, C., Garcia-Granada, A.: *Simulation approach for hydrophobicity replication via injection molding*, Polymers, Vol. 13, No. 13, p.p. 1-12, 2021.
[4] Pecas, P., Henriques, E.: *The need for agile manufacturing implementation in mould making business*. Proceedings of Business Excellence I, p.p. 321-326, Universiade do Minho, Braga, 2003.
[5] Galizia, F. G., ElMaraghy, W., ElMaraghy, H., Bortolini, M., Mora, C.: *The evolution of molds in manufacturing: from rigid to flexible*. Procedia Manufacturing, Vol. 33, p.p. 319-326, 2019.
[6] Mahshid, R., Zhang, Y., Hansen, H. N., Slocum, A. H.: *Effect of mold compliance on dimensional variations of precision molded components in multi-cavity injection molding*, Journal of Manufacturing Processes, Vol. 67, p.p. 12-22, 2021.
[7] Szabo, F., Suplicz, A., Kovacs, J. G.: *Development of injection molding simulation algorithms that take into account segregation*, Powder Technology, Vol. 389, p.p. 368-375, 2021.
[8] Matin, I., Vukelić, Đ., Hadžistević, M., Štrbac, B., Lukić, D.: *An integrated approach for design and manufacture of plastic products*, Applied Engineering Letters, Vol. 4, No. 1, p.p. 1-5, 2019.
[9] Geren, N., Akcali, O. O., Bayramoglu, M.: *Parametric design of automotive ball joint based on variable design methodology using knowledge and feature-based computer assisted 3D modelling*, Engineering Applications of Artificial Intelligence, Vol. 66, p.p. 87-103, 2017.
[10] Gaub, H.: *Customization of mass-produced parts by combining injection molding and additive manufacturing with Industry 4.0 technologies*, Reinforced Plastics, Vol. 60, No. 6, p.p. 401-404, 2016.
[11] Singh, G., Verma, A.: *A Brief Review on injection moulding manufacturing process*, Materials Today: Proceedings, Vol. 4, p.p. 1423-1433, 2017.
[12] Miranda, D. A. D., Nogueira, A. L.: *Simulation of an injection process using a CAE tool: Assessment of operational conditions and mold design on the process efficiency*, Materials Research, Vol. 22, No. 2, 2019.
[13] Pugliese, V., Mesa, J., Maury, H.: *Development of a design methodology for reconfigurable injection molds*, The International Journal of Advanced Manufacturing Technology Vol. 90, p.p. 153-166, 2017.
[14] Hohlweck, T., Fritsche, D., Hopmann, C.: *Validation of an extended objective function for the thermal optimisation of injection moulds*, International Journal of Heat and Mass Transfer, Vol. 198, p.p. 123-133, 2022.
[15] Crema, L., Sorgato, M., Lucchetta, G.: *Thermal optimization of deterministic porous mold inserts for rapid heat cycle molding*, International Journal of Heat and Mass Transfer, Vol. 109, p.p. 462-469, 2017.
[16] Torres-Alba, A., Mercado-Colmenero, J., Diaz-Perete, D., Martin-Donate, C.: *A New Conformal Cooling Design Procedure for Injection Molding Based on Temperature Clusters and Multidimensional Discrete Models*, Polymers, Vol. 12, p.p. 154-189, 2020.
[17] Mao, H., Wang, Y., Yang, D.: *Study of injection molding process simulation and mold design of automotive back door panel*, Journal of Mechanical Science and Technology, Vol. 36, No. 5, p.p. 2331-2344, 2022.
[18] Galati, N., Gherardini, F., Guaitoli, C., Vergnano, A.: *Simulation-Based Design of Reconfigurable Moulds for Injection Overmoulding*, Advances on Mechanics, Design Engineering and Manufacturing IV, Lecture notes in Mechanical Engineering, Vol. 4, p.p. 1159–1171, Springer, Cham, 2022.
[19] Guerrier, P., Tosello, G., Hatel, J. H.: *Flow visualization and simulation of the filling process during injection molding*, CIRP Journal of Manufacturing Science and Technology, Vol. 16, p.p. 12-20, 2017.

Authors: **Dr Ivan Matin, Prof. dr Branko Štrbac, Prof. dr Miodrag Hadžistević, M. Sc. Miloš Ranisavljev,** University of Novi Sad, Faculty of Technical Sciences, Department of Production Engineering, Trg Dositeja Obradovica 6, 21000 Novi Sad, Serbia, Phone.: +381 21 485 2332, Fax: +381 21 454 495.

E-mail: matini@uns.ac.rs
strbacb@uns.ac.rs
miodrags@uns.ac.rs
ranisavljev@uns.ac.rs

ETIKUM 2023 **INTERNATIONAL SCIENTIFIC CONFERENCE**
NOVI SAD, SERBIA, DECEMBER 7-9, 2023

Mešeljević, L., Hadžikadunić, F., Bajtarević-Jeleč, A.

THE IMPACT OF STIFFENER APPLICATION ON MATERIAL STRENGTH AND RESISTANCE OF ALUMINUM COMPOSITE METAL WALL PANELS

Abstract: *Aluminum composite metal panels, commonly referred to as ACM panels, are a type of building material used for cladding and covering the exteriors of buildings. In this paper, careful consideration is given to the studying and simulation of the impact of stiffeners used with ACM cladding in order to provide additional support and stability. Simulation done using SolidWorks shows that correct positioning of stiffeners behind panels significantly reduces material deflection caused by external factors such as strong wind loads and pressure. Also, different wind loads and pressures are applied through simulation and results are compared and discussed.*
Key words: *ACM panels, stiffeners, SolidWorks, simulation*

1. INTRODUCTION

Aluminum composite metal panels are a type of building material used primarily for exterior cladding, facades, and signage. These panels consist of a core material, typically made of polyethylene (PE) or a fire-resistant mineral core (FR), sandwiched between two aluminum sheets. Being made in such way, ACM panels provide excellent rigidity, strength and durability. Also, compared to many other building materials, ACM panels are lightweight which makes them easier to handle, transport and install. However, while ACM panels offer many advantages, it is essential to ensure proper installation to maximize their benefits and safety. One of the negative results of bad installation process, inadequate support or wrong size of metal panels is occurrence of "oil canning". This refers to a phenomenon where the metal surface appears to "pop" or "ripple" due to uneven stresses or deformations. However, oil canning is not classed as a defect of the metal panel and is seen as more of an aesthetic issue. More serious issues, such as bending or collapse of the system, happens when using large size panels without proper support and placement of stiffeners. Wall panels are stiffened by attaching and extruded profile to the back of a panel by using adhesives or tapes, and space them properly.

Stiffeners play a vital role in maintaining the structural integrity and appearance of ACM panels. Therefore, the impact of these stiffeners on panel resistance is being examined.

2. ANALYSIS PREPARATION

In order to create assembly of panel system in SolidWorks for analysis purposes, it is essential to determine some input parameters, such as type of material, mechanical properties, panel dimensions, allowable panel stress and deflection, etc. It is important to emphasize that ACM panels don't carry the dead load of other building components. However, they are designed to withstand wind pressures and transfer them to the supporting structures without causing bending failure of the aluminum or excessive deformation. In order to ensure panels meet the loading and deflection requirements, it is crucial to calculate both the aluminum stresses and panel deformations and compare them to allowable values, [2].

2.1 ACM mechanical properties

In order to perform structural calculations, the basic mechanical properties of the ACM panel need to be determined. Table 1. shows basic mechanical properties. Dimensions are given in inches, since the data is taken from US panel manufacturer.

Table 1. Basic Properties of PE and FR Cores [2]

	4mm	6mm
T_{ACM}	0.157 in	0.236 in
T_{Equal}	0.120 in	0.153 in
I_{ACM}	3.25×10^{-3} in^4/in	10.98×10^{-3} in^4/in
I_{Skin}	1.83×10^{-4} in^4/in	4.49×10^{-4} in^4/in
E_{ACM}	5770×10^3 psi	4220×10^3 psi
E_{Skin}	10000×10^3 psi	10000×10^3 psi

Using these basic mechanical properties, a close approximation of panel stress and deflection for a given panel size can be calculated,

Maximum panel stress is given as [1]:

$$\sigma_{max} = \frac{\beta \cdot W \cdot b^2}{T_{Equal}^2} \quad (1)$$

Maximum panel deflection is given as [1]:

$$\mathbf{y_{max}} = \frac{(-\alpha \cdot W \cdot b^4)}{E_{ACM} \cdot T_{ACM}^3} \quad (2)$$

W – Uniform load (psi)
b – Smallest panel dimension (width) (in), Fig. 1.
a/b – Ratio of largest panel dimension to smallest panel dimension (always ≥1)

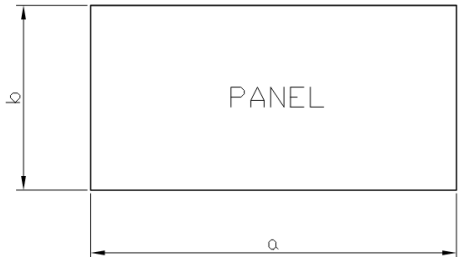

Fig. 1. Schematic view of simple rectangular ACM panel

The constant values α and β are given in Table 2., which shows these values depend on the a/b ratio and the type of support.

Table 2. Values of α and β [2]

	a/b	1	1.6	2
Simple supports all four sides	β	0.2874	0.5172	0.6102
	α	0.0444	0.0906	0.111
Fixed supports all four sides	β	0.3078	0.4680	0.4974
	α	0.0138	0.0251	0.0277

2.2 The selection of input parameters

Alloy 3105H14 is the most commonly used aluminum alloy for ACM sheets. However, any aluminum alloy sheets from the 3000 and 5000 series can be used in most cases. In this particular case, aluminum alloy 3003H14 is assumed for top and bottom skin and used for analysis. Also, material thickness of 4mm is being adopted. For the core of ACM, polyethylene (PE) is being adopted for analysis.

In order to start simulation in Solidworks, beside type of material, panel dimensions (width and lenght), as well as type of ACM system need to be determined. For this analysis, wet seal system has been adopted. Fig. 2. shows an example of a basic ACM panel sytem structure consisting of panel with returns and termination extrusions. It can be concluded that extrusions are used for panel attachment to building structure using proper types of fasteners. Extrusions are usually located 2 inches from panel edges, so vertical and horizontal extrusions don't overlap. It is important to emphasize that extrusions are also made of aluminum alloys.

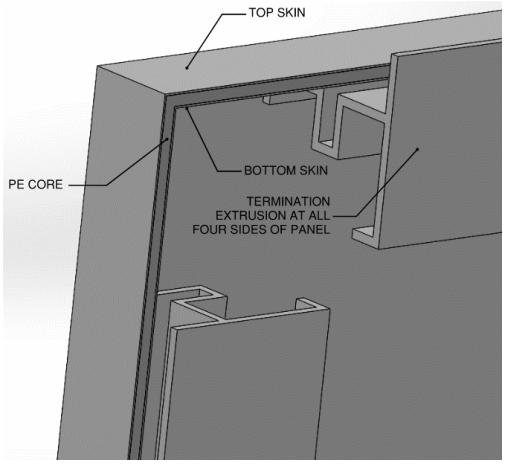

Fig. 2. Example of a basic ACM wet seal system

Other important input parameters are panel dimensions. For the analysis purposes, the following panel dimensions are being adopted:

- Panel width b=36 in (914.4mm)
- Panel length a=72 in (1828.8 mm)

According to these values and using Table 2., assuming fixed supports at all four sides of panel, the following parameters are being determined:

- Ratio a/b = 2
- α = 0.4972 and β = 0.0277

Design wind load can be adopted from charts, Fig. 3. According to these charts, using parameters b = 36 in, a/b = 2 ratio previously defined and assuming extrusions at all four sides, design wind load for panel of these characteristics is W=40 psf or 1915.21 Pa.

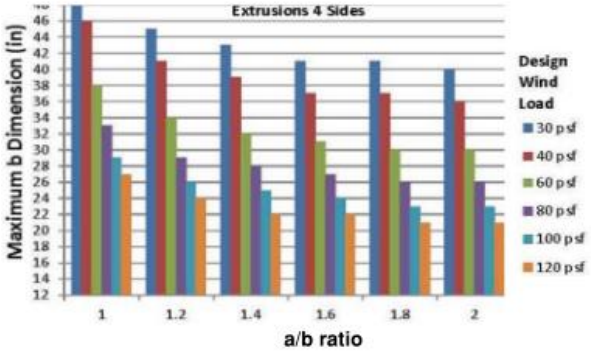

Fig. 3. Design wind load [2]

Thus, maximum bending stress can be calculated:

$$\sigma_{max} = \frac{\beta \cdot W \cdot b^2}{T_{Equal}^2} = \frac{0.4974 \cdot 0.28 \cdot 36^2}{0.120^2} \quad (3)$$

σ_{max} = 12 534.48 psi = 86.42 MPa (4)

Maximum panel deflection is given as:

$$y_{max} = \frac{(-\alpha \cdot W \cdot b^4)}{E_{ACM} \cdot T_{ACM}^3} = \frac{-0.0277 \cdot 0.28 \cdot 36^4}{5770 \cdot 10^3 \cdot 0.157^3} \quad (5)$$

y_{max} = -0.58341 in = -14.8 mm (6)

Calculated maximum stress and deflection for a panel of given dimensions are used as reference for simulation analysis.

3. SIMULATION IN SOLIDWORKS

After all input parameters are being determined and panel assembly is being made, the next step in analysis is preparing assembly for Simulation. This includes defining type of simulation, fixtures and external loads. For type of simulation, static simulation is being adopted. When wind is stopped by a surface, the dynamic energy in the wind is transformed to pressure. The pressure acting on the surface transforms to a force [1]:

$$F_W = p_d \cdot A = \frac{1}{2} \cdot \rho \cdot v^2 \cdot A \qquad (7)$$

F_W – Wind force (N)
A – Surface area (m^2)
p_d – dynamic pressure (Pa)
ρ – density of air (kg/m^3)
v – wind speed (m/s)

Surface area of the panel with previously defined dimensions is 1.67 m^2. Density of air is 1.2 kg/m^3. For analysis purposes, three different values of wind speed are used in simulations:
v_1 = 15 m/s – normal wind speed
v_2 = 35 m/s – category 1 hurricane
v_3 = 55 m/s – category 3 hurricane [4]

Thus, forces acting on a panel surface are:
F_1 = 225 N
F_2 = 1227 N
F_3 = 3031 N

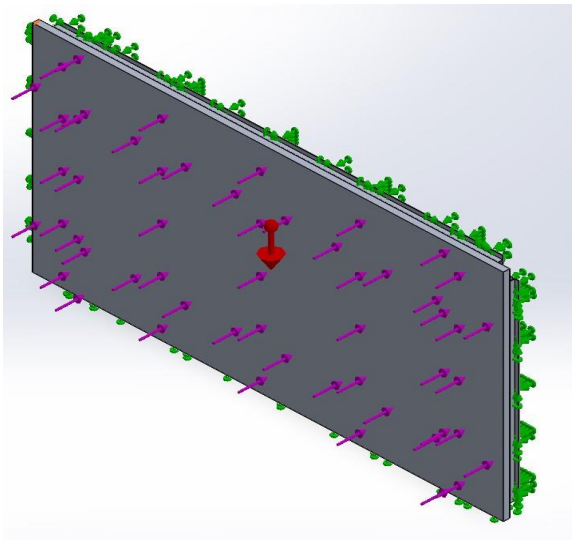

Fig. 4. Defining fixtures and external loads

These values are used for defining input parameters required for starting simulation. Fig. 4. shows force acting normal to panel surface. Also, gravity is considered as another external load in this case. Fixtures are placed at back of panel extrusion, since these surfaces are to be attached to building structure.

3.1 Simulation using no stiffeners behind panel

Results of simulation show that maximum bending stress is at inner connection of panel returns and extrusions. Also, maximum deflection is in the middle of panel. According to results, Fig. 5., maximum panel stress is 83.9 MPa, which is close to the allowable bending stress of 86.42 MPa. Also, maximum panel deflection is 8.32 mm, which is under allowable panel deflection of 14.8 mm.

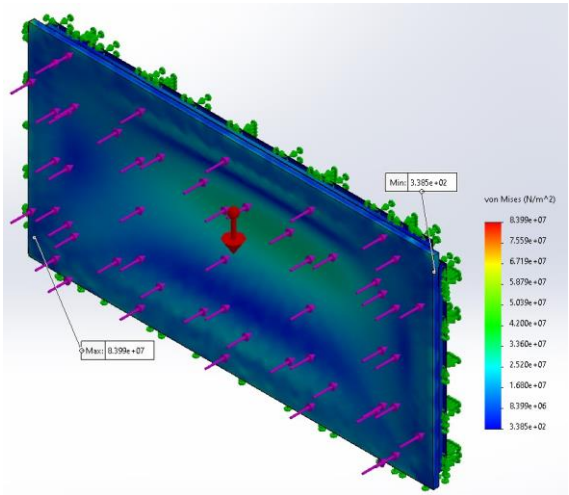

Fig. 5. Maximum and minimum stress for wind speed of 55 m/s for panel with no stiffeners

3.2 Simulation using stiffeners behind panel

Stiffeners behind ACM panel are generally used only for panels larger than 36x36 inches. However, there are some exceptions, especially if panels are to be installed on tall buildings and buildings exposed to extreme wind loads. Also, when defining stiffener spacing and position, it is important to pay attention to their orientation. Stiffeners need to be placed normal to the longer side of panel. Fig. 6. shows spacing and position of stiffeners on panel of previously defined dimensions.

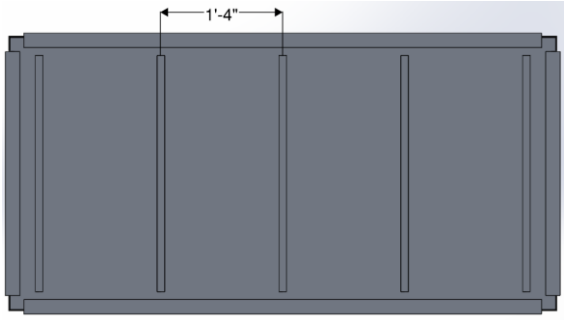

Fig. 6. Spacing and position of stiffeners

After defining stiffeners position, type of simulation, fixtures and external loads are being determined. For this analysis, the same input parameters are used, so the results can be compared. Simulation results show maximum bending stress when category 3 hurricane acts upon panel surface, Fig. 7.

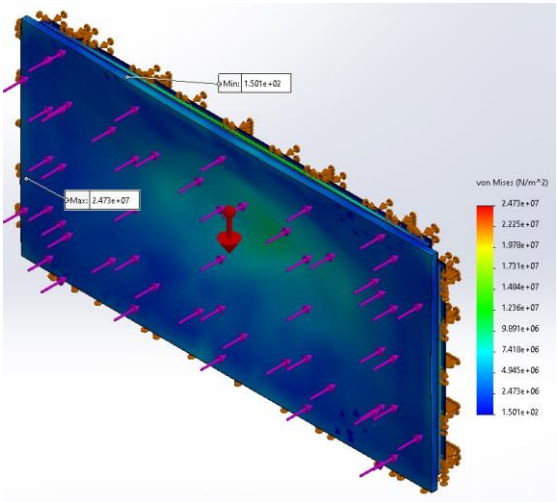

Fig. 7. Maximum and minimum values of stress for wind speed of 55 m/s for panel with stiffeners

3.3 Discussion of results

When comparing results of simulations for both cases, with and without stiffeners, it can be concluded that there are big differences between calculated stress and deflection values, Table 3.

Calculated maximum stress for the case with the highest wind speed when stiffeners are used behind panels is around 60 MPa lower than stress calculated when using no stiffeners. Also, maximum panel deflection is reduced by 7 mm for the highest wind speed. As simulation results show, when installed properly, stiffeners reduce stress and deflection of material, thus providing structural stability and wind resistance.

Table 3. Simulation results

	No stiffeners			Stiffeners		
v (m/s)	15	35	55	15	35	55
F (N)	225	735	1815	225	735	1815
p_d (Pa)	225	735	1815	225	735	1815
σ_{max} (MPa)	6.3	34	83.9	1.87	10	24.7
δ_{max} (mm)	0.618	3.37	8.32	0.089	0.486	1.2

4. CONCLUSION

As previously mentioned, stiffeners need to provide additional support and reinforcement, as well as to ensure that the panels perform as intended and withstand environmental and structural forces.

Through this research, it becomes evident that the addition of stiffeners to ACM panels significantly enhances their structural integrity and ability to withstand external forces. The incorporation of stiffeners not only bolsters the overall strength of the aluminum composite metal wall panels, but also plays a pivotal role in enhancing their resistance to deformation, deflection, and failure under stress. Also, stiffeners behind panels reduce occurrence of “oil canning” effect.

In summary, the implementation of stiffeners can lead to cost-effective solutions, as their use can potentially allow for the reduction in material thickness without compromising the desired performance. This, in turn, can result in lighter and more economical construction practices, which are increasingly important in the context of sustainable and eco-friendly building design. As the world continue to advance in the realm of construction materials and techniques, the role of stiffeners in optimizing material strength and resistance remains a topic of paramount importance for the industry.

5. REFERENCES

[1] Warren C. Y., Richard G. B.: *Roark’s Formulas for Stress and Strain*, Seventh Edition, McGraw-Hill, 2002.

[2] *Bending Strength & Stiffness, ALPOLIC Aluminum Composite Material Panels*, alpolic-americas.com, https://www.alpolic-americas.com/documents/tech-bulletins/, 19 September 2023.

[3] Hui, C., Wang, S., Liu, M., Han, W., Hai, R.: *Study on the Influence of Stiffeners on the Wind Resistance Performance of Aluminum Panel Curtain Wall*, International Journal of Steel Structures, 22, p.p. 1189-1199, 2022.

[4] Deiterich, A.: *At What Speed Does Wind Become a Hurricane?*, sciencing.com, https://sciencing.com/speed-wind-become-hurricane-5805814.html., 27 September 2023.

Authors: **Teaching assis. Lamija Mešeljević, Full prof. dr. Fuad Hadžikadunić, Senior teaching assis. Amna Bajtarević-Jeleč,** University of Zenica, Faculty of Mechanical Engineering, Fakultetska 1, 72000 Zenica, Bosnia and Herzegovina, Phone.: +387 32 449 129

E-mail: lamija.meseljevic@unze.ba
fuad.hadzikadunic@unze.ba
amna.bajtarevic@unze.ba

ETIKUM 2023 **INTERNATIONAL SCIENTIFIC CONFERENCE NOVI SAD, SERBIA, DECEMBER 7-9, 2023**

Miletić, S., Džunić, D., Mitrović, S., Kočović, V., Radisavljević, S., Vasiljević S., Kostić, S.

TRIBOLOŠKA KARAKTERIZACIJA MOTORNIH ULJA

Rezime: *Automobilska industrija se rapidno usavršava, a broj različitih automobila neprestano raste. a uporedo sa tim i mnogobrojna istraživanja u cilju unapređenja njihove efikasnosti. Jedno od tih istraživanja se odnosi i na motorna ulja. Eksperiment je izveden na tribometru sa „block on disc" kontaktnom geometrijom, pri čemu je analiziran uticaj različitih vrsta ulja na tribološke na trenje i habanje. Sva ulja su ospitivana u identičnim uslovima, pri konstantnoj brzini klizanja i opterećenju, pri čemu je svaki eksperiment ponovljen tri puta. Ulja imaju veliki uticaj na smanjenje gubitaka kod motora SUS, poznavanje njihovih karakteristika je od presudnog značaja za smanjenje trenja i habanja.*
Ključne reči: *motorna ulja, tribološka karakterizacija, podmazivanje, trenje, habanje*

1. UVOD

Motorno vozilo koje ima kao pogonski agregat motor sa unutrašnjim sagorevanjem (motor SUS) je veoma kompleksan sistem, sastoji se iz velikog broja delova koji su povezani u funkcionalnu celinu. Motorno vozilo ima pokretne i nepokretne delove, a kako bi se sprečili gubici usled trenja i habanja neophodno je delove koji se relativno kreću podmazivati. Motor SUS koji je sastavni deo motornog vozila, koji se sastoji od nepokretnih i pokretnih delova. Cilj brojnih istraživanja jeste smanjenje potrošnje goriva a samim tim i povećanje efikasnosti automobila, što se u velikoj meri može obezbediti adekvatnim podmazivanjem. Pravilno podmazivanje zahteva poznavanje tribomehaničkog sistema, karakteristika ulja, ali i vrstu i način samog procesa podmazivanja [1].

Razvoj tehnike doprineo je kvalitetnijim i tačnijim eksperimentima, a posebna tehnologija i oprema obezbedili su ispitivanja na nano nivou. Ulja koja su našla primenu u podmazivanju motora SUS ne treba samo da smanje trenje i habanje elemenata motora već i da utiču na druge karakteristike. Kako bi se postigli takvi rezultati ulju se dodaju različite vrste aditiva, čiji je cilj da u velikoj meri poboljšaju karakteristike ulja. Postoje mnoga istraživanja koja su vršena sa uljima. Eksperimenti su se zasnivali na dodavanju nanočestica različitih jedinjena kao aditivi uljima. Dodavanjem nanočestica CuO (50 nm), tačnije raspršivanje istih u ulje pokazalo je odlične rezultate. Nanočestice CuO su u velikoj meri poboljšale karakteristike ulja koje se ispitivalo. Širina traga habanja je za oko 50% smanjena, a koeficijent trenja je drastično smanjen [2]. Pored ispitivanja triboloških karakteristika ulja nakon dodavanja nanočestica CuO, vršena su ispitivanja i ulja nakon dodavanja nanočestica TiO_2. Pošto su nanočestice manje u odnosu na debljinu uljnog filma, one prodiru i deponuju se na kontaktnim površinama. Ove nanočestice, koje su prisutne u zoni kontakta, pretvaraju trenje klizanja u trenje kotrljanja što pomaže u smanjenju koeficijenta trenja. Analizom velikog broja radova može se zaključiti da se karakteristike ulja za podmazivanje poboljšavaju dodatkom aditiva u vidu TiO_2 nanočestica, što doprinosi smanjenju trenja i bolje antihabajuće ponašanje. Rezultati pokazuju da dodatkom ovog aditiva u motornom ulju dolazi do smanjenja koeficijenta trenja za čak 86%. Antihabajuće osobine motornih ulja su se takođe povećale usled aglomeracije ovih nanočestica. TiO_2 nanočestice su deponovane samo u slučajevima graničnog i mešovitog podmazivanja. Eksperiment je pokazao da ovi aditivi unapređuju tribološke karakteristike ulja. Ispitivanje korišćenjem UV spektrofoto metrije pokazuje da TiO_2 nanočestice poseduju dobru stabilnost i rastvorljivost u podmazajućem sredstvu [3]. Dodavanje mikrogranula cink oksida (ZnO) polivinilpirolidona (PVP - C_6H_9NO), i ugljeničnih čestica takođe je pokazalo odlične rezultate sa aspekta tribološke karakterizacije ulja koja se koriste kod motora SUS [4, 5]. Treba, takođe, naglasiti da i čestice čađi imaju određen uticaj na eksploataciju ulja za podmazivanje kod motora SUS. Čestice najčešće izazivaju abrazivno habanje što je apsolutno nepoželjno u ovakvom tribomehaničkom sistemu. Primenom adekvatnih ulja za podmazivanje nemoguće je eliminisati ovaj vid habanja ali se on može smanjiti [6].

Obzirom da su radne tmperature motora SUS uglavnom oko 100^{o}C u zavisnosti od vrste goriva, predstvaljena ispitivanja, izvedena na sobnoj temperaturi, bi se odnosila na uslove hladnog starta motora.

2. EKSPERIMENT

Određivanje triboloških karakteristika 4 komercijalna motorna ulja obavljeno je u Laboratoriji za tribologiju Fakulteta inženjerskih nauka u Kragujevcu. Eksperiment je obuhvatao merenje koeficijenta trenja i širine traga habanja pohabanih blokova. Zapremina pohabanog materijala određivana je analitički na osnovu poznavanja geometrije kontaktnih elemenata.. Merni lanac tribološkog ispitivanja prikazan je na slici 1. Na osnovu probnih ispitivanja definisani su uslovi ispitivanja, odnosno materijali kontaktnih parova, normalno opterećenjem brzina klizanja i vreme trajanja kontakta [6, 7]:

- Materijal: 50CrMo4
- Širina diska: 35 mm
- Dimenzije bloka: 6,3 x 10 x 15 mm
- Opterećenje: 20 N
- Vreme trajanja ispitivanja: 30 min po tragu

Tribološka ispitivanja izvedena su prema standardu ASTM G77, na tribometru sa „block-on-disc“ kontaktnom geometrijom. Prikazane dimenzije kontaktnih elemenata i način podmazivavanja definisan je standardom, odnosno donja strana diska je 3 mm uronjena u rezervorar sa uljem, ukupne zapremine 30 ml. Između površine bloka i obimne površine diska ostvaruje se linijski kontakt u početnim trenucima ekperimenta. Specijalna konstrukcija nosača bloka, oslanjanje preko ležaja, osigurava u svakom trenutku potpuno naleganje bloka, celom širinom na disk.

Univerzalni tribometar TR-95 namenjen je za tribološka ispitivanja, određivanje sile trenja i koeficijenta trenja pri određenim kontaktnim uslovima. Na ovom uređaju se mogu vršiti ispitivanja u uslovima kontakta sa podmazivanjem i bez podmazivanja. Osnovnu konfiguraciju tribometra čine: pogonski sistem, sistem za opterećenje, sistem za vođenje, sistem za podmazivanje, sistem za samopodešavanje bloka i merni sistem (Slika 1).

Pogonski sistem čini elektromotor sa remenicama, kaišem i varijatorom koji omogućuju variranje brojeva obrtaja od 100 do 1200 o/min. Na glavnom vratilu nalazi se rotacioni disk. Sistem za opterećenje pomoću tegova ili navojnim parom omogućuje opterećenje kontaktnih parova od 0 do 50 daN. Sistem za vođenje je realizovan pomoću linearnih valjkastih ležajeva, kod koga je prednaprezanjem eliminisan zazor. Sistem za podmazivanje čine različite posude za mazivo ili sistem za dovod ulja za podmazivanje u zonu kontakta (slika 3).

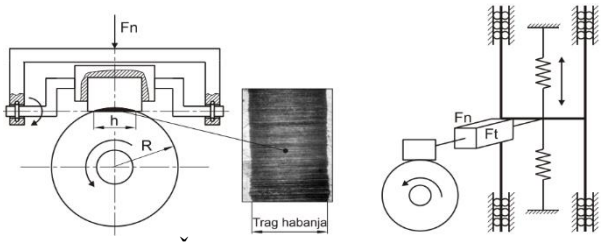

Sl. 1. Šema tribometra TR-95 [6]

Sistem za samopodešavanje bloka i diska ima zadatak da u svakom trenutku obezbedi prenošenje normalnog opterećenja u pravcu ose diska i kontakt celom dužinom bloka na disku. Ovaj sistem je realizovan konstrukcijom specijalnog rotirajućeg nosača bloka.

Kao osnovni parametar habanja korišćena je zapremina pohabanog materijala, koja je računata na osnovu širine traga habanja na kontaktnoj površini bloka.

Nakon merenja sile trenja, izmerena je širina traga habanja na univerzalnom mernom mikroskopu UIM-21. Namenjen za merenje dužine, uglova, parametara, spoljašnjih i unutrašnjih zavojnica, kontrolu alata, objekata složene konfiguracije, merenje tragova habanja.

Tokom ispitivanja je u zonu kontakta bloka i diska kontinualno dovođeno četiri različita motorna ulja tokom četiri ispitivanja.

Eksperiment se izvodi postavljanjem bloka u nosač bloka i njegovim pričvršćivanjem vijkom, kako bi se eliminisala i namanja mogućnost za pomeranjem. Nosač bloka se postavlja na tribometar i učvršćuje se. Kada se sve ovo postavi startuje se softver koji će pratiti da ne dođe do promene opterećenja, jer su ovde uslovi sa konstantnim opterećenjem, i pratiti promenu koeficijenta trenja. Softver ima mogućnost automatskog snimanja rezultata u realnom vremenu. Ispitivanja su vršena u uslovima konstantnog opterećenja i brzine klizanja, 200N i 0.5 m/s, respektivno. Vreme trajanja kontakta iznosilo je 1800s. Svaki eksperiment ponovljen je tri puta u identičnim uslovima kontakta.

Nakon tri ponovljena eksperimenta za sva četiri bloka, odnosno za sva četiri ulja, blokovi se čiste i meri se trag habanja. Na osnovu dobijenih rezultata koje je softver zabeležio dobijaju se dijagrami koeficijenta trenja, a na osnovu izmerenih širina traga habanja dobijaju se histogrami zapremine pohabanog dela bloka [6,7].

3. REZULTATI I DISKUSIJA

Rezultati merenja koeficijenta trenja na tribometru za ulje 1 pokazuju da nakon početnog rasta do maksimalne vrednosti, koeficijent trenja postepeno opada, da bi se u kasnijim fazama

ispitivanja njegova veličina stabilizovala i imala gotovo konstantnu vredost. Vremensko razdoblje u kojem se vrednost koeficijenta trenja intenzivno menja iznosi oko 60 sekundi i označava se kao faza uhodavanja. Fazu uhodavanja karakteriše značajna promena topografije površina bloka i diska zbog prelaska tehnološke u eksplatacionu topografiju i postizanja realne geometrije kontakta, odnosno površine teže „uravnoteženju“ topografije. Na slici 4 prikazan je koeficijent trenja u zavisnosti od jedinice vremena za prvo ulje, na slici 5 za drugo ulje, na slici 6 za treće ulje i na slici 7 za četvrto ulje. Na slici 8 prikazan je uporedni dijagram srednjih vrednosti koeficijenata trenja u jedinici vremena.

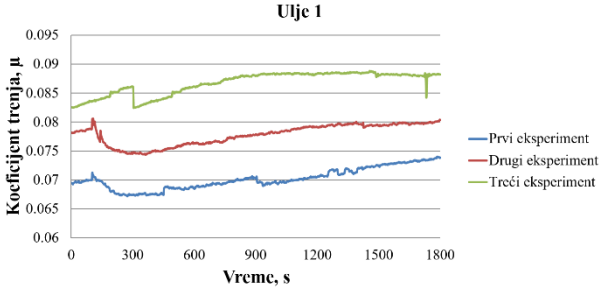

Sl. 4. Koeficijent trenja u jedinici vremena za motorno ulje 1

Dijagrami koeficijenata trenja za ulje 2 prikazani su na slici 5, gde se uočava pad koeficijenta trenja sa početne vrednosti, nakog čega sledi blagi porast do ustaljene vrednosti od u rasponu od 0.8-0.85, koju postiže nakon 900s trajanja kontakta.

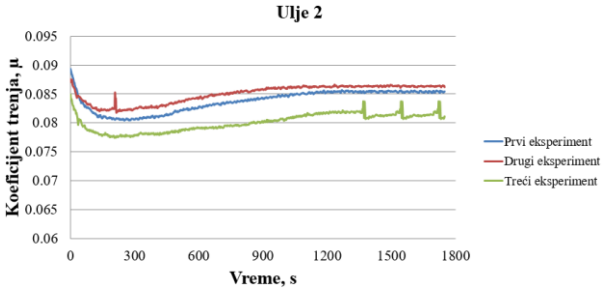

Sl. 5. Koeficijent trenja u jedinici vremena za motorno ulje 2

Sa dijagrama na slici 6 se vidi da u početku koeficijent u jednom slučaju konstantno blago raste do ustaljene vrednosti, a u druga dva slučaja na početku ostvarivanja kontakta brzo opada do gotovo ustaljene vrednosti. Sa dijagrama na slici 7 se u jednom slučaju vidi blagi početni pad koeficijenta trenja, dok se u drugim slučajevima vrednost koeficijenta trenja može smatrati gotovo konstantnom.

Slika 8 prikazuje uporedni dijagram srednjih vrednosti koeficijenata trenja u jedinici vremena za sva četiri ispitivana motorna ulja. Kod motornog ulja 1, srednja vrednost koeficijent trenja prvobitno opada do približno 300 sekundi trajanja eksperimenta, a zatim tokom ostatka vremena trajanja eksperimenta raste do vrednosti od približno 0.081.

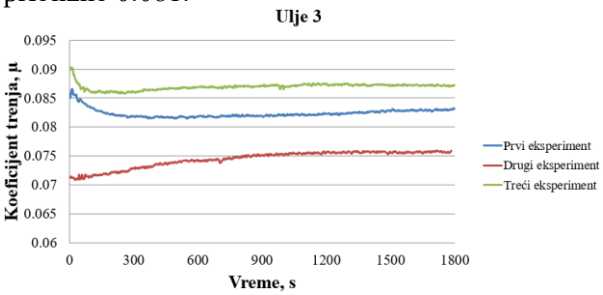

Sl. 6. Koeficijent trenja u jedinici vremena za motorno ulje 3

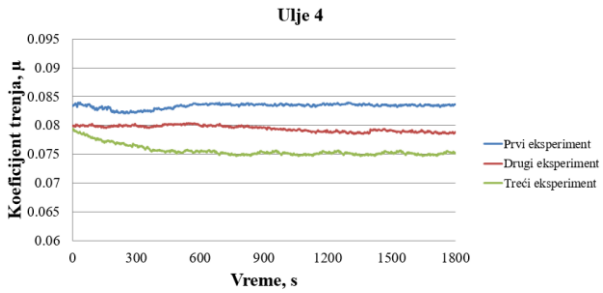

Sl. 7. Koeficijent trenja u jedinici vremena za motorno ulje 4

Kod motornog ulja 2, srednja vrednost koeficijent trenja prvobitno približno opada do prvih 300 sekundi trajanja eksperimenta, a zatim raste do ostatka vremena trajanja eksperimenta, gde nakon 1200 sekundi trajanja eksperimenta srednja vrednost koeficijenta trenja ovog motornog ulja ima približno konstantnu vrednost i iznosi približno 0.084, sa pojavom četiri pika koja označavaju nagli porast i brzi pad koeficijenta trenja zbog nailaženja kontaminenta.

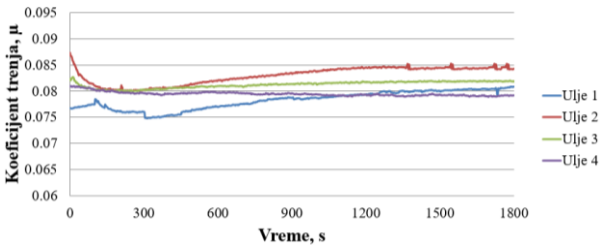

Sl. 8. Uporedni dijagram srednjih vrednosti koeficijenata trenja u jedinici vremena

Motorno ulje 3 ima prvobitni pad srednje vrednosti koeficijenta trenja u samom početku trajanja eksperimenta, a zatim dolazi do ostvarivanja približno konstantne srednje vrednosti koeficijenta trenja do ostatka vremena trajanja eksperimenta, gde je najveća srednja vrednost koeficijenta trenja ovog motornog ulja iznosila približno 0.0825. Kod motornog ulja 4 je ostvarena

približno konstantna srednja vrednost koeficijenta trenja tokom celog vremena trajanja eksperimenta, gde je ista iznosila manje od 0.08.

Na slici 9 je dat prikaz srednjih vrednosti zapremine pohabanog dela u zavisnosti od primenjenog ulja za podmazivanje. Na osnovu prikazanog se može zaključiti da ulje 4 ima najveći uticaj na antihabajuće karakteristike bloka, dok ulje 1 ima najmanje.

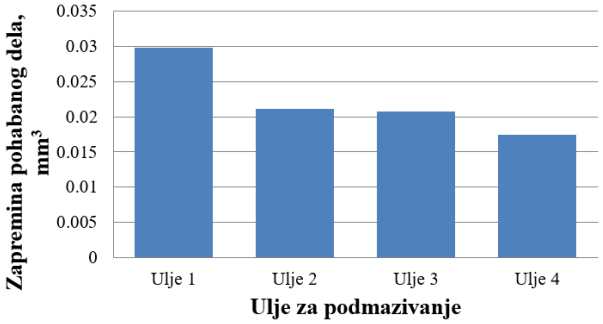

Sl. 9. Srednja vrednost zapremine pohabanog dela u zavisnosti od primenjenog ulja za podmazivanje

Na slici 10 je dat mikroskopski prikaz izgleda traga habanja blokova, sa kojih se jasno uočavaju brazde u pravcu kretanja, što ukazuje da je dominantan mehanizam habanja abrazivno habanje.

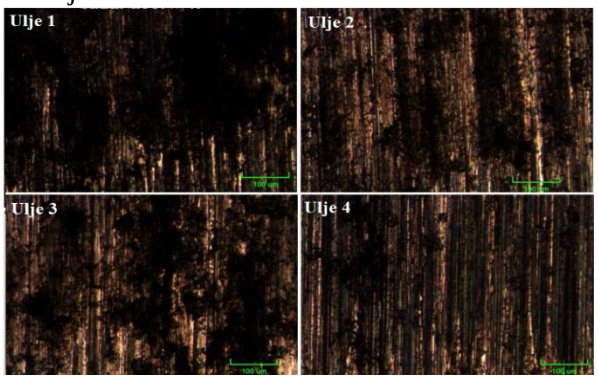

Sl. 10. Pohabana površina blokova

4. ZAKLJUČAK

Tribološka ispitivanja 4 komercijalna motorna ulja su ukazala na sledeće:

Sa aspekta vrednosti koeficijenta trenja sva 4 ispitivana komercijalna ulja pokazuju slične ustaljene vrednosti koeficijenta trenja. Mala razlika se može uočiti kada je u pitanju početni period, odnosno period uhodavanja, gde ulja 2 i 3 imaju veće inicijalne vrednosti u odnosu na ustaljenu vrednost, dok za ulja 1 je situacija obrnuta. Ulje 4 ima gotovo konstantu vrednost koeficijenta trenja tokom celog perioda trajanja kontakta. Sa aspekta habanja ulje četiri ima najveći uticaj, a ulje 1 najmanji na habanje bloka, dok su druga dva ulja gotovo ujednačena po pitanju izmerenih vrednosti habanja. Dominantan mehanizam habanja kod svih ispitivanih ulja predstavlja abrazivno habanje.

5. REFERENCE

[1] Gradin, Z.: *Tribološke karakteristike motora SUS*, 330-337, Beograd, Vojnotehnički glasnik, Beograd, 2003.

[2] Asrul M., Zulkiflia N.W.M., Masjukia H. H., Kalam M.A.: *Tribological properties and lubricant mechanism of Nanoparticle in Engine Oil*, The Malaysian International Tribology Conference, Volume 68, p.p. 320-325, 2013.

[3] Laad M., Jatti V. K. S.: *Titanium oxide nanoparticles as additives in engine oil*, Journal of King Saud University, Volume 30, p.p. 116-122, 2018.

[4] Wong D., Resendiz J., Egberts P., Park S. S.: *Reduction of friction using electrospun polymer composite microbeads emulsified in mineral oil*, p.p. 339-350, 45th SME North American Manufacturing Research Conference, NAMRC 45, LA, USA, , 2017.

[5] Hu E., Hu X., Liu T., Fang L., Dearn K.D., Xu H.: *The role of soot particles in the tribological behavior of engine lubricating oils*, Wear - An International Journal on the Science and Technology of Friction, Lubrication and Wear, Volume 304, p.p. 152-161, 2013.

[6] Babić, M., Mitrović S.: *Tribološke karakteristike kompozitnih materijala*, Mašinski fakultet u Kragujevcu, Kragujevac, 2007.

[7] Globoćki, Lakić, G., Perić, S., Bučko, M., Nedić, B., Borković, A., Babić, N.: *Technical system conditions monitoring via the lubricating oil analysis*, p.p. 379-390, International Conference on Tribology, Faculty of Engineering, Kragujevac, 2023.

Autori: **Mast. inž. maš. Stefan Miletić, vanr. prof. dr Dragan Džunić, red. prof. dr Slobodan Mitrović, docent dr Vladimir Kočović,** Univerzitet u Kragujevcu, Fakultet inženjerskih nauka, Sestre Janjić 6, 34000 Kragujevac, Srbija.
E-mail: stefan96miletic.finkg@gmail.com
dzuna@kg.ac.rs
boban@kg.ac.rs
vladimir.kocovic@kg.ac.rs

Autori: **Naučni saradnik Snežana Radisavljević,** Univerzitet u Kragujevcu, Prirodno-matematički fakultet, Radoja Domanovića 12, 34000 Kragujevac, Srbija.
E-mail: snezana.radisavljevic@pmf.kg.ac.rs

Autori: **Asistent Saša Vasiljević, Prof. strukovnih studija dr Sonja Kostić,** Akademija strukovnih studija Šumadija, Departman u Kragujevcu, Kosovska 8, Kragujevac, Srbija
E-mail: svasiljevic@asss.edu.rs
skostic@asss.edu.rs

ETIKUM 2023

INTERNATIONAL SCIENTIFIC CONFERENCE
NOVI SAD, SERBIA, DECEMBER 7-9, 2023

Milosevic, A., Agarski, B., Sokac, M., Simunovic, G., Kocovic, V., Vukelic, D.

IMPLEMENTATION OF LIFE CYCLE ASSESSMENT IN THE DESIGN PROCESS OF FIXTURE FOR REDUCER HOUSING MACHINING

Abstract: *This paper explores the application of Life Cycle Assessment in designing modular fixture for reducer housing machining, aiming to identify and reduce negative environmental impact. Through the four phases of LCA - goal definition, inventory analysis, impact assessment, and interpretation of results - key aspects influencing the environment throughout the life cycle of modular fixture have been identified.*
Keywords: *Fixture design, life cycle assessment, environment*

1. INTRODUCTION

Modern production systems, driven by growing market demands and rapid advancements in science and technology, are increasingly burdening the environment through the degradation of natural resources. Awareness of environmental preservation is becoming a global imperative, especially in the industrial sector [1].

Manufacturing systems are crucial in impacting the environment, both through direct emissions and waste materials during production, as well as through indirect influences such as energy and resource consumption. Reduction of the negative impact is possible through the optimization of all elements of the processing system, such as operations, machine tools, fixtures, cutting tools, etc.

Fixture, as an essential element of manufacturing systems, have a significant impact on the environment primarily through energy and material consumption during production. Reducing the impact can be achieved through proper fixture design, choosing materials with lower ecological impact, production techniques that minimize waste, using renewable energy sources for production, and other strategies [3].

The implementation of Life Cycle Assessment (LCA) in the fixture design process can be crucial for identifying potential issues and directing efforts towards reducing the negative impact. This research focuses on the application of LCA in the design of modular fixture for machining reducer housings, with the aim of identifying and reducing the fixture's negative impact on the environment.

2. METODOLOGY

LCA analyzes the impacts of a product or system on the environment throughout its entire life cycle, gathering data on materials, emissions, energy consumption, waste, and other factors [1, 2]. Based on this data, a quantitative assessment of environmental impacts is conducted, including greenhouse gas emissions, air pollution, and resource consumption. The goal of LCA is to provide objective information about the environmental profile of a product or system to identify potential issues and enhance environmental sustainability[1, 2].

According to ISO 14040 and ISO 14044 standards, LCA consists of four basic phases [4, 5]: goal definition, inventory analysis, impact assessment and interpretation of results. The goal definition and scope phase of LCA sets the foundation for the study by identifying the purpose and scope of the analysis to ensure relevant and reliable information about environmental impacts. The inventory analysis phase involves collecting and organizing data on all inputs and outputs throughout the product's life cycle, including raw materials, energy, and emissions. The life cycle impact assessment (LCIA) analyzes and quantifies the environmental impacts based on the inventory results. The results are interpreted to draw conclusions about the overall environmental impact of the product or service, identify challenges, and make decisions for sustainability improvements [1, 2].

LCA of the modular fixture for the reducer housing aims to evaluate the environmental impact of each component of the fixture and identify key aspects that may affect the environment. The analysis was conducted using the openLCA software. The functional unit for the LCA of the modular fixture is the modular fixture for locating and clamping the workpiece during machining. The workpiece is a cast reducer housing (Figure 1) that requires hole drilling on a CNC drilling machine.

For the workpiece, a designed modular fixture shown in Figure 2 is used. The body of the

modular fixture is a rectangular base plate that is attached to the machine worktable using four screws and centered with dowels through holes. Other fixture elements are fastened to the base plate through T-slots, centering holes, and fasteners. Workpiece locating is achieved using support pins and headless screws. Clamping is performed with three rotating clamps that utilize clamping screws. Since machining is planned on a CNC machine, a tool guiding element is not necessary.

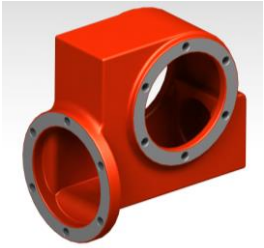

Fig. 1. 3D model of the workpiece

Fig. 2. 3D model of modular fixture

To obtain accurate and precise results during LCA, it is necessary to unambiguously define the system boundaries. System boundaries define the scope of the analysis and determine which phases of the life cycle will be included in the study. Within the LCA of the modular fixture for machining reducer housings, the system boundaries encompass all steps and activities related to the production of components, such as raw material extraction, raw material transportation, semi-finished product manufacturing, storage, and component production (Figure 3). In this context, the process of manufacturing fixture components is a foreground activity, while all other activities related to component production are background activities.

The use of fixtures and activities related to the end of the life cycle have not been specifically considered in the research, so they fall outside the boundaries of the system. Limitations for the LCA of modular fixture include the choice of materials for making the fixture components. Although it is possible to use various types of steel to make the components, only one type - carbon steel for reinforcement - was selected in the analysis.

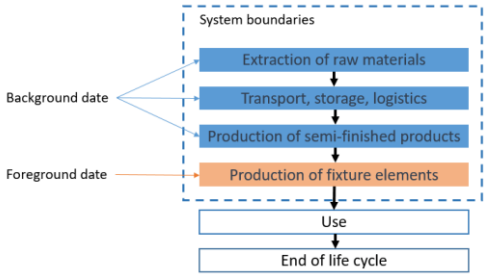

Fig. 3. System boundaries

LCI of modular fixture encompasses all the data and steps that allow for a numerical representation of the flow of materials and energy through the input and output phases of the life cycle. Ecoinvent 3.7 Cut-off database was used to collect the background data. The Ecoinvent database provides comprehensive data on various industrial sectors, processes, and materials. Table 1 lists the names of all production operations and materials from the Ecoinvent 3.7 Cut-off database that were used in the LCA.

Table 1. Input data from the Ecoinvent 3.7 Cut-off database

Processing or material	**Processing and material datasets selected from Ecoinvent 3.7 Cut-off**
Steel	market for hot rolling, steel | hot rolling, steel | Cutoff, S
Drilling	market for steel removed by drilling, computer numerical controlled | steel removed by drilling, computer numerical controlled | Cutoff, S
Milling	market for steel removed by milling, average | steel removed by milling, average | Cutoff, S
Turning	market for steel removed by turning, average, computer numerical controlled | steel removed by turning, average, computer numerical controlled | Cutoff, S
Grinding	Grinding [6]

In the Ecoinvent 3.7 Cut-off database, grinding is not listed as a separate activity. An inventory for grinding was created within the openLCA software to enable a proper LCA of modular fixture [6]. Grinding is a very important operation in the production of fixture components, especially clamping and base elements, but also for all other elements.

Table 2 provides an overview of all input and output flows of materials and energy for each individual element of the modular fixture. In the LCA analysis, numerical evaluation of manual human labor is not performed, as the assessment of such aspects is often subjective and difficult to measure. For this reason, assembly activities, which involve a significant amount of manual labor, are not included in the inventory table for modular fixture components.

The ReCiPe method LCIA was used to assess the environmental impact of the modular fixture for processing the reducer housing. ReCiPe is a method that allows for the quantification of environmental effects in various impact categories.

Table 2. Inventory for modular fixture

Element name	No. of pieces	Mass (kg)	Process
Base Plate	1	13	
Base Plate	1	3.5	Milling
Base Plate	1	0.8	Grinding
Mounting Block- 1	2	0.59	
Mounting Block- 1	2	0.73	Milling
Mounting Block- 1	2	0.06	Drilling
Mounting Block- 1	2	0.08	Grinding
Mounting Block- 2	1	1.15	
Mounting Block- 2	1	0.59	Milling
Mounting Block- 2	1	0.10	Drilling
Mounting Block- 2	1	0.12	Grinding
T-Slot Block	6	0.02	
T-Slot Block	6	0.01	Milling
T-Slot Block	6	0.01	Grinding
Nut for T-Slot	16	0.009	
Nut for T-Slot	16	0.01	Milling
Supporting Plate	3	0.07	
Supporting Plate	3	0.03	Milling
Supporting Plate	3	0.02	Drilling
Supporting Plate	3	0.01	Grinding
Grub Screw	1	0.01	
Grub Screw	1	0.01	Turning
Grub Screw	1	0.001	Grinding
Down-Thrust Clamp	3	0.22	
Down-Thrust Clamp	3	0.3	Milling
Down-Thrust Clamp	3	0.02	Drilling
Down-Thrust Clamp	3	0.01	Grinding
Height Cylinder	4	0.15	
Height Cylinder	4	0.05	Turning
Height Cylinder	4	0.01	Milling
Height Cylinder	4	0.01	Grinding
Height Cylinder	1	0.08	
Height Cylinder	1	0.02	Turning
Height Cylinder	1	0.01	Milling
Height Cylinder	1	0.01	Grinding
Pin	4	0.04	
Pin	4	0.02	Turning
Pin	4	0.01	Grinding
Collar Nut	2	0.01	
Collar Nut	2	0.02	Turning

3. RESULTS AND DISCUSSION

The results obtained using the ReCiPe LCIA method for environmental impact assessment are presented in the form of graphs (Figure 4). The graphical representations can serve as guidelines for designing fixture, selecting materials, and implementing sustainable practices to reduce the negative impact on the environment and achieve sustainable production of modular fixture components.

Based on the obtained results (Figure 4), it can be observed that the base plate has a dominant effect on all impact categories. This is due to its larger mass compared to all other fixture components. The impact of the other elements is also correlated with their mass. The amount of resources and energy required for the production, transportation, use, and disposal of the elements increases proportionally with their mass.

Since the base plate has the most significant environmental impact, its influence was specifically analyzed. In Figure 5, the assessment of the environmental impact of the production operations of the base plate is shown across different impact categories. Figure 5 provides insight into the percentage contributions that each production operation has on the environment. Based on the obtained results, it can be concluded that the mass of the element, the amount of waste material, and the type of material play important roles in environmental impact. When considering the impacts of machining processes and steel procurement, it is important to note several key factors. Machining processes can generate waste, dust, and emissions of harmful gases that have a negative impact on the quality of soil, water, and air. Therefore, machining has a more significant impact on freshwater ecotoxicity, marine ecotoxicity, natural land transformation, and terrestrial ecotoxicity compared to steel procurement. As for steel procurement, the main impact is related to metal depletion. The processes in steel production require resources and energy, and these requirements lead to a significant impact on metal depletion in the environment. On the other hand, machining has a significantly higher impact on water depletion compared to steel procurement due to the demanding machining process, which typically involves the use of larger quantities of water for cooling and lubricating the machines.

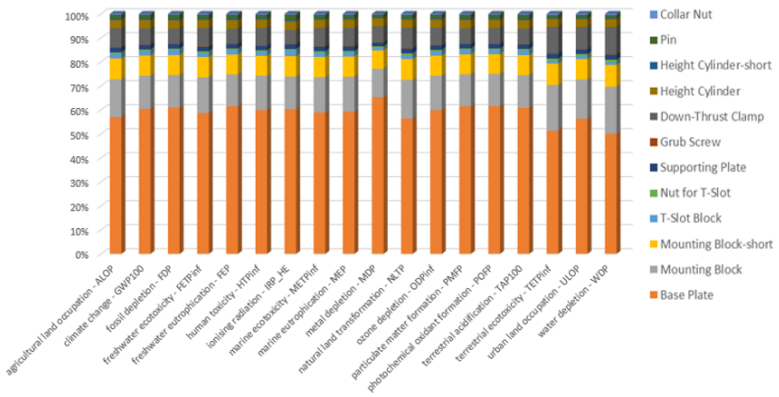

Fig. 4. Assessing the environmental impact of modular fixture components

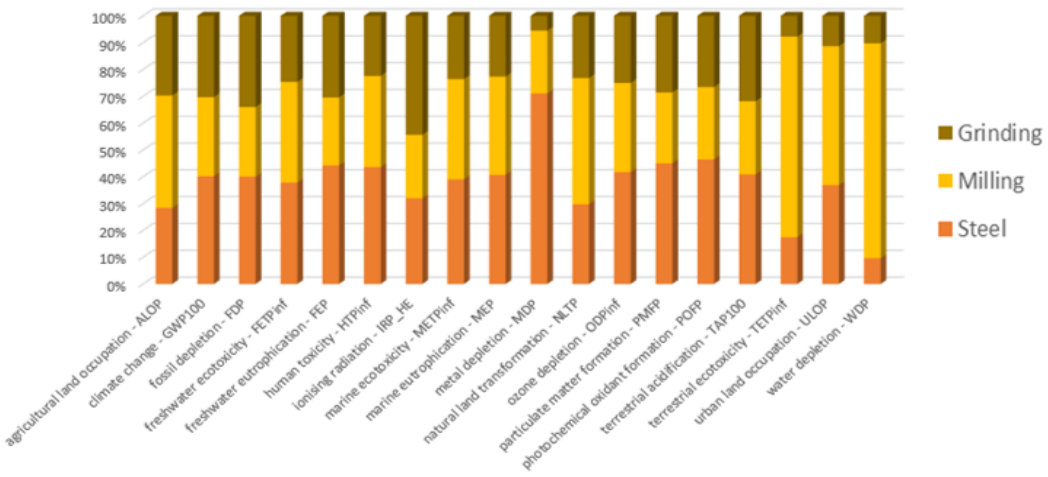

Fig. 5. Assessing the environmental impact of the production operations of the base plate

4. CONCLUSION

Manufacturing systems have a significant impact on the environment through energy production and consumption. At the same time, fixtures that are a crucial part of these systems contribute to waste generation and resource consumption. This paper focuses on the application of LCA in the process of designing fixtures for processing reducer housing. Key factors affecting the environment during the lifecycle of fixture have been identified. The results obtained show that it is possible to assess the negative impact of modular fixture in the process of designing their construction. The results indicate that the environmental impact is closely related to the mass and material from which the elements of the modular fixtures are made. The dominant influence in all impact categories was the base plate as the element with the highest mass. Therefore, special attention should be paid to the selection of materials and machining operations of the base plate in the process of designing fixture.

Future research will focus on exploring the exploitation and end-of-life stages of the modular fixture lifecycle, as well as integrating systems for designing environmentally-friendly fixtures with automated fixture design systems.

5. LITERATURE

[1] Prince, R., Rajeev, A., Jain, J.K.: *Life Cycle Assessment in Sustainable Manufacturing: A Review and Further Direction*, Operations Management and Systems Engineering, pp. 191-203, 2021.

[2] Budak, I., Vukelic, D., Agarski B., Ilic Micunovic, M.: *Life Cycle Design and Assessment Tools*, Faculty of Technical Sciences, Novi Sad, Novi Sad, 2020.

[3] Vukelic, D., Agarski B., Budak I., Simunovic G., Buchmeister B., Jakovljevic Z., Tadic B.: *Eco-design of fixtures based on life cycle and cost assessment*, International Journal of Simulation Modelling, Vol. 18, No. 1, pp. 72-85, 2019.

[4] ISO 14040: Environmental management - Life cycle assessment - Principles and framework, 2006.

[5] ISO 14044: Environmental management - Life cycle assessment - Requirements and guidelines, 2006.

[6] Murray, V. R., Zhao, F., Sutherland, J. W.: *Life cycle analysis of grinding: a case study of non-cylindrical computer numerical control grinding via a unit-process life cycle inventory approach*, Proceedings of the Institution of Mechanical Engineers, Part B: Journal of Engineering Manufacture, Vol. 226, No. 10, pp. 1604-1611, 2012.

Authors:

MSc Aleksandar Milosevic, PhD Boris Agarski, PhD Mario Sokac, PhD Djordje Vukelic University of Novi Sad, Faculty of Technical Sciences, Trg Dositeja Obradovica 6, 21000 Novi Sad, Serbia

E-mail: aleksandar.milosevic@uns.ac.rs
agarski@uns.ac.rs
marios@uns.ac.rs
vukelic@uns.ac.rs

PhD Goran Simunovic, University of Slavonski Brod, Mechanical Engineering Faculty, Trg Ivane Brlic Mazuranic 2, 35000 Slavonski Brod, Croatia
E-mail: gsimunovic@unisb.hr

PhD Vladimir Kocovic, University of Kragujevac, Faculty of Engineering, Sestre Janjic 6, 34000 Kragujevac, Serbia.
E-mail: vladimir.kocovic@kg.ac.rs

ETIKUM 2023 **INTERNATIONAL SCIENTIFIC CONFERENCE**
NOVI SAD, SERBIA, DECEMBER 7-9, 2023

Nemeš, T., Petković, B. Lj., Samardžić, S., Beljin-Čavić, M.

ODREĐIVANJE TOPLOTNE PROVODLJIVOSTI METALA – REALIZACIJA APARATURE I POSTUPKA MERENJA ZA POTREBE NASTAVE IZ FIZIKE

Rezime: *U okviru standarndog kursa opšte fizike vrlo često se izučava toplotna provodljivost. Međutim, za potrebe laboratorijskih vežbi, na tržištu se ne može naći aparatura koja će demonstrirati i omogućiti kvantitativna merenja vezana za toplotnu provodljivost različitih materijala u kratkom vremenskom periodu. Zbog toga je u ovom radu predstavljena konstrukcija jedne nove aparature za merenje toplotne provodljivosti. Za izradu aparature korišćena je 3D-tehnologija štampe, standardni EU aluminijumski profili kao i elektronske komponente koje se mogu naći na tržištu. U okviru rada razvijeno je nekoliko postupka merenja koji daju vrlo dobre rezultate za koeficijent provođenja toplote metalnih uzoraka.*
Ključne reči: *toplotna provodljivost, 3D-štampa, grejna ploča, kalorimetar, metalni cilindar, termometar*

1. UVOD

Provođenje toplote duž jedne ose i Furijeov obrazac izučava se u okviru standarnih kurseva fizike na tehničkim fakultetima [1]. Takođe moguća je i realizacija eksperimenta kojim se direktno posmatra proces provođenja i kvantitativno meri koeficijent toplotne provodljivosti [2]. U procesu modernizacije eksperimentalnih vežbi iz fizike, ponekad je nemoguće naći aparaturu koja će zadovoljiti sve zahteve. Međutim, pomoću 3D tehnologije štampe kao i prisustva velikog broja standarndih mehaničkih i električnih komponenti, aparaturu je moguće izraditi prema specifičnim zahtevima. Takođe, moguće je pronaći odgovarajući teorijski tretman kojim se dublje shvata proces provođenja toplote.

2. ODREĐIVANJE TOPLOTNE PROVODLJIVOSTI - LINEARNA APROKSIMACIJIA

Količina toplote koja je potrebna da promeni temperaturu vode u kalorimetru od t_0 do t je

$$Q = (m_v c_v + C_K)(t - t_0) \qquad (1)$$

gde je m_v masa vode u kalorimetru, c_v specifični toplotni kapacitet vode i C_K toplotni kapacitet kalorimetra. Sa druge strane količina toplote koja u vremenskom intervalu $d\tau$ prođe kroz poprečni presek cilindra je prema Furijeovom obrascu, uz pretpostavku da temperatura duž ose cilindra opada linearno sa rastojanjem:

$$dQ = KS\frac{t_p - t}{L}d\tau \qquad (2)$$

gde je t_p temperatura donje baze cilindra, t trenutna temperatura gornje baze (temperatura vode u kalorimetru), L dužina cilindra, S površina poprečnog preseka cilindra i K toplotna provodljivost materijala od koga je cilindar sačinjen.

Ako pretpostavimo da temperatura u kalorimetru sa vodom raste linearno sa vremenom:

$$t = t_0 + \alpha\tau \qquad (3)$$

onda se jednačina (2) može napisati u vidu

$$dQ = KS\frac{t_p - t_0 - \alpha\tau}{L}d\tau. \qquad (4)$$

Integracijom jednačine (4) u vremenskom intervalu od 0 do τ dobijamo ukupnu količinu toplote koja je prošla kroz poprečni presek cilindra i zagrejala vodu od temperature t_0 do t:

$$Q = \frac{KS\tau}{L}\left(t_p - t_0 - \frac{\alpha}{2}\tau\right) \qquad (5)$$

Izjednačavanjem (5) i (1) dobijamo izraz za određivanje toplotne provodljivosti:

$$K = \frac{(m_v c_v + C_K)(t - t_0)L}{S\tau\left(t_p - t_0 - \frac{\alpha}{2}\tau\right)}. \qquad (6)$$

U jedn. (6) je količnik $\frac{t - t_0}{\tau}$ zapravo koeficijent pravca linerane zavisnosti date sa (3), a $t_0 + \frac{\alpha}{2}\tau$ je srednja temperatura u vremenskom intervalu 0 do τ. Sledi izraz za eksperimentalno određivanje toplotne provodljivosti metalnog cilindra:

$$K = \frac{(m_v c_v + C_K)\alpha L}{S(t_p - \langle t \rangle)}. \qquad (7)$$

Dakle merenjem zavisnosti trenutne temperature vode u kalorimetru od vremena, moguće je na osnovu koeficijenta pravca α linearne funkcije i srednje vrednosti temperature vode u kalorimetru $\langle t \rangle$ odrediti toplotnu provodnost materijala.

3. ODREĐIVANJE TOPLOTNE PROVODLJIVOSTI – EGZAKTAN PRISTUP

Količina toplote koja promeni temperaturu vode u kalorimetru za beskonačno mali iznos je

$$dQ = (m_v c_v + C_K)dt. \qquad (8)$$

Količina toplote koja prođe kroz poprečni presek cilindra u vremenskom intervalu $d\tau$ je data jednačinom (2). Uz pretpostavku da nema toplotnih gubitaka, izjednačavanjem (2) i (8) dobijamo:

$$(m_v c_v + C_K)dt = KS\frac{t_p - t}{L}d\tau. \qquad (9)$$

U početnom trenutku $\tau = 0$ temperatura vode u kalorimetru je t_0, a nakon vremena τ temperatura vode u kalorimetru je t. Dakle, s obzirom na (9), iz integrala

$$\int_{t_0}^{t}\frac{dt}{t-t_p} = -\frac{KS}{(m_v c_v + C_K)L}\int_0^{\tau} d\tau \qquad (10)$$

sledi zavisnost temperature vode u kalorimetru od vremena

$$t = t_p + (t_0 - t_p)e^{-\frac{KS}{(m_v c_v + C_K)L}\tau}. \qquad (11)$$

Koeficijent u eksponentu

$$\beta = \frac{KS}{(m_v c_v + C_K)L} \qquad (12)$$

se može odredtii fitovanjem funkcije (11), na eksperimentalne podatke zavisnosti temperature vode u kalorimetru od vremena. Iz (12) sledi koeficijent toplotne provodljivosti:

$$K = \frac{(m_v c_v + C_K)L}{S}\beta \qquad (13)$$

4. ODREĐIVANJE TOPLOTNE PROVODLJIVOSTI NA OSNOVU DVE TAČKE

U prethodnim odeljcima opisane su procedure određivanja toplotne provodljivosti kada se prati zavisnost temperature vode od vremena u kalorimetru, što zahteva fitovanje podataka odgovarajućom funkcijom. Međutim, ako se meri samo početna temperatura vode u kalorimetru t_0 i krajnja temperatura t, kao i vremenski interval τ potreban da temperatura vode u kalorimetru poraste sa t_0 na t, iz (7) sledi izraz za merenje koeficijenta toplotne provodljivosti:

$$K = \frac{(m_v c_v + C_K)(t - t_0)L}{S\tau\left(t_p - \frac{t_0 + t}{2}\right)}. \qquad (14)$$

Slično iz izraza (11) sledi:

$$K = \frac{(m_v c_v + C_K)L}{S\tau}\ln\left(\frac{t_p - t_0}{t_p - t}\right). \qquad (15)$$

5. IZRADA APARATURE ZA MERENJE TOPLOTNE PROVODLJIVOSTI

Aparatura za merenje toplotne provodljivosti opisanim eksperimentima treba da obezbedi sledeće uslove:

1. Temperatura donje baze metalnog cilindra mora biti konstantna;
2. Gornja baza metalnog cilindra mora biti u termalnom kontanktu sa kalorimetrom koji je ispunjen određenom količinom vode;
3. Grejač, metalni cilindar i kalorimetar moraju biti stabilno postavljeni na odgovarajući stativ;
4. Rukovanje aparaturom mora bit bezbedno i jednostavno.

Stabilisano grejanje donje baze cilindra obezbeđeno je pomoću male grejne ploče (Sl. 1). Ova grejna ploča ima snagu od 65W, i radi na naponu od 20V.

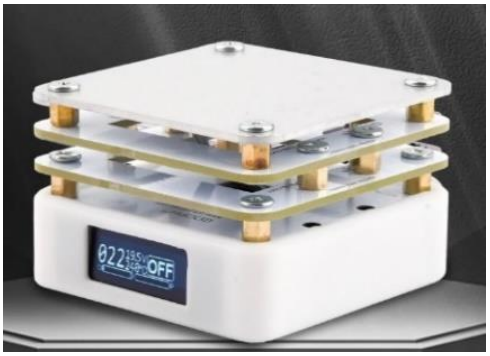

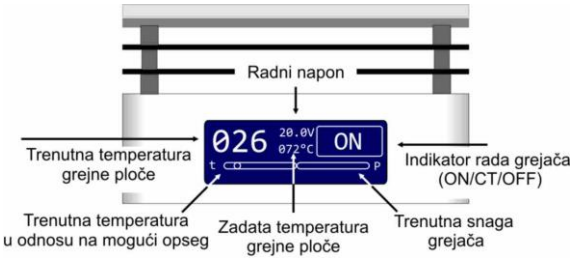

Sl. 1. Izgled grejne ploče sa indikatorom rada grejača (ON - grejanje, CT-prelazni režim, OFF - isključen grejač)

Kao izvor napajanja koristi se adapter za laptop računare ili punjač za mobilne telefone snage 65W sa USB-C priključkom. Grejna ploča ima PID protokol [3] koji obezbeđuje da se temperatura grejne ploče održava na zadatoj vrednosti sa što manjim odstupanjima za specifični proces. Sa zadnje strane nalaze se dva tastera koji služe za rukovanje grejačem. Sa prednje strane je ekran koji pokazuje zadatu temperaturu, trenutnu temperaturu, status rada grejača kao i radni napon (Sl. 1).

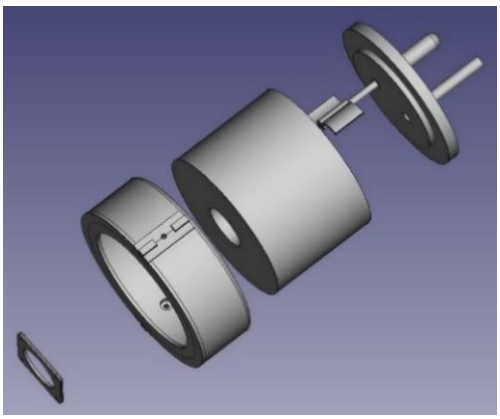

Sl. 2. Izgled kalorimetra i pratećih delova pripremljenih u programu FreeCAD

Kalorimetarski sud i prateći delovi s obzirom na specifične zahteve eksperimenta projektovan je u programu FreeCAD (Sl. 2). Delovi su izrađeni pomoću 3D-štampača Creality Ender5-pro. Materijal za izradu delova je bio PET-G zbog svojih dobrih mahaničkih i termičkih karakteristika kao i dobru otpornost na UV komponentu zračenja. Za posudu za vodu je iskorišćena metalna kutija instant kafe. Mešalica i digitalni termometar su postavljeni na poklopac kalorimetra. Sam kalorimetar i poklopac su štampani sa 10% punjenja, jer se time postiže dovoljno čvrsta mehanička struktura ali i dobra izolaciona svojstva.

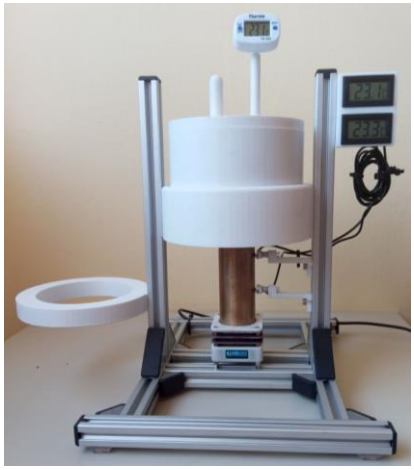

Sl. 3. Izgled sastavljene aparature

Stativ na kome je pričvršćena grejna ploča i nosač kalorimetra, napravljen je od standardnih EU profila 2020 i odgovarajućih spojnica. Konstrukcija od EU profila obezbeđuje da se uzorci metalnih cilindra jednostavno postavljaju na grejač na kome je postavljen žljeb za odgovarajući prečnik cilindra, takođe napravljen od PET-G materijala. Grejna ploča je pričvršćena za aluminijumski stativ pomoću četiri distancera dužine 30mm. Za noseću konstrukciju pričvršćen je i nosač kalorimetra pomoću kliznih navrtki, takođe napravljen na 3D-štampaču. Nosač kalorimetra obezbeđuje da kalorimetar stabilno stoji na metalnom cilindru tokom merenja jer se voda meša ručno pomoću mešalice. Vertikalni položaj nosača kalorimetra se može podesiti prema dužini metalnog cilindra čija se toplotna provodljivost meri. Izgled sastavljene aparature prikazan je na Sl. 3.

6. REZULTATI EKSPERIMENTA I DISKUSIJA

Za merenje toplotne provodljivosti opisanom aparaturom pripremeljni su cilindri od gvožđa, mesinga i duraluminijuma dužine 12cm i prečnika 4cm. Na kontaktnim površinama cilindar-grejna ploča i cilindar-kalorimetar nanešen je tanak sloj termalne paste (HY-610, K=3.05Wm^{-1}K^{-1}) kako bi se obezbedio bolji protok toplote. U kalorimetar je usuto 400ml vode koja je imala temperaturu oko 25℃. Temperatura grejne ploče je podešena na 70℃ koja se stabilisala nakon nekoliko minuta, a u trenutku kada je temperatura vode u kalorimetru porasla na 30℃ započeto je merenje temperature u zavisnosti od vremena. Na svakih 60s očitana je temperatura vode u kalorimetru tokom 20 minuta merenja. Rezultati merenja temperature za tri različita materijala prikazana su u Tabeli 1.

Tabela 1. Eksperimentalni podaci

	Gvožđe	Mesing	Aluminijum
τ [s]	t [℃]	t [℃]	t [℃]
0	30	30	30
60	30.5	30.8	31.2
120	31.1	31.6	32.3
180	31.6	32.5	33.4
240	32.1	33.4	34.4
300	32.5	34.2	35.5
360	32.9	35	36.5
420	33.4	35.8	37.5
480	33.9	36.5	38.5
540	34.3	37.1	39.4
600	34.6	37.8	40.2
660	35.1	38.6	41.1
720	35.4	39.2	41.9
780	35.8	39.8	42.7
840	36.2	40.4	43.5
900	36.6	41	44.2
960	36.9	41.6	44.9
1020	37.3	42.2	45.6
1080	37.6	42.8	46.3
1140	38	43.3	46.9
1200	38.4	43.9	47.6

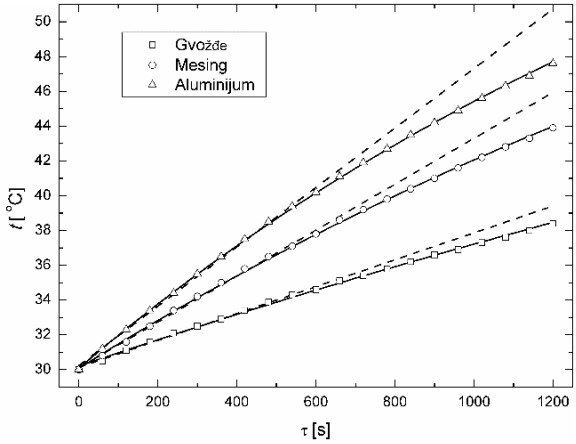

Sl. 4. Zavisnost temperature vode u kalorimetru pri provođenju toplote kroz gvožđe, mesing i duraluminijum. Linearni fit $t(\tau)$-isprekidana linija, jedn. (3)) za prvih 600s; egzaktan fit jedn. (11) u celom vremenskom intervalu (puna linija).

Na Sl. 4 prikazani su eksperimentalni podaci iz Tabele 1. Takođe, dati su linearni fitovi zavisnosti temperature vode u kalorimetru od vremena za tri različita materijala u prvih 600 s merenja. Sa grafika na Sl. 4 je jasno da je linearna aproksimacija strogo zadovoljena u sva tri slučaja u vremenskom intervalu 0s do nekih 500s.

Opšti podaci za merenje kao i rezultati fita i izračunate toplotne provodljivosti date su u Tabeli 2. Srednja temperatura vode je računata samo za prvih 11 tačaka (prvih 600s), jer je taj podatak potreban za izračunavanje toplotne provodljivosti u linearnoj aproksimaciji.

Dobijeni rezultati toplotne provodljivosti opisanim metodama su u međusobnoj saglasnosti u granicama eksperimentalne greške na nivou poverenja od 2σ (Tabela 2).

Tabela 2. Opšti eksperimentalni podaci i rezultati merenja toplotne provodljivosti.

		Gvožđe	Mesing	Aluminijum
Prečnik	d [mm]	40.00(5)		
Površina poprečnog preseka	S $[10^{-3}\mathrm{m}^2]$	1.257(3)		
Dužina	L [mm]	120.30(5)	122.60(5)	122.50(5)
Masa vode	m_v [g]	400.0(25)		
Specifični topl. kap. vode	c_v $[\mathrm{Jkg}^{-1}°\mathrm{C}^{-1}]$	4190		
Topl. kap. kal.	C_K $[\mathrm{J°C}^{-1}]$	1500		
Temperatura grejne ploče	t_p [°C]	70.0(5)		
Srednja temperatura vode	⟨t⟩ [°C]	32.445(16)	34.064(16)	35.354(16)
Linearni fit - Jedn. (3)	α $[10^{-2}\ °\mathrm{Cs}^{-1}]$	0.773(15)	1.320(22)	1.708(24)
Eksp. fit - Jedn. (11)	β $[10^{-4}\ \mathrm{s}^{-1}]$	1.926(19)	3.559(22)	4.835(20)
Linearni fit - Jedn. (7)	K $\left[\frac{\mathrm{W}}{\mathrm{m°C}}\right]$	63(3)	114(5)	153(6)
Eksp. fit - Jedn. (13)		58.6(12)	110.3(15)	149.7(14)
Dve tačke - Jedn. (14)		59(3)	112(4)	151(6)
Dve tačke - Jedn. (15)		59.6(20)	110(4)	150(5)

7. ZAHVALNICA

Ovaj rad je podržan od strane Ministarstva nauke, tehnološkog razvoja i inovacija kroz projekat broj 451-03-47/2023-01/200156 "Inovativna naučna i umetnička istraživanja iz domena delatnosti FTN-a" i Departmana zaopšte discipline u tehnici, Fakulteta tehničkih nauka u okviru projekta "Primena opštih disciplina u tehničkim i informatičkim naukama".

8. REFERENCE

[1] Resnick, R., Halliday, D., Krane, K.S.: *Physics*. 4thEd. Vol. 1. John Wiley and Sons, 1992.

[2] Samardžić, S., Nemeš, T.: *Praktikum Laboratorijskih vežbi iz fizike*, Fakultet tehničkih nauka, Novi Sad, 2021.

[3] Voldan, M., Strnad. R.: *PID control parameters optimization for temperature calibration laboratory*. 17th International Congress of Metrology, 15011, 2015.

Autori: **Assoc. prof. dr Tomas Nemeš, Full. Prof. dr Ljuba Budinski-Petković, Full. Prof. dr Selena Samardžić, Teaching Ass. M. Sc. Milica Beljin-Čavić,** Univerzitet Novi Sad, Fakultet Tehničkih Nauka, Trg Dositeja Obradovića 6, 21000 Novi Sad, Srbija.

Email: nemes.tomas@uns.ac.rs
ljupka@uns.ac.rs
selena@uns.ac.rs
milica.beljin@uns.ac.rs

ETIKUM 2023 **INTERNATIONAL SCIENTIFIC CONFERENCE**
NOVI SAD, SERBIA, DECEMBER 7-9, 2023

Petrović, Z., Tufegdžić, M., Brzaković, Lj., Nikolić, R.

PRIMENA PROGRAMSKOG SISTEMA ZA PRIPREMU SETOVA ALATA ZA OBRADU DELOVA SLOŽENE KONFIGURACIJE

Abstract: *Za realizaciju tehnoloških zadataka u okviru proizvodnje u fleksibilnom tehnološkom sistemu (FTS) neophodno je formirati setove alata koji se postavljaju u magacine obradnih centara na kojima se obrađuju delovi . Rešavanje problema setovanja alata za izvođenje ovih operacija je veoma značajno za povećanje produktivnosti tog FTS-a. U radu je prikazana primena programskog sistema za automatizovanu pripremu setova alata na osnovu analize NC programa dela koji se obrađuje. Programski sistem se oslanja na bazi tehnoloških podataka o elementima setova alata i geometrijskim parametrima o tehnološkim operacijama sadržanim u NC programu. Na osnovu predloženog algoritma u radu formiraju se liste setova alata za svaki učitan NC program.*
Key words: *Fleksibilni tehnološki sistem, Set alata*

1. UVOD

Upravljanje alatima u FTS-u sastoji se od izrade plana alata, određivanje njegovih karakterističnih geometrijskih veličina, izbora elemenata za komponovanje seta alata, sistema njegove identifikacije i monitoringa, i njegovoj dekompoziciji po završenoj tehnološkoj operaciji.

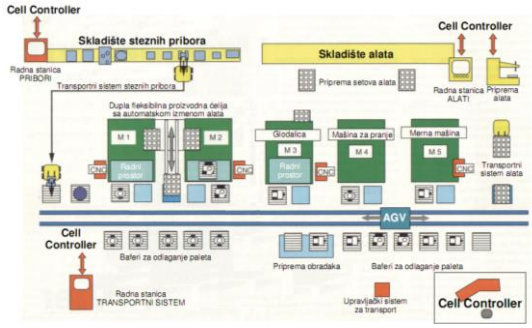

Sl. 1.Struktura fleksibilnog tehnološkog sitema[1]

U sekciji pripreme alata podaci o alatu se upisuju u bezkontaktni memorijski element a isčitavaju se posebnim čitačem povezanim sa računarsko upravljačkim sistemom alata. Svaki set alata mora biti izmeren i podešen a njegovi parmetri uneti u memorijski element nakon čega su spremni da se po redosledu izvšnih NC programa uključuju u obradne procese FTS-a prema instrukcijama cell kontrolera. Smanjenje vremena setovanja alata, u fleksibilnim tehnologijama, povećava produktivnost [2].

2. STRUKTURA SETA ALATA

Set alata je jedinstvena integrisana funkcionalna celina i sastoji se od elemenata: nosač, nastavak, reducir, pribor i rezni alat (slika 1). Elementi su modularno projektovani, zato se mogu komponovati na različite načine u zavisnosti od zahteva obradnog procesa i tehnološke operacije koju alat izvodi.

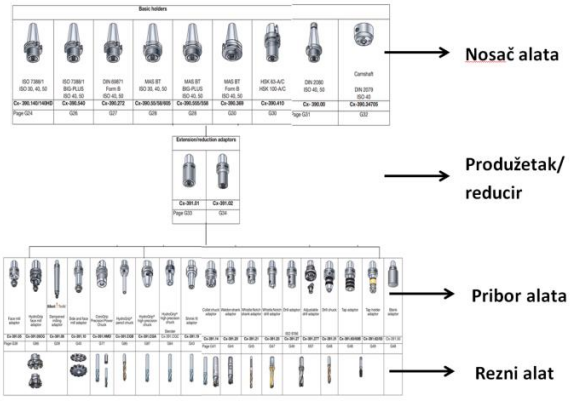

Sl. 2.Preporučeni elementi za sklapanje setova

Svaki set mora imati visoku krutost i da obezbedi dinamičku stabilnost reznog dela alata pri različitim režimima obrade. Kompatibilnost elemenata seta alata se određuje na osnovu njihovih dimenzija.

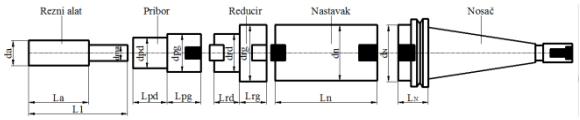

Sl 3. Opšta struktura seta alata [2]

Nosač uspostavlja vezu sa glavnim vretenom sa jedne strane i kompleta alata sa druge strane. Nastavak ima prednji cilindrični deo standardnog prečnika (d_N) dužine (L_N) koji se može postaviti ispred reducira ili pribora. Može se koristi da produži ukupnu dužinu seta alata ili da se smanji

prečnik seta alata. Prečnik nastavka (dn) određuju kompatibilnost sa sledećim elementom. U tehnološkoj praksi treba izbegavati setove alata sa višestrukim nastavcima, jer to smanjuje dinamičku stabilnost procesa obrade.
Reducir se koristi kada treba da se smanji prečnik seta. Reducir ima veći i manji prečnik (d_{RG}) i (d_{RD}) i dužine koje odgovaraju većem i manjem prečniku (L_{rg}) i (L_{RD}). Pribor sa jedne strane prihvata rezni alat (d_{PD}), sa druge strane ima konektor za ostale elemente (d_{PD}). Rezni alat i sve njegove karakteristike određuju se projektom tehnološkog procesa, a specificira se faza NC programa. Na osnovu NC programa alat obavlja tehničke operacije. Svaki niz NC programa obuhvaćenih tehnološkim ciklusom operacije, izvršava alat koji se nalazi u skupu. Jedan te isti alat može da izvrši više operacija ako njegove geometrijske i tehnološke karakterisitke to dozvoljavaju.
Set alata se postavjla u magacinu alata obradnog centra koji ima fiksno rastojanje između susednog sedišta alata i maksimalni prečnik reznog alata je ograničen.

3.SISTEM ZA AUTOMATIZOVANO SETOVANJE ALATA

Ulazni podaci za komponovanje seta alata se dobijaju analizom NC koda obrade:

- Mašina,
- vrsta alata,
- prečnik alata (d),
- dužina obrade (l) na osnovu vrednosti X,Y i Z iz NC programa.

Na osnovu mašine sistem bira koji nosač moraju imati setovi alata. Na osnovu vrste alata a za zadati prečnik (d) i dužinu obrade (l) sistem bira alate čiji su prečnici jednaki prečniku otvora ili rupe koja se obrađuje:

$$d=da \qquad (1)$$

Od tako izabranih alata bira onaj čija korisna dužina (la) sa dužinom obrade (l) pravi najmanju pozitivnu razliku:

$$\min\left[(l_{ai}-l)>0\right] \qquad (2)$$

Za ovako izabran nosač i alat sada postoje dva slučaja. Prvi slučaj je kada je Z koordinata iz NC programa manja od korisne dužine alata la:

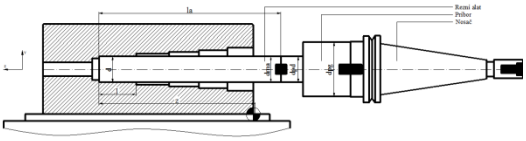

Sl. 4. Set alata kod koga je Z koordinata manja od korisne dužine alata[2].

U ovom slučaju sistem ima zadatak da izabere pribor koji mora imati kompatabilan prečnik sa prečnikom alata za spajanje dm:

$$dma=dpd \qquad (3)$$

i prečnikom nosača dN:

$$d_N=dpg \qquad (4)$$

U ovom slučaju ($Z<la$) setovi alata sadrže : alat, pribor koji ima ulogu reducira i nosač alata. Ovako izabran set mora da zadovolji uslov da je polovina najvećeg prečnika u setu veći od Y koordinate otvora ili rupe koja se obrađuje da nebi došlo do dodira elemenata seta alata sa radnim stolom ili priborom:

$$\frac{dpg}{2}<Y \qquad (5)$$

i da je ukupna dužina seta minimalna:

$$\min(l1+lpd+lpg) \qquad (6)$$

U drugom slučaju Z koordinata iz NC programa je veća od korisne dužine alata la:

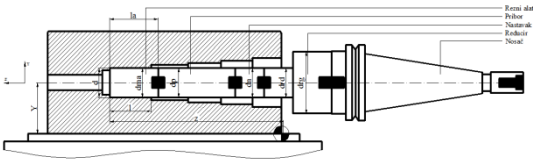

Sl. 5. Set alata kod koga je korisna dužina alata manja od Z koordinate[2].

U ovom slučaju inteligentni sistem takođe na osnovu mašine bira nosač koji moraju imati svi setovi alata. Zatim na osnovu tipa alata, prečnika obrade (d) i dužine obrade (l) sistem bira alate čiji su prečnici jednaki prečniku obrade:

$$d=da \qquad (7)$$

a nakon toga bira onaj alat čija korisna dužina (la) formira minimalnu pozitivnu razliku sa dužinom obrade (l):

$$\min\left[(l_{ai}-l)>0\right] \qquad (8)$$

Za ovako izabran alat i nosač a na osnovu poznate Z koordinate sistem proverava kolika je razlika između Z koordinate iz NC programa dužine alata u setu l_1. Veličinu ove razlike treba popuniti sa priborom, nastavkom, reducirom. Izabrani pribor mora da ima manji prečnik jednak prečniku za povezivanje alata a veći prečnik jednak prečniku za povezivanje kod nosača:

$$d_N=dpg$$
$$dma=dpd \qquad (9)$$

Ukoliko ukupna duzina seta još uvek nije veća od Z koordinate iz NC programa prazno mesto u setu se popunjava nastavcima. Cilj je pronaći nastavak sa kojim ukupna dužina seta alata i Z koordinatom pravi najmanju pozitivnu razliku:

$$\min\left\{\left[(Z-l1)-(lpd+lpg-l_N)\right]>0\right\} \qquad (10)$$

Pravila komponovanja setova alata su prikazana algoritmom:

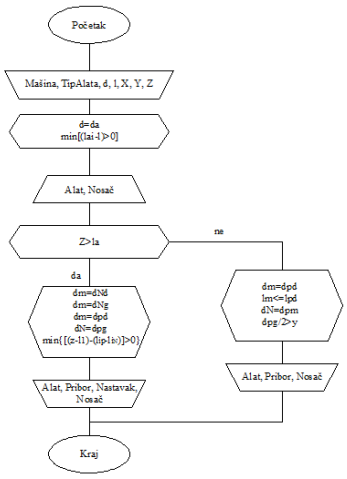

Sl. 6. Algoritam po kome se setuju alati.

Baza tehnoloških podataka o elementima seta alata se sastoji od devet objekata sa atributima kao na slici.

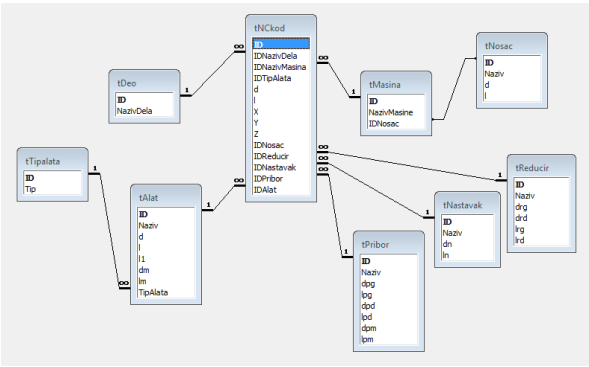

Sl. 7.Objekti i atributi baze podataka

Objekti odnosno tabele: tAlat, tPribor, tNastavak, tReducir, tNosač sadrže podatke o elementima seta alata, objekat tMašina sadrži podatke o mašinama koje su na raspolaganju, a objekat tDeo sadrži podatke o obratku.

4. PRIMENA PROGRAMSKOG SISTEMA ZA AUTOMATIZOVANO SETOVANJE ALATA

U svakoj tehnologiji za CNC obradu, a pogotovo u fleksibilnim tehnologijama koje se realizuju kroz izvođenje više hiljada različitih operacija pri obradi slženih delova u malim serijama, poseban problem predstavlja komponovanje setova alata za svaku operaciju [3].

Za prizmatični obradak, koji se proizvodi u velikoserijskoj proizvodnji, pomoću programskog sistema napravljen je spisak setova alata koji se koriste za realizaciju NC programa kojim se obrađuje ovaj komad.

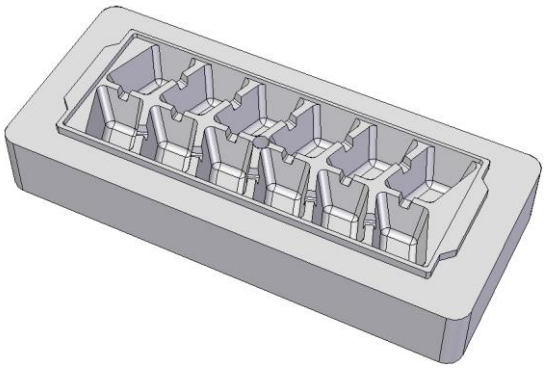

Sl. 8. Posuda za led [4]

Najpre se izaberu naziv obratka i mašina na kojoj se obradak obrađuje. Na osnovu redosleda tehnoloških operacija, koje se izvršavaju na osnovu NC koda na izabranoj mašini, unosi se prečnik i dužina obrade, tip alata i vrednosti X, Y i Z koordinate iz NC programa. Na osnovu tipa alata sistem zna iz koje grupe alata da izabere alat tog prečnika i dužine jednake ili veće od unete. Mašina na kojoj se izvode operacije je vertikalni obradni centar Mori Seiki NVD4000 DCG, sa upravljačkom jedinicom Fanuc MSX 501 MAPPS2, čiji je izgled dat na slici 6.10. Ova mašina pripada seriji troosnih obradnih centara posebno namenjenih za obradu kalupa za kovanje i livenje, čime omogućavaju veliku preciznost i veliki kvalitet obrade[4].

Sl. 9. Vertikalni obradni centar Mori Seiki NVD4000 DCG [4]

Redosled operacija za obradu radnih površina komada koji se obrađuje je sledeći:
1. Gruba čeona obrada
2. Gruba obrada kalupne šupljine
3. Gruba obrada džepova
4. Fina obrada džepova
5. Fina obrada ravnih površina kalupne šupljine
6. Fina obrada svih ostalih ravnih površina
7. Bušenje otvora

Za obradu radnih površina gnezda se koriste alati

firme Sandvik Coromant. Režimi obrade su usvojeni na osnovu preporuka proizvođača, i to iz kataloga CoroKey. Za čeonu i grubu obradu kalupne šupljine koristi se glodalo CoroMill® 200, prečnika 25 mm, čija je kataloška oznaka R200-015A20-10M, sa pločicom od tvrdog metala RCHT 10 T3 M0-ML. Za poluzavršnu obradu kalupne šupljine koristi se glodalo CoroMill® 300, prečnika 10 mm, čija je kataloška oznaka R300- 010A16L-05, sa pločicom od tvrdog metala R300- 0517E-MM. Za završnu obradu džepova se koristi glodalo CoroMill® Plura Ball nose endmill prečnika 8 mm, čija je kataloška oznaka R216.42-08030-AC16P. Za završnu obradu svih ravnih površina kalupne šupljine se koristi glodalo CoroMill® Plura Finishing endmill prečnika 4 mm, čija je kataloška oznaka R215.34-04045-AC11H, a za završnu obradu svih ostalih ravnih površina se koristi glodalo CoroMill® Plura Finishing endmill prečnika 16 mm, čija je kataloška oznaka R215.26- 16045DAC32H. Za bušenje otvora se koristi burgija CoroDrill Delta-C prečnika 10 mm, čija je kataloška oznaka R415.5-1000-50-AC0.. Ove podatke unosimo u poljima prikazanim na slici 13 a zadnjih pet polja inteligentni sistem sam popunjava.

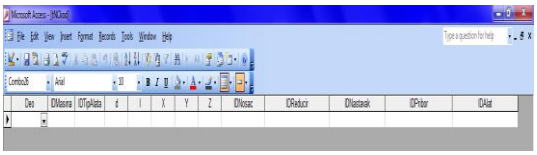

Sl. 10. Polja za unos podataka.

Na osnovu unetih podataka sistem bira elemente seta alata na osnovu definisanih pravila setovanja.
Sistem na osnovu oznake mašine bira nosač ISO40 koji moraju imati svi setovi alata, reducir ili nastavak ako treba zatim pribor a rezni alat je unapred definisan.

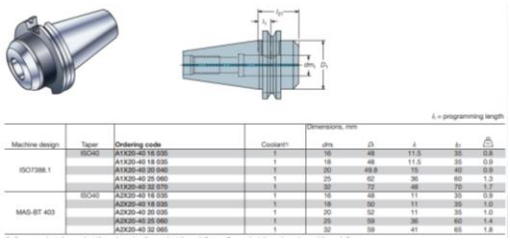

Sl. 11. Nosač alata

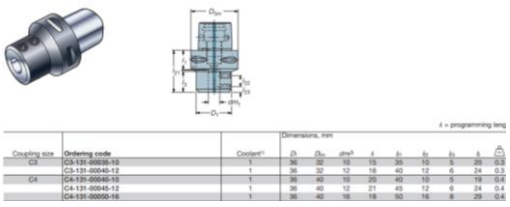

Sl. 12. Pribor za rezni alat

Potrebni setovi alata

ID	IDDeo	IDMasina	IDTipalata	IDNosač	IDReducir	IDNastavak	IDPribor	IDAlat
1	Posuda za led	More Seiki	Glodalo	ISO40	-	-	C5-131-00050-16	CoroMill200
2	Posuda za led	More Seiki	Glodalo	ISO40	-	-	C5-131-00050-16	CoroMill200
3	Posuda za led	More Seiki	Glodalo	ISO40	-	-	C5-131-00050-16	CoroMill300
4	Posuda za led	More Seiki	Glodalo	ISO40	-	-	C5-131-00050-16	CoroMill Plura Ball nose endmill
5	Posuda za led	More Seiki	Glodalo	ISO40	-	-	C5-131-00050-16	CoroMill Plura Finising endmill
6	Posuda za led	More Seiki	Glodalo	ISO40	-	-	C5-131-00050-16	CoroMill Plura Finising endmill
7	Posuda za led	More Seiki	Burgija	ISO40	-	-	C5-131-00035-10	CoroDrill Delta-C

Sl. 13. Lista setova alata potrebnih za obradu posude za led

5. ZAKLJUČAK

Algoritam za formiranje setova alata implementiran je u relacionu bazu tehnoloških podataka koja je razvijena u Microsoft Office Access-u. Baza podataka sadrži tabele sa podacima o alataima, priborima, nastavcima, reducirima i nosačima alata.

Smanjenje vremena setovanja alata direktno utiče na produktivnost proizvodnje, jer se fleksibilne tehnologije realizuju kroz izvođenje više hiljada različitih operacija. Vreme pakovanja setova alata za izvođenje ovih operacija se značajno skraćuje primenom ovakvog sistema.

6. REFERENCES

[1] Lukić, Lj.: *Fleksibilni tehnološki sistemi", Mašinski fakultet Kraljevo* , Kraljevo, 2008.

[2] Petrović, Z. , Lukić, Lj., Đapić, M., Petrović, A.: *Razvoj programskog sistema za pripremu setova alata u fleksibilnim tehnološkim sistemima*, 35th International Conference on Production Engineering, Kraljevo-Kopaonik, September 25, 2013-September 28,2013..

[3] Lukić, Lj., Šolaja, V.: *Ekspertni model za definisanje seta alata u fleksibilnim tehnologijama*, Zbornik radova 24. Savetovanja proizvodnog mašinstva Jugoslavije, knjiga I, Novi Sad, Vol. 2,str. 187- 192, 1992.

[4] Vranjevac, I.: *Automatsko generisanje NC programa za obradu radnog dela alata za proizvodnju delova od plastike*, Diplomski rad, Mašinski fakultet Kraljevo, 2008 godine.

Authors: **Zvonko Petrović, dr Milica Tufegdžić, Ljiljana Brzaković, dr Radovan Nikolić,** Akademija strukovnih studija Šumadija-Odsek Trstenik, Radoja Krstića 19, 37240 Trstenik, Srbija,
E-mail: zpetrovic@asss.edu.rs
mtufegdzic@asss.edu.rs
ljbrzakovic@asss.edu.rs
rnikolic@asss.edu.rs

ETIKUM 2023 **INTERNATIONAL SCIENTIFIC CONFERENCE**
NOVI SAD, SERBIA, DECEMBER 7-9, 2023

Pravdić, P., Đorđević, V., Erić-Obućina, J.

KONTROLA KVALITETA U MAŠINSTVU NA PRIMERU POGONSKOG ZUPČANIKA

***Rezime*:** *Cilj ovog rada je da na osnovu statističkih metoda ilustruje kontrolu kvaliteta pogonskog zupčanika koji je potrebno kontrolisati i prikazani su eksperimentalni podaci merenja, na osnovu dokumentacije preduzeća Petoletka DOO - Hidraulika. Na osnovu toga se zaključuje koje korektivne mere treba preduzeti da bi se osigurao stabilan i zadovoljavajući kvalitet u proizvodnji, a samim tim i povećanju rejtinga kompanija.*
Ključne reči: *pogonski zupčanik, kvalitet, mašinstvo, industrija.*

1. UVOD

Industrija se nalazi pod stalnim pritiskom da unapredi proizvodnju i poboljša kvalitet proizvoda. Postoji mnogo načina da se to uradi, ali je jako malo onih koji će pritom i smanjiti troškove proizvodnje. Zato se mnogo truda ulaže u pronalaženje i razvoj novih tehnoloških alatki za rešavanje ovih problema. Zahtev za kvalitetom star je gotovo kao i ljudska civilizacija i javlja se već u prvim oblicima "trgovine", odnosno materijalne razmene. Tokom vremena mnogo napora je uloženo u potvrđivanje kvaliteta i to ne samo proizvoda, već i proizvođača i isporučitelja. Možemo slobodno reći da kontrola kvaliteta ima dugu istoriju. Međutim, statistička kontrola kvaliteta je relativno nova metoda.

2. POGONSKI ZUPČANIK

Preduzeće Petoletka DOO – Hidraulika u svom proizvodnom programu ima veliki broj hidrauličnih pumpi koje proizvode u velikim serijama i za domaće i inostrano tržište i bitno je da obezbede precizan i kvalitetan proces izrade i kontrole zupčanika koji su sastavne komponente jednog dela njihovog proizvodnog programa. Na slici 1. je prikazan pogonski zupčanik ZPB F16 21 05, modeliran u programu ProEngineer Wildfire 5.0.

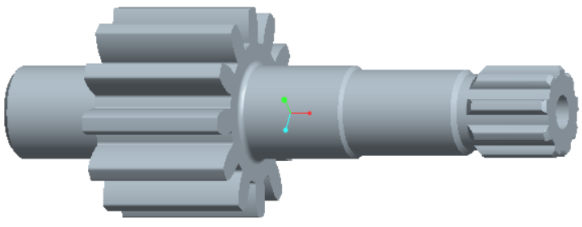

Sl. 1. Pogonski zupčanik

Sl. 2. Zupčanik ZPB F16 21 05

Realan prikaz istog pogonskog zupčanika iz procesa proizvodnje i kontrole je prikazan na slici 2. Na narednoj slici 3. prikazan je kontrolni list operacije za navedeni zupčanik. Na ovom dokumentu su navedeni svi podaci vezani za obradu zupčanika: mašina na kojoj se komad obrađuje, rezni alat i režimi obrade. Takođe, navedena je i kota koja se kontroliše, uz toleranciju i kvalitet obrade. Na skici zupčanika su dati i podaci o broju zuba (pravi zubi), modulu zupčanika, kvalitetu i polju tolerancije, uglu nagiba profila i meri preko dva zuba.

Deo	Naziv	I-šifra	br.crteža	Br. Dela
	Pogonski zupčanik,	757856		ZPB F16 21 05
Mašina	Naziv i tip	RC	I-šifra	Dat.pret.kon.
	0	3314085	0	
Režimi	Br.obrt.rad.kom.	Pomak	br.obrt.rez.	br.operac.
obrade	250	0,16		90
Rezni	Naziv	I-šifra	br.crt.alata	hladjenje
alat	nož za rendisanje	7280472		Ulje
Broj kontrolisanih komada:			30	

Sl. 3. Kontrolni list operacije

3. OCENA KVALITETA PROCESA

Osnovi koncept statističke kontrole procesa temelji se na upoređivanju podataka prikupljenih iz procesa, koji se kontroliše, sa kontrolnim granicama, koje su izračunate na osnovu istorijskih podataka pa na osnovu toga donošenje zaključaka o samom procesu. Statistička kontrola procesa u proizvodnji koristi se kako bi se osigurao kvalitet proizvoda koji će zadovoljiti zahteve kupca, u pogledu kvaliteta i cene koštanja [1]. Statistička kontrola procesa je skup metoda i procedura za prikupljanje, obradu, analizu, tumačenje i prikaz podataka. Koristi se u svrhu osiguranja kvaliteta proizvoda i procesa. Mehanizam statističke kontrole procesa zasniva se na upoređivanju podataka prikupljenih iz procesa sa unapred definisanim kontrolnim granicama za kvalitet proizvoda i proizvodnje, pa na osnovu toga donošenje zaključaka o samom procesu. Statistička kontrola procesa može da bude delimična i potpuna. Izbor jednog od dva moguća tipa statističke kontrole zavisi, pre svega, od tehničkih uslova i visine troškova. Po pravilu, delimična kontrola se primenjuje u uslovima masovne proizvodnje, gde bi potpuna kontrola uzrokovala izuzetno visoke troškove [2]. Ovi indeksi mere odnos između tekućih performansi procesa i zadatih performansi. Apsolutni minimum zahteva, da bi se proces smatrao sposobnim, je da se prirodna tolerancija procesa TP=X±3σ sadrži unutar zadatih tolerancija. Strožiji zahtev je da se obezbedi proizvodnja odgovarajućeg kvaliteta u dužem vremenskom periodu [3]. To obuhvata 99,73% proizvedenih proizvoda koji se nalaze u granicama 0,6÷0,7 polja tolerancije karakteristika proizvoda [5,6]. Analiza sposobnosti procesa ili opreme se izvodi sa ciljem ocene usaglašenosti parametara procesa ili opreme sa zahtevima definisanim crtežima, specifikacijama, u procesu proizvodnje ili u probnoj proizvodnji, pre i na poþetku serijske proizvodnje. Analiza obezbeđuje i identifikovanje karakteristika procesa potrebnih za projektovanje mera i primenu metoda i tehnika unapređenja kvaliteta [4]. Pet pokazatelja sposobnosti procesa i opreme Cp, CPU, CPL, k i Cpk predstavljaju potpun skup pokazatelja ocene sposobnosti - kvaliteta procesa, kao što je prikazano u tabeli 1 [3, 7]. Proces je sposoban kada su indeksi [3,7]:

- preciznosti Cp≥1,33 (atributivna ocena: precizan) i
- tačnosti Cpk≥1,33 (atributivna ocena: tačan-podešen).

Mogućnosti procesa, korišćenjem ovih navedenih indeksa, mogu se oceniti na sledeći način [3,7]:

- ako je Cp≥1,33 i |Cp–Cpk|≤0,1 |Cp| mogućnosti procesa su visoke (proces je precizan i tačan),
- ako je 1≤Cp≤1,33 i |Cp-Cpk|≤0,1 |Cp| mogućnosti procesa su zadovoljavajuće, ali je neophodno stalno praćenje i monitoring procesa,
- ako je Cp<1 mogućnosti procesa su nezadovoljavajuće i pod hitno je potrebno preduzeti mere unapređenja mogućnosti procesa (povećanje tačnosti tehnološkog procesa zamenom ili remontom opreme…).

Tabela 1. Pet pokazatelja sposobnosti procesa

Pokazatelji	Zavisnost	Naziv
Cp	$\frac{GGT - DGT}{6 \cdot \sigma}$	Potencijal procesa
CPU	$\frac{GGT - \overline{X}}{3 \cdot \sigma}$	Pokazatelj sposobnosti procesa u odnosu na gornju granicu odstupanja
CPL	$\frac{\overline{X} - DGT}{3 \cdot \sigma}$	Pokazatelj sposobnosti procesa u odnosu na donju granicu odstupanja
k	$\frac{2 \cdot \lvert m - \overline{X} \rvert}{GGT + DGT}$	Koeficijent odstupanja srednje vrednosti procesa od sredine tolerantnog polja
Cpk	$\min\{CPL, CPU\} = (1 - k) \cdot Cp$	Indeks sposobnosti procesa

4. MERENJE I OCENA PROCESA PREKO INDEKSA SPOSOBNOSTI

Mera koja se kontroliše u ovom primeru je data na skici sa slike 3. To je mera 16,30mm. Tolerancija je ±0,170. Ukupan broj kontrolisanih komada je 30.

Nakon obavljenih svih merenja, vidimo da se

izmerene vrednosti kreću u rasponu 16,400mm do 16,230mm, što odgovara navedenoj toleranciji. Sve dobijene vrednosti merenja su prikazane na slici 4.

r / n	1	2	3	4	5
1	16,250	16,260	16,250	16,260	16,250
2	16,250	16,240	16,250	16,250	16,240
3	16,260	16,260	16,260	16,250	16,250
4	16,240	16,240	16,240	16,250	16,250
5	16,250	16,260	16,250	16,260	16,250
6	16,260	16,260	16,260	16,250	16,250
Σx	97,510	97,520	97,510	97,520	97,490
$\bar{\bar{x}}$	16,252	16,253	16,252	16,253	16,248
w_i	0,020	0,020	0,020	0,010	0,010

Sl. 4. Rezultati merenja zupčanika

Na osnovu dobijenih rezultata merenja pristupa se obradi podataka, odnosno izračunavanju svih potrebnih indeksa potencijala i sposobnosti procesa. Obrada podataka se izvodi prema obrascima navedenim u tabeli 2.

Tabela 2. Obrasci i rezultati obrade podataka

Obrasci	Rezultati
$\bar{\bar{X}} = \frac{\sum_{i=1}^{r} \bar{X}_i}{r}$	$\bar{\bar{x}}$=16,25167
$\bar{\bar{\omega}} = \frac{\sum_{i=1}^{r} \bar{\omega}_i}{r}$	w=0,016
dn – usvojena vrednost	d_n =2,534
$\bar{\sigma} = \frac{\bar{\omega}}{d_n}$	$\bar{\sigma}$=0,006314
$\sigma = \sqrt{\frac{\sum_{i=1}^{r}\left(X_i - \bar{\bar{X}}\right)^2}{r \cdot n - 1}}$	σ=0,006989
TNM=6·σ	TNM=0,037885
TNP=6·σ	TNP=0,041936
$C_p = \frac{T}{6 \cdot \sigma}$	C_p=4,053805
$C_{pk} = \frac{\Delta krit.}{3 \cdot \sigma}$	C_{pk}=7,074607
$\Delta krit. = GGT - \bar{\bar{X}}$	0,148333333
$\Delta krit. = \bar{\bar{X}} - DGT$	0,021666667
$f_p = \frac{6 \cdot \sigma}{T} \cdot 100\%$	f_p = 24,66818

Svi izračunati rezultati iz obrade podataka i eksperimentalno dobijeni rezultati merenja se objedinjuju u jednom dokumentu, koji je prikazan na sledećim slikama.

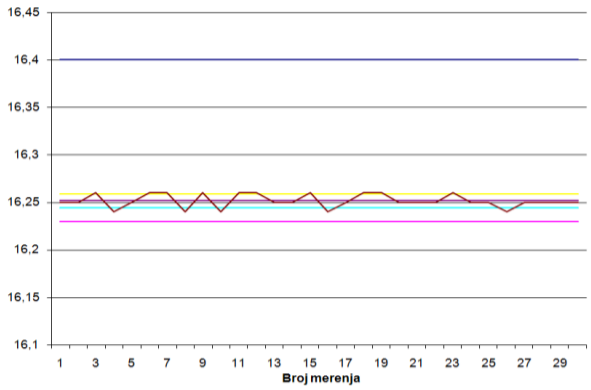

Sl. 5. Grafik rezultata merenja

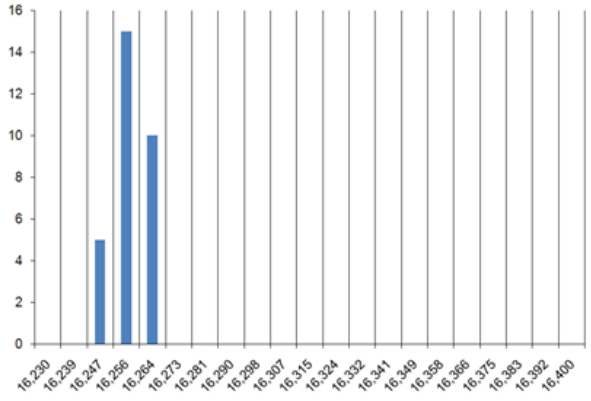

Sl. 6. Histogram raspodele rezultata merenja

Vrednosti koje su dobijene merenjem su prikazane i grafički, u dva grafika koji su prikazani na naredne dve slike.

Na prvom grafiku (slika 5) je prikazana zavisnost dobijenih brojčanih vrednosti merenja i broja izvršenih merenja. Vidimo da se izmerene vrednosti kreću u okviru tolerancije. Data je nazivna mera na crtežu, a minimalna i maksimalna izmerena vrednost se nalaze u okviru propisane tolerancije. Vrednost X treba da se nalazi između 16,230mm i 16,400mm i to je zadovoljeno, kao što vidimo iz izmerenih vrednosti.

X=16,252mm
Xmin=16,240mm
Xmax=16,260mm
T=0,170
šk%=0,000

Na drugom grafiku (slika 6) je prikazan histogram raspodele, odnosno zavisnost izmerenih vrednosti i broja ponavljanja istih vrednosti.

Svi ovi podaci su uneti u napomeni u dokumentu na kom se nalaze grafici i naveden je podatak o procentu škarta - 0%. Na kraju ostaje analiza rezultata merenja i izračunatih vrednosti. Iz rezultata dobijenih obradom podataka, vidimo da je vrednost potencijala procesa veća od 1,33 (Cp=4,053805), što nam govori da je proces precizan. Takođe, vrednost indeksa sposobnosti procesa je veća od 1,33 (Cpk=7,074607), što nam

govori da je proces tačan – podešen, što nam govori da su mogućnosti procesa visoke (proces je i precizan i tačan). Na osnovu svih ovih pokazatelja zaključujemo da mašina obezbeđuje precizan i tačan postupak i sve to unosimo u konačan izveštaj o sposobnosti tehnološkog procesa. Ovaj izveštaj je prikazan na slici 7. Takođe, naglašavamo da nije potrebno preduzimati nikakve korektivne mere.

IZVEŠTAJ O OCENI SPOSOBNOSTI TEHNOLOŠKOG SISTEMA
KONTROLNI LIST OPERACIJE/OCENA PROVERE

Deo	Naziv		I-šifra	br.crteža	Br. Dela
	Pogonski zupčanik		757856		ZPB F16 21 05
Mašina	Naziv i tip		RC	I-šifra	Dat.pret.kon.
	0		3314085	0	
Režimi	Br.obrt.rad.kom.		Pomak	br.obrt.rez.	br.operac.
obrade	250		0,16		90
Rezni	Naziv		I-šifra	br.crt.alata	hladjenje
alat	nož za rendisanje		7280472		Ulje
Broj kontrolisanih komada:			30		
Kontrolisane kote					
Kota	toler.	Ra	Kota	toler.	Ra
16,3	16,400	N7			
	16,230				
Kontrolisana karakteristika: 16,3			Veličina tolerantnog polja: 0,170		
Ocena provere: Mašina obezbedjuje precizan i tačan postupak					

Sl. 7. Izveštaj o oceni tehnološkog procesa

5. ZAKLJUČAK

Ocena sposobnosti procesa i opreme se može, pored pokazatelja sposobnosti procesa, izvesti i pomoću krivih rasipanja i kontrolnih karata. Bilo koja metoda da se koristi, ocenom se dobija odgovor da li se može obezbediti zahtevani nivo kvaliteta proizvoda, sa stanovišta procesa, radnika, mašina, alata i pribora. Nijedna aktivnost upravljanja kvalitetom nije moguća bez poznavanja sposobnosti procesa. Prednost indeksa pokazatelja sposobnosti je u tome što se aktivnost usmerava na prevenciju pojave neusaglašenosti, defektnih proizvoda, odnosno škarta. Naravno, pomoću ovih podataka proces može da se prati i stalno unapređuje. Da bi kvalitet došao na red, mora biti "prodat" rukovodstvu. Koristi moraju biti merljive i lako uočljive. Da bi se to ostvarilo treba krenuti od onih problema čijim se rešavanjem postižu najvidljiviji rezultati. Među ovim faktorima poslovnog neuspeha, polovina je objektivna i za većinu preduzeća je realnost sa kojom ne može samostalno da se bori. Međutim, druga polovina uzroka, odnosi se na odluke koje donosi rukovodstvo organizacije, na politike koje kreira, i na strategije koje sprovodi. To su faktori interne prirode na koje se može uticati unutar same organizacije.

6. REFERENCE

[1] Wu, C.W., Pearn, W.L., Kotz, S.: *An overview of theory and practice on process capability indices for quality assurance*, International Journal of Production Economics, Vol. 117, No. 2, pp. 338–359, 2009.

[2] Montgomery, D. C.: *Introduction to Statistical Quality Control*, John Wiley & Sons, Inc, 7th edition, 2013.

[3] Lazić, M.: *Sposobnost procesa - merenje i ocena kvaliteta procesa*, 38. nacionalna konferencija o kvalitetu festival kvaliteta, 2011.

[4] Chandra, M. J.: *Statistical quality control*, CRC Press, 2001.

[5] Kovačić, G., Kondić, Ž.: *Statistička analiza sposobnosti procesa proizvodnje stretch folije*, Tehnical journal - Tehnički glasnik, Vol. 6, No. 2, pp. 191-198, 2012.

[6] Alagić, I.: *Osiguranje kvaliteta procesa mašinske obrade kočionog diska 1J0 615 601 korištenjem SPC tehnika kvaliteta*, 3. Naučno-stručni skup sa međunarodnim učešćem KVALITET 2003, Zenica, B&H, 2003.

[7] Lazić, M.: *Alati, metode i tehnike unapređenja kvaliteta*, Mašinski fakultet, Kragujevac, 2006.

[8] Kolarević, M., Radičević, B., Premović, B., Živković, O.: *Indeksi za ocenu sposobnosti procesa*, IMK-14, Istraživanje i razvoj, Vol. 16, No. 4, pp. 31-36, 2010.

[9] Oakland, S. J.: *Statistical Process Control*, Fifth Edition, Butterworth Heinemann, 2003.

Autori:

Dr Predrag Pravdić, Akademija strukovnih studija Kruševac, Ćirila i Metodija 30, 37200 Krušavac, Srbija, Tel: +381 37 439 741, Fax: +381 37 439 416

E-mail: thepera81@gmail.com

M.Sc. Violeta Đorđević, M.Sc. Jelena Erić-Obućina, Akademija strukovnih studija Šumadija, odsek Trstenik, Radoja Krstića 19, 37240 Trstenik, Srbija, Tel: +381 37 714 121, Fax: +381 37 714 121

E-mail: vdjordjevic@asss.edu.rs
jobucina@asss.edu.rs

ETIKUM 2023 **INTERNATIONAL SCIENTIFIC CONFERENCE NOVI SAD, SERBIA, DECEMBER 7-9, 2023**

Pravdić, P., Đorđević, V., Erić-Obućina, J.

TEHNOLOŠKI PROCESI U INDUSTRIJI 4.0

Rezime: *Industriju 4.0 karakterišu tehnološka rešenja koja su omogućila veće upravljanje proizvodnim sistemima, fleksibilnost proizvodnje i savremeni način distribucije proizvoda. Ovakvim tehnologijama proizvodi i sredstva za proizvodnju postaju umreženi i mogu da „komuniciraju", omogućavajući nove načine proizvodnje i optimizaciju u realnom vremenu. Industrija 4.0, kao četvrta industrijska revolucija, već traje u mnogim zemljama. Time obezbeđuje opstanak industrije i njen konkurentan razvoj u savremenim uslovima.*
Ključne reči: *tehnologija, procesi, mašinstvo, industrija 4.0*

1. UVOD

Danas, u 21. veku, tehnologija je mnogo više od toga. Kako se rešenja probijaju direktnim putem do nas kroz mnogobrojne ponude tehnoloških giganata, tako se i kroz određene usluge kompanija i njihove operacije integrišu sa našim potrebama. Uzimajući u obzir pritisak inovacija i potreba novih generacija, kompanije su godinama preduzimale mere kako bi nadmudrile svoje konkurente i zadržale vodeću poziciju u igri gde je nebo granica. Kako bi lakše ispratilo ishode boljih, bržih, efikasnijih mera kompanija, čovečanstvo je kreiralo segmente revolucionarnih epoha, te tako danas u proizvodnim sistemima živimo četvrtu industrijsku revoluciju, poznatiju kao industrija 4.0. Istorijski gledano, svaka revolucija je donela nešto proizvodnom sektoru. Počevši od kraja 18. veka, prvom industrijskom revolucijom uvodi se proizvodni pogon koji koristi snagu vode i pare, pri čemu je čovek povećao svoju produktivnost osam puta. Zatim, na početku 20. veka, u tzv. eri fordizma, čovečanstvo podstiče kapitalističko društvo uvodeći standardizaciju sistema masivne i linijske proizvodnje, da bi, ubrzo zatim, sedamdesetih godina, došlo do razvoja poluatomatskih proizvodnih pogona pomoću elektronike i IT rešenja – treća industrijska revolucija.

2. NOVE TEHNOLOGIJE U INDUSTRIJI 4.0

Industrija 4.0 saopštena je prvi put kao pojam u 2011. godini, na sajmu u Hanoveru, gde je radna grupa nemačke vlade istakla ovaj pojam kao preokret konvencionalne logike proizvodnog procesa. Ovaj pojam karakterišu tehnološka rešenja koja su omogućila veće upravljanje proizvodnim sistemima, fleksibilnost proizvodnje i savremeni način distribucije proizvoda. Sajber-fizički sistemi, kao osnova industrije 4.0, koriste moderne softverske sisteme upravljanja koji raspolažu internet adresom za povezivanje i adresiranje putem interneta stvari (IoT). Ovakvim tehnologijama proizvodi i sredstva za proizvodnju postaju umreženi i mogu da „komuniciraju", omogućavajući nove načine proizvodnje i optimizaciju u realnom vremenu. Kombinovanjem razvoja pet osnovnih tehnologija koje podržavaju rast industrije 4.0 otvoriće se nove mogućnosti u ovoj oblasti. Konkretno, tehnologije prisutne u današnjim pametnim fabrikama koje pokreću ovu industriju pre svega su IoT rešenja, veštačka inteligencija, interfejsi, napredna robotika i 3D štampa. U praksi, danas imamo pametne fabrike opremljene naprednim senzorima, ugrađenim softverima i robotikom, koji prikupljaju i analiziraju podatke i omogućavaju bolje donošenje odluka. Takođe, ovakva rešenja dobijaju svoj pun potencijal kada se podaci iz proizvodnih operacija kombinuju sa operativnim podacima iz ERP-a, lanca snabdevanja, korisničke službe i drugih sistema preduzeća, kada dolazi do potpuno novih nivoa analize i uvida iz prethodno izdvojenih informacija. Neki od očekivanih ishoda ovakve industrijske transformacije, pre svega, jesu smanjenje troškova zaliha 15–20 odsto, povećanje produktivnosti 15–30 odsto, smanjenje perioda prestanka rada mašina 30–50 odsto i povećanje tačnosti predikcija od 85 odsto. Dobar primer kompanije koja je uspešno realizovala integraciju pametne fabrike, negde i očekivano, dolazi nam iz automobilske industrije. Naime, kompanija Seat je sprovela digitalnu transformaciju u postrojenju u Martorelju, gde se, pored mnogobrojnih benefita digitalizacije i konekcije sa digitalnom proizvodnom platformom Folksvagena, najviše ističe proračunata predikcija održavanja mašina kompletnog pogona do 2025. godine. Međutim, u jeku krize koja je zadesila ceo svet ovakav vid

transformacije predstavlja izazov i za najveće. Sa jedne strane, lideri su se susreli sa uticajima kovida, koji su svima nama već dobro poznati, dok, sa druge strane, imamo globalne uticaje koji su uslovili te iste lidere da se spreme za period recesije i inflacije. U oba slučaja, dok kompanije razmišljaju o obnavljanju poslovanja za suočavanje sa krizama, upotreba digitalnih tehnologija će mnogima biti na prvom mestu. Kada govorimo o proizvodnim kompanijama i njihovoj digitalnoj transformaciji operativnog modela, možemo slobodno da kažemo da svaki korak ka digitalnom poslovanju predstavlja korak ka industriji 4.0. Stoga, potrebno je jasno odrediti strateški put kompanije kako bi na efikasan način dostigla svoj potpuni potencijal. Kao temelj strategije, izdvojio bih pet ključnih segmenata integrisanih u dinamiku tržišta i ekosistema usmerenog ka industriji 4.0, kao i mogućnosti kojima treba težiti.

3. UNAPREĐENJE PROCESA PROIZVODNJE U INDUSTRIJI 4.0

Fleksibilna orijentacija ka klijentu: Kada govorimo o orijentaciji ka klijentima, koji pod uticajem tržišnih trendova frekventno menjaju svoje prohteve, bitnu komparativnu prednost u tom segmentu predstavlja fleksibilnost. Za takvu kompaniju važno je da ostvari mogućnost da individualno adaptira proizvod i proizvodne volumene prema željama kupaca. U tom slučaju postoje brojna rešenja koja omogućavaju takvu vrstu fleksibilnosti, na primer, automatizacija rukovanja porudžbinama, fleksibilni proizvodni sistemi, adaptivna logistika i drugo.

Operativna izvrsnost: U okviru operativne izvrsnosti, lično volim da stavim akcenat na način povećanja produktivnosti kroz kontinuiranu i dinamičku optimizaciju svih procesa duž lanca vrednosti radi postizanja efikasnosti u skladu sa zahtevima kupaca, koju je bitno sprovesti u periodu tehnološke tranzicije. Tehnologije koje podržavaju ovakav vid promena uglavnom se baziraju na automatizovanom upravljanju proizvodnjom u realnom vremenu i kontroli procesa, poboljšanju produktivnosti samih zaposlenih i sinhronizaciji dizajna proizvoda i proizvodnje.

Okolina, sigurnost i zdravlje: Kako bi se podsticale ljudske vrednosti i sprovela korporativna kultura koja neguje zdravu sredinu za rad u periodu tranzicije ka industriji 4.0, treba tražiti rešenja koja su namenjena HR aktivnostima i koja se bave poboljšanjem ergonomije i sigurnosti rada, kao i smanjenjem potrošnje resursa i energije.

Ljudi: Prema podacima Komisije za obrazovanje, predviđa se da do 2030. više od polovine od skoro dve milijarde mladih širom sveta neće imati veštine ili kvalifikacije neophodne za učešće u globalnoj radnoj snazi u razvoju. U praktičnom smislu, ovo znači da više od 50 odsto sutrašnjeg ljudskog kapitala potencijalno neće biti spremno da prati razvoj potrebnih veština za buduća radna mesta. Stoga, kompanije moraju da nađu način kako da razvijaju svoje zaposlene kroz edukaciju i pripreme za potrebe nove industrijske revolucije.

Rešenja: Prethodno spomenuti segmenti, u zavisnosti od industrije, mogu imati različitu interpretaciju i razradu do nivoa konkretnih aktivnosti. Postoje četiri osnove prilikom implementacije tehnološke transformacije ka industriji 4.0, koje se sastoje od usklađenih IT/klaud platformi, komunikacija mašina sa klaudom, operativnog modela za sveukupno usklađivanje i potencijalnih partnerstava za dodatne mogućnosti. Na kraju, bitno je naglasiti da rukovodstvo kompanije mora definisati konkretne mogućnosti kojima teži, zatim ih podeliti u određene projektne inicijative u skladu sa prioritetima, te odrediti tehnološka rešenja koja su potrebna kako bi se transformacija uradila na efikasan način, jer što se bolje spreme – duže će istrčati ovaj tehnološki maraton.

Pojam „industrijska revolucija" povezuje se s društvenim razvojem koji se događa u „kratkom" vremenskom periodu. Prelazak od ručne (zanatske) proizvodnje u drugoj polovini 18. veka i veće korišćenje parne mašine sredinom 19. veka, doveo je do promena političkih i privrednih sistema, pa se smatra početkom „prve industrijske revolucije". Čitav vek kasnije, primenom naizmenične električne energije i montažnih linija u proizvodnji, računa se kao početak „druge industrijske revolucije". Pojavom računara, razvojem telekomunikacija i interneta, automatizacijom proizvodnih procesa i bržom obradom podataka od sredine 20. veka, govori se o početku „treće industrijske revolucije". Neki istoričari nauke tvrde da se tek početkom trećeg milenijuma može govoriti o „četvrtoj industrijskoj revoluciji" ili „industriji 4.0", koju karakterišu digitalizacija, brzi internet, veća automatizacija proizvodnih procesa, razvoj fleksibilnih tehnologija, „inteligentnih mašina" i „pametnih fabrika" radi ekonomične proizvodnje visokog kvaliteta u malim serijama i sve kraćim rokovima. Opravdano je postaviti pitanje da li se ispravno koristi termin „industrijska revolucija", pošto su od prve do početka četvrte protekla dva i po veka. Za takve procese je pravilnije koristiti termine „evolucija", „trend" ili „proces razvoja", koji mogu biti sporiji ili brži. Treba imati u vidu i činjenicu da na trend razvoja (kompanija i zemalja) utiče mnoštvo parametara: nivo već

osvojenih tehnologija, postojeća znanja i sopstvena istraživanja, međunarodna saradnja, podrška bankarskog sektora, podsticaji države, kompetentnost vlasti i interesi donosilaca odluka.

4. INDUSTRIJI 4.0 KAO BUDUĆNOST

Industrija je danas suočena s novom generacijom potpuno digitalizovanih fabrika. Industrija 4.0, kao četvrta industrijska revolucija, već traje u mnogim zemljama. Time obezbeđuje opstanak industrije i njen konkurentan razvoj u savremenim uslovima. U digitalizovanoj fabrici obezbeđuje se inteligentno sadejstvo procesa proizvodnje i povezuju se fizički, digitalni i virtuelni svet. Digitalno preduzeće, osim digitalizovanih mašina, mora da ima i industrijski softver koji obuhvata proizvodne procese, komunikacionu infrastrukturu, bezbednosni sistem i digitalizovane industrijske servise. Softverska rešenja mogu se razvijati u sopstvenoj sredini, ali većina kompanija kupuje ih od specijalizovanih proizvođača. Sadašnjem razvoju Industrije 4.0, još osamdesetih godina prošlog veka, prethodili su CIM, CAM i CAD sistemi, ali oni zbog tadašnjeg tehnološkog nivoa nisu mogli da obuhvate ukupnu digitalizaciju poslovanja. Evropska komisija je, u okviru sprovođenja Strategije jedinstvenog digitalnog tržišta, u aprilu 2016. predstavila planove i mere za podršku digitalizaciji evropske industrije. Razvoj Industrije 4.0 je jedan od prioriteta i zato su osnovani podsticajni fondovi, usvojeni neki standardi i predloženi novi propisi. Nekoliko članica EU usvojilo je i posebne strategije za podršku razvoju Industrije 4.0. Procenjeno je da će se u narednih pet godina digitalizacijom povećati godišnji prihod evropskog industrijskog sektora za više od 110 milijardi evra. Gunther Oettinger, komesar za digitalnu ekonomiju i društvo, kaže: „Da bi Evropa zadržala vodeći položaj, mora uspešno i brzo da digitalizuje svu svoju industriju“. U Evropskoj uniji do 2030. godine planiraju se investicije od 1.350 milijardi evra u Industriju 4.0, što znači da je ona posvećena digitalizaciji i razvoju Industrije 4.0. Četvrta industrijska revolucija, 4IR ili Industrija 4.0, konceptualizuje brze promene tehnologije, industrija i društvenih obrazaca i procesa u 21. veku zbog sve veće međusobne povezanosti i pametne automatizacije. Pojam je popularizovao Klaus Švab, osnivač i izvršni predsednik Svetskog ekonomskog foruma, 2015. godine, i od tada se koristi u brojnim ekonomskim, političkim i naučnim člancima u vezi sa trenutnom eru nastajuće visoke tehnologije. Švab tvrdi da su promene koje se vide više od samo unapređenja efikasnosti, već izražavaju značajan pomak u industrijskom kapitalizmu. Deo ove faze industrijske promene predstavlja povezivanje tehnologija poput veštačke inteligencije, uređivanja gena i napredne robotike, koje zamagljuju granice između fizičkog, digitalnog i biološkog sveta. Tokom ovog procesa, fundamentalne promene se odvijaju u načinu funkcionisanja globalne proizvodne i snabdevačke mreže putem kontinuirane automatizacije tradicionalnih proizvodnih i industrijskih praksi, korišćenjem moderne pametne tehnologije, komunikacije između mašina (M2M) i interneta stvari (IoT). Ova integracija rezultira povećanom automatizacijom, poboljšanom komunikacijom i samopraćenjem, kao i upotrebom pametnih mašina koje mogu analizirati i dijagnostikovati probleme bez potrebe za ljudskim intervencijama. Takođe, predstavlja socijalni, politički i ekonomski pomak od digitalnog doba kasnih 1990-ih i ranih 2000-ih ka dobu ugrađene povezanosti koje se odlikuje sveprisutnom upotrebom tehnologije u društvu (npr. metavers), menjajući načine na koje ljudi doživljavaju i poznaju svet oko sebe. Tvrdi se da smo stvorili i ulazimo u unapređenu socijalnu stvarnost u poređenju sa samo prirodnim čulima i industrijskim sposobnostima ljudi. Očekuje se da će Četvrta industrijska revolucija biti praćena Petom industrijskom revolucijom.

5. ZAKLJUČAK

Velike i značajne promene u određenom trenutku nazivaju se revolucijom. Revolucija uključuje promene u kulturi, ekonomiji i društveno-političkim institucijama i, shodno tome, direktno utiče na živote ljudi. U tom kontekstu, Industrija 4.0, Industrijska revolucija 4.0 ili Četvrta industrijska revolucija usmerena je na stvaranje pametnih proizvoda, procedura, procesa i, na kraju, celokupne proizvodnje. Industrija 4.0 takođe produkuje i značajne poslovne implikacije, pružajući veću fleksibilnost i robusnost, zajedno sa najvišim standardima kvaliteta u inženjeringu, planiranju, proizvodnji i operativnim i logističkim procesima. To će dovesti do pojave dinamičkih, samoorganizujućih vrednosti u "realnom vremenu", koje je moguće optimizovati spram različitih kriterijuma kao što su troškovi, dostupnost i potrošnja resursa. Imajući u vidu gore navedeno, primarni cilj rada jeste sagledavanje efekata i problema Industrije 4.0 iz perspektive poslovne sfere u opštem smislu. Nalazi mogu biti od koristi i kompanijama (i kod nas) koje tek počinju sa implementacijom novih tehnologija, koje sa sobom donosi novi talas promena. U celini uzev, može se tvrditi, s obzirom na njegove karakteristike i promene, da je ovo najnapredniji i

najsofisticiraniji revolucionarni period koji potpuno menja tradicionalni način poslovanja. U suštini, Četvrta industrijska revolucija je trend ka automatizaciji i razmeni podataka u tehnologijama i procesima proizvodnje, uključujući kibernetičko-fizičke sisteme (CPS), internet stvari (IoT), industrijski internet stvari, cloud računarstvo, kognitivno računarstvo i veštačku inteligenciju. Mašine ne mogu zameniti dubinsko stručno znanje, ali često su efikasnije od ljudi u obavljanju ponavljajućih funkcija, a kombinacija mašinskog učenja i računarske snage omogućava mašinama da obavljaju veoma složene zadatke. Četvrta industrijska revolucija (4IR) definiše se kao tehnološki razvoj u kibernetičko-fizičkim sistemima kao što su visokokapacitivna povezanost; novi načini interakcije između ljudi i mašina kao što su interfejsi osetljivi na dodir i sistemi virtuelne stvarnosti; poboljšanja u prenosu digitalnih instrukcija u fizički svet, uključujući robotiku i 3D štampanje (aditivnu proizvodnju); internet stvari (IoT); "velike podatke" i cloud računarstvo; sistem zasnovan na veštačkoj inteligenciji; poboljšanja i usvajanje autonomnih energetskih sistema van mreže: solarnih, vetrovnih, talasnih, hidroelektričnih i litijum-jonskih sistema za skladištenje obnovljive energije (ESS) i električnih vozila.

6. REFERENCE

[1] Bai, Chunguang; Dallasega, Patrick; Orzes, Guido; Sarkis, Joseph (2020-11-01). *„Industry 4.0 technologies assessment: A sustainability perspective”*. International Journal of ProductionEconomics, 229:107776. ISSN 092 55273. S2CID 218941878. doi:10.1016/j.ijpe. 2020.107776.

[2] McGinnis, Devon (2023-02-02). *„What Is the Fourth Industrial Revolution?”*.

[3] *„The Fourth Industrial Revolution will be peoplepoweredMcKinsey”*. *www.mckinsey.com.*

[4] Signé, Njuguna Ndung'u and Landry (2020-01-08). *„The Fourth Industrial Revolution and digitization will transform Africa into a global powerhouse”*. Brookings

[5] Marr, Bernard. *„Why Everyone Must Get Ready For The 4th Industrial Revolution”*.

[6] Park, H. A. (2016). *„Are We Ready for the Fourth Industrial Revolution?”*. Yearbook of Medical Informatics (1): 1—3. PMC 5171547 . PMID 27830223.

[7] Philbeck, Thomas; Davis, Nicholas (2018). *„The Fourth Industrial Revolution: Shaping a New Era”. Journal of International Affairs.* 72 (1):17—22. ISSN 0022-197X. JSTOR 26588339.

Autori: **Dr Predrag Pravdić, M.Sc. Violeta Đorđević, M.Sc. Jelena Erić-Obućina,** Akademija strukovnih studija Kruševac, Ćirila i Metodija 30, 37200 Krušavac, Srbija, Tel: +381 37 439 741, Fax: +381 37 439 416;
Akademija strukovnih studija Šumadija, odsek Trstenik, Radoja Krstića 19, 37240 Trstenik, Srbija, Tel: +381 37 714 121, Fax: +381 37 714 121;
E-mail: thepera81@gmail.com
vdjordjevic@asss.edu.rs
jobucina@asss.edu.rs

ETIKUM 2023 INTERNATIONAL SCIENTIFIC CONFERENCE
NOVI SAD, SERBIA, DECEMBER 7-9, 2023

Ranisavljev, M., Strbac, B., Santosi, Z., Sokac, M., Matin, I., Hadzistevic, M., Jotic, G.

APPLICATION OF SEGMENTATION ALGORITHMS FOR MONO AND MULTI-MATERIAL COMPONENTS IN COMPUTED TOMOGRAPHY

Abstract: *This paper presents the most commonly used methods for determining the surface of models created using computer tomography. Surface determination comes down to the application of different CT image segmentation algorithms. The most frequently applied algorithms are based on the threshold of gray values (global method - ISO-50% and the local threshold method), region growing method, and other more advanced methods like neural networks and genetic algorithms. Different segmentation methods were applied to two different workpieces, VGCube (mono-material component) and Pedal (multi-material component). After surface determination step, an analysis of the dimensional and geometric specifications of the product was performed. A comparison of the results of different methods was made concerning the nominal values of the quality characteristics.*
Key words: *Computed tomography, segmentation algorithms, multi-material components*

1. INTRODUCTION

X-ray computed tomography (CT) has made a significant impact in the field of industrial metrology, due to its ability to provide numerous benefits over conventional coordinate measuring systems. These advantages include non-destructive digitalization of internal geometric characteristics, verification of assembled parts, concurrent oversight of dimensional and material quality, as well as the generation of densely populated point clouds [1].

One of the most demanding stages in the data analysis process involves surface extraction, which is the procedure for identifying surfaces from the CT volume data. The CT volume reflects the varying levels of attenuation within the object, influenced by the distance the X-rays travel through the absorbing material. This is determined by the material's attenuation coefficient and the energy of the X-rays. At each point within the measurement volume, X-ray attenuation data is produced and stored in a volume element referred to as a voxel. A voxel can be thought of as a single component within a three-dimensional image, possessing a numerical value denoting its gray level [2].

To be able to perform dimensional measurements of a part, a threshold value has to be carefully determined, as it is a critical parameter for accurate image segmentation and surface data determination, and therefore, has a great influence on the final measurement results. A typical way is to use an ISO-50% value, determined as a ratio between the air (background) and the material (object), where 50% is assigned to the air and 50% to the material of the part. This is generally illustrated by a histogram showing a gray value distribution of the scanning volume, i.e., frequency (number of voxels) on *y*-axis and gray values on *x*-axis. When scanning a homogeneous object (only one material) and assuming no artefacts in the reconstructed volume, this method, also called global method would be sufficient. However, this is not the case for real CT scans, where occurrence of image artefacts, caused by, e.g., beam hardening, scattered radiation or artefacts created by insufficient penetration of the object is common. Thus, ISO-50% method can only be applied as a first estimate for surface determination. For a more accurate surface determination, resulting in a more accurate coordinate measurement, a local adaptive threshold method shall be applied, where the surface is determined in each voxel locally. In principle, this method is based on searching of a sharp edge in gray level perpendicularly to the originally defined surface through global method within a predefined (by user) search distance at both sides of the original surface [3].

Measuring multi-material objects yields typical problems related to edge detection, artefacts and increased noise. A first problem is to find an adequate threshold. The optimal threshold (edge value) to distinguish material 1, for example, from material 2 may differ from the optimal threshold to distinguish material 3 from material 1. A second problem relates to proper selection of the X-ray power or energy when measuring different materials: high energy exposure (high voltage, current or exposure time) is needed to penetrate high absorbing material with sufficient photons reaching the detector, but does not allow

visualizing low absorbing material [4].

This paper aims to perform a systematic analysis of the most commonly used methods for the segmentation of CT images and apply them to two different workpieces. The workpieces analyzed in the study are VGCube and Pedal. VGCube is made of one type of material (mono-material), and Pedal belongs to a group of products that are composed of several different materials (MMC). Emphasis is placed on the analysis of the dimensional and geometrical specifications of the product using various surface area determination methods available in the commercial software VGStudio Max 2022.4. from Volume Graphics.

2. SURFACE DETERMINATION

Surface determination plays a pivotal role in the post-processing of CT scans when conducting dimensional analyses. The presence of a clearly defined surface is imperative for the accurate fitting of geometric shapes such as planes, circles, cylinders, and even isolated points on the surface. Segmentation, as a concept, refers to the partitioning of 2D or 3D data into distinct regions to extract relevant information for particular analytical purposes. The two most common surface determination techniques used in dimensional CT are ISO-50% and local threshold methods [5].

2.1 The global method – ISO-50%

The widely employed approach for surface determination, rooted in a fixed threshold value, such as the commonly used ISO-50%, was the initial segmentation technique introduced in the CT-based dimensional metrology. This method relies on the overall behavior of grey values within the reconstructed CT volume and is typically defined as the midpoint (i.e., 50%) between the peaks of the background distribution (representing air) and the material distribution (representing the workpiece). However, the global algorithm exhibits certain limitations, particularly when dealing with overlapping distributions. This constraint implies that a sole threshold value is insufficient for accurate segmentation of a 3D dataset. Moreover, challenges arise from the presence of image artefacts, which further complicates the task of surface determination. Factors like beam hardening, noise, and other image irregularities introduce non-uniformity in the CT dataset's grey values, potentially leading to surface offset. Consequently, the ISO-50% method is susceptible to systematic errors [5].

Figure 1. shows the ISO-50% global segmentation method on the VGCube workpiece. From the zoomed-in segment, the gradient transition of shades of gray pixels is clearly visible. On the histogram of gray values, two blue lines indicate the peaks with the highest frequency for material and air, while the red line represents the specific numerical value of the pixel (threshold).

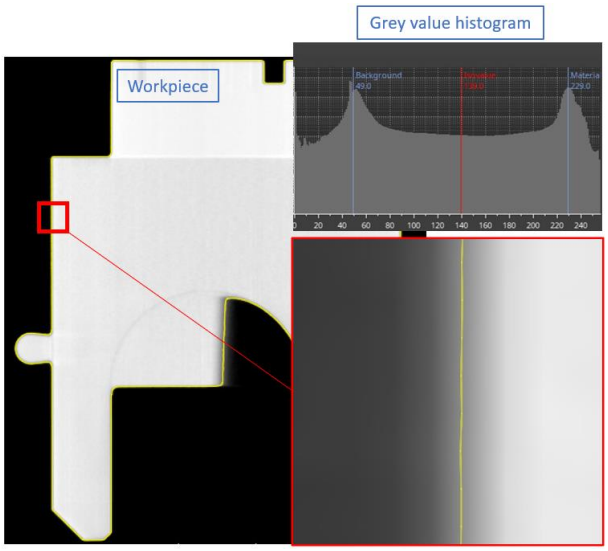

Fig. 1. ISO-50% segmentation method

2.2 The local thresholding method

The local thresholding method has been developed aiming to segment the dataset locally, providing reliable information even in an artefact-corrupted dataset. Such algorithms allow selecting a threshold for a small group of voxels, while taking into consideration their intensity within a definable bidirectional search distance over a preliminary surface defined by the algorithm. This preliminary surface is assumed to be, e.g. obtained from the global threshold. The local accuracy of local thresholding, in a mono-material scenario, may lie within less than 1/10th of a voxel size under optimal conditions [5].

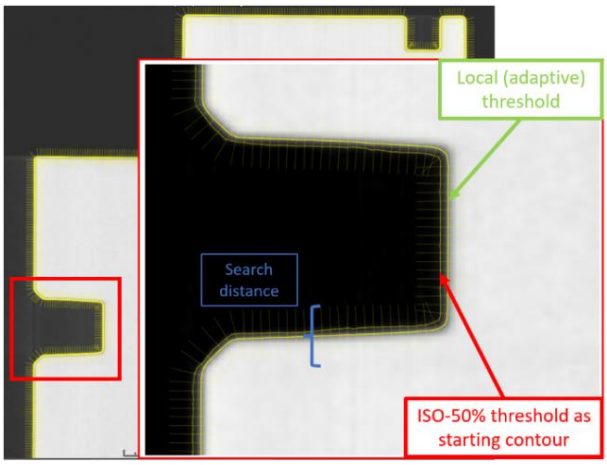

Fig. 2. The local thresholding method

2.3 Region growing method

Region-based methods rely on the postulate that neighboring pixels within the one region have similar value. This leads to the class of algorithms known as region growing of which the “split and merge” technique is probably the best known. The general procedure is to compare one pixel to its neighbor(s). If a criterion of homogeneity is satisfied, the pixel is said to belong to the same class as one or more of its neighbors. The choice of the homogeneity criterion is critical for even moderate success, and in all instances the results are upset by noise. Figure 3 shows a) the selection of the initial seed for growing the region, b) the determination of the surface on the region of interest (ROI), and c) the visualization of the ROI in the assembly.

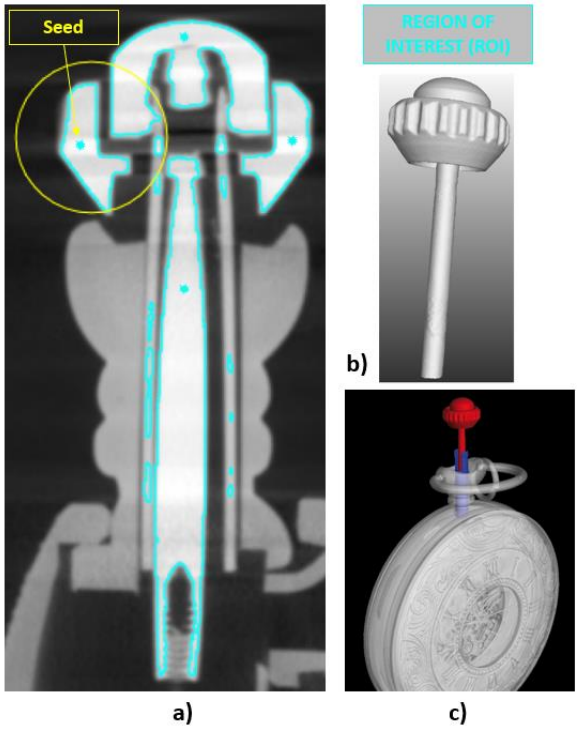

Fig. 3. a) The selection of the initial seed for growing the region, b) the determination of the surface on the region of interest (ROI), and c) the visualization of the ROI in the assembly.

3. EXPERIMENTAL RESEARCH

Using the VGStudio Max 2022.4 software, two segmentation methods, ISO-50%, and the local threshold method, are shown in a practical example. Dimensional and geometric analyses were performed on "demo" workpieces, the data of which are available during software installation, and their purpose is to train personnel to use the software.

The VGCube is shown in Figure 4. and the Pedal is shown in Figure 5.

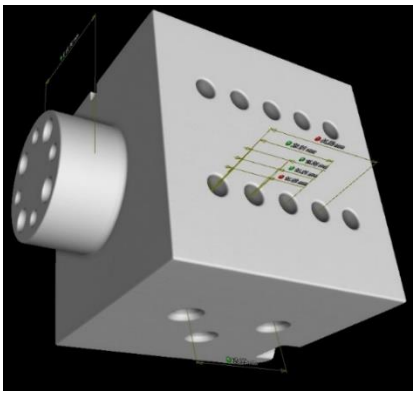

Fig. 4. VGCube (mono-material component)

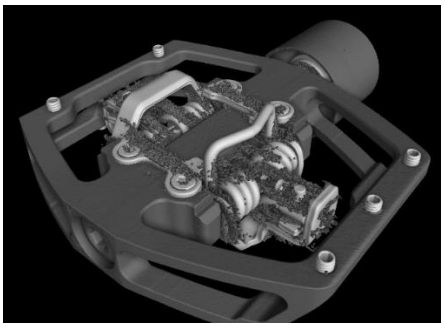

Fig. 5. Pedal (multi-material component)

VGCube is segmented according to the ISO-50% method and the local threshold method (called the Advanced method in the software). The Pedal is segmented with Advanced methods and Advanced multi-material options. After each segmentation, a substitute geometry was fitted and the deviations from the nominal values were analyzed.

4. RESULTS AND DISCUSSION

The diagram in Figure 6. shows deviations of quality characteristics from nominal values when using ISO-50% and the local thresholding method. It can be seen that there are no significant deviations in the results when applying these two methods to most of the characteristics. There are deviations in certain characteristics such as cylindricity 2 and distances 2, 3, and 4, with the local thresholding method giving closer results to nominal values than ISO-50%. Deviations are expressed in mm.

The diagram in Figure 7. shows the deviations from the nominal values for the Pedal. The designation LTM MONO means that an advanced segmentation method has been applied that recognizes one type of material, similarly, LTM MMC recognizes several different materials.

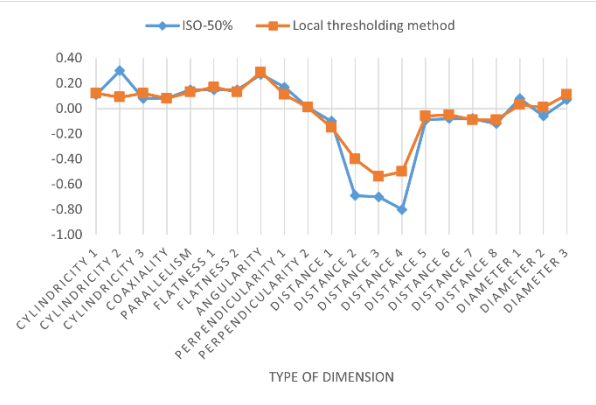

Fig. 6. Difference from nominal values for the VGCube

The only correct thing to do in this case is to use LTM MMC because the Pedal is intended to evaluate both external and internal characteristics, which can be reached if one of the two materials is excluded from the total volume in this case.

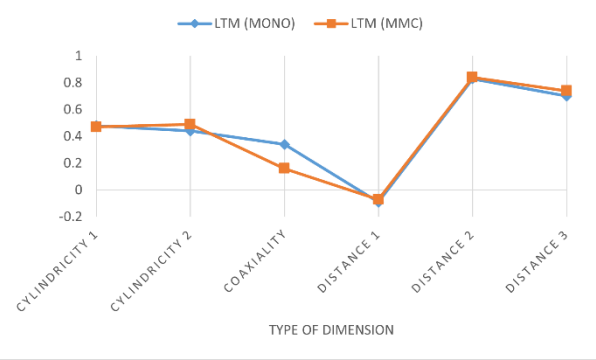

Fig. 7. Difference from nominal values for the Pedal

Again, there is no significant difference between the measurement results. It should be reminded of the fact that these examples are not on real-world scenarios, but that they are intended for learning, and that they are largely free of errors (artifacts) in the data that occur due to the nature of the process for obtaining results from a CT. Also, the operator has a great influence on the measurement results by choosing the number and arrangement of fitted points, the calculation method of the substitute geometry, etc.

5. CONCLUSION

The choice of an adequate method for surface determination in the data obtained by computer tomography is a demanding task. The segmentation methods directly affect the value of the measurement results. By using the "wrong" method, significant systematic errors are introduced into the evaluation process of the workpiece.

In the case of workpieces consisting of several different materials, choosing a method that does not recognize different materials within the assembly results in neglecting a large amount of data, that is, not fulfilling the potential that computer tomography offers.

6. REFERENCES

[1] S. Carmignato, “Accuracy of industrial computed tomography measurements: Experimental results from an international comparison,” CIRP Annals - Manufacturing Technology, vol. 61, no. 1. pp. 491–494, 2012.

[2] J. A. Yagüe-Fabra, S. Ontiveros, R. Jiménez, S. Chitchian, G. Tosello, and S. Carmignato, “A 3D edge detection technique for surface extraction in computed tomography for dimensional metrology applications,” CIRP Ann. - Manuf. Technol., vol. 62, no. 1, pp. 531–534, 2013.

[3] P. Müller, “Coordinate Metrology by Traceable Computed Tomography by Pavel Müller For fulfilment of the degree PhilosophiæDoctor Department of Mechanical Engineering,” p. 181, 2013.

[4] J. P. Kruth, M. Bartscher, S. Carmignato, R. Schmitt, L. De Chiffre, and A. Weckenmann, “Computed tomography for dimensional metrology,” CIRP Ann. - Manuf. Technol., vol. 60, no. 2, pp. 821–842, 2011.

[5] F. Borges de Oliveira, A. Stolfi, M. Bartscher, L. De Chiffre, and U. Neuschaefer-Rube, “Experimental investigation of surface determination process on multi-material components for dimensional computed tomography,” Case Stud. Nondestruct. Test. Eval., vol. 6, pp. 93–103, 2016.

Authors: **Teaching Assis. Ranisavljev Milos, Assoc. prof. dr Strbac Branko, Assis. prof. dr Santosi Zeljko, Assis. prof. dr Mario Sokac, dr Matin Ivan, Full prof. dr Hadzistevic Miodrag,** University of Novi Sad, Faculty of Technical Sciences, Trg Dositeja Obradovica 6, 21000 Novi Sad, Serbia, Phone.: +381 21 485 2350, Fax: +381 21 454-495.
E-mail: ranisavljev97@uns.ac.rs
strbacb@uns.ac.rs
zeljkos@uns.ac.rs
marios@uns.ac.rs
matini@uns.ac.rs
miodrags@uns.ac.rs
Teaching Assis. Goran Jotic University of Banja Luka, Faculty of Mechanical Engineering
goran.jotic@mf.unibl.org

ETIKUM 2023 **INTERNATIONAL SCIENTIFIC CONFERENCE**
NOVI SAD, SERBIA, DECEMBER 7-9, 2023

Skakun, P., Rajnović, D., Janjatović, P., Dramićanin, M.

EXPERIMENTAL DETERMINATION OF STRAIN STATE IN METAL FORMING

Abstract: *Process parameters determination in metal forming, such as forming load and work, are based on stress and strain analysis. However, experimental ways of strain state determination are not numerous. One way to determine strain values is through material hardness measurement. In sheet metal forming it is possible to get information about deformation of surface by digital image correlation technique. A method based on dependence of recrystallized grain size and prior deformation can be used in bulk metal forming. In this paper mentioned experimental methods for strain state determination in metal forming processes are described and presented.*
Key words: *metal forming, strain state*

1. INTRODUCTION

In order to develop, design and perform a metal forming process it is necessary to determine basic process parameters, such as forming load, work or punch pressure. To obtain values of these parameters, stress and strain analysis of a formed workpiece has to be done.

Numerical simulations are currently a very common tool when it comes to stress and strain analysis, especially because results can be obtained in a relatively short period of time. On the other hand, experimental methods can also be used for these analyses. Experiments usually involve more challenging procedures which require longer periods of time compared to numerical simulations, however experimental results give more realistic insight into analysed parameters.

In this paper three experimental methods for strain values determination of a workpiece obtained by metal forming processes are presented: method based on the relation between hardness of the deformed metal material and obtained strain; the digital image correlation method; and a metallographic method which enables strain determination through values of recrystallized grain size.

2. HARDNESS - STRAIN RELATION

Determination of a material hardness is one of the most common procedures when it comes to bulk material testing. The hardness of a solid material is usually defined as a measure of its resistance to a permanent deformation [1]. For some materials, such as metals, ceramics and most of polymers indentation hardness is measured. The measured hardness is related to a plastic deformation of a surface by tool of different shapes. Although special equipment is required for hardness measurement, a test by itself is not complicated, thus allowing results to be reached relatively easily. Because of that, if relation is made between hardness and some other mechanical properties, hardness test can be used for determination of properties such as yield stress [2], strength [3], flow stress [4,5] or strain [5,6,7].

In the paper [7], this method was used to determine the state of effective strain in a tooth of a cold forged spur gear (Fig. 1).

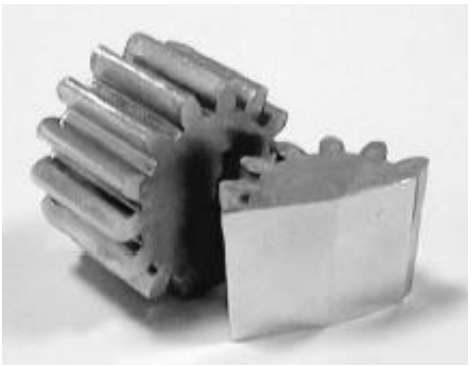

Fig. 1. Cold forged spur gear [7]

In this case determination of hardness-strain relation was based on the Vickers microhardness measurement of specimens with known values of effective strain. Those specimens were obtained in test of uniaxial compression in which Teflon foil was used for friction elimination. Microhardness indentations were made around the center of each specimen, to eliminate the influence of strain inhomogeneity. Based on the data obtained by measurement, relation between Vickers microhardness and effective strain was determined in following form:

$$HV=-9.505\varepsilon^2+24.064\varepsilon+77.469 \quad (1)$$

Strain values obtained through microhardness measurement were compared to results of numerical simulation (Fig. 2). As it can be seen from Fig. 2 the accordance between numerical simulation and experimental results is good. At the contact surface between the workpiece and the tool the highest values of strain were found.

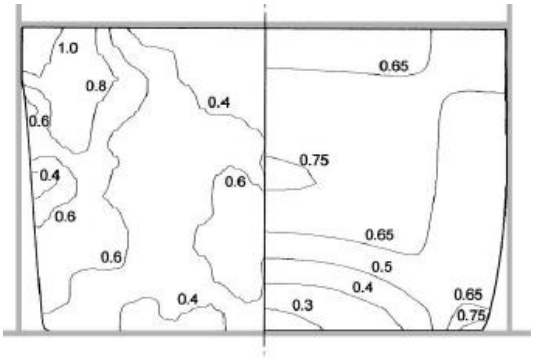

Fig. 2. Experimental values (left) and values obtained in numerical simulation (right) [7]

3. DIGITAL IMAGE CORRELATION

Digital image correlation is a non-contact optical method used for displacement and deformation measurement on the surface of an object [8,9]. To apply this technique digital images of an analysed object at different loadings have to be obtained. After that, image analyses with correlation-based matching algorithms are performed to determine displacements and strains [8,9]. Fields of application are wide, from material science, biomechanics, civil engineering all the way to geotechnical and aerospace engineering, namely displacements of materials, components, structures and biological tissues can be obtained. [8,9]. Application of this method for strain determination in formed metal material are numerous [10,11,12].

In the paper [12] digital image correlation technique was used to characterize the hardening behavior of different materials so that stress-strain curve obtained from a conventional tensile test could be extent beyond the necking point (Fig. 3). Stress strain curves can be obtained from the tensile test, but the main disadvantage of this way of the flow curve determination is that maximal uniform strain is reached when necking occurs, and that happens for small amount of strain. This experiment was conducted in two stages: the first measuring stage was called Before Necking Measurement (BNM, Fig. 3, left), and the second measuring stage was called After Necking Measurement (ANM, Fig. 3, right). In the first stage pre-necking values were obtained, where strain distribution in surface area of test piece was determined. In the second stage the goal was to acquire material properties after the necking. This part of the experiment was based on the theory that if necking zone still has a homogeneous strain distribution, the stress state is considered uniaxial. In that way mechanical properties of the material can be obtained, beyond the necking point and true stress–strain curve can be extended to greater strains.

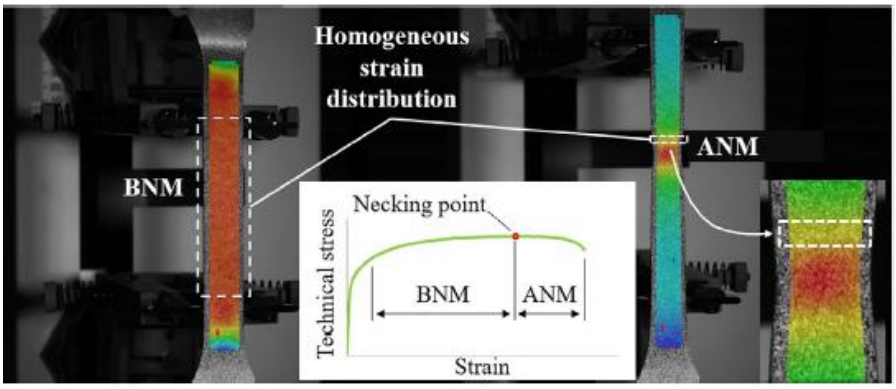

Fig. 3. Strain distribution of a specimen during tensile test [12]

4. GRAIN SIZE - STRAIN RELATION

During cold forming of a metal amount of the stored energy increases providing the driving force for the transformation of microstructure. When the cold formed part is heated to the recrystallization temperature, growth of the new grains occurs, and finer grain size is obtained in the parts of volume with higher strain values. This phenomenon is used for strain state determination in cold formed metal parts [13,14].

As well as in the hardness-strain relation method described in chapter 2, to apply this method it is necessary to establish relation between a value which can be measured (in this case size of the recrystallized grain) and the value that has to be

determined (in this case strain value). That means that the calibration curve, which shows dependence between recrystallized grain size and obtained deformation, needs to be determined.

Samples which are used to establish the calibration curve must undergo the same preparation procedure as samples which will be used in the forming process where strain values have to be determined. That procedure generally consists of several steps (starting heat treatment, uniaxial compression for amount of φ=0.25, final heat treatment-recrystallization). The type of starting heat treatment depends on the type of material that is used in the forming process. This procedure is designed to achieve uniform initial microstructure, as in the case of Al99.5 presented in Fig. 4a [14]. To determine the calibration curve, samples obtained in this way were deformed for different amount of strain values. After heat treatment (recrystallization) each sample will have a different size of grains (Fig. 4b, c, d) Measuring grain size in those samples and relating them with strain values, calibration curve is determined.

In Fig. 5 calibration curve for material Al99,5 is illustrated [14].

This curve has analytical interpretation in the general power function form:

$$\varphi = 44.357 \cdot d^{-0.973} \qquad (2)$$

where: φ is logarithmic strain, and *d* is grain diameter [μm].

When calibration curve for certain material is determined it can be used for strain determination within the volume of the part obtained by bulk metal forming process. Results of application of this method for strain state determination of cold extruded gear-like element made of Al99.5 are presented in Fig. 6 [14].

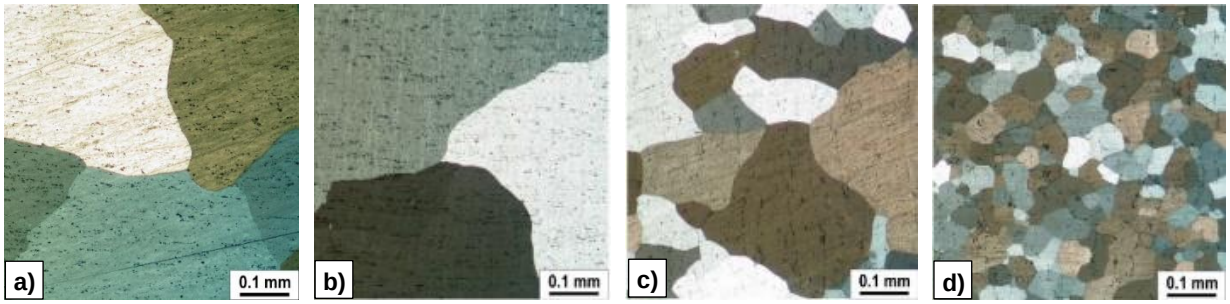

Fig. 4. Starting microstructure for Al99.5: a) φ=0, d = 287±52 μm; and recrystallization microstructures after different deformation: b) φ=0.1, d = 445.6 μm; c) φ=0.45, d = 104.2 μm; d) φ=1.07, d = 53.1 μm

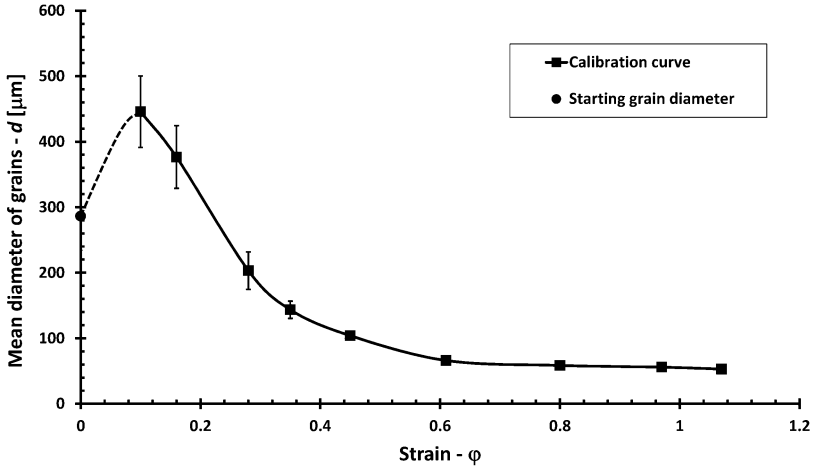

Fig. 5. Calibration curve for Al99.5 [14]

5. CONCLUSION

Each experimental method for strain state determination presented in this paper has its advantages and disadvantages. One general disadvantage of the every experimental method is that experimental equipment is needed and that experimental procedure is usually time consuming.

In the case of hardness measurement or digital image correlation technique, that is not entirely true, because equipment is easily available and measuring procedure is not complicated. On the other hand, digital image correlation can be used only for strain determination on the surface of the formed part, and hardness measurement is affected by microstructure inhomogeneity. Method based

on the relation between strain values and recrystallized grain size has a demanding preparation procedure and has certain limits when it comes to applied materials. However, the results give not only good insight in strain values within a formed part, and also the way material flows for certain forming conditions can be seen.

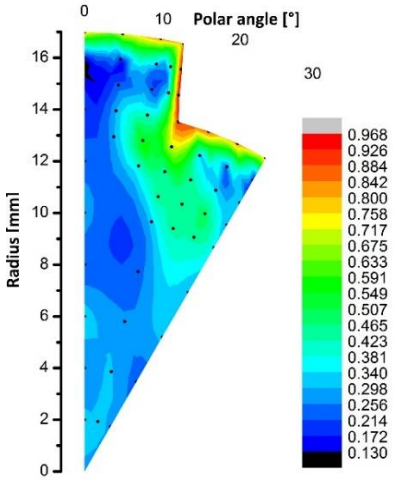

Fig.6. Strain state in cold extruded gear-like element [14]

6. ACKNOWLEDGEMENT

This research has been supported by the Ministry of Science, Technological Development and Innovation through project no. 451-03-47/2023-01/200156 "Innovative scientific and artistic research from the Faculty of Technical Sciences activity domain".

7. REFERENCES

[1] Broitman, E.: *Indentation hardness measurements at macro-, -micro-, and nanoscale: a critical overview*, Tribology letters, Vol. 65, Article number 65, 2017.

[2] Tiryakioglu, M.: *On the relationship between Vickers hardness and yield stress in Al–Zn–Mg–Cu Alloys*, Materials Science & Engineering A, Vol. 633, pp.17-19, 2015.

[3] Zhang, P., Li, S.X., Zhang, Z.F.: *General relationship between strength and hardness*, Materials Science and Engineering: A, Vol. 529, pp.62-73, 2011.

[4] Rudnytskyj, A., Varga, M., Krenn, S., Vorlaufer, G., Leimhofer, J., Jech, M., Gachot, C.: *Investigating the relationship of hardness and flow stress in metal forming*, International Journal of Technical sciences, Vol. 232, Article 107571, 2022.

[5] Sundararajan, G., Tirupataiah, Y.: *The hardness - flow stress correlation in metallic materials*, Bulletin of Materials Science, Vol. 17, No. 6, pp. 747-770, 1994.

[6] Sonmez, F.O., Demir, A.: *Analytical relations between hardness and strain for cold formed parts*, Journal of Materials Processing Technology, Vol. 186, pp.163-173, 2007.

[7] Alves, M. L., Rodrigues, J. M. C., Martins, P. A. F.: *Cold forging of gears: experimental and theoretical investigation*, Finite Elements in Analysis and Design, Vol. 37, Issues 6-7, pp. 549-558, 2001.

[8] Pan, B.: *Digital image correlation for surface deformation measurement: historical developments, recent advances and future goals*, Measurement Science and Technology, Vol. 29, No. 8, 082001, 2018.

[9] https://www.correlatedsolutions.com/ (2023)

[10] Tarigopula, V., Hopperstad, O.S., Langseth, M., Clausen, A.H., Hild, F., Lademo, O.G., Eriksson, M.: *A study of large plastic deformations in dual phase steel using digital image correlation and FE analysis*, Experimental mechanics Vol. 48, pp.181-196, 2008.

[11] Cheong, K., Omer, K., Butcher, C., George, R., Dykeman, J.: *Evaluation of the VDA 238-100 tight radius bending using digital image correlation strain measurement*, Journal of Physics: Conference Series, Vol. 896, 012075, 2017.

[12] Agirre, J., Galdos L., de Argandona, E.S., Mendiguren, J.: *Hardening prediction of diverse materials using the Digital Image Correlation Technique*, Mechanics of Materials, Vol. 124, pp. 71-79, 2018.

[13] Oyekanmi B. O., Hughes T. A., Bramley A. N.: *A microstructural evaluation technique for deformation studies in metal forming processes*, Journal of Materials Processing Technology, Vol. 21, Issue 1, pp. 75-89, 1990.

[14] Skakun, P., Rajnovic D., Janjatovic P., Balos S., Shiskin A., Novak P., Sidjanin L.: *Metallographic determination of strain distribution in cold extruded aluminium gear like elemen*t, Metals, Vol.10, 589, 2020.

Authors: **Assoc. prof. dr Plavka Skakun, Assoc. prof. dr Dragan Rajnović, Teaching assistant Petar Janjatović, Assis. prof. dr Miroslav Dramićanin,** University of Novi Sad, Faculty of Technical Sciences, Trg Dositeja Obradovica 6, 21000 Novi Sad, Serbia, Phone.: +381 21 485 2317, Fax: +381 21 454-495.

E-mail: plavkas@uns.ac.rs
draganr@uns.ac.rs
janjatovic@uns.ac.rs
dramicanin@uns.ac.rs

ETIKUM 2023 **INTERNATIONAL SCIENTIFIC CONFERENCE NOVI SAD, SERBIA, DECEMBER 7-9, 2023**

Spasojević, S., Dramićanin, M.

UTICAJ TEMPERATURE I DEFORMACIJE NA TVRDOĆU ČELIKA AISI 304L

Rezime: *Čelične konstrukcije na povišenim temperaturama odnosno prilikom požara su osetljivije od betonskih konstrukcija. Kod konstrukcionih materijala prilikom požara dolazi do pada mehaničkih karakteristika, kao što su čvrstoća i krutost materijala, što može da dovede do kolapsa cijele konstrukcije. U ovom radu se izvršilo ispitivanje konstrukcionog nerđajućeg čelika AISI 304L na povišenim temperaturama, tom prilikom ispitivane su zatezne karakteristike od sobne temperature do 800 °C. Nakon čega je na istim uzorcima izvršena priprema za metalografsko ispitivanje i mjerenje tvrdoće, kako bi se vidjele promjene na mikrostrukturi i uvidjelo da li postoji zavisnost sa vrijednostima tvrdoće. Predstavljen je uticaj deformacije pri povišenim temperaturama na tvrdoću čelika u oblasti izraženog deformacionog ojačavanja. Takođe, objašnjen je način promjene tvrdoće kroz mehanizme ojačavanja, oporavljanja i rekristalizacije.*

Ključne reči: *Nerđajući čelik, čelik 304l, rekristalizacija, deformaciono ojačavanje.*

1. UVOD

Nerđajući čelici sa austenitnom mikrostrukturom spadaju u materijale koji su kao što sam naziv kaže otporni prema koroziji, zahvaljujući austenitnoj osnovi imaju i dobre mehaničke osobine u širokom temperaturnom opsjegu. Mogu se koristiti za kriogene proizvode odnosno dijelove, elemente koji rade na temperaturama oko -200 °C, tako i dijelove koji rade na 800 °C. Svakako da temperature utiču na mehaničke osobine, ali kod ove vrste materijala taj uticaj je mnogo manji u odnosnu na obične konstrukcione čelike. Kako bi se ispunili današnji zahtevi u pogledu bezbjednosti, otpornosti na koroziju i postojanosti na izloženost otvorenom plamenu povećava se potražnja za upotrebom skupljih materijala, premaza i lakova, međutim austenitni nerđajući čelici mogu da ispune date zahteve uz niže troškove[1].

2. ČELIK 304L

Čelik 1.4307 ili 304L je niskougljenični austenitni nerđajući čelik koji sadrži hrom i nikl. Ovaj tip čelika je najrasprostranjeniji u upotrebi u građevini, koristi se za teške komponente jer poboljšava zavarljivost. Zbog svoje autentitne strukture dobar je za primjenu u slučajevima gdje je potrebna niska magnetna propustljivost.

Sadrži do 0,03% ugljenika, od 17,5 do 19,5% hroma, od 8-10,5% nikla, do 2% mangana kao, i do 1% silicijuma [2].

3. EKSPERIMENTALNI DIO

U okviru eksperimentalnog dijela sprovedeno je ispitivanje uticaja povišene temperature na niskougljenični austenitni nerđajući čelik. Za ispitivanje je odabran najviše primjenjivani nerđajući čelik oznake X2CrNi19-11 (AISI 304L) u toplovaljanom stanju, a mehaničke karakteristike i hemijski sastav je dat u tabelama 1 i 2.

Tabela 1. Hemijski sastav čelika AISI 304L prema atestu proizvođača i prema EN 10088-4 [2]

Sadržaj elemenata (%)	Atest	EN 10088-4
C	0,025	≤0,07
Si	0,508	≤1,00
Mn	1,502	≤2,00
P	0,0213	≤0,045
S	0,0077	≤0,0015
Cr	18,317	17,5-19,5
Ni	8,126	8,0-10,5
N	0,0452	≤0,10

Tabela 2. Mehaničke karakteristike čelika AISI 304L prema atestu proizvođača i prema EN 10088-4 [2]

	Atest	EN 10088-4
Konvencionalni napon tečenja MPa)	431	≥210
Zatezna čvrstoća (MPa)	631	≥520
Izduženje A (%)	52,4	45

Mikrostruktura osnovnog materijala prije ispitivanja zatezanjem pri uvećanju od 200x nalazi se na slici 1.

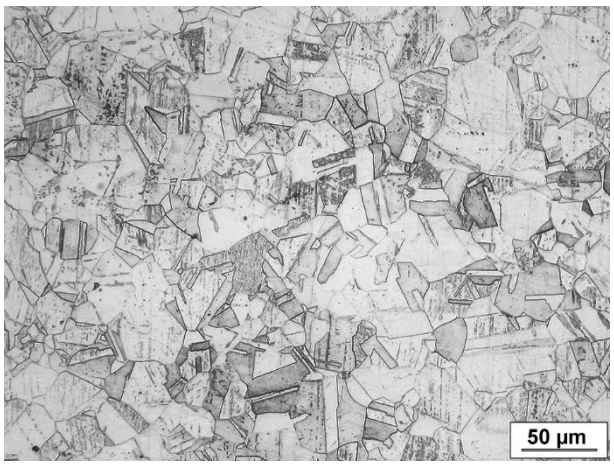

Sl. 1. Mikrostruktura čelika 304L

Pri izradi rada su izvršena sledeća ispitivanja na uzorcima:

- ispitivanje zatezanjem na sobnoj i povišenim temperaturama,
- analiza mikrostrukture osnovnog materijala,
- analiza mikrostrukture nakon zatezanja na povišenoj temperaturi,
- mjerenje tvrdoće osnovnog materijala,
- mjerenje tvrdoće nakon zatezanja na povišenoj temperaturi.

Iz table lima debljine 3 mm izrezane su epruvete za zatezanje tehnikom vodenog mlaza (eng. Water jet). Epruvete koje su isječene na mašini imaju pravugaoni poprečni presjek čije su izmjerene dimenzije date u tabeli 3, a nominalne dimenzije epruveta su prikazane na slici 2.

Tabela 3. Dimenzije ispitanih epruveta

Oznaka	Temperatura ispitivanja (°C)	Širina epruvete (mm)	Debljina epruvete (mm)
01	20	12,60	3,02
31	300	12,58	3,03
61	600	12,32	2,98
71	700	12,66	3,01
81	800	12,70	2,92

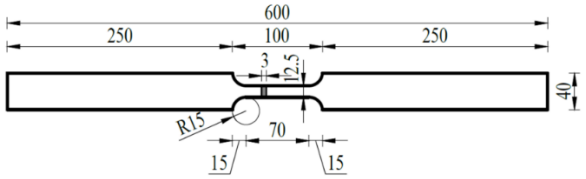

Sl. 2. Nominalne dimenzije epruveta u mm

Ispitivanje je izvršeno na hidrauličnoj kidalici kapaciteta 250 kN Schenk Hydropuls PSB 250. Na kidalicu je postavljena peć za zagrijavanje uzoraka koja radi na principu infracrvenog zračenja (IC), a prenos toplote se odvija radijacijom, a sama kontrola zagrijevanja je dinamički promjenljiva. U peći temperatura na površini uzorka je kontrolisana pomoću termoparova, koji su bili pričvršćeni uz sam uzorak kako ne bi došlo do odstupanja temperature. Upotrebom ovakvog tipa peći sa dinamičkom kontrolom temperatura na površini uzorka se postizala za veoma kratko vrijeme. Tokom procesa zagrijevanja uzorka, jedna strana uzorka nije bila pričvršćena u čeljust mašine i time je dopušteno njegovo slobodno širenje. Nakon postizanja odgovarajuće temperature, uzorak je ostavljen 5 min na zadatoj temperaturi kako bi bili sigurni da je temperatura po cijelom poprečnom prijeseku ista, kao i da je prestalo širenje uzorka. Dok je trajalo zagrijevanje uzoraka u peći, na računaru koji je u sklopu kidalice su unijeti početni podaci u vidu dimenzije poprečnog presjeka i početne mjerne dužine. Podešena je brzina prirasta napona prilikom zatezanja koja je automatski kontrolisana i iznosila je 15 MPa/s. Po isticanju 5 minuta koje je uzorak proveo u peći, zateže se druga čeljust i mašina se startuje. Na osnovu mjernih ćelija za dužinu i silu prikuplja podatke u brzini deset puta u sekundi, odnosno 10Hz. Tokom prikupljanja podataka na ekranu se može vidjeti sam izgled dijagrama zatezanja.

Nakon zatezanja uzorka, odnosno loma uzorka pristupljeno je slijedećim ispitivanjima, kao što su metalografska ispitivanja i mjerenje tvrdoće. Ispitivanja su vršena na uzorku koji je uzet sa mjesta loma u dužini od 10 mm.

Mikrostruktura uzoraka zabilježena je pomoću svjetlosnog mikroskopa „Leitz Orthoplan“, pri uvećanju od 100x. Mikrostruktura uzorka zabilježena na vrhu uzorka u zoni loma i 10 mm od zone loma pri uvećanju od 100x.

Mjerenje tvrdoće je vršeno na uređaju za ispitivanje mikrotvrdoće „Wilson Tukon 1102“ po metodi Vikers. Opterećene prilikom mjerenja tvrdoće je HV1 odnosno 1 kg. Prvi otisak je zabilježen na mjestu loma na rastojanju od 1 mm od same ivice loma i nastavljeno je mjerenje u dužini od 10 mm sa rastojanjem od 0,5 mm od otiska do otiska.

Takođe, na datim uzorcima je izvršeno mjerenje dimenzija mjesta loma, odnosno suženja gdje je došlo do stvaranja vrata.

4. REZULTATI I DISKUSIJA

Rezultati ispitivanja u vidu zatezne čvrstoće (Rm) i izduženja (A) na zadatim temperaturama od 20 , 300, 600, 700 i 800 °C nalaze se u tabeli 4.

Dijagram napon-deformacija koji je dobijen prilikom zatezanja uzoraka prikazan je na slici 3.

Tabela 4. Zatezna čvrstoća i izduženje

Oznaka uzorka	Zatezna čvrstoća Rm (MPa)	Izduženje A (%)
01	641	58,0
31	461	40,5
61	271	44
71	197	50,5
81	141	54,5

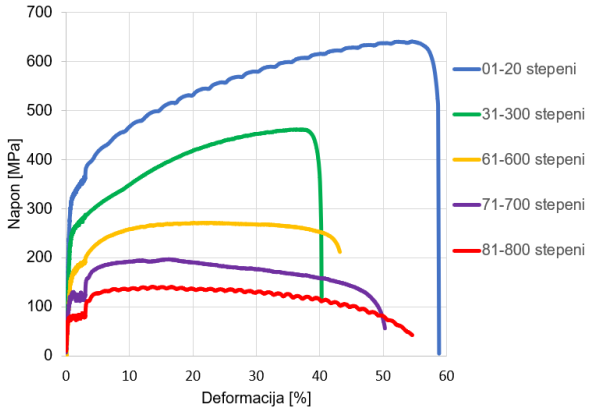

Sl. 3. Dijagrami napon-deformacija

Posmatrajući oblik dijagrama pri zatezanju na različitim temperaturama, uočljivo je da je kod uzoraka zatezanih na 700 °C i 800 °C izražena oblast napona tečenja nakon koje slijedi skok napona. Ovakav oblik dijagrama javlja se zbog dinamičke rekristalizacije i viđen je u radu [3]. Takođe se može uočiti da kod uzoraka na sobnoj temperaturi i 300 °C ubrzo nakon postizanja maksimalno napona dolazi do pucanja.

Tabela 5. Širina i debljina vrata uzorka nakon loma

Oznaka uzorka	Debljina	Širina
01	0,72	8,55
31	0,96	9,51
61	1,73	9,22
71	1,78	7,25
81	1,6	6,32

Na osnovu izmjerenih vrijednosti ne može se sa sigurnošću reći da li je porast temperature uticao na povećanje deformacije, zato je izvršeno izračunavanje procentualnog suženja u odnosu na početne vrijednosti koje su date u tabeli 3, a dobijene vrijednosti su prikazane u tabeli 4. Primjetno je da se sa povećanjem temperature dobija povećanje deformacije na osnovu procentualnog suženja (Tabela 5) osim kod uzoraka 01 koji je zatezan na sobnoj temperaturi ima veći procenat suženja od uzoraka na temperaturama 300°C i 600°C. Posmatrajući dijagrame na slici 3 može se vidjeti da uzorak 01 ima najveće izduženje (58%) u odnosu na uzorke 31 i 61, dok sa druge strane ima veće izduženje nego i uzorci 71 i 81 koji imaju preko 30% veće procentualno suženje.

Tabela 6. Procentualno suženje

Oznaka uzorka	Procentualno suženje Z (%)
01	64,0
31	55,6
61	56,6
71	81,7
81	87,7

Mikrostruktura uzoraka zatezanih na temperaturama 600 i 800 ˚C je prikazana na slikama 4 i 5, gdje je pod a) prikazana mikrostruktura na mjestu loma, a pod b) mikrostruktura na udaljenosti 10 mm od mjesta loma.

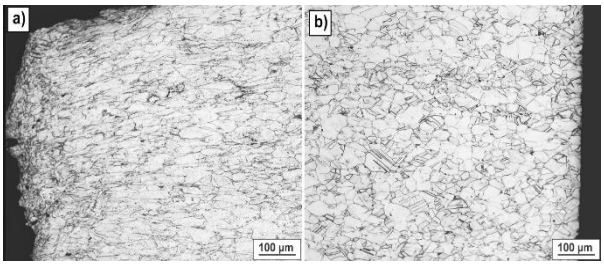

Sl. 4. Mikrostruktura uzorka 61(T= 600°C) sa uvećanjem 100x, a) mjesto loma, b) 10 mm od mjesta loma

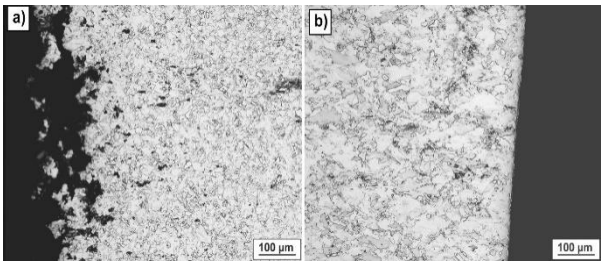

Sl. 5. Mikrostruktura uzorka 81 (T=800°C) sa uvećanjem 100x, a) mjesto loma, b) 10 mm od mjesta loma

Mikrostruktura austenitnog čelika AISI 304L na temperaturama 20, 300, 600 i 700 ˚C je slična nakon zatezanja. Na većini uzoraka uočljivo je da se radi o mjestu gdje je došlo do loma uzorka, odnosno sužavanja i stvaranja vrata. Na slici 4a zrna početne mikrostrukture nisu jasno uočljiva, jer su tu bile najveće deformacije, stoga su se zrna izdužila u pravcu tih deformacija, dok kod uzorka ispitanog na 800°C se ne vide deformisana zrna (slika 5), već zrna koja odgovaraju austenitnoj strukturi samo sitnija u odnosu na početno stanje. Slika 4b) prikazuje mikrostrukturu pri zatezanju na 600˚C, ali 10 mm udaljeno od mjesta loma i na njoj nisu uočljiva deformisana zrna, niti ima vidljivih tragova deformacije. Takođe ovakvo stanje imamo

i kod uzoraka 01, 31, 71.

Dobijena mikrotvrdoća je prikazana preko krive kako bi se jasnije uočila razlika između dobijenih rezultata.

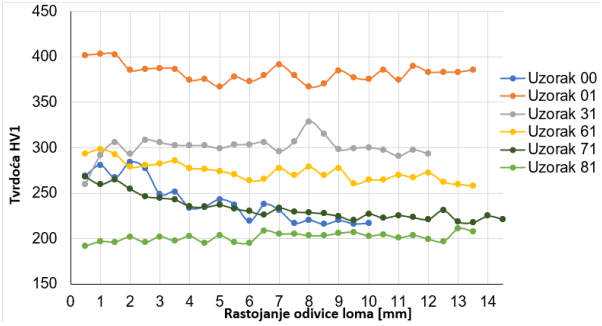

Sl. 6. Krive tvrdoće za sve uzorke

Na dijagramu se može uočiti da je tvrdoća kod uzorka 01 koji je zatezan na sobnoj temperaturi veća od uzorka koji nije zatezan. Primjetno je da uzorak 01 koji je zatezan na sobnoj temperaturi ima najveću tvrdoću. Dok uzorci koji su zatezani na temperaturama 300 °C i 600 °C imaju manju tvrdoće od uzorka 01, ali i dalje je tvrdoća veća od nultog uzorka.

Porast tvrdoće kod uzoraka ispitanih na sobnoj temperaturi, 300 °C i 600 °C može se objasniti pojavom deformacionog ojačavanja što se slaže sa padom izduženja kod ispitivanja zatezanjem. Ovakva pojava je vidljiva u tehničkom izveštaju [4], ali i u radu [5], gdje je tvrdoća zavisna od stepena deformacije, ali i temperature i vremena provedenoj na temperaturi. Tokom ojačavanja pored pada izduženja i rasta tvrdoće, trebalo bi dolaziti i do porasta zatezne čvrstoće, međutim kako je već rečeno porastom temperature smanjuju se vrednosti zatezne čvrstoće.

5. ZAKLJUČAK

Prilikom zatezanja zatezna čvrstoća (Rm) sa porastom temperature opada. Dok kod uzoraka na 700 °C i 800 °C imamo izražen napon tečenja i nagli skok nakon toga, a kod temperatura 20, 300 i 600 °C nemamo izražen napon tečenja.

Kod mikrostrukture čelika uočeno je izduženje zrna na uzorcima koji su zatezani na temperaturama 20, 300, 600 i 700 °C, što je poslijedica deformacije. Dok je kod uzorka koji je zatezan na 800 °C uočljiva sitnozrna struktura. Što je poslijedica rekristalizacije, pa možemo reći da se rekristalizacija čelika 304L događa na temperaturi između 700 – 800 °C.

Uzorak koji je zatezan na sobnoj temperaturi (Uzorak 01) ima najveću tvrdoću i možemo reći da je prilikom zatezanja došlo do deformacionog ojačavanja materijala koji je uzrokovao veliku tvrdoću u odnosu na nulti uzorak. Što je slučaj i sa uzorcima koji su ispitivani na 300, 600 i 700 °C, koji takođe imaju veću tvrdoću od nultog uzorka, ali manju od uzorka 01 i koja opada sa porastom temperature zatezanja. Uzorak koji je imao najmanju tvrdoću je uzorak 81 (T=800 °C), što možemo reći da je poslijedica rekristalizacije.

6. ZAHVALNICA

Ovaj rad je rezultat rada autora u okviru projekta pod naslovom „Savremeni materijali, tehnologije spajanja i srodni postupci“ Laboratorije za ispitivanje materijala i Laboratorije za zavarivanje, Departmana za proizvodno mašinstvo, Fakulteta tehničkih nauka.

7. LITERATURA

[1] Rajić, N.: *Izvijanje stubova i preseka od nerđajućeg čelika pri dejstvu požara sa uticajem istorije opterećenja*, Doktorska disertacija, Fakultet tehničkih nauka, Novi Sad, 2022.

[2] DIN EN 10088 -3, Vol. 108, No. 0, pp. 0–1.

[3] Liang, Y., Manninen, T., Zhao, O., Walport, F., Gardner, L.: *Elevated temperature material properties of a new high-chromium austenitic stainless steel*, Journal of Constructional Steel Research, Vol. 152, pp. 261–273, 2019.

[4] Smith, W. H.: *Characterization of the Deformation and Annealing of 304L Stainless Steel*, Available: https://www.osti.gov/servlets/purl/10181340, 1994.

[5] Deibler, L., Brown, A., Puskar, J.: *Experiments and Modeling to Characterize Microstructure and Hardness in 304L*, Metallography, Microstructure, and Analysis, Vol. 6, No. 1, pp. 3–11, 2017.

Authors: **Asis. Stanko Spasojević, Doc. dr Miroslav Dramićanin,** Univerzitet Novi Sad, Fakultet Tehničkih Nauka, Trg Dositeja Obradovica 6, 21000 Novi Sad, Serbia, Tel: +381 21 485 2340.
E-mail: spasojevic@uns.ac.rs
dramicanin@uns.ac.rs

ETIKUM 2023

INTERNATIONAL SCIENTIFIC CONFERENCE
NOVI SAD, SERBIA, DECEMBER 7-9, 2023

Stojišić, N., Jevtić, N., Borović, Z., Pećanac, M., Baloš, S.

UTICAJ BRZINE LASERSKOG ZAVARIVANJA NA OBLIK METALA ŠAVA

Rezime: *U ovom radu izvršeno je eksperimentalno ispitivanje uticaja brzine laserskog zavarivanja na oblik metala šava, sa ciljem optimizacije tehnologije spajanja, što će doprineti većoj produktivnosti, smanjenju troškova obrade, a takođe je i osnova za inovativne pristupe čija će primena biti široko rasprostranjena u budućnosti. Nakon zavarivanja, rađena je metalografska priprema uzoraka a zatim i merenje vrednosti nadvišenja, širine šava i dubine uvara pomoću svetlosnog mikroskopa. Obradom rezultata došlo se do pozitivnih zaključaka koji predstavljaju jaku osnovu za dalja istraživanja.*
Ključne reči: *lasersko zavarivanje, parametri, metal šava*

1. UVOD

Proučavanje laserskog zavarivanja od velikog je značaja kako bi se unapredile tehnike, optimizovali procesi i omogućilo šire usvajanje u industrijskim aplikacijama. Laseri omogućavaju visoku preciznost i kontrolu nad procesom zavarivanja. Zbog fokusa i intenziteta laserskog zraka, smanjuje se toplotni uticaj na okolni materijal, što dovodi do manjih deformacija i oštećenja. Ovo je posebno važno kod zavarivanja tankih materijala. Lasersko zavarivanje ima manju termičku zahvaćenost okolnog materijala u poređenju sa drugim metodama zavarivanja. Takođe, omogućava brži proces zavarivanja u poređenju sa tradicionalnim metodama. [1] [2]

U ovom radu, izvršeno je ispitivanje uticaja brzine laserskog zavarivanja na oblik metala šava.

2. EKSPERIMENTALNI DEO

2.1 Koncept istraživanja

Cilj eksperimenta bio je ispitivanje uticaja brzine laserskog zavarivanja konstrukcionog čelika na izgled i dimenzije zavarenog spoja. Prvi deo eksperimenta jeste sam postupak zavarivanja, dok je drugi deo obuhvatao proces metalografske pripreme uzoraka, a zatim i samo ispitivanje.

Iz flaha debljine 3mm isečeno je deset jednakih uzoraka dimenzija 150 x 50 mm. Uzorci bili su pozicionirani i pričvršćeni na radnu površinu za zavarivanje. Osnovni materijal korišćen u eksperimentu je čelik sa oznakom S355. Spada u grupu nelegiranih konstrukcionih čelika. [3]

Tabela 1. Hemijski sastav čelika S355, dobijen hemijskom analizom

C	Si	Mn	P	S	Cr	Ni	Mo
0,16	0,31	0,78	0,014	0,015	0,63	0,15	0,03

2.2 Oprema za zavarivanje

Oprema za zavarivanje sastoji se iz 3 celine, sl. 1:

1. Uređaja za lasersko zavarivanje marke *GWEIKE*, model *LW1500H* [4]
2. Glave (pištolja) za lasersko zavarivanje proizvođača *AU3TECH*, model *HW970* [5]
3. Prenosivog traktora za zavarivanje proizvođača *PROMOTECH*, model *GECKO BATTERY* [6]

Sl. 1. Konfiguracija uređaja za zavarivanje

2.3 Tok eksperimenta

Na deset pripremaka dimenzija 150 x 50 mm vršeno je ručno uklanjanje masnoće sredstvom za odmašćivanje koje je bilo naneseno na polipropilensku krpu, a zatim su pripremci prebrisani sa 70% medicinskim alkoholom.

Glava za zavarivanje vođena je traktorom za zavarivanje, tj. sprovedena je potpuna automatizacija procesa, koja je doprinela doslednosti rezultata eksperimenta. Svi pripremci su pričvršćeni na zavarivački sto, dimenzija 1000 x 2000 mm. Tokom probnog zavarivanja zapažena je mogućnost izvođenja više zavara na istom

pripremku, pri čemu ne dolazi do njihovog međusobnog uticaja, čime je postignuta značajna ekonomska efikasnost i ušteda u materijalu. Početna udaljenost vrha mlaznice od radnog predmeta je iznosila 3mm, što se pokazalo previše blisko jer je pri toj visini isparavanje materijala neminovno, pri čemu su ostali parametri bili nepromenjeni. Nakon probnog pripremka, zavarivanje pretapanjem je vršeno na još dva pripremka.

Formirano je 11 zavara, koji su realizovani bez dodatnog materijala, u atmosferi zaštitnog gasa argona i upotrebom traktora za zavarivanje, slika 2.

Konstantni parametri:

- Snaga laserskog snopa: P=1500 W
- Zaštitni gas: Argon
- Protok gasa: Q=20 l/min
- Udaljenost vrha mlaznice od pripremka: l_{vm}=10mm
- Širina laserskog snopa: d=3 mm
- Režim rada lasera: Kontinualni režim
- Maksimalna snaga: 80%

Promenljivi parametri:

- Brzina zavarivanja: V_z=20, 25, 30, 40, 50, 60, 70, 80, 90, 100, 110 cm/min

Sl. 2. Izgled ploče nakon postupka zavarivanja pretapanjem

2.4 Metalografsko ispitivanje preseka

Postupak metalografske pripreme uzoraka standardih dimenzija 15 x 15 x 10 mm obuhvata:
1. Uzorkovanje - uzorci su dobijeni iz poprečnog preseka zavarenog spoja.
2. Isecanje - vršeno je pomoću silicijum karbidnog (SiC) tocila na uređaju STRUERS DISCOTOM.
3. Zatapanje - realizovano je automatski, pomoću uređaja STRUERS PRONTOPRES. Uzorak postavljen u kalup prekriven je određenom količinom polimernog granulata (polietilena).
4. Brušenje - izvedeno je na uređaju *STRUERS KNUTH ROTOR*, postepenim prelaskom sa najgrubljeg, na najfiniji silicijum - karbidni (SiC) brusni papir (P120 do P3000), pod konstantnim vodenim mlazom.
5. Poliranje – sprovedeno je mehaničkom procedurom, na uređaju *STRUERS DP-U2*, upotrebom dijamantske suspenzije, granulacije od najgrublje 6μm, preko 3μm i 1μm, do najfinije 0,25μm.
6. Nagrizanje - sredstvo za nagrizanje je bio *NITAL* (rastvor 3% azotne kiseline u alkoholu). [3]

Metalografsko ispitivanje vršeno je na svetlosnom mikroskopu *LEITZ ORTHOPLAN*. Za potrebe ovog eksperimenta korišćeno je uvećanje 20x. Merene su vrednosti nadvišenja, širine šava i dubine uvara. Nakon merenja, svi šavovi su fotografisani, nakon čega su fotografije spajane u programskom paketu „Adobe Photoshop", u okviru kog su formirane panorame za svaki šav pojedinačno. Širina ZUT-a za svaki od pripremaka izmerena je na osnovu formiranih panorama, u okviru programskog paketa „ImageJ".

3. REZULTATI I DISKUSIJA

3.1 Prikaz dobijenih rezultata

Na slici 3 prikazani su makro preseci zavara, evidentno je značajno smanjenje dubine uvara, širine šava i zone uticaja toplote sa povećanjem brzine zavarivanja.

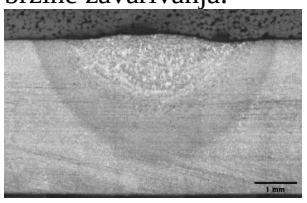
a) uzorak 23, (υ=20 cm/min)

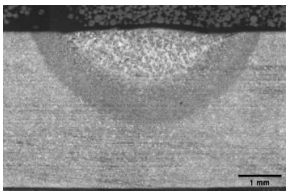
b) uzorak 24, (υ=25 cm/min)

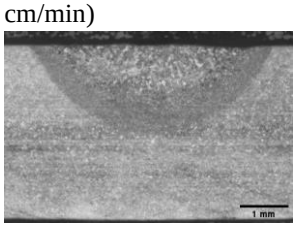
c) uzorak 25, (υ=30 cm/min)

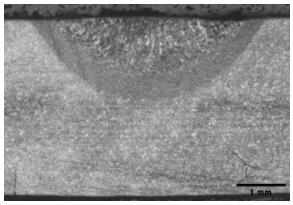
d) uzorak 26, (υ=40 cm/min)

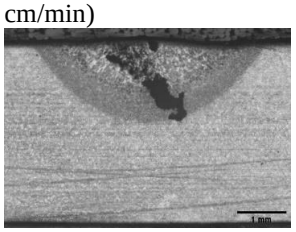
e) uzorak 27, (υ=50 cm/min)

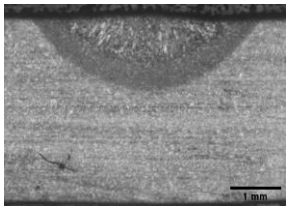
f) uzorak 28, (υ=60 cm/min)

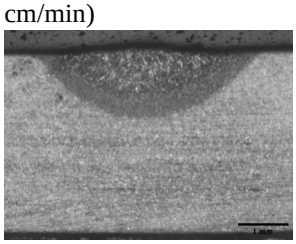
g) uzorak 29, (υ=70 cm/min)

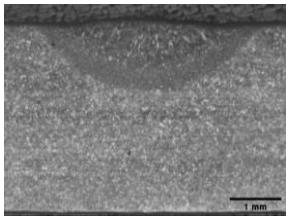
h) uzorak 30, (υ=80

cm/min)

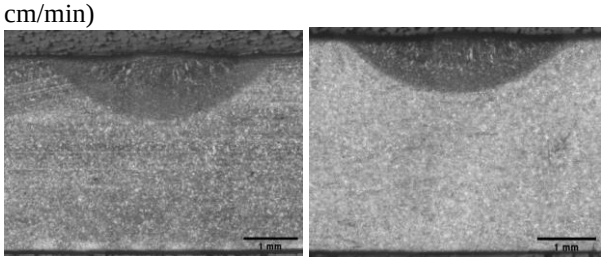

i) uzorak 31, (υ=90 cm/min) j) uzorak 32, (υ=100 cm/min)

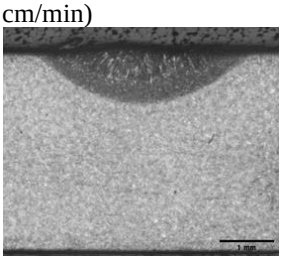

k) uzorak 33, (υ=110 cm/min)

Sl. 3. Mikrostrukturni pregled šavova u uslovima variranja brzine zavarivanja

Kod dubine uvara, pored toga što je sa povećanjem brzine zavarivanja vidljiva promena strukture zrna, što se može najviše uočiti počevši od uzorka 26, jasno je da se dubina smanjuje pri brzini od 25 cm/min (uzorak 24). Povećanje brzine zavarivanja takođe rezultuje manjom širinom šava. Brže kretanje zavarivačke glave smanjuje vreme izloženosti toploti i smanjuje količinu rastopljenog metala koja se dodaje u spoj. Ovakav način može generisati da šav postane tanji i uži. Najveća zona uticaja toplote formirana je pri brzini od 20 cm/min (uzorak 23). Međutim, lako se uočava da se sa porastom brzine zavarivanja smanjuje dubina i širina ZUT – a. Shodno tome, već pri brzini od 25 cm/min se vidi jasno smanjenje kada je reč o njenoj dubini.

U fazi formiranja šavova, brzina je bila promenljiva, dok su svi ostali parametri ostali nepromenjeni. U eksperimentu, postignuta je maksimalna brzina zavarivanja od 110 cm/min, što odgovara maksimalnoj brzini traktora za zavarivanje (uzorak 33). U tabeli 2, prikazane su vrednosti dimenzija šavova dobijenih očitavanjem sa okulara svetlosnog mikroskopa. Nakon toga, iz preventivnih razloga, dimenzije su proverene u programu ImageJ.

Tabela 2. Prikaz izmerenih osnovnih dimenzija metala šava

Br. uzorka	Brzina zavarivanja (cm/min)	Širina šava (mm)	Nadvišenje (mm)	Dubina uvara (mm)	Širina ZUT (mm)
23	20	3,7	0,1	1,3	0,921
24	25	3,6	0,075	1,15	0,817
25	30	3,6	0	1	0,623
26	40	3,3	0	1	0,476
27	50	3,2	0,075	0,8	0,485
28	60	3,1	0,075	0,75	0,499
29	70	3	0,05	0,7	0,409
30	80	2,8	0,05	0,7	0,360
31	90	2,65	0,05	0,6	0,390
32	100	2,55	0,025	0,55	0,289
33	110	2,45	0,05	0,5	0,277

Na osnovu tabelarnih rezultata merenja, formiran je dijagram zavisnosti dubine uvara, visine nadvišenja, širine šava i ZUT-a, u odnosu na brzinu zavarivanja.

Sl. 4. Uticaj brzine zavarivanja na vrednosti nadvišenja, širine šava, dubine uvara i širine ZUT-

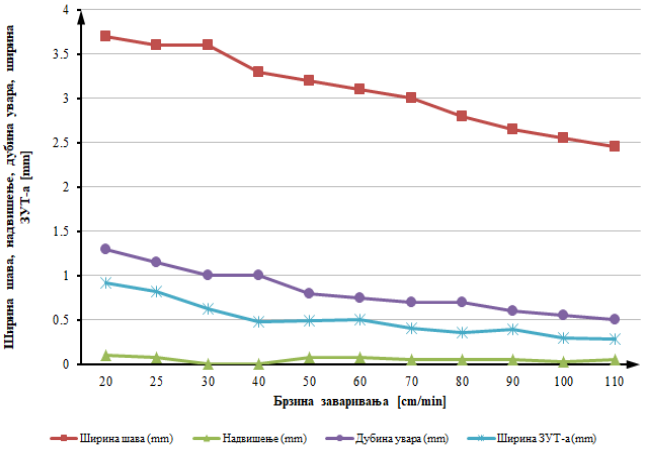

a

Analizom dobijenih rezultata, kako su predstavljeni na grafikonu, može se zaključiti da povećanje brzine zavarivanja rezultuje smanjenjem širine šava u većoj meri, smanjenjem penetracije materijala i širine ZUT-a u nešto manjoj meri, dok je odstupanje nadvišenja suštinski zanemarljivo. Zapažena je nepromenjena dubina uvara pri porastu brzine zavarivanja (sa 30 na 40 cm/min) koja je praćena najvećim padom širine šava. Slika 4 prikazuje skoro identičan trend opadanja širine šava i dubine uvara i nagoveštava da svaki formirani šav ima višestruko veću širinu šava od dubine uvara. Ova konstatacija je i računski dokazana u sledećoj tački gde su preko izračunatih koeficijenata uvara i nadvišenja definisani sami šavovi.

3.2 Proračun koeficijenata uvara i nadvišenja

U tabeli 3 date su brojčane vrednosti koeficijenta uvara. Za vrednosti koeficijenta uvara veće od 5, smatra se da je u pitanju navarivanje. Kada je koeficijent nadvišenja veći od 10, radi se o širokom šavu sa malim nadvišenjem. [5]

Tabela 3. prikaz koeficijenata uvara

Br. uzorka	$\Psi_u = \frac{b}{h_u}$	Rezultat
23	2,85	$\Psi_u = \Psi_{u(opt.)}$
24	3,13	$\Psi_u = \Psi_{u(opt.)}$
25	3,6	$\Psi_u = \Psi_{u(opt.)}$

26	3,3	$\Psi_u = \Psi_{u(opt.)}$
27	4	$\Psi_u = \Psi_{u(opt.)}$
28	4,43	$\Psi_u = \Psi_{u(opt.)}$
29	4,29	$\Psi_u = \Psi_{u(opt.)}$
30	4	$\Psi_u = \Psi_{u(opt.)}$
31	4,42	$\Psi_u = \Psi_{u(opt.)}$
32	4,64	$\Psi_u = \Psi_{u(opt.)}$
33	4,9	$\Psi_u = \Psi_{u(opt.)}$

$* \Psi_{u(opt.)} = (1{,}3 \div 5)$

Ispitivanjem rezultata do kojih se dolazi analizom koeficijenata uvara, pružaju se dokazi koji potvrđuju prethodno navedenu konstataciju da se formirani šavovi dobro uklapaju u optimalne vrednosti date ispod tabele 3. Koeficijenti uvara rastu sa povećanjem brzine zavarivanja.

4. ZAKLJUČCI

Povećanje brzine zavarivanja značajno doprinosi povećanju produktivnosti, pri čemu ne dolazi do smanjenja kvaliteta i izgleda zavara. Ako se brzina poveća bez gubitka kvaliteta, može doći do smanjenja troškova rada po zavaru, čime se povećava efikasnost proizvodnje. Primećeno je da pri parametrima primenjenim u eksperimentu, za brzine veće od 70 cm/min laser predstavlja pogodniju opciju za postupak navarivanja. Kod zavarivanja, osnovni materijal se obično potpuno topi kako bi se postigao trajni spoj, dok kod navarivanja, samo dodatni materijal prolazi kroz fazu topljenja dok se spaja s osnovnim materijalom. Pored toga, pri zavarivanju limova tanjih od 3 mm, mogao bi da se ostvari provar bez značajnih deformacija, što predstavlja veliki izazov kod tradicionalnih postupaka zavarivanja. Laseri omogućavaju visoku preciznost u usmeravanju toplote, laserski zrak ima mali fokus, što rezultuje manjom zahvaćenošću okolnog materijala toplotom.

5. ZAHVALNICA

Ovaj rad je rezultat rada autora u okviru projekta pod naslovom „Savremeni materijali, tehnologije spajanja i srodni postupci“ Laboratorije za ispitivanje materijala i Laboratorije za zavarivanje, Departmana za proizvodno mašinstvo, Fakulteta tehničkih nauka.

6. REFERENCE

[1] Bauer, B.: Optimiranje parametara laserskog zavarivanja čelika za poboljšavanje (Disertacija), Hrvatska: Sveučilište u Zagrebu, Fakultet strojarstva i brodogradnje, 2006.

[2] Antolić, A.: Zavarivanje laserom (Završni rad), Hrvatska: Sveučilište u Zagrebu, Fakultet strojarstva i brodogradnje, 2016.

[3] Šiđanin, L., Gerić, K.: Mašinski materijali sveska 1.

[4] „Gweike,“ [Na mreži]. Available: https://www.gwklaser.com/welding/LCW.html. [Poslednji pristup 17. 11. 2023.].

[5] „Handhend Laser Welder,“ [Na mreži]. Available: https://m.au3laser.com/fiber-laser-welding-solution/2000w-hw970-3in1-handheld-laser-torch-welding.html. [Poslednji pristup 10. 10. 2023.].

[6] „Gecko | Compact Welding Carriage,“ [Na mreži].Available: https://www.promotech.eu/en/product/gecko-fillet-welding-carriage/. [Poslednji pristup 11. 10. 2023.].

[7] Baloš, S.: Tehnologija zavarivanja, Fakultet tehničkih nauka, Novi Sad.

Autori: **Sar. u nas. Nikolina Stojišić, Dipl. maš. inž. Nikola Jevtić, Dipl. maš. inž. Zoran Borović, Asistent – master Milan Pećanac, Red. prof. Sebastian Baloš**
Univerzitet Novi Sad, Fakultet Tehničkih Nauka, Trg Dositeja Obradovića 6, 21000 Novi Sad, Serbia, Tel: +381 21 485 2350, Fax: +381 21 454-495.

E-mail: stojisicnikolina@gmail.com
pecanac.milan@uns.ac.rs
sebab@uns.ac.rs

ETIKUM 2023 **INTERNATIONAL SCIENTIFIC CONFERENCE NOVI SAD, SERBIA, DECEMBER 7-9, 2023**

Šokac, M., Katić, M., Milošević, A., Ranisavljev, M., Santoši, Ž., Vukelić Đ.

PRIMENA INDUSTRIJSKOG CT-A KAO ALATA ZA DIMENZIONALNU ANALIZU I DETEKCIJU DEFEKATA KOD ODLIVAKA

Rezime: *Uzimajući u obzir veliki napredak računarske tehnologije, danas dolazi do sve veće primene naprednih sistema kao što je kompjuterizovana tomografija (CT) za vizuelizaciju i inspekciju u oblasti mašinske industrije. Ovi sistemi obezbeđuju jedan efikasan način za mapiranje, vizuelizaciju i analizu kompleksnih struktura skeniranih objekata. U okviru ovog rada će biti prikazana primena i analiza industrijske kompjuterizovane tomografije za analizu defekata kod aluminijumskog odlivka, kao i alata CAD inspekcije za sprovođenje dimenzionalne analize.*
Ključne reči: *Kompjuterizovana tomografija, CT, defekti, poroznost, analiza*

1. UVOD

Kompjuterizovana tomografija ili CT danas ima sve veću primenu u različitim oblastima kao što su mašinsko inženjerstvo, automobilska industrija, avio industrija i dr. zahvaljujući svojim ne-destruktivnim osobinama [1,2]. Posvećeni su veliki istraživački napori za obradu i analizu snimaka generisanih primenom CT sistema kako bi se iz njih izvukle važne informacije o objektu, kao što su njegove dimenzionalne i geometrijske karakteristike, podaci o zapremini, unutrašnjoj strukturi objekta i materijalu objekta. Sama analiza snimaka generisanih primenom CT-a ima sve veću potrebu za novim načinima i što većim stepenom automatizovanosti postupka ekstrakcije ovih informacija iz složenih pod-struktura iz velikih skupova podataka.

Industrijska kompjuterska tomografija predstavlja bilo koji oblik kompjuterski navođenog tomografskog procesa sa x-zracima kako bi se generisala trodimenzionalna (3D) slika skeniranog objekta, kako njegove spoljašnje, tako i njegove unutrašnje geometrije [3]. Industrijski CT sistemi se koriste u mnogim područjima industrije za interni pregled različitih komponenata. Primena CT skeniranja je veoma rasprostranjena kod otkrivanja defekata, analize otkaza, metrologije, analize sklopova i kod reverzibilnog inženjerstva [2]. Industrijski CT sistemi otvaraju velike mogućnosti u polju ne-destruktivnog ispitivanja, i kao takva zauzima važno mesto u oblasti industrije [4,5].

Kako bi se ustanovila poroznog odlivka, tradicionalno se on morao uništiti kako bi se mogla ispitati njegova unutrašnja struktura. Tehnologija livenja danas omogućuje izradu odlivaka od različitih vrsta materijala, kao što su različiti metali ili polimeri, ali koji su skloni prisutnosti poroznosti, različitih uključaka itd. Ovi problemi nastaju tipično zbog procesa hlađenja kao i u prelazima između debelih i tankih zidova predmeta, a takođe zavise i od vrste materijala odlivka. Računarom podržana inspekcija ovakvih CT snimaka može biti primenjena za pronalaženje, merenje i analizu nastalih praznina i nepravilnosti kod plastičnih ili metalnih komponenata [6]. Primena industrijskih CT sistema za NDT (engl. *Non-Destructive Testing*) ispitivanja ima veliki potencijal za otkrivanje ovih nepravilnosti i da otkrije defekte unutar bilo koje geometrije. Ovi defekti se mogu otkriti analizom voksel (3D pixel) podataka primenom softvera za 3D vizuelizaciju. Pored toga, takođe se mogu rekonstruisati i površinski 3D modeli na bazi ovih voksel podataka i nakon toga se sprovode analize za otkrivanje defekata ili nepravilnosti unutar objekta. Na bazi presečnih 2D ravni, može se takođe dobiti bolji uvid u prikaz i stanje ovih nepravilnosti u objektu [6].

Danas na tržištu postoje softveri koji se koriste za analizu ovakvih CT snimaka, a koji omogućavaju korisnicima da na adekvatan način detektuju i analiziraju ovakve predmete sa ciljem dobijanja više informacija o njihovoj raspodeli, veličini, broju, itd.

Uzimajući u obzir aktuelnost polja istraživanja u okviru ovog rada je predstavljena primena softverskih alata na rezultujuće CT snimke dobijene na industrijskom CT sistemu, a sa ciljem ekstrakcije i analize različitih nesavršenosti koje se mogu javiti kod ovakvih odlivaka. Detaljna analiza pora i uključaka daje veći uvid u ponašanje tehnologije, kao i potencijalnih izmena u tehologiji njihove izrade sa ciljem dobijanja kvalitetnijih finalnih proizvoda.

2. PRINCIP RADA

Industrijska tomografija je našla svoju primenu kod analize unutrašnjih struktura materijala (npr. vlaknima ojačana plastika) i kod otkrivanja nedostatka materijala, gde se pri tome ne koriste pribori za njegovo stezanje i pozicioniraje. U skorije vreme, CT tehnologija je ušla i u oblast dimenzione metrologije, kao alternativa za taktilne ili optičke koordinatne merne sisteme, merne ruke, itd [7].

Primena metode kompjuterizovane tomografije, odnosno CT-a predstavlja nedestruktivnu metodu skeniranja unutrašnjosti dela (Slika 1). Na bazi slike se vidi da objekat izvodi rotaciju na obrtnom stolu dok su izvor X-zraka i detektor stacionarni.

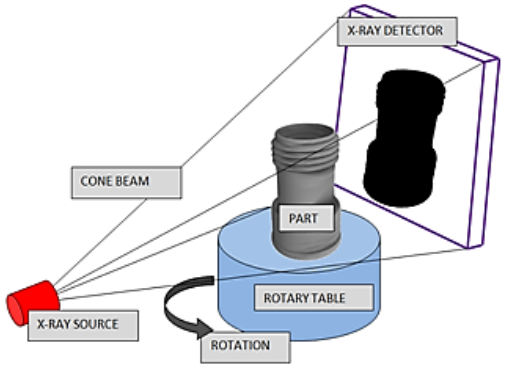

Sl. 1. Princip rada industrijskog CT-a [5]

CT skeniranje omogućava adekvatan pregled i lociranje problematičnih regiona unutar komponenti, kao i pronalaženje mesta nastanka eventualnih nepravilnosti u samom materijalu predmeta, i to bez potrebe za eventualnom demontažom kompletnih sklopova ili razaranjem predmeta [8].

3. ANALIZA CT SNIMAKA - STUDIJA SLUČAJA

3.1 Analiza unutrašnjosti materijala objekta

U okviru studije slučaja je izvršena rekonstrukcija aluminijumskog odlivka. Eksperimentalna analiza je sprovedena na računaru (FUJITSU CELSIUS M470-2) sa Intel(R) Xeon (R) CPU E5645, 2.40 GHz procesorom i sa 32 GB RAM memorije. Za analizu su korišćeni industrijski CT snimci odlivka dobijenih na industrijskom CT sistemu Nikon XT H 225 sa ciljem sprovođenja analize (Slika 2). Podaci o CT snimcima su prikazani u tabeli 1.

Tabela 1. Podaci o CT snimcima

Parametar	Vrednost	Jedinice
X rezolucija	434	pix
Y rezolucija	533	pix
Broj CT snimaka	480	/
Veličina piksela	0,06432	mm
Vidno polje (engl. FOV)	27,92	mm
Debljina slajsa	0,064	mm

FOV – engl. field of view

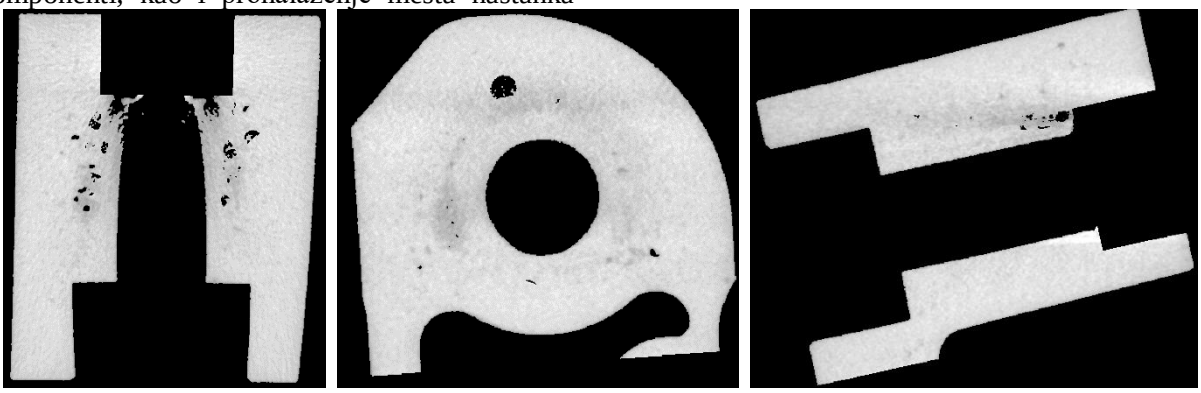

Sl. 2. Prikaz jednog 2D CT snimka aluminijumskog odlivka u sva tri pogleda

Sa ciljem rekonstrukcije 3D modela prvi korak predstavlja generisanje maski primenom alata segmentacije. Za potrebe segmentacije primenjena je metoda praga (engl. *Threshold method*). Prilikom segmentacije CT snimaka primenjena su dva različita seta parametara. Ovo je izvršeno sa cilejm lokalizacije porozne strukture unutar aluminijumskog odlivka, a koje zbog zadržanog vazduha u materijalu imaju drugačiji intenzitet piksela prilikom akvizicije CT snimka. Segmentacija odlivka (uključujući i pore) je prikazana na slici 3a. Uzimajući u obzir da je poroznost prikazana crnom bojom (prisutnost vazduha), segmentacija je izvršena gde je kao rezultat generisana kompletna zapremina vazduha na CT snimcima (uključujući i pore) prikazano na slici 3b. Bazičnom subtakcijom zapremina je naknado izdvojena poroznost unutar odlivka prikazana crvenom bojom (Slika 3c). U tabeli 2 su prikazani parametri koji su primenjeni prilikom segmentacije odlivka, kao i porozne strukture primenom predstavljene metode.

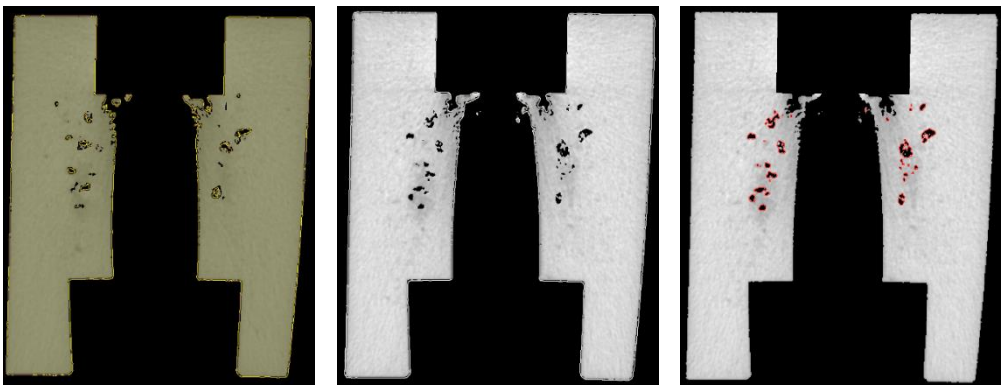

Sl. 3. Segmentacija a) kompletnog odlivka, b) spoljašnje geometrije, i c) porozne strukture

Tabela 2. Parametri segmentacije

Parametri segmentacije			
ODLIVAK		PORE	
Mix.	Max.	Min.	Max.
14337	30467	0	15813

Na bazi segmentiranih 2D granica izvršena je rekonstrukcija površinskih 3D modela kompletnog odlivka, kao i porozne strukture. Na slici 4a je prikazan kompletno rekonstruisan aluminijumski odlivak. Na slici 4b je prikazana ekstraktovana porozna struktura unutar odlivka. Na slici 4c je prikazana pozicija porozne strukture unutar transparentnog odlivka.

a) b) c)

Sl. 4. Prikaz a) rekonstruisanog aluminijumskog odlivka, b) porozne strukture i c) pozicije porozne strukture unutar odlivka

U tabeli 3 su prikazani neki od osnovnih parametara kod analize poroznosti.

Tabela 3. Parametri analize poroznosti u odlivku

Br.	Zapremina [mm^3]	Površina [mm^2]	Max. dimenzija [mm]
1	2,28	15,67	2,01
2	2,29	19,45	3,46
3	2,03	23,27	3,60
4	1,83	17,54	2,12
5	2,54	23,12	2,87
6	3,16	32,41	5,14
7	1,93	24,35	3,72
---	---	---	---
1034	1,87	13,26	2,47

3.2 Dimenzionalna analiza objekta

Sa ciljem dobijanja informacija o dimenzionalnoj tačnosti rekonstruisanog površinskog 3D modela aluminijumskog odlivka sprovedena je CAD inspekcija jer omogućava prikaz devijacija u vidu boja na 3D modelu. Kako bi se mogla sprovesti inspekcija, neophodan je CAD model aluminijumskog odlivka, pored rekonstruisanog površinskog 3D modela. Nakon toga je potrebno izvršiti postupak registracije (poravnavanja) CAD modela i rekonstruisanog površinskog 3D modela sa ciljem sprovođenja CAD inspekcije. Rezultati CAD inspekcije u vidu devijacija boja su prikazani na slici 5a, a na slici 5b je prikazana analiza u 2D poprečnom preseku.

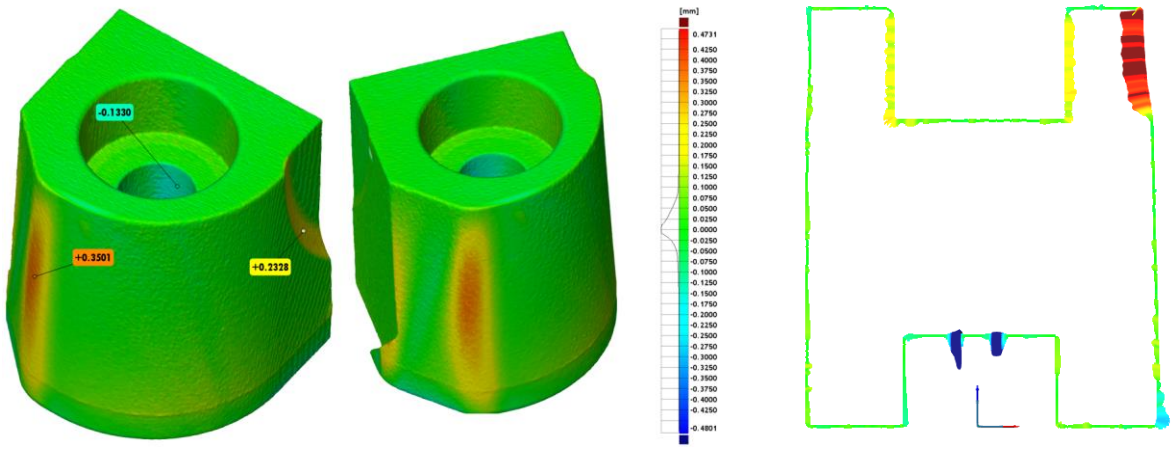

a) b)

Sl. 5. CAD inspekcija a) kompletne geometrije odlivka i b) inspekcija u 2D poprečnom preseku

Na bazi rezultata CAD inspekcije može se videti kako spoljašnja geometrija odlivka se nalazi unutar definisanih tolerancija (prikazano zelenom bojom). Devijacije se kreću u rasponu oko ±0,1 mm. Takođe se može videti prisutnost devijacija u otvoru (-0,133 mm), na radijusu odlivka (+0,232 mm) i zaobljenju (+0,35 mm) koja ukazuju na odstupanja u ovim zonama.

4. ZAKLJUČAK

Uzimajući u obzir rasprostranjenu primenu industrijskih CT sistema u oblasti industrije, kroz ovaj rad je prikazana primena rezultata na konkretnom predmetu, gde se kroz detaljne analize unutrašnjosti materijala, kao i dimenzionalne analize, mogu dobiti informacije o, kako spoljašnjoj, tako i unutrašnjoj geometriji radnih predmeta.

5. ZAHVALNICA

Ova rad je podržan od strane Ministarstva nauke, tehnološkog razvoja i inovacija kroz projekat broj 451-03-47/2023-01/200156 „Inovativna naučna i umetnička istraživanja iz domena delatnosti Fakulteta tehničkih nauka“.

6. REFERENCE

[1] L. De Chiffre, S. Carmignato, J.-P. Kruth, R. Schmitt, A. Weckenmann: *Industrial applications of computed tomography*, CIRP Annals, Vol. 63, pp. 655–677, 2014.

[2] A. Flisch, J. Wirth, R. Zanini, M. Breitenstein: *Industrial computed tomography in reverse engineering applications*, Computerized Tomography for Industrial Applications and Image Processing in Radiology, Berlin, 1999.

[3] R. Hanke, T. Fuchs, N. Uhlmann: *X-Ray based Methods for Non-destructive Testing and Material Characterization*, Nuclear Instruments and Methods in Physics, Vol. 591, pp. 1–6, 2008.

[4] M. Bartscher, U. Neuschaefer-Rube, F. Wäldele: *Computed tomography a highly potential tool for industrial quality control and production near measurements*, VDI Berichte, pp. 3–8, 2014.

[5] F. Gschwantner: *Advanced Measurement and Quantification of Industrial CT Data*, PhD thesis, 2011.

[6] C. Reinhart, C. Poliwoda, T. Günther: *How industrial computer tomography accelerates product development in the light metal casting and injection moulding industry*, 10th European Conference on Non-Destructive Testing - ECNDT, Moskva, Rusija, pp. 1–10, 2010.

[7] J.P. Kruth, M. Bartscher, S. Carmignato, R. Schmitt, L. De Chiffre, A. Weckenmann: *Computed tomography for dimensional metrology*, CIRP Annals, Vol. 60, pp. 821–842, 2011.

[8] A. du Plessis, P. Rossouw: *X-ray computed tomography of a titanium aerospace investment casting*, Case Studies in Nondestructive Testing and Evaluation, Vol. 3, pp. 21–26, 2015.

Autori: **Doc. dr Mario Šokac, M.Sc. Aleksandar Milošević, M.Sc. Miloš Ranisavljev, doc. dr Željko Santoši, prof. dr Đorđe Vukelić,** Univerzitet Novi Sad, Fakultet Tehničkih Nauka, Trg Dositeja Obradovica 6, 21000 Novi Sad, Serbia, Tel: +381 21 485 2332.
E-mail: marios@uns.ac.rs
aleksandar.milosevic@uns.ac.rs
mranisavljev97@uns.ac.rs
zeljkos@uns.ac.rs
vukelic@uns.ac.rs

Vanr. prof. dr Marko Katić, Sveučilište u Zagrebu, Fakultet Strojarstva i Brodogradnje, Zagreb, Republika Hrvatska. E-mail: marko.katic@fsb.hr

ETIKUM 2023 **INTERNATIONAL SCIENTIFIC CONFERENCE**
NOVI SAD, SERBIA, DECEMBER 7-9, 2023

Urekar, M.

NOVA VERZIJA STANDARDA SRPS EN IEC 61557-9 OPREMA ZA LOCIRANJE KVARA IZOLACIJE U IT SISTEMIMA

Rezime: *Predstavljena je nova verzija standarda SRPS EN IEC 61557-9:2023 „Električna bezbednost u niskonaponskim distributivnim mrežama do 1000 V naizmeničnog napona i 1500 V jednosmernog napona – Oprema za ispitivanje, merenje ili praćenje zaštitnih mera – Deo 9: Oprema za lociranje kvara izolacije u IT sistemima“. Dat je kontekst standarda, njegov značaj u savremenom IT i medicinskom okruženju, sadržaj i napomene za ključna poglavlja, ključne izmene u odnosu na prethodnu verziju, veze sa drugim standardima i metrologijom, te analiza istorijskog razvoja i budućnost ovog dokumenta.*
Ključne reči: *merenje, kvar izolacije, standard, IEC 61557-9, IT sistem*

1. UVOD

Nagli i sveobuhvatni razvoj IT tehnologije krajem 20. i početkom 21. veka je doveo do eksponencijalnog rasta IT industrije koju danas smatramo za lidera u inovacijama i profitabilnosti, jer svakako predstavlja najvidljiviji primer moderne industrije, ali i je takođe i integralno-neizostavni deo modernog života. Mora se naglasiti da osim razvoja IT tehnološkog sektora, ogroman uticaj ima i širenje ove tehnologije na sve postojeće industrijske sektore, što je dovelo i do paradigme Industrije 4.0. Ne postoji industrija i privredna grana gde IT nije ušao na neki način, od elementarne administracije do potpune kontrole svih procesa, zavisno od spremnosti za inovaciju u tom polju [1, 2].

Ono što je manje vidljivo i što se često zaboravlja je neophodnost da za svu tu stalno šireću tehnologiju mora postojati i adekvatna IT infrastruktura koja će omogućiti rad, komunikaciju i pouzdanost. Jasno je da ogromna količina računara i računarski podržanih tehnologija koristi veliku količinu energije za napajanje, te je potrebno obezbediti stabilno i kvalitetno napajanje. Za ovo je potrebno da postoji mreža niskonaponskih instalacija prema neposrednim korisnicima, takva da zadovoljava kako zahteve za kvalitetom, tako i visoke zahteve za bezbednost.

Da bi se ove karakteristike proverile i pratile, potrebno je postojanje jasnih metroloških normi i postupaka koji će ovo omogućiti, usaglašenih na međunarodnom nivou.

Odavde postaje jasno da su za moderne potrebe industrije potrebni i novi, aktuelni standardi koji će omogućiti pouzdan rad u savremenom okruženju Industrije 4.0.

2. STANDARDI VEZANI ZA ISPITIVANJE AC I DC INSTALACIJA U IT SISTEMIMA

Međunarodna elektrotehnička komisija (IEC) redovno donosi nove i ažurira postojeće standarde koji se tiču, između ostalog, i zahteva za ispitivanje IT infrastrukture. Ove standarde usvaja i Srbija kao članica IEC putem Nacionalnog komiteta koji predstavlja Institut za standardizaciju Srbije (ISS) [3].

Standard SRPS EN IEC 61557-1:2023 „Električna bezbednost u niskonaponskim distributivnim mrežama naizmeničnog napona do 1000 V i jednosmernog napona do 1500 V – Oprema za ispitivanje, merenje ili praćenje zaštitnih mera – Deo 1: Opšti zahtevi“ je u novoj verziji postavio opšte zahteve koji se primenjuju na opremu za merenje, praćenje i ispitivanje električne bezbednosti u sistemima za distribuciju AC napona do 1000 V i DC napona do 1500 V [4].

Uslovi za energetsku mrežu IT infrastrukture su dati u standardu SRPS HD 60364-4-41:2017 „Električne instalacije niskog napona – Deo 4-41: Zaštita radi ostvarivanja bezbednosti – Zaštita od električnog udara“. Ovaj standard daje suštinske zahteve koji se odnose na zaštitu od električnog udara - osnovnu zaštitu od direktnog dodira i zaštitu u slučaju kvara tj. od indirektnog dodira (odnosi se na ljude i životinje), uređuje primenu i koordinaciju definisanih zahteva u odnosu na spoljašnje uticaje, kao i primenu dopunske zaštite tamo gde je to primenljivo [5].

Što se tiče metrološkog aspekta ove oblasti, SRPS EN IEC 61557-9:2023 „Električna bezbednost u niskonaponskim distributivnim mrežama do 1000 V naizmeničnog napona i 1500 V jednosmernog napona – Oprema za ispitivanje, merenje ili praćenje zaštitnih mera – Deo 9:

Oprema za lociranje kvara izolacije u IT sistemima“ je standard trenutno u finalnom postupku usvajanja (novembar 2023). Ovaj standard specificira zahteve za *sistem lociranja kvara izolacije* (IFLS) kojim se lokalizuje kvar izolacije u bilo kom delu sistema u neuzemljenim IT sistemima naizmenične struje i neuzemljenim IT sistemima naizmenične struje sa galvanski povezanim jednosmernim kolima nominalnog napona do 1000 V AC, kao i u neuzemljenim IT jednosmernim sistemima sa naponima do 1500 V DC, nezavisno od principa merenja [6].

Osnovna ideja ovog rada je da predstavi formu i osnovnu strukturu SRPS EN IEC 61557-9:2023, sadržaj, izmene u odnosu na prethodnu verziju, ali i da naglasi njegovu važnost i potrebu u kontekstu modernog IT okruženja.

3. IEC 61557-9

Ovaj standard je deo povezane porodice standarda serije počevši od IEC 61557-1:2019, koji utvrđuje opšte zahteve primenjene na opremu za praćenje, merenje i ispitivanje električne bezbednosti u niskonaponskim distributivnim sistemima sa nazivnim naponima do 1000 V AC i 1500 V DC. Kada merna oprema ili merne instalacije uključuju različite merne zadatke obuhvaćene ovom serijom standarda, onda je primenljiv onaj deo serije standarda koji je relevantan za svaki od pojedinačnih zadataka merenja.

Istorija razvoja IEC 61557-9 ilustruje i prati razvoj globalnog IT sektora. Prva verzija je objavljena 1999. godine kao odgovor na nove uslove u industriji koje je donelo širenje interneta. Sledeća verzija je izdata tek 2009. godine, potom 2014. praćene izmenama u revizijama 2016. i 2017. godine, da bi 4. edicija u 2023. donela najnovije izmene koje reflektuju nove prakse i zahteve u pogledu bezbednosti i načina ispitivanja. Ovo jasno pokazuje kako se IT oblast razvijala i postajala sve zastupljenija, postojala je i potreba za češćim ažuriranjem standarda [7].

Prvi zadatak nove verzije je da isprati značajne promene koje su se desile u „krovnom“ standardu IEC 61557-1 koji 2017 potpuno izmenjen u odnosu na verziju iz 2007. godine. Ove izmene se tiču prvenstveno:

a) terminologije usklađene sa IEC 60050;

b) merna nesigurnost je izražena u skladu sa tzv. GUM-om, tj. ISO/IEC Guide 98-3:2008 [8].;

c) ažurirane su zahtevi za bezbednosti i zahteve za elektromagnetnu kompatibilnost (EMC);

d) ažurirani su zahtevi za obeležavanje i uputstva za upotrebu;

e) ažurirane su zahtevi za ispitivanje bezbednosti i EMC.

IEC 61557-9 je ažuriran u skladu sa strukturom ovog dokumenta i navedenim sadržajima.

U tehničkom smislu, najveće promene su izvršene u novim pojmovima, definicijama i zahtevima za maksimalno dozvoljenih vrednosti AC i DC ispitnih struja i napona, izmenjene su granične vrednosti kod pojedinih metoda ispitivanja i dodati novi zahtevi za performanse.

4. STRUKTURA I SADRŽAJ SRPS EN IEC 61557-9:2023

Srpska verzija standarda je identična sa IEC 61557-9:2014 ED4, tj. verzijom iz 2023. godine [6, 9, 10].

Sadržaj standarda sa napomenama:

1 Obim
Obim ili područje primene ovog standarda je dat u poglavlju 2 ovog rada
2 Normativne reference
Navedena su čak 22 IEC dokumenta čiji zahtevi se odnose na ovaj standard.
3 Termini, definicije i skraćenice
Vrlo koristan rečnik pojmova koji se koriste u ovom dokumentu, sa potrebnim definicijama, oznakama, jedinicama i napomenama.
4 Zahtevi
Ovde su navedeni osnovni tehnički zahtevi koji se odnose na metode, načine, opremu i vrednosti merenja izolacije u IT sistemima.
4.1 Opšti zahtevi
Oprema za lociranje kvara izolacije mora biti sposobna da lokalizuje simetrične i asimetrične greške u izolaciji u IT sistemu uz davanje upozorenja o lokaciji ako je na nekom mestu došlo do smanjena otpornosti ispod praga osetljivosti.
4.2 Obavezne funkcije IFLS
Normativ obaveznih funkcija koje mora da obezbeđuje sistem ili instrument za lociranje kvara izolacije (IFLS).
4.2.1 Upozorenje o lokaciji
IFLS mora posedovati ugrađenu i/ili udaljenu indikaciju kvara, uz mogućnost resetovanja.
4.2.2 Lokalno (ugrađeno) upozorenje o lokaciji kvara (LLV)
Vizuelni ili audio signal upozorenja kada otpor izolacije prema uzemljenu padne ispod praga osetljivosti uz lociranje kvara.
4.2.3 Upozorenje o lokaciji kvara preneto na udaljenu lokaciju (RLV)
Mogućnost da se gorenavedeni signal pošalje na udaljenu lokaciju.
4.3 Opcione funkcije IFLS
Indikacija vrednosti izolacije, Alarm u slučaju

prekida gubitka veze sa lociranje strujnog senzora (LCS), Samotestiranje.

4.4 Zahtevi za performanse

Tehničke specifikacije dozvoljenih/potrebnih vrednosti**.**

4.4.1 Osetljivost

Struje curenja za date vrednosti kapacitivnosti u odnosu na prag osetljivosti mernog sistema.

4.4.2 Ispitni naponi i struje (struje i naponi za lociranje kvara) U_L i I_L

Unete su izmene kojima se propisuju maksimalno dozvoljene vrednosti AC i DC ispitnih struja i napona, frekvencije, za koje otpornosti i uslove su definisani.

4.4.3 Dozvoljena vrednost trajnog nazivnog napon U_{pa}

Nov pojam. Definiše maksimalno dozvoljeni napon od minimalno 105% nominalnog napona, primenjen na između ulaznih kontakata sistema/IFLS i uzemljenja.

4.4.4 Napon napajanja Us

Nov pojam. Definiše se napon kojim se napaja IFLS a potiče od napona koji se meri.

4.5 Bezbednosni zahtevi

Definisani su zahtevi razmake, naponske zazore, IP klase zaštite i uzemljenje.

4.7 Mehanički zahtevi

Definišu se zahtevi za mehaničku robusnost i zahtevi za klasu zaštite (IP) za IFLS.

4.8 Uslovi okoline

Definišu se uslovi okoline radne sredine u kojima IFLS mora da funkcioniše ispravno.

5 Označavanje i uputstvo za upotrebu

Definišu se jasni načini obeležavanja tj. označavanja na IFLS i priloženog uputstva za rukovanje.

6 Ispitivanje

Definišu se načini i metode ispitivanja izolacije pomoću IFLS. Metode su ilustrovane šemama spajanja mernih sistema za potrebe praktičnih merenja

6.1 Opšti zahtevi

Definisani su uslovi za ispitivanja.

6.2 Tipska ispitivanja

Definisana su tipska ispitivanja

6.2.1 Klimatska ispitivanja

6.2.2 Test osetljivosti reakcije IFLS

6.2.3 Ispitivanje struje za lociranje (ispitne struje) I_L i napona lociranja (ispitnog napona) U_L

Ovaj deo poglavlja je doživeo najveće tehničke izmene u odnosu na prethodnu verziju. Obavezno obratiti pažnju na sve navode u slučaju praktične primene. *Kritičan (ključni) deo standarda*!

6.2.4 Ispitivanje upozorenja o lokaciji kvara

6.2.5 Ispitivanje indikacije vrednosti otpora izolacije

6.2.6 Provera usklađenosti izolacije

Usklađenost sa zahtevima razmaka i naponskih zazora (*clearance and creepage distance*).

6.2.7 Ispitivanje EMC

6.2.8 LCS ispitivanje

Loss of the connection ispitivanje u slučaju gubitka veze.

6.2.9 Ispitivanje klase zaštite IP i spoja uzemljenja IFLS

6.2.10 Provera obeležavanje i uputstva za rukovanje

6.2.11 Mehanička ispitivanja

Pad sa visine i vibracija.

6.2.12 Zapisi o vrsti ispitivanja

6.3 Rutinska ispitivanja

Opšti zahtevi, Ispitivanje napona, Dokumentovanje rutinskih ispitivanja.

7 Pregled zahteva i ispitivanja za IFLS

Tabelarni pregled zahteva i ispitivanja prema poglavljima ovog standarda.

Aneks A (normativni)

Sistem lociranja kvara izolacije na medicinskim lokacijama (MED-IFLS). Ovo se odnosi se na električne instalacije na medicinskim lokacijama kako bi se osigurala sigurnost pacijenata i medicinskog osoblja.“Medicinskim lokacijama“ su obuhvaćene bolnice, klinike, medicinske i stomatološke ordinacije, domovi zdravlja, sanatorijumi, ambulante, namenske medicinske prostorije na radnom mestu ili ekvivalentne ustanove (uključujući ekvivalentne pokretne i mobilne lokacije). Dati su opšti zahtevi (za performanse, EMC), zahtevi za dodatna ispitivanja (performanse, vreme odziva, EMC).

Aneks B (normativni)

Prenosiva oprema za lociranje kvara izolacije.

Definisani su opšti zahtevi, dodatni zahtevi (za performanse), zahtevi za obeležavanje IFLS i uputstvo za rukovanje, te dodatni testovi.

Aneks C (informativni)

Primer realnog IFLS i parazitnih kapacitivnosti.

5. DISKUSIJA

Iz navedenih kratkih opisa sadržaja poglavlja i novosti koje su implementirane, vidi se da je SRPS EN IEC 61557-9:2023 usklađen sa velikim brojem IEC normi, da su uključene sve izmene i dopune koje su razvijane od prve verzije ovog standarda. Takođe se mora naglasiti da je očigledan uticaj LVD direktive Evropske Komisije (*Low Voltage Directive*) [11], kako bi se izbegle neusaglašenosti.

Praksa i razvoj tehnologije, ali i realno “stanje na terenu”, uslovili su neke potrebne izmene koje dodatno definišu i unapređuju pojmove bezbednosti, daju jasno definisane vrednosti koje

su uputstvo kako proizvođačima, tako i korisnicima, koje su primenjene i van usko definisanog područja IT sistema (opšte električne instalacije) [12].

Mnoge stvari nisu menjane, pa su tako aneksi koji su postojali u prethodnoj verziji samo ažurirani, a vezani su za posebno osetljiv aspekt IT uređaja u medicini, tačnije u medicinskim ustanovama (ova terminološka razlika potiče od toga što se u medicinskim ustanovama ne moraju koristiti samo medicinski IT uređaji, na primer obični kompjuteri).

Drugi aneks se odnosi na prenosive uređaje koji zahtevaju poseban set modifikacija i dodatnih zahteva koji su usko vezani sa mobilnom (prenosivom) prirodom ovakvih uređaja [13].

6. ZAKLJUČAK

Standard SRPS EN IEC 61557-1:2023 je doneo ažurirane zahteve i normative u polju ispitivanja grešaka izolacije u IT sistemima, kao jedne od oblasti industrije koja se najviše i najbrže razvija i širi. Jasno je da je potreba za pouzdanom i proverivom energetskom infrastrukturom, posebno u medicinskim ustanovama, ovde od vitalnog značaja i uloga električnih merenja i metrologije ovde dolazi do izražaja ispunjavajući jednu od svojih osnovnih namena: merenje radi bezbednosti i usklađenosti sa normativnim standardima [14].

Jedan od jasnih pokazatelja kritičnog aspekta ove oblasti je i tzv. *stability date* podatak ovog standarda, koji je dat do 2028. godine. Ovo znači da se najkasnije do tog datuma očekuje nova verzija, a postojeća će do tada da bude ili dopunjavana ili potpuno povučena i zamenjena novom. Rok od 5 umesto uobičajenih 10 godina, ukazuje na svest koliko se ova oblast menja, koliko će se brzo i sveobuhvatno promeniti, te se predviđa da će dalji progres dovesti do potrebe za neminovnim izmenama i ažuriranjima kako bi zahtevi ostali relevantni i upotrebivi.

7. ZAHVALNICA

Ovaj rad je podržan od strane Fakulteta tehničkih nauka u Novom Sadu, Departmana za energetiku, elektroniku i telekomunikacije, u okviru realizacije projekta pod nazivom: “Istraživanja u cilju unapređenja nastavnog procesa i razvoja naučno–stručnih oblasti Departmana za energetiku, elektroniku i telekomunikacije”. Zahvaljujem se Institutu za standardizaciju Srbije i Komisiji N085 „Oprema za merenje električnih i elektromagnetskih veličina“ na pomoći i tehničkoj podršci tokom izrade ovog rada.

8. REFERENCE

[1] Urekar, M., Đorđević Kozarov, J.: *10 ključnih tačaka za metrologiju u konceptu Industrije 4.0*, ISBN 978-86-6022-320-5, pp. 1-27, 5. Merno-informacione tehnologije MIT, Fakultet tehničkih nauka, Novi Sad, 2020.

[2] Urekar, M., Pejić, D., Gazivoda, N., Novaković, Đ., Mirković, S., Bulat, M.: *Značaj merenja i metrologije u konceptu Industrije 4.0*, ISBN 978-86-6022-233-8, pp. 1-34, 4. Mernoinformacione tehnologije MIT, Fakultet tehničkih nauka Novi Sad, 2019.

[3] Institut za standardizaciju Srbije, https://iss.rs/sr_Cyrl/

[4] *SRPS EN IEC 61557-1:2023*, https://iss.rs/sr_Cyrl/project/show/iss:proj:64254

[5] *SRPS HD 60364-4-41:2017*, https://iss.rs/sr_Cyrl/project/show/iss:proj:65272

[6] *SRPS EN IEC 61557-9:2023*, https://iss.rs/sr_Cyrl/project/show/iss:proj:102389

[7] *IEC 61557-1:2019 RLV*, https://webstore.iec.ch/publication/65550

[8] *ISO/IEC Guide 98-3:2008 Uncertainty of measurement Part 3: Guide to the expression of uncertainty in measurement (GUM:1995)*, https://www.iso.org/standard/50461.html

[9] *IEC 61557-9:2014*, https://webstore.iec.ch/publication/5583

[10] *IEC 61557-9 ED4*, https://iss.rs/sr_Cyrl/project/show/iec:proj:105391

[11] *Low voltage directive (LVD) (2014/35/EU)*, https://single-market-economy.ec.europa.eu/sectors/electrical-and-electronic-engineering-industries-eei/low-voltage-directive-lvd_en

[12] *A Practical Guide to the Measurements on Electrical Installations in Accordance with IEC 60364-6 standard*, Kyoritsu Electrical Instruments, LTD, 2008.

[13] *The Complete Guide to Electrical Insulation Testing*, Megger, 2006.

[14] Bender, W.: *IT systems, The basis for a reliable power supply*, Technical information No.1, Power in electrical safety, Bender GmbH, 2004.

Autor: **Vanr. prof. dr Marjan Urekar**
Univerzitet u Novom Sadu, Fakultet tehničkih nauka, Trg Dositeja Obradovića 6, 21000 Novi Sad, Srbija, Tel: +381 21 485 4543
E-mail:
urekarm@uns.ac.rs

ETIKUM 2023

INTERNATIONAL SCIENTIFIC CONFERENCE
NOVI SAD, SERBIA, DECEMBER 7-9, 2023

Vasiljević, S., Kostić, S., Kočović, V., Tanasković, A., Miletić, S., Džunić, D.

STATISTICAL PROCESSING OF 3D PRINTER PRINTING TIME DATA AND ANALYSIS OF INFLUENTIAL FACTORS

Abstract: *The use of 3D printers is very common in industry today due to the easy production of parts or prototyping of some products. One of the problems that can occur when printing is the length or time of printing. In this paper, statistical analysis was used to process data on the printing time of 3D printers, and based on such statistical analysis, a conclusion was reached about the factors that have an impact on printing time. Six parameters were taken into account, on the basis of which the analysis of the printing time was performed.*
Key words: *Statistical, analysis, time, printing, 3D printer*

1. INTRODUCTION

3D printing is a technological paradox that is constantly evolving and bringing changes in various industries. This technology brings numerous benefits, including faster production, waste reduction and product personalization. With increasing interest and investment in research and development, 3D printing can be expected to become ubiquitous in manufacturing and significantly impact the way we make and use objects in the future [1]. The basic idea of 3D printing lies in the additive process of creating objects, contrary to traditional methods of processing materials that are often subtractive, such as CNC machines. This process involves the layering of materials, such as plastic, metal, ceramic or even biological materials, to create a three-dimensional object [2].

The speed of 3D printing depends on a number of factors, the most important of which include, design complexity, object size, printer speed, layer thickness, material, printer settings, support and infill, software optimization, post-processing, … All these factors should be considered when planning 3D printing in order to optimize the printing speed according to the needs and requirements of the project [3].

The aim of this paper is to use a statistical tool to analyze the influence of some of the parameters of the 3D printer on the printing time of one model. In this case, six different factors were analyzed, which are mostly adjusted before the actual printing. The paper consists of three more chapters, namely: research methodology, where the methodology of data collection, analysis results and the final conclusion are explained.

2. RESEARCH METHODOLOGY

2.1 Calculating of printing time

The software used to write the printer code Flashforge Creator Pro was used to calculate the time required to print the 3D model. That is, the software used in this case is FlashPrint version 3.23.1 64 bit. Figure 1 shows the layout of the desktop of the applied software.

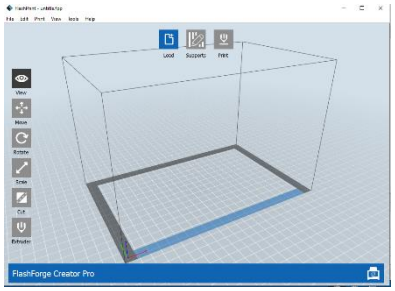

Fig. 1. Software FlashPrint software 3.23.1

The model that was applied in this case, i.e. for which the printing time was calculated, is the model shown in Figure 2.

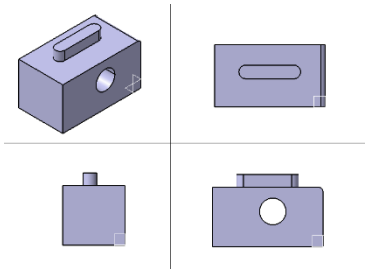

Fig. 2. 3D model that has been selected for printing

The displayed model is loaded into the printing software as shown in Figure 3.

Then, by selecting the print option, the print parameters are set as shown in Figure 4.

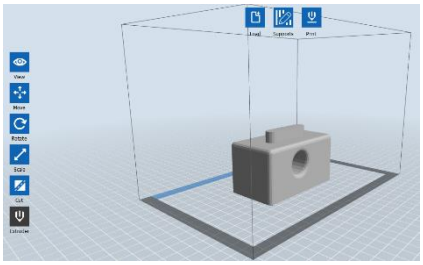

Fig. 3. 3D model in FlashPrint 3.23.1 software

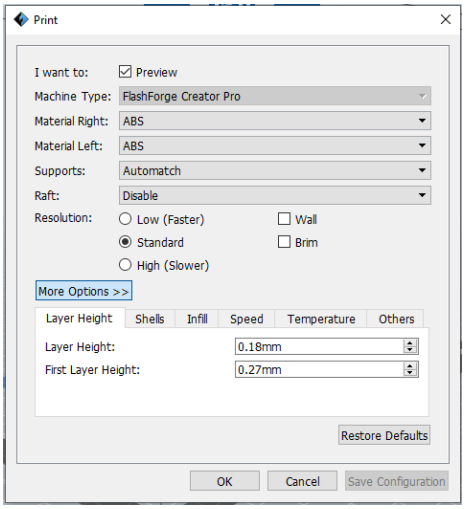

Fig. 4. A window in the software for setting print parameters

After setting the printing parameters of the 3D printer, information about the time required for the printer to print the selected model appears. An example of time is shown in Figure 5. This data was collated and analyzed based on software calculations.

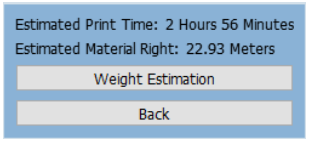

Fig. 5. Data on the required time of model printing

The time required for printing directly depends on the size of the model and the selected printing parameters. Keeping in mind that in this case, the analysis only includes the influencing factors of molding and setting, the model and its size were not taken into account. parameters that were applied and varied in this case are layer height, first layer height, travel speed of extruder, print speed, infill, extruder temperature. In this case, it was applied that the infill should be on the entire model without every other layer, except for the initial and final layers, being made of 100% material (full material). ABS plastic was always used as plastic. The fill pattern is set to always be a hexagon. The temperature of the platform is 60°C.

In the case of six combined parameters, a total of five parameters were applied. The applied values of the parameters that were varied are shown in Table 1.

Table 1. Applied print parameter values

Parameter	Values
Layer height (mm)	0.10, 0.18, 0.25, 0.30, 0.40
Print speed (mm/s)	40, 50, 60, 80, 90
Infill (%)	0, 25, 50, 75, 100
Extruder temperature (°C)	180, 190, 200, 210, 220
Travel speed (mm/s)	60, 70, 80, 90, 100
First layer height (mm)	0.18, 0.23, 0.27, 0.35, 0.42

Figure 6 shows the layout of the model's internal print. In this case, the layout of the interior of the model is shown for the selected infill values of 0%, 50% and 100%. Where the interior for 0% is completely hollow while in the case of 100% the interior is solid material.

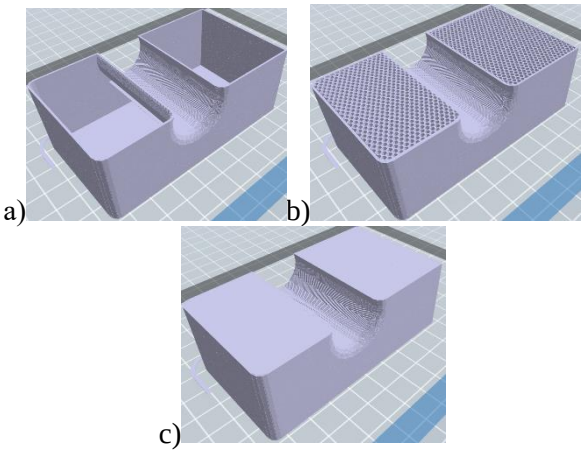

Fig. 6. Applied infill, where: a) 0%, b) 50%, c) 100%

2.2 Applied statistical analysis

Taguchi data analysis typically includes a design-of-experiments phase, where the factors, levels, and design of experiments are determined, and a data analysis phase, where the effects of factors on response are evaluated. By using mathematical models and statistical techniques, engineers and researchers can identify optimal settings of factors to improve the quality and performance of a product or process.

Taguchi data analysis is widely used in industry, especially in the automotive, electronics, pharmaceutical and other sectors where product

quality and process efficiency are important. A detailed explanation of the method of calculation and analysis using Taguchi is presented in references [4].

In this case, a combination of parameters was determined by applying the Taguchi design of the experiment. Given that six factors with five levels were chosen, the combination model L25 was chosen. This means there are 25 combinations of factors. Also having in mind that the goal is to optimize the parameter so that the printing time is the shortest, a Taguchi analysis of the parameters for the shortest printing time was performed. Thus, the possibility of "smaller is better" was analyzed first. Parameters were also optimized to determine the combination that would result in the longest printing time using the "larger is better" option.

3. RESULTS

As 25 combinations of factors were taken into account, the result was that the minimum printing time is 70 minutes (combination 21), while the maximum time is 2936 minutes (combination 4). The results are shown in Figure 7. The average time is 823.64 minutes.

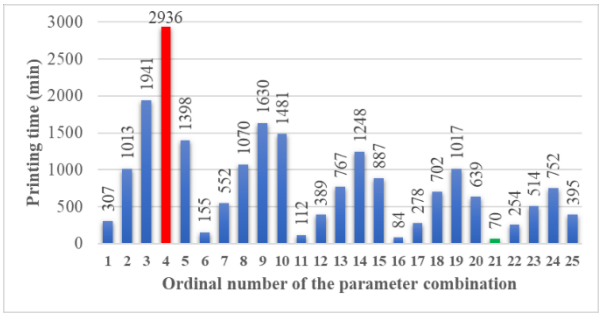

Fig. 7. Printing time depending on the combination of parameters

Taking into account that it is necessary to analyze the influence of various factors on the printing time, then it is necessary to make that time as short as possible. Thus, in this case, in Taguchi's analysis, it was assumed that the time should be as short as possible, that is, the "smaller is better" option was chosen. The results of the analysis are shown in Table 2. It can be seen that the largest influence is the occupancy within the model, followed by the height of one layer, the extruder print speed, the extruder travel speed, then the extruder temperature and finally the first layer height (FLH), which is shown in Table 2 The table shows the parameter values according to the assigned impact rank (R). Figure 7 graphically shows the aforementioned and the obtained values of influencing factors based on response for signal to noise (Rang S/N) and response for threats (Rang RM) are shown graphically.

Table 2. Analysis of the ranking of factors influencing the printing time

Level	Rang S/N	Rang RM
Layer height	2	2
Infill	1	1
Print speed	3	6
Extr. temp.	5	5
Travel of extr.	4	5
FLH	6	3

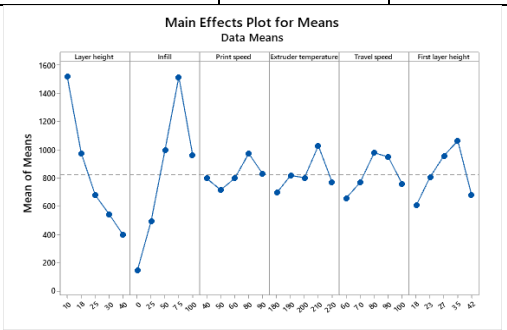

Fig. 7. Analysis of the influence of certain factors on the printing time based on effect for means

The analysis of the parameters to achieve the shortest printing time is shown graphically in Figure 8, while the values of the analysis of the parameters are given in Table 3. The table indicates the optimal values according to the parameter, i.e. according to the order of listing in Table 1.

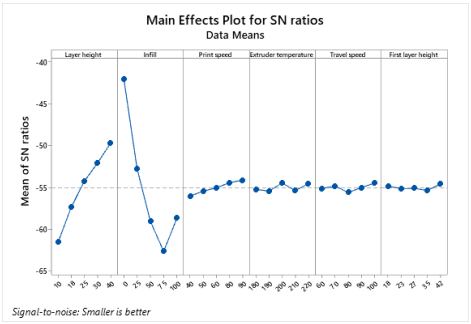

Fig. 8. Graphical analysis of the most favorable combination of factors for the shortest printing time

Table 3. Value analysis of the most favorable factors for the shortest printing time

Level	**1**	**2**	**3**	**4**	**5**
Layer height	-61.58	-57.38	-54.27	-52.11	**-49.73**
Infill	**-41.98**	-52.75	-59.04	-62.64	-58.66
Print speed	-56.02	-55.45	-55.04	-54.43	**-54.13**
Extr. temp.	-55.22	-55.45	**-54.46**	-55.4	-54.55
Travel of extr.	-55.14	-54.84	-55.6	-55.01	**-54.48**
FLH	-54.87	-55.13	-55.11	-55.37	**-54.59**

Considering that the highest quality print of the model with the highest resolution is obtained with the longest print time, the factors that would give the longest print time were analyzed. Thus, Figure 9 shows a graphic representation of the optimal values for the longest printing time. Table 4 shows the values of the analysis according to each parameter, and the most favorable parameter is marked according to the order of listing in table 1.

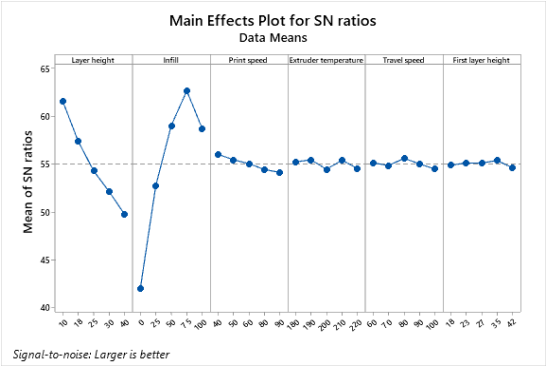

Fig. 9. Graphical analysis of the most favorable factors for the longest print time

Table 4. Analysis values of the most favorable factors for the longest printing time

Level	1	2	3	4	5
Layer height	**61.58**	57.38	54.27	52.11	49.73
Infill	41.98	52.75	59.04	**62.64**	58.66
Print speed	**56.02**	55.45	55.04	54.43	54.13
Extr. temp.	55.22	55.45	54.46	**55.4**	54.55
Travel of extr.	55.14	54.84	**55.6**	55.01	54.48
FLH	54.87	55.13	55.11	**55.37**	54.59

4. CONCLUSION

Statistical analysis of the printing time of the model on a 3D printer was performed using the Taguchi method. Based on the applied printer programming software, the printing time of the given model is determined. The result was that the filling inside the model has the greatest influence on the molding time, followed by the height of one layer, the press speed of the extruder, the travel speed of the extruder, then the temperature of the extruder and finally the height of the first layer. It was also determined by the application of statistical analysis which parameter values should be applied in this case for the shortest and longest printing time of the task model. Thus, it was determined what the influencing factors are, where it turned out that the height of the layer, the occupancy of the model and the printing speed are one of the most important factors that affect the printing time.

Future research will be limited to the statistical analysis of influential factors depending on the form of filling the interior of the model. In this case, only the model with hexagonal filling was analyzed. So the shape of the clean line and the triangular infill will be analyzed in the following researches.

5. REFERENCES

[1] Sandeep, B., Kannan, T. T. M., Chandradass, J., Ganesan, M., John Rajan, A.: *Scope of 3D printing in manufacturing industries-A review.* Materials Today: Proceedings, 45, p.p. 6941-6945, 2021.

[2] Jandyal, A., Chaturvedi, I., Wazir, I., Raina, A., Ul Haq, M.I. *3D printing – a review of processes, materials and applications in industry 4.0*, Sustainable Operations and Computers, 3, pp. 33-42, 2022.

[3] Geng, P., Zhao, J., Wu, W., Ye, W., Wang, Y., Wang, S., Zhang, S. *Effects of extrusion speed and printing speed on the 3D printing stability of extruded PEEK filament*. Journal of Manufacturing Processes, 37, 266–273, 2019.

[4] Vasiljević, S.; Taranović, D.; Lukić, J.; Miloradović, D.; Glišović, J. *Design of experimental research on influencing factors on the particle emission caused by brake wear*. Proceedings of 16th International Conference on Accomplishments in Mechanical and Industrial Engineering, p.p 368-375, Banja Luka, Faculty of Mechanical Engineering, Banja Luka, 2023.

Authors: **Teaching Assis. Saša Vasiljević, Prof. of App. Studies. dr Sonja Kostić, Teaching Assis. Aleksandra Tanasković,** Academy of Professional Studies Šumadija, Department in Kragujevac, Kosovska 8, Kragujevac, Serbia.
E-mail: svasiljevic@asss.edu.rs
skostic@asss.edu.rs
tanaskovicsaska@gmail.com

Assis. prof. dr Vladimir Kočović, MEng. Stefan Miletić, Assoc. prof. dr Dragan Džunić, University of Kragujevac, Faculty of Engineering, Sestre Janjić street, no. 6 - 34000 Kragujevac, Serbia.
E-mail: vladimir.kocovic@kg.ac.rs
stefan96miletic.finkg@gmail.com
dzuna@kg.ac.rs

INTERNATIONAL SCIENTIFIC CONFERENCE - ETIKUM 2023

PROCEEDINGS

Session 2:

METROLOGY AND QUALITY CONTROL IN THE BIOMEDICAL ENGINEERING

Novi Sad, 07 – 09th December 2023

ETIKUM 2023 **INTERNATIONAL SCIENTIFIC CONFERENCE NOVI SAD, SERBIA, DECEMBER 7-9, 2023**

Adamov, L., Petrović, N., Putnik, I., Đoćoš, M., Petrović, B., Vejin, M., Kojić, S.,

AUTOMATED DENTAL AGE ASSESSMENT WITH CAMERIERE'S THIRD MOLAR INDEX: A PRECISION APPROACH AND FUTURE DEVELOPMENTS

Abstract: *Dental age signifies the extent of development in teeth, thus the estimation of dental age holds significant implications in dentistry, legal medicine and criminology. Cameriere's method offers a straightforward and noninvasive approach to determine the dental age. Even though the manual assessment approach through measuring the mandibular third left molar has its advantages, it reveals numeral constraints. This study focuses on addressing the limitations by the process of automation on a randomized sample. Similar values were identified and the automated implementation of this method enhances result objectivity while simplifying the procedure.*
Key words: *Chronological age; Dental age; OPT; Third molar index; Legal age*

1. INTRODUCTION

In contrast to the chronological age which refers to time elapsed since birth, measured in years, biological age reflects the development of organic systems within the body. Dental age, as a form of biological age represents the development of teeth [1]. Given that teeth are the most resilient tissue in the human body, dental age acts as a crucial element in odontology, investigative and legal matters [2-5].

Methods for determining dental age can take various routes. Radiological methods are common due to their non-invasive nature and simplicity. Cameriere's method, amongst many methods which assess stages of tooth development, represents a radiological method used for the purpose of this research. To be more precise, the method used in this research is the modified Cameriere's method for determining legal age [2,3,6].

Adulthood, also referred to as legal age, represented in years, for most European countries is considered as the age of 18 and above, while the age below 18 represents minors of the population.

The original Cameriere's method assesses dental age by measuring the open apex projections in seven left mandibular teeth.

The adapted Cameriere's approach is used to determine the legal age of individuals, examining the tooth 38 introducing the same formula using the third molar index (I_{3M}). The assessment relies on measurements of the projections of open apices of the third molar ($Ai=A_1+A_2$) and the height of the said tooth (Li) [6-9].

Formula. Measurements of the projections of open apices of the third molar (Ai) and the height of the tooth (Li):

$$I_{3M} = [Ai / Li] \qquad (1)$$

Cameriere and various other authors proved that the optimal value separating adults from minors is $I_{3M} < 0.08$. The value of $I_{3M} < 0.08$ is assigned to adults, leaving the value of $I_{3M} \geq 0.08$ to minors [6,7].

2. MATERIALS AND METHODOLOGY

The aim of this research was to highlight the importance of precision and practicality in Cameriere's method in situations where chronological age is unknown. A total of fifty orthopantomographic (OPG) images were randomly selected from the author's baseline study database, sourced from the Dentistry Clinic of Vojvodina's radiographic database.

To conduct a more comprehensive evaluation, a Graphical User Interface (GUI) application was created. This application provides dentists with the capability to load radiographic images and accurately identify the specific tooth under consideration, which in this case is the mandibular left third molar. Furthermore, the application allows dentists to make adjustments to the image's contrast, thereby facilitating their interpretation of radiographic results, while simultaneously aiding the program in processing the data. The process of adjusting the contrast involves altering the power of the pixel value, which can range from 0 to 2. The algorithm employed in this application distinguishes the tooth within the designated region

by detecting pixels that surpass a predetermined brightness threshold. It is important to note that this threshold is automatically established through the utilization of the k-means algorithm, which effectively separates the teeth from the background structures.

Fig. 1. Result of using k-means on desired region

A binary mask of the tooth is subsequently created through the implementation of various morphological operations such as opening and dilatation. These operations involve the manipulation and transformation of the tooth's binary representation, resulting in the generation of a distinct and discernible binary mask. Once this binary mask has been obtained, it serves as the foundation for the subsequent steps in the dental image analysis process. Specifically, an algorithm designed for the purpose of detecting apices is developed and employed. This algorithm effectively identifies and locates the apices within the tooth, allowing for a comprehensive and detailed analysis of its structure and characteristics. Through the utilization of this algorithm, the intricate features and properties of the tooth can be accurately assessed and evaluated, contributing to a more comprehensive understanding of its overall condition.

Fig. 2. Result after morphology operations to clear

This algorithm, utilizing a meticulously crafted methodology, is designed with the sole purpose of identifying the local minimum of the binary region.

It achieves this feat by employing an intricate searching technique, which systematically scans each and every pixel within the said region and discerns those possessing a true value. Furthermore, the algorithm proceeds to isolate these identified pixels, effectively filtering out any extraneous noise or irrelevant data, and meticulously analyzes their respective positions. Through this meticulous analysis, it successfully identifies and pinpoints the pixels that reside in the lowest positions, thus unequivocally determining the local minimum of the binary region.

Fig. 3. Detected root ending marked with red

The distance between red pixels (walls of the undeveloped root canal) is calculated as Euclidean distance and that distance is multiplied by pixel size in the real world, which is known from the DICOM file format created by X-Ray apparatus (Sidexis, 60 kV, 2 mA, and 8.82 s). Euclidean distance of two pixels is described as:

$$D = \sqrt{(x_1 - x_2)^2 + (y_1 - y_2)^2} \qquad (2)$$

where x and y are x and y coordinates of the pixel on the image. Similarly, local maximums of the tooth were found. Height of the tooth is calculated as Euclidean distance between equidistant pixel from two red colored pixels (distance between dentinal wall of the apex) of one channel and its corresponding local maximum.

Equation for equidistant pixel coordinates can be written as:

$$E_q x, E_q y = \frac{x_1 + x_2}{2}, \frac{y_1 + y_2}{2} \qquad (3)$$

Acquired distances are used as parameters in calculating I_{3M} index as can be seen in equation:

$$I3M = \frac{A_1 + A_2}{L} \qquad (4)$$

where A_1 and A_2 are dimensions of apex openings, and L stands for tooth height.

3. RESULTS

Comparing results acquired from manual calculations of I_{3M} index and results acquired from calculations done automatically with described algorithm matched with precision of 99.54%. Algorithm perform the same calculations consistently, which helps eliminate human error and variability in measurements.

Fig. 4. Manual dental age assessment

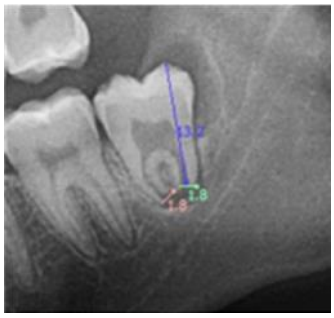

Fig. 5. Manual calculations of the third molar index

Fig. 6. Effect of changing the pixel value power

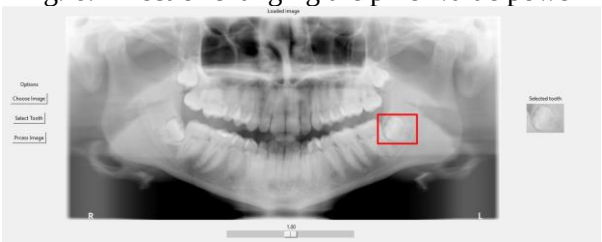

Fig. 7. Selection of the tooth of interest

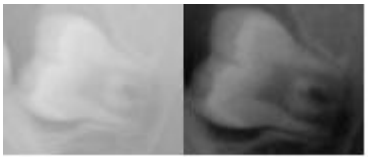

Fig. 8. Difference between not applied contrast and applied contrast

Manual measurements can be prone to inconsistencies due to factors such as human fatigue, different operators, and variations in measurement techniques.

4. DISCUSSION AND CONCLUSION

In this study, our main objective was to highlight and emphasize the importance of precision and practicality in the assessment of dental age, especially in situations where the chronological age of the individual is unknown. To achieve this goal, we decided to employ an approach that involved the integration of Cameriere's method with a customized Graphical User Interface (GUI) application. This specialized application was developed to accurately identify teeth and analyze images, thereby ensuring the reliability and accuracy of the results. To analyze the structure of the tooth, we utilized morphological operations and a specialized algorithm that was designed to detect apices. By focusing on the local minimum and maximum within the tooth root, our methodology was able to provide a comprehensive understanding of the various characteristics of the tooth. Furthermore, our calculation of distances, coupled with the subsequent application of these calculations in the I_{3M} index formula, greatly enhanced the accuracy of our assessments. As a result, our method contributed to the development of a more reliable and precise technique for estimating dental age.

To validate the effectiveness of our automated algorithm, we compared its results with manual calculations of the I_{3M} index.

This comparison revealed an extraordinary precision rate of 99.54%. This level of accuracy clearly demonstrates the efficacy of our approach in eliminating human error and reducing the variability that is often associated with manual measurements [10]. On the other hand, manual calculations are highly susceptible to inconsistencies due to various factors, such as differences among operators and variations in measurement techniques [11]. In contrast, our automated method not only ensures consistent results but also significantly minimizes the likelihood of inaccuracies that can arise from human factors. The consistency provided by our approach is particularly essential in fields like forensic dentistry, where precise age estimation is of utmost importance. By enhancing the reliability of the conclusions that can be drawn from the assessments, our method greatly enhances the overall trustworthiness and validity of the results.

Moreover, the development and successful implementation of our GUI application represent a

major advancement in terms of the practicality of dental age assessment techniques. With the help of this user-friendly tool, dentists and practitioners are now able to easily load radiographic images, accurately identify specific teeth, and interpret the results with the aid of enhanced contrast adjustments. The practicality of our method is further underscored by the fact that it seamlessly integrates into dental practice, thanks to its user-friendly interface. By combining precision and practicality in our study, we not only contribute to the advancement of the field of dental age assessment but also provide dental professionals with a valuable tool.

In conclusion, our study sheds light on the importance of precision and practicality in dental age assessment. By employing a novel approach that incorporates Cameriere's method and a customized GUI application, we were able to ensure the reliability and accuracy of our assessments. The results obtained from our automated algorithm demonstrated an impressive precision rate, highlighting the effectiveness of our approach in eliminating human error and reducing variability. Furthermore, the development and successful implementation of our user-friendly GUI application marks a significant step forward in the practicality of dental age assessment techniques. Overall, our study not only advances the field of dental age assessment but also provides dental professionals with a valuable tool that enhances the reliability and efficiency of dental age estimation.

5. REFERENCES

[1] Galic I, Vodanovic M, Cameriere R, Nakas E, Galic E, Selimovic E et al. *Accuracy of Cameriere, Haavikko, and Willems radiographic methods on age estimation on Bosnian Herzegovian children age groups 6-13*. Int J Legal Med., Vol 125, pp.315-21, 2011.

[2] Jurisic A, Galic I. *Willemsova metoda za određivanje dentalne dobi u hrvatske djece*. zir.nsk.hr., Vol. 44, pp. 6-8, 2016.

[3] Perišić T, Galic I. *Procjena punoljetnosti analizom trećih kutnjaka metodom po Demirjianu*. zir.nsk.hr., Vol. 46, pp. 1-10, 2018.

[4] Srabović A, Zukić S, Jesenković DžA, Srabović N. *Dental age estimation using the pulp/tooth ratio in lower canines in population of Bosnia and Herzegovina*, Balkan Journal of Dental Medicine, Vol. 27, pp. 78-84, 2023.

[5] Trivunov N, Petrović B, Milutinović S, Subašić M, Šipovac M, Milekić B et al. *Sex and age determination of human mandible using anthropological parameters and TCI and Kvaal methods: study of a Serbian medieval sample*. Surg. Radiol. Anat., Vol 44, pp. 1485-1494, 2022.

[6] Kilic K, Galic I. *Procjena punoljetnosti analizom donjih trećih kutnjaka metodom po Camerieru,* zir.nsk.hr., Vol, 35, pp. 6-9, 2017.

[7] Zelic K, Galic I, Nedeljkovic N, Jakovljevic A, Milosevic O, Djuric M et al. *Accuracy of Cameriere's third molar maturity index in assessing legal adulthood on Serbian population,* Forensic Science International 259, Vol. 6, pp. 1-6, 2016.

[8] Trbojevic D, Galic I. *Određivanje dentalne dobi u hrvatske djece metodom po Cameriere*, zir.nsk.hr., Vol. 42, pp. 6-8, 2016.

[9] Cameriere R, Ferrante L, Cingolani M. *Age estimation in children by measurement of open apices in teeth.* Int J Legal Med., Vol. 5, pp. 2-5, 2006.

[10] Quentin R., Futian Z., Daniel V. *Automation Accuracy Is Good, but High Controllability May Be Better*. in CHI '19: Proceedings of the 2019 CHI Conference on Human Factors in Computing Systems, May 2019, pp, 1–8.

[11] Sanjana B., Simon F., Takeshi M., Craig D. *Accuracy of an automated method of 3D soft tissue landmark detection*, European Journal of Orthodontics, Vol. 43, pp. 622-630, 2021.

Authors: **dr Luna Adamov[1], Nikol Petrović[2], Igor Putnik[2], Miroslav Đoćoš[2], Marija Vejin[2], prof. dr Bojan Petrović[1], dr Sanja Kojić[2]**

[1]University of Novi Sad, Faculty of Medicine Hajduk Veljkova 3, Novi Sad, Srbija, Tel.: +381 21 661 2222.

[2]University of Novi Sad, Faculty of Technical Sciences, Trg Dositeja Obradovica 6, 21000 Novi Sad, Serbia, Tel: +381 21 485 2350
E-mail:
luna.adamovnew@yahoo.com
nikolpetrovic@uns.ac.rs
putnik.igor@uns.ac.rs
djocos.miroslav@uns.ac.rs
vejinmarija@uns.ac.rs
sanjakojic@uns.ac.rs
bojan.petrovic@mf.uns.ac.rs

ETIKUM 2023 **INTERNATIONAL SCIENTIFIC CONFERENCE NOVI SAD, SERBIA, DECEMBER 7-9, 2023**

Bobić Z., Terek V., Kovačević L., Csik A., Čapo I., Rodič P., Drljača J., Terek P.

PRELIMINARY INVESTIGATION OF BIOCOMPATIBILITY AND CORROSION RESISTANCE OF SURGICAL STEEL COATED WITH TiAlSiN AND TiAlN/CNx COATINGS

Abstract: *Surgical steel, commonly used in orthopedic implants, is susceptible to localized corrosion in biological environment. Physical Vapor Deposition (PVD) coatings offer a dual advantage, enhancing both biocompatibility and corrosion resistance. This study delves into the biocompatibility and corrosion resistance of surgical steel, as well as surgical steel coated with nanolayer TiAlSiN and TiAlN/CNx PVD coatings. The coating growth defects has opposite effect on biocompatibility. Growth defects in PVD coatings increase the surface roughness, which lead to increase in biocompatibility. However, a higher quantity of defects correlates with reduced corrosion resistance. The results of this study indicate that the impact of increased surface roughness prevails.*

Key words: *Biocompatibility, PVD, Corrosion resistance, TiAlSiN, CNx, PVD growth defects*

1. INTRODUCTION

Surgical steel is frequently utilized in orthopedic implants, particularly for short-term applications, as it is prone to localized corrosion in long term use in biological environments [1]. The application of Physical Vapor Deposition (PVD) coatings offers the advantage of simultaneously enhancing biocompatibility [2–5] and corrosion resistance [6]. However, PVD coatings often exhibit growth defects that can modify surface roughness, potentially influencing cell adhesion [2–4]. Additionally, these defects contribute to a reduction in corrosion resistance [6]. Due to the changes in local pH values and surface potential, galvanic and crevice corrosion processes alter the cell adhesion [5,7]. Therefore, the aim of this study was to examine the combined influence of changes in surface topography and corrosion resistance on biocompatibility for various PVD coatings.

2. EXPERIMENTAL

Nanolayer TiAlSiN and dual layer TiAlN/CNx coatings were deposited on surgical steel 316L. substrates with a 20 mm diameter using the unbalanced magnetron sputtering system (CC800/9). Prior to deposition, the samples underwent polishing and cleaning, with an additional step of sputtering etching to activate the surface. In Table 1 sample denotation is given.
Electrochemical impedance spectroscopy measurements were conducted in Hank solution using the Autolab device. Employed Hank's solution composition is given in Table 2. A three-electrode electrochemical cell was utilized, applying an Ag/AgCl (KCl saturated) reference electrode and a graphite counter electrode.

Table 1. Sample denotation

Sample	Coating
316 L	/
HSN	TiAlSiN
CN_x	$TiAlN/CN_x$

Table 2. Hank's composition

Component	Concentration
NaCl	0.14 M
KCl	0.005 M
$CaCl_2$	0.001 M
$MgSO_4 \cdot H_2O$	0.0004 M
$MgCl_2 \cdot 6H_2O$	0.0005 M
$Na_2HPO_4 \cdot 2H_2O$	0.0003 M
KH_2PO_4	0.0004 M
D-glucose	0.006 M
$NaHCO_3$	0.004 M

The sample areas exposed to corrosive environments were 0.785 cm^2. All measurements were taken after a one-hour stabilization period at open circuit potential (OCP), with frequency sweeping spanning from 1×10^6 Hz to 0.01 Hz. Measurements were performed 1, 4, 6, 12 and 24 hour after exposure.

Bruker Dektak XT device was employed for 3D tactile profilometry, Measurements covered were performed on 1.5 × 1 mm areas with lateral resolutions of 0.3 µm and 2 µm in X and Y directions, respectively. Surface analysis and calculation of surface roughness parameters were performed using SPIP 6.2.0 imaging software.

Biocompatibility was investigated by observing fibroblast cells response on examined surface. Cells were cultured in DMEM medium supplemented with 10% FBS and 1% penicillin-streptomycin, maintained in an incubator at 37 ℃ with 5% CO2. Experiments were conducted using cells in the logarithmic growth phase, seeded at a density of 5x104 cells per well in a 24-well plate. At the conclusion of the 3-day treatment period, cells were washed with PBS (containing Ca/Mg). Subsequently, sufficient glutaraldehyde was added to cover the surface, and after a 20-minute incubation, paraformaldehyde was introduced. Following another 20-minute incubation, cells were thoroughly washed at least five times with PBS.

3. RESULTS

Figure 1a and 1b presents surface morphology (confocal microscopy) and 3D surface topography of evaluated samples. Results for 316L sample stands for both the steel sample and substrates used for coatings deposition. It is evident that the deposition process results in surface roughening for both coatings. The darker spots in confocal images indicate growth defects in the coating. HSN sample displays a higher number of larger defects. Surface topography measurements reveal that these defects manifest as either needle-like or nodular defects and craters. After deposition, Sa and Spk surface roughness parameters also indicate an increase in surface roughness for both coatings (Figure 2a). Notably, HSN coatings exhibit a greater material ratio in peaks, suggesting a higher prevalence of nodular defects or larger defects compared to CNx coatings.

Corrosion test results, presented in Figure 2b, demonstrate that the uncoated sample exhibits the highest impedance value, indicating superior corrosion resistance. HSN coating, while still exhibiting corrosion resistance, shows a slightly lower impedance value. Additionally, it is observed for all samples that impedance values increase over time, which is most likely associated with substrate oxidation.

In Figure 2c, representative confocal microscopy images of samples covered by fibroblast cells are displayed. It is apparent that fibroblasts cover a larger portion of the surface on both coatings compared to the uncoated stainless steel sample (316L).

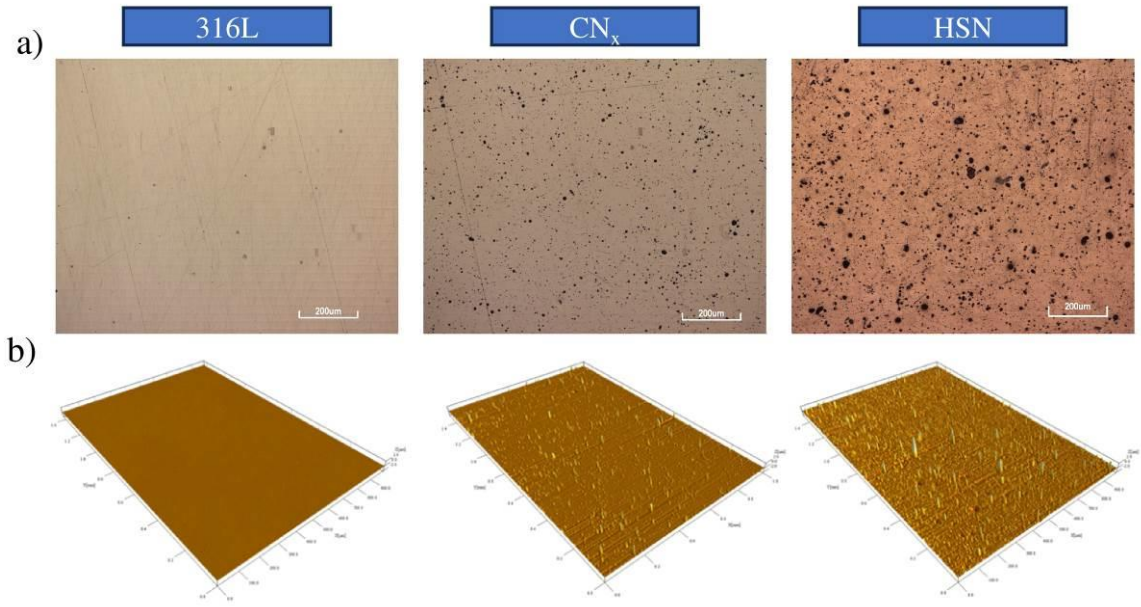

Fig. 1. a) Representative confocal microscopy images and b) 3D surface topography images

4. DISSCUSION

Considering confocal images, 3D topographic images and surface roughness parameters it is evident that the increased roughness can be attributed predominantly to nodular growth defects. These characteristic peaks, originating from the deposition process, represent a form of growth defects in PVD layers, as categorized by Panjan et. al under nodular growth defects [8].

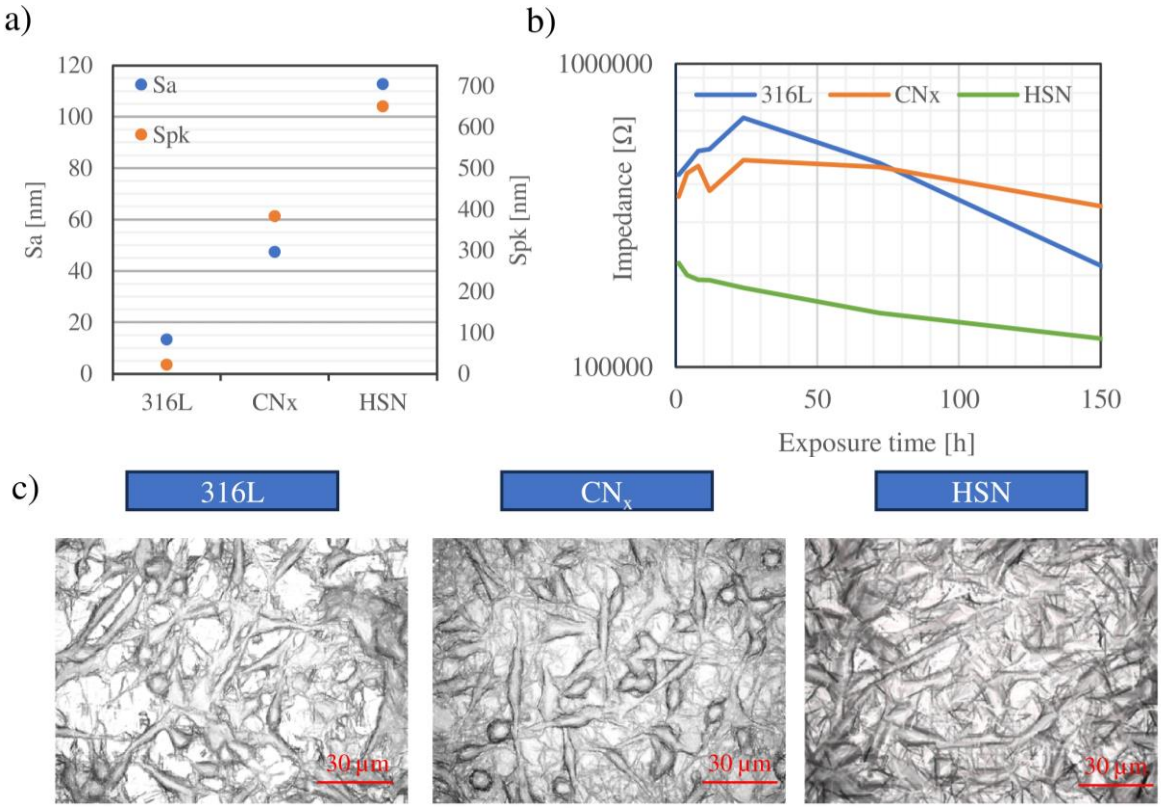

Fig. 2. a) Surface roughness parameters, b) impedance spectroscopy measurements, c) and representative images of fibroblast adhesion

The increase in the Spk parameter implies an augmentation in the overall material volume at the peaks. This increase can be attributed to a higher frequency of nodular growth defects or an increase in the size of these defects. A closer examination of confocal images revealed that the number of these defects remained consistent, suggesting that the rise in this parameter was predominantly due to generally larger nodular growth defects.

Results indicate that the uncoated sample exhibited the highest impedance value, which suggests superior corrosion resistance. These results corelate with previous investigation where it was reported that deposition of PVD coating leads to decrease in impedance of surgical steel used substrate [1,6]. This means that localized pitting corrosion of steel can be increased by deposition of PVD coatings. The cause of such behavior is penetration of liquid to coating-surface interface through coating growth defect. This results in intensify the galvanic corrosion and crevice corrosion effects [6].

The size of nodular growth defects can serve as an indicator of their potential to facilitate the passage of media to the interface [9]. In other words, an increase in the size of these defects enhances their likelihood of reaching the coating-substrate interface. Therefore, the lower impedance values for HSN sample specimen are likely to be caused by a higher number of permeable defects.

Analyzing the coverage of fibroblast cells on the surface revealed superior coverage of specimens with CNx and HSN coatings. Being a barrier between the biological environment and steel substrate, CNx and HSN-coated samples demonstrated enhanced biocompatibility. Examination of roughness parameters for these samples showed significantly higher roughness compared to 316L specimen. Hence, variations in biocompatibility, particularly in fibroblast cell coverage, can be attributed not only to the type of coating material but also to the effects of increased surface roughness [2–4]. Existing literature supports the notion that adjusting surface roughness can lead to improved protein deposition and consequently cell adhesion [3,5].

By comparing the results of corrosion tests and biocompatibility tests, contrasting trends become apparent. Specifically, the uncoated sample with surgical steel exhibited the best corrosion properties and the least coverage by fibroblast cells, whereas the opposite trend was observed for the sample with subsequently deposited HSN. These findings suggest that within the examined time interval, corrosion effects are not so intensive and do not significantly impact the results of fibroblast cell adhesion. However, there is also a

possibility that corrosion effects on defect sites cause increased fibroblast cell attachment due to altered localized pH values and surface potential [5,7]. In other words, the effect of increased roughness, caused by a higher number of larger nodular growth errors, seems to dominates the effects fibroblast cell adhesion.

5. CONCLUSIONS

In this study, we investigated the corrosion behavior and biocompatibility of 316L steel, as well as steel coated with CNx and TiAlSiN. From this study the following conclusion are drawn.

- The deposition of PVD coatings may reduce the corrosion resistance, which is primarily attributable to the presence of PVD growth defects.
- The increase of surface roughness, caused by PVD growth defects, correlates with an increase in surface area covered by fibroblasts.
- In the initial days of coating exposure to fibroblasts cells, surface roughness had a more influential effect on biocompatibility than the effects of corrosion.

6. ACKNOWLEDGEMENT

This research was founded by Serbian-Hungarian bilateral project (2021-2023) grant No.1. We would like to express our gratitude to the companies Narcissus d.o.o., Ada, and Termometal d.o.o., Ada, for their support in preparing the samples for this research.

7. REFERENCES

[1] Ali, S., Abdul Rani, A.M., Baig, Z., Ahmed, S.W., Hussain, G., Subramaniam, K., Hastuty, S., Rao, T.V.V.L.N. *Biocompatibility and Corrosion Resistance of Metallic Biomaterials*, Corros. Rev., Vol. 38, pp. 381–402, 2020.

[2] Giljean, S., Bigerelle, M., Anselme, K. *Roughness Statistical Influence on Cell Adhesion Using Profilometry and Multiscale Analysis*, Scanning, Vol. 36, pp. 2–10, 2014.

[3] Giljean, S., Bigerelle, M., Anselme, K. *Roughness Statistical Influence on Cell Adhesion Using Profilometry and Multiscale Analysis*, Scanning, Vol. 36, pp. 2–10, 2014.

[4] Barfeie, A., Wilson, J., Rees, J. *Implant Surface Characteristics and Their Effect on Osseointegration*. Br. Dent. J., Vol. 218, pp. E9–E9, 2015.

[5] Barberi, J., Spriano, S. *Titanium and Protein Adsorption: An Overview of Mechanisms and Effects of Surface Features*, Materials (Basel), Vol. 14, pp. 1590, 2021.

[6] Panjan, P., Čekada, M., Panjan, M., Kek-Merl, D.; Zupanič, F., Čurković, L., Paskvale, S. *Surface Density of Growth Defects in Different PVD Hard Coatings Prepared by Sputtering*, Vacuum, Vol. 86, pp. 794–798, 2012.

[7] Pierre R. Roberge, Ph.D., P.E. *Corrosion Engineering Principles and Practice*; Vol. 1; ISBN 0071640878, 2008.

[8] Panjan, P., Drnovšek, A., Gselman, P., Čekada, M., Panjan, M. *Review of Growth Defects in Thin Films Prepared by PVD Techniques*, MDPI AG, Vol. 10, 2020.

[9] Ling, X., Shao, J., Fan, Z. *Thermal-Mechanical Modeling of Nodular Defect Embedded within Multilayer Coatings*, J. Vac. Sci. Technol. A Vacuum, Surfaces, Film, Vol. 27, pp. 183–186, 2009.

Authors: **M.Sc. Zoran Bobić, Associate Prof. Lazar Kovačević, M.Sc. Vladimir Terek, Associate Prof. Pal Terek,** University of Novi Sad, Faculty of Technical Sciences, Trg Dositeja Obradovića 6, 21000 Novi Sad, Serbia, Phone.: +381 21 485 2330
E-mail: zoranbobic@uns.ac.rs
lazarkov@uns.ac.rs
vladimirterek@uns.ac.rs
palterek@uns.ac.rs

PhD Attila Csik, Institute for Nuclear Research, Laboratory of Materials Science, Bem tér 18/c, Debrecen, Hungary, Phone.:+36 52 509 212
E-mail: csik.attila@atomki.mta.hu

PhD Peter Rodič, Jožef Stefan Institute, Department of Physical and Organic Chemistry - F3, Jamova cesta 39, Ljubljana, Slovenia, Phone.: +386 1 477 3261
E-mail: peter.rodic@ijs.si

Associate Prof. Čapo Ivan, Drljača Jovana,, University of Novi Sad, Faculty of Medicine, Hajduk Veljkova 3, 21000 Novi Sad, Serbia.
E-mail: ivan.capo@mf.ac.rs
jovana.drljaca@uns.ac.rs

ETIKUM 2023 **INTERNATIONAL SCIENTIFIC CONFERENCE NOVI SAD, SERBIA, DECEMBER 7-9, 2023**

Đurović Koprivica, D., Jeremić Knežević. M., Maletin, A, Milekić, B., Puškar. T., Ilić Mićunović, M.

COMPUTER GUIDED DENTAL IMPLANT PLACEMENT

Abstract: *The goal of dental implant therapy is the accurate and predictable restoration of a patient's dentition. According to a computer-generated virtual treatment plan this is now a reality, transferring the virtual plan from the computer to operative treatment. To minimize implant malposition, advances in 3D digital implantology have made it possible to introduce computer-guided implant surgery (CGIS). Surgical and prosthetic phases can be virtually simulated by importing 3D data into implant planning software. The process of ideal implant planning and surgical placement is prosthetically driven, technically challenging, and requires considerable training and experience to execute well.*
Key words: *dental implants; CAD/CAM technology; dental implant placement; guided-surgery*

1. INTRODUCTION

Computer-guided implant planning and treatment workflows were developed to improve the accuracy and precision of dental implant placement while placing implants in a minimally invasive manner. Virtual engineering combined with digitization of information in dentistry has led to a new and innovative direction for dental diagnostics and treatment. In particular, computer-based implant-guided surgery has been developed to overcome the limitations associated with traditional surgical plans and has significantly improved the accuracy of implantation and enabled minimally invasive surgery [1, 2]. Placing implants in this manner reduces tissue trauma, reduces postoperative pain and swelling in patients, improves the postoperative experience, and can improve patient outcomes. Dental implants are usually placed under direct visualization of the bony bed after soft tissue elevation. Computer-guided dental implant placement uses an advanced technology to allow oral surgeons to precisely place the new teeth for patients. Fortunately, this technique offers a number of benefits for any patient who is considering the option for replacing missing teeth. Advances in computed tomography (CT) technology, which allow better visualization of bone morphology than standard two-dimensional (2D) radiographs, along with the development of planning software, have improved the predictability of implant treatment [1]. With these new approaches, implant placement can be based on computerized three-dimensional (3D) plans, making it less dependent on surgeon experience, knowledge of the prosthetic treatment plan, and the specific anatomy of a given patient.

2. BACKGROUND

Dental implant placement planning is currently based on sophisticated diagnostic imaging. The exact positioning of the fixtures is one of the more important goals of the surgical phase [1, 2, 3]. Modern surgery is based on improved diagnostic technologies that give the surgeon more precise information on patient anatomy, allowing the surgeon to interact dynamically with a 3D reconstruction and to simulate the result of the surgery to evaluate different surgical approaches before the actual surgical treatment. Then, the virtual treatment plan can be transferred to clinical practice through the use of surgical guides, which allow fixture insertion the ideal position as predetermined virtually [2, 3, 4].

Computer-guided implantation was introduced to improve diagnosis, treatment planning, and to aid surgery. The use of this technology reduces surgical time and post-operative surgical complications, including pain and swelling resulting from minimally invasive surgery .In addition, complications from the misalignment of dental implants can be significantly reduced by using computer-guided implantation, due to its greater placement accuracy in comparison with freehand placement.

3. METHODOLOGY

Since the late 1990s, cone beam computer tomography (CBCT) has become an important diagnostic tool in implant dentistry . CBCT allows dentists to visualize the three-dimensional anatomical structure, particularly of the inferior alveolar nerve, the bony defects, and the maxillary sinus before placing the dental implant. However,

placing dental implants in the correct position is usually difficult in conventional implant placement, even with prior CBCT imaging [1, 2]. One main outcome of computer-assisted surgery is the possibility of inserting implants in a more accurate manner in limited bony volumes using a precise guide and these modern techniques allow less invasive approaches like flapless surgery and simplify the prosthetic procedures involved with immediate-loading protocols [1, 2, 4].

In clinical practice, the increasing interest among clinicians in flapless procedures allowing immediate loading has led to the development of software that can use CT data to produce an elaborate, virtual 3D model for simulating the implant surgery and prosthetic phase. The computer-assisted surgery protocol involves three successive phases: the planning, the surgical phases, the prosthetic phase. The accurate planning of every step in each phase has a strong influence on the subsequent stages and therefore on the precision of the final result.

To establish an implant placement plan and create a digital implant guide, there was several steps to follow. It usually include a few very important steps. At first, patient scanning or preliminary prosthetic diagnosis which indicate the future placement of the implant in the desired position [3, 4]. After collecting the digital imaging data the next step is conversion those inputs and importation of the digital images into the special software program. Then we have everything needed for completion and finalization of virtual implant treatment planning. The most important step is integration of a virtual model of the teeth with the cone beam computed tomography model (CBCT) which can be derived from an intraoral surface scan or an extraoral scan of stone casts [3, 5]. After precise final virtual plan next step in this procedure would be the selection and fabrication of surgical guide based on the computed tomography model and, at the end, implant placement using the fabricated surgical guide [3].
In clinical practice, there are many software systems that are compatible with appropriate scanners, as well as many ways of manufacturing and using surgical guides for the placement of dental implants. As an example we are introducing the protocol utilized by other researchers in their retrospective cohort study. First, they sent preoperative CBCT data. Second, a conventional gypsum material dental cast made from polyvinyl siloxane was scanned and imported to the Dentium Digital Center (Dentium, Suwon, Korea). Third. each model was scanned using Rainbow Scanner Prime (Dentium, Suwon, Korea) and superimposed with CBCT data based on the teeth. Fourth, a computer-guided implant plan was developed, including a digital wax-up of the edentulous region and accurate 3D location of the implants (Figure 1). Based on the plan, finally, the tooth and mucosa supportive surgical guide was fabricated by using a stereolithography (SLA) 3D Printer (Dentium, Suwon, Korea) (Figure 2). The manufactured guides were assessed for preoperative fitness in the oral cavity and adjusted as needed [3].

Each protocol must contain the specified steps and every procedure must be carefully performed with the aim that the procedure of computer-guided placement of dental implants meets all the necessary criteria. Very often it is not possible to place the implants completely precisely according to the virtual fabricated guide, and need to be displaced compared with the planned position mainly due to poor bone quality and insufficient bone volume compared with the CBCT inputs.

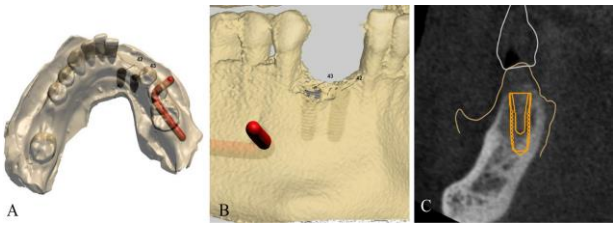

Fig. 1. Superimposing the cone beam computed tomography and the intraoral scan. a), b) Three-dimensional virtual images of the surgical site, c) Virtual implant position planning with the relation of the implant to the surrounding bone structure [3]

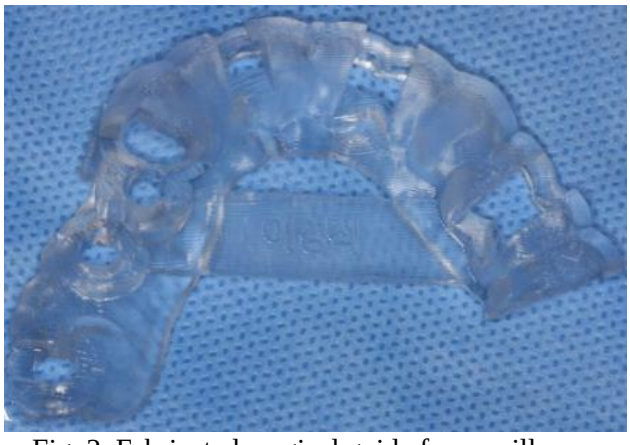

Fig. 2. Fabricated surgical guide for maxillary partial edentulism [3]

4. ADVANTAGES AND DISADVANTAGES OF CGIS

Nowadays, computer-guided placement of dental implants is widely used and more and more surgeons are deciding for virtual planning of installation and computer flow of diagnosis and treatment of edentulous and edentulous patients.

Implant therapy is and must be guided by the patients' restorative needs and dependent of the esthetic and functional demands of every particular case, although very often implant therapy can be limited by anatomic limitations. Because of that, correct and precise positioning of the implant is essential if we want to achieve an aesthetically and functionally acceptable restoration that can be maintained with proper oral hygiene. The placement of dental implants must also respect the various critical anatomical elements that are often present near the implant site dictated by the restoration [6]. Consequently, during diagnosis and individual treatment planning, the implant surgeon must pay much attention to restorative and anatomical limitations while selecting an alveolar bone space of adequate quality and quantity to provide both appropriate and safe implant placement. Implant therapy diagnosis and treatment planning during the early years of osseointegration was based on clinical examination, study casts, and radiographs (periapical and panoramic) [4, 5, 6].

4.1 Advantages

The fact that bone tissue is becoming part of the treatment plan is extensively corroborated by the concept of prosthetically-guided bone regeneration as a direct evolution of the restoration-driven implant placement. In order to insert implants in the correct prosthetically-guided position, optimal conditions of the recipient bone in terms of quality and quantity are mandatory in the first instance. At the beginning of diagnostics and treatment planning it is essential to involve all dental professionals providing complete diagnosis and treatment planning and better outcomes. Like any innovative and computer-guided procedure, this one also has its many advantages over conventional methods. Expected benefits of computer-guided surgery for dental implants with a computerized implant guide are: more efficient procedure and shorter appointment, smaller and cleaner incisions, reduced discomfort, faster recovering and healing, less risk for complications and implant failure and a lessened need for additional sinus surgeries or bone grafts.

At first, many, usually serious, potential complications of implant surgery can be minimized by guided implant surgery – such as injury of critical anatomical structures (sinus, nerves, vessels and teeth) [5, 7, 8].

CGIS also allows flapless implant placement , which reduces crestal bone resorption associated with routinely used flap elevation [7, 9]. Also, avoidance of flap elevation and sutures makes postoperative period less painfull, reduce edema, and bleeding, and enables immediate uninterrupted resumption of oral hygiene procedures [7]. So, when flap elevation and sutures are avoided, postoperative pain, edema, and bleeding are reduced, and oral hygiene practices can be resumed right away which could not be imagined in the case of flap operations using conventional methods. In contrast, even for experienced surgeons, flapless implant placement without guided implant surgery can pose considerable hazards [7, 9,10]. More important is that there are many evidence which indicate that putting an implant through the gingiva has no effect on osseointegration, bone levels, or aesthetic outcomes, as long as the soft tissue punch employed is not greater than the implant diameter [7-11]. From the aspect of the future aesthetic appearance of the implant-supported restoration, also great advantage of CGIS is much better maintenance of the soft tissue profiles such as gingival margin position and interdental papilla.

On the other hand, that is, from the aspect of better time consuming and easier and better organization in terms of keeping evidence and data availability for each individual patient, this innovative method of implant placement has undoubtedly great advantages compared to the conventional approach.

Certainly, when all the presented advantages are taken into account, it is obvious that the placement of dental implants in this way represents a great progress in dental prosthetics and surgery, but regardless of all the benefits mentioned, all the possible complications and risks that this method carries with it should clinicans have in mind. with its all disadvantages that must not be ignored. That is why the approach to patients who require the creation of implant-supported restorations should always be always very carefull and thorough .

4.2 Disadvantages

Many of the challenges that can potentialy result in implant failure can be avoided with proper planning and surgical execution that places the implant atraumatically in an ideal position.

The biggest disadvantages that can be attributed to this implant placement technique are, at first, expensive initial cost for the purchase of adequate computer hardware and software programs and special instructions and drills. Increased preoperative treatment planning time and additional cost of guide fabrication for each individual case could also be one of the disadvanages.Also, the routine and correct use of

guided implant surgery demands a change in philosophy regarding implant placement and need for training and familiarization with the software and the tools provided which is usually the main problem for surgions which are experienced in the conventional approach [7-12].

5. CONCLUSION

The process of ideal implant planning and surgical placement is prosthetically driven, technically challenging, and requires con-siderable training and experience to execute well. Computer software that facilitates virtual implant planning and placement can enhance the dental implant treatment plan. Furthermore, utilizing computer-generated surgical guides derived from such a plan can improve the predictability of achieving an optimal surgical placement.

6. AKNOWLEDGMENT

The results presented in this paper were realized as a part of the project no. 142-451-2576/2021-01/01, titled “Investigation of dentists’ exposure to microbiological agents from respiratory aerosols during dental interventions” funded by the Provincial Secretariat for Higher Education and Scientific Research, Autonomous Province of Vojvodina, Republic of Serbia.

7. REFERENCES

[1] Yafi F, Camenisch B, Al-Sabbagh M. *Is digital guided implant surgery accurate and reliable?*, Dent Clin N Am., Vol. 63, pp. 381–397, 2019.

[2] D'Haese J, Ackhurst J, Wismeijer D, De Bruyn H, Tahmaseb A. *Current state of the art of computer-guided implant surgery*, Periodontology, Vol. 73, pp. 121–133, 2017.

[3] Ku JK, Lee J, Lee HJ, Yun PY, Kim YK. *Accuracy of dental implant placement with computer-guided surgery: a retrospective cohort study*, BMC Oral Health., Vol. 16, pp.1-8, 2022.

[4] Schnitman PA, Hayashi C, Han RK. *Why guided when freehand is easier, quicker, and less costly?*, J Oral Implantol., Vol. 40, pp. 670-678, 2014.

[5] Greenstein G, Tarnow D. *The mental foramen and nerve: clinical and anatomical factors related to dental implant placement: a literature review*, J Periodontol., Vol. 77, pp. 1933-1943, 2006.

[6] Jung RE, Schneider D, Ganeles J, Wismeijer D, Zwahlen M, Hämmerle CH, Tahmaseb A. *Computer technology applications in surgical implant dentistry: a systematic review*, Int J Oral Maxillofac Implants, Vol. 24, pp. 92-109, 2009.

[7] Sindhusha BV, Rajasekar A. *A short review on guided implant surgery and its efficiency*, Bioinformation,Vol. 30. pp. 764-767, 2022.

[8] Apostolakis D, Brown JE. *The anterior loop of the inferior alveolar nerve: prevalence, measurement of its length and a recommendation for interforaminal implant installation based on cone beam CT imaging*, Clin Oral Implants Res., Vol. 23, pp. 1022-1030, 2012.

[9] Maier FM. *Initial Crestal Bone Loss After Implant Placement with Flapped or Flapless Surgery-A Prospective Cohort Study*, Int J Oral Maxillofac Implants., Vol. 31, pp. 876-883, 2016.

[10] Becker W, Wikesjö UM, Sennerby L, Qahash M, Hujoel P, Goldstein M, Turkyilmaz I. *Histologic evaluation of implants following flapless and flapped surgery: a study in canines*, J Periodontol., Vol. 77, pp. 1717-1722, 2006.

[11] Rocci A, Martignoni M, Gottlow J. *Immediate loading in the maxilla using flapless surgery, implants placed in predetermined positions, and prefabricated provisional restorations: a retrospective 3-year clinical study*, Clin Implant Dent Relat Res., Vol. 5, pp. 29-36, 2003.

[12] Mandelaris GA, Rosenfeld AL, King SD, Nevins ML. *Computer-guided implant dentistry for precise implant placement: combining specialized stereolithographically generated drilling guides and surgical implant instrumentation*, Int J Periodontics Restorative Dent., Vol. 30, pp. 275-81, 2010.

Authors:

Assoc. prof. dr Daniela Đurović Koprivica[1], Assoc. prof. Dr Milica Jeremić Knežević[1], Assoc. prof. dr Aleksandra Maletin[1], Assoc. prof. dr Bojana Milekić[1], Prof. dr Tatjana Puškar[1], Asist. prof. dr Milana Ilić Mićunović[2]

[1]University of Novi Sad, Medical faculty, Hajduk Veljkova 3, 21000 Novi Sad, Serbia, Phone: +381 21 6420 677.

[2]Faculty of Technical Sciences, Trg Dositeja Obradovica 6, 21000 Novi Sad, Serbia, Phone: +381 21 485 2350, Fax: +381 21 454-495.

E-mail: daniela.djurovic-koprivica@mf.uns.ac.rs; milica.jeremic-knezevic@mf.uns.ac.rs; aleksandra.maletin@mf.uns.ac.rs; bojana.milekic@mf.uns.ac.rs; tatjana.puskar@mf.uns.ac.rs; milanai@uns.ac.rs

ETIKUM 2023 **INTERNATIONAL SCIENTIFIC CONFERENCE NOVI SAD, SERBIA, DECEMBER 7-9, 2023**

Ilić Mićunović, M., Kuzmanović, M., Budak, I., Agarski, B., Vukelić, Đ.

ISPITIVANJE PRISUSTVA RESPIRATORNIH AEROSOLA PRILIKOM STOMATOLOŠKIH INTERVENCIJA

Rezime: *Stomatološki radnici, zbog svoje bliske interakcije sa pacijentima i radnim okruženjem koje podrazumeva prisustvo aerosola i mikročestica, izloženi su različitim respiratornim opasnostima. Ovaj rad ima za cilj istraživanje i analizu respiratornih čestica prisutnih u stomatološkim ordinacijama kako bi se identifikovale potencijalne pretnje po zdravlje. Osim identifikacije čestica, analiza će takođe obuhvatiti ispitivanje veličine ovih čestica, što će pružiti važne informacije o nivou izloženosti i stepenu prodora u organizam stomatološkog osoblja i picijenata i procenu rizika od respiratornih i drugih oboljenja.*
Ključne reči: *SEM, stomatologija, aerosol, respiratorne čestice*

1. UVOD

U stomatološkim ordinacijama i stomatološko osoblje kao i sami pacijenti su svakodnevno izloženi velikom broju zaraznih agenasa i toksičnih materija koje se prenose aerosolima i kapljičnim putem, nastale tokom stomatoloških operativnih zahvata i rutinskih stomatoloških intervencija, uz povećan rizik i od unakrsne infekcije [1].

Aerosolizovani stomatološki materijali kao suspenzije čvrstih ili tečnih čestica u vazduhu su grupa ozbiljnih štetnih agenasa u stomatološkim ordinacijama. Aerosoli su čestice dovoljno male da ostanu u vazduhu duži period pre nego što se talože na površinama sredine u kojoj su prisutne. Ove čestice mogu ostati suspendovan do 30 minuta nakon završetka procedure i lako se šire po operativnom okruženju vazdušnim strujama. Pri tom 75% od ove čestice padaju u dijametru od 1-3 m od položaja pacijenta [2]. Zbog ugroženosti samog pacijenta i stomatološkog osoblja veoma je važno ispitati prisustvo i sastav samog aerosola. Iz usne duplje pacijenta zbog prisustva tečnosti u samim procesima u velikoj meri vazduh je kontaminiran bakterijama, uglavnom aerobnim bakterijama (streptokoke i stafilokoke) i virusima [3]. Same stomatološke procedure, koje koriste različite instrumente i uređaje za obradu i skidanje materijala, kao i operativni zahvati pored prisustva bakterija i virusa emituju veliku količinu različitih čestica i po veličini i obliku.

Saznanja o kvalitetu vazduha u zatvorenom prostoru u stomatološkim klinikama iz hemijske perspektive su i dalje zastrašujuća. Pokazalo se da postupci bušenja zuba mogu da dovedu do povećanja koncentracije čestica u stomatološkoj ordinaciji, a da je koncentracija bila najveća za čestice ispod 0,5 μm [4].

Aerosoli se obično klasifikuju prema njihovom fizičkom stanju oblik i način generisanja. U ovom slučaju veličina suspendovanog čestice imaju najznačajniji uticaj na svojstva aerosola.

Iako izloženost svim česticama aerosola u vazduhu mogu nose rizike, studije se danas koncentrišu uglavnom na fine (<2,5 mm) i ultrafine čestice (<0,1 mm) kao i nanočestice. Oni mogu predstavljati rizik po ljudsko zdravlje, tim više su dovoljno mali da prodru duboko u alveolarni region pluća. Takođe, jedna od često korišćenih podela čestica u radnoj sredini je prema stepenu prodora u ljudski organizam gde se ove čestice mogu klasifikovati u inhalatorne (maseni udeo od ukupnih lebdećih čestica koje se udišu kroz nos i usta), torakalne (masena frakcija udahnutih čestica koje prodiru do grkljana) i respiratorne (masena frakcija udahnutih čestica koje prodiru u donje disajne puteve) frakcije aerosola [5].

Prisutne čestice mogu dovesti do niza zdravstvenih problema i profesionalnih bolesti, kao što su upale pluća i hronične opstrukcije plućne bolesti, povećan rizik od raka pluća, silikoze, kardiovaskularne bolesti i alergijske reakcije kod atopijskih pacijenata [6,7]. Do sada su se koristili različiti pristupi za mapiranje aerosolnih zagađivača u stomatološkom radnom okruženju, od bojenja preparata do procena kontaminacije vazduha i površine različitim česticama. Literatura pokazuje da stomatološki tretmani značajno povećavaju biološku kontaminaciju stomatoloških ordinacija i to na viši nivo nego javne površine [8].

Cilj ove studije je da se proceni kontaminacija aerosola iz respiratorne frakcije prilikom obavljanja rutinskih stomatološki tretmani i da se analizira njihovo prisustvo i veličina ovih čestica. Čestice su analizirane na skenirajućem elektronskom mikroskopu (SEM). Drugi cilj ove studije je bio da se proveri kvalitet atmosfere stomatološke klinike.

2. MATERIJALI I METODE

2.1 Uzorkovanje

Merenja aerosola izvršena su na Klinici za stomatologiju Vojvodine u Novom Sadu. Stomatološka ordinacija (slika 1a.) koja predstavlja nastavnu bazu Medicinskog fakulteta u Novom Sadu se nalazila na prvom spratu dvospratnice u ulici izdvojenoj od prometog saobraćaja.

Čestice su prikupljene prilikom rutinske stomatološke intervencije brušenja akrilatnih zuba na "fantomskoj" glavi (slika 1b.). Tokom celog period merenja sistem klimatizacije je isključen i prozori u ordinaciji su bili zatvoreni. Mikroklimatski parametri su bili normalni (temperatura 21^{o}C, strujanje vazduha nije registrovano, vlažnost vazduha 36%).

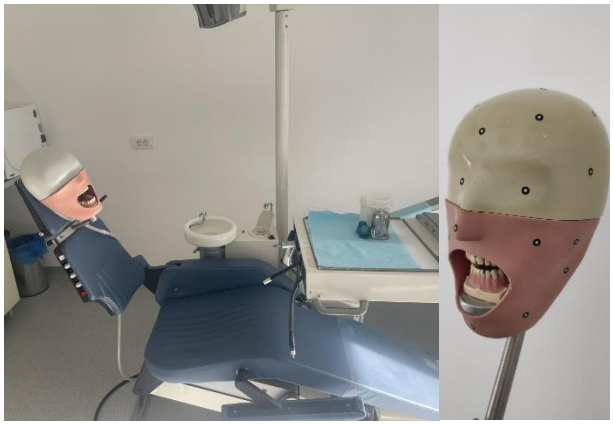

a) b)

Sl. 1. a) stomatološka ordinacija u kojoj je izvršeno uzorkovanje; b) fantomska glava

Merenja su izvršena pomoću personalnog uređaja EGO PLUS TT, koji radi na principu pumpe i predstavlja vremenski integrisanu metodu prikupljanja. Čestice se uvlače preko nastavka za respiratornu frakciju aerosola, koji je povezan sa držačem za filter i preko silikonske cevi za uređaj (slika 2.). Nastavak za prikupljanje respiratornih frakcija čestica je ciklon, koji spade u grupu centrifugalnih separatora i koje simulira respiratorni trakta prekriven bronhijama. Kvadratni filter je od mešavine celuloznih estara, prečnika 25 mm, veličine pore 0,2 μm, da bi mogao da zadrži čestice manjih promera. Personalni uređaj, tj. nastavak za prikupljanje čestica se smešta u disajnoj zoni ne dalje od 30cm od usta stomatologa (uglavnom na ključnu kost). Protok vazduha je podešen pomoću merača protoka na 1,7 l/min, po preporuci proizvođača uređaja (Zambelli), a što simulira količinu vazduha koja bi bila udahnuta od strane čoveka, pa samim time i potencijalnu količinu čestica koja bi dospela u disajne puteve stomatologa u toku određenog vremena.

Sl. 2. Peronalni uzorkivač EGO PLUS TT sa nastavkom za resiratornu frakciju

2.2 SEM analiza

Ispitivanje čestica na filter izvršeno je na skenirajućem elektronskom mikroskopu (SEM) JEOL JSM 6460 LV na Prirodno-matematičkom fakultetu u Novom Sadu, Departman za biologiju i ekologiju, Univerzitetski centar za elektronsku mikroskopiju - Novi Sad.

SEM merenje respiratornih čestica u stomatološkoj ordinaciji obično se koristi za proučavanje čestica u vazduhu koji se mogu pojaviti tokom stomatoloških postupaka ili drugih aktivnosti koje mogu generisati čestice.

Ključni aspekati kada je reč o SEM merenju respiratornih čestica u stomatološkoj ordinaciji:

1. **Identifikacija čestica**: SEM omogućava visoku rezoluciju, što je korisno za identifikaciju vrsta čestica u vazduhu, uključujući bakterije, viruse, čestice prašine, ili druge potencijalno opasne materije.
2. **Analiza veličine čestica**: SEM može pružiti informacije o veličini respiratornih čestica, što je važno jer manje čestice mogu prodirati dublje u disajne puteve i pedstavljveći rizik za zdravlje.
3. **Praćenje porekla čestica**: Identifikacija izvora čestica može pomoći u razumevanju kako i odakle dolaze čestice u stomatološkoj ordinaciji. To može biti korisno za usmeravanje mera kontrole zagađenja.
4. **Procena uticaja ventilacije i zaštitne opreme**: SEM merenje može pomoći u proceni efikasnosti ventilacijskih sistema i lične zaštitne opreme u smanjenju izloženosti respiratornim česticama.

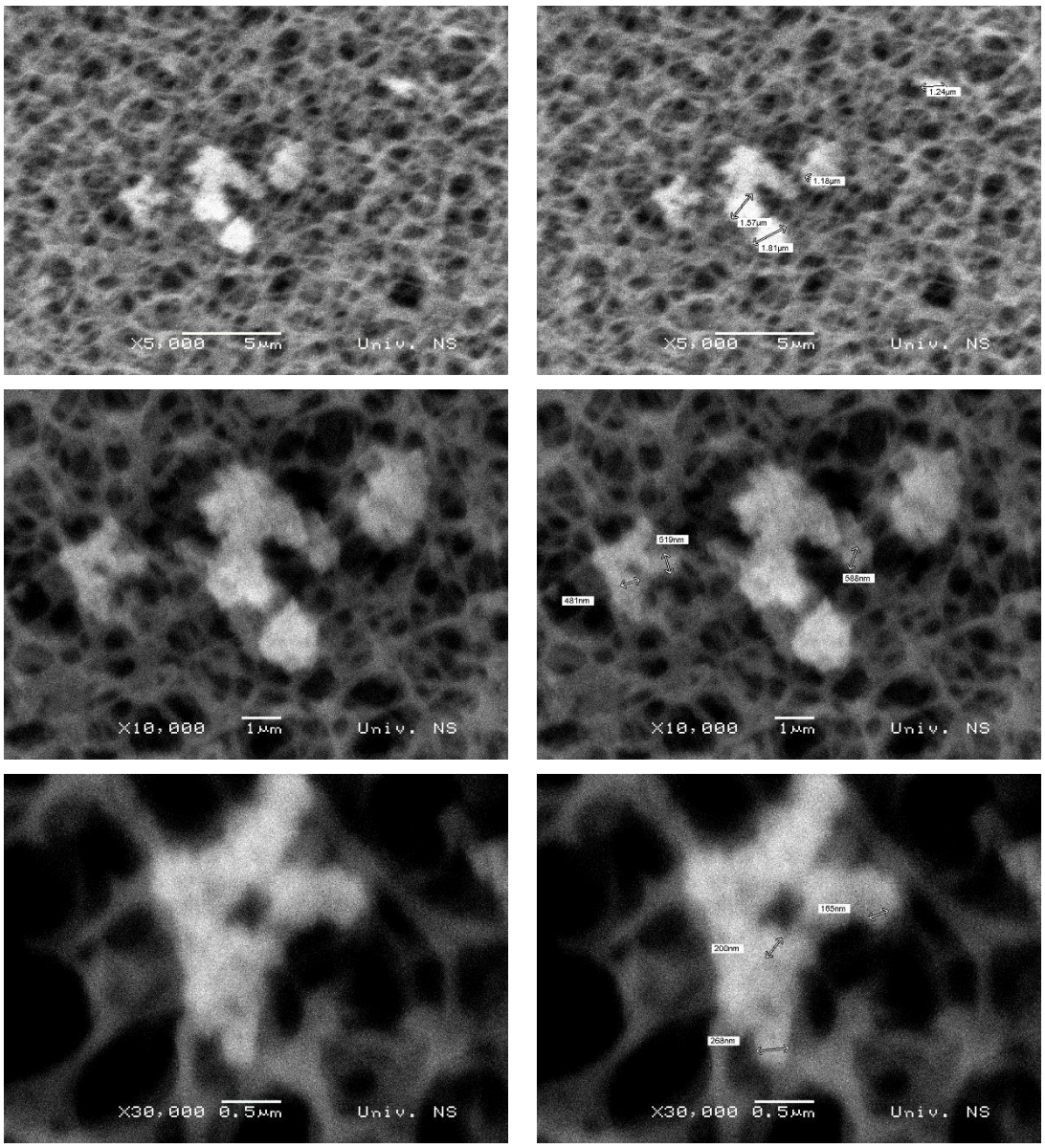

Sl. 3. SEM mikrografije

5. **Naučni i istraživački pristup**: SEM može biti koristan alat u istraživačkim studijama koje proučavaju uticaj stomatoloških postupaka na kvalitetu vazduha u stomatološkim ordinacijama.

Za potrebe ovog ispitivanje pre svega je bila potrebna identifikacija čestica i analiza veličine čestica, radi sprovođenja i definisanja ostalih aspekata. Čestice su predstavljale izazov za detektovanje zbog veličine koja je bila na granici rezolucije SEM instrumenta. Korišćeno uvećanje je bilo od 5.000 – 100.000x (slika 3.).

3. REZULTATI I DISKUSIJA

Uzorkovanje aerosola u stomatološkoj ordinaciji je trajalo 15 minuta, da bi se pre svega indetifikovalo prisustvo čestica i da se čestice ne bi preklapala, radi njihove lakše analize, kao i analize njihove veličine.

Rezultati sa skenirajućeg elektronskog mikroskopa indetifikovali su prisustvo čestica, sa ravnomernom distribucijom na filteru. Čestice su bile prisutne i na središnjem delu i na rubovima filtera. Čestice su submikronske veličine i mada su SEM mikrografije lošije rezolucije, vidno je da su u uzorku uglavnom prisutni aglomerati.

Aglomerati se formiraju međusobnim pridruživanjem čestica i stvoranjem veće strukture. Prisutnost aglomerata respiratornih čestica može biti značajna, posebno s obzirom na potencijalne rizike koje aglomerati mogu predstavljati za zdravlje radnika u stomatološkoj praksi.

S obzirom da je u pitanju aerosol nastao kao posledica procesa brušenja akrilatnih zuba, pri kojoj je prisutna i velika količina vode u samom procesu, i ovo prisustvo vode takođe može uticati na formiranje aglomerata respiratornih čestica na više načina. Voda može uticati i na razgradnju

samog akrilatnog materijala na manje čestice koje formiraju aglomerate, a može biti i medijum koji povezuju manje čestice u aglomerat. Na osnovu SEM mikrografija mogu se definisati i ivice manjih čestica prisutnih u ovim agregatima, koje spadaju u red veličina nanočestica (1-100 nm).

Vrednosti faktora kontaminacije i doze koje je udahnuo stomatolog utvrđeni su primenom uzorkovanja lične izloženosti. Dobijeni rezultati ukazuju na to da procedure sprovedene u stomatološkoj ordinaciji doprinose povećanju indeksa izloženosti i impliciraju da izloženost stomatološkog osoblja i pacijenata generisanom aerosolu može imati štetne posledice po zdravlje.

Značaj doza inhaliranih čestica aerosola može biti rezultat štetnih svojstava takvih čestica koji se odnose, između ostalog, na njihov hemijski ili biološki sastav i njihovu veličinu. Ta činjenica proizilazi i iz toga da je infektivnost čestica opterećenih virusom u korelaciji sa veličinom i da su manje čestice (<5 μm) potencijalno zaraznije nego veće. Prethodno ukazuje na neophodnost korišćenja sredstava zaštite u stomatološkim ordinacijama, s obzirom na dobijene rezultate i veličine čestica vidljive na SEM analizi.

4. ZAKLJUČCI

SEM analiza je omogućila identifikaciju i karakterizaciju respiratornih submikronskih čestica nastalih tokom procesa brušenja akrilatnih zuba. Ova metoda nam daje uvid u morfologiju i veličinu čestica na mikroskopskom nivou. Rezultati pokazuju značajnu raznolikost u morfologiji respiratornih čestica, uključujući sferične i nepravilne oblike. Takođe, primetili smo varijacije u veličini čestica unutar submikronskog spektra. SEM analiza je potvrdila formiranje aglomerata čestica tokom procesa. Ovi aglomerati često formiraju složene strukture, koje mogu dalje uticati na karakteristike aerosola.

Pokazalo se da je prisustvo vode tokom brušenja važan faktor koji utiče na karakteristike čestica. Voda može da posreduje u formiranju aglomerata i modifikuje oblik i veličinu respiratornih čestica.

Analiza ukazuje na potencijalni rizik po zdravlje radnika u stomatološkoj ordinaciji, s obzirom na prisustvo submikronskih čestica i aglomerata. Udisanje ovih čestica može predstavljati rizik za respiratorni sistem.

Na osnovu dobijenih rezultata preporučuje se primena preventivnih mera i razvoj efikasne strategije zaštite radnika, ističući važnost pridržavanja mera bezbednosti i potrebu za daljim istraživanjem za unapređenje prakse u stomatološkim ustanovama sa ciljem očuvanja zdravlja radnika.

5. ZAHVALNICA

Rezultati prezentovani u ovom radu su realizovani u okviru dugoročnog projekta „Istraživanje izloženosti stomatologa mikrobiološkim agensima iz respiratornih aerosola prilikom stomatoloških intervencija“ (br. 142-451-3157/2022-01) finansiranog od strane Pokrajinskog sekretarijata za visoko obrazovanje i naučnoistraživačku delatnost.

6. REFERENCE

[1] Polednik, B.: *Exposure of staff to aerosols and bioaerosols in a dental office*, Build. Environ., 187, pp. 1-13, 2021.

[2] Checchi, L., Montevecchi, M., Moreschi, A., Graziosi, F., Taddei, P., Violante, F.S.: *Efficacy of three face masks in preventing inhalation of airborne contaminants in dental practice*. J. Am. Dent. Assoc., 2005.

[3] Manarte-Monteiro, P., Carvalho, A., Pina, C., Oliveira, H., Manso, M.C.: *Air quality assessment during dental practice: Aerosols bacterial counts in an universitary clinic*, Rev Port Estomatol Med Dent Cir Maxilofac, 54, pp. 2-7, 2013.

[4] Sotiriou, M., Ferguson, S.F., Davey, M., Wolfson, J.M., Demokritou, P., Lawrence, J.: *Measurement of particle concentrations ina dental office*, Environ. Monit. Assess., 137, pp. 351–361, 2008.

[5] SRPS EN 1540:2015 - Vazduh na radnom mestu — Terminologija.

[6] Munoz, M.M., Soriano,Y.J., R. Roda, P., Sarrion, G.: *Cardiovascular diseases in dental practice, Practical considerations*, Med. Oral Patol. Oral Cir. Bucal., 13, pp. 296–302, 2008.

[7] Syed, M., Chopra, R., Sachdev, V.: *Allergic reactions to dental materials-A systematic review*, J. Clin. Diagn. Res. 9, 2015.¶

[8] Zemouri, C., de Soet, H., Crielaard, W., Laheij, A.: *A scoping review on bio-aerosols in healthcare and the dental environment*. PLoS One.,12, 2017.

Autori: **Doc. dr Milana Ilić Mićunović, Miloš Kuzmanović, Prof. dr Igor Budak, Vanr. prof. dr Boris Agarski, Prof. dr Đorđe Vukelić,** Univerzitet Novi Sad, Fakultet Tehničkih Nauka, Trg Dositeja Obradovica 6, 21000 Novi Sad, Serbia, Tel: +381 21 485 2350.
E-mail: milanai@uns.ac.rs
milos.kuzmanovic021@gmail.com
budaki@uns.ac.rs
agarski@uns.ac.rs
vukelic@uns.ac.rs

ETIKUM 2023

INTERNATIONAL SCIENTIFIC CONFERENCE
NOVI SAD, SERBIA, DECEMBER 7-9, 2023

Jeremic Knezevic, M., Knezevic, A., Djurovic Koprivica, D., Milekic, B., Maletin, A., Puskar, T.

MOUTH OPENER FOR MAGNETIC RESONANCE IMAGING OF THE TEMPOROMANDIBULAR JOINT

Abstract: *In order to examine TMJs in adequate positions during MR examination, an MRI compatible mouth opener is required, which allows the articular surfaces to maintain their position stably. The mouth opener device proved to be adequate in case of MRI of the TMJ for different ranges of mouth opening with the proper protocol for provoked imaging, because the incisures are located at a distance of 1mm and no objective artifacts were observed in any examination that degraded the diagnostic quality of the examination. The design of the acrylate mouth opener is precisely defined, and it has a purpose in the MRI diagnosis of TMJ disorders.*
Key words: *TMJ, MRI, mouth opener, TMD, MRI compatible.*

1. INTRODUCTION

TMJ is part of the orofacial system, which belongs to the group of condylar synovial diarthroses, which enables it to have a wide range of motion in all three planes. The basic anatomical components of the TMJ are condyle or head of the mandible, mandibular fossa, articular disc, joint capsule, joint ligaments, and lateral pterygoid muscle.

Epidemiological studies show that 50–75% of the general population have some sign of dysfunction in the orofacial system during their lifetime, and the most common reason for being referred to a physician is pain. Some authors estimate that the prevalence of TMDs is 5–12% in the general population, thus representing the second most frequent location of musculoskeletal pain (after low back pain) and a very frequent cause of absenteeism. A recent report of Valesan et al. in 2021 estimated that the prevalence of TMD was 31% for adults and 11% for children and adolescents. In the past, clinical examinations and specific protocols were the only possible way to diagnose TMDs. With the development of modern technologies, through arthrography (1944), arthrotomography (1970), and computerized tomography (CT) and MRI in 1984, new valuable knowledge was gained. Today, MRI, as an imaging method, represents the "gold standard" for establishing the position of the articular disc, the presence of synovial fluid in the TMJ, the condition of the retrodiscal tissue, and the bone marrow signal of the mandibular canal. Moreover, MRI is a non-invasive, non-ionizing, and non-contrast method for diagnosing internal disorders of the TMJ. Today, MRI is routinely used in patients with suspected or known TMDs.

Fig. 1. Magnetic resonance imaging

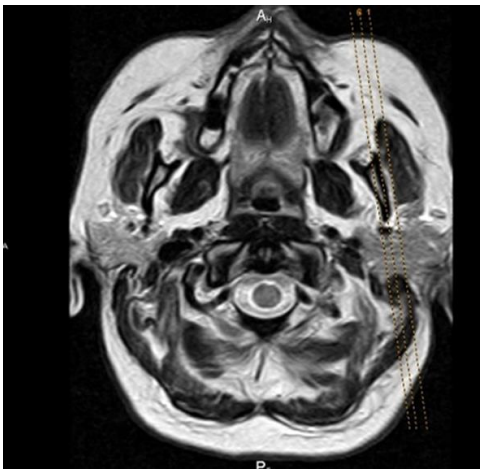

Fig. 2. The position of parasagittal sections of the TMJ following the plane of the body of the mandible.

2. MATERIAL AND METHODS

200 patients underwent MRI on a 3 T unit (Siemens Trio Tim, Erlangen, Germany), with Standard MR protocol for brain and dedicated

imaging of TMJ: proton density sequence was used, time of repetition 1850ms, time of echo 15ms, field of view 13 cm, matrix size 256 x256, and slice thickness 2 mm. The MRI was performed after clinical examination, using TMJ surface coil, with parasagittal and coronal tomograms of both condyles. All the patients were scanned with a mouth opener and, immediately after this scanning, with a syringe (20 ccm) as a standard device used for mouth opening in a clinical setting.

One experienced radiologist in head and neck imaging with over 15 years of work in the field of maxillofacial radiology and neuroradiology examined TMJs by MRI (J.B.). The second rater was dental medicine doctor, specialist of prosthodontics, with over 15 years of experience and special focus on TMDs (M.J.K.). If two raters made a different diagnosis, final diagnosis was established by consensus.

A polymeric mouth opener made of polymethyl methacrylate (PMMA) was used for dynamic imaging of the TMJ. The device is in the form of an arrow, with incisures on upper and lower surfaces (places to put incisors inside) 1 mm apart; these match possible variations in jaw opening. The thickness of the device is 2.5 mm. While inside the MRI unit, after having completed sequences performed with closed jaw, the patient placed the applicator in their mouth, according to instructions given by the radiographer.

Fig. 3. Position of the polymethyl methacrylate mouth opener in the patients' mouth during MRI examination.

The basic protocol for MRI of TMJ is comprised of the closed and maximally open jaw positions. In order to record both TMJs in the maximally open jaw position, a mouth opener is required, which enables the articular surfaces to maintain stable position during one MRI sequence (Figure 4). In a closed-mouth position, the examination was performed without the opening device.

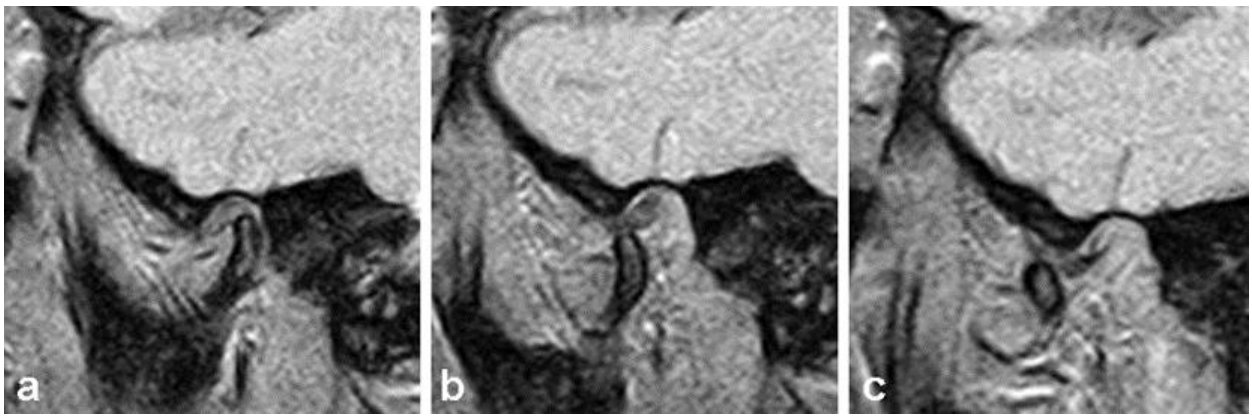

Fig. 4. Sagittal view of TMJ on MRI. (a) Closed mouth position. (b) Semi-opened mouth position, 25 m distance between upper and lower incisors. (c) Maximum mouth opening position

3. RESULTS

Patients did not report any significant discomfort during MR examination of TMJ. On the MRI, no artifacts were detected derived by the mouth opener (MR compatible) and diagnosis could be established by two independent examiners. Based on MR examination, two experienced raters separately diagnosed various levels of conditions of TMD. The largest number of TMJs were without pathological changes, 198 of them (49.5%). Anterior disc dislocation with reduction was found in 46 TMJs (11.5%),

followed by anterior disc dislocation without reduction (18 TMJs (4.5%)), posterior dislocation 4 TMJs (1), osteoarthritis (OA) in (100 TMJs (25%)). The combination of disc dislocation with reduction and OA was found in 20 TMJs (5%), disc dislocation without reduction and OA in 6 TMJs (1.5%), while the combination of posterior dislocation and OA was detected in 8 TMJs (2%).

4. DISCUSSION

The goal of designing and manufacturing an acrylate mouth opener is to obtain a standardized device for determining the condition of patients with both emergency and long-term problems of the TMJ and therefore provide the adequate treatment after MRI examination. The presented mouth opener is an original clinical device for examination of the TMJ by MRI. The results of this study show that accurate diagnoses of the TMDs without artifacts and the evaluation of the TMJ by MRI can be performed by polymethyl methacrylate mouth opener.

Our study was performed on a 3 T MRI unit. High-resolution of 3 T magnetic field strengths have better overall image quality, better visibility, and delineation of both TMJ disc and part near to the condylar neck of pterygoid muscle. Due to higher signal-to-noise ratios, 3 T MRI magnets have the advantage of depicting improved anatomic and pathologic details of the TMJ compared with 1.5 T. Our idea was to compare the quality of images using the new solution (mouth opener) and the standard device used in the clinical setting (syringe), so we decided to evaluate the images acquired on a higher field strength which is also more susceptible to the artifacts.

Many clinical and scientific centers dealing with the diagnosis of TMJ diseases, and in the absence of the above-mentioned mouth openers, use plastic syringes of a certain volume (20-cc syringe-diameter approximately 20 mm) that are placed in patients' mouths in a horizontal position during the TMJ MR examination. In this way, it is not possible to ensure a fixed position of the mandible during imaging, and it is very uncomfortable for the patient, given that the syringe has only one diameter and the position of fully opened jaw is not adequately achieved in all patients. An additional problem is that the use of a syringe allows the opening of the mouth to the same extent for each patient, that is, individualized access to the examination is lost.

The principles of all the above-mentioned mouth openers is to open and close the mouth in exactly defined steps and to provide motion-free images. When choosing the material for making this device, it should be ensured that it is compatible with the strong MR field, it should be made of materials that do not possess ferromagnetic or paramagnetic properties, so as not to endanger the patient or degrade the quality of the examination due to the presence of artifacts. For this reason, polymethyl-methacrylate is the material of choice for mouth openers used in TMJ imaging using MRI.

These materials are the most commonly used materials in some fields of dentistry, such as prosthetics and orthodontics, and they also have a well-documented history of use as biomaterials in the manufacturing of different types of dental appliances and devices. Many positive properties of PMMA, such as low density, aesthetics, cost-effectiveness, ease of manipulation, and efficient mechanical and biological features, make it a suitable and popular biomaterial for these dental applications.

The TMJ is anatomically, embryologically, and physiologically a complex structure, functionally tightly connected to the rest of the craniomandibular complex. Contemporary imaging modalities, if used properly and according to adequate clinical implications and criteria, are able to depict different pathological processes and play a crucial role in establishing the right diagnosis and monitoring therapeutic effect. The key to the right diagnosis, however, still lies in thorough familiarity with the TMJ developmental and functional anatomy, as well as with the TMJ dysfunction related to the jaws, teeth, and cranial base.

The final but not neglectable advantage of our mechanical mouth opener is low production cost.

5. CONCLUSION

The use of a specially designed mouth opener for TMJ imaging with high-field magnetic resonance imaging of 3 T and an appropriate protocol leads to an adequate assessment of the TMJ condition.

6. ACKNOWLEDGMENTS

The results presented in this paper were realized as a part of the project no.142-451-2576/2021-01/01, titled "Investigation of dentists' exposure to microbiological agents from respiratory aerosols during dental interventions" funded by the Provincial Secretariat for Higher Education and Scientific Research, Autonomous Province of Vojvodina, Republic of Serbia.

7. REFERENCES

[1] Wilkie, G.; Al-Ani, Z. *Temporomandibular joint anatomy, function and clinical relevance*. Br. Dent. J., Vol. 233, pp. 539–546, 2022.

[2] Sharma, S.; Ohrbach, R. *Definition, aetiology, and epidemiology of temporomandibular disorders. In Temporomandibular Disorders: Manual Therapy, Exercise and Needling Therapies*, 7th ed.; Fernández-de-las-Peñas, C., Mesa, J., Leon, C., Eds.; Handspring Publishing: Edinburgh, Scotland, pp. 243–255, 2018.

[3] Valesan, L.F.; Da-Cas, C.D.; Reus, J.C.; Denardin, A.C.S.; Garanhani, R.R.; Bonotto, D.; Januzzi, E.; de Souza, B.D.M. *Prevalence of temporomandibular joint disorders: A systematic review and meta-analysis*, Clin. Oral. Investig., Vol. 25, pp. 441–453, 2021.

[4] Xiong, X.; Ye, Z.; Tang, H.; Wei, Y.; Nie, L.; Wei, X.; Liu, Y.; Song, B. *MRI of Temporomandibular Joint Disorders: Recent Advances and Future Directions*, J. Magn. Reson. Imaging, Vol. 54, pp. 1039–1052, 2021.

[5] Zafar, M.S. *Prosthodontic Applications of Polymethyl Methacrylate (PMMA): An Update*, Polymers, Vol. 12, pp. 2299, 2020.

Authors: **Assoc.prof. Milica Jeremic Knezevic, Prof.dr Aleksandar Knezevic, Assoc.prof. Daniela Djurovic Koprivica, Assoc.prof. Bojana Milekic, Assoc.prof. Aleksandra Maletin, prof.dr Tatjana Puskar;**

University of Novi Sad, Faculty of Medicine Novi Sad, Hajduk Veljkova 12, 21000 Novi Sad, Serbia, Phone.: +381 21 6612222.

E-mail:
milica.jeremic-knezevic@mf.uns.ac.rs
aleksandar.knezevic@mf.uns.ac.rs
daniela.djurovic-koprivica@mf.uns.ac.rs
bojana.milekic@mf.uns.ac.rs
aleksandra.maletin@mf.uns.ac.rs
tatjana.puskar@mf.uns.ac.rs

ETIKUM 2023 **INTERNATIONAL SCIENTIFIC CONFERENCE NOVI SAD, SERBIA, DECEMBER 7-9, 2023**

Maletin, A., Đurović Koprivica, D., Jeremić Knežević, M., Milekić, B., Puškar, T., Ristić, I.

EVALUATION OF ADHESIVE BOND STRENGTH OF COMPOSITE RESIN BASED CEMENT MATERIALS-DROPLET DEBONDING TEST

Abstract: *While different approaches can be adopted in the assessment of bond strength between composite resin-based cement materials and fiber posts, push-out test remains the most dominant. However, as it involves a series of very intricate and demanding phases, and requires extensive sample preparation, there is evident need for developing a simplified testing method that could be easily applied in everyday dental practice and would yield comparable results in terms of precision and reliability. The proposed droplet debonding test method is highly useful, as it is the simplest method for testing the adhesive bond strength of composite resin-based cement materials.*
Ključne reči: *bond strength; droplet debonding test; composite resin based cement;*

1. INTRODUCTION

In order to assess the clinical performance of different adhesive materials, the bond strength is usually verified [1]. Shear bond strength [2], macro-tensile [3-5] (pull-off [6] and push-out [7-10]) and micro-tensile tests are the usual bond strength testing methods applied to dental composite resin-based materials. When aiming to ascertain the adhesion strength between dentin and a particular resin-based material, both pull-off and push-out macro-tensile tests can be applied, whereby the specimen is extracted or expelled from the apparatus, respectively. These tests are rarely used in practice, as they are protracted and require extensive and complex specimen preparation. Nonetheless, as a dynamic test, push-out test is deemed appropriate for evaluating adhesive bond strength between fiber post and resin-based dental cement materials [2. Still, the significant number of specimen preparation phases that need to be executed prior to testing render the push-out approach highly technically demanding method for evaluating dental material bond strength. Owing to the aforementioned issues, the testing procedure cannot be standardized, due to which the data reported in pertinent literature is difficult to compare, as the test results are influenced by a wide range of factors, including those noted above. Hence, there is evident need for developing a simplified testing method that could be easily applied in everyday dental practice and would yield comparable results in terms of precision and reliability.

This was the motivation behind the present study, as a part of which the authors developed and applied a modified droplet debonding test. Compared to the standard push-out test, the proposed droplet debonding test is highly simplified, as it requires fewer specimen preparation as well as test execution steps, thus reducing the potential for specimen damage, while limiting failure and error rates. Specifically, the proposed test dispenses with the need for human material preparation and storage, as well as eliminates the specimen cutting phase, thus not only simplifying the testing process, but also requiring fewer tools. Most importantly, the testing apparatus and procedure can be standardized, allowing the obtained results to be compared across materials or studies. In the droplet debonding test, the interfacial shear strength is calculated by determining the force required to debond the cement droplet from the contact area between the droplet and the fiber [11]. In their study, Liu et al. made a disc-shaped droplet using a pinhole, whereas Morlin and Czigany developed a new method for producing a cylindrical droplet [12].

In the present study, the size and shape of the resin materials deviate from those typically adopted in droplet debonding tests, as the aim was to replicate the natural tooth slice shape and thickness that were used when conducting the push-out test (1.0 mm ± 0.1 mm), as shown in Figure 1.

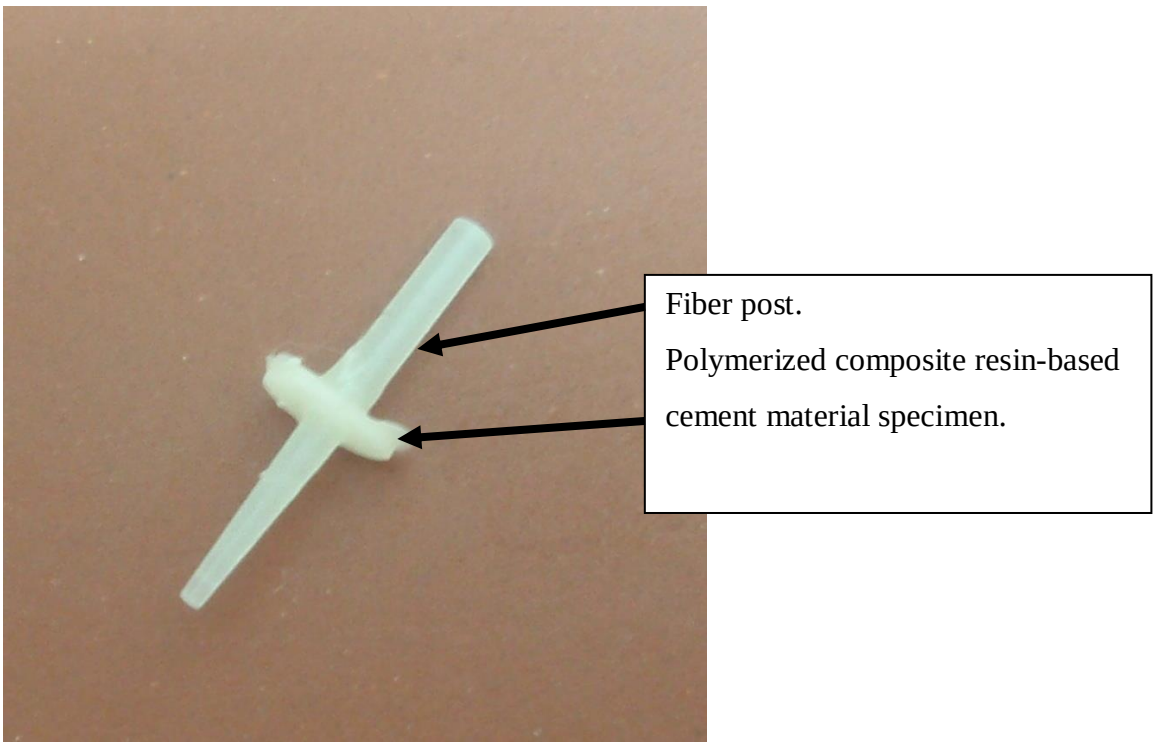

Fig. 1. Fiber post with the resin-based cement material specimen

The droplet debonding test, developed by Miller et al. in 1987, is one of the widely used single fiber-matrix interfacial bond tests in polymer material studies. It consists of applying a polymer droplet on a single reinforcing fiber and by pulling a fiber out in addition to the debonding at the fiber−matrix interface, as shown in Figure 2. [13].

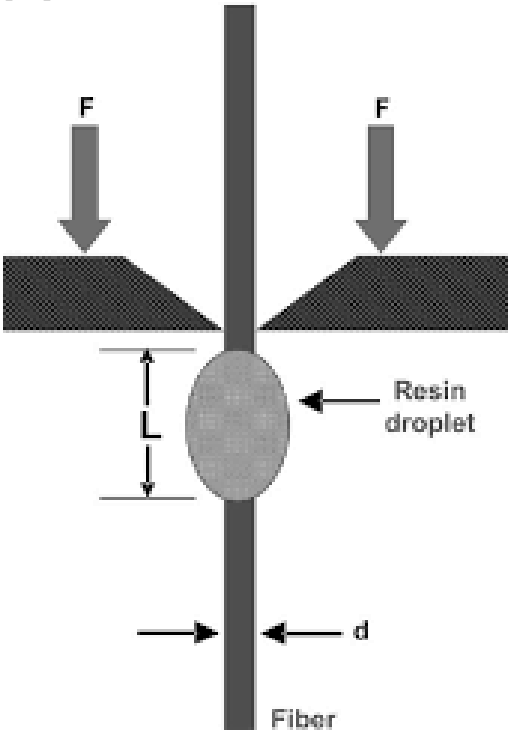

Fig. 2. Schematic representation of the basic microbond test apparatus

This method is commonly used to determine polymer adhesive bond strength [12]. However, the droplet debonding test method has not been previously applied as a method of choice in the bond strength testing of dental composite resin-based materials.

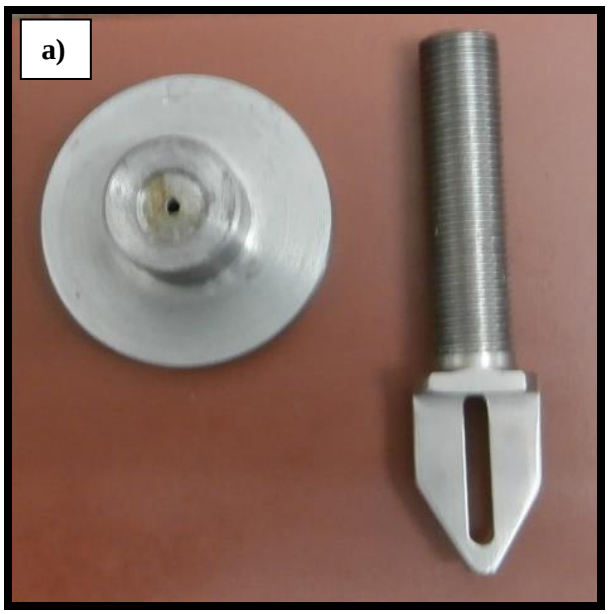

Fig. 3. Showing a) The tool specifically designed for the droplet debeonding test that is affixed to the universal testing device head in order to induce the breakage in the adhesive bond between the composite resin-based cement material being tested and the fiber post and b) breakage in the adhesive bond at the interface between the resin-based cement material and the fiber post.

During the test, the aforementioned cylindrical cone-shaped steel part was moved towards the cement material at 0.5 mm/min speed in an attempt to sever the cement−post bond. The bond strength (in MPa) was calculated according to the formula:

$$\text{Bond strength} = F/2r\pi h \qquad (1)$$

where F is the force applied to the material in N, r is the post radius in mm (with the cervical third of $2r$ = 2 mm, the middle third of $2r$ = 1.5 mm, and the apical third of $2r$ = 1 mm), π is 3.14, and h is the thickness of the resin cement segment in mm.

2. CONCLUSION

The droplet debonding test method employed in the present study was shown to be of high practical value, as it is simple to use and can yield reliable information on the adhesive bond strength of composite resin-based dental cements. It is worth noting that, unlike in the push-out test, no special sample preparation is needed prior to conducting the test, and there is no potential for damaging the specimen.

3. REFERENCES

[1] Welington L, Piva E, Fernandes A. *Bond strength of universal adhesives: A systematic review and meta-analysis.* J Dent., Vol. 43, pp. 765-776, 2015.

[2] Meerbeek BV, Peumans M, Poitevin A, Mine A, Van Ende A. Neves A. *Relationship between bond-strength tests and clinical outcomes.* Dent Mater., Vol. 26, pp. 100-121, 2010.

[3] Wu H, Hayashi M, Okamura K, Koytchev EV, Imazato S, Tanaka S, et al. *Effects of light penetration and smear layer removal on adhesion of post-cores to root canal dentin by self-etching adhesives.* Dent Mater.,. Vol. 25, pp. 1484-1492, 2009.

[4] Aksornmuang J, Nakajima M, Senawongse P, Tagami J. *Effects of C-factor and resin volume on the bonding to root canal with and without fibre post insertion.* J Dent., Vol. 39, pp. 422-429, 2011.

[5] Mortazavian S, Fatemi Ali. *Effects of fiber orientation and anisotropy on tensile strength and elastic modulus of short fiber reinforced polymer composites.* Compos B Eng., Vol 72, pp. 116-129, 2015.

[6] Heintze SD. *Crown pull-off test (crown retention test) to evaluate the bonding effectiveness of luting agents.* Dent Mat., Vol. 26, pp. 193-206, 2010.

[7] Kececi AD, Ureyen Kaya B, Adanir N. *Micro push-out bond strengths of four fibre-reinforced composite post systems and 2 luting materials.* Oral Surg Oral Med Oral Pathol Oral Radiol Endod. Vol. 105, pp. 121-128, 2008.

[8] Giachetti L, Grandini S, Calamai P, Fantini G, Scaminaci Russo D. *Translucent fiber post cementation using light- and dual-curing adhesive techniques and a self-adhesive material: Push-out test.* J Dent., Vol. 37, pp. 638-642, 2009.

[9] Juloski J, Fadda, GM, Radovic I, Chieffi N, Vulicevic ZR, Aragoneses M. *Push-out bond strength of an experimental self-adhesive resin cement.* Eur J Oral Sci., Vol. 121, pp. 50-56, 2013.

[10] De Long C, He J, Woodmansev K. *The effect of obturation technique on the psuh-out bond strength of calcium silicate sealers.* J Endodont., Vol.41, pp. 358-388, 2015.

[11] Day RJ, Cauich Rodrigez JV. *Investigation of the micromechanics of the microbond test.* Compos Sci Technol., Vol. 58, pp. 907-914, 1998.
[12] Sockalingam S, Nilakantan G. *Fiber-matrix interface characterization through the microbond test.* Int J Aeronaut Space Sci., Vol. 13, pp. 282-295, 2012.
[13] Miller B, Muri P, Rebenfeld L. *A microbond method for determination of the shear strength of a fiber/resin interface.* Compos Sci Technol., Vol. 28, pp. 17-32, 1987.

Authors: **Vanr. prof. dr Aleksandra Maletin, Vanr. prof. dr Daniela Đurović Koprivica, Vanr. prof. dr Milica Jeremić Knežević, Vanr. prof. dr Bojana Milekić, Red. prof. dr Tatjana Puškar, Vanr. prof. dr Ivan Ristić.**
Univerzitet u Novom Sada, Medicinski fakultet, Tehnološki fakultet, 21000 Novi Sad, Serbia,

E-mail:
aleksandra.maletin@mf.uns.ac.rs
daniela.djurovic-koprivica@mf.uns.ac.rs
milica.jeremic-knezevic@mf.uns.ac.rs
bojana.milekic@mf.uns.ac.rs
tatjana.puskar@mf.uns.ac.rs
ivan.ristic@uns.ac.rs

ETIKUM 2023 **INTERNATIONAL SCIENTIFIC CONFERENCE NOVI SAD, SERBIA, DECEMBER 7-9, 2023**

Milekić, B., Jeremić Knežević, M., Đurović Koprivica, D., Maletin, A., Gušić, I., Puškar, N.

PROCENA KVALITETA FUNKCIONALNE SPOSOBNOSTI MASTIKATORNOG SISTEMA ELEKTROMIOGRAFIJOM

Rezime: *Cilj ovog rada bio je da se utvrde mogućnosti procene kvaliteta fuunkcionalne sposobnosti mastikatornog sistema primenom različitih funkcijskih testova. Takav vid procene neophodan je zbog definisanja pojma funkcionalno optimalnog mastikatornog sistema i zbog određivanja granica koje ga dele od onog što smatramo oštećenjem – orofacialni sistem sa disfunkcijama. Na osnovu kliničkih procena i uzimajući u obzir posebne metodološke preporuke, elektromiografija (EMG) omogućava dobijanje validnih i pouzdanih kvantitativnih podataka o funkcionalnom stanju mastikatornih mišića.*

Ključne reči: *mastikatorni mišići, elektromiografija, primena instrumenata*

1. UVOD

Elektromiografiju (EMG) definišemo kao metod pomoću kojeg registrujemo akcione potencijale nastale u mišiću pri različitim aktivnostima, kao i stimulisane impulse iz motornih i senzitivnih nerava. Predstavlja invazivnu elektrofiziološku dijagnostičku metodu, ukoliko metod snimanja i detektovanja podrazumeva uvođenje tanke igle - elektrode u ispitivani mišić [1]. Za razliku od nje neinvazivna elektromiografska metoda se sprovodi sa površnim elektrodama, pa je i njeno izvođenje bezbolno i lako, kao i dobijanje preciznih podataka, pa samim tim u ovoj metodi leži budućnost u ovoj oblasti [2]. Mnogi ispitivači su upoređivali rezultate vrednosti dobijenih sa obe tehnike (iglenim i površnim elektrodama) i po njima nema statistički značajnih razlika u vrednostima merenim sa obe tehnike na mišićima elevatorima u položaju izometričke maksimalne kontrakcije [3].

Grafički prikaz dobijen elektromiografskom metodom naziva se elektromiogram i njegovom detaljnom analizom dobijamo uvid u osnovno stanje mišića, zatim prisustvo ili odsustvo poremećaja, kao i mogućnost prognostike za ozdravljenje i terapijsku primenu [2].

U sklopu svih funkcijskih ispitivanja orofacijalnog sistema, EMG kao metoda je našla važno mesto i primenu kako u dijagnostici tako i u terapiji poremećaja mastikatornih mišića. Područja njene primene su:

- Definisanje i merenje performansi mastikatornih mišića i kraniofacijalne morfologije;
- Metoda za detekciju jačine okluzalnih kontakata;
- Metoda u određivanju međuviličnih odnosa;
- Dijagnostika obolenja i poremećaja mastikatornih mišića;
- Praćenje funkcionalnog oporavka mastikatornih mišića i terapijskih procedura;
- Diferencijalna dijagnostika mišićnih obolenja;
- Utvrđivanje obima i težine patološkog procesa.

EMG se može koristiti kao detekciona metoda - kada se registruju akcioni potencijali nastali u mišiću spontano ili izazvani voljnom kontrakcijom ispitanika i kao stimulaciona metoda - kod koje se registruju akcioni potencijali nastali elektrostimulacijom odgovarajućih nervnih završetaka.

Specifičnost ove elektromiografske metode u okviru stomatologije je i praćenje kvaliteta funkcijskih performansi orofacijalnog sistema, tačnije mastikatorne efikasnosti u sklopu mastikacije [4]. Grafički prikaz koji se dobija u toku mastikacije naziva se elektromiomastikaciogram. On se može analizirati kvalitativno i kvantitativno.

Kvantitativna analiza obuhvata:

- ukupno vreme mastikacije (A/t) - odnos maksimalne amplitude i ukupnog trajanja mastikacije. Prosečna vrednost kod zdravih osoba iznosi 32-36s, dok je kod osoba sa CMD značajno prolongirana na 48-56s;

- broj žvačnih ciklusa između mastikacijskog mira (A/f) - je odnos amplitude i ukupnog broja žvačnih ciklusa. Kod zdravih osoba je taj odnos 42/32s a kod osoba sa CMD se broj žvačnih ciklusa povećava;

Kvalitativna analiza podrazumeva opis jednog žvačnog ciklusa (sve tri faze), sa osnovnim karakteristikama mišićnih akcionih potencijala koji su sinhronizovani:

- Oblik akcionih potencijala – broj faza koje skreću sa bazne linije. Normalni mišićni akcioni potencijali su bifazni ili trifazni i čine 80% ukupnih potencijala. Ukoliko potencijali imaju više od četiri faze zovu se polifazni i samo ih je 10%.

- Amplituda akcionog potencijala - meri se od vrha pozitivnog do dna negativnog otklona. Prosečno kod zdravih osoba iznosi oko 0,1-3mV. Ona je mera depolarizovanih mišićnih vlakana u jednoj motornoj jedinici. Ovaj raspon različitih veličina amplituda je posledica različitog broja mišićnih vlakana u jednoj motornoj jedinici.

- Trajanje akcionog potencijala - obično iznosi od 2-12ms, to je vreme potrebno da se izvrši ekscitacija ili depolarizacija svih mišićnih vlakana jedne motorne jedinice, tj. vreme od početka prvog otklona do kraja zadnjeg otklona od izoelektrične linije.

- Frekvencija - predstavlja učestalost aktivacije jedne motorne jedinice. Prosečno iznosi od 2-25Hz i određuje se u toku umerene voljne mišićne kontrakcije.

2. PRIMENA ELEKTROMIOGRAFIJE U STOMATOLOŠKOJ PROTETICI

Postoje mnogi načini za procenu kvaliteta uspešnosti protetske terapije i vrednovanje kvaliteta same protetske nadoknade. Međutim ti parametri su često nedovoljni i pretežno subjektivni. Upravo u tom domenu se EMG izdvaja zbog svoje objektivnosti, preciznosti, ponovljivosti i mogućnosti za posmatranje i ocenjivanje efekata uspešnosti protetske rehabilitacije, sa aspekta funkcijskih promena [5, 6].

Vrednosti bioelektričnih potencijala m. massetera i m. temporalisa pre i posle adaptacionog perioda u toku protetske rehabilitacije, mogu da nam ukazuju na uključivanje većeg broja motornih jedinica u mastikatornim mišićima zahvaljujući dejstvu primenjenih totalnih proteza. Može se reći da je totalna proteza imala efekat na povećanje bioelektričnih potencijala u tim mišićima. Pošto je merenje vršeno u položaju maksimalne interkuspacije, dakle u stanju izometrijske kontrakcije ovih mišića, može se shvatiti i da je to rezultat povećanja mišićne snage, zagrižajnih sila i svakako mastikatorne efikasnosti tih ispitanika [7].

Važan parametar evoluacije elektromiografskih merenja je registrovanje perioda tišine. To je kratka inhibicija aktivnosti mastikatornih mišića izazvana porastom mišićnog tonusa ili period posle mišićne kontrakcije. Trajanje ovog peroda je 8-32ms za mastikatorne mišiće. Kod ispitanika sa kraniomandibularnim disfunkcijama je ovaj period duži tako da se ova pojava koristi kao klinički preduslov definitivne dijagnostike promena u mastikatornom sistemu [8].

Prevremeni kontakti i neuravnotežena okluzija kod nosilaca totalnih proteza usloviće promenu vrednosti perioda tišine. Neurofiziološko objašnjenje za ovu pojavu je draženje Goldžijevih tetivnih receptora od kojih se impulsi prenose do nucleusa motoricusa n. trigemini u ponsu, a odatle eferentnim vlaknima do efektora mišića [9].

M. masseter ispoljava svoju maksimalnu EMNG aktivnost pri voljnom stiskanju zuba u položaju maksimalne interkuspacije . To se objašnjava time, da je to najstabilniji položaj mandibule i osnova je sklada koji je neophodan kod fiziološki optimalne okluzije [10].

Polazeći od definicije izometrijske kontrakcije, kao stanja pri kojem se mišić za vreme kontrakcije ne skrati, već samo povećava refleksnu napetost do momenta postsinaptičke inhibicije skeletnomotornih neurona, izazvanih nervnim impulsima senzitivnih završetaka Goldžijevih tetivnih receptora. Izometrijska kontrakcija mišića dovodi do povećanja njihovog tonusa (mišićne

snage ili napetosti), pa je on sposoban da se odupire različitim silama. Skraćenje ili istezanje mišića smanjuje snagu njegove kontrakcije [8].

Ukoliko mišići nemaju normalnu potporu, kao što je slučaj sa gubitkom zuba, oni vremenom podležu fizičkoj kontrakturi, čime se i smanjuje snaga njihove kontrakcije. Dakle, produženo stanje bezubosti dovodi do trajnih promena na mišićima, što je praćeno smanjenjem mastikatorne efikasnosti, gubitkom tonusa mišića i promenama u izgledu lica.

Krstić u svom radu mereći EMG metodom vrednosti bioelektrične aktavnosti mastikatornih mišića, zaključuje da ispitanici sa totalnim protezama kod kojih je vertikalna dimenzija okluzije snižena u odnosu na ispitanike sa zdravom prirodnom denticijom imaju: manje vrednosti bioelektrične aktivnosti, kraći period tišine i duži period adaptacije na proteze. Time ona ove faktore svrstava u parametre za ocenu vrednosti protetske nadoknade, kao i da vrednosti bioelektričnih aktivnosti kod osoba sa totalnim protezama, pravilno izrađenim, moraju da teže vrednostima kod osoba sa zdravom denticijom [11].

Razlozi za izvođenje EMG na m. masseteru i m. temporalisu su višestruki. Najbliže su površini kože, time i lako dostupni, glavni su elevatori donje vilice, poseduju najveći broj proprioceptora (m. temporalis 217, a m. masseter 160), kao i najveću bioelektričnu aktivnost u položaju centralne okluzije.

3. IZVOĐENJE EMG METODE

Svi rezultati merenja ovom metodologijom sprovode se po standardizovanim procedurama datim od međunarodno priznatih udruženja. Elektrode se aplikuju na kožu pacijenta u projekcionim tačkama za date mišiće koje su prethodno precizno određene šematskim profilima. Aparat je povezan sa kompjuterom i na njegovom ekranu se prate i analiziraju svi podaci merenja. Signal elektromiograma se direktno pretvara u digitalizovani, razumljiv računaru, koji softverski obrađuje sve željene podatke. Merenje se izvodi više puta zbog objektivnosti rezultata.

4. ZAKLJUČAK

Svi funkcijski testovi daju donekle odgovor na postojeće dileme oko razgraničenja funkcionalno optimalnog mastikatornog sistema, od onog što smatramo nezadovoljavajućim, odnosno postojanja smetnji i disfunkcija u okviru orofacijalnog sistema. Samo elektromiografija je najpouzdanija upravo zbog preciznosti i objektivnosti dobijenih rezultata. Na žalost, ni do danas ova metodologija nije u potpunosti prihvaćena da bi je svaki stomatolog mogao koristiti u svakodnevnoj kliničkoj praksi. Nameće se stav da bi to trebao biti jedan od ciljeva u budućnosti, njena brža, efikasnija i jednostavnija primena u svakodnevnom kliničkom radu.

5. LITERATURA

[1] Tankis, H., at all. *Standards of instrumentation of EMG. Clinical of Neurophysiology*; Vol. 131, pp. 235-236, 2020.

[2] Hugger, A., Hugger, S., Schindler, HJ. *Surface electromyography of the masticatory muscles for application in dental practice. Current evidence and future developments.* Int J Comput Dent, Vol. 11, pp. 81-106, 2008.

[3] Koole, P., Jough, HJ., Boering, G. *A comparative study of electromyograms of the masseter, temporalis and anterior digastric muscles obtained by surface and intramuscular electrodes: raw-EMG.* J Cranio Practise, Vol. 9, pp. 228-240, 1991.

[4] Woda, A., Foster, K., Mishellany, A., Peyron, MA. *Adaptation of healthy mastication to factors pertaining to the individual or the food.* Physiology and Behavior, Vol. 89, pp. 28-35, 2006.

[5] Neves, BR., Costa, RTF., at all *Muscle activity between dentate and edentulous patients rehabilitated with dental prostheses: A systematic review.* J of Oral Rehabilitation, Vol. 50, pp. 1508-1517, 2023;

[6] Ibrahim, S., Elkholy, S., Swelem, A. *Electromyography: a qualitative mesure of the degree of prosthesis retention.* Basic

Research Journal of medicine and Clinical Science, Vol. 1, pp. 25-31, 2012.

[7] Jefić, B. *Procena functionalne sposobnosti mastikatornog sistema kod osoba sa mobilnim zubnim nadoknadama*. Magistarska teza, Medicinski fakultet Novi Sad, 2003.

[8] Đurć, S. *Klinička neurofiziologija.* Niš: Prosveta, 1992.

[9] Stanišić Sinobad, D. *Zglobna veza mandibule sa kranijumom. Normalne funkcije i poremećaji.* Stomatološki fakultet, Beograd; 2001.

[10] Okeson, JP., T*emporomandibularni poremećaji i okluzija.* 5. izdanje-1. hrvatsko izdanje. Zagreb: Medicinska naklada, 2008.

[11] Krstić, M. *Elektromiografija u stomatološkoj protetici. Dostignuća u stomatološkoj protetici 2.* Zavod za udžbenike i nastavna sredstva, Beograd; 1985.

Autori: **Vanr. prof. dr Bojana Milekic, Vanr. prof. dr Milica Jeremic Knezevic, Vanr. prof. dr Daniela Djurovic Koprivica, Vanr. Prof. Dr Aleksandra Maletin, Vanr. Prof. Dr Ivana Gušić, Nataša Puškar.**

Univerzitet u Novom Sadu, Medicinski Fakultet, Hajduk Veljkova 12, 21000 Novi Sad, Serbia, Phone.: +381 21 6612222.

E-mail:

bojana.milekic@mf.uns.ac.rs
milica.jeremic-knezevic@mf.uns.ac.rs
daniela.djurovic-koprivica@mf.uns.ac.rs
aleksandra.maletin@mf.uns.ac.rs
ivana.gusic@mf.uns.ac.rs
905005d23@mf.uns.ac.rs

ETIKUM 2023 **INTERNATIONAL SCIENTIFIC CONFERENCE NOVI SAD, SERBIA, DECEMBER 7-9, 2023**

Panić, M., Movrin, D., Milutinović, M., Stefanović, Lj.

UTICAJ BRZINE EKSTRUDIRANJA FARMACEUTSKOG FILAMENTA NA TAČNOST MASE TABLETA U TEHNOLOGIJI DEPONOVANJA ISTOPLJENOG FILAMENTA

Rezime: *Primena aditivnih tehnologija ili tehnologija 3D štampe u farmaciji poprima sve veći značaj. Jedan od segmenata primene jeste izrada tableta sa tačno propisanom dozom aktivne materije, čime bi se omogućilo individualno doziranje lekova za svakog pacijenta. Deponovanje istopljenog filamenta (FDM) predstavlja najpovoljniju tehnologiju 3D štampe za izradu tableta. Pored jednostavnosti tehnologije, prednost FDM-a u odnosu na ostale aditivne tehnologije predstavlja relativno jednostavno i jeftino dobijanje filamenta punjenog aktivnom materijom. Problematika izrade tableta primenom FDM-a ogleda se u nejednakosti prečnika dobijenog filamenta koja za posledicu ima dobijanje mase tablete koja se razlikuje od propisane. U ovom radu izvršena su istraživanja odnosa brzine ekstrudiranja filamenta i mase dobijene tablete u zavisnosti od tipa korišćenog farmaceutskog filamenta. Cilj rada predstavlja dobijanje relacije zavisnosti mase izrađene tablete od brzine ekstrudiranja filamenta pomoću koje bi se jednostavnim podešavanjem štampača izrađivale tablete zadate mase i dimenzija sa tačno propisanom količinom aktivne materije.*

Ključne reči: *3D štampa, filament, deponovanje istopljenog filamenta, ekstruzija*

1. UVOD

Prvi fizički model trodimenzionalnog objekta (prototip), formiran po principu sloj po sloj primenom kompjuterski potpomognutog dizajna (CAD) izrađen je 1980-tih godina, a tehnologija izrade je nazvana brza izrada prototipova (rapid prototyping). U današnje vreme ove tehnologije se nazivaju aditivne tehnologije. Glavne prednosti ovih tehnologija su smanjenje vremena i troškova proizvodnje, minimalni gubitak materijala, mogućnost formiranja proizvoda različitih geometrijskih oblika, formiranje gotovih sklopova, nije potrebna posebna priprema uređaja i opreme, mogućnost kombinovanja više različitih materijala [1].

Poslednjih nekoliko godina, aditivne tehnologije su proširile svoju primenu i u oblasti farmacije. Najviše zastupljena tehnologija u farmaceutskoj industriji jeste tehnologija deponovanja istopljenog filamenta, odnosno FDM. Glava prednost 3D štampe u farmaceutskoj industriji ogleda se kroz mogućnost izrade lekova koji su u potpunosti prilagođeni svojstvenim potrebama pacijenta [2].

2. 3D ŠTAMPA

Trodimenzionalna štampa, poznata još kao aditivna ili slojevita proizvodnja, predstavlja savremenu i sve više zastupljenu proizvodnu tehnologiju. Pri trodimenzionalnoj štampi predmet se formira uzastopnim nanošenjem slojeva materijala. Izrada delova vođena je digitalnim informacijama iz kompjuterski podržane datoteke za projektovanje, bez potrebe za specijalnim alatima koji su karakteristični za deo koji se izrađuje na konvencionalan način [3].

Na slici 1 prikazan je redosled operacija pri formiranju proizvoda, gde ceo proces počinje od ideje, koja se prenosi u računarski program pri čemu se formira CAD model. Tako formiran model se konvertuje u STL datoteku koja je čitljiva uređaju za 3D štampu, vrši se proces štampe i na kraju procesa dobija se željeni proizvod.

Sl. 1. Redosled operacija pri formiranju proizvoda primenom 3D štampe [4]

3. DEPONOVANJE ISTOPLJENOG FILAMENTA (FDM)

Jedna od najrasprostranjenijih tehnologija aditivne proizvodnje jeste modelovanje deponovanjem istopljenog filamenta. Ova tehnologija 3D štampe zasnovana je na procesu ekstruzije polimernih materijala. Ekstruziona glava je pokretna u više pravaca i omogućava topljenje i deponovanje polimernog filamenta na

radnu ploču [5]. Proces ekstrudiranja istopljenog filamenta vrši se pomoću mlaznice prečnika koji se kreće od 0.1 do 2 mm, a najčešće je prečnika 0.4 mm [6].

3.1 Parametri FDM procesa

Da bi se obezbedile zahtevane karakteristike proizvoda, potrebno je u zavisnosti od materijala definisati različite parametre procesa. U slučaju neadekvatnog podešavanja parametara, može se javiti niz problema, kao što je odvajanje predmeta sa radne ploče ili pojava raslojavanja. Iz svega navedenog može se zaključiti značaj razumevanja parametara u cilju dobijanja željenog štampanog proizvoda [7].

Najvažniji parametri koji utiču na kvalitet proizvoda su temperature procesa (ekstruzione glave i radne ploče), brzine štampe, procenat ispune i debljina zida radnog komada [7].

Ukoliko postoji velika fluktacija u protoku filamenta kroz mlaznicu ili nedovoljna/prevelika zapremina filamenta, dolazi do značajnih odstupanja od zadate geometrije i do grešaka modela. Kako bi se eliminisali navedeni problemi potrebno je poznavati koeficijent brzine ekstruzije.

3.1.1 Koeficijent brzine ekstruzije (KE)

Koeficijent brzine ekstruzije predstavlja parametar koji definiše protok filamenta kroz glavu ekstrudera, odnosno određuje zapreminu filamenta koja ističe iz mlaznice. Preporučena vrednost koeficijenta se kreće u intervalu od 0.8 do 1.2, ali je najčešće njegova vrednost 1.0. Promena vrednosti ovog parametra se koristi pri rešavanju dva problema:

- Premala ekstruzija – mala količina materijala ističe iz mlaznice, odnosno protok je prenizak. Problem koji nastaje kao posledica ove pojave jesu male praznine koje se nalaze između linija slojeva (slika 2) i tada se vrednost koeficijenta povećava;
- Prekomerna ekstruzija – previše materijala je isteklo, odnosno protok je previsok. Kao posledica toga dolazi do pojave nakupljanja nepotrebnog materijala na gornjim slojevima modela (slika 2) i tada se vrednost koeficijenta smanjuje [8].

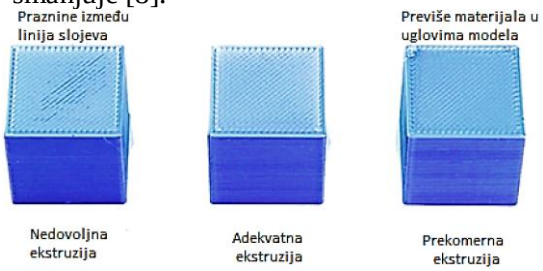

Sl. 2. Greške usled nedovoljne ili prekomerne ekstruzije [8]

4. PRIMENA FDM TEHNOLOGIJA U FARMACEUTSKOJ INDUSTRIJI

Tehnologija 3D štampanja je naročito pogodna za personalizovanu medicinu, koja zahteva fleksibilnu i efikasnu kontrolu doze leka, u zavisnosti od stanja i potreba pacijenta [9].
Trenutno, istraživanja su fokusirana na unapređenje FDM štampača, obzirom da imaju veliki potencijal da postanu glavna alternativa u proizvodnji lekova. Na tom putu glavna prepreka jeste ograničenje izbora materijala koji se mogu primenjivati u FDM štampi. Materijali koji se primenjuju jesu termoplastični polimeri i niske doze termostabilnih aktivnih farmaceutskih sastojaka (API-ja) [10].

Kompletan proces kreiranja 3D štampane formule putem FDM štampača u čiji sastav ulaze navedene komponente prikazan je na slici 3 [9].

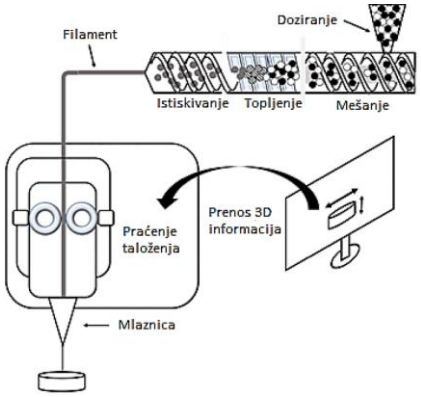

Sl. 3. Proces formiranja 3D štampane formule pomoću FDM tehnologije [9]

5. EKSPERIMENTALNA ISTRAŽIVANJA

Eksperimentalna istraživanja imala su za cilj ispitivanje uticaja koeficijenta brzine ekstruzije na masu tableta u tehnologiji deponovanja istopljenog filamenta. S obzirom da je standardna vrednost prečnika filamenta 2.85 mm, eksperiment je izveden na Ultimaker 2+ 3D štampaču, prikazanom na slici 4.

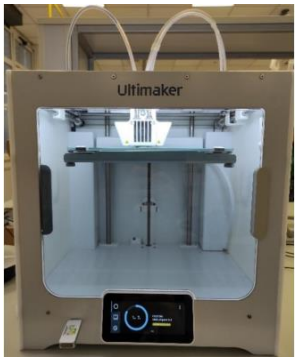

Sl. 4. Prikaz Ultimaker 2+ štampača [11]

5.1 Određivanje koeficijenta brzine ekstruzije za Ultimaker 2+ 3D štampač

U okviru eksperimenta za izradu farmaceutskih tableta korišćeni su filamenti različitih formulacija, prečnika 2.85 mm. Izrađene tablete su štampane po standardnim dimenzijama Ø5x3 mm, Ø8x2 mm i Ø12x4 mm. Različite dimenzije su uzete u obzir kako bi se utvrdila promena mase pri korigovanju koeficijenta brzine ekstruzije (KE). 3D računarski model tableta odgovarajućih dimenzija nacrtan je u SolidEdge programu, a potom konvertovan u STL datoteku. U okviru PrusaSlicer programa sprovedena su potrebna podešavanja parametara štampe, dok je g – kod eksportovan na SD karticu.

Jedan od nedostataka Ultimaker uređaja jeste tzv. Bowden drive, gde se posredstvom koračnog motora filament ubacuje sa suprotne strane PTFE creva, na oko 400 mm od zone topljenja što izaziva visoko trenje i pritiske u samom filamentu, kao i na izlaznom delu mlaznice, što naročito izaziva veliki problem pri štampi fleksibilnih filamenata.

Tokom štampe korišćeni su filamenti oznake F2 i F3 sledećih formulacija:

F2 - API (25% ibuprofen),
- plastifikator (25% manitol),
- superdezintegrator (5% kroskarmeloza – natrijum),
- fabrički filament (45% polivinilalkohol)

F3 - API (25% ibuprofen),
- plastifikator (10% manitol),
- superdezintegrator (0.5% kroskarmeloza – natrijum),
- fabrički filament (64.5% polivinilalkohol).

Na osnovu tabela 1, 2 i 3 formirani su grafički prikazi promene dužine filamenta u zavisnosti od promene koeficijenta brzine ekstruzije u slučaju tablete dimenzija Ø5x3 mm, Ø8x2 mm i Ø12x4 mm (slike 5, 6 i 7).

Tabela 1. Parametri 3D štampe tablete dimenzija Ø5 x 3 mm

Димензија таблете Ø5 x 3 mm	Коефицијент брзине екструзије	Теоријска маса [g]	Потребна дужина филамента [m]	Време штампе [min]	Стварна маса [g]
	0.8	0.127	0.013	3	0.053
	0.9	0.133	0.017	3	0.058
	1	0.143	0.017	3	0.064
	1.1	0.150	0.020	3	0.080
	1.2	0.157	0.020	3	0.081

Tabela 2. Parametri 3D štampe tablete dimenzija Ø8 x 2 mm

Димензија таблете Ø8 x 2 mm	Коефицијент брзине екструзије	Теоријска маса [g]	Потребна дужина филамента [m]	Време штампе [min]	Стварна маса [g]
	0.8	0.173	0.023	4	0.100
	0.9	0.187	0.023	4	0.103
	1	0.197	0.023	4	0.113
	1.1	0.210	0.027	4	0.123
	1.2	0.223	0.027	4	0.130

Tabela 3. Parametri 3D štampe tablete dimenzija Ø12 x 4 mm

Димензија таблете Ø8 x 2 mm	Коефицијент брзине екструзије	Теоријска маса [g]	Потребна дужина филамента [m]	Време штампе [min]	Стварна маса [g]
	0.8	1.18	0.15	9	0.962
	0.9	1.3	0.16	9	1.06
	1	1.42	0.18	9	1.094
	1.1	1.54	0.19	9	1.163
	1.2	1.66	0.21	9	1.259

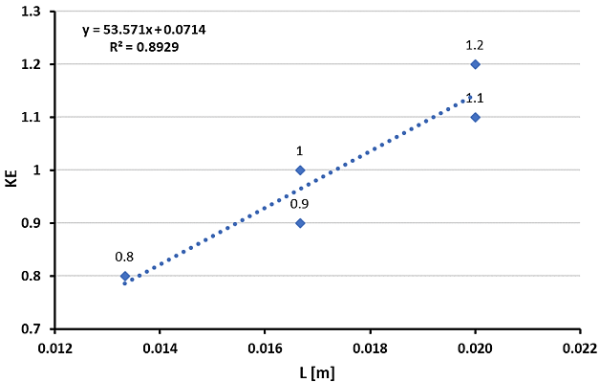

Sl. 5. Zavisnost koeficijenta ekstruzije u odnosu na dužinu filamenta za dimenziju Ø5 x 3 mm

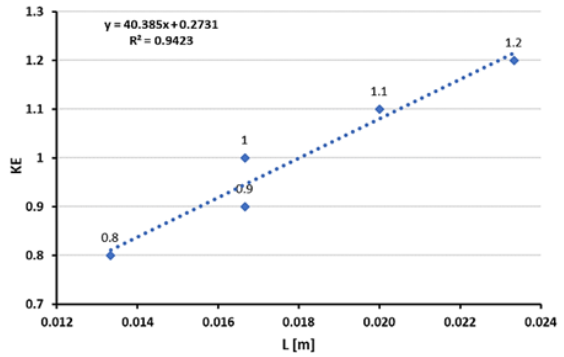

Sl. 6. Zavisnost koeficijenta ekstruzije u odnosu na dužinu filamenta za dimenziju Ø8 x 2 mm

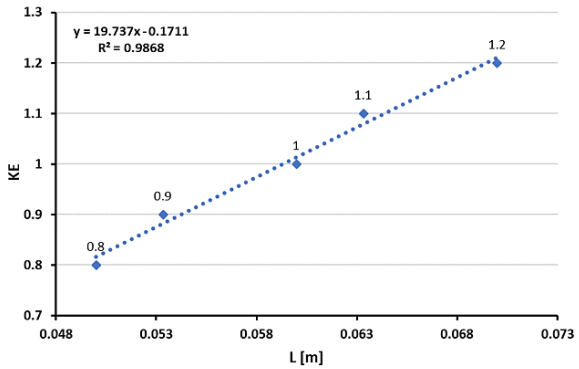

Sl. 7. Zavisnost koeficijenta ekstruzije u odnosu na dužinu filamenta za dimenziju Ø12 x 4 mm

Glavni problem eksperimenta jeste velika elastičnost farmaceutskih filamenata i bowden drive sistem štampača, usled čega nije ni dolazilo do ekstruzije ili je ekstruzija bila delimična, pa samim time i štampa neuspešna, što se može uočiti sa slike 8.

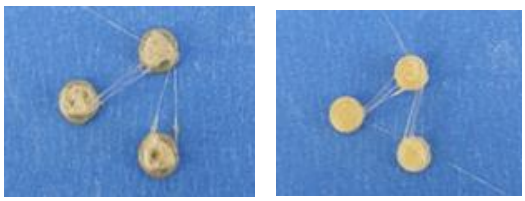

Sl. 8. Prikaz farmaceutskih tableta odštampanih filamentima F3 i F2

Jedini merljivi rezultati dobijeni su korišćenjem filamenta formulacije F2, ali kao što je prikazano u tabeli 4 razlike u zadatoj i iskorišćenoj dužini filamenta su veoma značajne.

Tabela 4.Verifikacija relacija KE i dužine filamenta

Dimenzija tablete					
5x3		8x2		12x4	
Zadata dužina	Iskorišćena dužina	Zadata dužina	Iskorišćena dužina	Zadata dužina	Iskorišćena dužina
0.065	0.035	0.022	0.011	0.15	0.05

6. ZAKLJUČAK

U radu su prikazana eksperimentalna istraživanja određivanja relacije između koeficijenta brzine ekstruzije i mase dobijenih delova, u konkretnom slučaju tableta. Cilj istraživanja je bio uspostaviti relaciju koja bi omogućila štampanje tableta tačno zadate mase. Problem izrade tableta upotrebom filamenta dobijenog ekstruzijom farmaceutskih komponenti jeste njegov neravnomerni prečnik, a samim tim i nejednaka masa po istoj dužini filamenta. Zbog toga je potrebno prvo tačno izmeriti masu filamenta, izmeriti njegovu dužinu, a zatim na osnovu dužine i utvrđene jednačine odrediti potreban koeficijent ekstruzije.

Prilikom upotrebe farmaceutskog filamenta uočena je velika elastičnost filamenta koja je uticala na krajnje rezultate zbog same konstrukcije štampača koja zahteva veliku dužinu filamenta prilikom rada. Ceo pritisak ekstrudiranja se prenosi kroz čitavu dužinu filamenta koji se usled elastičnosti sabija i stvara oscilacije pritiska na izlazu iz mlaznice. Zbog malih dimenzija, mase tableta i kratkog vremena štampe ne stvara se dovoljno veliki pritisak i finalna tableta ima nepotpuni oblik i masu preko 50% manju od zadate. Takođe, određene dužine filamenata ekstrudirane su tek oko polovine svoje dužine.

7. LITERATURA

[1] S. Ashley, *Rapid prototyping systems*, Mechanical Engineering, Vol. 113, pp. 34, 1991.

[2] Varghese R, Sood P, Salvi S, Karsiya J, Kumar D. *3D Printing in the Pharmaceutical Sector: Advances and Evidences,* Sensors International, Vol. 3, pp.100177, 2022.

[3] ASTM Committee F42 on Additive Manufacturing Technologies. http://www.astm.org/COM MITTEE/F42.htm

[4] https://voxellab.rs/3d-stampa/ (14.7.2023.)

[5] W.S.W. Harun, S. Safian, M.H. Idris, *Evaluation of ABS patterns produced from FDM for investment casting process,* WIT Trans. Eng. Sci., Vol. 64, pp. 319-328, 2009.

[6] I. Gibson, D.W. Rosen, B. Stucker, *Additive Manufacturing Technologies*, Springer Science Business Media, LLC, 2010

[7] Pietrzak K, Isreb A, Alhnan MA., *A fexible-dose dispenser for immediate and extended release 3D printed tablets*. Eur J Pharm Biopharm. Vol. 96, pp. 380–387, 2015.

[8] https://help.prusa3d.com/article/extrusion multiplier-calibration_2257 (2.10.2023).

[9] Korte C., Quodbach J. *3D-printed network structures as controlled-release drug delivery systems: dose adjustment, API release analysis and prediction*, AAPS Pharm Sci Tech., Vol. 19, pp. 3333–3342, 2018.

[10] Shaqour, B., Samaro, A., Verleije, B., Beyers, K., Vervaet, C., Cos, P. *Production of Drug Delivery Systems Using Fused Filament Fabrication: A Systematic Review,* Pharmaceutics, Vol. 12, pp. 517, 2020.

[11] Smiljić Đ., *Ispitivanje potencijala farmaceutskih materijala za primenu u tehnologiji deponovanja istopljenog filamenta*, Master rad, Fakultet tehničkih nauka, 2023.

Autori: **Sar. u nas. MSc Milica Panić, Vanr. prof. dr Dejan Movrin, Red. prof. dr Mladomir Milutinović, Ass. MSc Ljiljana Stafanović,** Univerzitet Novi Sad, Fakultet Tehničkih Nauka, Trg Dositeja Obradovica 6, 21000 Novi Sad, Serbia, Tel: +381 21 485 2334, Fax: +381 21 454-495.

E-mail: milicapanic@uns.ac.rs
movrin@uns.ac.rs
mladomil@uns.ac.rs
ljiljanastefanovic@uns.ac.rs

ETIKUM 2023 **INTERNATIONAL SCIENTIFIC CONFERENCE NOVI SAD, SERBIA, DECEMBER 7-9, 2023**

Puškar, M., Puškar, N., Jeremić Knežević, M., Đurović Koprivica, D., Maletin, A., Milekić, B.

NEAR-INFRARED LIGHT TRANSILLUMINATION FOR EARLY PROXIMAL CARIES DETECTION

Abstract: *The aim of this manuscript is to present Near Infrared Transillumination (NILT) as a method for early caries detection and to compare it with other available methods. Although the importance of management of non-cavitated lesions has been recognized, dental caries has been traditionally detected at the cavitation stage and its management has focused strongly on operative treatment. NILT can help in early caries detection, specially on the proximal surfaces. That can enable the therapist to move away from the surgical model, towards a preventive approach aiming to control the initiation of the disease process.*
Key words: *Near-infrared light transillumination, Caries detection, Proximal caries*

1. INTRODUCTION

Dental caries, otherwise known as tooth decay, is a microbial disease of the calcified tissues of the teeth, caused by the complex interaction, over time, between acids and many host factors such as teeth and saliva [1]. It is the localised destruction of susceptible hard tissues by acid by-products from bacterial fermentation of the dietary carbohydrates [1]. The disease process is initiated within the bacterial biofilm, dental plaque, that covers a tooth surface. The signs of carious demineralisation are seen on the hard dental tissues, but the very early changes in the enamel are not detected with traditional clinical and radiographic methods. The disease is initially reversible and can be halted at any stage, even when some enamel or dentine is destroyed. It is a chronic disease that progresses very slowly in most people and can be seen in both the crown and root parts of primary and permanent teeth on smooth and pitted and fissured surfaces [1]. Depending on the area of the crown in which caries is developed there can be occlusal caries, approximal, lingual and buccal caries. Approximal surfaces are not readily accessible for visual-tactile inspection and it is more difficult to make early stage diagnosis of caries disease [2].

Over a long period of time, from the beginning of the 20th century dental professionals have thought of tooth restoration as a cure for dental caries. Todays international trend in caries management is to move away from the surgical model (to excise and replace diseased tooth tissue) towards a preventive approach aiming to control the initiation of the disease process over a patient's lifetime [1]. Therefor, a major challenge for the clinician is to detect lesions at an early stage, before surgical intervention is needed.

2. CARIES DETECTION AND DIAGNOSTIC METHODS

2.1 Visual Inspection

The most commonly used caries detection, diagnostic and assessment method is the visual-tactile inspection (clinical examination) [3]. The technique is easy and it is routinely performed in clinical practice. It can be performed easily on smooth surfaces that are available for inspection like occlusal, buccal and lingual aspect of the tooth. Its use is limited on proximal sides due to its limited accessibility [4]. In posterior teeth visualisation of interproximal caries is particularly complicated by overlying tooth structure at the marginal ridge. Visual inspection has presented high specificity (proportion of sound sites correctly identified), but low sensitivity (proportion of carious sites correctly identified) and low reproducibility, because of its subjective nature [5].

The International Caries Detection and Assessment System (ICDAS) is one of the most widely used methods for visual inspection of dental caries in terms of comparability [4]. According to the ICADS criteria, detection of smooth surface caries requires visual inspection from the occlusal, buccal and lingual aspects. ICADS criteria are classified with codes from 0 to 6. Code 0 means there is no evidence of caries; 1, when viewed there is no colour changes, but after a prolonged air drying, a caries opacity (white or brown) are seen from the buccal or lingual surface; 2, caries opacity can be seen directly from

the buccal or lingual aspects and as a shadow bounded by enamel, seen through the marginal ridge; 3, when dried for 5 seconds, visible loss of enamel integrity is viewed from the buccal or lingual aspect; 4, in wet condition the lesion seems as an intrinsic shadow of discoloured dentin which appears as grey, blue and brown; 5, there is cavitation in opaque or discoloured with visible dentin; 6, there are distinct loss of tooth structure and deep cavity with visible dentin [4].

2.2 Radiography

Radiography is additional diagnostic tool for detection and diagnosis of dental caries. It is the most common additional method with its advantages and limitations [6]. The superiority of radiographic techniques over clinical examination for the detection of caries, specially interproximal caries lesions has been verified [7]. The major disadvantage is that the patient should be exposed to ionizing radiation. The restriction of x-ray exposure may comprise pregnancy, frequent follow ups in epidemiological studies or patient's antipathy. Bitewing X-ray radiograms are usually used for caries detection, but the sensitivity and accuracy have been reported as low, specially if caries is in enamel [2]. The presence and/or extent of initial caries assessed by radiographs is generally underestimated [2]. Also, it has been pointed out that there is a high risk of false positive errors and the radiographic detection and differentiation of non-cavitated caries is insufficient [8]. Achieving acceptable bitewing radiography in children and teenagers is frequently difficult and occasionally impossible [4]. In patients with fixed orthodontic appliances the detection of caries is more difficult because of overlapping images [4].

2.3. LED based devices

LED based devices have also been developed for detection of dental caries [9]. The hand piece of LED based device uses light transmitted by optical fibres to detect dental caries. The reflectance and refraction of LED that are captured by fibre optics are turned into electrical signal. When the detection is positive, the light at the tip changes to red. The speed of the audible signal is proportional to the amount of the caries detected. Although the LED- based device provides both optical and acoustic feedback, the examiners have difficulty in clearly discriminating between the midlevel and continuous beeping noise [4]. It was suggested that understanding of four different colours would be easier than three different tones [4].

2.4. Transilumination

Transilumination is one of the oldest alternative caries detection methods besides radiographs, especially for detection of approximal caries [6, 10]. Fibre optic transillumination is based on the phenomenon of light scattering to increase contrast between normal and carious enamel [11]. Sound enamel is comprised of modified hydroxyapatite crystals that are densely packed, producing an almost transparent structure. Caries causes changes in enamel structure and increases its porosity. When light passes through the changed enamel with modified optical properties increased scattering will occur [10].

Visible light, used for fibre optic transillumination (FOTI), has evolved to digital fibre optic transillumination (DIFOTI) to allow digital recording and monitoring of early enamel lesions. DIFOTI replaces human eye with CCD sensor. Those methods are very useful in treatment decision making, but they are not suitable for monitoring the caries lesions.

Near-infrared transillumination (NILT) uses longer wavelengths (λ=780 nm) than fibre-optic transillumination (DIFOTI, λ=400-700 nm) which decreases light scattering and at the same time allowing a deeper penetration of the tissues [3]. As a result there is sufficiently good contrast achieved between a caries lesion and the surrounding sound hard tissue.

3. CARIES DETECTION USING NILT

In the last decade NILT has been developed for occlusal and proximal caries detection. The DIAGNOcam device (KaVo, Biberach, Germany), using 780 nm NIR transillumination technology recently entered the marketplace. This intraoral camera has two flexible extensions: one NIR light that transilluminates the tooth and the other that captures the images from the occlusal surface of the examined tooth [4]. The set consists of camera with smaller tip for kids and bigger one for adults and KaVo integrated desktop (KID) software (DIAGNOcam software V 3.1.6). (Figure 1.)

Fig. 1. Diagnocam camera

When capturing the images care should be taken to capture each image as best centered as possible over the region of interest with as little overlap as possible for each investigated tooth. (Figure 2.)

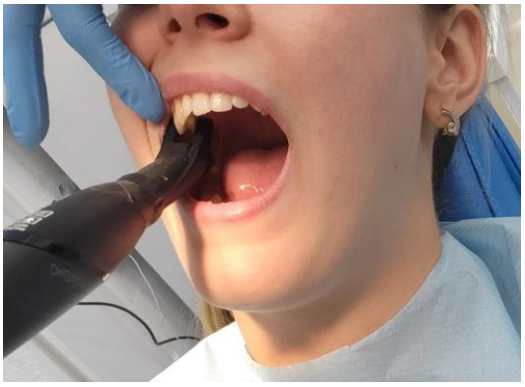

Fig. 2. Capturing images with Diagnocam camera

After capturing the images should be stored with KID software and then analysed independently from the diagnostic findings. Illustration of sound dental structure seen on Diagnocam image can be seen on Figure 3.

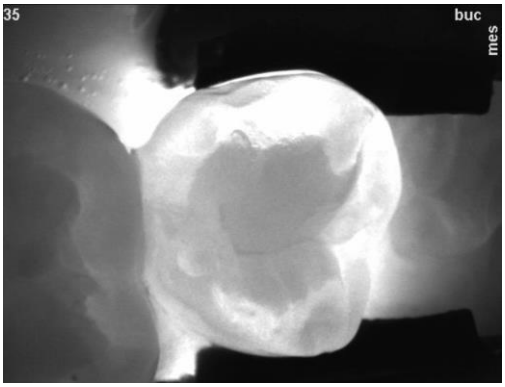

Fig. 3. Sound dental structure on Diagnocam image

Caries tissue is appearing as a dark area, (Figure 4.), while amalgam filling is presented as dark area (Figure 5.). Saliva bubbles shouldn't be misdiagnosed as caries disease. An example of saliva bubbles can be seen on Figure 6.

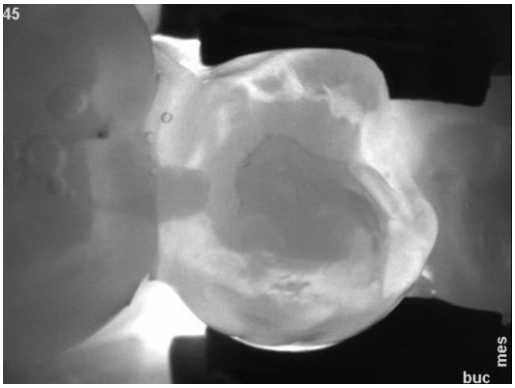

Fig. 4. Proximal region suspicious to caries on Diagnocam image

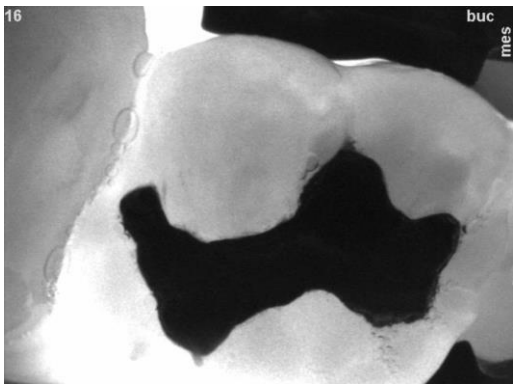

Fig. 5. Amalgam filling on Diagnocam image

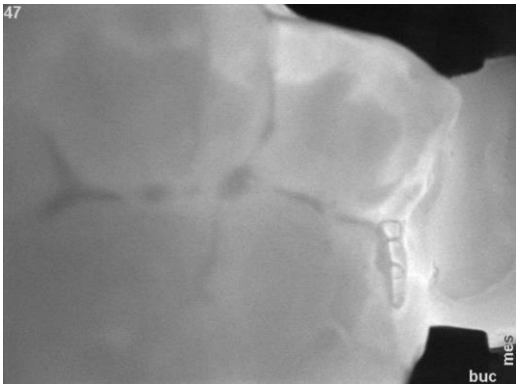

Fig. 6. Saliva bubbles in dental fissure on Diagnocam image

4. DISCUSSION

Dental status assessment and caries detection are still one of the main elements of the daily dental practice. NILT is a promising method in daily clinical practice as primary screening for detection of proximal caries, on tooth surfaces that are hard to be seen and inspected. NILT may very well serve as a reliable device to monitor primary caries lesions, without exposing the patients to unnecessary ionizing radiation, especially for the more susceptible patient groups, such as pregnant women and growing patients [3]. NILT is photo-optical method for caries detection by employing a long-wave light against the side of the tooth [12]. It uses light within the invisible spectrum, so it reduces light scattering and absorption in the solid dental enamel and penetrates objects more deeply, achieving good contrast between healthy and carious tissue [2, 12]. A considerable amount of retrospectively and prospectively designed studies on NILT reported an acceptable diagnostic accuracy compared to bite wing radiography despite different trial designs, diverging number of subjects or examined teeth and surfaces [2-4,6, 10]. There are attempts to introduce a computer aided automated methodologies for the detection and classification of caries disease [13-16]. They can improve and make more user friendly the use of NILT for caries detection in every day practice.

5. CONCLUSION

Although visual-tactile and radiographic diagnostics are still considered the gold standard methods in the caries diagnostic field NILT is valuable diagnostic tool. A visual-tactile examination, followed by NILT might be considered as first line diagnostic method and only in same cases of proximal caries detection if the diagnosis can not be achieved, radiographic method should be used.

6. REFERENCES

[1] Selwitz, R.H., Ismail A.I., Pitts N.B.: *Dental caries*, The Lancet, Vol. 369, p.p. 51-59, 2007.

[2] Ortiz, M., De Melo Alencar, C., De Paula, B.,Magno, M., Cople Maia, L., Silva, C.: *Accuracy of near-infrared transillumination (NILT) compared to bitewing radiograph for detection of interproximal caries in the permanent dentition: A systematic review and meta-analysis*, Journal of Dentistry, Vol. 98, p.p.103351, 2020.

[3] Stratigaki, E., Jost, F., Kuhnish, J., Litzenburger, F., Lussi, A., Neuhaus, K.: *Clinical validation of near-infrared light transillumination for early proximal caries detection using composite reference standard*, Journal of Dentistry, Vol. 103S, p.p.100025, 2020.

[4] Dundar, A., Ciftci, M., Isman, O., Aktan, A.: *In vivo performance of near-infrared transillumination for dentine proximal caries detection in permanent teeth*, Saudi Dental Journal, Vol. 32, p.p.187-193, 2020.

[5] Hibst, R., Paulus, R., Lussi, A.: *Detetion of occlusal caries by laser fluorecence: basic and clinical investigations*, Medical laser Application, Vol. 16, p.p. 205-213, 2001.

[6] Abdelaziz, M., Krejci, I., Perneger, T., Feilzer, A., Vazquez, L.: *Near infrared transillumination compared with radiography to detect and monitor proximal caries: A clinical retrospective study*, Journal of dentistry, Vol. 70, p.p. 40-45, 2018.

[7] Feldens, C.A., Tovo, M.F., Kramer, P.F., Feldens, E.G., Ferreira S.H., Finkler, M.: *An in vitro study of the correlation between clinical and radiographic examinations of proximal caries lesions in primary molars.* Journal of clinical pediatric dentistry, Vol. 27, 143-147, 2003.

[8] Baelum, V.: *What is an appropriate caries diagnosis?*, Acta Odontologica Scandinavica, Vol. 68, p.p. 65-79, 2010.

[9] Aktan, A.M., Cebe, M.A., Ciftci, M.E., Sirin Karaarslan, E.: *A novel LED-based device for occlusal caries detection.* Lasers in medical science, Vol. 27, p.p. 1157-1163, 2012.

[10] Fried, D., et al. *Early caries imaging and monitoring with near- infrared light,* Dentistry Clinical of North America, Vol. 49, p.p. 771-793, 2005.

[11] Gomez, J. *Detection and diagnosis of the early caries lesion,* BMC Oral health, Vol. 15, p.p. 1-7, 2015.

[12] Kuhnisch, J. et al., *In vivo validation of near-infrared light transillumination for iner-proximal dentin caries detection,* Clinical Oral Investgation, Vol. 20, p.p. 821-829, 2016.

[13] Berdouses, E.D. et al., *A computer aided automated methodology for the detection and classification of occlusal caries from photographic color images,* Computers in Biology and Medicine, Vol. 62, p.p. 119-135, 2015.

[14] Mohammad-Rahimi H. et al., *Deep learning for caries detection: A systematic review,* Journal of Dentistry, Vol. 122, p.p.1-16, 2022.

[15] Ghaedi, L., et al., *An automated dental caries detection and scoring system for optical images of tooth occlusal surface, Proceedings of the 36th Annual International Conference of the IEEE Engineering in Medicine and Biology Society*, p.p. 234-241, 2014.

[16] Kumara,C., Singhb, B.: A Comparative Study of Machine Learning Regression Approach on Dental Caries Detection, Procedia Computer Science, Vol. 215, p.p. 519–528, 2022.

Authors: **Milica Puškar, dr Nataša Puškar, Assoc. prof. Milica Jeremić Knežević, Assoc. prof. Daniela Đurović Koprivica, Assoc. prof. Aleksandra Maletin, Assoc. prof. Bojana Milekić,** University of Novi Sad, Faculty of Medicine, Hajduk Veljkova 3, 21000 Novi Sad, Serbia, Tel: +381 21 526 120

E-mail:

tatjana.puskar@mf.uns.ac.rs
905005d23@mf.uns.ac.rs
milica.jeremic-knezevic@mf.uns.ac.rs
daniela.djurovic-koprivica@mf.uns.ac.rs
aleksandra.maletin@mf.uns.ac.rs
bojana.milekic@mf.uns.ac.rs

ETIKUM 2023 **INTERNATIONAL SCIENTIFIC CONFERENCE**
NOVI SAD, SERBIA, DECEMBER 7-9, 2023

Putnik, I., Petrović, N., Adamov, L., Vejin, M., Đoćoš, M., Movrin, D., Kojić, S.

SLA PRINTED MICROFLUIDIC CHIPS: PRINTING ORIENTATION INFLUENCE ON PRINTING QUALITY

Abstract: *This paper presents the influence of microfluidic chip model orientation on printing quality within the context of SLA printing technology. SLA technology is 3D printing, which involves the production of three-dimensional objects by UV laser light polymerization of liquid material (photopolymer) layer by layer. The orientation of the model on the build plate can significantly affect the outcome, potentially distinguishing between a successful print and a failed one. Incorrect positioning during printing may lead to object malfunctions. To quantify these effects, all chip dimensions were measured using 3D microscopic imagery and specialized measurement software.*
Key words: *SLA, 3D Printing, Microfluidics*

1. INTRODUCTION

Microfluidics is an innovative interdisciplinary field, focusing on precise control of small fluid volumes, often at the microliter scale, within microscale channels and chambers. It plays a vital role in numerous scientific and engineering domains, transforming applications in medical diagnostics, drug delivery, chemical synthesis, and environmental monitoring. By merging physics, chemistry, and engineering principles, microfluidics enables efficient fluid manipulation for complex tasks on a miniature scale. These systems offer benefits like reduced reagent usage, faster analysis, and the development of portable and point-of-care devices, driving scientific and technological advancements.

Microfluidic chips come in diverse shapes and dimensions, often featuring intricate designs. This is why 3D printing is increasingly popular in this field.

The emergence of 3D printing technology has brought about a revolution in various industries, including the fabrication of microfluidic chips. Microfluidic chips are essential components in fields such as biotechnology, chemistry, and medical diagnostics, as they enable precise control and manipulation of small volumes of fluid. Microfluidic chips have potential applications in the field of medicine. They can be used to create in vitro models of the blood-brain barrier to assess drug efficacy and toxicity for central nervous system diseases [1,2].

The achievement of optimal performance and accuracy in these chips relies on the flawless fabrication of intricate channels and structures. Therefore, it is of utmost importance to understand and optimize the orientation of the microfluidic chip model during the SLA printing process [3,4,5]. The effects of different orientations of the microfluidic chip model during the SLA printing process on the resulting performance and accuracy have been studied. It was found that vertical 3D-printing is superior to the horizontal printing approach in terms of both dimensional fidelity and shape conformity. The base wall roughness was approximately the resolution of current 3D-printers, and a spatial periodicity was found along the channel length. These findings suggest that the orientation of the microfluidic chip model during SLA printing can significantly impact its performance and accuracy.

This paper explores SLA printing technology for microfluidic chip fabrication, focusing on optimizing model orientation during printing. Proper orientation is critical in 3D printing, as it affects print accuracy and final product functionality. In SLA printing, distortions can occur in large rectilinear plots. Therefore, optimizing the microfluidic chip model's orientation is crucial for desired performance and accuracy. This study delves into the intricacies of orientation optimization in SLA-based microfluidic chip fabrication, highlighting the interplay between orientation, stability, surface finish, and printability.

2. METHODS

The microfluidic mixer, which is based on serpentine patterns, has been implemented utilizing SLA (Stereolithography) printing. The active (middle layer) is printed in SLA while for carrier and top coverage a PMMA layer was used. This microfluidic mixer active layer consists of two inlets designed for the combination of two

liquids. At the conclusion of the extended serpentine mixer, an outlet has been installed.

The investigation made use of the Huvitz Bioimager microscope, which had magnification capabilities of 25x and 50x, in order to obtain highly detailed images. These images were then subjected to rigorous analysis and processing through the utilization of Panasis software, a tool renowned for its ability to manipulate and measure obtained images. Within the Panasis software platform, we employed 3D profiling techniques for 3D optimal profile and all-in-focus 2D imaging. By employing this comprehensive methodology, we were able to thoroughly examine the fabricated microfluidic chips from various perspectives and depths, thereby ensuring a nuanced evaluation of the optimal printing orientations for microfluidic chip production. The measurements taken during this process included the design depth (D), which was averaged across the entire structure. Additionally, we considered the width between the highest points in the channel (CW), and the width of the deepest part (CUW) to assess the useful section of the channel. Measurements were also taken for the serpentine width and serpentine useful width (SW and SUW) and the connection points from the channel to the I/O ports, both at the highest and lowest points (I/O CW and I/O CW, respectively). Furthermore, we analyzed the depth within the serpentine (SD) and the deviation from that depth (SD dev). Finally, the pouring angle (□) was a crucial part of our analysis. The pouring angle refers to the angle at which the material descends from the highest to the deepest part of the channel, and applies to both serpentines and channel confluence. These parameters are drafted in Fig. 1.

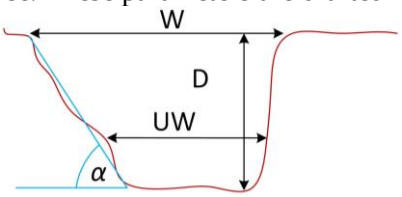

Fig. 1. Measurements labels

These numerical values are presented in Table 1, in which it is evident that the print quality was assessed across seven different prints in relation to nine metric variables.

In order to ensure a comprehensive and representative analysis of the printed structures, each microfluidic chip was meticulously imaged in 12 different locations. Furthermore, the utilization of 3D profiling techniques provided a holistic view of the microfluidic chips, capturing not only their surface characteristics but also their internal structures. This in-depth analysis was instrumental in the identification of any inconsistencies or defects within the printed microfluidic devices. The integration of advanced imaging technology, sophisticated software analysis, and comprehensive measurements allowed for a robust exploration of the optimal orientations for SLA 3D printing of microfluidic chips. This meticulous methodology served as the fundamental basis for our findings, offering valuable insights into the intricate relationship between printing orientations and the quality of microfluidic chip fabrication. The detailed outcomes of these analyses will be discussed in the subsequent section, shedding light on the key factors that influence the optimal orientation of microfluidic chip models in SLA 3D printing.

3. RESULTS

In the scope of our investigation, we conducted an analysis of four orientations and support presence variations that were employed during the printing of microfluidic chips.

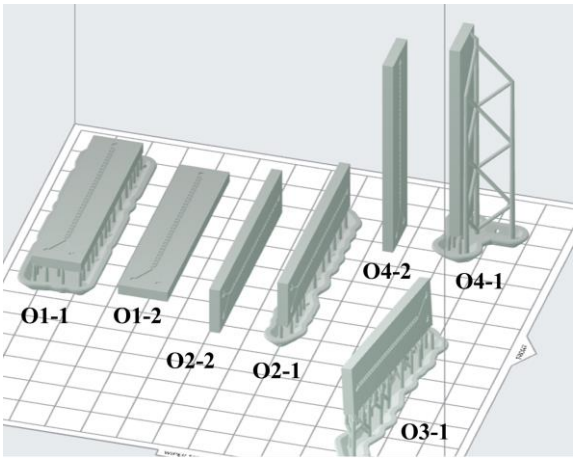

Fig. 2. Tested orientations of a microfluidic chip functional layer

On the Fig. 2. all four examined orientations and support variations are presented and labeled. Three of them are manually determined (according to experience) and positioned on the printing table (O1, O2 and O4) while the fourth (O3) is the software PreForm suggested optimal orientation. Every (but software suggestion) orientation of the part is analyzed for two variations, printed with (marked with Ox-1) and without (marked with Ox-2) supporting structures to examine if they make a difference in microfluidic channel print quality.

The findings that have been presented in Table 1 provide a clear and unambiguous indication of the presence of significant differences among the various orientations that were examined.

Table 1. Measured dimensions (in □m)

	O1-1	O1-2	O2-1	O2-2	O3-1	O4-1	O4-2
D	326,75	328,22	216,83	201,75	202,13	257,55	245,27
CW	465,79	412,27	489,57	457,81	483,55	503,39	477,93
CUW	187,07	187,23	186,48	312,90	251,88	281,09	303,69
SW	629,32	339,08	529,02	469,34	477,15	498,31	502,90
SUW	372,51	227,96	166,50	234,38	288,65	78,74	335,89
I/O CW	485,95	519,08	539,26	521,88	555,13	46,84	493,77
I/O CUW	242,25	299,75	284,78	392,72	294,84	375,56	396,44
SD	272,09	251,32	154,26	155,73	133,58	112,76	147,69
SD deviation	9,42	19,12	6,13	1,91	0,99	35,50	82,21
□	74,35	70,33	35,24	52,58	67,87	64,78	69,53

Among all the orientations that were considered, it was found that O1-1 emerged as the most favorable choice for the printing of microfluidic chips Fig. 3 b, c and e. This conclusion was drawn based on the observation of a highest level of quality and accuracy in the chips that were produced using this particular configuration compared to other orientations. The superiority of O1-1 can be attributed to its ability to more closely match the dimensions provided in the original 3D model of the microfluidic chip since □ is closest to 90° and D is near projected 400 □m. The only parameter that is not satisfactory in O1-1 is CUW which should be larger. This can be obtained by widening the channel in the design. The same could be done with O1-2 and O2-1, but since the other parameters (such as SUW, SD, and □) are not satisfactory the superior orientation remains O1-1. Conversely, it was discovered that O3-1, which was recommended by the computer model, proved to be not nearly the best choice among the orientations that were examined. The chips that were manufactured using this orientation exhibited a low level of quality due to the deviation of the design measurements which lead to the constriction of serpentines, channels and confluences. Furthermore, this particular orientation not only demonstrated a lower level of efficiency in terms of production but also resulted in frequent damage to the products during the printing process.

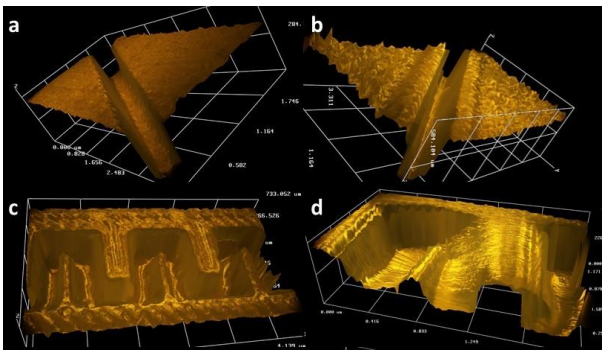

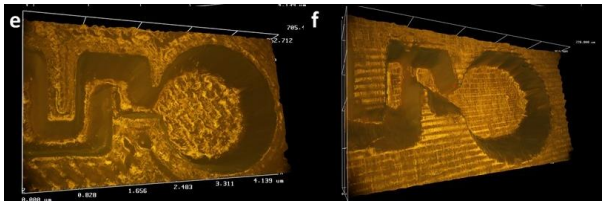

Fig. 3. 3D model of a channel a (O4-1), b (O1-1); serpentine c (O1-1), d (O4-1) and I/O to channel e (O1-1), f (O4-1).

It is crucial to highlight that O1-1, which involves the propagation of channels in a direction that is perpendicular to the printing direction and the presence of supports, yielded satisfactory results. These results serve to emphasize the critical importance of carefully considering the orientation in comparison of a design during the process of microfluidic chips printing. By making the appropriate choice of orientation, it is possible to significantly enhance the performance of the final product and optimize the overall manufacturing process.

4. DISCUSSION AND CONCLUSION

The microfluidic mixer, which is introduced in this investigation and manufactured utilizing Stereolithography (SLA) 3D printing, represents a notable advancement in the fabrication of microfluidic chips. The primary objective of this research was to determine the most optimal printing orientation for microfluidic chips, while considering various factors such as the distribution of channels, support structures, and the overall quality of the final product. By employing a meticulous approach that combines advanced imaging techniques, precise measurements, and thorough analysis, several crucial insights were obtained.

The outcomes of this study reveal significant differences among various printing orientations. Among these orientations, O1-1 stands out as the

most favorable choice due to its ability to ensure an optimal dimension of microfluidic structures. This specific orientation, characterized by channels propagating perpendicular to the printing direction and possessing adequate support, demonstrates superior quality and accuracy in the resulting chips. In contrast, O3-1, which was recommended by the computer model, proved to be effective only in maintaining serpentine depth (low SD deviation). In other parameters, O3-1 did not emerge as the best orientation.

Additionally, all other orientations in which the channel was not horizontally aligned with gravity exhibited lower printing quality. Chips manufactured using these orientations showed suboptimal serpentine dimensions, inadequate support, low production efficiency, and frequent damage during the printing process. Furthermore, despite being slightly less efficient than O1-1, O1-2 still delivers an acceptable level of product quality. This highlights the critical importance of carefully selecting the appropriate orientation in the microfluidic chip printing process. Choosing the correct orientation significantly enhances the performance of the final product and streamlines the manufacturing process. Moreover, this underscores that orientation is more crucial than the presence of support.

In conclusion, this study provides a demonstration of the paramount importance of selecting an appropriate printing orientation in SLA 3D printing of microfluidic chips. By conducting a comprehensive analysis that encompasses detailed imaging, precise measurements, and sophisticated software analysis, O1-1 emerges as the optimal choice, ensuring superior product quality and accuracy. The findings underscore the necessity for a nuanced approach in the design of microfluidic structures, taking into consideration aspects such as channel distribution and support structures.

These results not only make a substantial contribution to the field of microfluidics but also offer valuable insights for researchers and manufacturers involved in 3D printing technologies. By comprehending the intricate relationship between printing orientations and product quality, this research lays the groundwork for the development of more efficient and reliable microfluidic devices, with potential applications spanning from medical diagnostics to chemical analysis.

5. ACKNOWLEDGEMENT

This research has received funding from the European Union's Horizon 2020 research and innovation programme under the Marie Skłodowska-Curie grant agreement No. 872370.

6. REFERENCES

[1] Dan L. *Blood–brain barrier microfluidic chips and their applications.* Organs-on-a-chip, Vol. 5, 2023.

[2] Sanapathi, J.; Vipparthi, P.; Sosnik, A.; Kumarasamy, M. *Microfluidics for Brain Endothelial-Astrocytic Interactions.* Preprints, 2023.

[3] E., Yankov., Maria, P., Nikolova, *Orientation of the Digital Model for SLA 3D Printing and Its Influence on the Accuracy of the Manufactured Physical Objects for Micro- and Nano Technologies*, in book: Materials Design and Applications II, pp. 283-291, 2019.

[4] Norouzi, N., Bhakta, H. C., Grover, W. H.: *Orientation-Based Control of Microfluidics*, PLoS ONE, Vol. 11, 2016.

[5] Kim, Y.J., & Chun, K.: *Novel Sperm Sorting Microfluidic Chip With Feedback Channel and Vertical Orientation*, IEEE Sensors, pp. 1-4, 2019.

Authors: **Igor Putnik[1], Nikol Petrović[1], dr Luna Adamov[2], Marija Vejin[1], Miroslav Đoćoš[1], dr Dejan Movrin[1], dr Sanja Kojić[1]**

[1]University of Novi Sad, Faculty of Technical Sciences, Trg Dositeja Obradovica 6, 21000 Novi Sad, Serbia, Tel: +381 21 485 2350
[2]University of Novi Sad, Faculty of Medicine Hajduk Veljkova 3, Novi Sad, Srbija, Tel.: +381 21 661 2222
E-mail:
putnik.igor@uns.ac.rs
nikolpetrovic@uns.ac.rs
luna.adamovnew@yahoo.com
vejinmarija@uns.ac.rs
djocos.miroslav@uns.ac.rs
movrin@uns.ac.rs
sanjakojic@uns.ac.rs

ETIKUM 2023 **INTERNATIONAL SCIENTIFIC CONFERENCE**
NOVI SAD, SERBIA, DECEMBER 7-9, 2023

Qureshi, S., Kumar, P., Stojanović, G.

ELECTRO-MECHANICAL TESTING OF SILVER CONDUCTIVE TEXTILES FOR STRAIN SENSING APPLICATIONS

Abstract: *Strain sensors that are flexible and stretchable have become increasingly important for measuring various movements and forces and are now being used more frequently in smart textiles. They can be utilized to monitor movements of arms, legs, or individual joints, and have a high sensitivity for detecting large movements. However, there are only a few that are able to measure small movements. In this study, three different stretchable and flexible conductive textiles were tested electromechanically for their application as strain sensors. The conductive textiles exhibited the maximum change in resistance at 0.6N, with an observed sensitivity of 6.97 N^{-1} at a very small applied force of 0.1 N. These interesting finding exhibited the potential of conductive textiles as the promising wearable strain sensors to carry out important health measurements, such as breathing, bending, heartbeat, and vibrations.*
Keywords: *conductive textile, strain sensor, low strain*

1. INTRODUCTION

The demand for soft electronics has led to the development of smart textiles, which are getting popular day by day. Traditional strain sensors such as metal foil or semiconductor-based sensors are bulky and rigid, which makes them unsuitable for wearable applications. One of the most notable types of smart sensors is the wearable, skin-mountable, and stretchable strain sensor. The sensor has numerous applications in fields like personalized health monitoring [1], human motion detection [2], and soft robotics or human-machine interfaces [3]. Smart textiles have the advantage of being able to interact naturally with the human body, which enables long-term monitoring. The sensors operate through capacitive or resistive means and are designed to convert physical deformation into electrical signals [4]. Resistive sensors are simple and suitable for a wide range of applications, as they detect changes in electrical resistance resulting from physical deformation. Conductive materials are necessary for both capacitive and resistive sensors, but conventional textile materials are typically insulators, so conductive materials must be added externally. This can be achieved through the integration of conductive materials [5] into the polymer matrix. Although numerous strain sensors with a large strain range and high sensitivity have been reported, there is relatively little documentation on sensors with high sensitivity at small strain ranges (< 5%). Textile strain sensors have become increasingly popular for detecting motion and measuring strain levels across a wide range.

Despite significant progress in the area, it remains a challenge to produce flexible and textile-based strain sensors with sensitivity to slight variations in load. This is why there is a growing need to develop textile strain sensors that are easy to manufacture and have exceptional sensitivity to small loads. These sensors can provide valuable information about an individual's health status, such as heartbeat, vibrations, torsions, or bending.

Our study proposes conductive clothes as strain-sensing material that holds promise for overcoming this challenge. These are silver-coated conductive clothes. The conductive clothes provide the benefits of both components, including the high electrical conductivity and flexibility of silver by using these conductive clothes, we can create highly sensitive, easy-to-manufactured textile-based sensors that can detect the smallest strains. The functionality of resistive strain sensors is based on the equation (1) [4].

$$R = \rho \frac{L}{A} \qquad (1)$$

The electrical resistance (R) is determined by multiplying the material's specific electrical resistance (ρ) with the quotient of the distance between the measuring electrodes (L) and the cross-sectional area of the sample (A). For a change in electrical resistance to occur, the sensor load needs to alter either the geometry (L/A) or the specific electrical resistance of the material

(ρ). The operational mechanism of resistive strain sensors is a complex process that is influenced by multiple factors, including the textile structure, manufacturing process, and components utilized. These factors can significantly impact the sensor's accuracy and performance, emphasizing the need for careful consideration of these aspects to ensure optimal sensor performance.

In the present research, we have tested silver-based conductive textiles for strain sensing by choosing the textiles of different knitting styles. The sensitivity and resistive response of the textiles were investigated to examine their potential use as a strain sensor in the wearable health monitoring applications.

2. MATERIALS AND METHODOLOGY

Three silver conductive fabrics namely Technik-tex P130 + B, Silitex, and Technik-tex P130 + B were purchased from Sheildex and labelled as C1, C2, and C3 respectively. All fabrics are knitted in warp and weft direction. The composition, electrical properties and knitting of these conductive textiles are summarized in Table 1.

Table 1. Composition and electrical properties of conductive textiles

Sample	Composition	R (Ω/m^2)	Knitting
C1	A hybrid knitted fabric consisting of (78% polyamide and 22% elastane).	2	warp and weft
C2	Silver metallized knitted fabric(78% polyamide and 22% elastane).	2	warp and weft
C3	Knitted fabric metalized with pure silver consists of 94% polyamide and 6% Dorlastan.	2	warp

The morphology of conductive clothes was performed by 3D Optical Profilometer (Huvitz BioImager® HRM-300) with Huvitz microscope. The associated Panasis software was used to analyze the surface of textile samples.

The electromechanical measurement of the conductive clothes was performed using a tensile testing machine (Instron 34SC-2, city of Norwood, Massachusetts, USA) and the output is recorded as DC resistance (R_{dc}) by impedance analyzer (Hioki IM3590, Nagano, Japan). The textile samples were prepared by cutting the conductive clothes in size of 12 cm x 1 cm (W x L). During the measurement, these samples were fixed between the clamp of the machine. The testing set-up is shown in Fig. 1.

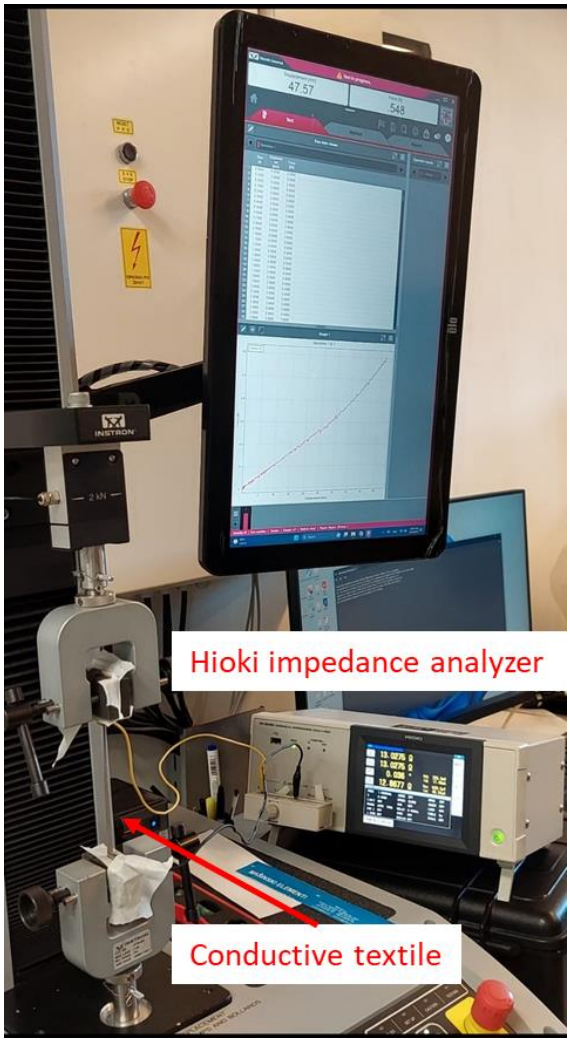

Fig. 1. Conductive textile is fixed between the clamps of the tensile testing machine, both ends of the textiles are also connected with the HIOKI impedance analyzer to record the resistance change due to tensile force

3. RESULTS AND DISCUSSION

Fig. 2 represents the 2D profilometry images of the conductive textiles. Fig. 2(a)-2(c) show the photographs of different textiles. Fig. 2(d)-(f) displays the knitting styles of different textile samples. The knitting direction of the textile can be seen in the images. Sample C1 and C2 showed the knitting in the horizontal and vertical directions. The yarns were found to be looped

horizontally showing a weft knit whereas the parallel yarns were observed to be looped vertically at the same time, indicating warp knit. The wrap and weft knitting makes the textile stretchy in both directions. The conductive textile C3 was found to be knitted only in warp and stretchable in the vertical direction only. We also observed the change in the knitting after stretching the textile. The small gaps in samples C2 and C3 were observed as highlighted by the marked area in Fig. 2(g), Fig. 2(h) whereas a few broken yarns are observed in Fig. 2 (i).

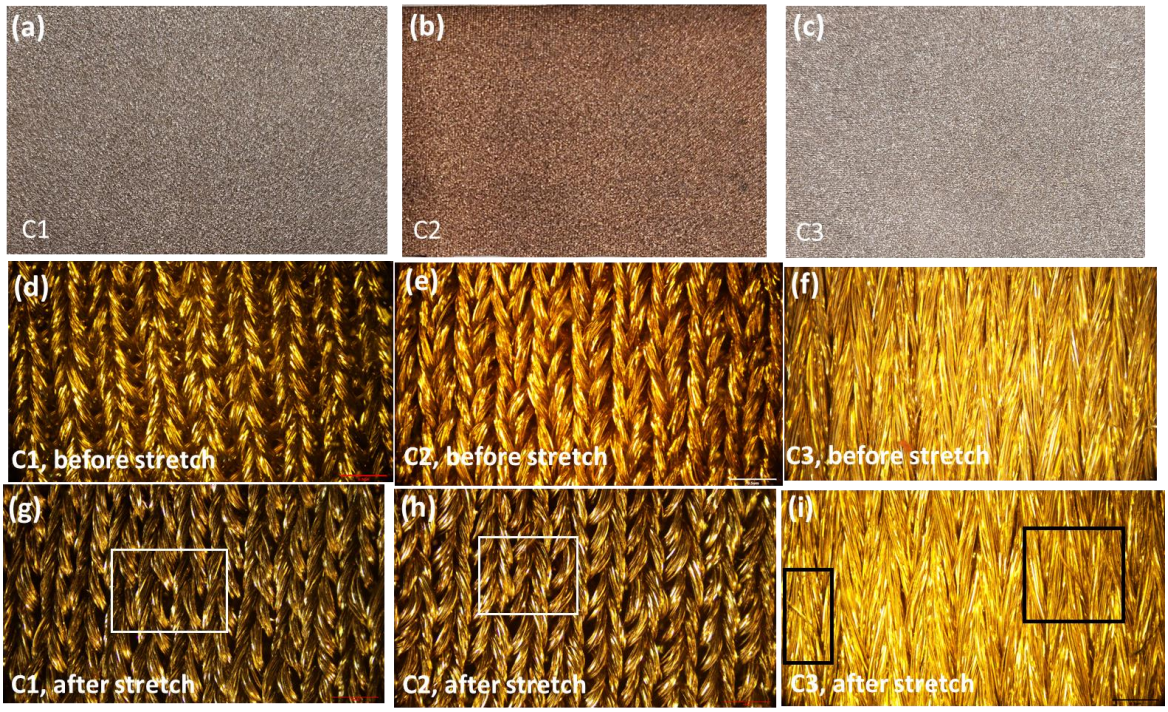

Fig. 2. a),b),c) photographs of conductive textiles d),e),f) 2D optical profiler images of the conductive textiles before applying tensile force g),h),i) 2D optical profiler images of the conductive textiles after applying tensile force

Fig. 3 represents the change in resistance of conductive clothes with applied strain at the rate of 0.05 N/s. The maximum force of 1N is applied with a step size of 0.1 N.

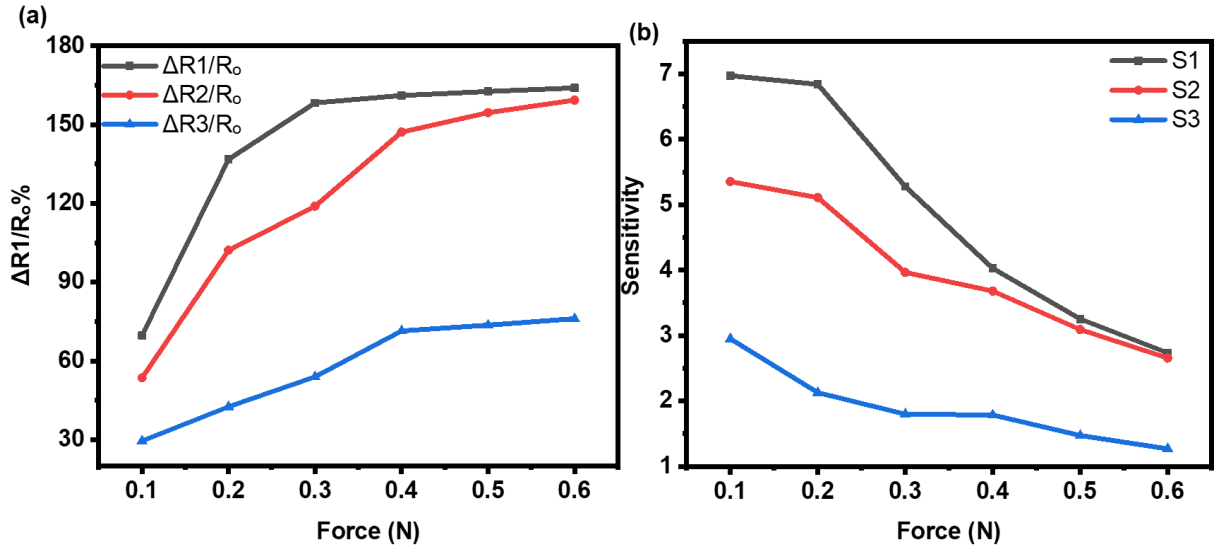

Fig. 3. The resistive response of the conductive clothes a) relative change in resistance of conductive clothes and b) sensitivity of the conductive clothes with respect to applied force

From Fig. 3(a), it was observed that the resistance of conductive clothes increased with the applied forces. For the three conductive clothes, the maximum resistive response was observed at the applied force of 0.6 N. In the case of samples C1 and C3, the change in resistance was observed until an applied force of 0.4 N. After 0.4 N, the applied force showed a negligible effect on the resistance change whereas sample C2 showed a slight change in resistance after 0.4 N.

Fig. 3(b) represents the sensitivity of samples C1, C2 and C3. The sensor's sensitivity was calculated using equation (2)

$$S = \frac{\Delta R/R_0}{\Delta F} \qquad (1)$$

The sensitivity of the samples was found to be decreased in sensitivity with an increase in applied force. The sensitivity of sample C1 was obtained higher than the other two conductive textiles. The sensitivity of samples C1, C2 and C3 were 6.97 N^{-1}, 5.35 N^{-1} and 2.95 N^{-1} respectively at 0.1 N force.

4. CONCLUSION

In this work, silver-based textiles were tested as strain sensors. These textiles showed a promising response in the form of resistance variations even at a small value of applied force. This work demonstrates the potential use of conductive textiles as strain sensors capable of detecting smaller movements such as breathing, bending, heartbeat, and vibrations.

5. ACKNOWLEDGEMENT

This research was funded by the European Union's Horizon 2020 research and innovation programme under grant agreement No. 854194.

6. REFERENCES

[1] Min, S.H., Lee, G.Y., Ahn, S.H., *Direct printing of highly sensitive, stretchable, and durable strain sensor based on silver nanoparticles/multi-walled carbon nanotubes composites*, Compos. Part B Eng., Vol. 161, pp. 395–401, 2019.

[2] Zhang, H., Zhang, D., Guan, J., Wang, D., Tang, M., Ma, Y., Xia, H., *A flexible wearable strain sensor for human-motion detection and a human–machine interface*, J. Mater. Chem. C, Vol. 10, pp. 15554–15564, 2022.

[3] Hu, X., Yang, F., Wu, M., Sui, Y., Guo, D., Li, M., Kang, Z., Sun, J., Liu, J., *A Super-Stretchable and Highly Sensitive Carbon Nanotube Capacitive Strain Sensor for Wearable Applications and Soft Robotics*, Adv. Mater. Technol., Vol. 7, pp. 2100769, 2022.

[4] Seyedin, S., Zhang, P., Naebe, M., Qin, S., Chen, J., Wang, X., Razal, J.M., *Textile strain sensors: A review of the fabrication technologies, performance evaluation and applications*, Mater. Horizons, Vol. 6, pp. 219–249, 2019.

[5] Rashid, I.A., Saif, I., Usama, M., Umer, M., Javid, A., Rehan, Z.A., Zubair, U., *Highly resilient and responsive fabric strain sensors: Their effective integration into textiles and wireless communication for wearable applications*, Sensors Actuators A Phys., Vol. 346, pp. 113836, 2022.

Authors: **Saima Qureshi, Pradeep Kumar, Prof. Goran Stojanović,** University of Novi Sad, Faculty of Technical Sciences, Trg Dositeja Obradovica 6, 21000 Novi Sad, Serbia, Phone.: +381 21 485 2350, Fax: +381 21 454-495.

E-mail: saima.qureshi@uns.ac.rs
pradeep.kumar@uns.ac.rs
sgoran@uns.ac.rs

ETIKUM 2023 **INTERNATIONAL SCIENTIFIC CONFERENCE NOVI SAD, SERBIA, DECEMBER 7-9, 2023**

Vučinić, P., Petrović, Đ., Ivić, S., Puškar, T., Radumilo, D., Puškar, N., Vučinić T.

CONTEMPORARY ADVANCES IN AUTOMATED LANDMARK DETECTION IN CEPHALOMETRICS

Abstract: *Contemporary methods for automatic landmark detection in cephalometrics are based on the results and positive experiences of traditional techniques such as edge detection or AAM and utilize cutting-edge technologies, including deep learning and machine learning algorithms. These advanced approaches harness convolutional neural networks and other sophisticated models to achieve robust and accurate identification of anatomical landmarks on cephalometric images. These methods transcend traditional limitations, accommodating variations in anatomy and enhancing precision. The synergy of these contemporary methods not only revolutionizes orthodontic practices but also contributes to interdisciplinary research, propelling the field towards a future of enhanced diagnostics and treatment planning.*

Key Words: *Artificial intelligence; Cephalometric landmarks; Computer vision; Deep Learning*

1. INTRODUCTION

Cephalometrics, the study of the head's skeletal and soft tissue structures, plays a pivotal role in orthodontics, anthropology, and forensic science. Traditionally, cephalometric analysis involved manual identification of landmarks on X-ray images, a time-consuming and error-prone process. However, with the advent of advanced computational techniques, automated landmark detection has revolutionized this field [1,2]. This introduction provides an overview of the contemporary knowledge in automated landmark detection in cephalometrics, exploring the techniques, challenges, and applications that have emerged in recent years.

2. HISTORICAL PERSPECTIVE

The journey of automated landmark detection in cephalometrics traces back to the early applications of computer vision and pattern recognition in the mid-20th century. Early attempts focused on basic geometric features, paving the way for more sophisticated algorithms in subsequent decades. Progress accelerated with the availability of high-resolution imaging technologies and computational power.

Early attempts (1950s - 1970s): The roots of automated landmark detection in cephalometrics can be traced back to the 1950s when computer technology began to emerge. Early attempts focused on basic geometric features and edge detection algorithms. Researchers explored methods to identify specific points on X-ray images manually, which laid the foundation for subsequent automated approaches [3,4].

Introduction of computer vision (1980s - 1990s): The 1980s and 1990s witnessed significant progress in computer vision techniques. Researchers started applying image processing algorithms to identify edges and shapes within cephalometric images. Template matching methods were also explored, where predefined templates of landmarks were compared with the image data to detect specific points [5,6].

Integration of machine learning (1990s - 2000s): As machine learning gained traction, researchers began integrating these techniques into cephalometric landmark detection. Supervised learning algorithms, such as neural networks and support vector machines, were employed to train models on labeled datasets. These models could identify landmarks based on learned patterns from the training data, marking a shift from rule-based systems to data-driven approaches [7,8].

Advancements in 3D imaging (2000s - 2010s): With the advent of 3D imaging technologies, such as cone-beam computed tomography (CBCT), the scope of cephalometric analysis expanded. Automated landmark detection algorithms evolved to handle 3D data, allowing for more comprehensive analyses of craniofacial structures. These advancements paved the way for a more detailed understanding of anatomical landmarks in three-dimensional space.

Rise of deep learning (2010s - present): The 2010s marked a significant turning point with the rise of deep learning techniques, especially convolutional neural networks (CNNs). CNNs excel at learning hierarchical features from images, making them highly effective for landmark detection tasks. Deep learning models were trained on large datasets, enabling them to automatically extract complex features and accurately identify landmarks in cephalometric images [9].

Integration of augmented reality (present and future): In recent years, the integration of automated landmark detection with augmented reality (AR) technologies has gained attention. AR applications overlay virtual information onto the real world, allowing clinicians to visualize cephalometric landmarks in real-time during patient examinations. This integration enhances the precision of landmark identification and facilitates better communication between clinicians and patients.

2.1 Traditional image processing techniques:

- Edge detection algorithms

- Template matching methods

Active Appearance Models (AAMs) are statistical models used in computer vision and image analysis to capture shape and texture variations in images. In the context of automated detection of landmarks in cephalometrics, AAMs are employed to model the appearance and shape of craniofacial structures, allowing for accurate and robust landmark detection. AAM approach involves the following series of procedures:

1. Data acquisition and preprocessing: High-quality cephalometric images of patients are collected using X-ray imaging techniques, ensuring consistent positioning and image resolution. Cephalometric images then undergo preprocessing steps, including noise reduction, contrast enhancement, and normalization, to standardize the image quality and make them suitable for analysis.

2. Shape and texture modeling: A set of manually annotated landmarks is used to create a shape model, representing the spatial arrangement of landmarks. Principal Component Analysis (PCA) is commonly employed to reduce the dimensionality of shape variations, capturing the main modes of shape variation in the data. The texture of the cephalometric image is modeled using pixel intensities within a local region around each landmark. PCA is again applied to reduce the dimensionality of texture variations, capturing the main modes of texture variation in the data.

3. Building the Active Appearance Model: The shape and texture models are combined to create the Active Appearance model. This model represents the relationship between the shape and texture variations observed in the training dataset. The combined model encapsulates the statistical information necessary to generate new instances of cephalometric images with plausible landmark locations.

4. Landmark localization: During the landmark detection process, an initial estimate of landmark locations is obtained either manually or using a simpler algorithm. This initialization serves as a starting point for the AAM-based optimization. The AAM then optimizes the landmark positions iteratively, aligning the shape and texture models with the input image. The optimization process seeks the best-fitting instance of the AAM in the image space, refining the landmark positions to match the actual landmarks in the cephalometric image. AAMs can be constrained to ensure plausible deformations, preventing unrealistic shapes and textures. Constraints are often derived from anatomical knowledge and incorporated into the optimization process.

5. Evaluation and refinement: The accuracy of landmark detection is evaluated by comparing the automatically detected landmarks with manually annotated ground truth landmarks. Metrics such as Euclidean distance or mean squared error are commonly used to measure the accuracy of landmark localization. Based on the evaluation results, the AAM can be refined by incorporating additional training data, refining the shape and texture models, or adjusting the initialization and optimization strategies to improve landmark detection accuracy.

In our research, which we conducted and published in 2010, an average accuracy in cephalometric landmark detection of 1.68 mm was obtained, with 61 per cent of landmarks detected within 2 mm and 95 per cent of landmarks detected within 5 mm precision. A noticeable increase in overall precision and detection of low-contrast cephalometric landmarks was achieved compared with other automated systems of that time [10].

2.2 Machine learning approaches:

- Supervised learning algorithms (e.g., neural networks, support vector machines).

- Unsupervised learning techniques (e.g., clustering algorithms) [11,12].

2.3 Deep learning architectures:

- Convolutional Neural Networks (CNNs) and their variants.

- Recurrent Neural Networks (RNNs) for sequential data analysis [13,14].

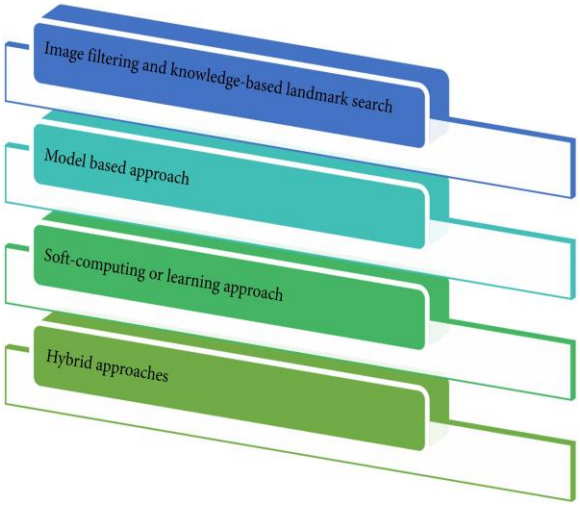

Fig. 1. Artificial intelligence approaches to identify landmarks

3. CHALLENGES AND LIMITATIONS

Despite significant advancements, automated landmark detection faces several challenges, including image noise, anatomical variations, and occlusions. Additionally, ensuring robustness, accuracy, and real-time processing remains a persistent challenge.

Image quality and noise: Cephalometric images can vary in quality due to factors like exposure settings, patient positioning, and equipment differences. Noise, artifacts, and distortions in the images can hinder accurate landmark detection. Preprocessing techniques, such as noise reduction and contrast enhancement, are applied to improve image quality.

Anatomical variations: Human anatomy exhibits natural variations, and landmarks may appear differently and can deviate significantly from the standard positions in different individuals. Training machine learning models on diverse datasets encompassing various demographics and conditions can improve the system's ability to handle anatomical variations.

Occlusions and overlapping structures: Landmarks may be obscured by other anatomical structures, dental appliances, or radiopaque materials, leading to partial or complete occlusions. Detecting obscured landmarks accurately is a complex task. Techniques like semantic segmentation can help identify regions of interest, aiding in landmark localization even when they are partially visible.

Landmark ambiguity: Some anatomical features might lack distinct boundaries, making it difficult to pinpoint exact landmark locations. Expert knowledge and anatomical constraints can guide landmark detection algorithms. Integrating domain-specific rules and constraints into the algorithms can help resolve ambiguity to some extent.

Computational complexity and processing time: Deep learning models, especially complex architectures like deep neural networks, demand significant computational resources. Researchers are continually working on optimizing algorithms and developing hardware accelerators tailored for deep learning tasks (parallel processing, distributed computing, etc.)

Algorithmic bias: Automated landmark detection algorithms can be biased based on the training data, leading to inaccurate results, especially for underrepresented demographic groups. Addressing algorithmic bias requires diverse and representative training datasets. Techniques like adversarial training and fairness-aware machine learning are employed to reduce bias [15].

4. CONCLUSION

Automated landmark detection in cephalometrics represents a transformative paradigm shift, enhancing the accuracy, efficiency, and reliability of craniofacial analyses. The AI is a promising tool for facilitating cephalometric tracing in routine clinical practice as well as analyzing large databases for research purposes. Despite the advancements, challenges such as anatomical variations, occlusions, and ethical concerns persist. Ongoing research focuses on addressing these challenges through diverse and representative datasets, advanced algorithms, and ethical frameworks.

Additionally, the future of automated landmark detection in cephalometrics is likely to see further integration with artificial intelligence, leading to more intelligent and adaptive systems. The main objective of this narrative review was to assist clinicians and researchers in comprehending various features of this study area.

5. REFERENCES

[1] Khanagar S.B., Al-Ehaideb A., Maganur P.C et al.: *Developments, application, and performance of artificial intelligence in dentistry - a systematic review*, Journal of Dental Sciences, 16(1), p.p. 508–522, 2021.

[2] Hwang H.W., Park J.H., Moon J.H. et al.: *Automated identification of cephalometric landmarks: part 2-might it be better than human*, The Angle Orthodontist, 90(1), p.p. 69–76, 2020.

[3] Alam M.K., Alfawzan A.A.: *Evaluation of Sella Turcica bridging and morphology in different types of cleft patients*, Frontiers in Cell and Developmental Biology, 8, p.p. 656, 2020.

[4] Cohen, A.M., Ip H.S., Linney A.: *A preliminary study of computer recognition and identification of skeletal landmarks as a new method of cephalometric analysis*, British Journal of Orthodontics, 11(3), p.p. 143–154, 1984.

[5] Leonardi R., Giordano D., Maiorana F, Spampinato C.: *Automatic cephalometric analysis*, The Angle Orthodontist, 78(1), p.p. 145–151, 2008.

[6] Richardson A.: *A comparison of traditional and computerized methods of cephalometric analysis*, The European Journal of Orthodontics, 3(1), p.p. 15–20, 1981.

[7] Subasi M.K., Kiymik A., Alkan A., Koklukaya E.: *Neural network classification of EEG signals by using AR with MLE preprocessing for epileptic seizure detection*, Mathematical and Computational Applications, 10(1), p.p. 57–70, 2005.

[8] Baxt W.G.: *Application of artificial neural networks to clinical medicine*, The Lancet, 346(8983), p.p. 1135–1138, 1995.

[9] Y. M. Bichu, Y.M., Hansa, I., Bichu, A.Y., Premjani, P., Flores-Mir, C., Vaid, N.R.: *Applications of artificial intelligence and machine learning in orthodontics: a scoping review*, Progress in Orthodontics, 22 (1), p.p. 1–11, 2021.

[10] Vučinić, P., Trpovski, Ž., Šćepan, I.: *Automatic landmarking of cephalograms using active appearance models*, The European Journal of Orthodontics, 32(3), p.p. 233–241, 2010.

[11] Ahmed, N., Abbasi M.S., Zuberi F. et al.: *Artificial intelligence techniques: analysis, application, and outcome in dentistry—a systematic review*, BioMed Research International, 2021, Article ID 9751564, 15 pages, 2021.

[12] Shetty, V., Rai, R., Shetty, K.: *Artificial intelligence and machine learning: the new paradigm in orthodontic practice*, International Journal of Orthodontic Rehabilitation, 11(4), p.p. 175–175, 2020.

[13] Arik, S.Ö., Ibragimov, B., Xing, L,: *Fully automated quantitative cephalometry using convolutional neural networks*, Journal of Medical Imaging, 4(1), p.p. 014501, 2017.

[14] Nishimoto, S., Sotsuka, Y., Kawa,i K., Ishise, H., Kakibuchi, M.: *Personal computer-based cephalometric landmark detection with deep learning, using cephalograms on the internet*, Journal of Craniofacial Surgery, 30(1), p.p. 91–95, 2019.

[15] Talaat, S., Kaboudan, A., Talaat, W., et al.: *Improving the accuracy of publicly available search engines in recognizing and classifying dental visual assets using convolutional neural networks*, International Journal of Computerized Dentistry, 23(3), p.p. 211–218, 2020.

Authors: **Assoc. Prof. dr Predrag Vučinić, Full Prof. dr Đorđe Petrović, Assist. Prof. dr Stojan Ivić, Full. Prof. dr Tatjana Puškar, Assist. dr Danijela Radumilo, dr Nataša Puškar, Tijana Vučinić,** Univerzitet u Novom Sadu, Medicinski fakultet, Hajduk Veljkova 3, 21000 Novi Sad, Serbia, Tel: +381 21 6420 677

E-mail: predrag.vucinic@mf.uns.ac.rs
djordje.d.petrovic@mf.uns.ac.rs
stojan.ivic@mf.uns.ac.rs
tatjana.puskar@mf.uns.ac.rs
danijela.radumilo@mf.uns.ac.rs
905005d23@mf.uns.ac.rs
310252@mf.uns.ac.rs

ETIKUM 2023 **INTERNATIONAL SCIENTIFIC CONFERENCE**
NOVI SAD, SERBIA, DECEMBER 7-9, 2023

Žigić, M.

THE APPLICATION OF INERTIAL MEASUREMENT UNITS (IMUs) IN BIOMECHANICS AND ROBOTICS

Abstract: *In the fields of biomechanics and robotics, the integration of Inertial Measurement Units (IMUs) has proven to be very useful, providing data that opens new frontiers in understanding human movement and enhancing the capabilities of robotic systems. This paper deals with rigid body position and attitude estimation using IMU sensor data. The earlier developed numerical algorithm including quaternions is applied for the analysis of a human or robotic lag motion.*
Key words: *quaternions, rigid body, IMU*

1. INTRODUCTION

IMUs serve as invaluable tools in capturing and dissecting the intricacies of human motion. By measuring parameters such as joint angles, accelerations, and angular velocities, biomechanists gain unprecedented insights into the mechanics of movement. This is particularly crucial in sports science, rehabilitation, and ergonomics. The application of IMUs in gait analysis has revolutionized our ability to comprehend walking patterns, [1-4]. Researchers leverage IMU data to diagnose gait abnormalities, monitor rehabilitation progress, and tailor interventions to enhance mobility. Understanding and optimizing body posture is paramount in various fields. IMUs aid in real-time posture analysis, offering valuable feedback for ergonomics, rehabilitation protocols, and performance optimization in both everyday activities and specialized tasks. Athletes benefit from IMUs in sports performance monitoring. Whether analyzing running strides, cycling techniques, or swim strokes, IMUs provide precise data to fine-tune training regimens and prevent injuries, ultimately optimizing athletic performance. In rehabilitation settings, IMUs are instrumental in tracking and evaluating patients' movements. By ensuring the correct execution of prescribed exercises, IMUs contribute to more effective rehabilitation programs and improved patient outcomes.

The integration of IMUs in both biomechanics and robotics represents a symbiotic relationship where the precision and versatility of IMU technology empower researchers, healthcare professionals and engineers. The rigid body attitude estimation problem is of great importance in various fields such as aerospace and automotive engineering, robotics and human movement analysis, [5,6]. Mobile phones typically incorporate micro-electromechanical systems (MEMS) inertial sensors, which are a type of IMU. The two primary components of a MEMS-based IMU found in many mobile phones are accelerometers and gyroscopes. These sensors work together to provide information about the device's motion and orientation.

In order to demonstrate the analysis including rigid body position estimation by the use of IMU, the numerical algorithm developed in [7] is applied to problem of human body part motion.

2. THE PROBLEM

Consider the body with the center of mass C and IMU attached to the body at an arbitrary point A. The reference frame $Cxyz$ is fixed to the body and moves together with it, while $O\xi\eta\zeta$ represents the inertial coordinate system, Fig 1.

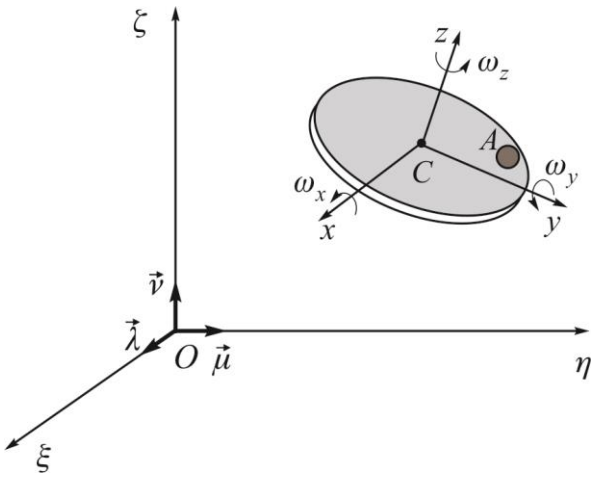

Fig. 1. System under consideration. Rigid body with an IMU positioned at the point A

It is necessary to determine the attitude of the body on the basis of sensor data. The body can represent a human body part or a robotic segment. Input data are angular velocity components ω_x, ω_y, ω_z, as well as the projections of the acceleration of the point A on axes fixed to the body. Position vectors of C and A read:

$$\begin{aligned}\mathbf{r}_C &= \xi_C\boldsymbol{\lambda} + \eta_C\boldsymbol{\mu} + \zeta_C\boldsymbol{\nu},\\ \mathbf{r}_A &= \xi_A\boldsymbol{\lambda} + \eta_A\boldsymbol{\mu} + \zeta_A\boldsymbol{\nu}.\end{aligned} \qquad (1)$$

while the acceleration of the center of mass can be expressed using the Rival's theorem:

$$\mathbf{a}_C = \mathbf{a}_A - \mathbf{a}_A^C = \ddot{x}_A\mathbf{i} + \ddot{y}_A\mathbf{j} + \ddot{z}_A\mathbf{k} - \begin{vmatrix}\mathbf{i} & \mathbf{j} & \mathbf{k}\\ \dot{\omega}_x & \dot{\omega}_y & \dot{\omega}_z\\ x_A^C & y_A^C & z_A^C\end{vmatrix} - \begin{vmatrix}\mathbf{i} & \mathbf{j} & \mathbf{k}\\ \omega_x & \omega_y & \omega_z\\ I_{C1} & I_{C2} & I_{C3}\end{vmatrix}, \qquad (2)$$

where:

$$\begin{aligned}I_{C1} &= \omega_y z_A^C - \omega_z y_A^C,\\ I_{C2} &= \omega_z x_A^C - \omega_x z_A^C,\\ I_{C3} &= \omega_x y_A^C - \omega_y x_A^C.\end{aligned} \qquad (3)$$

The relation between acceleration of the mass center expressed in the inertial (I) and in the body (M) reference frames can be obtained by the use of a rotation matrix R:

$$\mathbf{a}_C^{(I)} = R\cdot\mathbf{a}_C^{(M)}, \qquad (4)$$

where the elements of the rotation matrix $c_{i,j}$, (i, j=1,2,3):

$$\begin{aligned}&c_{11}=\cos\angle(\boldsymbol{\lambda},\mathbf{i}),\ c_{12}=\cos\angle(\boldsymbol{\lambda},\mathbf{j}),\ c_{13}=\cos\angle(\boldsymbol{\lambda},\mathbf{k}),\\ &c_{21}=\cos\angle(\boldsymbol{\mu},\mathbf{i}),\ c_{22}=\cos\angle(\boldsymbol{\mu},\mathbf{j}),\ c_{23}=\cos\angle(\boldsymbol{\mu},\mathbf{k}),\\ &c_{31}=\cos\angle(\boldsymbol{\nu},\mathbf{i}),\ c_{32}=\cos\angle(\boldsymbol{\nu},\mathbf{j}),\ c_{33}=\cos\angle(\boldsymbol{\nu},\mathbf{k}),\end{aligned} \qquad (5)$$

can be calculated by the use of quaternions, containing Euler parameters q_0, q_1, q_2, q_3, see [7]. Quaternions can be considered as quadrinomial expressions which consist of a real and an imaginary part. The singularity problem which might occur using Euler angles can be avoided by the application of quaternions.

Rotation matrix elements can be represented as:

$$\begin{aligned}&c_{11}=q_0^2+q_1^2-q_2^2-q_3^2, \quad c_{12}=2(q_1q_2-q_0q_3),\\ &c_{13}=2(q_0q_2+q_1q_3), \quad c_{21}=2(q_1q_2+q_0q_3),\\ &c_{22}=q_0^2-q_1^2+q_2^2-q_3^2, \quad c_{23}=2(q_2q_3-q_0q_1),\\ &c_{31}=2(-q_0q_2+q_1q_3), \quad c_{32}=2(q_2q_3+q_0q_1),\\ &c_{33}=q_0^2-q_1^2-q_2^2+q_3^2,\end{aligned} \qquad (6)$$

while the time derivative of Euler parameters, expressed by the use of the correction factor λ are:

$$\begin{aligned}\dot{q}_0 &= -\frac{1}{2}\left(q_1\omega_x + q_2\omega_y + q_3\omega_z\right) + \lambda q_0,\\ \dot{q}_1 &= \frac{1}{2}\left(q_0\omega_x + q_2\omega_z - q_3\omega_y\right) + \lambda q_1,\\ \dot{q}_2 &= \frac{1}{2}\left(q_0\omega_y + q_3\omega_x - q_1\omega_z\right) + \lambda q_0,\\ \dot{q}_3 &= \frac{1}{2}\left(q_0\omega_z + q_1\omega_y - q_2\omega_x\right) + \lambda q_1.\end{aligned} \qquad (7)$$

3. THE SOLUTION

In order to solve the problem, time is discretized, $t_n=n\cdot h$, (n=1,2,...), where h is the time step. The approximation of the first derivative is taken in the following form:

$$\dot{q}_{0_n} = \frac{q_{0_{n+1}} - q_{0_n}}{h}. \qquad (8)$$

Output data from the IMU are. Euler parameters can be calculated by the numerical algorithm:

$$\begin{aligned}q_{0_{n+1}} &= h\left[-\frac{1}{2}\left(q_{1_n}\omega_{x_n} + q_{2_n}\omega_{y_n} + q_{3_n}\omega_{z_n}\right) + \lambda_n q_{0_n}\right] + q_{0_n},\\ q_{1_{n+1}} &= h\left[\frac{1}{2}\left(q_{0_n}\omega_{x_n} + q_{2_n}\omega_{z_n} - q_{3_n}\omega_{y_n}\right) + \lambda_n q_{1_n}\right] + q_{1_n},\\ q_{2_{n+1}} &= h\left[\frac{1}{2}\left(q_{0_n}\omega_{y_n} + q_{3_n}\omega_{x_n} - q_{1_n}\omega_{z_n}\right) + \lambda_n q_{2_n}\right] + q_{2_n},\\ q_{3_{n+1}} &= h\left[\frac{1}{2}\left(q_{0_n}\omega_{z_n} + q_{1_n}\omega_{y_n} - q_{2_n}\omega_{x_n}\right) + \lambda_n q_{3_n}\right] + q_{3_n},\end{aligned} \qquad (9)$$

while the rotation matrix elements can be obtained in the following way:

$$\begin{aligned}&c_{11_n}=q_{0_n}^2+q_{1_n}^2-q_{2_n}^2-q_{3_n}^2, \quad c_{12_n}=2(q_{1_n}q_{2_n}-q_{0_n}q_{3_n}),\\ &c_{13_n}=2(q_{0_n}q_{2_n}+q_{1_n}q_{3_n}), \quad c_{21_n}=2(q_{1_n}q_{2_n}+q_{0_n}q_{3_n}),\\ &c_{22_n}=q_{0_n}^2-q_{1_n}^2+q_{2_n}^2-q_{3_n}^2, \quad c_{23_n}=2(q_{2_n}q_{3_n}-q_{0_n}q_{1_n}),\\ &c_{31_n}=2(-q_{0_n}q_{2_n}+q_{1_n}q_{3_n}), \quad c_{32_n}=2(q_{2_n}q_{3_n}+q_{0_n}q_{1_n}),\\ &c_{33_n}=q_{0_n}^2-q_{1_n}^2-q_{2_n}^2+q_{3_n}^2,\end{aligned} \qquad (10)$$

and the correction factor λ_n reads:

$$\lambda_n = 1 - \left(q_{0_n}^2 + q_{1_n}^2 + q_{2_n}^2 + q_{3_n}^2 \right). \qquad (11)$$

Euler parameters are calculated iteratively by the described procedure, while Euler angles of the type (3,2,1) can be obtained as follows:

$$\psi_n = \arctan\left[\frac{2(q_{1n}q_{2n} + q_{0n}q_{3n})}{q_{0n}^2 + q_{1n}^2 - q_{2n}^2 - q_{3n}^2} \right], \qquad 0 \le \psi_n \le 2\pi,$$

$$\theta_n = -\arcsin\left[2(q_{1n}q_{3n} - q_{0n}q_{2n}) \right], \qquad -\frac{\pi}{2} \le \theta_n \le \frac{\pi}{2},$$

$$\phi_n = \arctan\left[\frac{2(q_{2n}q_{3n} + q_{0n}q_{1n})}{q_{0n}^2 - q_{1n}^2 - q_{2n}^2 + q_{3n}^2} \right], \qquad -\pi \le \phi_n < \pi. \qquad (12)$$

Acceleration of the point C can now be expressed in the inertial reference frame using the expressions (2)-(4) in a discretized form. After that, the velocity and position of the center of mass C can be easily obtained by integration.

4. RESULTS

The numerical algorithm for rigid body position and attitude estimation can be demonstrated on the examples of human body part or robotic segment motion. For this purpose a human leg motion is chosen, with the anthropometric data taken from [8]. The leg is modeled by a homogeneous rectangular cuboid of mass m and dimensions a, b and c. The body is connected to a spherical joint representing the hip, at the center of the base $a \cdot b$. Instead of using IMU data, input data are obtained solving the problem of a heavy symmetrical gyroscope, [7]. Coordinates of points A(where the IMU is positioned) and C are (a/2,b/2,c) and (0,0,c/2), respectively. Lagrange's equations of the second kind are solved for the following initial conditions $\psi(0) = \theta(0) = \varphi(0) = 0, \dot{\psi}(0) = 0.1, \dot{\theta}(0) = 0.2, \dot{\varphi}(0) = 0,$ with the values m=12.176 kg, a=b=0.125 m, c=0.428 m, g=9.81 m/s^2, and the Euler angles are obtained. Angular velocity $\boldsymbol{\omega}$ is calculated for the body fixed coordinate system, which is presented in Fig. 2. The acceleration of the center of mass C in the moving reference frame is obtained by the Rival's theorem, while the acceleration expressed in the inertial reference frame is calculated by Eq. (4). Projections of the acceleration of point C in the inertial coordinate system are presented in Fig. 3 - Fig. 5.

To determine the consistent acceleration $\boldsymbol{a}_C^{(\mathrm{I})}$ through the quaternion-based algorithm, we use the acceleration $\boldsymbol{a}_A^{(\mathrm{M})}$ and the angular velocity $\boldsymbol{\omega}$ as input parameters.

These inputs are derived from pre-computed Euler angles and kinematic relationships. The outcomes for acceleration $\boldsymbol{a}_C^{(\mathrm{I})}$, computed using the quaternion method with a time step h=0.01 seconds, are depicted in Figures 3 to 5 by dots.

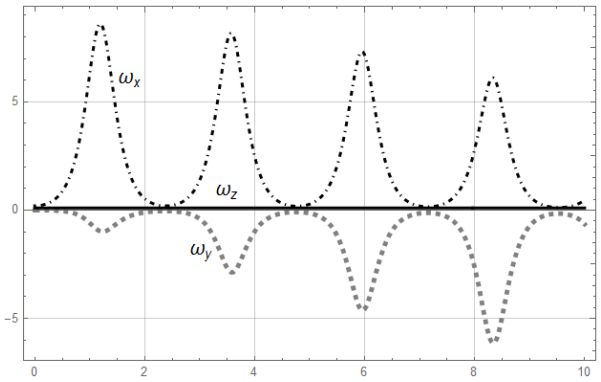

Fig. 2. Angular velocity of the body. Projections of the angular velocity on moving axes x, y and z

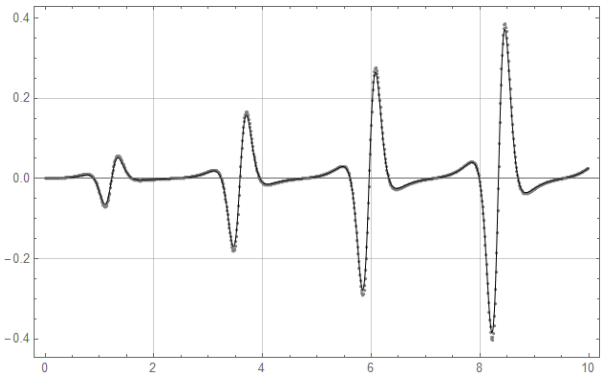

Fig. 3. Projection of the absolute acceleration of point C on ξ axis

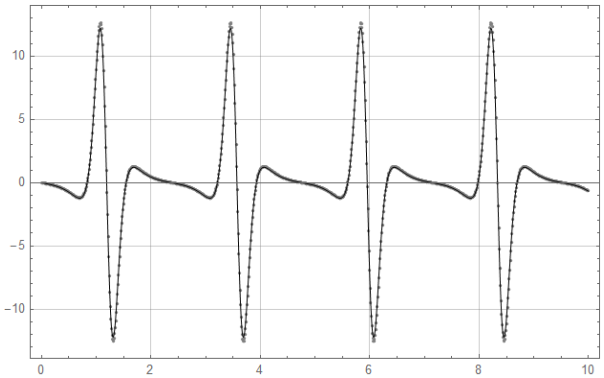

Fig. 4. Projection of the absolute acceleration of point C on η axis

Last three figures demonstrate a good agreement between the outcomes derived from the quaternion approach and those acquired through solving the system of differential equations governing the spherical motion of the human leg.

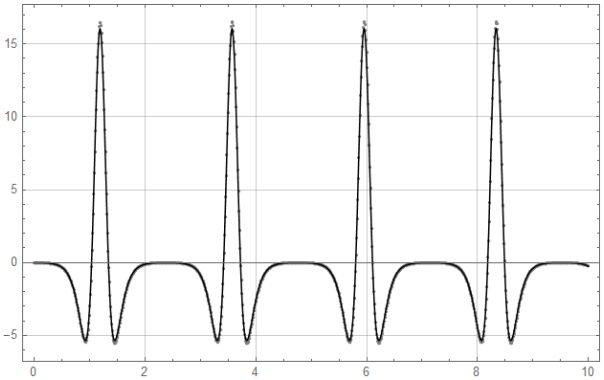

Fig. 5. Projection of the absolute acceleration of point C on ζ axis

5. CONCLUSIONS

In this paper, an analysis of the unrestricted motion of a rigid body is conducted to ascertain its orientation and the acceleration of any arbitrary point on the body. We used previously published numerical algorithm for computing both the acceleration of the center of mass and any selected point on the body, along with Euler angles within an inertial coordinate system. These calculations rely on the acceleration data from a specific body point, denoted as A and the angular velocity expressed in the body reference frame. The input data can be acquired through an Inertial Measurement Unit (IMU) attached to the body, measuring kinematic data in the sensor reference frame with axes parallel to those of the body reference frame.

The quaternion representation is employed to construct the rotation matrix for transformations from the body to inertial reference frame. Utilizing quaternions offers an advantage over Euler angles as it avoids singularities that may arise in the latter. The initial quaternion values are chosen based on the system's initial state.

The algorithm is applied to the case of a heavy symmetrical gyroscope, aiming to determine the acceleration of the center of mass in an inertial coordinate system. Instead of relying on an IMU, input data is obtained through the solution of differential equations of motion and the application of Rivals' theorem. The numerical algorithm calculates the rotation matrix during each time step, yielding the acceleration of the center of mass C in the inertial reference frame. The obtained results are compared with those derived from general theory, demonstrating satisfactory agreement. This proposed numerical approach holds applicability across a wide range aerospace and marine engineering problems, as well as in unmanned aerial vehicles and robotic systems.

6. ACKNOWLEDGMENTS

The research was supported by the Faculty of Technical Sciences of the University of Novi Sad, Project number 2023-054.

7. REFERENCES

[1] Karatsidis, A., Bellusci, G., Schepers, H., De Zee, M. Andersen, M., Veltink, P.: *Estimation of Ground Reaction Forces and Moments During Gait Using Only Inertial Motion Capture*, Sensors, Vol.17, p.p. 1-22, 2017.

[2] Sabatini, A.M.: *Estimating three-dimensional orientation of human body parts by inertial/magnetic sensing*, Sensors, Vol. 11, p.p. 1489-1525, 2011.

[3] Prayudi, I., Kim, D.: *Design and Implementation of IMU-based Human Arm Motion Capture System*, Proceedings of IEEE International Conference on Mechatronics and Automation, p.p. 670-675, Chengdy, China, 2012.

[4] Filippeschi, A., Schmitz, N., Miezal, M. Bleser, G., Ruffaldi, E., Stricker, D.: *Survey of Motion Tracking MEthods Based on Inertial Sensors: A Focus on Upper Limb Human Motion*, Sensors, Vol. 17, p.p. 1-40, 2017.

[5] Grauer, J.A., Hubbard, J.E.Jr.: *Flight Dynamics and System Identification for Modern Feedback Control*, Woodhead Publishing, Philadelphia, USA, 2013.

[6] Barshan, B., Durrant-Whyte, H.F.,: *Inertial navigation systems for mobiel robots*, IEEE Transactions on Robotics and Automation, Vol. 11, p.p. 328-342, 1995.

[7] Zigic, M., Grahovac, N.: *Numerical Algorithm for Rigid Body Position Estimation Using the Quaternion Approach*, Acta Mechanica Sinica, Vol. 34, p.p. 400-408, 2018.

[8] Plagenhoef, S., Evans, F.G., Abdelnour, T.: *Anatomical data for analyzing human motion*, Research Quarterly for Exercise and Sport, Vol. 54, p.p. 169-178, 1983.

Author: **Assoc. prof. dr Miodrag Žigić,** University of Novi Sad, Faculty of Technical Sciences, Trg Dositeja Obradovica 6, 21000 Novi Sad, Serbia, Phone.: +381 21 485 2248.

E-mail: mzigic@uns.ac.rs

INTERNATIONAL SCIENTIFIC CONFERENCE - ETIKUM 2023

PROCEEDINGS

Session 3:

METROLOGY AND QUALITY IN THE FIELD OF ENVIRONMENTAL PROTECTION AND OCCUPATIONAL SAFETY

Novi Sad, 07 – 09th December 2023

ETIKUM 2023 **INTERNATIONAL SCIENTIFIC CONFERENCE NOVI SAD, SERBIA, DECEMBER 7-9, 2023**

Adamović, S., Milošević, R., Banjanin, B., Tomić, I., Adamović, D., Mihailović, A., Dramićanin, M.

GASOVITE ZAGAĐUJUĆE MATERIJE U RADNOM OKRUŽENjU TAMPON MAŠINE

Rezime: *Koncentracije formaldehida i ukupnih lakoisparljivih ogranskih komponenti detektovane su u neposrednom okruženju tampon mašine. U cilju procene inhalacione bezbednosti rada operatera za tampon mašinom, detektovane koncentracije gasovitih zagađujućih materija su upoređene sa graničnim vrednostima emisije koje propisuju Standardi bezbednosti i zdravlja na radu i Nacionalni institut za bezbednost i zdravlje na radu. Detektovane vrednosti formaldehida su više od 84,8 do 95,5% u odnosu na preporučenu granicu izloženosti prema Nacionalnom institutu za bezbednost i zdravlje na radu. Navedeno odstupanje zahteva upotrebu ventilaciong sistema u okruženju tampon mašine radi inhalacione bezbednosti operatera.*

Ključne reči: *Tampon tehnika štampe, formaldehid, ukupne lakoisparljive organske komponente, UV-VIS spektrofotometrija, gasna hromatografija*

1. UVOD

Tampon štampa, kao indirektna duboka štampa, u poslednje dve decenije usavršavanjem tehnologije i zahvaljujući svojim fleksibilnim mogućnostima primene, razvila se u nezavisnu tehniku štampe koja danas ima veoma široku primenu. Najveća prednost tampon štampe jeste mogućnost otiskivanja boje na različitim materijalima (papir, karton, plastika, staklo, metal, laminirane podloge, keramika, itd.) nepravilnih oblika [1].

Danas se široka paleta proizvoda za svakodnevnu upotrebu štampa tampon tehnikom. Neki od tipičnih tampon proizvoda su [1, 2]:

- elektronske komponente (kablovi, konektori, čipovi, releji, prekidači, itd.),
- električni kućni uređaji (paneli za monitore, video i dvd uređaje, tv uređaji, mašine za pranje veša i sušenje, kuhinjski aparati, itd.),
- igračake i oprema za decu (figure, lutke, automobili, dečije flašice, noćne lampe, itd.),
- reklamni materijali (olovke, upaljači, privesci, satovi, lica ručnih satova, itd.) i
- sportska oprema (lopte za fudbal, košarku, golf, teniski i drugi reketi, itd.).

Većina gasovitih zagađujućih materija se emituje skladištenjem, upotrebom i odlaganjem tečnih i čvrstih grafičkih materijala, kao i generisanjem otpada [3]. U zatvorenom grafičkom prostoru isparljiva organska jedinjenja emituju sledeći izvori zagađenja: boje, lepila, rastvarači, sredstva za čišćenje, građevinski materijali, itd. [4]. Grafičke boje, toneri i ketridži sadrže isparljive organske komponente koje mogu izazvati ozbiljan zdravstveni rizik. Mnogobrojnim istraživanjima ustanovljeno je da su zaposleni u štamparijama prilikom udisanja izloženi dejstvu gasovitih zagađujućih materija, poput benzena, toluena, ksilena, formaldehida (HCHO), ukupnih lakoisparljivih organskih komponenti (Total Volatile Organic Compounds, TVOCs), itd. [3-6]. Analizom je ustanovljeno da je u štamparijama sa većim brojem mašina za štampu i više štampača i fotokopirnih mašina, glavni uzrok akumulacije zagađujućih materija visok obim proizvodnje [4,6]. Su i saradnici (2018) sproveli su procenu rizika od udisanja benzena, toluena, ksilena i HCHO u štamparijama u Pekingu (Kina) 2017. godine. Studija je pokazuja da su vrednost rizika od raka kod inhalacije HCHO u intervalu od 1,35 do 3,45 × 10^{-6}, što je više od propisane granice (1 × 10^{-6}). Rizik od raka udisanja benzene, u intervalu od 1,09 do 4,65 × 10^{-6}, viši je od granice (1 × 10^{-6}) i ukazuje na rizik od leukemije [5].

Al-Awadi i saradnici (2019) su u svom radu procenili kvalitet vazduha u zatvorenom prostoru ofset štamparije merenjem: TVOCs, ugnjen-dioksida, temperature, vlažnosti, ozona i suspendovanih čestica. Nivoi TVOCs tokom 8 radnih sati su dostigli koncentraciju od 7,72 ppm. Dok su u radu Pongboonkhumlarp-a i Jinsartan-a (2022) srednje koncentracije TVOCs za osmočasovno radno vreme: 2,68, 5,02, 21,86 i 0,67 ppm, redom za tri ofset i jednu digitalnu štampariju na Tajlandu [6].

Uticaj zagađenja vazduha u zatvorenom prostoru na zdravlje radnika u industriji širom svet izaziva veliku zabrinutost. Studije su pokazale da lakoisparljive organske komponente mogu biti potencijalno štetne po osoblje u zatvorenom prostoru, pa je njihova kvalitativna i kvantitativna

analiza neohodna da bi se procenio njihov uticaj na grafičko okruženje. U cilju procene inhalacione bezbednosti rada operatera za tampon mašinom, u radu su detektovane koncentracije HCHO i TVOCs u neposrednom okruženju mašine.

2. EKSPERIMENTALNI DEO

2.1 Materijali i mašina za tampon štampu

Tampon štamparija nalazi se na teritoriji Novog Sada. Za tampon štampu hemijskih olovaka (tiraž 2.000 za 8 sati) upotrebljeni su sledeći materijali i mašine:

- polipropilenske BRIDGE C plastične hemijske olovke, poreklom iz Kine,
- polivinilhloridna (PVC) boja METALINK, proizvođača Manoukian Argon, Italija,
- PVC razređivač za boje Hemmax (proizvođača Zorka Šabac, Srbija),
- PAD PRINTER tampon mašina (model 2-1010PG, 2008) proizvođača SGIA TSH PRINT, Kina. i
- sušara MOELLER (Nemačka) sa ručno nadograđenim ventilatorom.

2.2 Apsorpciona i spektrofotometrijska analiza formaldehida

Analiza HCHO u vazduhu flekso štamparije sprovedena je kombinacijom apsorpcione i UV-VIS spektrofotometrijske metode.

Apsorpciona metoda za uzorkovanje HCHO sprovedena je u tampon štampariji prema standardnoj 3500 metodi Nacionalnog instituta za bezbednost i zdravlje na radu (National Institute for Occupational Safety and Health, NIOSH). Vazduh štamparije sproveden je brzinom od 0,5 l/min kroz četvorokanalni uzorkivač vazduha (PRO-EKOS AT-401X, Srbija) sa četiri Drekslerove (Drechsel) staklene ispiralice ispunjene sa apsorpcionim rastvorom za HCHO. Apsorpcioni rastvor za HCHO pripremljen je sa 95 cm^3 koncentrovane sumporne kiseline i 0,5 cm^3 1% hromotropne kiseline, koja reaguje sa HCHO i daje hidroxidifenilmetan derivat ljubičaste boje [7].

Po završetku uzorkovanja koncentracije HCHO u apsorpcionim rastvorima sakupljenim na terenu detektovane su spektrofotometrijskim merenjem apsorpcije rastvora na 580 nm na uređaju UV-VIS spektrofotometar DR 5000 (HACH LANGE, Nemačka) sa optičkim kivetama od 1 cm [7].
Koncentracije HCHO u jedinicama $\mu g/m^3$, u sakupljenim uzorcima na terenu određena je prema izrazu (1), [7]:

$$C_{HCHO} = \frac{A \cdot f}{V_{kor}} \qquad (1)$$

gde su:

- A –apsorbanca uzorka na 580 nm,
- f – nagib krive (0,015) i
- V_{kor} – zapremina propuštenog vazduha u m^3 korigovana na normalne uslove (T_k = 25°C i P_k = 101325 Pa). Faktor konverzije na T_k i P_k za HCHO iznosi: 1,228 mg/m^3 = 1 ppm.

Uzorkivač vazduha za apsorpciju HCHO je postavljen na udaljenost od 1,5 m u odnosu na tampon mašinu i na visinu (koja odgovara zoni disanja) od 1,5 m iznad poda. Na svakih sat vremena sakupljena su po četiri apsorpciona uzorka sa HCHO.

2.2 Gasno hromatografska analiza ukupnih lakoispranjivih organskih komponenti

Primenom gasno hromatografske metode sa mobilnim gasnim hromatografom Voyager-Photovac (PHOTOVAC INTERNATIONAL, INC., Sjedinjene Američke Države) detektovani su koncentracioni nivoi TVOCs u okruženju tampon mašine. Softverski paket (Site Chart) upotrebljen je za obradu dobijenih rezultata. Funkcija za analizu TVOCs, koristi samo fotojonizujući detektor i automatsko injektovanje uzorka vazduha uz upotrebu interne pumpe [8].

Tokom uzorkovanja TVOCs u okruženje tampon mašine mobilni gasni hromatograf Voyager-Photovac postavljen je na udaljenost od 1,5 m u odnosu na tampon mašinu i na visinu (koja odgovara zoni disanja) od 1,5 m iznad poda.
Vreme potrebno za uzorkovanje, analizu i obradu podataka za TVOCs od strane mobilnog gasnog hromatografa Voyager-Photovac iznosi 1 sat.

3. REZULTATI I DISKUSIJA

3.1 Koncentracioni nivoi formaldehida i ukupnih lakoispranjivih organskih komponenti u okruženju tampon mašine

Rezultati apsorpcione i spektrofotometrijske analize koncentracionih nivoa HCHO izmerenih na četiri merna mesta (ispiralice od 1 do 4) ukazuju na prisustvo HCHO u neposerednom okruženju tampon mašine. Koncentracije HCHO tokom 8 radnih sati rastu u intervalima: od 0,11 do 0,35 ppm (ispiralica 1), od 0,10 do 0,35 ppm (ispiralica 2), od 0,10 do 0,36 ppm (ispiralica 3) i od 0,11 do 0,37 ppm (ispiralica 4).

Najviša srednja koncentracija HCHO (0,358 ppm) je viša za: 70,6, 65,7, 55,9, 46,2, 37,1, 26,6 i 9,8% u odnosu na srednje vrednosti od prvog do sedmog radnog sata, redom. Uočava se da pojedinačne i srednje vrednosti koncentracionih nivoa HCHO za sve četiri ispiralice, u neposerdnom okruženju tampon mašine, rastu tokom osmočasovnog radnog vremena sa povećanjem obima proizvodnje (slika 1).

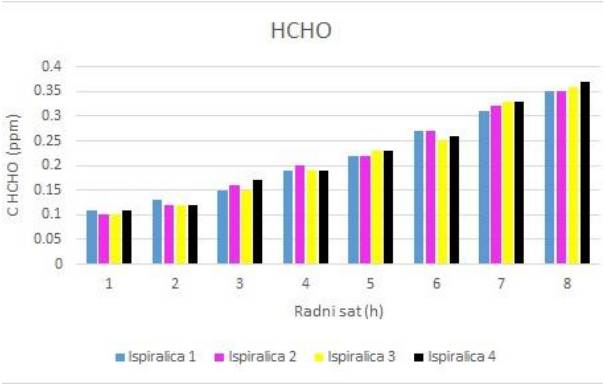

Sl. 1. Koncentracioni nivoi HCHO izmerenih na četiri merna mesta tokom osmočasovnog uzorkovanja

Sa povećavanjem radnih sati i višim obimom tampon proizvodnje, povećavaju se i koncentracioni nivoi TVOCs u intervalu od 1,67 do 15,77 ppm tokom osmočasovnog radnog vremena. Ako se uporedi najviši koncentracioni nivo sa detektovanim nivoima od prvog do sedmog radnog sata, uočavaju se povećanja za 89,4, 83,6, 72,4, 63,3, 45,9, 35,9 i 21,6%, redom.

Poređenjem srednjih vrednosti koncentracionih nivoa HCHO sa detektovanim koncentracionim nivoima TVOCs tokom osmočasovnog uzorkovanja (slika 2) uočava se da su koncentracije TVOCs više u intervalu od 93,7 do 97,7% u odnosu na HCHO.

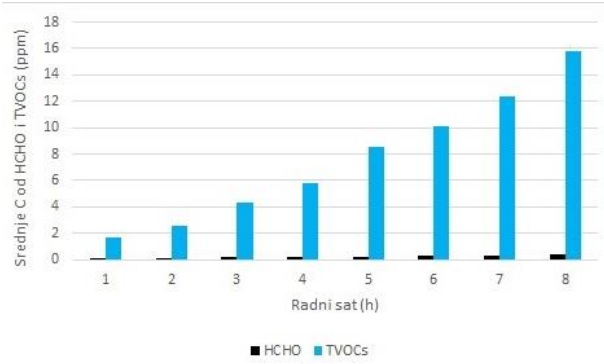

Sl. 2. Komparacije srednjih koncentracionih nivoa HCHO i TVOCs tokom osmočasovnog uzorkovanja

3.2 Poređenje detektovanih koncentracionih nivoa gasovitih zagađujućih materija sa zakonskim uredbama

U Republici Srbiji definisana je Uredba o graničnim vrednostima emisija (GVE) zagađujućih materija u vazduhu iz stacionarnih izvora zagađivanja, osim postrojenja za sagorevanje. Navedena Uredba propisuje GVE za HCHO od 30 mg/m^3 (odnosno 36,84 ppm) samo za postrojenje za impregnaciju i sušenje mineralnih vlakana [9]. Nažalost, u Republici Srbiji ne postoji Uredba u kojoj su definisane GVE HCHO za tampon štampu i druge grafičke procese.

Sa druge strane, Standardi bezbednosti i zdravlja na radu (Occupational Safety and Health Standards, OSHA) propisuju sledeće vrednosti za HCHO [10]:

- dozvoljenu graničnu vrednosti izlaganja (Permissible Exposure Limit, PEL) od 0,75 ppm i
- granicu kratkotrajnog izlaganja (Short-Term Exposure Limit, STEL) od 2 ppm.

Takođe, i NIOSH propisuje sledeće vrednosti za HCHO [11]:

- preporučenu granicu izloženosti (Recommended Exposure Limit, REL) od 0,016 ppm i
- granicu odmah opasnu po život i zdravlje (Immediately Dangerous to Life and Health, IDLH) od 20 ppm.

Na osnovu intervala srednjih vrednodnosti koncentracionih nivoa HCHO od 0,105 do 0,358 ppm, zaključuje se da detektovane vrednosti HCHO ne prelaze PEL i STEL vrednosti prema OSHA i IDLH vrednost prema NIOSH-u. Detektovane vrednosti su niže u intervalu od 52,3 do 86% u odnosu na PEL i u intervalu od 82,1 do 94,5% u odnosu na STEL vrednosti. U odnosu na IDLH vrednosti prema NIOSH-u izmerene vrednosti HCHO su niže od 98,2 do 99,5%. Jedino su sve detektovane vrednosti HCHO više od 84,8 do 95,5% u odnosu na REL prema NIOSH-u. Navedeno odstupanje zahteva upotrebu ventilaciong sistema u okruženju tampon mašine radi inhalacione bezbednosti operatera.

Kada su upitanju TVOCs, njihove GVE nisu definisane ni u nacionalnoj ni u navedenim međunarodnim zakonskim regulativama. Usled nepostojanja GVE za TVOCs nije moguće definisati inhalacionu bezbednost operatera u neposrednom okruženju tampon mašine.

4. ZAKLJUČAK

Na osnovu detektovanih koncentracionih nivoa emitovanih gasova zaključuje se da:

- Srednje vrednosti koncentracionih nivoa HCHO (od 0,105 do 0,358 ppm) i TVOCs (od 1,67 do 15,77 ppm)u neposerdnom okruženju tampon mašine, za sve četiri ispiralice, rastu tokom osmočasovnog radnog vremena sa povećanjem obima proizvodnje.
- Koncentracije TVOCs su više 16 do 44 puta u odnosu na koncentracije HCHO, tokom osmočasovnog uzorkovanja.
- U Republici Srbiji ne postoje Uredbe koje definišu MDK za HCHO i TVOCs za tampon štampu, što zahteva neophodnost monitoringa

istih.

- Najviši koncentracioni nivo HCHO (0,358 ppm) je niži 2 puta u odnosu na dozvoljenu graničnu vrednosti izlaganja i 5,6 puta u odnosu na granicu kratkotrajnog izlaganja koje propisuju Standardi bezbednosti i zdravlja na radu, čime inhalaciona bezbednost operatora za tampon mašinom nije narušena.
- Prema Nacionalnom institutu za zaštitu i zdravlje na radu, najviši koncentracioni nivo HCHO je niži 55,9 puta u odnosu granicu odmah opasnu po život i zdravlje. Međutim, detektovana vrednost je viša 22,4 puta od preporučene granice izloženosti.
- Odstupanje od preporučene granice izloženosti (0,016 ppm) zahteva upotrebu ventilaciong sistema u okruženju tampon mašine radi inhalacione bezbednosti operatera.

5. ZAHVALNICA

Ovaj rad je podržan od strane Ministarstva nauke, tehnološkog razvoja i inovacija kroz projekat broj 451-03-47/2023-01/200156 "Inovativna naučna i umetnička istraživanja iz domena delatnosti FTN-a".

6. REFERENCE

[1] Novaković, D., Pavlović, Ž., Kašiković, N.: *Tehnike štampe – praktikum za vežbe*, FTN Izdavaštvo, Novi Sad, 2011.

[2] Centropapir (2010) Naučite osnovno o tampon štampi, URL: http://www.centropapir.rs/CP_PLUS_novi_kurs_o_tampon_stampi_2010.pdf (Pristupljeno, 11.10.2023.)

[3] Al-Awadi, L., Al-Rashidi, M., Pereira, B., Pillai, A., Khan, A.: *Indoor air quality in printing press in Kuwait*, International Journal of Environmental Science and Technology, 16, p.p. 2643-2656, 2019.

[4] Martins, E.M., Falcão de Sá Borba, P., Espindola dos Santos, N., Bermudez dos Reis, P.T., Simões Silveira, R., Machado Corrêa, S.: *The relationship between solvent use and BTEX concentrations in occupational environments*, Environmental Monitoring and Assessment, 188, 608, 2016.

[5] Su, M.; Sun, R., Zhang, X., Wang, S., Zhang, P., Yuan, Z., Liu, C., Wang, Q.: *Assessment of the inhalation risks associated with working in printing rooms: a study on the staff of eight printing rooms in Beijing, China*, Environmental Science and Pollution Research, 25, p.p. 17137-1714, 2018.

[6] Pongboonkhumlarp, N., Jinsart, W.: *Health risk analysis from volatile organic compounds and fne particulate matter in the printing industry*, International Journal of Environmental Science and Technology, 19, p.p. 8633-8644, 2022.

[7] Adamović, D., Čepić, Z., Adamović, S., Stošić, M., Obrovski, B., Morača, S., Vojinović Miloradov, M.: *Occupational exposure to formaldehyde and cancer risk assessment in an anatomy laboratory*, International Journal of Environmental Research and Public Health, 18, 11198, 2021.

[8] Photovac Monitoring Instruments (n.d.) PE Photovac Voyager Portable Gas Chromatograph, URL: https://clu-in.org/products/site/camp/photovac.htm (Pristupljeno, 28.10.2023.)

[9] Službeni glasnik Republike Srbije ("Sl. glasnik RS", br. 111/2015 i 83/2021): Uredba o graničnim vrednostima emisija zagađujućih materija u vazduh iz stacionarnih izvora zagađivanja, osim postrojenja za sagorevanje. URL: https://www.paragraf.rs/propisi/uredba-granicnim-vrednostima-emisija-zagadjujucih-materija-vazduh.html (Pristupljeno, 06.11.2023.)

[10] Occupational Safety and Health Administration (2011) Formaldehyde, URL: https://www.osha.gov/sites/default/files/publications/formaldehyde-factsheet.pdf (Pristupljeno, 06.11.2023.)

[11] The National Institute for Occupational Safety and Health (2014) Formaldehyde, URL: https://www.cdc.gov/niosh/idlh/50000.html (Pristupljeno, 06.11.2023.)

Autori: **Van. prof. dr Savka Adamović, Asistent sa doktoratom dr Rastko Milošević, Doc. dr Bojan Banjanin, Van. prof. dr Ivana Tomić, Van. prof. dr Dragan Adamović, Van. prof. dr Aleksandra Mihailović, Doc. dr Miroslav Dramićanin,** Univerzitet u Novom Sadu, Fakultet tehničkih nauka, Trg Dositeja Obradovića 6, 21000 Novi Sad, Srbija, Tel: +381 21 485 2634.

E-mail: adamovicsavka@uns.ac.rs
rastko.m@uns.ac.rs
bojanb@uns.ac.rs
tomic@uns.ac.rs
draganadamovic@uns.ac.rs
zandra@uns.ac.rs
dramicanin@uns.ac.rs

ETIKUM 2023 **INTERNATIONAL SCIENTIFIC CONFERENCE NOVI SAD, SERBIA, DECEMBER 7-9, 2023**

Andreeva, I., Gabechaya, V., Morev, D., Samardžić, M., Vasenev, I.

COMPARATIVE ASSESSMENT OF THE ECOLOGICAL STATE OF VINEYARD SOILS USING BIOLOGICAL AND CHEMICAL METHODS OF ANALYSIS

Abstract: *The assessment of the functional and ecological status of Eutric Cambisols with archaic and intensive vineyard cultivation system in the Fruška gora region of the Autonomous Province of Vojvodina, Republic of Serbia, is presented using a number of agrochemical, ecotoxicological and biological indicators. The study has showed significant differences between studied soil plots in the content of organic matter, the content of mobile sulfur and the gross content of copper in the upper horizons of the studied soils, which reflects the specifics of agrotechnical methods used in viticulture. The greatest contrast was in the biological activity of the soil indicator, determined by the rate of basal respiration, which in the soil with an archaic cultivation system was on average 5-11 times higher compared to the same indicator in the soil with an intensive industrial cultivation system, depending on the position on the vineyard's slope. The combination of chemical and biological methods seems to be the most effective methodological approach for a comprehensive assessment of the current ecological state of soils in ampelocenoses due to their special sensitivity to anthropogenic influences, and are best suited as express methods of soil-ecological monitoring.*

Key words: *soil assessment, ecological condition, vineyard, basal respiration, copper.*

1. INTRODUCTION

Vineyards are a unique type of agroecosystem, distributed in mountainous and hilly landscapes with their inherent regional and local climatic, geomorphological, hydrological and pedological conditions. In this regard, vineyards are complex, but extremely interesting objects of research from the point of view of studying the accumulation and migration of matter from autonomous to subordinate elementary landscapes under the conditions of the combined actions of natural and agrogenic factors.

Long-term cultivation of grapes on slopes of varying steepness, exposure, shape and length using mechanized agrotechnical operations, numerous treatments with pesticides and agrochemicals is accompanied by significant environmental risks. Thus, the long-term input of copper and other heavy metals into the soil of vineyards led to their intensive accumulation in the upper part of the soil profile and migration to associated components of ecosystems, especially in historical wine-growing regions [1].

Due to the scale of pollution and other negative processes in the soils of ampelocenoses, early diagnosis of changes in the normal course of chemical and biological processes in them is of particular importance. Soil chemical and biological indicators, such as organic carbon and microbial biomass, are important in terms of reflecting soil health and quality [2].

The soil microbial community responds rapidly to the presence of pollutants, exhibiting alterations in the total number of microorganisms, species diversity, soil enzyme activity, soil respiration, and processes influencing the cycling of essential nutrients. This, in turn, makes it possible to promptly adjust existing agrotechnical practices in order to increase the sustainability of ampelocenoses [3].

Among the numerous ascertainable microbiological indicators, the assessment of the ecophysiological status of the soil microbial community warrants special consideration. In particular, an indirect indicators, such as respiratory activity of the microbiome, are highly informative for evaluating organic matter decomposition efficiency, reflecting a wide range of ecosystem services, exhibiting considerable reliability and recognition, and possessing standardized and relatively straightforward methods for their determination [4].

Previous studies, aimed at identifying environmental risks for vineyard soils in the Northern Black Sea region, showed that the use of indicators of the biological state of the soil can provide valuable information for the decision-making system in viticulture, along with chemical indicators [5]. At the same time, there is an assumption that the possibility of using such indicators largely depends on local conditions and agricultural technologies used at the specific farm. In this work, an attempt is made to comparatively assess the ecological state of soils of vineyards of

different ages grown in the conditions of the Autonomous Region of Vojvodina of the Republic of Serbia, using both chemical and biological research methods.

2. OBJECTS AND METHODS

The research was carried out on the soil (Eutric Cambisols according to FAO) of two private wineries' vineyards, of different age, located near the town of Sremski Karlovci, Autonomous Region of Vojvodina, Republic of Serbia, in a slope landscape of Middle Danube Upland. The climate of the study area is temperate continental with elements of subhumid and mesothermal in some locations. The average annual air temperature in the study area is 11.8°C, the average annual precipitation is 764 mm.

The studied farms practice different systems of grape cultivation: the farm near the locality of Lipovac an intensive trellis-row system of management, including the complete mechanization of labor-intensive processes for caring for plants and the cultivation of row spacing under black fallow; farm near the Čerat locality - an archaic bush (standard) system of maintaining grape bushes, evenly distributed along the slope and processed entirely by hand.

Soil samples were collected under grape plants using a soil auger at depths of 0–5, 5-15 and 15–30 cm (Čerat) and 0-15 and 15-30 cm (Lipovac). Soil sampling was carried out within the conjugate transit landscapes of the slopes: transeluvial (upper Тэ1, middle Тэ2) and transaccumulative (lower Тэа) parts according to the scheme presented in Fig. 1.

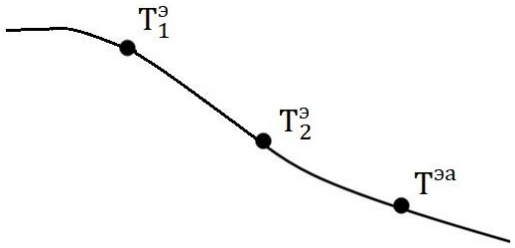

Fig. 1. Location schemes of soil sampling points in the transit landscape under vineyards

The soil was sieved through a 1-mm sieve, and plant roots, stones, and other inclusions were removed. pH in water was analyzed potentiometrically with glass electrode using a Mettler Toledo SevenCompact s220 pH-meter. Organic matter content is measured by the titrimetric method using a strong oxidizing agent ($K_2Cr_2O_7$) in the presence of H_2SO_4 with a Leki UV2107 spectrophotometer. Mobile sulfur (S) was determined by using 0.15 per cent $CaCl_2$ solution. All analyses were performed in triplicate. Determination of basal respiration (BR) was conducted in accordance with CEN EN ISO 16072-2011 Soil quality - Laboratory methods for determination of microbial soil respiration (ISO 16072:2002). Carbon dioxide content was analyzed using a Chromatec-Crystall 5000.1 gas chromatograph. BR rate was expressed in μg CO_2 C g^{-1} soil h^{-1}, with a fivefold repeatability.

The data were statistically processed using the R language.

3. RESULTS

The obtained data on pH, organic matter content, mobile sulfur, gross copper content and basal respiration rate of the soil of the studied vineyards are presented in Tables 1 and 2.

Agrochemical indicators were selected taking into account according to their most likely correlation with microbiological indicators and copper due to long-term use of copper-containing pesticides.

Table 1. pH value, content of organic carbon (Corg, %), mobile sulfur (S, mg/kg) and total copper content (Cu, mg/kg), basal respiration (BR) (μg CO_2 C g^{-1} soil h^{-1}) in soils of ampelocenoses at Lipovac locality

Part of slope	Depth, cm	pH	Corg	S	Cu	BR
Тэ1	0-15	8,6	1,2	23,8	21,4	0,20
	15-30	8,6	1,1	1,8	23,7	
Тэ2	0-15	8,6	3,0	42,3	41,9	0,43
	15-30	8,7	2,7	1,1	20,3	
Тэа	0-15	8,7	3,2	53,8	21,0	0,58
	15-30	8,9	3,0	1,7	20,8	

In the soil of the studied vineyards near the locality of Lipovac, the pH varied within a narrow range from 8.6 to 8.9, and in the locality of Čerat from 8.5 to 8.8, with a general tendency to increase with depth.

The content of organic matter (Corg) varied in the range of 1.1-3.0% in the Lipovac farm, and this indicator depended both on the part of the slope on which samples were taken and on the depth. Corg in the upper and middle parts of the slope was 2.7 and 1.1 times lower, respectively, than in the lower part. Apparently, this is due to the manifestation of the process of planar erosion of the top layer of soil and deposition on the lower part of the slope. Such processes contribute to the redistribution of matter along the slope from autonomous elementary landscapes to subordinate ones with accumulation in the latter. This is confirmed by data on the content of mobile sulfur and the content of copper

in the surface soil horizon in both farms studied. Thus, the content of mobile sulfur in the soil of the Lipovac locality in the upper and middle parts of the slope was 23.8 and 42.3 mg/kg, respectively, while in the lower transaccumulative part of the slope it was 53.8 mg/kg. The analogous situation of increasement of organic matter and mobile sulfur in surface horizons downslope was observed at Čerat locality.

Table 2. pH value, content of organic carbon (Corg), mobile sulfur (S) and basal respiration (BR) (μg CO_2 C g^{-1} soil h^{-1}) in soils of ampelocenoses at Čerat locality

Part of slope	Depth, cm	pH	Corg	S	Cu	BR
Тэ1	0-5	8,5	5,7	2,2	109,0	3,34
	5-15	8,8	4,4	4,1	95,1	2,49
	15-30	8,7	2,4	6,5	61,9	1,02
Тэ2	0-5	8,6	5,5	38,8	132,7	3,57
	5-15	8,8	3,6	37,4	72,3	1,92
	15-30	8,8	2,3	9,8	59,4	0,92
Тэа	0-5	8,5	8,0	36,2	128,3	7,52
	5-15	8,7	5,7	24,4	146,1	2,68
	15-30	8,7	5,8	2,4	247,5	1,52

It can be noted that the archaic system of grape cultivation on the Čerat, with its uniform distribution of individual grape bushes along a naturally grassed slope without mechanical tillage, contributed to a noticeably greater accumulation of organic matter in the soil than in an intensive vineyard with constant mechanical tillage of the rows.

The total Cu content in the soil at the Lipovac locality varied from 20.3 to 41.9 mg/kg. Copper accumulated predominantly in the 0-15 cm horizon of the middle part of the slope, and its content in the 0-15 and 15-30 cm horizons was almost equal.

In the soil of the Čerat locality, the Cu content was for an order of magnitude higher than in the Lipovac locality, with statistical significance (p-value=0.004) (Fig. 2). It can be assumed that this is due to the duration of continuous grape cultivation on given locality. The age of the vineyard at the Čerat is 200 years, while in Lipovac it is 15 years old. Thus, in the 0–5 cm horizon of the middle part of the slope, the copper content increased by 22% compared to the upper part of the slope, which was not observed in the 5–15 and 15–30 cm horizons. On the contrary, in the lower part of the slope, the accumulation of copper covered the entire studied part of the soil profile, which also indicates the process of deposition. The copper content in this part of the slope reached 247.5 mg/kg, which is 2.8 times higher than the maximum permissible amount of copper in medium loamy soils established in the Republic of Serbia.

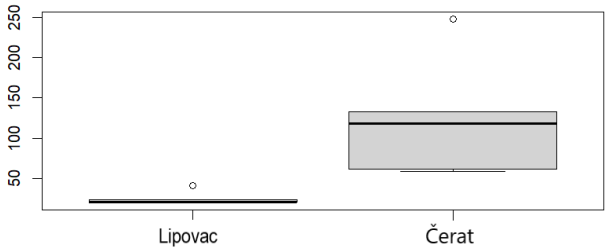

Fig. 2. Total copper content (mg/kg) in the upper horizon of the studied vineyard soils according to the Kruskal–Wallis criterion (p=0.004)

Taking into account the high steepness of the slope, on which the vineyard at Čerat is located, the active migration of copper from the upper to the lower part of the slope can also be related to the increased frequency of rainfall, which has been fixed in the last years in the Autonomous Region of Vojvodina [6].

By absolute value, basal respiration (BR) in the soil of the Čerat farm with an archaic cultivation system, on average 5-11 times higher compared to the same indicator in the soil with an intensive industrial cultivation system with statistical significance (p-value=0.02), depending on the position on the vineyard's slope (Fig. 3). At the same time, a common pattern was observed for the both farms in the change in BR along the slope and soil profile.

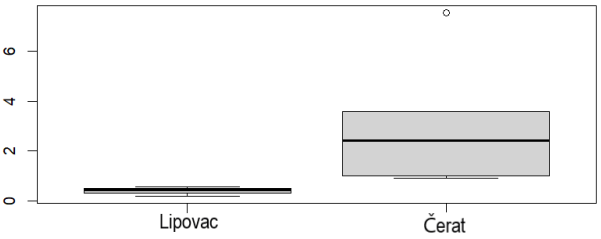

Fig. 3. Basal respiration (μg CO_2 C g^{-1} soil h^{-1}) in the studied vineyard soils according to the Kruskal–Wallis criterion (p=0.02)

The BR value increased from the upper to the lower part of the slope by 2.9 times in the Lipovac soil and by 2.3; 1.1 and 1.5 times in horizons 0-5, 5-15 and 15-30 cm, respectively, in Čerat soil. The BR indicator reached its maximum value for two farms, 7.52 μg CO2 C g−1 soil h−1, in the surface horizon of the lower part of the Čerat slope. Here, too, there was a tendency for BR to decrease from the surface horizon to the underlying ones. The correlation analysis showed that the observed patterns in BR changes fully correlate with the above-mentioned changes in organic matter content along the soil profile and slope (r = 0.83) (Fig. 4).

In addition, a positive and strong correlation (r = 0.81) was found between BR and gross copper content in soil. Typically, low BR values are interpreted as a sign of low biological activity of the soil, which can be caused in agroecosystems by various agricultural practices (mechanical tillage, pollution, application of pesticides and agrochemicals, low biodiversity, etc.). At the same time, too high BR values are also regarded as a response of the soil microbial community to the action of unfavorable environmental factors. In this study, such a factor was the excess of copper in the soil of Čerat as a result of many years of systematic use of copper-containing fungicides to protect grapes.

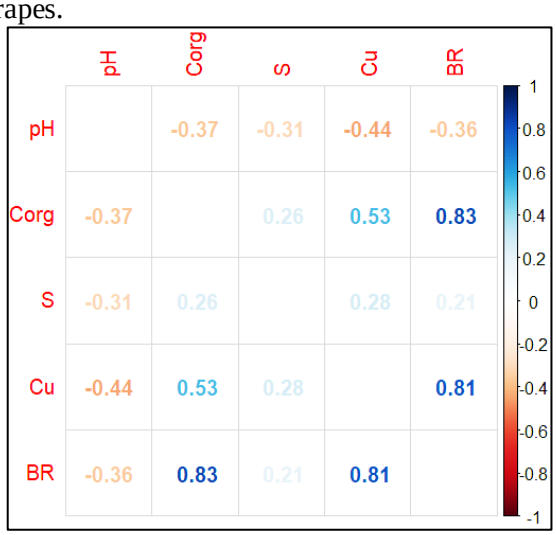

Fig. 4. Correlogram of Spearman's correlation analysis

Thus, using the example of basal soil respiration, studies have demonstrated the effectiveness of using not only individual chemical indicators (such as organic matter content in our research) but also the biological activity of ampelocenosis soils criteria to assess the changes occurring in it. This will make it possible to better characterize the direct response of the agroecosystem to anthropogenic impacts.

4. CONCLUSION

The use of criteria for the biological activity of soil, reflecting the occurrence of biological processes in it, is especially important for the environmental assessment of the current state of soils in ampelocenoses due to the environmental risks that accompany the cultivation of grapes.

The combination of chemical and biological methods seems to be the most effective methodological approach for a comprehensive assessment of the current ecological state of soils in ampelocenoses due to their special sensitivity to anthropogenic influences, and are best suited as express methods of soil-ecological monitoring.

5. FUNDING

The research was financed by the Ministry of Science and Higher Education of Russian Federation (Agreement № 075-15-2021-1030).

6. REFERENCES

[1] Lamichhane, J.R., Osdaghi, E., Behlau, F., Köhl, J., Jones, J., Aubertot, J.-N.: *Thirteen decades of antimicrobial copper compounds applied in agriculture. A review*, Agronomy for Sustainable Development, Vol. 38, 2018.

[2] Lehmann, J., Bossio, D.A., Kögel-Knabner, I., Rillig, M.C.: *The concept and future prospects of soil health.* Nature Reviews Earth & Environment, Vol. 1, p.p. 544-553, 2020.

[3] Amaral, H., Schwan-Estrada, K., Sena, J., Colozzi-Filho, A., Andrade, D.: *Seasonal variations in soil chemical and microbial indicators under conventional and organic vineyards*, Acta Scientiarum, Agronomy, Vol. 45, 2022.

[4] Ananyeva, N.D., Ivashchenko, K.V., Sushko, S.V.: *Microbial indicators of urban soils and their role in the assessment of ecosystem services (review)*, Soil Science, Vol. 54, p.p. 1517–1531, 2021.

[5] Gabechaya, V., Andreeva, I., Morev, D., Yaroslavtsev, A., Neaman, A., Vasenev, I.: *Exploring the Influence of Diverse Viticultural Systems on Soil Health Metrics in the Northern Black Sea Region*, Soil Systems, Vol. 7, p.p. 73, 2023.

[6] Malinović-Milićević, S., Mihailovic, D., Radovanovic, M., Dreško vić, N.: *Extreme Precipitation Indices in Vojvodina Region (Serbia)*, Journal of the Geographical Institute "Jovan Cvijić" SASA, Vol. 68, p.p. 1-15, 2018.

Authors: **Assoc. prof. PhD Irina Andreeva, Assis. Valeria Gabechaya, Assoc. prof. PhD Dmitry Morev, Prof. dr Miljan Samardžić, Prof. dr Ivan Vasenev**, Russian State Agrarian University - Moscow Timiryazev Agricultural Academy, Ecology Department, Timiryazevskaya str., 49, 127434 Moscow, Russian Federation, Phone: +7 499 976 4560.

E-mail: i.andreeva@rgau-msha.ru
lera.gabechaya@mail.ru
dmorev@rgau-msha.ru
miljan.samardzic@gmail.com
vasenev@rgau-msha.ru

ETIKUM 2023 **INTERNATIONAL SCIENTIFIC CONFERENCE NOVI SAD, SERBIA, DECEMBER 7-9, 2023**

Brborić, M., Nakomčić Smaragdakis, B., Turk Sekulić, M.

HUMAN HEALTH RISK ASSESSMENT DUE TO CONTAMINATION OF DANUBE RIVER SEDIMENTS WITH POLYAROMATIC HYDROCARBONS

***Abstract**: In the framework of the study, for the purposes of risk calculation due to the exposure of the human population to polyaromatic hydrocarbons (PAHs) detected in the Danube River, different data were used for human indicators depending on their gender and age. Using different scenarios, it was observed that the risk of cancerous outcomes for the human population exceeded prescribed safety limit of 10-6 for all ages in all localities , and the groups of children aged 5-11 (due to ingestion) and adolescents aged 12-19 (dermal contact) were the most at risk.*
***Key words:** Danube, sediment, PAHs, human health risk assessment*

1. INTRODUCTION

Polycyclic aromatic hydrocarbons (PAHs) are a type of carcinogens that come from the incomplete combustion of organic items and exist ubiquitously in the general and occupational environments [1,2]. Over 100 PAHs may be present in the environment as a mixture, and 16 of them are prioritized by the US EPA according to such factors as their toxicity, potential exposure, and carcinogenicity to human and animals [3,4].
Risk assessment for the human population is an integral part of complex hazard identification processes, with the defined probability and impact of each risk in the research with the possibility of proposing appropriate mitigation measures. Risk assessment is a quantitative parameter of the risk value that refers to the studied contamination phenomena and is directly related to the negative consequences that the risk causes. Consequently, for the purpose of assessing the risk to the human population due to exposure to the tested PAHs, an indirect approach was chosen, by performing a calculation based on available data from the literature, as well as by modifying the usual way of interpreting results through several different scenarios in order to assess as precisely and reliably as possible the negative impacts of contaminants accumulated in sediment of the Danube River.

2. MATERIAL AND METODS

Carcinogenic risk (CR) for the human population, expressed in ($mg^{-1}\cdot kg\cdot d$), at different ages (babies, children, adolescents and adults), as well as for the total life span, was calculated for the sum of 6 PCBs, 6 DDT, and 5 HCHs, through the two most significant routes of exposure, i.e., ingestion and dermal. The US Environmental Protection Agency [5] proposed the following equations to calculate the carcinogenic risk:

$$CR_{ing} = \frac{C_{sed} \cdot ingR \cdot EF \cdot ED \cdot CF \cdot SFO}{BW \cdot AT} \quad (1)$$

$$CR_{der} = \frac{C_{sed} \cdot SA \cdot AF_{sed} \cdot ABS \cdot CF \cdot SFO}{BW \cdot AT} \quad (2)$$

Where:
C_{ing} and C_{der} are the measured concentrations of contaminants due to ingestion and dermal contact, respectively, (μg/kg); ingR - ingestion rate (mg/day); EF - frequency of exposure (day/year); ED - duration of exposure (years); CF - unit conversion factor (-); SFO - oral slope factor (mg/kg·day); BW - body weight (kg); AT - average exposure time (day); SA - exposed skin area (cm^2); AFsed - adhesion factor of skin to sediment (mg/cm^2); ABS - dermal absorption from sediment (-).

The cumulative risk to human health for each examined locality was calculated as the sum of individual risks for each group of pollutants, with two ways of exposure of human indicators being considered. The characteristics of carcinogenic risk can be qualitatively described as follows (USEPA, 2009): $CR < 10^{-6}$: very low risk; $10^{-6} < CR < 10^{-4}$: low risk; $10^{-4} < CR < 10^{-3}$: moderate risk; $10^{-3} < CR < 10^{-1}$: high risk; $CR < 10^{-1}$: very high risk. Exposure where the risk factor exceeds $1E^{-6}$ (1 case per million people) is considered significant.

Different values of ingestion rate, body mass and exposed skin surface were used for each age depending on gender. Although reference values of the ingestion rate of 200 mg/day for children and 100 mg/day (values for land) for adolescents

and adults were used in the literature, modified values are stated in the article. Ingestion rate was calculated according to Wilson et al. [6], where the final value was obtained by adding the rate of ingestion via hand-to-mouth contact and contact with suspended sediment. The obtained value was multiplied by the number of hours of daily exposure of the population to contaminated sediment (3, 5 and 8 hours). For the exposure frequency, the most extreme scenario was applied, assuming that the human indicators were exposed to the sediment throughout the year. The average exposure time is calculated as the product of the exposure frequency and the average lifetime (according to USEPA [5] it is 70 years). The reference values previously used for the surface of skin exposed to sediment were 5700 cm^2 (values for land). This value represented the average value of the skin surface of the legs of an adult man. In order to obtain a more precise assessment of the risk due to dermal contact of the human population with sediment, the study used individual values for the area of the legs and the area of the entire body for all ages and genders. AF_{sed} and ABS values are taken from USEPA [5].

3. RESULTS AND DISCUSSION

In the framework of the research, for the purposes of calculating the risk due to the exposure of the human population, different data were used for human indicators depending on their gender and age. The values used in the calculation of the risk of ingestion and dermal contact for babies (from 7 months to 4 years), children (from 5 to 11 years), adolescents (from 12 to 19 years) and adults/able-bodied (older than 20 years).

3.1. Risk assessment due to ingestion

Based on the obtained values of the carcinogenic risk factor (CR) due to the presence of 29 PAHs contaminants in the sediment of the Danube River, it was established that in certain selected localities there is a significant connection with the occurrence of carcinogenicity caused by the exposure of the human population through ingestion. In Table 1. the cumulative risk values for the tested pollutants are shown depending on the degree of ingestion, i.e. time exposure (scenario 1: 3h, scenario 2: 5h and scenario 3: 8h) to contaminated sediment.

Table 1. Cumulative risk to human health (mg^{-1}·kg·d) for the tested pollutants due to ingestion

	Babies (7m-4)	**Children (5-11)**		**Adolescents (12-19)**		**Adults (>20)**	
		M	**Ž**	**M**	**Ž**	**M**	**Ž**
Scenario 1	$9.3E^{-5}$	$1.5E^{-4}$	$1.6E^{-4}$	$4.1E^{-5}$	$4.3E^{-5}$	$7.2E^{-5}$	$8.3E^{-5}$
Scenario 2	$1.5E^{-4}$	$2.5E^{-4}$	$2.6E^{-4}$	$6.8E^{-5}$	$7.2E^{-5}$	$1.2E^{-4}$	$1.4E^{-4}$
Scenario 3	$2.5E^{-4}$	$4.0E^{-4}$	$4.2E^{-4}$	$1.1E^{-4}$	$1.2E^{-4}$	$1.9E^{-4}$	$2.2E^{-4}$

It is observed that with increasing exposure time, the carcinogenic risk factor also increases. For the group of carcinogenic PAHs compounds, the prescribed safety limit of 10^{-6} for all ages was exceeded in all localities (Figure 1). 71% of the obtained values were above 10^{-4}. The research showed that all human indicators were equally threatened, with slightly higher values for the female sex. However, the highest values of risk factors were registered for children aged 5-11 years and both sexes in the locality D9, near Pančevo (women: $8.56 \cdot 10^{-4}$ mg^{-1}·kg·d and men: $8.14 \cdot 10^{-5}$ mg^{-1}·kg·d for an eight-hour exposure to sediment), while the lowest values were determined for male adolescents at the locality Ratno ostrvo (D5), in the vicinity of Novi Sad.

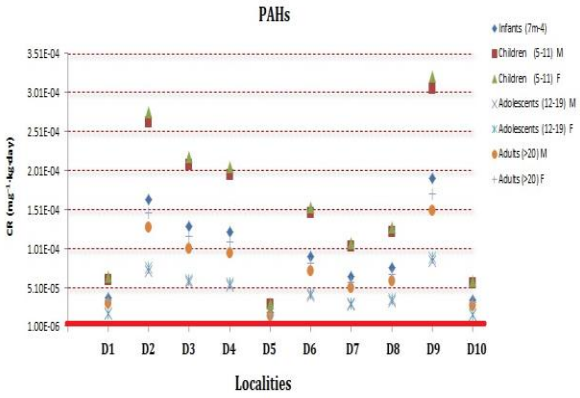

Fig. 1. Risk assessment due to ingestion of human population exposed to PAHs contamination of Danube sediment

3.2. Risk assessment due to dermal contact

During the risk assessment, two scenarios of dermal exposure to contaminated sediment were considered: 1) if only the legs were exposed to the human indicator and 2) if the whole body was exposed to the human indicator. Obtained carcinogenic risk values for different groups of tested pollutants are shown in Table 2. The results of the carcinogenic risk point to the fact that the potential risk is conditioned by the equal presence of the studied groups of pollutants in the sediment, but also that the risk increases significantly if the dermal surface in contact with the sediment increases.

Table 2. Cumulative risk to human health (mg^{-1}·kg·d) for the examined pollutants due to dermal contact

	Babies (7m-4)	Children (5-11)		Adolescents (12-19)		Adults (>20)	
		M	Ž	M		M	Ž
Scenario 1	$1.6E^{-5}$	$6.1E^{-5}$	$6.4E^{-5}$	$6.9E^{-5}$	$7.3E^{-5}$	$4.5E^{-5}$	$5,2E^{-5}$
Scenario 2	$5.8E^{-5}$	$2.0E^{-4}$	$2.1E^{-4}$	$2.1E^{-4}$	$2.3E^{-4}$	$1.4E^{-4}$	$1,6E^{-4}$

Based on the obtained values for the detected concentration levels of PAHs in aquatic sediment, it can be concluded that if a child, adolescent or adult comes into contact with the sediment with the entire surface of their body instead of only the skin on their feet, the risk of cancer exceeds the permitted prescribed limit (10^{-6}) and can be considered very significant. Also, this is the case if scenario 1 is replaced by scenario 2 for babies, there will be a higher probability of carcinogenic consequences due to the presence of PAHs in the sediment.

Graphic representations of carcinogenic risk due to dermal contact are shown in Figure 2. CR values during dermal contact with Danube sediment contaminated with PAHs in all localities significantly exceeded the prescribed limit of 10^{-6} for all ages and sexes. Even 80% of the results exceeded the coefficient of 10^{-5}, and about 14% exceeded 10^{-4}. The highest values were recorded in the locality Ritopek (D9) for female adolescents if the whole body surface was exposed to the sediment ($4.65 \cdot 10^{-5}$ mg^{-1}·kg·d), while the lowest values characterized the locality Ratno ostrvo (D5) for babies from 7 months to 4 years ($3.18 \cdot 10^{-6}$ mg^{-1}·kg·d).

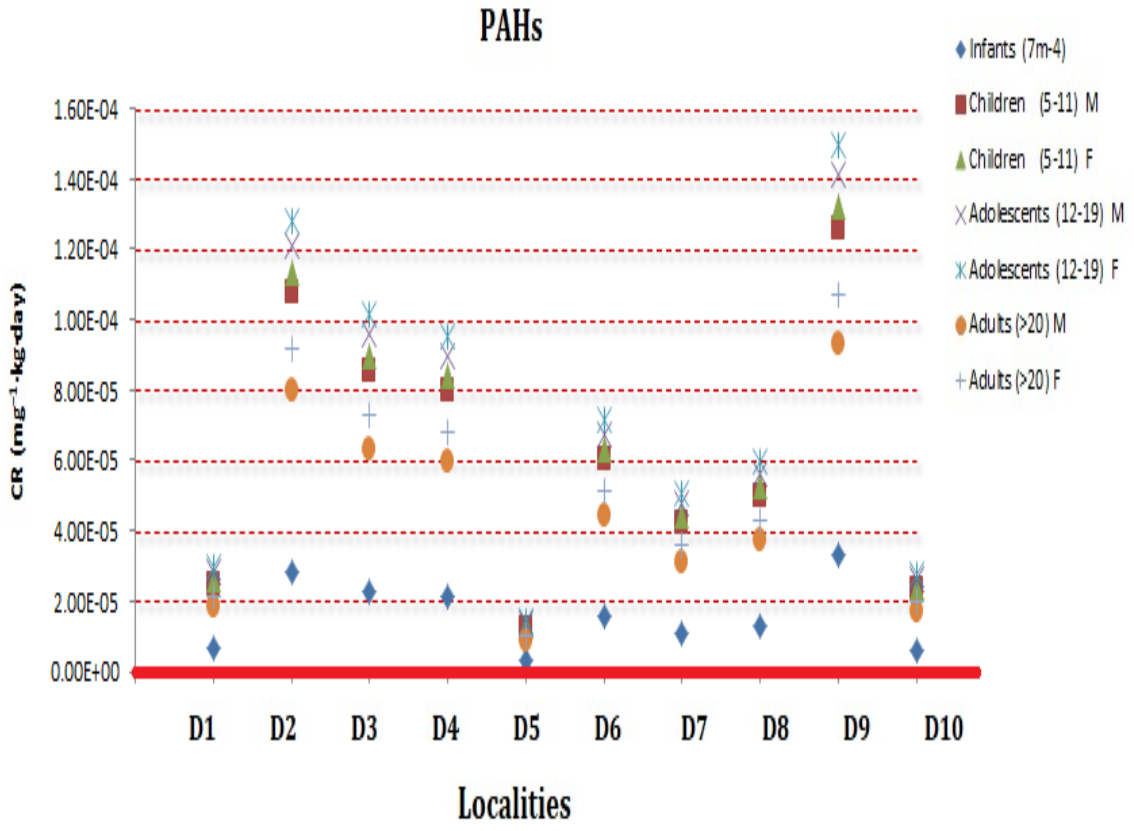

Fig. 2. Risk assessment due to dermal contact of human population exposed to PAHs contamination of Danube sediment

4. CONCLUSION

Based on the overall analysis of the obtained results, it can be concluded that the Danube River bank flow at the territory of Serbia still has significant potential pollution sources of aquatic systems with PAHs, which is important information to conduct more extensive monitoring and prevent further disposal of equipment that containing these pollutants by adequate controls, thus diminishing the extremely negative ecotoxicological effects currently present in the aquatic system. Within the framework of such a systematized research process, it would be necessary to include more media (biotic and abiotic) in the analysis as well as more specific points.

5. ACKNOWLEDGMENTS

This research was supported by the Science Fund of the Republic of Serbia, grant number 6707, REmote WAter quality monitoRing anD IntelliGence – REWARDING and the Ministry of Science, Technological Development and Innovation through project no. 451-03-47/2023-01/200156 "Innovative scientific and artistic research from the FTS (activity) domain".

6. REFERENCES

[1] Kamal, A., Cincinelli, A., Martellini, T., Malik, R.N., 2015. A review of PAH exposure from the combustion of biomass fuel and their less surveyed effect on the blood parameters. Environ. Sci. Pollut. Res. 22, 4076–4098

[2] Shen, H., Huang, Y., Wang, R., Zhu, D., Li, W., Shen, G., et al., 2013. Global atmospheric emissions of polycyclic aromatic hydrocarbons from 1960 to 2008 and future predictions. Environ. Sci. Technol. 47, 6415–6424.

[3] Morales P, Roscales J, Muñoz-Arnanz J, Barbosa A, Jiménez B, Evaluation of PCDD/Fs, PCBs and PBDEs in two penguin species from Antarctica, Chemosphere (2022) 286(Pt 3):131871. doi: 10.1016/j.chemosphere.2021.131871.

[4] Xie J, Tao L, Wu Q, Bian Z, Wang M, Li Y, Zhu G, Lin T, Bioaccumulation of organochlorine pesticides in Antarctic krill (Euphausia superba): Profile, influencing factors, and mechanisms. J Hazard Mater (2022) 15;426:128115. doi: 10.1016/j.jhazmat.2021.128115. Epub 2021 Dec 22.

[5] USEPA (2009) Risk Assessment Guidance for Superfund, Vol. I: Human Health Evaluation Manual (Part F, Supplemental Guidance for Inhalation Risk Assessment): Final. Environmental Protection Agency, Washington. EPA/540/R/070/ 002.

[6] Wilson J., Berntsen H.F., Zimmer K.E., Verhaegen S., Frizzell C., Ropstad E., Connolly L. (2015) Do persistent organic pollutants interact with the stress response? Individual compounds, and their mixtures, interaction with the glucocorticoid receptor. Toxicologye Letters 241:121-32.

Authors: **Scien. Assoc. dr Maja Brborić, Full prof. dr Branka Nakomčić Smaragdakis, Full prof. dr Maja Turk Sekulić**

University of Novi Sad, Faculty of Technical Sciences, *Department of Environmental Engineering and Occupational Safety and Health*, Trg Dositeja Obradovića 6, 21000 Novi Sad, Serbia

E-mail: majabrboric@uns.ac.rs
nakomcic@uns.ac.rs
majaturk@uns.ac.rs

ETIKUM 2023 **INTERNATIONAL SCIENTIFIC CONFERENCE NOVI SAD, SERBIA, DECEMBER 7-9, 2023**

Brborić, M., Nakomčić Smaragdakis, B., Turk Sekulić, M.

OCCURRENCE AND CHARACTERIZATION OF DIOXIN CONTAMINATION IN DANUBE SEDIMENTS

***Abstract**: Since dioxins are detected in all environmental matrices and have been identified as harmful substances due to their toxicity, persistence, and bioaccumulation in humans and wildlife, they are still one of the important groups of POPs. For this reason, this original approach studies the toxicological influence of dioxins, quantified in sediment samples collected at ten sites along the river Danube, by an application of advanced classification and clustering method such as hierarchical cluster analysis. Selected multivariate technique was applied to the monitoring dataset in order to obtain visual images of the components distributed at each sampling site when all components are included in the classification and data projection procedure.*
***Key words:** Danube, sediment, dioxins, hierarchical cluster analysis*

1. INTRODUCTION

Organochlorine compounds have been in the focus of interest and research for the past several decades due to their prevalence in the entire environment and their toxic effects on human and animal health[1]. The most widespread of this group of compounds are polychlorinated biphenyls (PCBs), organochlorine pesticides (OCPs) and dioxins, which will be discussed in this paper. Groups of compounds called dioxins for short belong to polychlorinated dibenzop-dioxins (PCDD) and polychlorinated dibenzofurans (PCDF).

Dioxins are undesirable by-products in various combustion processes at temperatures between 200 °C and 400 °C, especially in the presence of metals as catalysts and carbon and chlorine. All these compounds have in common the properties of persistence, lipophilicity, toxicity, bioaccumulation and the possibility of long-distance airborne transmission, and are part of the group of persistent organic pollutants (POPs) [1,2]. Due to these properties, they are found together in all parts of the environment and are distributed in them.

Due to the presence of organic matter in soil and sediment, POPs bind very tightly, and soil and sediment particles act as environmental collectors and reservoirs. In this way, these particles become a secondary source of pollution of water, plants, animals and, ultimately, humans. Due to their lipophilicity in humans and animals, they accumulate in tissues containing fat (liver, kidneys, adipose tissue) and in serum and milk [3,4]. A wide range of toxic and biochemical effects have been observed in laboratory animals treated with these compounds, while some of these effects have also been observed in humans after accidents or prolonged occupational exposure. Today, their production and use is prohibited and/or limited, and in recognized sources of dioxins and furans, efforts are being made to limit or completely eliminate their emission. Despite this, they are still present in all parts of the environment and circulate among them, thus keeping their level at the so-called steady state. In order to assess their distribution in the environment, and thus possible human exposure, organochlorine pollutants are analyzed in food, air, soil, sediment, plants, various animal species and humans[5,6]. Out of a total of 210 PCDD and PCDF congeners, the most toxic congeners, of which there are a total of 17, are most often analyzed individually.

In 1997, the International Agency for Research on Cancer classified 2,3,7,8-tetrachlorodibenzo-p-dioxin (eng. 2,3,7,8-tetrachlorodibenzo-p-dioxin, TCDD) as the most prominent representative of the dioxin group and as proven carcinogenic substance. Due to its chemical, physical and biological stability, TCDD is extremely stable in the environment [7], with a half-life of 8 to 15 years for surface and 25 to 100 years for deep sediment [8] with a tendency to bioaccumulate in biological tissues, including human tissues. Tetrachlorodibenzo-p-dioxin is formed as a by-product of incomplete combustion. It is released into the environment during the burning of fossil fuels and wood and during the incineration of industrial waste.

2. MATERIAL AND METODS

2.1. Sediment samples collection

The sampling was performed in October 2012. For this investigation, 10 samples of bottom sediment from different sites of Danube River through Serbia (Apatin- D1 (1401 km), Labudnjača- D2 (1367 km), Neštin- D3 (1264 km), Begeč- D4 (1275 km), Ratno Ostrvo- D5 (1257 km), Šangaj- D6 (1250 km), Knićanin- D7 (1214 km), Belegiš- D8 (1199 km), Ritopek- D9 (1141 km), Dubravica- D10 (1103 km)) were collected using a grab sampler (Fig. 1). Samples were taken to the laboratory in an ice cooler, where they were weighed and sealed to avoid contamination. All sediment samples were analyzed in the laboratory of Research Centre for Toxic Compounds in the Environment - *RECETOX* (Brno, Czech Republic) after two days. Before analysis, wet sediment samples were sieved through 2 mm sieve to remove leaves, stoned and roots. The sediments were well homogenized and subsamples were taken in 150 ml glass jar for freeze-drying.

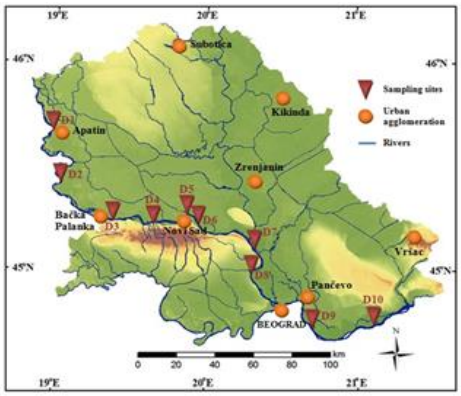

Fig. 1. Danube River sampling sites

2.2. Sample analysis

Freeze-dried sediment samples were extracted with dichloromethane in a Büchi System B-811 automatic extractor. One laboratory blank and one reference material were analyzed in parallel with each set of ten samples. Surrogate "recovery" standards (13C labeled standard for dioxins and furans (800 pg tetra-hexa PCDDs/Fs, 1600 pg hepta-octa PCDDs/Fs) were injected into each sediment sample before extraction.

After Soxhlet extraction, the concentrated extracts were purified with silica gel modified with sulfuric acid (30% w/w) and eluted with 40 ml of a mixture of DCM/n-hexane (1:1). Fractionation was achieved in a micro column (6 mm) containing from bottom to top: 50 mg silica gel, 70 mg charcoal/silica gel (1:40) and 50 mg silica gel. The column was previously washed with 5 ml of toluene and with 5 ml of a mixture of DCM/cyclohexane (30%). The sample was then eluted with 9 ml of a mixture of DCM/cyclohexane (30%) in fraction 1 (mono-ortho dl-PCBs) and 40 ml of toluene in fraction 2. Fractions were concentrated using a stream of nitrogen in a TurboVap II (Caliper LifeSciences, USA) and transferred to a GC-MS vial. Standard was injected into all samples to a final volume of 50 µl.

For the quantification of PCDD/Fs, instrumental analysis, high resolution gas chromatography–high resolution mass spectrometry (HRGC/HRMS) was applied.

2.3. Data analysis

In order to increase the performance of the modelling procedure, applying the hierarchical cluster analysis (HCA) approach to recognize and group the subsets of the large amount sediment samples data with a similar pattern can be helpful [8]. HCA allowed grouping the sampling localities depending on the concentration levels of PCSS/Fs in the Danube sediment. Statistical analysis was implemented applying the IBM SPSS Statistics 22 software (IBM Corporation, Armonk, New York, U.S.). The proposed methodologies and results obtained in this paper provided valuable assessment using the HCA visualization capabilities and highlighted zones of priority that might require additional investigations and also provide productive pathway for effective decision making and remedial actions.

3. RESULTS AND DISCUSSION

The concentration levels of compounds from the group of polychlorinated dibenzo-p-dioxins and dibenzofurans in Danube sediment samples collected as part of the research at 10 investigated sites are shown in Figure 2. At the investigated sites, significant spatial fluctuations of concentrations during the deposition of PCDDs and PCDFs were recorded.

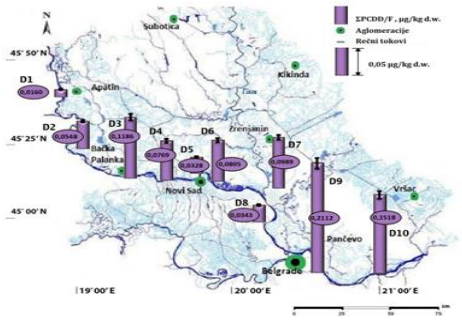

Fig. 2. Spatial distribution of PCDDs and PCDFs in sediment samples

In sediment samples, the highest content of PCDDs/Fs, expressed as the sum of seven polychlorinated dibenzo-p-dioxins and ten dibenzofurans, was detected at the Ritopek site (0.211 µg/kg, with a median of 0.00079 µg/kg and a mean value of 0 .01242 µg/kg), while the lowest value was recorded at the Apatin locality (0.016 µg/kg), with a mean value of 0.088 µg/kg and a median±SD of 0.079±0.060 µg/kg.

When analyzing the compositional profile, i.e. the share of individual compounds in the total contribution of PCDD/Fs contamination in sediment samples of the Danube River in the territory of Serbia (Figures 7.9 and 7.10), a clear dominance of PCDD/Fs with eight substituted chlorine atoms was observed, where the OCDD content represented from 83.3 (D8) % to 94.5 % (D10) of the total concentrations of detected dioxins, while the share of OCDF ranged from 36.6 % (D7) to 60.4 % (D8) of the total concentrations of furans. The fractions of tested compounds detected in Zlin district were lower for octa dioxins and furans and amounted to 84.85 and 41.3 %, respectively. In most samples, the proportion of 2378-TCDD was very low and the highest values were registered at the Labudnjača locality (0.6%). In the locality Knićanin, fraction 2378-TCDF of 6.6% was registered.

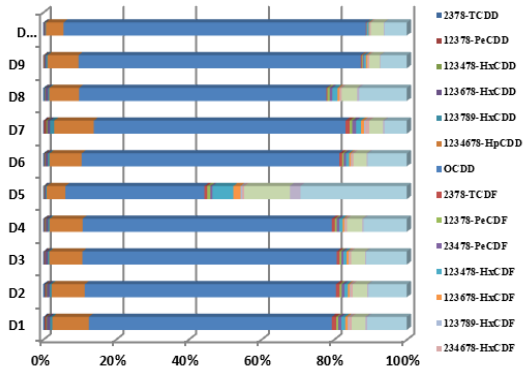

Fig. 3. Composition of PCDD and PCDF congeners in the riverbed sediment from Danube River

3.1. Hierarchical cluster analysis

Hierarchical cluster analysis using the Ward method was applied to the results of the analysis of the main components in order to group the examined locations according to the similarity in the composition of the Danube sediment. The obtained dendograms, with isolated clusters of localities, of the sampled Danube sediment are shown in Figure 4.

On the dendogram, four clusters were distinguished. The **first** cluster includes the localities of Apatin (D1), Belegiš (D8) and Ratno ostrvo (D5). The lowest concentration levels of the tested pollutants were recorded at the investigated localities. Uncontrolled burning of waste and industrial activities in the past, however, caused the quantification of PCDD/Fs in the examined parts of the Danube basin. The **second** cluster included the localities of Labudnjača (D2), Begeč (D4), and Šangaj (D6) and reflects a moderate load of contaminants, due to industrial activities and the presence of incomplete combustion processes. Localities D4 and D6, which are located upstream and downstream of Novi Sad, were exposed to the long-term negative impact of the factory of parts for the automotive industry "Motins", the cable factory "Novkabel" and the industry for the production and processing of paper/cardboard ("A-REA" d.o.o.- Kartonaža Novi Sad", "Neopak", Sremska Kamenica). The **third** caster separated the localities Neštin (D3), Ritopek (D9) and Dubravica (D10), while the **fourth** separated only the locality Knićanin (D7) with the dominant influence of the Tisa River on the Danube sediment. The increased levels of PCDD/Fs at sites D3 and D9 were contributed by the pulp and paper industry in Belgrade (cardboard factory "Umka" and company for the production of transport, commercial and laminated packaging "Avala Ada") and Bačka Palanka ("Grafokartonka"), in the immediate vicinity of the sampling site. Also, the elevated concentration levels at the site D10 are interpreted as a consequence of the proximity of the factory for the production of steel (in a radius of 10 km), hot and cold rolled products and white sheet in the village of Radinac (Company "HBIS GROUP Serbia Iron & Steel" d.o.o. Belgrade, former "Železara Smederevo" d.o.o.).

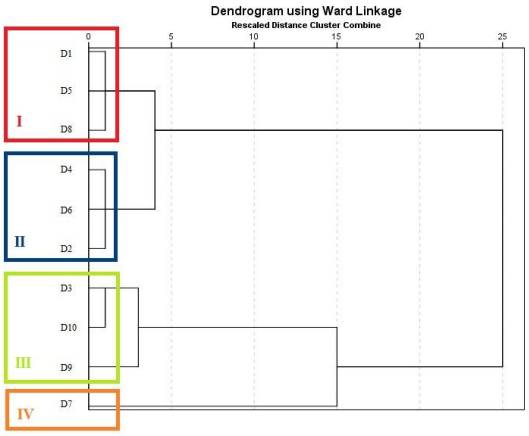

Fig. 4. Hierarchical dendogram for sediment data clustering of sampling sites from the Danube

4. CONCLUSION

Quantified total concentrations of examined lipophilic persistent organic pollutants, PCDDs and PCDFs, in sediment samples were relatively low. The obtained results are highly valuable information about the current status of the observed heterogeneous river system. At localities in the Republic of Serbia, both in the total concentration levels and in the fractions of individual analytes, there are significant oscillations of the detected concentrations, partly conditioned by the primary emission sources. While the sampling points varied from rural to highly industrial locations, the total measured concentrations in the sediment mass showed values of ΣPCDD/Fs: min 0.016 μg/kg - max 0.211 μg/kg.

Based on the overall data analysis of the obtained results, it can be established that the Danube riverbank flow at the territory of Serbia still has significant potential pollution sources of aquatic systems with PCDD/Fs, which is important information to conduct more extensive monitoring and prevent further disposal of equipment that containing these pollutants by adequate controls, thus diminishing the extremely negative ecotoxicological effects currently present in the aquatic system. Within the framework of such a systematized research process, it would be necessary to include more media (biotic and abiotic) in the analysis as well as more specific points.

5. ACKNOWLEDGMENTS

This research was supported by the Science Fund of the Republic of Serbia, grant number 6707, REmote WAter quality monitoRing anD IntelliGence – REWARDING and the Ministry of Science, Technological Development and Innovation through project no. 451-03-47/2023-01/200156 "Innovative scientific and artistic research from the FTS (activity) domain".

6. REFERENCES

[1] Abad E, Sauló J, Caixach J, Rivera J. *Evaluation of a new automated cleanup system for the analysis of polychlorinated dibenzo-p-dioxins and dibenzofurans in environmental samples*. J Chromatogr A 2000;893:383-91.

[2] Hosomi M, Matsuo T, Dobashi S, Katou S, Abe H. *Survey of dioxins in Tokyo Bay bottom sediment*. Mar Pollut Bull 2003;47:68-73.

[3] Srogi K. *Levels and congener distributions of PCDDs, PCDFs and dioxin-like PCBs in environmental and human samples: a review*. Environ Chem Lett 2008;6:1-28.

[4] Shan G, Leeman WR, Gee SJ, Sanborn JR, Jones AD, Chang DPY, Hammock BD. *Highly sensitive dioxin immunoassay and its application to soil and biota samples*. Anal Chim Acta 2001;444:169-78.

[5] Reiner EJ, Clement RE, Okey AB, Marvin CH. *Advances in analytical techniques for polychlorinated dibenzo-p-dioxins, polychlorinated dibenzofurans and dioxin-like PCBs*. Anal Bioanal Chem 2006;386:791-806.

[6] Nichkova M, Park E-K, Koivunen ME, Kamita SG, Gee SJ, Chuang J, Van Emon JM, Hammock BD. *Immunochemical determination of dioxins in sediment and serum samples*. Talanta 2004;63:1213-23.

[7] Bjurlid F., Roos A., Jogsten I.E., Hagberg J. *Temporal trends of PBDD/Fs, PCDD/Fs, PBDEs and PCBs in ringed seals from the Baltic Sea (Pusa hispida botnica) between 1974 and 2015*. Science of The Total Environment 2018,616–617: 1374-1383.

[8] Wang P., Shang H., Li H., Wang Y., Li Y., Zhang H., Zhang Q., Liang Y., Jiang G. *PBDEs, PCBs and PCDD/Fs in the sediments from seven major river basins in China: Occurrence, congener profile and spatial tendency*. Chemosphere , 2016, 144: 13-20.

[9] Yang, Y., Shu, G., Liang, Z., Yunwei, W., Gaocong, l., Yaping, W., Zhuochen, H., Peihong, J. *Classifying the sedimentary environments of the Xincun Lagoon, Hainan Island, by system cluster and principal component analyses*. Acta Oceanologica Sinica 2017, 36, 64–71.

Authors:
Scien. Assoc. dr Maja Brborić,
Full prof. dr Branka Nakomčić Smaragdakis,
Full prof. dr Maja Turk Sekulić

University of Novi Sad, Faculty of Technical Sciences, *Department of Environmental Engineering and Occupational Safety and Health*, Trg Dositeja Obradovića 6, 21000 Novi Sad, Serbia
E-mail: majabrboric@uns.ac.rs
nakomcic@uns.ac.rs
majaturk@uns.ac.rs

ETIKUM 2023 **INTERNATIONAL SCIENTIFIC CONFERENCE**
NOVI SAD, SERBIA, DECEMBER 7-9, 2023

Đorđević, G., Petković, M., Zarev, I., Jocić, N., Klikovac, A.

RISK MANAGEMENT IN FIRE PROTECTION AS A CONSEQUENCE OF ELECTROSTATIC ELECTRICITY

***Abstract**: Electrostatic charge, even if it does not represent a large amount of charge in terms of its quantity, represents a permanent danger of occurrence and explosions, and a series of negative events warns that the damage caused by this phenomenon is a danger both to human life and causing great material damage. Knowing how electrostatic charge is created, the places where this charge poses a great danger and how we must protect ourselves from this charge is the basis for managing the risk of hazards caused by electrostatic charge.*
***Key words:** electrostatic charge, risk, conductivity*

1. INTRODUCTION

Electrostatic discharge is a phenomenon that is increasingly mentioned as a cause of fires or explosions. Even if, due to its quantity, it falls into the category of relatively small non-electricity, its occurrence and manifestation represent a great danger during certain technological processes, which as such must be observed and the method of treatment and method of protection determined, in order to prevent fires and explosions.

The charge that leads to electrostatic electricity most often arises as a result of the contact of two unequal materials, be it solid or solid and liquid, while this is not a characteristic for gaseous substances.

The danger from electrostatic charging is particularly pronounced:

1. In places threatened by explosive mixtures of gases, steam or dust with air
2. When working with explosive substances and ammunition
3. In production processes where there is no danger of explosive mixtures, but electrostatic electricity is a potential source of fire and damage due to disruptions in production.

2. ELECTROSTATIC CHARGING OF SOLID MATERIALS

From the aspect of charge accumulation, solid materials that have a specific volume conductivity of less than 1 pS/m and a surface conductivity of less than 1 pS and that are able to hold the created charge for a long time, i.e. with a charge relaxation time of more than 20 seconds, are particularly dangerous.

Solid materials can most often be charged by contact charging due to separation, friction, etc.

Non-conductive materials that are applied as coverings to metal parts pose a lower risk than such materials that are not in contact with metal. In certain cases, increasing conductivity gives good results. For example, by adding graphite to rubber products, such items have a lower possibility of accumulating electrostatic charge.

Protection against electrostatic charging - technical measures

Dangers from electrostatic charging occur when so much charging accumulates in one place that when a discharge occurs and the limit of flammability and explosiveness can lead to an explosive mixture of gases, steam, dust or explosive substances upon ignition.

Accumulation of static electricity in production facilities is prevented:

Grounding

Grounding must be applied to all electrically conductive parts in the production plant, regardless of whether other preventive measures against static electricity have been applied. Grounding is performed by galvanically connecting all conductive parts of the plant to the object's grounding device. The moving parts of the plant, via copper, bronze or carbon brushes, are connected to the grounding system. The brushes must be vertically and firmly mounted on the rotating shaft, with adequate pressure on the surface of the shaft.

Air ionization using appropriate ionizers

There are several types of air ionizers such as:

- stick air ionizers
- fan air ionizers
- ionizers with nozzles, etc.

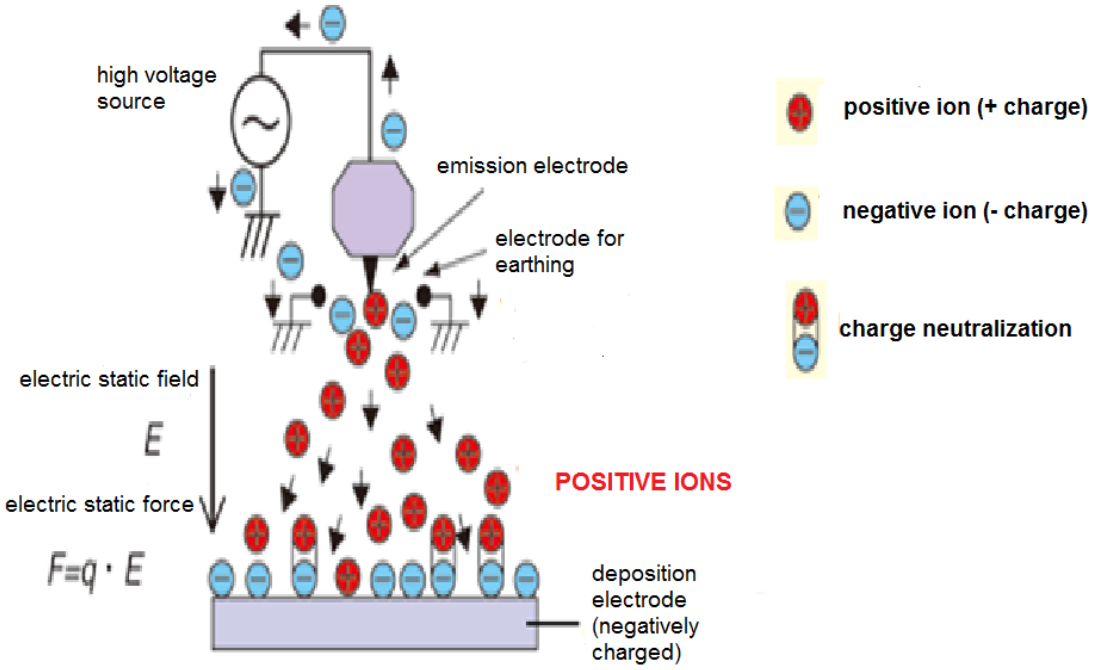

Fig. 1. Principle of operation of the air ionizer [2]

The principle of operation of the static electricity eliminator (ionizer) is based on the application of high voltage (direct DC or alternating AC) on the emission electrode (discharge electrode). It causes the formation of corona discharges between the emission electrode and the ground electrode. An electrostatic eliminator (ionizer) actually ionizes the air using a corona discharge, thus creating positive and negative ions. Of the obtained ions, those required for static elimination (q) are moved to the charged object (precipitation electrode) by means of the Coulomb force (F) acting in the direction of the obtained electrostatic field (E). In this way, the neutralization of the static charge is achieved, that is, the so-called electrostatic removal is performed. In order to achieve better conductivity of insulating materials, colloidal graphite must be added to natural or synthetic rubber. Metal oxides can also be used as additives. Higher conductivity of poorly conductive liquids is increased by adding e.g. ethyl alcohol. Instead of increasing the conductivity of the entire material, it is often sufficient to increase only the surface conductivity. For this purpose, the surface of the material is coated with colloidal graphite, carbon black or glycerin. These coatings should be periodically renewed.

Dissipating static electricity with flue

Metal arresters of static electricity in the form of grounded brushes, combs, barbed arresters, etc. should be placed as close as possible to the material from which static electricity is to be removed, but at such a distance that it does not touch the protected material (about 15 mm above the material). On parts of the plant that are rotated during the technological process, i.e. from which it is separated, e.g. textile or foil material, above the place of greatest accumulation of static electricity, a grounded brass rod must be placed on which brass chains are attached at intervals of 50 mm. During the movement of the

material, the chains come into contact with its surface and slide away static electricity from it.

3. MEASURES OF PROTECTION AGAINST ELECTROSTATIC CHARGING IN CERTAIN TECHNOLOGICAL PROCESSES

Manipulation of commercial explosives, transport and storage of explosive materials and protection against electrostatic charging

Places where explosive substances are used, such as: mines, quarries, road construction, tunnels, etc., which have permanent or temporary storage places for explosive substances must take measures to protect against electrostatic charging.

The clothing of workers who manipulate explosive substances must not be made of silk, nor must it contain fibers of synthetic material. Clothing should be made of cotton material to prevent the formation and discharge of electrostatic charges. The footwear of workers who manipulate explosive substances must be made of leather and conductive rubber. Brass plates should be installed in the soles of the shoes in order to establish a galvanic connection between the shoes and the ground. Workers who handle explosive materials should not wear rings, bracelets and metal objects.

Floors in rooms with explosive materials must be conductive in the role of removing electrostatic charge, handles, doorknobs, locks should be connected to the grounding system.

When packing explosive materials in bags, they must be made of electrically conductive materials with embedded metal strips in the fabric.

When packing explosive materials, tables, chairs, ventilation systems must be properly grounded. It is also necessary to maintain a relative humidity of 70% in those rooms.

Transportation of flammable and combustible liquids and gases, dangers and protection against electrostatic charging

Tanks for the transport of flammable liquids and gases are subject to a high concentration of electrostatic charge. Vehicles and tanks have many metal parts and these parts must be electrostatically connected (galvanic connection) so that the electrostatic charge has a path to earth.

Conditions for electrostatic discharge of explosive atmosphere during transportation of dangerous goods

In order for an explosive atmosphere to ignite, two conditions must be met at the same time:

- that the permitted concentration of vapors of flammable liquids and air should be between the lower and upper limit of flammability or explosiveness
- that the electrostatic discharge is greater than the minimum ignition energy of the mixture of flammable liquids and air

Factors that affect the amount of electrostatic charge are:

- type of material
- environmental conditions
- repetition of the process

Electrostatic charging must be controlled to avoid electrostatic discharge and ignition of the explosive mixture. Control of electrostatic charge can be done in one of the following ways:

- by reducing the accumulated charge (for example, by reducing the flow rate of petroleum products and the like)
- discharge removal (grounding, equalization of potential, adding additives to oil derivatives, etc.)

Electrostatic charging can occur in tank vehicles, lifting devices, pipelines, tanks and people who handle flammable substances. Electrostatic charging in humans can occur due to:

- movement on the surface
- wearing inappropriate clothes
- combining and separating clothes on people with objects (chairs, etc.)
- manipulations with non-conductive objects or objects

Protection of people from the creation of electrostatic charge and prevention of ignition is done by installing electrically conductive floors, grounding things and objects, using appropriate clothing and footwear.

Electrostatic discharge during the transportation of dangerous goods

Electrostatic charging during the transportation of dangerous goods, where it is created on the means of transport due to the movement of the vehicle, due to friction, the accumulation of charges occurs. As a protection measure, it is mandatory to ground the tanks during filling and emptying. When filling and emptying tanks, the supply pipe must be grounded. At the end of the cable used for grounding, an insulated handle with a switch is placed, the stationary part of which is connected to the movable part only when the cable on the tank is turned on. The switch and plug for the earthing cable must be in Ex protection, degree II A T3.

All connection connections should be inspected in detail and only when it is concluded that they are properly connected and grounded can the filling or emptying of the tank be allowed. The pipe for filling the cistern should be immersed in the cistern so that it is at least 50 mm away from the bottom of the cistern.

When filling and emptying a cistern with a plastic tank, it must be discharged after galvanic connection and earthing due to the movement of electrostatic charge. From the moment of connection to the ground when filling and emptying the tank, you must wait at least 15 minutes before starting the filling or emptying of the tank.

When pouring oil derivatives into a tank vehicle, the surface tension on the liquid itself in the tank increases depending on the amount of derivative, and then the charge for flammable liquids is transferred to the metal tank of the tank, where the inside of the tank is charged negatively and the outside of the tank is positively charged.

Figure 2 shows the potential voltage and discharge energy during tank filling

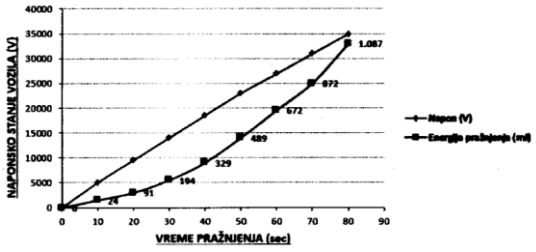

Fig. 2. Potential voltage and discharge energy during tank filling

Protection measures against uncontrolled electrostatic discharge during loading and unloading of dangerous goods

In order to reduce and eliminate the possibility of electrostatic discharge when loading or unloading dangerous goods, appropriate protection measures must be applied, namely:

- grounding the tank
- filling the tank with flammable liquid must not be filled at a speed greater than 1 m/s until the pipe is below the liquid level
- the filling pipe must be at the bottom of the tank
- the tank must be cleaned before filling
- it is necessary to check what substance was in the tank before filling
- if there was another liquid in the tank before, it must be cleaned
- the filling hose should be fixed before filling
- after filling, the hose is removed after a period of time of one minute to avoid the possibility of a spark due to electric charges.

Figure 3 shows the danger zones of tanks with flammable liquids during transfer, where there is a risk of fire and explosion due to electrostatic charging.

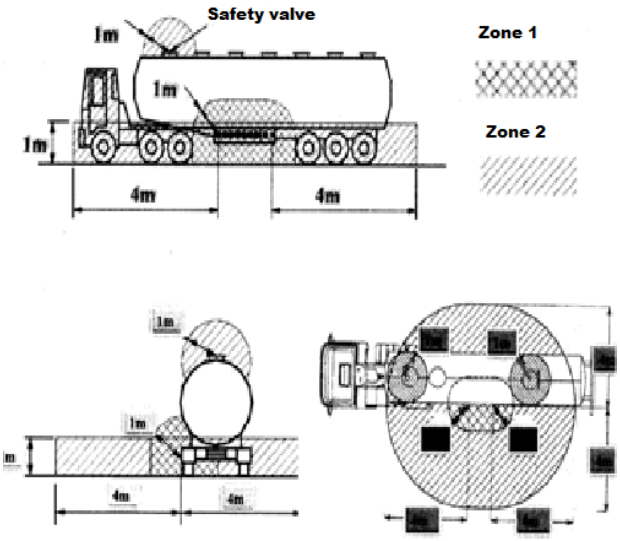

Fig. 3. Danger zones of tanks with flammable liquids during transfer

4. EXAMPLE OF FIRE AND EXPLOSION AS A RESULT OF ELECTROSTATIC CHARGING

As an example of the incident, the fire and explosion at the Bradarac-Naruljevac crude oil well No. 3 in the Braničevo district, which belongs to "NIS" a.d., was taken. Novi Sad, "NIS Naftagas" Novi Sad, the cause of which was electrostatic charging.

Event description:

On September 20, 2018, around 7:30 p.m., there was a fire and an explosion at the well for the exploitation of crude oil in the Bradarac - Maruljevac field, at well No. 3. The wells are located in the municipality of Požarevac in the Braničevo district.

The fire occurred at a crude oil well during overhaul and maintenance by "NIS" workers. d. Novi Sad-pogon remont, department for overhaul works Zrenjanin.

According to the statements and according to the work order, in the process of overhauling the well, hot water is injected into the well under pressure, and paraffin and natural gas, which are also products accompanying the extraction of crude oil, are released through the mounted hose. Paraffin and natural gas are delivered to open plastic tanks-tubs with partitions where they are stored and then transported via tankers for transporting dangerous goods-cargo.

The entire procedure should take place according to special rules prescribed by the company act.

Dangers

Natural gas is heavier than air and collects in the lower parts of the tank-tub, and since the tank is open, mixtures of natural gas and air can also be found around the tank.

By injecting hot water under pressure into the well, an electrostatic charge is created, which absorbs both paraffin and natural gas, as well as the vessel in which they are stored.

The occurrence of a suitable discharge (spark and the like) can cause a fire to explode.

Documents issued during the renovation works:

- Decision on overhaul works on the Bradarac-Maruljevac well No. 3 dated September 8, 2018, issued by the research and production block - plant "Srednji Banat".
- The program of ongoing overhaul of the Bradarac-Maruljevac borehole No. 3 signed by the manager of the geological survey, which was signed on behalf of the workers who carried out the overhaul, which is illegal.
- In chapter In the program of the current overhaul, fire protection measures were given, which the employees did not adhere to during the overhaul work.

Disadvantages and improper work that day during repair work:

1. Adequate protection against electrostatic charging was not provided because the tank-tub in which paraffin and natural gas were stored was not grounded and connected to the grounding system.
2. When loading the dangerous cargo into the tank, there was no proper grounding with a handle and a proper switch in Ex protection as a basic protection against electrostatic charging.
3. The electrical equipment that was in use at the time of the fire and that was used in the danger zones of the tub-reservoir is not in the appropriate degree of Ex protection.
4. In the video before the fire broke out, it can be seen that the worker is illuminating the workplace with a mobile phone, which is prohibited and described in the overhaul program.
5. The equipment that was used during the overhaul works does not have certificates that it is non-sparking equipment.
6. There was no training for the workers who carried out the overhaul on the dangers and measures of protection against fire and explosions at the place where they worked and the dangers of electrostatic charging.
7. The workers did not have certificates of completion of special training in the field of fire protection.
8. Workers did not wear appropriate footwear and clothing as a measure of protection against electrostatic charging.

Jobs that were not intended as repair work and that led to (caused) a fire and explosion:

During the work that day, at the time when the fire broke out, the workers carrying out the repair work used a hose and a nozzle to wash the tank-tub under water pressure, and due to the speed and impact of the water, it was discharged and due to the presence of electrostatic charge and the presence of flammable gas vapors with air there was a spark discharge and a fire.

Consequences

As a result of the fire and explosion, three workers were injured, two seriously with life-threatening first-degree burns and one with minor burns, who were taken to the health centers in Belgrade, and the less injured to the Požarevac health center.

The fire spread to other buildings, but was stopped by the intervention of the fire department.

Part of the equipment and plant near the origin of the fire and explosion was damaged, with major material damage.

Other defects important for fire protection:

1. No consent was obtained for the safe installation of buildings and tanks with flammable liquids.
2. Approval was not obtained for the technical documentation and implemented fire protection measures for the plant.
3. Improvised overhead electric lines pass above buildings and tanks with flammable liquids, which is not allowed and is dangerous.
4. An open container was used as a tank-tub, which widens the danger zones and increases the risk.
5. The bathtub-reservoir was made of plastic, which is susceptible to electrostatic charging due to poor electrical conductivity.

Special aggravating circumstances when determining the cause of the fire and explosion: The company deleted part of the video, which shows the type of work during the overhaul when the fire and explosion occurred, which was recorded by security cameras (washing the tank-tub with a pressurized water jet).

5. STATISTICAL DATA ON FIRES CAUSED BY ELECTROSTATIC CHARGING IN THE REPUBLIC OF SERBIA FOR THE PERIOD 2011-2021

In the Republic of Serbia in the last ten years, there have been fires caused by electrostatic charging. And if that number seems to be very small, it must not be ignored that fires and explosions caused by electrostatic charging cause great danger, often great material damage and the constant threat to human life. Also, determining the cause of a fire when it comes to electrostatic charging is often enough complex and without concrete and clear indications, so the number of fires with this cause is certainly higher, and often there are in the part where the cause of the fire is undetermined. Table 4 shows the number of fires in the Republic of Serbia caused by electrostatic charging in the period from 2011 to 2021.

Table 4. Number of fires in the Republic of Serbia caused by electrostatic charging in the period from 2011 to 2021

The number of fires in the Republic of Serbia that were investigated in the period 2011-2021	Number of fires caused by electrostatic charging
257 521	25
100 %	0,009%

Proposal for improvements in the protection against electrostatic charge

When we look at the area related to electrostatic charging, what can be concluded is that there are very few legal and by-laws that must follow this area. The Rulebook that regulated this area (the Rulebook on Technical Normatives for Protection from Static Electricity (Official Gazette of SFRY 62/73) [4]) has been repealed, so it is necessary to pass a by-law that should regulate this area as the basis for the system protection and risk management of electrostatic charge.

As much as it seems that electrostatic discharge is small and does not represent a permanent danger, the very events where this discharge led to large fires and explosions, endangering human lives and great material damage warn us that we must pay special attention to this risk. That is why it is necessary, first of all, in the part of the basic training program for fire protection workers, which is characteristic of a legal entity in whose facilities and space there is a risk of electrostatic charging, to include and separately process this type of risk with all risks, and especially with the part that refers to taking measures for protection against possible discharge, which causes fire or explosion.

In the special part of the training that is carried out for persons who work in fire protection, it is necessary to carry out special training for persons who in their legal and other subjects have plants, plants, vehicles and equipment that are threatened by electrostatic charging.

Inspection bodies that carry out inspections in legal and other subjects in which there is a danger and risk of electrostatic charging must pay special attention and prompt control to this risk in order to avoid the immediate danger of fire and explosions such as the oil industry, dedicated production, production of explosive substances, gas stations, transportation of dangerous goods and similar facilities. For all facilities and objects and objects, especially technological processes that are subject to the dangers of electrostatic charging, it is necessary to create appropriate technical documentation in which the dangers will be dealt with in detail and prescribed protection measures that should prevent the occurrence and discharge of electrostatic charges and cause fire and explosion.

In all these entities, it is necessary to prescribe and adopt regulations for the operation and application of protection measures against electrostatic charging, and all hazards and protection measures should be detailed in the fire protection plan.

6. CONCLUDING CONSIDERATION

The concept of electrostatic charging is a phenomenon that must be seriously understood and treated as a danger that can cause fires and explosions with serious consequences, both for objects and for people. Knowing how this phenomenon occurs, how to collect it and how to initiate and cause fires and explosions is important if we want to reduce the dangers of this risk and bring the risk management system to the level of comprehensive protection against the manifestation of this risk. Where this phenomenon is expressed, appropriate protection measures must be applied, both in the organizational and in all other segments of appropriate training and the application of appropriate preventive measures, so that the risk and danger management system from electrostatic charging is effective.

7. LITERATURE

[1] Law on Flammable and Combustible Liquids and Combustible Liquids (Official Gazette of RS No. 62/73)

[2] https://www.smc.eu/hr-hr/proizvodi/istaknuti-proizvodi/ionizatori

[3] Despotović Ž. *Basic principles of operation of ionizers for industrial air purification, Power Point Presentation*, College of Electrical Engineering and

Computing of Vocational Studies, Belgrade, 2015.
[4] Rulebook on technical standards for protection against static electricity (Official Gazette SFER 62/73) - out of force
[5] Sremac S., Matijašević, M.: *Transport of dangerous goods*, Faculty of Technical Sciences Novi Sad, 2021
[6] Vladimir Kapor: Static electricity-scientific meeting, fires, explosions, prevention, Sarajevo 1987.
[7] Recommended practice on static electricity, NFPA 77
[8] Directive 2004/54 EC
[9] Directive 2010/35 EU

Authors: Goran Đorđević, PhD, Academy of Vocational Technical Studies Belgrade, Dr. Martina Petković, PhD - Kosovo and Metohija academy of applied studies, Department Zvečan, Nušićeva br.6, Zvečan, Serbia, Tel: +381 28 664-179, Fax: +381 28 664-179. Ivan Zarev, PhD, Fire Protection Expert, Belgrade, Nenad Jocić, UP RS-Sector for Emergency Situations, Administration for Prevention Belgrade, Anita Klikovac, Msc, Department of Emergency Situations in Smederevo, Sector for Emergency Situations, Ministry of the Interior, Serbia
E-mail**:** goranzop@gmail.com
martinaeco@yahoo.com
ivan.zarev@mup.gov.rs
nenad.jocic@mup.gov.rs
anitaklikovac@yahoo.com

ETIKUM 2023 **INTERNATIONAL SCIENTIFIC CONFERENCE NOVI SAD, SERBIA, DECEMBER 7-9, 2023**

Gvoić, V., Agarski, B., Kerkez, Đ., Vukelić, Đ., Prica, M.

OCENJIVANJE ŽIVOTNOG CIKLUSA I ISPITIVANJE UTICAJA SINTEZE HETEROGENOG FENTON KATALIZATORA NA ŽIVOTNU SREDINU

Rezime: *Primena različitih Fenton katalizatora u tretmanu otpadnih voda ostvaruje veliki potencijal sa aspekta uklanjanja brojnih organskih polutanata, ali se neretko zaobilazi tumačenje uticaja primenjene metode na životnu sredinu. Razmatranje ekoloških i ekonomskih aspekata u svim fazama sintetičkog postupka i razvoj novih materijala za sintezu Fenton katalizatora je od velikog značaja. Stoga je u radu izvršeno ocenjivanje životnog ciklusa (eng. life cycle assessment – LCA) sinteze heterogenog Fenton katalizatora, gvožđe(III)-molibdata, koje ima za cilj da ustanovi sve materijalne i energetske tokove u svakoj fazi procesa, odnosno da ispita ekološke performanse sinteze, identifikujući kritične faze navedenog procesa.*

Ključne reči: *ocenjivanje životnog ciklusa, gvožđe(III)-molibdat, heterogena Fenton kataliza, otpadne vode*

1. UVOD

Kako se svest o očuvanju životne sredine povećava, industrija sve veću pažnju usmerava ka razmatranju činjenice kako se sprovedeni proizvodni procesi odražavaju na životnu sredinu. Određivanje najbolje raspoloživih tehnika zahteva odabir najučinkovitijih tehnika uz postizanje visokog nivoa očuvanja životne sredine u celini, što dalje zahteva implementaciju ekoloških sirovina i procesa, kao i praksu koja se bazira na minimizaciji otpada, nultoj emisiji i odgovornosti proizvođača. Na taj način se podstiče integracija eko-dizajna u razvoju proizvodnog procesa [1].

Metodologija ocene životnog ciklusa (eng. *life cycle assesment analysis* - LCA), usled sveobuhvatnog pogleda i međunarodne standardizacije, predstavlja studiju koja razmatra sve materijalne i energetske tokove u svim fazama životnog veka proizvoda, uz procenu uticaja životnog ciklusa materijala na životnu sredinu, od ekstrakcije sirovine do završne faze kada proizvod postane otpad [2]. U okviru tretmana industrijskih otpadnih voda, LCA metodologija je prevashodno korišćena za ekološku ocenu tehnologija zasnovanih na fizičko-hemijskim procesima [3] i u okviru poređenja konvencionalnih i alternativnih tretmana optimizovanih za životnu sredinu [4]. Ipak, primena bilo koje tehnologije otpadnih voda trebala bi da se odnosi ne samo na efikasnost degradacije, mineralizacije ili smanjenja toksičnosti, već da obuhvati celokupan uticaj na životnu sredinu. Ovo bi moglo biti posebno relevantno u slučaju unapređenih procesa oksidacije, koji su obično veoma zahtevni sa aspekta potrošnje hemikalija, električne energije i generisanja degradacionih proizvoda sa potencijalnim uticajem na životnu sredinu (mulj obogaćen metalima, iskorišćeni čvrsti katalizatori, itd.) [5].

U radu je izvršeno ocenjivanje životnog ciklusa u cilju razmatranja ekoloških aspekata sinteze heterogenog Fenton katalizatora (gvožđe(III)-molobdata – $Fe_2(MoO_4)_3$), uzimajući u obzir sve materijalne i energetske tokove u svakoj fazi procesa sinteze pomenutog katalizatora.

2. EKSPERIMENTALNI DEO

Za procenu uticaja životnog ciklusa na životnu sredinu (eng. *life cycle impact assessment* - LCIA) primenjena je The ReCiPe Endpoint (H) 2016 metoda sa Europe ReCiPe H/A setom normalizacionih i težinskih faktora [6], dok su za inventar životnog ciklusa korišćeni procesi iz Ecoinvent v3.4 baze podataka sa sistemom modeliranja alokacije na tački supstitucije (eng. *Allocation at point of substitution* - APOS) [7], uz podršku programa OpenLCA 1.7. Ceo proces je preračunat na funkcionalnu jedinicu (1 kg katalizatora) koja je uvedena za poređenje funkcionalno ekvivalentnih proizvoda ili procesa. Granice sistema za sintezu gvožđe(III)-molibdata obuhvataju: potrošnju destilovane vode, iskorišćeni filter papir, potrošnju amonijum-hidroksida, amonijum molibdata-tetrahidrata, gvožđe(III)-nitrata nonahidrata, potrošnju električne energije usled rada magnetne mešalice, pumpe za filtraciju, sušnice i peći za žarenje i odlaganje papira (slika 1).

U tabeli 1 je prikazan inventar životnog ciklusa za sintezu gvožđe(III)-molibdata.

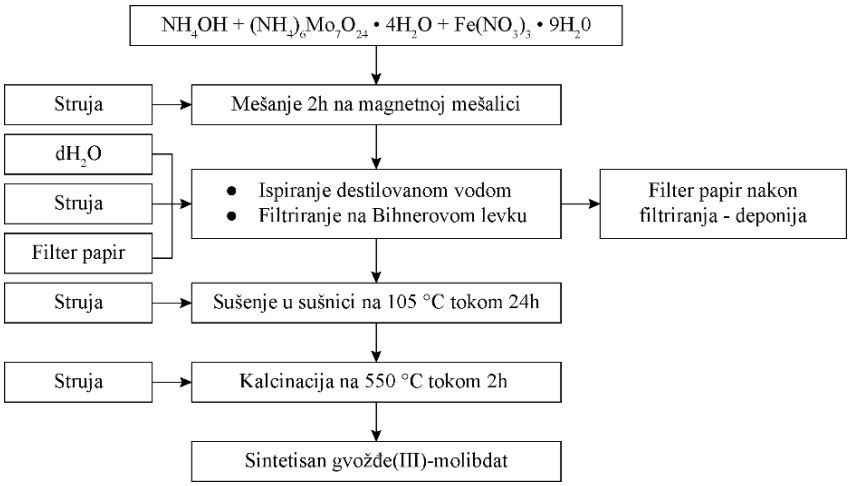

Sl. 1. Granice sistema za sintezu heterogenog Fenton katalizatora, gvožđe(III)-molibdata

Tabela 1. Inventar životnog ciklusa sinteze gvožđe(III)-molibdata po funkcionalnoj jedinici

Aktivnost	**Naziv iz Ecoinvent baze**	**Količina**	**Jedinica**	**Komentar**
	Ulazni tokovi			
Destilovana voda	Market for water, deionised, from tap water, at user | water, deionised, from tap water, at user – APOS, S – Europe without Switzerland	350	kg	Ukupna potrošnja destilovane vode
Filter papir	Market for paper, newsprint | Paper, newsprint | APOS, S - RER	0,070	kg	Suv filter papir korišćen za filtraciju
Amonijum-hidroksid (NH_4OH)	Market for ammonia liquid | ammonia liquid | APOS, S - RER	1,380	kg	Amonijum-hidroksid korišćen za sintezu katalizatora
Amonijum molibdat-tetrahidrat **(**$(NH_4)_6Mo_7O_{24}$ * $4H_2O$**)**	Market for ammonium molybdate terahydrate| ammonium heptamolybdate | APOS, S - RER	2,470	kg	Amonijum molibdat-tetrahidrat korišćen za sintezu katalizatora
Gvožđe(III)-nitrat nonahidrat ($Fe(NO_3)_3$ * $9H_2O$)	Market for iron(III) nitrate nonahydrate | iron(III) nitrate nonahydrate | APOS, S - RER	3,750	kg	Gvožđe(III)-nitrat nonahidrat korišćen za sintezu katalizatora
Potrošnja struje usled rada magnetne mešalice	Market for electricity, low voltage | Electricity, low voltage | APOS, S - RS	40	kWh	Potrošnja struje usled rada magnetne mešalice
Potrošnja struje usled rada pumpe za filtraciju	Market for electricity, low voltage | Electricity, low voltage | APOS, S - RS	50	kWh	Potrošnja struje usled rada pumpe za filtraciju
Potrošnja struje usled rada sušnice	Market for electricity, low voltage | Electricity, low voltage | APOS, S - RS	5280	kWh	Potrošnja struje usled rada sušnice
Potrošnja struje usled rada peći za žarenje	Market for electricity, low voltage | Electricity, low voltage | APOS, S - RS	4000	kWh	Potrošnja struje usled rada peći za žarenje
	Izlazni tokovi			
Iskorišćen filter papir	Market for waste newspaper | APOS, S - GLO	0,220	kg	Iskorišćen filter papir koji ide na deponiju
Sintetisan gvožđe(III)-molibdat **(**$Fe_2(MoO_4)_3$**)**	-	1	kg	Sintetisan $Fe_2(MoO_4)_3$

3. REZULTATI I DISKUSIJA

Rezultati ispitivanja mehanizama za ocenjivanje uticaja putem kategorija uticaja krajnjeg nivoa prikazani su na slici 2 u bezdimenzionim bodovima. Interpretacijom rezultata u vidu kategorija uticaja: kvalitet ekosistema, ljudsko zdravlje i izvori, uočava se najizraženiji negativan uticaj sinteze gvožđe(III)-molibdata u pogledu ljudskog zdravlja (1135 bodova).

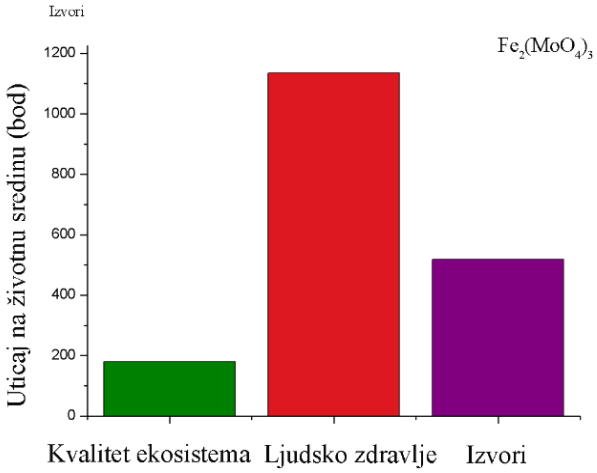

Sl. 2. Uticaj na životnu sredinu po kategorijama uticaja krajnjeg nivoa

Analizirajući detaljnije doprinose unutar svake kategorije uticaja (slika 3), zaključuje se da sinteza heterogenog Fenton katalizatora u okviru kategorije uticaja ljudskog zdravlja ostvaruje najveći doprinos putem uticaja na klimatske promene, toksičnosti po ljude i formiranje čestičnih materija. Posmatrajući kategoriju izvora uočava se izražen uticaj na potrošnju resursa fosilnih goriva i potrošnju resursa metala, dok je u slučaju kvaliteta ekosistema izražen uticaj na klimatske promene. Ovakav ishod je očekivan budući da je u sintezi katalizatora korišćeno više polaznih supstanci, izvršeno je sušenje i kalcinacija sintetisanog materijala, što rezultuje izraženom upotrebom konvencionalne električne energije i dovodi do većeg negativnog uticaja na životnu sredinu. Treba uzeti u obzir da je sinteza heterogenog Fenton katalizatora sprovedena u laboratorijskim uslovima i da bi tokom industrijske proizvodnje bile korišćene znatno veće količine osnovnih resursa, što bi ujedno predstavljalo i energetski zahtevnije procese.

Doprinos različitih procesa u sintezi heterogenog Fenton katalizatora prikazan je na slici 4, gde se zaključuje da tržište električne energije ostvaruje najveći uticaj budući da su u toku sintetičkog procesa korišćeni uređaju poput laboratorijske mešalice, sušnice, peći za žarenje i pumpe za filtraciju.

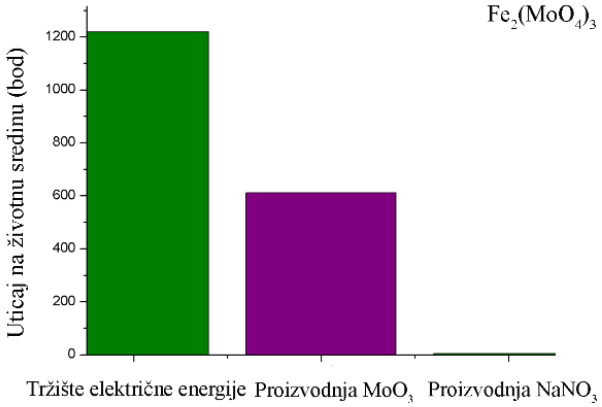

Sl. 4. Doprinos odabranih procesa u sintezi katalizatora gvožđe(III)-molibdata

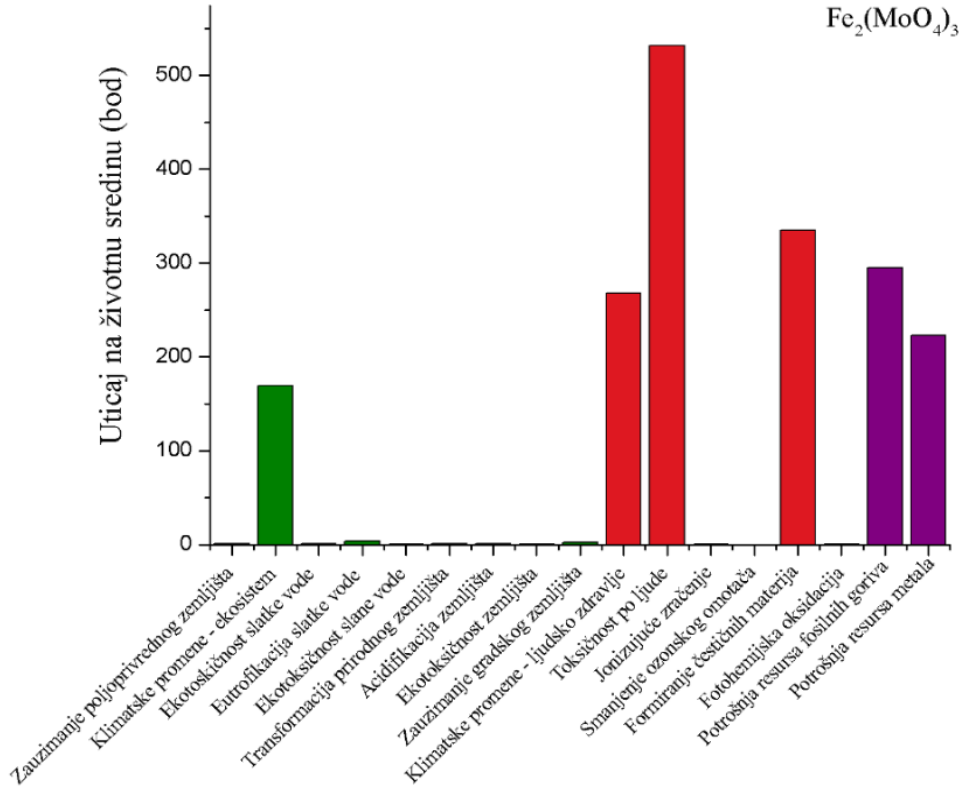

Sl. 3. Rezultati kategorija uticaja krajnjeg nivoa za katalizator gvožđe(III)-molibdat

4. ZAKLJUČAK

Iako su brojna istraživanja potvrdila da heterogeni Fenton proces prevazilazi brojne nedostatke homogenog Fenton procesa, poput smanjene reaktivnosti, primene visokih doza gvožđa i rad u ograničenom pH opsegu, rezultati ove studije ukazuju na izražen negativan uticaj sinteze heterogenog Fenton katalizatora na životnu sredinu.

Najveći doprinos sinteze heterogenog Fenton katalizatora je ustanovljen putem uticaja na klimatske promene, toksičnost po ljude, formiranje čestičnih materija, potrošnju resursa fosilnih goriva i potrošnju resursa metala. Usled izražene potrebe za potrošnjom električne energije za izvedbu energetski zahtevnih procesa, manji ukupan uticaj na životnu sredinu bi mogao da se ostvari proizvodnjom električne energije koja se zasniva na primeni obnovljivih izvora energije i manjim udelom fosilnih izvora. Pored toga, manji ukupan uticaj na životnu sredinu bi mogao da se ostvari primenom alternativne osnovne sirovine za sintezu katalizatora, odnosno druge soli gvožđa.

Buduća istraživanja bi trebala da budu usmerena u pravcu poboljšanja sinteze heterogenog Fenton katalizatora, ali i u pravcu sinteze, razvoja i primene alternativnih „zelenih“, ekološki prihvatljivih Fenton katalizatora, koji bi bili favorizovani kako sa aspekta uticaja na životnu sredinu, tako i sa aspekta ekonomske isplativosti celokupnog sintetičkog postupka.

5. ZAHVALNICA

Istraživanja predstavljena u radu su realizovana u okviru projekata 451-03-47/2023-01/200156 i 451-03-47/2023-01/200125, finansiranih od strane Ministarstva nauke, tehnološkog razvoja i inovacija Republike Srbije.

6. REFERENCE

[1] Oldfield, T., White, E., Holden, N.: *The implications of stakeholder perspective for LCA of wasted food and green waste*, Journal of Cleaner Production, 170, p.p. 1554-1564, 2018.

[2] Agarski, B., Nikolić, V., Kamberović, Z., Anđić, Z., Kosec, B., Budak, I.: *Comparative life cycle assessment of Ni-based catalyst synthesis processes*, Journal of Cleaner Production, 162, 7-15, 2017.

[3] Conde, J., Abelleira, S., Estevez, S., Gonzalez-Rodriguez, J. *Improving the sustainability of heterogeneous Fenton-based methods for micropollutant abatement by electrochemical coupling*, Journal of Environmental Management, 332, 117308, 2023.

[4] Awad, H., Alalam, M., El-Etriby, H.: *Environmental and cost life cycle assessment of different alternatives for improvement of wastewater treatment plants in developing countries*, Science of the Total Environment, 660, p.p. 57-68, 2019.

[5] Liu, D., Huang, C., Hunag, Y., Hseih, P., Lee, M.: *Technological suitability and improvement for shaping environmental performance: A life cycle perspective on Fenton-based wastewater treatment processes*, Journal of Cleander Production, 428, 139307, 2023.

[6] Huijbregts, M., Steinmann, Z., Elshout, P., Stam, G., Verones, F., Vieira, M. Hollander, A. Zijp, M., van Zelm R.: *A harmonized life cycle impact assessment method at midpoint and endpoint level Report I: Characterization*, National Institute for Public Health and the Environment, Bilthoven, 2016.

[7] Wernet, G., Bauer, C., Steubing, B., Reinhard, J., Moreno-Ruiz, E., Weidema, B.: *The ecoinvent database version 3 (part I): overview and methodology*, The International Journal of Life Cycle Assessment, 21, p.p. 1218-1230, 2016.

Autori: **dr Vesna Gvoić, Vanr. prof. dr Boris Agarski, Prof. dr Đorđe Vukelić, Prof. dr Miljana Prica,** Univerzitet u Novom Sadu, Fakultet Tehničkih Nauka, Trg Dositeja Obradovića 6, 21000 Novi Sad, Serbia, **Vanr**. **prof. dr Đurđa Kekrez,** Univerzitet u Novom Sadu, Prirodno-matematički fakultet, Trg Dositeja Obradovića 3, 21000, Novi Sad.

E-mail: kecic@uns.ac.rs
agarski@uns.ac.rs
djurdja.kerkez@dh.uns.ac.rs
vukelic@uns.ac.rs
miljana@uns.ac.rs

ETIKUM 2023 **INTERNATIONAL SCIENTIFIC CONFERENCE NOVI SAD, SERBIA, DECEMBER 7-9, 2023**

Jovanović, S., Budak, I., Ilić Mićunović, M., Agarski, B.

POTROŠNJA ELEKTRIČNE ENERGIJE I UTICAJ HOTELA NA POTENCIJAL GLOBALNOG ZAGREVANJA

Rezime: *Hoteli značajno doprinose uticaju na životnu sredinu, pomenute uticaje ne treba zanemariti i treba ih detaljno istražiti i pratiti. Potrebna su naučna istraživanja koja će omogućiti bolji uvid u čitavu situaciju i koja će koristiti efektivne metode za rešavanje problema. U radu su analizirani rezultati ocenjivanja životnog ciklusa iz prethodnih istraživanja hotelskih usluga. Upoređeni su dosadašnji rezultati za različite hotele u pogledu potrošnje električne energije i uticaja na potencijal globalnog zagrevanja. Upoređeni rezultati otkrivaju da kako se hotelski sadržaji povećavaju, tako se povećava i njihov uticaj na potencijal globalnog zagrevanja. Hoteli u Južnoj Americi troše znatno više struje od hotela u Iranu. Hoteli u Iranu za grejanje koriste prirodni gas, dok se hoteli u Južnoj Americi za grejanje oslanjaju na struju, što pokazuje kako nastaje razlika u potrošnji električne energije za ispitane hotele. Navedeno istraživanje obuhvatilo je sve slučajeve korišćenja energije u hotelskom poslovanju u sledeće svrhe: boravak gostiju (uključujući pranje veša), ugostiteljstvo, slobodno vreme, poslovanje. Slučajevi indirektnog/neoperativnog korišćenja energije (energija sadržana u nabavci hrane, hotelskih zgrada, nameštaja i opreme) isključeni su iz analize zbog (ne)dostupnosti podataka. Upoređivanjem rezultata dolazi se do zaključka da granice sistema u dve analizirane studije nisu iste za hotele u Iranu i Južnoj Americi, pa se poređenje ne preporučuje prema ISO 14044.*

Ključne reči: *hoteli, potencijal globalnog zagrevanja, potrošnja električne energije*

1. UVOD

Pružaoci turističkog smeštaja, kao što su hoteli, značajno doprinose globalnom uticaju na životnu sredinu [3]. Zbog dominacije stambenih zgrada u postojećem građevinskom fondu, one su odgovorne za 2/3 ukupne potrošnje energije i emisije gasova sa efektom staklene bašte (engl. Greenhouse gases - GHG) u građevinskom sektoru [1]. Uprkos tome, specifične tipove komercijalnih zgrada često karakteriše intenzivnija praksa korišćenja energije. Hoteli su, na primer, jedan od najzahtevnijih potrošača energije među svim kategorijama građevinskog fonda [1]. Građevinski sektor proizvodi 20-30% globalnog povećanja emisije ugljen dioksida (CO_2), a pretpostavlja se dalji rast [1]. Hoteli imaju visok energetski i materijalni intenzitet jer imaju obimne zalihe proizvoda i usluga kako bi ispunili potražnju potrošača [3]. Energetika omogućava razvoj različitih industrija, a istovremeno izaziva i zagađenje životne sredine [6]. Ovaj intenzitet dovodi do ekoloških problema kao što su emisije GHG [2], potrošnja i zagađenje vode, zagađenje česticama, oštećenje ozonskog omotača i stvaranje čvrstog otpada [3]. Poslednjih godina globalno zagrevanje nije samo ekološko pitanje već i jedan od najvećih izazova za međunarodnu zajednicu. U Deklaraciji iz Djerbe iz 2003 Svetska turistička organizacija je priznala složene interakcije između turizma i klimatskih promena. Turizam utiče na klimatske promene koristeći fosilna goriva i emisije GHG. Emisije CO_2 iz turizma, kao važnog odnosa čoveka i zemlje u turističkoj industriji u 21. veku, predstavljaju vitalni indeks koji odražava njegove efekte na promene životne sredine.

Cilj rada je da se uporedi potrošnja energije hotela u Iranu i hotela u Južnoj Americi (Brazil i Peru) i njihov uticaj na potencijal globalnog zagrevanja (engl. Global Warming Potential - GWP). Informacije koje su bile potrebne za rad preuzete su iz naučnih radova [3] i [4]. Skupovi podataka iz baze podataka Ecoinvent [8] na osnovu studije [3] prvo su analizirani u openLCA softveru [7] u okviru diplomskog rada [5]. U ovom radu su isti rezultati predstavljeni dijagramima da bi se detaljnije prikazao uticaj hotelskih usluga na GWP.

2. METODOLOGIJA

Slika 1 predstavlja prikaz okvira za analizu potrošnje električne energije na uticaj GWP iz hotelskih usluga. Prvo, kao ulazne informacije uzeti su rezultati LCA hotelskih usluga u Brazilu i Peruu [3], kao i LCA potrošnje električne energije hotela u Iranu [4]. Zatim su analizirani Ecoinvent

skupovi podataka [8] za hotelske usluge u Brazilu i Peruu da bi se dobio prikaz uticaja navedenih usluga na GWP. Na kraju, urađena su poređenja vrednosti GWP-a za potrošnju električne energije u hotelima u Brazilu, Peruu i Iranu. Cilj je da se uporedi potrošnja energije hotela u Iranu i hotela u Južnoj Americi (Brazil i Peru) i njihov uticaj na GWP.

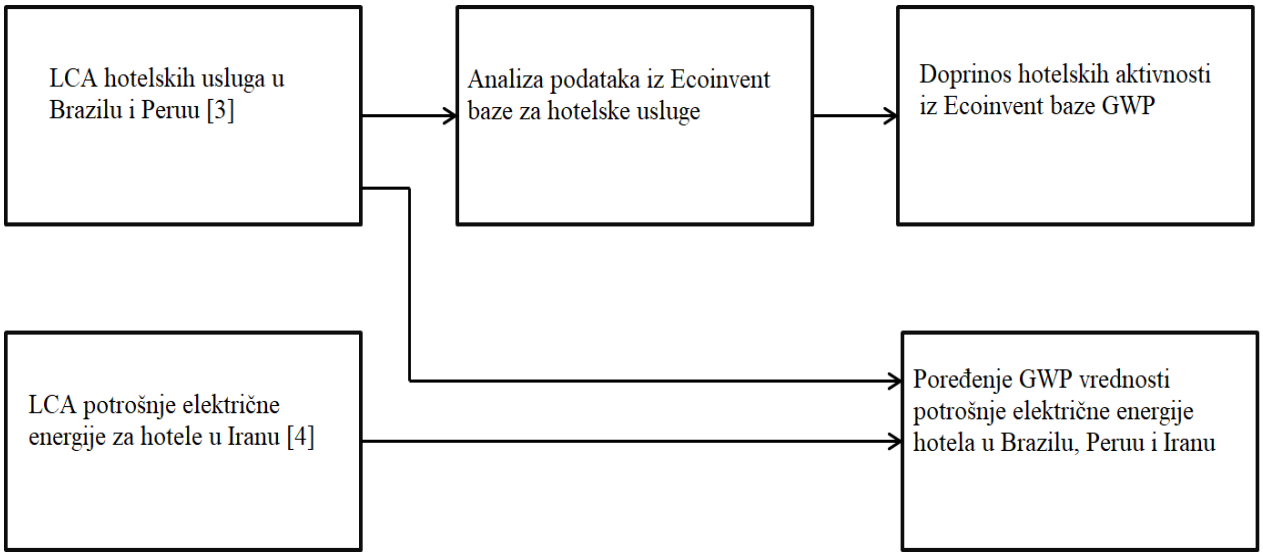

Sl. 1. Okvir za analizu potrošnje električne energije i uticaj na GWP, iz hotelskih usluga

Rezultati preuzeti iz studije [3] sadrže podatke o hotelskim aktivnostima, kao što su upotreba papirnih maramica, televizije, izgradnja hotela, odlaganje otpada i ostalo. Pomenute aktivnosti imaju određeni uticaj na GWP, u većoj ili manjoj meri. Hoteli koji su analizirani nalaze se u Brazilu i Peruu. Studija je obuhvatila svakodnevno poslovanje različitih kategorija hotela za određeni period tokom 2017. godine, uključujući sve operativne i neoperativne faze životnog ciklusa hotelskog poslovanja, odnosno počev od proizvodnje građevinskog materijala potrebnog za izgradnju hotelskih zgrada pa do odlaganja materijala na kraju životnog ciklusa hotelske zgrade. Granice iz studija [3] i [4] nisu iste. Studija [4] obuhvata sve slučajeve korišćenja energije u hotelskom poslovanju u svrhe kao što su: boravak gostiju (uključujući pranje veša), ugostiteljstvo, slobodno vreme, posao i nabavka hrane. Slučajevi indirektne/neoperativne upotrebe energije (energija sadržana u nabavci hrane, zgrada hotela, nameštaj i oprema) isključeni su iz analize zbog dostupnosti podataka. Studija [3] uključuje sve operativne i neoperativne faze životnog ciklusa hotela poslovanje, odnosno počevši od proizvodnje građevinskog materijala potrebnog za izgradnju hotelskih zgrada i završavajući odlaganjem ovog materijala na kraju životnog ciklusa hotelske zgrade. Glavni izuzeci studija [3] su nabavka hrane i isključivanje stvari i putovanja gostiju što predstavlja glavno ograničenje studije. Tabela 1 i 2 prikazuju inventar potrošnje električne energije za navedene hotele.

Tabela 1. Inventar potrošnje električne energije za hotele u Iranu

Hoteli	Potrošnja električne energije - Struja (kWh/gost po noći)
Hotel A	0,32
Hotel B	0,22
Hotel C	0,29
Hotel E	0,33
Hotel F	0,18
Hotel X	0,03

Tabela 2. Inventar potrošnje električne energije za hotele u Južnoj Americi

Hoteli	Potrošnja električne energije - Struja (kWh/gost po noći)
Jeftiniji hotel Brazil	0,84
Jeftiniji hotel Peru	4,46
Hostel Brazil	1,72
Hostel Peru	2,73
Luksuzni hotel Brazil	8,07
Luksuzni hotel Peru	23,18
Skuplji hotel Peru	3,04

3. REZULTATI

Slika 2 predstavlja vrednosti GWP-a za sve hotele prema rezultatima iz openLCA softvera za Ecoinvent bazu podataka. Slika 2 jasnije pokazuje

uticaj podataka iz Ecoinvent baze, koji nije prikazan na ovaj način u studiji [3]. Najniže vrednosti GWP se beleže za hostele. Najveće vrednosti GWP-a pripisuju se luksuznim hotelima i jeftinijim hotelima u Peruu. Ovi rezultati ukazuju na vezu između kategorije hotelskog komfora i emisije GHG. Doprinos hotelske zgrade ukupnim vrednostima GWP značajno varira. Doprinos izgradnje hotela emisijama GHG može biti značajan i ne treba ga zanemariti [3]. Slika 2 pokazuje da je učešće potrošnje električne energije značajno malo u poređenju sa ostalim hotelskim delatnostima (osim luksuznog hotela u Peruu). Zbog poređenja studija, treba naglasiti da granice sistema nisu iste.

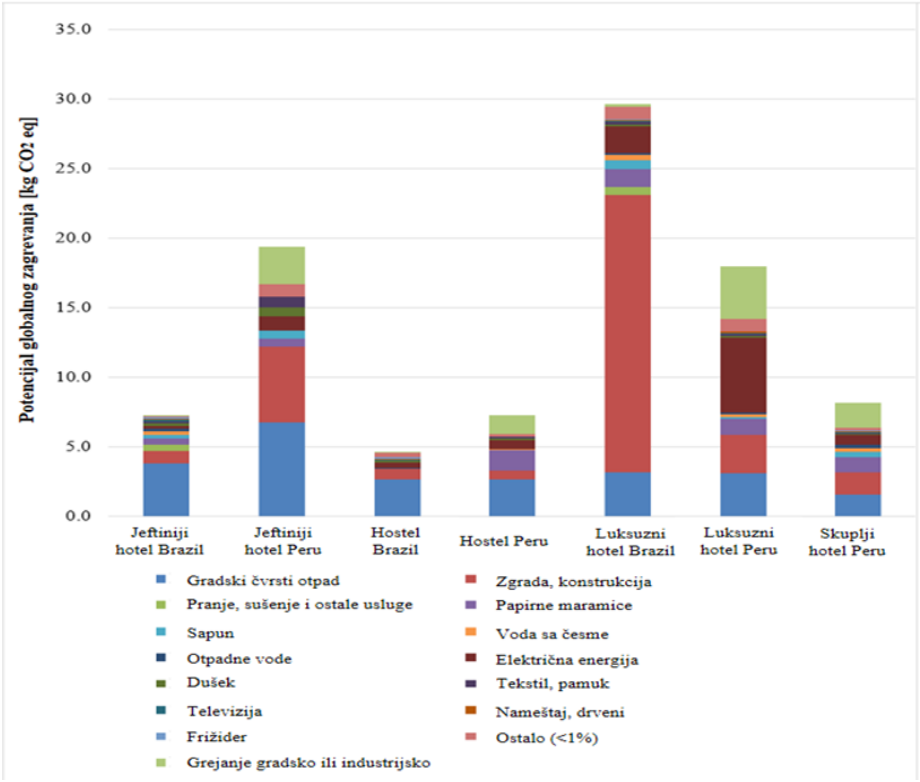

Sl. 2. Uticaj hotelskih aktivnosti, hotela iz Južne Amerike, na GWP

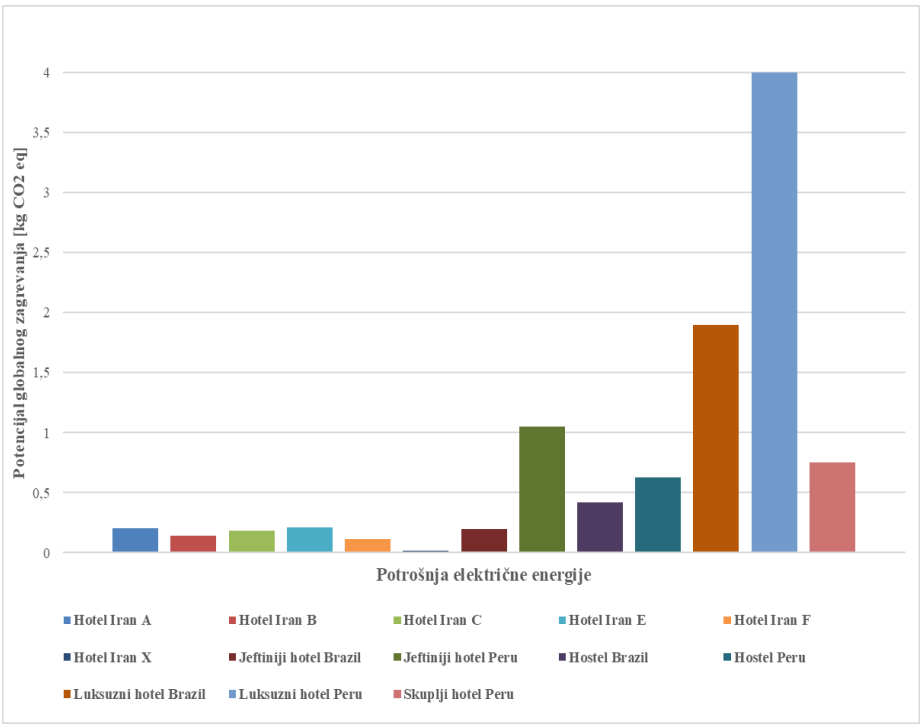

Sl. 3. Potrošnja električne energije za hotele u Iranu i Južnoj Americi

Na slici 3 prikazane su upoređene vrednosti potrošnje električne energije za različite hotele. Kada se uporede ovi hoteli, nameće se zaključak da hoteli u Iranu imaju znatno manju potrošnju električne energije u odnosu na hotele u Južnoj Americi, bez obzira na kategoriju komfora hotela. Hoteli u Iranu su uglavnom dizajnirani da budu „održivi“, takođe hoteli u Iranu koriste mnogo više prirodnog gasa nego električne energije. Hoteli u Južnoj Americi koriste energiju iz hidroelektrana, kao i fosilna goriva u manjoj meri, a više se oslanjaju na električnu energiju za grejanje objekata.

4. ZAKLJUČAK

LCA metodom su istaknuti rezultati uticaja na GWP koji su od značaja za dato istraživanje. Upoređivanjem rezultata dolazi se do zaključka da granice sistema u dve analizirane studije nisu iste za hotele u Iranu i Južnoj Americi, pa se poređenje ne preporučuje prema ISO 14044. Na osnovu prethodnih istraživanja [3, 4], ustanovljeno je da najveći uticaj na GWP imaju čvrsti gradski otpad i električna energija, odnosno najveće emisije CO_2 se odnose na ove aktivnosti. Sa povećanjem komfora i usluga koje nude hoteli, povećava se negativan uticaj na životnu sredinu, pri čemu najveći uticaj imaju luksuzni hoteli, što bi se moglo pretpostaviti. Prikazani rad naglašava i pomaže boljem razumevanju uticaja hotelskih usluga na GWP, rezultati su analizirani i grafički predstavljeni.

Velika potrošnja energije povezana je sa hotelima u Južnoj Americi, bez obzira na kategoriju komfora hotela. Preporuka je da analizirani hoteli preduzmu određene mere u cilju očuvanja i smanjenja potrošnje električne energije.

Budući pravci istraživanja mogu uključivati istraživanje hotelskih usluga u Srbiji i drugim zemljama i poređenje dobijenih rezultata sa rezultatima prethodnih istraživanja. Buduća istraživanja bi mogla koristiti različite metode ocene uticaja na životni ciklus kako bi se ispitali drugi uticaji hotelskih usluga koji nisu obuhvaćeni prethodnim istraživanjem.

5. LITERATURA

[1] Filimonau, V., Dickinson, J., Robbins, D., Huijbregts, M. A. J.: *Reviewing the carbon footprint analysis of hotels: Life Cycle Energy Analysis (LCEA) as a holistic method for carbon impact appraisal of tourist accommodation*, Journal of Cleaner Production 19, pp. 1917-1930, 2011.

[2] Yu-guo, T., Zhen-fang, H.: *Review of accounting for carbon dioxide emissions from tourism at different spatial scales*, Acta Ecologica Sinica 34, pp 246-254, 2014.

[3] Filimonau, V., Rosa, M. S., Franca, L. S., Creus, A. C., Ribeiro, G. M., Molanarova, J., Piumatti, R. G., Valsasina, L., Safaei, A.: *Environmental and carbon footprint of tourist accommodation: A comparative study of popular hotel categories in Brazil and Peru*, Journal of Cleaner Production 328, pp 129561, 2021.

[4] Salehi, M., Filimonau, V., Asadzadeh, M., Ghaderi, E.: *Strategies to improve energy and carbon efficiency of luxury hotels in Iran*, Sustainable Production and Consumption 26, pp 1-15, 2021.

[5] Jovanović, S.: *Ocenjivanje životnog ciklusa hotelskih usluga*, Diplomski rad, Fakultet tehničkih nauka, Novi Sad, Srbija, 2022.

[6] Zhang, X., Zhang, M., Zhang, H., Jiang,Z., Liu, C., Cai, W.: *A review on energy, environment and economic assessment in remanufacturing based on life cycle assessment method*, Journal of Cleaner Production 255, pp 120160, 2020.

[7] https://www.openlca.org/ Pristupljeno 10.03.2023.

[8] Wernet, G., Bauer, C., Steubing, B., Reinhard, J., Moreno-Ruiz, E., Weidema, B.: *The ecoinvent database version 3 (part I): overview and methodology*, The International Journal of Life Cycle Assessment 21(9), pp.1218–1230, 2016.

Autori: **Msc. Slađana Jovanović, Prof. dr Igor Budak, Doc. dr Milana Ilić Mićunović, Vanr. prof. dr Boris Agarski,** Univerzitet Novi Sad, Fakultet Tehničkih Nauka, Trg Dositeja Obradovića 6, 21000 Novi Sad, Serbia, Tel: +381 21 485 2350, Fax: +381 21 454-495.

E-mail: sladjanajovanovic76@yahoo.com
budaki@uns.ac.rs
milanai@uns.ac.rs
agarski@uns.ac.rs

ETIKUM 2023 **INTERNATIONAL SCIENTIFIC CONFERENCE NOVI SAD, SERBIA, DECEMBER 7-9, 2023**

Kadušić, E., Birdahić, V., Imamović, N.

APPLICATION OF REVERSE OSMOSIS FOR TREATING WASTEWATER FROM THE COKING INDUSTRY

Abstract: *This paper focuses on the analysis of the reverse osmosis (RO) application in the context of treating wastewater generated in the coke industry. The coke industry produces wastewater with high concentrations of hazardous chemicals and suspended particles, posing a significant challenge for conventional wastewater treatment methods. It examines the RO technical aspects and efficiency, compares combined treatment method (coagulation+RO) with individual (coagulation) method, as well as against other traditional and newer techniques. By applying Spearman's rank correlation matrix for the mentioned two processes, it was found that all parameters except pH have a coefficient of "1", which indicates a perfect positive linear correlation between these two variables. A comparative analysis of the purification efficiency revealed a significant advantage of using the coagulation+reverse osmosis process. The study also discusses the benefits and challenges of implementing RO in coke industry wastewater treatment, offering a concise overview of its environmental role in this sector.*
Key words: *coke industry, wastewater treatment, reverse osmosis, coagulation+reverse osmosis.*

1. INTRODUCTION

One of the primary challenges confronting industries is the effective treatment of wastewater, especially in sectors that produce highly polluted and intricate effluents, such as the coke industry. The coke industry is a pivotal segment within the chemical sector, involved in the manufacturing of coke, a solid fuel material widely used in metallurgical and energy processes. [1]

The wastewater generated by coke production presents a significant environmental concern, demanding meticulous management and treatment to minimize its adverse ecological impact. These wastewater streams contain substantial concentrations of ammonium salts and various compounds like phenols, oils, tars, suspensions, polycyclic aromatic hydrocarbons (PAHs), toxic organic nitrogen compounds, cyanide, and ammonia, along with hydrogen sulfide. [2]

It is imperative to subject coke industry wastewater to multi-stage purification processes before its release into municipal sewage systems or surface waters. The recommended approach involves the utilization of integrated systems that combine biological, chemical, and physical treatment methods. Remarkably high treatment efficiency for these wastewater streams is achieved through the adoption of membrane processes, with reverse osmosis (RO) standing out as a particularly effective technique. [3]

RO, as a membrane-based process, utilizes semi-permeable membranes to exert pressure and compel water to pass through them, leaving contaminants behind on one side of the membrane. This technology has proven to be exceptionally proficient in the removal of diverse pollutants, including heavy metals, organic substances, salts, and other impurities from wastewater.

2. THE PRINCIPLE OF REVERSE OSMOSIS

The concept of reverse osmosis was first introduced in the early 1960s. Initially, this technology was primarily focused on concentrating solutions, and only later was its potential application in wastewater treatment recognized. The reverse osmosis process is complex and involves multiple steps to achieve high water purity [4]:

- Pretreatment: removing suspended matters, oils, fats, and other impurities that could potentially damage the membrane or reduce its efficiency.
- Pumping: using high pressure (usually from 7 to 70 bar) enables the passage of water through the semipermeable membrane while blocking the passage of larger molecules and impurities.
- Membrane: semipermeable membrane with extremely fine pores (size from 1 to 100 nm) allowing only water molecules to pass through while retaining almost all salts, impurities, bacteria, viruses etc.
- Additional Permeate Treatment: additional treatment may be required depending on law regulations. This may involve additional

filtration, disinfection steps, and possibly remineralization. Shematic representation of RO process is showed at Figure 1.

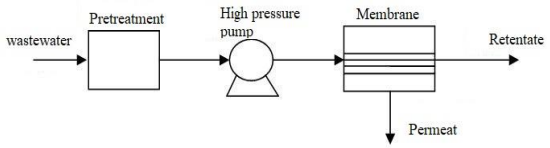

Fig. 1. Reverse osmosis process scheme

3. APPLICATION OF REVERSE OSMOSIS IN COKING INDUSTRY – CASE STUDY

Coke production wastewaters result from diverse processes and activities in the coke manufacturing, including oil extraction and coal processing. Key features of coke industry wastewater encompass a high concentration of suspended particles, the presence of phenolic compounds, ammonia, heavy metals, and various organic substances.[3] In Table 1., standard characteristics of wastewater from one specific coke plant are presented, along with a comparison to the effluents limits according to the Regulation on the Conditions for Discharging Wastewater into the Environment and Public Sewerage Systems (Official Gazette of FBiH 26/20 and 96/20 – Annex 16). As can be seen from the table, all values of wastewater from the coke industry exceed the effluents limits.

Table 1. Comparison of characteristics of wastewater from coke industry and regulatory limits [5,6]

Parameter	Unit	Coke plant wastewater	Limit values of effluents into the surface water	Limit values of effluents into the public sewage system
pH	-	7.56	6.0-9.0	6.5-9.5
Temp.	°C	47	30	40
COD	mg O_2/l	6080.4	125	700
TC[1]	mg C/l	496.9	ns.[2]	ns.
TOC[3]	mg C/l	386.1	15	30
TN[4]	mg N/l	609.1	15	100
Amonium nitrogen	mg N-NH_4^+/l	168.0	10	40
Turbidity	NTU	375.1	ns.	ns.

The paper presents an integrated wastewater treatment system for the coke industry: coagulation + reverse osmosis for the removal of organic and inorganic contaminants from wastewater. Before the wastewater from the coking plant enters the coagulation-reverse osmosis treatment system, it undergoes pretreatment involving denitrification, nitrification and organic carbon oxidation. Figure 2 illustrates a schematic representation of such a facility. A polyamide reverse osmosis membrane is used for this treatment, operating within a pH range of 1-11 and temperatures up to 50°C. [5]

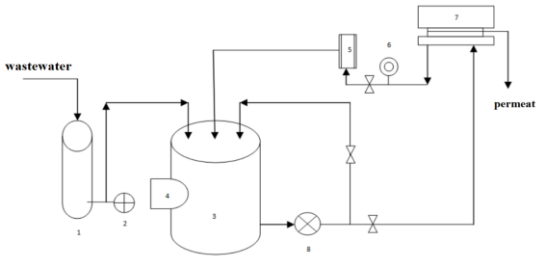

Fig. 2. Schematic layout of the coke industry Wastewater Treatment Plant (1 - Mixer Reactor, 2 - Dosing Pump, 3 - Wastewater Tank, 4 - Cooler, 5 - Flow Meter, 6 - Pressure Gauge, 7 - Membrane Module, 8 - Pump)

The efficiency of wastewater treatment in the coke industry was assessed based on the degree of removal of pollutants, as shown in Table 2. As can be seen in Table 2. the pH of the wastewater showed a slight decrease from 7.56 to 7.34; however, it remained within permissible limits for discharge into the public sewer system or natural receiving bodies. The COD (Chemical Oxygen Demand) value decreased to 2984.9 mg O_2/L after coagulation and to 507.2 mg O_2/L after reverse osmosis, making it suitable for discharge into the public sewer system.

Table 2. Wastewater treatment results

Parameter	Unit	Results by coagulation+reverse osmosis
pH	-	7.34
Temperature	°C	33
COD	mg O_2/l	507.2
TOC	mg C/l	40.1
TC	mg N/l	28
TN	mg N/l	89.8
Amonijum nitrogen	mg N-NH_4^+/l	5.6
Turbidity	NTU	0.99

As seen in the Figure 4, the highest level of purification was achieved for the turbidity parameter with a 99.74% reduction in turbidity after reverse osmosis. Additionally, high levels of purification were attained for ammonium nitrogen at 96.67%, COD at 91.66%, and total carbon at 94.37%.

[1] TC-Total Carbon
[2] ns – it is not standardized
[3] TOC- Total Organic Carbon
[4] TN-Total Nitrogen

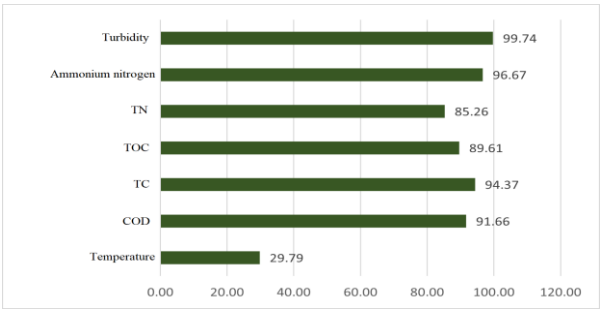

Fig. 3. Purificatio efficiency rate by using coagulation+reverse osmosis

4. BENEFITS AND CHALLENGES OF REVERSE OSMOSIS-COMPARATIVE ANALYSIS

The use of reverse osmosis for wastewater purification offers numerous advantages, making it an attractive option for various applications. Key benefits of this process include high efficiency in removing various pollutants, adaptability to different types of wastewater, low energy consumption, reduced waste generation, straightforward operation and maintenance, minimal spatial requirements, and environmental friendliness. Despite challenges and limitations, such as costs and water losses, reverse osmosis remains a valuable technology for wastewater treatment and the production of clean water for diverse purposes. [7]

4.1. Coagulation and coagulation+reverse osmosis

Figure 4. presents a comparative analysis of the efficiency of wastewater treatment in the coke industry using only the coagulation process versus using the coagulation-reverse osmosis process. The purification efficiency achieved with the combination of coagulation and reverse osmosis is significantly higher than that achieved using the coagulation process alone. More specifically, using the coagulation process alone would not meet the requirements outlined in the Regulation [6]. The correlation between reverse osmosis and coagulation can be complex and depends on the specific input parameters and purification objectives of individual cases. The correlation between these processes can be viewed in the following context:

- Coagulation is employed as a preparatory step before reverse osmosis to reduce the amount of suspended particles in the water to extend the lifespan of RO membranes.
- Reverse osmosis is often used for additional purification of water that has undergone coagulation to remove dissolved salts and other harmful substances.

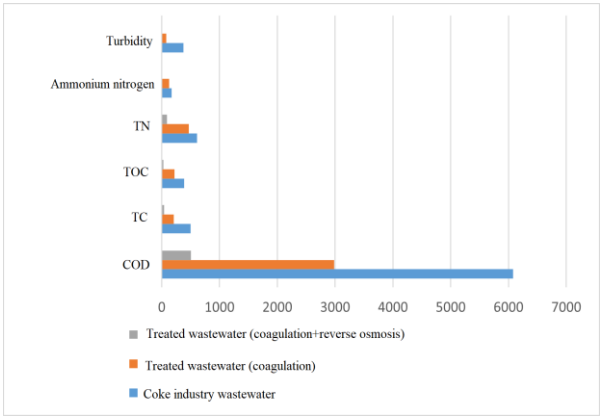

Fig. 4. A comparative analysis coagulation versus the coagulation+reverse osmosis process [5]

Correlation between theese two processes is confirmed by implementation of Spearman rank correlation matrix (Table 3.) where can be seen that all parameters except pH have a coeficient „1“ which indicates a perfect positive linear correlation between these two variables. The reason why pH value goes slightly to acidic side after coagulation (precisely to 5.4) is probably because of the choice of coagulant used in the process, which is then treated by reverse osmosis membrane, so it is back to the value allowed by the regulations. This matrix is as well a vital step to select appropriate treatment method as removal of one parameter shows the possible removal of related parametance.

Table 3. Spearman rank correlation matrix for certain parameters in different treatment processes

	pH	**COD**	**TC**	**TOC**	**Turbidity**
pH	1	-0.4	-0.4	-0.4	0.4
COD		1	1	1	1
TC			1	1	1
TOC				1	1
Turbidity					1

4.2. Coagulation+reverse osmosis and other coke wasterwater treatments

Figure 5. presents a comparative analysis of individual wastewater treatment methods for parameters such as COD while Figure 6. focuses on ammonium nitrogen. While individual treatment methods may offer economic advantages, they cannot be used independently for treating this type of wastewater [8]. Compared to other treatment methods such as biological treatment, aeration, sedimentation, and anaerobic digestion, RO integrated with physicochemical treatments can consistently achieve a high level of

pollutant removal. Advanced treatment technologies, such as advanced oxidation or photocatalytic oxidation, are also viable options for more efficiently treating wastewater than RO. However, these processes require investment and specialized knowledge for maintenance. The choice of treatment should be based on an analysis of specific plant needs, pollution characteristics, and financial capabilities.

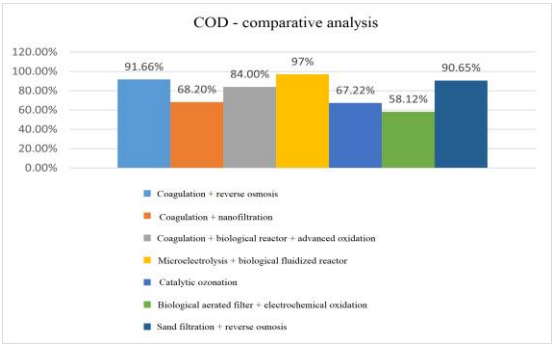

Fig. 5. A comparative analysis for the parameter COD [8,9]

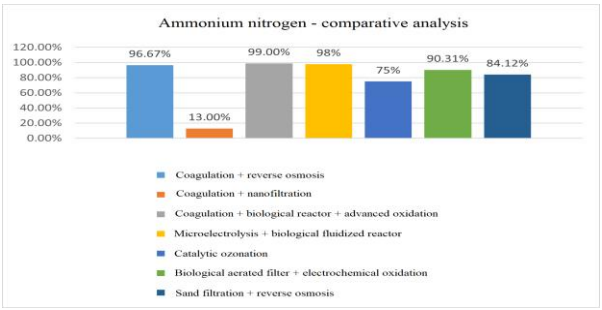

Fig. 6. A comparative analysis for the parameter ammonium-nitrogen [8,9]

5. CONCLUSIONS

Based on the presented analyzes and the results of the processed data for the application of the reverse osmosis process for the purification of waste water from the coke industry, the following can be concluded:

- Reverse osmosis is a very efficient process of wastewater treatment in the coke industry, and in general in the chemical industry,
- By analyzing a case study through the application of reverse osmosis in the coke industry, the significant efficiency of using this technology was unequivocally determined by removing 96.67% of ammonium nitrogen, COD to 91.66%, and total carbon to 94.37%,
- Using Spearman's correlation matrix, a correlation between coagulation and reverse osmosis is evident, whereby a decrease in the parameter value in one treatment leads to a continued decrease in the other, except in the case of pH due to the nature of the coagulant,
- Analyzes show that the use of reverse osmosis for the purification of wastewater in the chemical industry represents a high-quality and key solution for numerous challenges in terms of protection and improvement of the quality of the recipient, which significantly reduces the costs of wastewater treatment procedures and thereby increases economic profit,
- As an innovative technology, the application of reverse osmosis should take its place in the future and play a significant role in achieving sustainability in the chemical industry as well.

6. REFERENCE

[1] Chen L., *Research on the Energy Management and Development of Semi Coke Industry*, Advanced Materials Research 962-965, VI. 2014.

[2] Kwiecinska A., Lajnert R., *Coke oven wastewater–Formation, treatment and utilization methods–a review*, ECOpole 2017.

[3] Čistije tehnologije – lecture material P-9, dr.sc. Zoran Ilicković – University of Tuzla

[4] Garud R.M., *A short review on process and applications of Reverse Osmosis*, Universal Journal of Environmental Research and Technology, Volume 1, Issue 3: 233-238

[5] Smol M., Bohdziewicz J., *The use of integrated membrane systems in the removal of selected pollutants from pre-treatreed wastewater in coke plant*, Membranes and Membrane Processes in Environmental Protection, 2014, 143-152,

[6] Regulation on the Conditions for Discharging Wastewater into the Environment and Public Sewerage Systems (Official Gazette of FBiH 26/20 and 96/20 – Annex 16).

[7] Cruver, J. E., and I. Nusbaum. , *Application of Reverse Osmosis to Wastewater Treatment*, Journal (Water Pollution Control Federation) 46, no. 2 (1974): 301

[8] A. Tutić et al.: *An Overview of Coking Wastewater Characteristics and Treatment Technologies*, Kem.Ind.72(5-6.2023)349-358,

[9] Tamang M., Advances in treatment of coking wastewater – a state of art review, Water Science & Technology Vol 00 No 0, 1

Auhtors: **Bach.mech.eng. Emina Kadušić, Doc. dr Vehid Birdahić, Vanr. prof. dr Nusret Imamović,** University of Zenica, Mechanical engineering faculty, Fakultetska 1, 72000 Zenica, B&H, Tel: +387 32 449111

E-mail: emina.kadusic@unze.ba
vehid.birdahic@unze.ba
nusret.imamovic@unze.ba

ETIKUM 2023 **INTERNATIONAL SCIENTIFIC CONFERENCE NOVI SAD, SERBIA, DECEMBER 7-9, 2023**

Kadušić, E., Imamović, N.

EVALUATION OF EFFLUENT CHARACTERISTICS IN POULTRY INDUSTRY – A COMPARISION BETWEEN ACTUAL MEASUREMENTS AND GPS-X SIMULATION

Abstract: *This paper examines the characteristics of effluent generated in the poultry industry through a comparison between actual measurements and simulations obtained using the water waste modeling software, GPS-X. Genuine wastewater characteristic data were amassed from the processes inherent to the poultry industry. The same processes were modeled using GPS-X to generate virtual effluent characteristic results. A comparative analysis between simulated results and actual measurements was conducted, highlighting discrepancies and their causes. This paper also explores the applicability of the GPS-X software for simulating effluent characteristics in the context of changing input parameters of wastewater.*

Key words: *poultry industry wastewater, effluent analysis, GPS-X simulation*

1. INTRODUCTION

The poultry industry holds a prominent position within the agro-industrial sector and often takes a leading role in food production. Wastewater from the poultry industry contains a complex mixture of pollutants, including ammonia, nitrates, phosphates, fats, and organic substances, necessitating specialized treatment processes to minimize their adverse effects on the environment and water resources. [1] In last two decades, several different wastewater treamtments modelling softwer have been developed. The results of several studies have indicated that values of only a few coefficients need to be adjusted during model calibration in order to get acceptable results. [2] GPS-X is an advanced software tool developed by Hydromantis for modeling and simulating wastewater treatment processes in industrial facilities.. GPS-X allows users to virtually model various scenarios and treatment conditions, including monitoring changes in pollutant concentrations, operational regimes, and process dynamics. This tool holds significant importance across various industries, including the poultry industry, as it provides precise predictions of how different substances and components will react during wastewater treatment processes. This is particularly valuable for evaluating and optimizing existing facilities and developing new strategies for wastewater treatment to reduce environmental impact and improve economic efficiency. [3]

In this study, attention is directed towards comparing actual measurements of wastewater characteristics from this industry with results obtained through simulation using the GPS-X software tool. This provides a deeper understanding of the accuracy and reliability of GPS-X simulations in the specific context of the poultry industry, contributing to an enhanced comprehension and management of wastewater in this sector.

2. METHODOLOGY

2.1 Influent charateristics

Technological wastewater is generated in the process of slaughtering and meat processing. Production takes place continuously throughout the year, operating 14-16 hours per day. Within the facilities, two types of wastewater are produced: slaughter wastewater and meat processing wastewater. The daily average quantity of wastewater is recorded at 400 m3/d. The quantity of discharged wastewater from the facility is measured using a Parshall flume with an ultrasonic flow meter installed in a measurement chamber integrated into the outlet pipeline. The values of parameters for poultry processing wastewater, which will be considered in the study, are provided in the Table 1. Since the effluent is discharged in natural receptor, parameters values should be in limit regulated by the Regulation on the Conditions for Discharging Wastewater into the Environment and Public Sewerage Systems (Official Gazette of FBiH 26/20 and 96/20 – Annex 16). As can be seen in the Table 1. most of the parameters exceeds the limit values which leads to conclusion that wastewater from this poultry industry needs to undergo the certain treatments so the values are in the limits according to the law regulation.

Table 1. Poultry wastewater charateristic [4,5]

Parameter	Value	Limit values	Unit
BOD	2630	25	mg/L
COD	4550	125	mg/L
Suspended particles	1630	35	mg/L
Oils and fats	700	20	mg/L
P_{tot}	4	2	mg/L
N_{tot}	330	15	mg/L
Cl	20	-	mg/L
T	10-25	30	°C
pH	6-8	6.5-9.5	-
Nitrates	22	10	mg/L
Nitrites	0,245	-	mg/L
Ammonia	7.8	10	mg/L

2.2 Principles of wastewater treatment and effluent charateristics

The treatment process consists of the following technological units [4]:

- Automatic mechanical "pre-treatment" for wastewater from the slaughterhouse and water that passes through the receiving depot.
- Pumping station
- Mechanical "pre-treatment"
- Equalization tank
- Physico-chemical treatment
- Biological treatment in two lines
- Sludge tank
- Mechanical sludge dewatering
- Electrical control unit The technological wastewater treatment device is under the automatic control of the central control unit.

At the entrance of treatment plant there is pumping station that lifts wastewater to the mechanical treatment on a fine 1mm screen, after which the water enters the equalization tank.

Wastewater is mixed in the equalization tank, after which the water is pumped to the physico-chemical treatment in a pipe mixer and a flotation unit. In the pipe mixer, a neutralization, coagulation, and flocculation agent is dosed and mixed with the technological wastewater.

The purpose of the chemical "pre-treatment" is to adjust the pH value and improve the removal of impurities from wastewater. After the physico-chemical treatment in the flotation unit, partially purified water goes for further biological treatment. Biological treatment with denitrification and nitrification stages (D-N denitrification - nitrification) is provided, along with a sludge regeneration tank to enable a more stable operation of the biological process and achieve a higher concentration of active sludge. D-N biological reactors for industrial wastewater treatment operate based on the biological degradation of organic substances using active sludge.

The mixture of treated water and active sludge goes to a secondary sedimentation tank where active sludge and treated water are separated by gravity. The treated water gravitates into a control chamber and passes through a flow meter before being discharged to the recipient. Excess sludge collected from the flotation unit and the biological part of the device is mechanically dewatered and disposed of in accordance with legal regulations.

By finishing this treatment, the effluent characteristics are in the limits of Regulation on the Conditions for Discharging Wastewater into the Environment and Public Sewerage Systems (Official Gazette of FBiH 26/20 and 96/20 – Annex 16) as can be seen in Table 2. It should be mentioned that theese values are the results of using the input values of Table 1 and water of flow of 400 m^3/h and effluent flow of 250 m^3/h.

Table 2. Poultry industry effluent charateristic [5]

Parameter	Value	Limit values	Unit
BOD	12	25	mg/L
COD	86,4	125	mg/L
Suspended particles	15	35	mg/L
P_{tot}	0.54	2	mg/L
N_{tot}	6,36	15	mg/L
T	23,9	30	°C
pH	6,94	6.5-9.5	-
Nitrates	0,716	10	mg/L
Nitrites	0,078	-	mg/L
Ammonia	3,53	10	mg/L

2.3. GPS-X modelling and simulation

Since GPS-X creates dynamic process models based on a graphical depiction of unit processes, the first step was to create a graphical representation of real wastewater treatment plant in poultry industry. The WWTP[1] process flow diagram was built by selecting items (process unit icons) from the process table (GPS-unit X's process library) and connecting them through flow pathways, as shown in Figure 1. It is important to choose a library that is appropriate for the entire WWTP facility. The characterisation of the influent wastewater is considered the basis of the simulated system as the characteristics of the

[1] WWTP – wastewater treatment plant

influent affect the rest of the WWTP's behaviour. GPS-X offers six different models for the influent characterisation: bodbased, codfractions, codstates, sludge, states and tsscod. Since the data available from project documentation concerned mainly the total COD, total nitrogen and total phosphorus, the model chosen for influent characterisation was the codstates. Using this model, most of the state variables whose value was not a user input value were calculated as a fraction of total COD. Since here was the focus in removing nitrogen, phosphorus compands as well as COD and BOD, it was chosen to use mantis2 library for the WWTP which contains the imput parameters taken from the project documentation for this WWTP, such as wastewater parameters and dimension and performances of each treatment stage.

The assumptions are adopted for the development of the model in this study are as follows [6]:

- WWTP operates at a content temperature,
- a constant concentration of dissolved oxygen (DO) is maintained, and there is sufficient mixing within the reactor
- pH is steady and near-neutral value,
- the model's coefficients are assumed to be constants for any influent characteristics
- there are enough inorganic nutrients to ensure sufficient growth,
- there is simultaneous hydrolysis of organic and nitrogenous compounds.

The obtain effluent charateristics model was simulated for a day and the simulation was done under steady-state conditions. Simulations results are presented in Table 3.

Table 3. Effluent charateristic obtained by GPS-x

Parameter	**Unit**	**Value**
Flow	m^3/d	250.0
TSS	mg/L	13,37
cBOD5	mg/L	11,53
COD	mg/L	88,58
Ammonia N	mgN/L	3,42
Nitrite N	mgN/L	0.101
Nitrate N	mgN/L	0.7524
TN	mgN/L	3,97
TP	mgP/L	0.36
pH	-	7.0

3. RESULTS DISCUSSION

The effluent charateristics comparision obtained by GPS-X and on-site measurements is shown in Figure 2. In Table 4. are shown average predicition errors for the selected parameters. Analysing these data, it can be observed certain discrepancies between the results obtained using GPS-X and actual measurements. Simulational models are not always perfect and may encompass errors or simplifications that are not entirely faithful to real-world conditions. It is important to consider factors that could impact these discrepancies, such as environmental conditions or technical characteristics of the instruments used, or lack of data from project documentation so some of the input parameters are taken as pre-set in softwer. The highest accuracy is for parameters BOD with error of just 0,47 mg/l and ammonium with error of 0,11 mg/l. system.

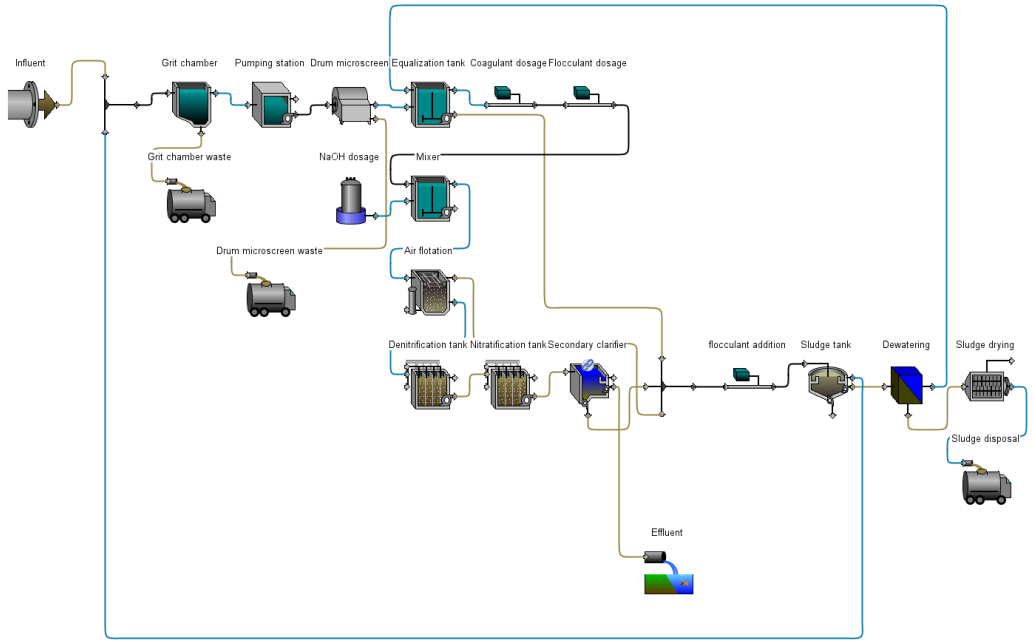

Fig. 1. WWTP scheme obtained by GPS-X modelling

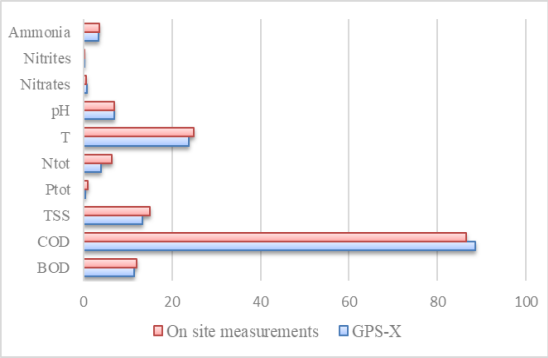

Fig. 2. GPS-X and on-site measurements

Table 4. Predicted errors of GPS-X simulation

Parameter	Unit	Prediction error
TSS	mg/L	1.63
cBOD5	mg/L	0.47
COD	mg/L	2.18
Ammonia N	mgN/L	0.11
Nitrite N	mgN/L	0.023
Nitrate N	mgN/L	0.034
TN	mgN/L	2.39
TP	mgP/L	0.18
pH	-	0.06

However, by observing the results of this case study, it can be adopted that all errors are negligible and this model can be used for prediction and further improvement During simulation in GPS-x, modifying input parameters, including water temperature and flow can significantly influence output characteristics, including COD and BOD concentrations, as well as nitrates and nitrities. An increase in water temperature typically accelerates chemical reactions and biological processes within the water treatment system which results in an enhanced rate of organic matter degradation, leading to a reduction in COD values. Moreover, a warm environment can promote denitrification that can lead to a decrease in nitrate and nitrite concentrations, as shown in Figure 3.

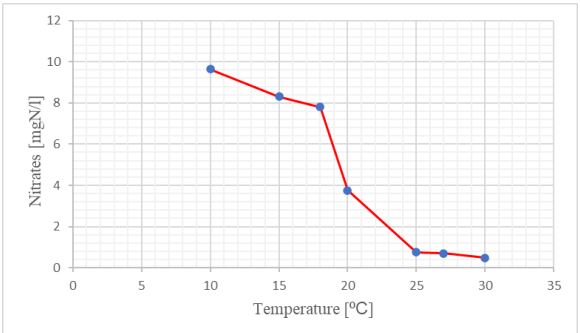

Fig. 3. Impact of temperature on effluent nitrates values

4. CONCLUSION

Through the comparison of actual and modeled effluent characteristics, differences was effectively identified, which, for the most part, proved negligible. This underscores the validity and utility of GPS-X simulation as a tool for predicting the effects of various scenarios across seasons and system load variations. This research provides valuable guidance for engineers and industry professionals, facilitating the optimization of wastewater treatment processes in poultry facilities. The findings also underscore the adaptability of simulation models in predicting effluent characteristics under varying seasonal conditions and flow-rate loads, which is of importance for effective planning and management in the poultry industry.

5. REFERENCES

[1] Maizatul Y., Radin S., Radin M., Adel A., Amir K., Characteristics of Chicken Slaughterhouse Wastewater, Chemical Engineering Transactions, Vol. 63, 2018, ISBN 978-88-95608-61-7; ISSN 2283-9216

[2] Makinia. J., Swinarski M., Experiences with computer simulation at two large wasterwater treatment plants in northern Poland, Water Science and Technology Vol 45 No 6 pp 209–218 © IWA Publishing 2002

[3] GPS-X (Hydromantis), available at: https://www.hydromantis.com/GPSX-innovative.html (september 2023)

[4] Operativne upute za rad i održavanje postrojenja , ASIO, Osijek 2019

[5] Regulation on the Conditions for Discharging Wastewater into the Environment and Public Sewerage Systems (Official Gazette of FBiH 26/20 and 96/20 – Annex 16).

[6] Alagha O., Anil I., Systematic Modeling of Municipal Wastewater Activated Sludge Process and Treatment Plant Capacity Analysis Using GPS-X, Sustainability 2020, 12(19), 8182; https://doi.org/10.3390/su12198182

Auhtors: **bach.mech.eng. Emina Kadušić, associate.prof. Nusret Imamović,** University of Zenica, Mechanical engineering faculty, Fakultetska 1, 72000 Zenica, B&H, Tel: +387 32 449111
E-mail: emina.kadusic@unze.ba
nusret.imamovic@unze.ba

ETIKUM 2023 **INTERNATIONAL SCIENTIFIC CONFERENCE NOVI SAD, SERBIA, DECEMBER 7-9, 2023**

Kerac, J., Prica, M.

PRINTING INKS: ENVIRONMENTAL IMPACTS, INNOVATIONS, AND FUTURE DIRECTIONS

Abstract: *Focusing on the environmental and health implications of printing inks, this paper provides an examination of the challenges posed by synthetic inks within the printing industry. The discussion includes the composition of inks, the release of volatile organic compounds, and the associated health hazards. The paper adresses recent research on natural printing inks, aiming to create safer products and reduce the overall environmental impact of the printing industry. The structured approach covers key components, historical overviews, ink classifications, environmental impact of printing inks and natural alternatives.*
Key words: *Natural ink, green printing, eco printing, synthetic ink.*

1. INTRODUCTION

The environmental ramifications of printing inks within the realm of the printing industry are both pervasive and consequential. The composition of printing inks, specifically synthetic ones, generates a negative impact on the environment. Globally, the production of printing inks precipitates the release of approximately 3 million tons of volatile organic compounds (VOCs) annually [1]. This emission not only contributes significantly to the exacerbation of the greenhouse effect but also compromises air quality and poses a direct threat to public health. The resultant formation of oxides and photochemical smog further underscores the far-reaching implications of ink-related environmental degradation. Moreover, the inherent nature of some of the printing inks introduces a wide range of health hazards, accentuated by the inclusion of toxic heavy metal ions in certain kinds of pigments, and dyes. This compositional complexity of inks poses an additional threat to human well-being, with its carcinogenic properties. The use of diverse organic solvents in the formulation of printing inks introduces the peril of residual solvents persisting and potentially migrating into consumable items, thereby magnifying the health hazards confronting consumers [1]. Despite efforts within the industry to address these concerns, persistent challenges endure. This paper offers a review of the literature concerning the environmental impacts associated with printing inks. It delves into recent research and development endeavors aimed at enhancing the quality of natural printing inks. The objective of this paper is to examine the ecological ramifications of traditional printing inks and to explore the latest strides made in creating natural alternatives that uphold high-quality standards.

Apart from Introduction and Conclusion sections, this paper is structured as follows. Section two outlines the key components of printing inks and offers a brief historical overview of both natural and synthetic inks. In section three, various classifications of printing inks are presented, underscoring the sometimes complex, nature of ink categorization, even within a single printing technique. The environmental impact of printing inks, with a specific focus on Volatile Organic Compounds, is examined in section four. Section five takes a closer look at natural inks, presenting recent research dedicated to implementing and enhancing these inks. These efforts are not only striving to create safer products for human interaction but also working towards addressing and improving the overall environmental impact of the printing industry.

2. TYPES OF PRINTING INKS

The constituents of printing inks are generally categorized into four fundamental components: binder, colorant, additives, and solvents. Binders, fulfill essential functions within ink composition. Primarily, they facilitate the dispersion of pigments in the base material and secure pigments onto the printing substrate. Additionally, binders play a role in adjusting the ink's rheological and mechanical properties. Conventional materials like phenolic resins derived from tall oil resin (colophony) or alkyd resins have historically been employed, while synthetic resins, such as polyacrylates, also serve this purpose. In order to enhance the ink properties, various additives are incorporated. These compounds encompass a diverse range of functions such as the inclusion of surfactants to reduce surface tension and mitigate wetting issues. Furthermore, plasticizers contribute to increased

flexibility in dried ink, while driers aid in the oxidative drying process. Other additives, such as adhesion promoters or wetting agents, serve to augment the ink's binding characteristics to the printing substrate. Additives can also prevent microbial degradation of inks, with biocides. Solvents are utilized to dissolve binders and regulate ink viscosity. Their properties are adapted based on the intended application, with variations in vapor pressure. These solvents may evaporate during the printing process. In certain printing procedures and considering the viscosity of the binder, the use of additional solvent might be unnecessary, resulting in a solvent-free ink (referred to as a 100% system) [2]. When it comes to the color of printing inks, they are commonly comprised of either pigments or dyes as colorants [2]. Pigments, available in both inorganic and organic forms, are predominantly utilized in printing processes. Organic pigments are derived from sources such as natural gas, petroleum, or various carbon-containing raw materials [3]. Pigment particles typically range in size from 0.01 µm to 0.5 µm [4]. When examining process color inks, the specific printing method does not significantly impact the pigments chemistries [3]. These dispersed solid particles remain insoluble in the ink's base material (solvent). In contrast, despite being favored originally dyes are soluble in the base and they possess certain drawbacks compared to pigments, notably lower light fastness and decreased resistance to water [2, 3]. Nowadays dyes can be natural and synthetic. Natural dyes, used for millennia across diverse cultures, were largely superseded by synthetic dyes after their discovery in 1856 due to their muted tones, limited variety, and susceptibility to fading [5, 6].

3. INK CLASSIFICATION

There are various ways to classify printing inks. These methods offer different ways to group them based on their characteristics, composition, and application. For example, printing inks, despite the generally consistent chemistries [3], can be classified based on the printing method used, such as offset printing inks, digital printing inks, screen printing inks, or flexographic printing inks. They can be further classified within one printing method [7]**.** In thesis written by Gvojić [8] printing inks are classified based on the following methods:

- origin of color as:
  - organic and inorganic
- application method as, among others:
  - direct, basic, acidic, reactive, disperse, corrosive, etc.
- solubility as:
  - insoluble (e.g. vat, azo, disperse, and sulfur ink) and soluble (e.g. direct, basic, reactive, metal-complex, and acidic ink)
- chemical structure, as, among others:
  - e.g. azo, nitro, phtalocyanine, xanthene, indigoid, etc.

4. ENVIRONMENTAL IMPACT OF SYNTHETIC INKS

According to [2, 9, 10] among the pollutants in printing inks the most attention is given to the solvents. Solvents encompass a variety of hydrocarbon compounds, including small, aerosolized aromatic molecules that vaporize as Volatile Organic Compounds (VOCs), alongside alkanes, alcohols, ketones, aldehydes, esters, and ethers [9]. Volatile Organic Compounds (VOCs) constitute a group of organic compounds characterized by one or more carbon atoms possessing high vapor pressures, facilitating rapid evaporation into the atmosphere [11]. According to Okubo et al. [12] Organic chemicals can be classified as:

- VVOCs (very volatile organic compounds) with boiling point, $Tb < 50\text{-}100°C$
  - Such as dichloromethane (CH_2Cl_2), methane (CH_4), formaldehyde (HCHO), acetaldehyde (CH_3CHO), etc.
- VOCs (volatile organic compounds) with boiling points, of $50\text{-}100°C \leq Tb < 240\text{-}260°C$
  - Such as toluene (C_7H_8), benzene (C_6H_6), ethanol (C_2H_5OH), xylene ($C_6H_4(CH_3)_2$), etc.
- SVOCs (semi-volatile organic compounds) with boiling points, of $240\text{-}260°C \leq Tb < 380\text{-}400°C$
  - Such as chlorpyrifos ($C_9H_{11}C_{l3}NO_3PS$), bis(2-ethylhexyl) phthalate ($C_{24}H_{38}O_4$), dibutyl phthalate ($C_{16}H_{22}O_4$), etc
- POM (particulate organic matter) with a boiling point, of $380°C \leq Tb$
  - Such as polychlorinated biphenyl (PCB) ($C_{12}H_{(10-n)}Cl_n$), benzo[a]pyrene ($C_{20}H_{12}$), etc.

Volatile Organic Compounds (VOCs), among the most serious pollutants in the printing industry, not only affect the external environment around printing facilities but also compromise indoor air quality (IAQ). While indoor air pollution (IAP) resulting from low and short-term VOC exposure may not lead to serious health issues, workers in printing facilities where VOC presence is consistently high, may experience severe and long-term health consequences. This prolonged exposure could even contribute to the development of health issues such as cancer over time [13]. Thus, it is crucial to invest efforts in researching and producing printing inks that are free from Volatile

Organic Compounds.

5. NATURAL INKS

The initial inks and dyes were of natural origin. In recent times, the growing environmental awareness has led to an increased demand and motivation to develop inks that are natural, green, or eco-friendly. In research by Ozcan et al. [14] it is stated that natural inks can be safely used in close contact with human skin, particularly in printing fabrics, products intended for children, and various types of food packaging, including smart packaging. However, a significant challenge with natural inks lies in their low yield during industrial production. Recent studies have shifted their focus on to the extraction of the dye from plants like red beet, red onion, potato, quince, hibiscus, black carrot, etc. [15]. In the experiment done by Ozcan and Arman [14] researchers demonstrated the feasibility of obtaining a dye with a wavelength determined at 538 nm through UV spectroscopy, which is perceivable as a red-magenta color. The dye was not only produced using natural resins and solvents but is also entirely edible. This literature indicates that natural dyes, depending on the solvent components could be edible [14, 15]. Karademir et al. [16] examined *P. pinaster* resins ink rheology, printability, water interaction test of ink, print gloss, color density, set-off, rub resistance, color change following light fastness and surface energy, and contact angle. They have found that *P. pinaster* resin was compatible with general requirements for ink resins that contain vegetable and mineral oils, as well as positive results in high light fastness, high print gloss, rub resistance of ink, and good set-off. However, Karademir et al. [16] suggest a hybrid use of this type of resin, which while still a better solution, indicates that there is a gap in research and production of fully VOC-free *P. pinaster* resins. Furthermore, it is worth noting that the use of such resins can reduce the levels of VOCs affecting IAQ, while also raising questions about sourcing the necessary ingredients for these resins in an environmentally friendly manner.

The research and development of natural inks for printing purposes have proven crucial, particularly for printing on substrates in close contact with humans. Recent literature highlights a growing emphasis on research exploring printing techniques for various textiles, with a focus on utilizing natural dyes and inks. One such method employed in textile printing is the use of inkjet technology. Savvidis et al. [17] tested six natural dyes: Annatto, 2: *Bixa Orellana*, Natural Orange; Annatto, 4: *Bixa Orellana*, Natural Orange; Cutch, 2: *Acacia Catechu*, Natural Brown; Cutch, 4: *Acacia Catechu*, Natural Brown; Pomegranate fruit rind, 2: *Punica granatum*, Natural Yellow; and Golden dock, 2: *Rumex maritimus*.

These six natural inks, printed on textiles with the ink-jet technology were tested on light fastness, rub test, and regular wash test. Savvidis et al. [17] authors found that by itself inks rub and wash fastness are low, but with the addition of fixators these properties become similar to other low-molecular-weight direct dyes on cotton. However the same cannot be said about the light fastness test, despite the use of fixators. In paper by Yeo and Shin [18] the development of environmentally friendly CMYK inks compatible with piezo-type printing on textiles involved the formulation of inks by researchers. These inks utilized biodegradable natural dyes, including amaranth, gardenia blue, gardenia yellow, lac, and logwood as well as water-soluble solvents, surfactant, distilled water, wetting agent, and anti-foaming agent. The researchers conducted a comprehensive assessment of the ink's physical properties, including surface tension, viscosity, and pH, over a 60-day period in order to ascertain the storage stability of the ink. Printing sharpness, rubbing, light, and washing fastness were tested as well. Yeo and Shin [18] have found positive results when testing for printing sharpness, rubbing, light, and washing fastness on both cotton and silk fabrics. This research suggests a promising direction for the utilization of natural dyes in textile printing and serves as a valuable model for future research.

6. CONCLUSION

This paper has looked into the landscape of printing ink, highlighting the environmental impact of synthetic inks in the printing industry. The classification of printing inks based on origin, application, method, solubility, and chemical structure offered a perspective on the diverse nature of these inks. The environmental impact of synthetic inks, particularly the attention on solvents as pollutants, emphasized the urgent need for sustainable alternatives in the industry. Volatile organic compounds emerged as a critical focus, impacting not only the external environment but also posing long-lasting health risks for workers in indoor settings of printing facilities. The shift towards natural inks, showcased ongoing research and development endeavors aimed at producing safer products and addressing the environmental footprint of the printing industry. The challenges of low yield in industrial production were highlighted, along with recent studies focusing on extracting dye from natural sources. The exploration of

natural inks in textile printing demonstrated promising results. By synthesizing current knowledge and ongoing efforts in the domain of natural printing inks, this paper could contribute to a deeper understanding of the environmental implications of printing processes and underscore the importance of sustainable alternatives in the field of printing inks.

Future research is needed in the field of natural inks, in order to optimize the production yield of natural inks. Literature outlined an issue of adapting current ink production facilities to better support the production of natural inks, which indicates the need for future research not only in ink composition but also in production process optimization.

7. REFERENCES

[1] Gu, W., Li, Y,, Zhang, X.: *Printing industry and the environment,* Advanced Materials Research, p.p. 759–762, 2013.

[2] Robert T.: *'green ink in all colors' - Printing ink from renewable resources,* Progress in Organic Coatings, 78, p.p. 287–292, 2015.

[3] Pekarovicova A., Husovska V.: *Printing Ink Formulations*, Printing on Polymers: Fundamentals and Applications, Elsevier Inc., p.p. 41–55, 2015.

[4] Prica M,, Adamović S.: *Grafički Materijali*, 1st ed. Novi Sad: FTN: Grafički Centar GRID, 2017.

[5] Katheresan V., Kansedo J., Lau SY.: *Efficiency of various recent wastewater dye removal methods: A review,* Journal of Environmental Chemical Engineering 6, p.p. 4676–4697, 2018.

[6] Kant R.: *Textile dyeing industry an environmental hazard,* Nat Sci (Irvine), 04, p.p. 22–26, 2012.

[7] Tawiah B., Howard E.K., Asinyo B.K., et al.: *the chemistry of inkjet inks for digital textile printing-review,* nternational Journal of Management, InformationTechnology and Engineering, 4, p.p. 61-78, 2019.

[8] Gvojić, V.: *Ispitivanje mogućnosti primene fenton-procesa u tretmanu obojenih otpadnih voda grafičke industrije*, Doktorska disertacija, Univerzitet u Novom Sadu, 2019.

[9] Aydemir, C., Özsoy, S.A.: *Environmental impact of printing inks and printing process,* Journal of Graphic Engineering and Design 11, p.p. 11–17, 2021.

[10] Yang, S., Chen, S., He, T.F., et al.: *Preparation of sustainable mineral oil-free offset printing ink with vegetable oil esters,* Environmental Science and Pollution Research 30, p.p. 97404–97415, 2023.

[11] Goverment of Canada: *Volatile organic compounds in products overview. Volatile organic compounds in products overview,* 2023, [Online] Available at*:* https://shorturl.at/xFLM4. [Accessed: 08.11.2023.]

[12] Okubo, M., Kuwahara, T.: *Prospects for marine diesel engine emission control,* New Technologies for Emission Control in Marine Diesel Engines, Elsevier, p.p. 211–266, 2020.

[13] Van Tran, V., Park, D., Lee, Y.C.: *Indoor air pollution, related human diseases, and recent trends in the control and improvement of indoor air quality,* International Journal of Environmental Research and Public Health; 17. Epub ahead of print DOI: 10.3390/ijerph17082927, 2 April 2020.

[14] Ozcan, A., Arman, K.E.: *Natural ink production and printability studies for smart food packaging,* Color Res Appl 45, p.p. 495–502, 2020.

[15] Pallottino, F., Hakola, L., Costa, C., et al.: *Printing on Food or Food Printing: a Review,* Food and Bioprocess Technology 9: p.p. 725–733, 2016.

[16] Karademir, A., Aydemir, C., Yenidogan, S., et al.: *The use of natural (Pinus pinaster) resin in the production of printing ink and the printability effect*, Color Res Appl 45, p.p. 1170–1178, 2020.

[17] Savvidis, G., Karanikas, E., Nikolaidis, N., et al.: *Ink-jet printing of cotton with natural dyes*, Coloration Technology 130: p.p. 200–204, 2014;.

[18] Yeo, Y., Shin, Y.: *Inkjet Printing of Textiles Using Biodegradable Natural Dyes,* Fibers and Polymers 24, p.p. 1695–1705, 2023.

Authors: **Jelena Kerac, Full prof. dr Miljana Prica,** University of Novi Sad, Faculty of Technical Sciences, Trg Dositeja Obradovica 6, 21000 Novi Sad, Serbia, Phone.: +381 21 485 2350, Fax: +381 21 454-495.

E-mail: jelena.kerac@uns.ac.rs
miljana@uns.ac.rs

ETIKUM 2023 **INTERNATIONAL SCIENTIFIC CONFERENCE**
NOVI SAD, SERBIA, DECEMBER 7-9, 2023

Kiss, F.

IMPACT OF INVENTORY MODELLING CHOICES ON LCA RESULTS: A CASE STUDY WITH ELECTRIC VEHICLES

Abstract: *Life Cycle Assessment (LCA) is considered an essential method for evaluating the environmental impact of product systems, often hailed as the best. While LCA follows a standardized approach, relevant ISO standards allow for the utilization of various methods to address identical methodological concerns. This flexibility can lead to highly disparate outcomes, creating uncertainty and doubt about the assessment's reliability. This study aims to demonstrate how the chosen modelling approach can significantly influence LCA results when assessing the environmental impacts of electric vehicles. Furthermore, it aims to discuss the advantages and disadvantages of these approaches in terms of their effectiveness in facilitating decision-making processes.*
Key words: *life cycle assessment, modelling choice, electric vehicles.*

1. INTRODUCTION

Battery electric vehicles (BEVs) have gained significant attention as a presumably more sustainable and environmentally friendly alternative to traditional internal combustion engine vehicles (ICEVs). They are lauded for their increased efficiency and complete absence of tailpipe emissions [1]. However, recent examinations of life cycle assessment (LCA) studies for BEVs have uncovered a notable variability in results, leading to conflicting conclusions about their overall environmental benefits in comparison to ICEVs [2]. The divergence in LCA findings can be attributed to several factors, including variations in data quality, differences in vehicle types, sizes, battery technologies, and efficiency, as well as assumptions about electricity sources [3] and considerations related to end-of-life (EoL) scenarios for vehicles and batteries [4]. Nonetheless, prior research frequently overlooked a potentially significant source of variability: the methodological choices made in the life cycle inventory phase (LCI) of the LCA of BEVs. While LCA follows a standardized approach, relevant ISO standards offer flexibility in defining system boundaries and addressing multifunctionality. This flexibility has given rise to two distinct LCA approaches: the attributional life cycle assessment (ALCA) and the consequential life cycle assessment (CLCA) [5].

The primary aim of this study is to demonstrate the substantial influence of choosing either the ALCA or CLCA approach on the LCA results of electric vehicles. Additionally, the LCA results will be compared to the environmental impacts of ICEVs to assess whether the modelling approach choice can alter conclusions regarding the environmental benefits of BEVs.

2. METHOD

A process-based Life Cycle Assessment (LCA) was conducted in accordance with ISO 14040 and 14044 standards to evaluate the environmental impacts of BEVs and ICEVs. The life cycle inventory data were sourced from the ecoinvent LCI database, which enables assessments based on both attributional (represented in this study by the ecoinvent's "Allocation, cut-off by classification" system model) and consequential principles (represented by the "Substitution, consequential, long-term" system model in ecoinvent) [6]. The environmental impacts of BEV is estimated based on ecoinvent 3.7 processes "*transport, passenger car, electric | transport, passenger car, electric | Cutoff or Consequential*" while processes *"market for transport, passenger car with internal combustion engine | transport, passenger car with internal combustion engine | Cutoff or Consequential"* were used to estimate the impact of the average ICEV in Europe.

The functional unit corresponds to one km of driving. This entails that environmental impacts are computed across the entire life cycle of the vehicle and distributed over the total kilometres driven during the vehicle's lifetime. The ecoinvent process covers all the processes involved in vehicle manufacturing, including material extraction and processing, component manufacturing, vehicle assembly, and end-of-life (EoL) as well as the life cycle of the energy carrier for vehicle propulsion. Battery recycling is only

included in the LCI data for BEVs. In the ecoinvent process, the original electricity mix has been substituted with the Serbian electricity mix in both the cut-off and consequential processes. This alteration aims to provide a more accurate representation of the potential impact of BEVs in Serbia.

The LCA calculations were computed using the OpenLCA software version 10 (https://openlca.org) and the ecoinvent database version 3.7. The life cycle impact assessment (LCIA) method employed is the ReCiPe (H) v.1.04 [7]. Six midpoint impact categories were selected for discussion in detail. Beside global warming potential (GWP) and fossil resource scarcity (FRS), which are priority indicators in the current environmental decision-making [8], fine particulate matter formation (FPMF), mineral resource scarcity (MRS), human non-carcinogenic toxicity (HnCT), and human carcinogenic toxicity (HCT) are also discussed.

3. RESULTS AND DISCUSSION

The results section is structured as follows: firstly, the environmental impacts of the BEVs assessed with both modeling approaches are compared to ICEVs; secondly, the environmental impact hotspots of the ALCA and CLCA of the BEVs are presented.

As depicted in Table 1, the environmental performance of BEVs, compared to conventional ICEVs, varies significantly depending on the LCA modelling and the selected impact category. Based on both ALCA and CLCA results, the assessed BEV exhibits lower fossil fuel depletion (27% reduction in ALCA and 71% in CLCA) and global warming impact (10% reduction in ALCA and 49% in CLCA) compared to ICEVs. There is also a consensus for particulate matter formation and human carcinogenic toxicity between the two models, emphasizing the advantages of BEV technology. However, for MRS and HnCT, the ALCA and CLCA models draw different conclusions. In these impact categories, the CLCA model indicates benefits for BEVs, whereas the ALCA calculates higher impacts than ICEVs.

The overall breakdown of the cradle-to-grave environmental impact of BEVs is illustrated in Fig. 1. In the case of ALCA, it can be observed that supply of electricity is the most relevant environmental hotspot (45-88% of the cradle-to-grave environmental burden) in all categories except for mineral resource scarcity. Vehicle and battery life cycle (production and EoL) are the second and third largest contributors to overall impacts except in MRS impact category where these two processes are responsible for 92% of the impacts. Other processes have only a minor share in overall impacts.

Similar to the results from the ALCA, in CLCA, supply of electricity, vehicle (production and EoL) and battery life cycle are responsible for most of the impacts within specific impact categories. Differing from the ALCA, the consequential modeling leads to the results that impacts associated with additional demand for batteries are the most important contributors to particulate matter formation and emissions of carcinogenic substances (whereas in ALCA, this was electricity). It is crucial to highlight that in the cut-off model, results are consistently positive numbers, whereas in CLCA, these values can be either positive or negative (refer to Table 1). In the context of LCA, positive impact category indicators signify environmental burden, while negative results denote an overall reduction in environmental impact. Negative outcomes in CLCA arise from employing the substitution method, i.e., the avoided burden approach, particularly when addressing multifunctional processes and modeling the effects of providing recyclable materials (e.g., batteries and vehicle parts) in the process. This aspect will be explored further in subsequent discussions.

Given the considerable disparities in results between ALCA and CLCA, two pivotal questions emerge: why do such pronounced differences exist, and which approach stands as the superior choice for assessing the environmental impact of

Table 1. The estimated life cycle environmental impacts of BEVs and ICEVs depending on the modelling approach (per 1 km driven)

Impact category	Unit	BEVs		ICEVs	
		ALCA (cut-off)	CLCA	ALCA (cut-off)	CLCA
Fine particulate matter formation (FPMF)	kg $PM_{2.5\ eq}$	1.52E-03	3.80E-04	3.70E-04	2.10E-04
Fossil resource scarcity (FRS)	kg oil $_{eq}$	7.54E-02	2.98E-02	1.03E-01	1.02E-01
Global warming (GWP)	kg $CO_{2\ eq}$	2.97E-01	1.62E-01	3.31E-01	3.17E-01
Human carcinogenic toxicity (HCT)	kg 1,4-DCB	6.17E-02	8.50E-02	4.94E-02	6.81E-02
Human non-carcinogenic toxicity (HnCT)	kg 1,4-DCB	7.89E-01	8.09E-02	2.24E-01	1.76E-01
Mineral resource scarcity (MRS)	kg Cu $_{eq}$	3.16E-03	-1.88E-02	3.07E-03	1.66E-03

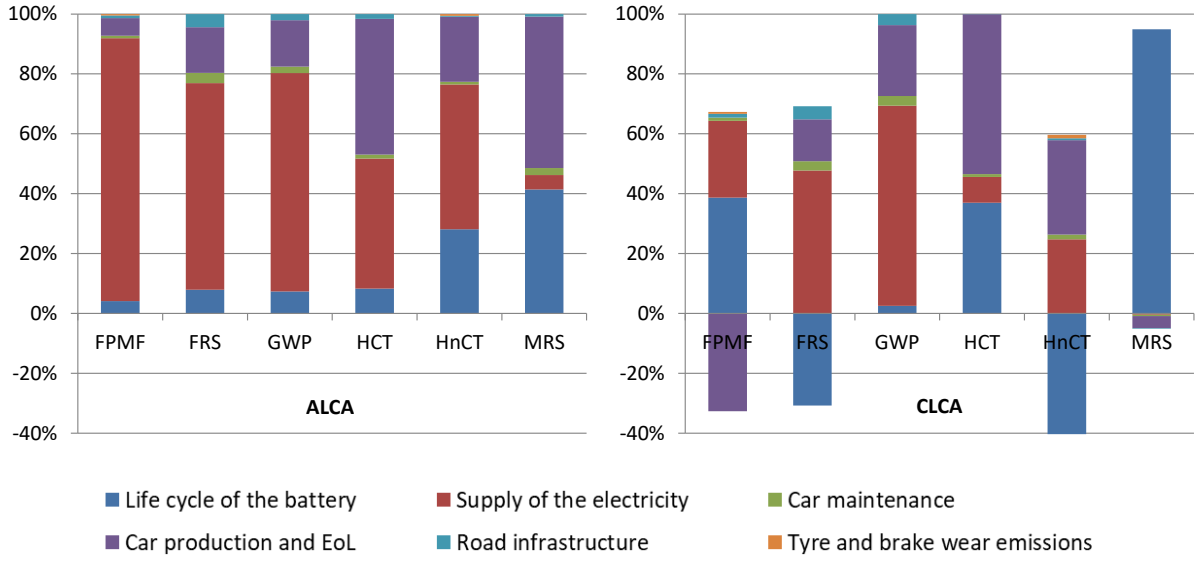

Fig. 1. Contribution of processes to impact category indicator results depending on the modelling approach

vehicles? The notable disparities in outcomes between ALCA and CLCA stem from the fundamental distinctions in the systems they model, the input data they employ, and the methodologies they apply to address the challenges associated with multifunctionality and recycling. ALCA relies on average data, while CLCA ideally employs marginal data [5]. For example, in this specific case study, ALCA calculates based on the average electricity mix in Serbia from the preceding period (60% lignite, 24% hydropower, 16% other). CLCA calculates with marginal electricity data and assumes that the long-term marginal electricity supply will be predominantly from natural gas power plants, with a relatively low share of the highly polluting lignite in the overall electricity mix in Serbia. The lower environmental impact of the marginal electricity mix and the substantial contribution of electricity to the overall results (Fig. 1) partly explain why CLCA yielded lower impacts in five out of the six impact categories compared to ALCA.

A notable distinction between ALCA and CLCA lies in how they handle multifunctional processes and recycling. In the ecoinvent's cut-off system model, multifunctionality is addressed through a partitioning approach, wherein the overall impact of a multifunctional process is divided among its co-products, typically in proportion to their economic value (or exergy value for specific processes) [6]. In contrast, the consequential approach addresses multifunctionality through the substitution approach, also referred to as the avoided burden approach. This method involves subtracting the impact of processes replaced by by-products from the overall impact of the multifunctional process [6]. The distinction in how these approaches handle recycling becomes particularly significant when considering BEVs, given the recyclability of both electric vehicles and batteries. In the consequential approach, it is assumed that recyclable materials replace virgin materials, and the impact of the avoided production of virgin material can be subtracted from the overall impact of the analyzed process. This stands in stark contrast to the cut-off modeling approach, where the primary producer receives no credit for providing recyclable materials [6]. The application of the avoided burden approach in CLCA of BEVs explains the negative values obtained in the MRS impact category (Table 1). Additionally, there are environmental benefits (negative emissions), derived from battery and vehicle recycling, which are also evident in the FPMF, FRS, and HnCt impact categories (Fig. 1). Another differentiation between the cut-off and consequential approaches lies in the assumption in the former that recycled products used as inputs in the production process are always available burden-free. In contrast, the consequential approach may assign a certain environmental value to consumed recycled materials based on the dynamics of the scrap market [9].

So, which modelling approach is better to estimate the environmental impact of BEVs? Unfortunately, it cannot be definitively stated that one is universally better than the other, as the two types of LCA come with distinct advantages and disadvantages [5]. It is widely acknowledged that the choice between these approaches should not be

arbitrary but based on the study's goal, as they address different questions. The attributional approach seeks to quantify the portion of global burdens associated with the specific product under assessment [5]. CLCA gives and estimated of how the global environmental burdens are affected by the production and use of the product [5]. Attributional LCAs have found broad applications in ecolabeling and policy support since their results are generally less sensitive to assumptions and have lower uncertainties [8]. Consequential LCAs, in contrast, have primarily been applied for policy support in understanding the consequences of policy decisions, especially for biofuels [8]. It is broadly acknowledged in the literature that CLCAs are more sensitive to uncertainties than ALCAs due to the inclusion of market prospects [8]. In the case of BEVs, uncertainties regarding the prediction of the future marginal electricity mix, as well as the end-of-life fate of electric vehicles and batteries, are major concerns in CLCA models. Nevertheless, an argument for CLCA is that checks on the consequences linked with the indirect causal-effect effects of BEVs' utilization are necessary for a policy perspective aiming to avoid unintended counterfactual effects.

4. CONCLUSIONS

The main goal of this article was to compare the results of ALCA and CLCA in evaluating BEVs. In this specific case study, environmental burdens were higher when using attributional modelling than consequential modelling, leading to contrasting conclusions in several impact categories compared to conventional ICEV technology. The reason is that ALCA and CLCA are two conceptually different approaches, particularly in defining system boundaries and dealing with multifunctional processes and recycling. Given the substantial differences in results and conclusions obtained with these approaches, it is crucial to appropriately select the right methodological approach. While it is widely acknowledged that the choice of modeling approach should align with the goals and scope of the study, the absence of clear goal definitions and precise guidelines for selecting a modeling approach based on the study's goals remain a significant challenge.

5. ACKNOWLEDGMENTS

This research was supported by the Ministry of Education, Science and Technological Development of the Republic of Serbia, contract number 451-03-47/2023-01/200134.

6. REFERENCES

[1] Kukreja, B. (2018). *Life Cycle Analysis of Electric Vehicles—Quantifying the Impact*. City of Vancouver: Vancouver, BC, Canada.

[2] Verma, S., Dwivedi, G., & Verma, P. (2022). *Life cycle assessment of electric vehicles in comparison to combustion engine vehicles: A review.* Materials Today: Proceedings, 49, 217-222.

[3] Marmiroli, B., Messagie, M., Dotelli, G., & Van Mierlo, J. (2018). *Electricity generation in LCA of electric vehicles: A review.* Applied sciences, 8(8), 1384.

[4] Koroma, M. S., Costa, D., Philippot, M., Cardellini, G., Hosen, M. S., Coosemans, T., & Messagie, M. (2022). *Life cycle assessment of battery electric vehicles: Implications of future electricity mix and different battery end-of-life management.* Science of the Total Environment, 831, 154859.

[5] Ekvall, T. (2019). *Attributional and consequential life cycle assessment.* In Sustainability Assessment at the 21st century. IntechOpen.

[6] Wernet, G., Bauer, C., Steubing, B., Reinhard, J., Moreno-Ruiz, E., & Weidema, B. (2016). *The ecoinvent database version 3 (part I): overview and methodology.* The International Journal of Life Cycle Assessment, 21, 1218-1230.

[7] Huijbregts, M. A., Steinmann, Z. J., Elshout, P. M., Stam, G., Verones, F., Vieira, M., ... & Van Zelm, R. (2017). *ReCiPe2016: a harmonised life cycle impact assessment method at midpoint and endpoint level.* The International Journal of Life Cycle Assessment, 22, 138-147.

[8] Moretti, C., Vera, I., Junginger, M., López-Contreras, A., & Shen, L. (2022). *Attributional and consequential LCAs of a novel bio-jet fuel from Dutch potato by-products.* Science of the Total Environment, 813, 152505.

[9] Ekvall, T., Johannesson, C. (2020). *Modeling recycling in life cycle assessment.* Project report. IVL Swedish Environmental Research Institute.

Author: **Dr. Ferenc E. Kiss, research assistant,** University of Novi Sad, Faculty of Technology, Bul. cara Lazara 1, 21000 Novi Sad, Serbia, Phone.: +381 21 485 3667.

E-mail: fkiss@uns.ac.rs

ETIKUM 2023 INTERNATIONAL SCIENTIFIC CONFERENCE
NOVI SAD, SERBIA, DECEMBER 7-9, 2023

Kuhnová, L., Szaryszová, P., Bosák, M.

THE BOOM IN NUCLEAR ENERGY AND ITS IMPACT ON THE ENVIRONMENT

Abstract: *Energy is one of the most important factors affecting the development of society, and the demands for its consumption are constantly increasing. European energy and its gradual transition to climate neutrality, planned until 2050, is significantly affected by the Russian invasion of Ukraine. As a result, many countries (such as France, the Czech Republic and Slovakia) were forced to increase their coal consumption in 2022, which the EU aims to reduce. The aim of the paper is to outline possible scenarios for the future development of European energy until 2050, when several countries begin to prioritize nuclear energy.*
Key words: *nuclear energy, life cycle, environment, sustainability*

1. INTRODUCTION

The current European context, affected by the dramatic conflict between Russia and Ukraine and the related lack of energy and food, is putting a strain on the availability of natural gas in European member countries. They are forced to new negotiations with other potential energy suppliers, to urgent internal measures to reduce energy demand, and at the same time to fulfil obligations towards internationally agreed climate goals, where energy transformation is a key strategy. A sustainable energy transition strategy is also necessary for the implementation of the circular economy, which requires replacing fossil energies with renewable ones. In turn, the energy transformation should meet the principles of the circular economy with the aim reduce the consumption of natural resources and the contribution to climate change. In this context, this study assesses the environmental impacts of nuclear power under various government and research scenarios as well as individual perspectives.

2. HISTORY OF NUCLEAR ENERGY

After the use of atomic bombs at the end of World War II in Japan and the subsequent tests of nuclear weapons by world powers, the question of using nuclear energy in other areas also arose. In the field of research and development of nuclear energy, work was carried out mainly in the Soviet Union, the USA, UK and Canada. The most widespread use found the fission of uranium in nuclear power plants [1]. The history of nuclear energy as we know it today began to be written in the world in 1950. In this year, the construction of the world's first nuclear power plant began near the village of Obninsk, southwest of Moscow. The power plant was connected to the power grid in 1954 and was shut down on April 29, 2002. Today, a museum of nuclear energy has been established in its place. A nuclear reactor was first used in 1951 in the state of Idaho in the USA to produce electricity [2].

2.1 Advantages of nuclear energy

Due to the importance of clean energy, nuclear power has become the subject of considerable interest among academics and policy makers in achieving a low-carbon economy with sustainable energy and has been identified as one way to reduce CO_2 emissions [3]. It can be said that the energy systems of countries across Europe are distinctly different, but countries that are geographically close to each other often have them somewhat similar [4, 5].

In the process of transition to clean energy, all options for measures to reduce carbon emissions can and should be considered. New innovative projects of nuclear power plants have a real chance to reduce initial construction costs, which are probably the biggest obstacle to the widespread use of nuclear energy [6]. Another important aspect to consider when choosing an energy source is the waste generated during energy production. Renewable energy sources generate a significant amount of waste due to the materials used to produce electricity and their comparatively shorter lifetime, in contrast to radioactive waste from nuclear power plants, which can be disposed of using deep geological repositories and the radioactivity of the waste decreases over time [7].

2.2 Nuclear energy as a tool for emission reduction

On an international scale, the importance of

clean energy is highly valued in the context of Sustainable Development and air protection. According to the authors Azam et al. [8] it is important to identify the impact of the consumption of renewable energy, natural gas and nuclear energy on economic growth and CO_2 emissions. However, several authors agreed that decarbonization takes place in all countries at different speeds based on the regional situation [9].

In general, nuclear energy is an important part of the transition to a more sustainable society because of its minimal carbon emissions, high energy and energy density, and rapid power generation capacity with less land requirement [10]. Its development has been prioritized over renewable energy sources because it offers significant advantages in optimizing the energy structure, ensuring ecological stability, and reducing air pollution [11,12]. In a study for China, Dong et al. [13] considered the impacts of nuclear power on environmental pollution consider fossil fuels and renewable energy in 1993–2016. The results of their study confirmed the existence of the environmental Kuznets curve hypothesis and found that nuclear power has a positive impact and contributes to pollution mitigation.

3. METHODOLOGY OF THE STUDY

This study used bibliometric and visualization methods for data analysis. Using the VOSviewer application to create a collaboration network of authors, institutions, and countries with a network of common concepts. Due to the global nature of issues in the field of energy, the Web of Science database was selected as a literature source for this study. As an important database for global access to academic information, it includes multidisciplinary content from nearly 9,000 of the most prestigious and influential scientific journals and more than 33,000 academic conferences worldwide. In this study, we identified the subject term "Nuclear Energy" in the core collection of Web of Science (SCIE, SSCI), obtaining 11,237 documents (published from 1987 to 2023) for the study (as of 11/14/2023).

4. BIBLIOGRAPHIC ANALYSIS AND NUCLEAR ENERGY SCENARIOS

As part of the study, an analysis of the co-occurrence of key words in the field of nuclear energy was carried out. The results of the analysis are shown in Fig. 1 and Fig. 2. Fig. 1 shows eight thematic categories defined by keywords with their colour differentiation, where red means keywords related to the topic of low-carbon transitional routing, blue means keywords related to the topic of low-carbon policy support, yellow means keywords related to the topic of low-carbon infrastructure network planning, green means keywords related to the topic of the circular economy, orange means keywords related to the theme of innovation, purple means keywords related to the concept of sustainability, brown means keywords related to the logistics management mechanism and green financing strategy, and light blue reflecting the social aspect of climate change.

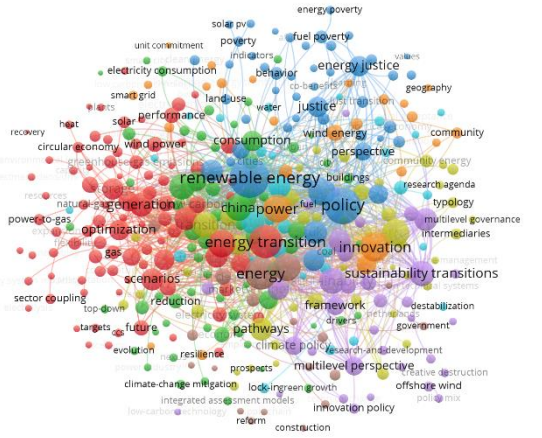

Fig. 1. The connection of scientific and research terms in connection with the nuclear low-carbon transformation

The reasons why this field has not become mainstream in the field of energy transformation may be the assumption that the two main research tasks of energy supply, which correspond to the current needs of socio-economic development and energy sustainability, have not yet been realized. In the field of energy transformation, probably most researchers have not shifted their focus to this subfield.

In terms of cluster connectivity, researchers have studied both the internal and external constraints of energy systems. Internal constraints include energy categories, carbon emissions, and energy demands within the energy system we focus on, while external constraints include economic growth, government policies, and citizen participation.

On the other side, it has been found that some previously popular technologies (e.g., biogas technologies and nuclear technologies) may not meet the growing demands of the low-carbon transition of energy systems, which requires careful evaluation studies. In addition, scientists have shown that renewable energies cannot completely replace fossil fuels in the short term. Co-existing

models of emerging renewables and traditional fossil fuels are thus essential for the process of low-carbon transition of energy systems. It is difficult to support the low-carbon transition in carbon-intensive industries due to high costs. Additional research could further transform the industry from fossil fuel-based power generation to low-carbon technologies using nuclear power.

The low-carbon transformation plays an important role in shaping future energy systems. Through content analysis of highly cited papers from the WOS database, we identified that researchers have focused on designing transformations that depend on different spatiotemporal scales and transition constraints. Fig. 2 illustrates the topic of low-carbon transformation at the level of individual countries.

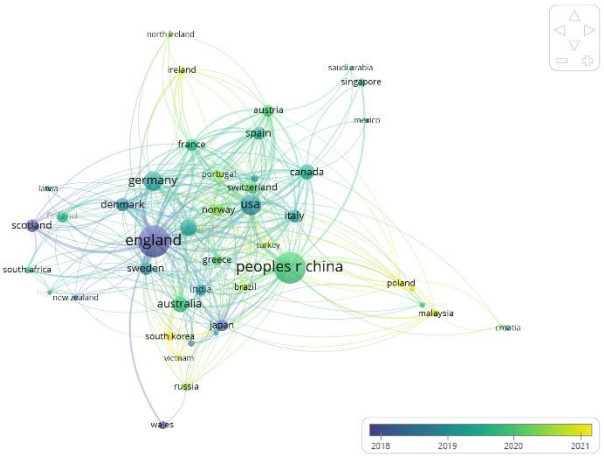

Fig. 2. World network of scientific and research cooperation

According to analysis of the existing literature, research on the low-carbon transition of energy systems has been growing rapidly in the past decade, where China, the United Kingdom, and the United States playing a leading role in this field. The interdisciplinarity of studies on the low-carbon transition of energy systems has brought together scientists from various fields, including energy engineering, environmental sciences, and social sciences, who have produced publications in academic journals in various fields. With the growing practical need to support the low-carbon transition of energy systems, it is likely that an ever-increasing number of scientists from different regions and academic disciplines will be drawn into the study of low-carbon transition of energy systems. Efficient and effective collaboration will be key in generating valuable and practical knowledge in this area. Building cooperative relationships between scientists from developed and developing countries can be mutually beneficial, allowing scientists from developing countries to learn from the experiences of developed countries and scientists from developed countries to test theories in broader contexts. Researchers would particularly benefit from collaborating with scientists from China, the United Kingdom, and the United States to study the low-carbon transition of energy systems, as these three countries play a central and leading role in this field.

5. NUCLEAR ENERGY IN THE WORLD

The biggest boom in the construction of nuclear power plants occurred in the 1970s and 1980s. According to the International Atomic Energy Agency, there are currently 441 nuclear reactors in operation in 30 countries. The world leader is the USA with 93, followed by France with 56 reactors, China with 52 and Russia with 38 reactors. Nuclear power plants can be found in 30 countries around the world. China holds the lead in the number of reactors under construction.

Thirteen countries produced at least one quarter of their electricity from nuclear in 2020. France gets about three-quarters of its electricity from nuclear power, Slovakia (53.1 %) and Ukraine more than half from nuclear power, while Hungary, Belgium, Slovenia, Bulgaria, Finland, and the Czech Republic get one-third or more. South Korea routinely gets more than 30 % of its electricity from nuclear, while the USA, UK, Spain, Romania and Russia get about a fifth of their electricity from nuclear. Japan used to rely on nuclear power for more than one quarter of its electricity and is expected to return to somewhere close to that level [1].

France is the European leader, Ukraine with 15 reactors and Great Britain with 13 reactors have the highest number of units compared to other countries.

Renewable energy is growing impressively in many parts of the world, but it is still not at the level to achieve net zero emissions by mid-century. Nuclear energy does not pollute the air with harmful emissions, does not produce greenhouse gases and mitigates the excessive use of other fuel stocks. As the world's energy demand grows at an alarming rate, both developed and developing economies are seeking access to stable and clean sources of energy in cost-effective and environmentally friendly ways. The main advantages of nuclear energy are that they use less energy, use cheap, highly efficient materials, and do not emit greenhouse gases. Therefore, it is the only stable source of energy with a base load that does not harm the environment.

6. CONCLUSIONS

Studies indicate that nuclear power significantly reduces CO_2 emissions in all countries except Canada and the USA. Renewable energy also significantly reduces CO_2 emissions only in Canada and France. In line with these findings, it is important for the G7 countries to increase the use of nuclear power for the purpose of reduction the dependence on fossil fuels in most of the G7 countries to reduce CO_2 emissions. In addition, it is also suggested that these countries adopt relevant policies for other ecological processes of consumption and production to ensure complementarity between economic growth and environmental development.

7. ACKNOWLEDGEMENT

This research was supported by the Scientific Grant Agency of the Ministry of Education, Science, Research, and Sport of the Slovak Republic as part of the research project KEGA 035EU-4/2022: Achieving the Goals of the 2030 Agenda for Sustainable Development under the influence of the Global Pandemic COVID-19.

8. REFERENCES

[1] World-nuclear. 2022. *Nuclear energy's contribution to climate change mitigation.* [Online] (cited 14.11.2023). Retrieved from: www.world-nuclear.org.

[2] Markard, J., Bento, N., Kittner, N., & Nuñez-Jimenez, A. 2020. Destined for decline? Examining nuclear energy from a technological innovation systems perspective. *Energy Research & Social Science*, 67, 101512.

[3] Sadiq, M., Shinwari, R., Wen, F., Usman, M., Hassan, S. T., & Taghizadeh-Hesary, F. 2023. Do globalization and nuclear energy intensify the environmental costs in top nuclear energy-consuming countries?. *Progress in Nuclear Energy*, 156, 104533.

[4] Wang, J; Yin, Y. 2018. Fermentative hydrogen production using various biomass-based materials as feedstock. *Renewable and sustainable energ.* 92, 2018. (online). Cit. 16.10.2023. doi: 10.1016/j.rser.2018.04.033.

[5] Nasim, I. 2023. Role of Green Finance for Sustainable Environment So Far: A Bibliometric Analysis and Policy Framework. *Pakistan Journal of Humanities and Social Sciences*, 11(2), 899-912.

[6] Mignacca, B., Locatelli, G., & Sainati, T. 2020. Deeds not words: Barriers and remedies for Small Modular nuclear Reactors. *Energy*, 206, 118137.

[7] Tazi, N.; Kim, J.; Bouzidi, Y.; Chatelet, E.; Liu, G. 2019. Waste and material flow analysis in the end-of-life wind energy system. Res. Conserv. *Recycl.* 2019, 145, 199–207.

[8] Azam, A., Rafiq, M., Shafique, M., Zhang, H., & Yuan, J. 2021. Analyzing the effect of natural gas, nuclear energy and renewable energy on GDP and carbon emissions: A multi-variate panel data analysis. *Energy*, 219, 119592.

[9] Fankhauser S, Jotzo F 2018 Economic growth and development with low-carbon energy. Wiley Interdisciplinary Reviews: *Climate Change*, 9(1), e495, doi: 10.1002/wcc.495.

[10] C. McCombie, M. Jefferson. Renewable and nuclear electricity: comparison of environmental impacts. *Energy Pol.*, 96 (2016), pp. 758-769, doi: 10.1016/J.ENPOL.2016.03.022.

[11] L.S. Lau, C.K. Choong, C.F. Ng, F.M. Lie w, S.L. Ching. Is nuclear energy clean? Revisit of Environmental Kuznets Curve hypothesis in OECD countries. *Econ. Modell.*, 77 (2019), pp. 12 20, doi: 10.1016/j.econmod.2018.09.015.

[12] H. Iwata, K. Okada, S. Samreth. Empirical study on the determinants of CO2 emissions: evidence from OECD countries. Appl. *Econ.*, 44 (2012), pp. 3513-3519, doi: 10.1080/00036846.2011.577023.

[13] K. Dong, R. Sun, H. Jiang, X. Zeng CO2 emissions, economic growth, and the environmental Kuznets curve in China: what roles can nuclear energy and renewable energy play? J. Clean. *Prod.*, 196 (2018), pp. 51-63, doi: 10.1016/j.jclepro.2018.05.271.

Authors: **Assis. prof. Ing. Lenka Kuhnová, PhD., MBA, Assis. prof. Ing. Petra Szaryszová, PhD., Assis. prof. prof. h. c. Ing. Martin Bosák, PhD., Ing.Paed.IGIP, MBA.** University of Business Economics, Faculty of Business Economics with seat in Košice, Tajovského 13, 042 30 Košice, Slovak republic, Phone.: +421 55 722 3254

E-mail: lenka.kuhnova@euba.sk
petra.szaryszova@euba.sk
martin.bosak@euba.sk

ETIKUM 2023 **INTERNATIONAL SCIENTIFIC CONFERENCE NOVI SAD, SERBIA, DECEMBER 7-9, 2023**

Morev, D., Vasenev, I., Andreeva, I.

COMPARATIVE ANALYSIS OF THE METROLOGICAL FEATURES OF SOIL CARBON MEASUREMENT IN CONDITIONS OF AGROECOLOGICAL RESEARCH STATION OF TIMIRYAZEV ACADEMY

Abstract: *Soil carbon is the most important factor influencing the processes that widely determine global climate change. However, its assessment requires different approaches, including the use of specific methods of analysis. The classic and most common nowadays are the analysis of soil total carbon by the Dumas dry combustion method and Walkley-Black for measuring of organic carbon (wet method). Paper presents the results of a comparative analysis of these two methods, as well as the method of Valeeva et al., based on the evaluation of reflective characteristics in the red channel of RS.*
Key words: *soil total carbon, soil organic carbon, comparative analysis*

1. INTRODUCTION

Problems associated with global climate change raise the issue of assessing carbon pools and fluxes in ecosystems at various levels. Agroecosystems play a significant role in the global carbon cycle and can both accumulate it and release it during land use, depending on a set of environmental conditions and anthropogenic factors [1,2]. The distribution of organic matter in the soil and carbon as its main component is often characterized by high variability and its accounting requires an integrated approach and selection from a wide range of research methods [3,4]. Approaches and methods for determining carbon in soil cover its various fractions and are characterized by both positive and negative aspects [5-7].

The widely used method for determining organic carbon using potassium dichromate in soil has proven to be reliable and reproducible, although it is indirect. However, it should be noted that the accuracy of the results obtained using this method may be influenced by temperature conditions, wet ashing time, the presence of chlorides in the soil and a few other conditions [8,9].

On the other hand, the dry combustion method, which is now implemented in automatic carbon analyzers, also depends on the temperature regime and the presence of inorganic compounds in the soil that form carbon dioxide [10,11]. At the same time, even considering the presence of carbonates in soil samples, the obtained data have significantly greater reliability and reproducibility even with interlaboratory comparative tests, while indirect ones have more modest metrological indicators even with intra-laboratory control.

With the development and reduction in cost of remote sensing systems, interest in approaches and methods for estimating carbon from reflected radiation is growing [12-14]. The method proposed by Valeeva et al. [15] using reflected radiation in the red channel has the potential to allow carbon assessment over large areas when a camera is mounted on a drone. However, the quality of the calculated carbon values obtained in this case does not always provide the required level of reliability and reproducibility.

Thus, the available literature data indicates greater reliability and better metrological characteristics of the dry combustion method for carbonate-free soils.

2. OBJECTS AND METHODS

2.1 Objects

As an object of research, we used a field agroecosystem with aestivum spring wheat with disturbed soddy-podzolic soils of the field agroecological station of the Russian State Agrarian University - Moscow Timiryazev Agricultural Academy, which is located in the northern part of the Moscow metropolis (55°50'25.5"N 37°33'03.4"E).

The area of the site is about 2.2 hectares and, with a slope steepness of less than 1°, has a pronounced complex microrelief represented by microdepressions. The structure of the soil cover is disturbed as a result of a complex history of land use, including melioration (drainage unit).

2.2 Methods

Field research methods included preparing a grid of points for soil sampling and measurement of plant yields using a GNSS Stonex S9 III

system. To differentiate site conditions, the points were divided into 4 areas according to yield amount. Aerial photography was carried out using a DJI Phantom 4 drone with a visible camera and an RTK system. Soil sampling was carried out with an Edelman drill from a depth of 0-10 cm. The mowing of the above-ground mass of plants, followed by threshing to consider the yield, was carried out at each sampling point from an area of 0.25 м^2.

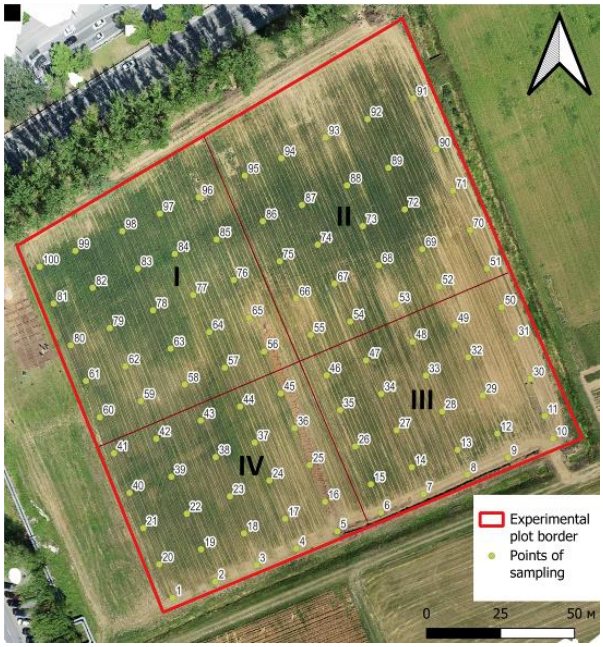

Fig. 1. Scheme of sampling and station view

Laboratory studies included the determination of soil organic carbon by the Walkley-Black method with photometry (using leki SS2107UV spectrophotometer (Finland)). Total soil carbon was determined by dry combustion using a Vario El Cube analyzer (Germany) at 950 °C.

Statistical data processing (calculation of mean, median, variance, standard deviation, standard error of mean and coefficient of variation) was carried out using the MS Excel spreadsheet processor from the Office 365 package and using the R programming language.

3. RESULTS AND DISCUSSION

Sites formed considering crop yields (Fig. 2) are characterized by significant variations in all-form carbon content, which is largely consistent with the localization of points of increased yield.

Fig. 2. Map of spring wheat yield

Thus, analysis of descriptive statistics of organic soil carbon content shows a decrease in variance values for areas with high crop yield values, while in all variants there is an increase in the standard error of the mean (Table 1). It should also be noted that the correlation coefficient with yield in area IV becomes significant (r = 0.462 with a critical value of 0.396 (p = 0.05, n = 25) where the average soil organic carbon content is higher than in the rest.

Table 1. Descriptive statistics of SOC in conditions of Agroecological research station

Parameter	Subset				
	I	II	III	IV	General
Size	25	25	25	25	**100**
Mean	1,903	1,716	2,100	2,297	**2,004**
Median	1,880	1,710	2,110	2,180	**1,900**
Variance	0,182	0,179	0,431	0,353	**0,325**
St. deviation	0,427	0,423	0,657	0,594	**0,570**
St. error of mean	0,085	0,085	0,131	0,119	**0,057**
Coefficient of variation	22%	25%	31%	26%	**28%**

The minimum coefficient of variation is also observed on the first site.

Similar calculations for the indicator of total soil carbon content (Table 2) revealed different trends in the distribution of measures of scatter of a random variable. It should be noted that the greatest variation is observed on the first site with the highest yield and soil total carbon. The same site has the highest coefficient of variation, twice the carbon variability at other sites.

Table 2. Descriptive statistics of STC in conditions of Agroecological research station

Parameter	Subset				
	I	II	III	IV	**General**
Size	25	25	25	25	**100**
Mean	2,713	1,534	1,738	2,539	**2,131**
Median	2,535	1,493	1,776	2,430	**1,908**
Variance	1,452	0,062	0,073	0,258	**0,704**
St. deviation	1,205	0,249	0,270	0,508	**0,839**
St. error of mean	0,241	0,050	0,054	0,102	**0,084**
Coefficient of variation	44%	16%	16%	20%	**39%**

As in the case of organic carbon, the correlation coefficient with yield in plot IV becomes significant (r = 0.486 with a critical value of 0.396 (p = 0.05, n = 25).

Separately, measures of position and variance were calculated for calculated carbon content values using remote sensing data (Table 3).

Table 3. Descriptive statistics of soil carbon calculated with RS data in conditions of Agroecological research station

Parameter	Subset				
	I	II	III	IV	**General**
Size	25	25	25	25	**100**
Mean	2,022	1,714	1,940	2,346	**2,006**
Median	1,900	1,600	1,950	2,550	**2,025**
Mode	1,750	1,550	1,900	2,550	**2,150**
Variance	0,243	0,351	0,189	0,447	**0,350**
St. deviation	0,493	0,592	0,270	0,669	**0,592**
St. error of mean	0,099	0,118	0,054	0,134	**0,059**
Coefficient of variation	24%	35%	14%	29%	**29%**

In the case of the analysis of the red channel, an increase in the correlation coefficient with yield to a significant level is not observed. It should also be noted that the values of all measures of dispersion are low in area III, while the lowest average is typical for area II.

Correlation analysis between carbon distribution indicators and yield shows a significant relationship only with the dry combustion method (R = 0.232 with a significant 0.197, p = 0.05, n = 100). In general, the distribution of yield by sector of the site shows the greatest standard deviation in the southeast (Fig. 3). The minimum yield is also noticeable on the orthophotomap.

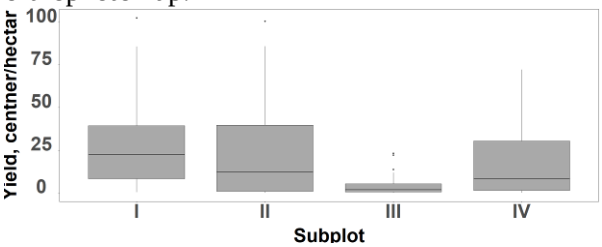

Fig. 3. Yield variability

A correlation was also revealed between the values of soil total carbon and carbon calculated using remote sensing (R = 0.232 with a significant 0.197, p = 0.05, n = 100), although no significant relationship was found between the latter and yield.

4. CONCLUSIONS

The studies have shown that the lowest values of dispersion measures are characteristic of the Walkley-Black and Valeeva methods; the values of variance, standard deviation and standard error of the mean are lower here relative to the dry combustion method. At the same time, when dividing a site into subsections, stability indicators begin to fall, and variations begin to increase. In the case of the dry combustion method, dividing the sample into subgroups allows, in some cases, to reduce variation and increase the accuracy of calculations.

At the same time, new correlations also appear, which can be useful when analyzing limiting factors in areas with contrasting properties.

5. FUNDING

The research was financed by the Ministry of Science and Higher Education of Russian Federation, Agreement No. 075-15-2021-1030

6. REFERENCES

[1] Srivastava P., Singh R., Tripathi S., Singh H., Raghubanshi A. S.: *Soil carbon dynamics and climate change: current agro-environmental perspectives and future dimensions Energy*, Ecol. Environ. Vol. 1, pp. 315–22, 2016.

[2] Meshalkina J. L., Yaroslavtsev A. M., Vasenev I. I., Andreeva I. V., Tihonova M. V.: *Carbon balance assessment by eddy covariance method for agroecosystems with potato plants and oats & vetch mixture on sod-podzolic soils of Russia* IOP Conf. Ser. Earth Environ. Sci., Vol. 107, pp. 012119, 2018.

[3] Vizirskaya M., Sheydgen A., Akanova N., Zhdanov V., Tihonova M., Buzylev A.: *Agroecological efficiency of periodic use of neutralized phosphogypsum in rice crops* E3S Web Conf., 175 07004, 2020.
[4] Kogut B.M., Milanovsky E.Yu., Hamatnurov Sh.A.: *Methods for determining the organic carbon content in soils (critical review)*, Dokuchaev Soil Bulletin, Vol. 114, pp. 5-28, 2023.
[5] Wang X., Sheng L., Li Y., Jiang H., Lv Z., Qi W., Luo W.: *Soil labile organic carbon indicating seasonal dynamics of soil organic carbon in northeast peatland* Ecol. Indic., Vol. 138, 108847, 2022.
[6] Kiš A., Andreeva I., Novačić Z., Gavranović A., Samardžić M., Ponjarac R., Galić Z.: *Prostorna analiza tala i utjecaj na produktivnost u gospodarskoj jedinici* Mužljanski rit Šumarski List, Vol. 145, pp. 456–7, 2021.
[7] Samsonova V. P., Meshalkina J. L., Blagoveschensky Y. N., Yaroslavtsev A. M., Stoorvogel J. J.: *The role of positional errors while interpolating soil organic carbon contents using satellite imagery Precis*. Agric., Vol. 19, pp. 1085–99, 2018.
[8] Chatterjee A., Lal R., Wielopolski L., Martin M. Z., Ebinger M. H.: *Evaluation of Different Soil Carbon Determination Methods* CRC. Crit. Rev. Plant Sci., Vol. 28, pp. 164–78, 2009.
[9] FAO: *Standard operating procedure for soil organic carbon. Walkley-Black method: titration and colorimetric method* (Rome: FAO), 2020.
[10] FAO: *Standard operating procedure for soil total carbon - Dumas dry combustion method* (Rome: FAO), 2020.
[11] Sato J. H., Figueiredo C. C. de, Marchão R. L., Madari B. E., Benedito L. E. C., Busato J. G., Souza D. M. *Methods of soil organic carbon determination in Brazilian savannah soils* Sci. Agric., Vol. 71, pp. 302–8, 2014.
[12] Angelopoulou T., Tziolas N., Balafoutis A., Zalidis G., Bochtis D.: *Remote Sensing Techniques for Soil Organic Carbon Estimation: A Review*, Remote Sens., Vol. 11, pp. 676, 2019.
[13] Van Wesemael B., Chabrillat S., Sanz Dias A., Berger M., Szantoi Z.: *Remote Sensing for Soil Organic Carbon Mapping and Monitoring*, Remote Sens., Vol. 15, pp. 3464, 2023.
[14] Thaler E. A., Larsen I. J., Yu Q.: *A New Index for Remote Sensing of Soil Organic Carbon Based Solely on Visible Wavelengths* Soil Sci. Soc. Am. J., Vol. 83, pp. 1443–50, 2019.
[15] Valeeva A. A., Aleksandrova A. B., Koposov G. F.: *Color estimation of forest-steppe soils by digital photography under laboratory conditions* Eurasian Soil Sci., Vol. 49, pp. 1033–7, 2016.

Authors: **Assoc. prof. PhD Dmitry Morev, Prof. PhD Ivan Vasenev, Assoc. prof. PhD Irina Andreeva,** Russian State Agrarian University – Moscow Timiryazev Agricultural Academy, Ecology Department, Timiryazevskaya Ul., 49, 127434 Moscow, Russia, Phone.: +7 905 728 9421.
E-mail: dmorev@rgau-msha.ru
vasenev@rgau-msha.ru
i.andreeva@rgau-msha.ru

ETIKUM 2023 **INTERNATIONAL SCIENTIFIC CONFERENCE NOVI SAD, SERBIA, DECEMBER 7-9, 2023**

Prcanović, H., Duraković, M., Beganović, S., Lemeš, S.

STANJE KVALITETA ZRAKA U DUBOKOJ KOTLINI NAKON UKLANJANJA DOMINANTNOG IZVORA ZAGAĐIVANJA SUMPOR DIOKSIDOM

Rezime: *U radu je predstavljeno istraživanje uticaja na kvalitet zraka dominantnog izvora zagađivanja sumpor dioksidom u kotlini dubokoj 600 m koja se nalazi u središnjem dijelu toka rijeke Bosne (Zenička kotlina - Bosna i Hercegovina) u kojoj je smještena najveća željezara dugih čeličnih proizvoda na Balkanu (Arcelor Mittal Zenica). U sastavu željezare nalazi se toplana za proizvodnju toplotne energije za tehnološke potrebe same željezare te za potrebe centralnog grijanja Grada Zenice. Rezultati istraživanja pokazuju da prestankom rada stare toplane na ugalj i uklanjanjem više od polovine emisija sumpor dioksida iz zeničke kotline, nije došlo do značajnijeg smanjenja prosječne godišnje koncentracije sumpor dioksida u zraku. Zabilježen je samo pad broja prekoračenja dozvoljene vrijednosti dnevnih prosjeka sumpor dioksida u naselju Tetovo koje se nalazi neposredno uz granicu tog termoenergetskog postrojenja.*
Ključne reči: *sumpor dioksid, modeliranje, disperzija, toplana.*

1. UVOD

Loš kvalitet zraka u zeničkoj kotlini uzrokovan je velikim brojem različitih izvora zagađivanja (industrijski izvori, energetska postrojenja, kućna ložišta, male kotlovnice, saobraćaj i dr.). Emisije zagađujućih materija iz tih izvora u kombinaciji sa slabim strujanjem zraka i formiranjem inverznih slojeva atmosfere uzrokuju značajnu zagađenost prizemnog sloja atmosfere, naročito u hladnijem dijelu godine kada su svi izvori zagađivanja aktivni i kada najčešće dolazi do pojave temperaturne inverzije i slabog strujanja zraka.

Procjenjuje se da emisija SO_2 u zrak iz industrijskih postrojenja i malih kotlovnica u Zenici iznosi oko 12.353 tona godišnje, pri čemu emisija SO_2 iz stare toplane iznosi 7.786 tona godišnje [1]. Prema podacima iz popisa stanovništva BiH 2013. godine procjenjuje se da se na području grada Zenice godišnje sagori oko 28.000 tona uglja, uglavnom iz zeničkih rudnika koji sadrži oko 3,6% sumpora. Prema podacima iz registra o postrojenjima i zagađivanjima Zeničko-dobojskog kantona, a shodno utrošenoj količini uglja, ukupna godišnja emisija SO_2 iz malih kućnih ložišta, iznosi 2.006 tona [2].

Najveći izvor emisija u zrak bila je stara toplana, smještena u sjevernom dijelu industrijske zone. Toplana je proizvodila energetsku paru i električnu energiju za tehnološke potrebe željezare, te toplotnu energiju za potrebe centralnog grijanja grada. Visina dimnjaka toplane iznosi 120 m, a godišnje je trošila oko 150.000 tona uglja. Toplana je u ljetnom periodu radila s polovinom kapaciteta, dok je u zimskom periodu radila optimalnim kapacitetom (94,3%). Prema podacima sa sistema automatskog monitoringa emisija, navedena potrošnja uglja uzrokovala je emisije sumpor dioksida u iznosu od 7.786 t/godišnje.

Pored toplane, u gradu se koristi 20 malih kotlovnica sa ukupnom godišnjom emisijom od oko 277 tona SO_2. Svi dimnjaci kotlovnica su niži od 20 m, osim dimnjaka Kantonalne bolnice, čija visina iznosi 60 m. U okviru željezare izvori emisija su pogon Aglomeracija sa ukupnom godišnjom emisijom od 2.087 t SO_2 i pogon Koksara sa ukupnom godišnjom emisijom od 2.203 tone SO_2 [1]. Pogon Aglomeracija ima dva dimnjaka visine 150 m, dok pogon Koksara ima jedan dimnjak visine 120 m.

Zenička kotlina nalazi se u središnjem dijelu Bosne i Hercegovine, u dolini rijeke Bosne, i okružena je brdima Smetovi i Vepar na sjeveru (1.000 m), Klopački vrh na jugoistoku (1000 m n.v.) i Janjički vrh na jugozapadu (800 m n.v.), te planinom Vilenicom na sjeverozapadu sa najvišim vrhom Lisac nadmorske visine 1.400 m. Položaj zeničke kotline, okolnih planina i brda prikazan je na slici 1.

Teren ovako složene konfiguracije može u velikoj mjeri modificirati vremenske prilike blokiranjem strujanja orografskom preprekom, različitim zagrijavanjem i hlađenjem slobodne atmosfere i tla, uticajem trenja i sl., što uzrokuje specifičnu cirkulaciju zraka manjih razmjera. U tim uslovima teško je generalizovati promjene u prizemnom sloju atmosfere, odnosno detaljna slika cirkulacije zraka jedinstvena je za svaki teren posebno [3].

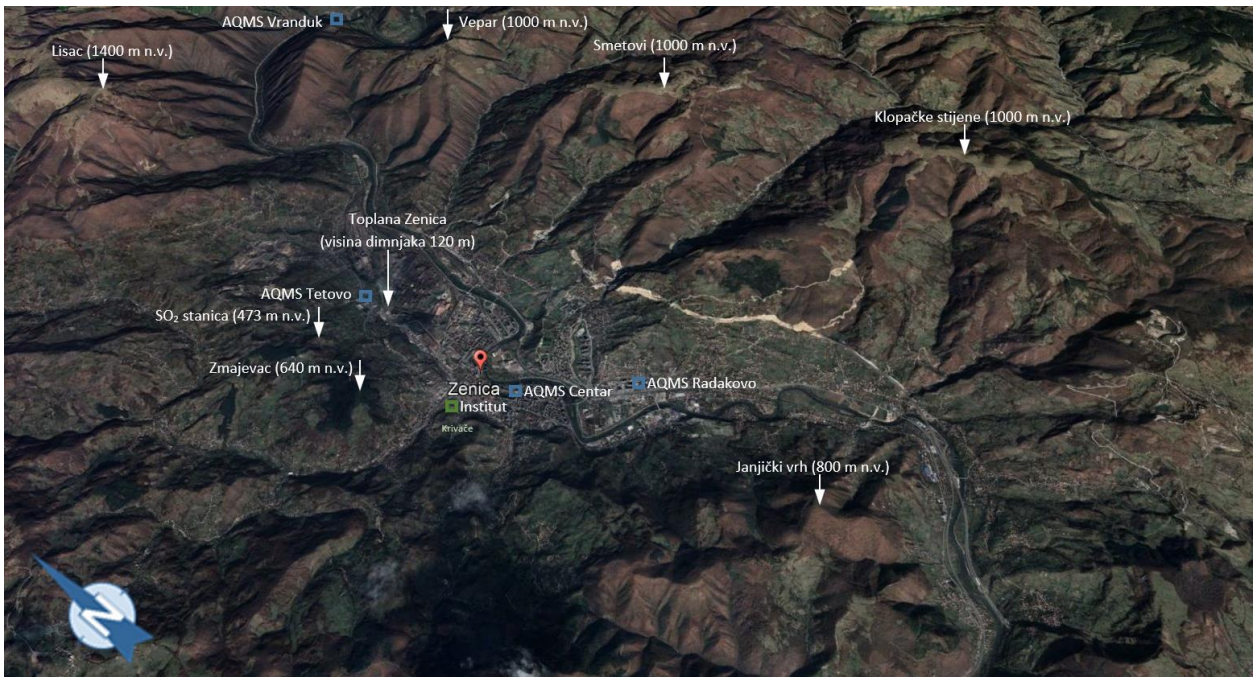

Sl. 1. Položaj planina, brda i stanica za mjerenje kvaliteta zraka u zeničkoj kotlini

2. TEMPERATURNA INVERZIJA

Dosadašnja istraživanja povezuju osobine inverznog sloja i kvaliteta zraka. Bez poznavanja karakteristika inverznog sloja nije moguće uraditi kvalitetnu procjenu uticaja emisija zagađujućih materija na kvalitet ambijentalnog zraka.

Provedena istraživanja uticaja visine inverzionog sloja na kvalitet zraka [3, 5, 6, 7, 8, 9, 10, 11, 12] ukazuju da je vezu između inverznog sloja stepena zagađenosti ambijentalnog zraka jako teško kvantifikovati. Većina istraživanja zaključuje da je zagađenost zraka u dane inverzije veća, ali autori navode da se rezultati analiza uticaja osobina inverznog sloja atmosfere na stepen zagađenosti zraka u jednoj kotlini ne mogu primjeniti na drugu kotlinu, bez obzira na orografsku sličnost.

3. KVALITET ZRAKA U ZENICI

Kvalitet zraka u gradu Zenici prati se skoro 50 godina. Dozvoljene koncentracije SO_2 i prašine često su bile višestruko premašene. 1989. godine maksimalna dnevna koncentracija SO_2 u zraku na jednom mjernom mjestu iznosila je 2.663 µg/m^3, a godišnji prosjek koncentracija SO_2 iznosio je 209 µg/m^3. To mjerno mjesto nalazi se na nadmorskoj visini od oko 470 m i pod direktnim je uticajem najvećeg izvora emisija SO_2 (stara toplana). Na ostalim mjernim mjestima srednje dnevne koncentracije SO_2 bile su znatno niže i kretale su se od 573 µg/m^3 u naselju Lukovo Polje (na krajnjem južnom dijelu kotline) do 1.472 µg/m^3 u naselju Tetovo, neposredno uz metalurška postrojenja [1]. Nakon privremenog gašenja integralne metalurške proizvodnje 1992. godine došlo je do poboljšanja kvaliteta zraka, ali i dalje značajno iznad graničnih vrijednosti. U januaru 2007. godine, kada nije bilo integralne proizvodnje, ali se toplana koristila za centralno grijanje grada, maksimalna srednja dnevna koncentracija SO_2 iznosila je 903 µg/m^3 na mjernom mjestu "Institut" u urbanom dijelu grada (slika 1).

Od 2012. godine kvalitet zraka prati se na 4 automatske mjerne stanice, čiji je razmještaj prikazan na slici 1. Tri stanice su u urbanom dijelu kotline a četvrta mjerna stanica (AQMS Vranduk) udaljena je oko 8 km zračne linije od dominantnih izvora emisija u zeničkoj kotlini – metalurških postrojenja.

U tabeli 1 date su godišnje koncentracije SO_2 u periodu od 2015. do 2022. godine. Od marta 2022. godine ugašena je stara toplana na ugalj.

Tabela 1. Srednja godišnja vrijednost sumpor dioksida (µg/m^3)

Lokacija AMS	2015	2016	2017	2018	2019	2020	2021	2022	GV
Zenica-Tetovo	90	78	82	73	60	86	91	72	50
Zenica-Centar	107	61	147	79	58	92	71	77	
Zenica-Radakovo	126	352	108	79	116	78	73	58	
Vranduk	-	-	-	137	63	84	59	92	

Tabela 2. Broj prekoračenja srednje dnevne vrijednosti SO_2 > 125 µg/m^3

Lokacija AMS	2015	2016	2017	2018	2019	2020	2021	2022	GV
Zenica-Tetovo	56	6	51	88	117	66	32	19	3
Zenica-Centar	75	54	65	57	42	75	67	43	
Zenica-Radakovo	102	39	50	77	44	78	7	21	
Vranduk	-	-	-	13	41	46	32	62	

Izmjerene vrijednosti maksimalnog satnog i maksimalnog dnevnog prosjeka varirale su u skladu s meteorološkim prilikama, osim što je na mjernim mjestima Tetovo i Radakovo došlo do smanjenja maksimalne dnevne vrijednosti nakon obustave rada stare toplane. Modeliranjem obavljenim u sklopu istraživanja [3, 12], utvrđeno je da emisije SO_2 iz stare toplane doprinose maksimalnoj satnoj koncentraciji sa preko 350 µg/m^3. Analizom podataka o kvalitetu zraka može se uočiti da modeli nisu obuhvatili sve uticajne faktore na disperziju zagađujućih materija u orografski složenoj kotlini.

Prema podacima iz tabele 2 vidljivo je da je u periodu nakon obustave rada stare toplane 2022. godine smanjen broj prekoračenja dozvoljene dnevne koncentracije SO_2 od 125 µg/m^3 na urbanim stanicama Tetovo i Radakovo.
Zanimljivo je da je u 2021. i 2022. godini na mjernom mjestu Vranduk zabilježeno povećanje broja prekoračenja srednje dnevne koncentracije SO_2, te da je na mjernim mjestima Centar i Vranduk u tom periodu zabilježen znatno veći broj prekoračenja maksimalne satne vrijednosti.

Analiza sezonske varijacije koncentracija SO_2 [4] pokazuje da su koncentracije SO_2 na mjernim mjestima koja nisu pod direktnim uticajem termoenergetskih i metalurških postrojenja značajno veće tokom hladnog dijela godine (kad se koristi centralno grijanje), dok je na mjernom mjestu Tetovo neposredno uz metalurška postrojenja ta razlika značajno manja. Zabilježeni su i periodi kada je godišnji prosjek koncentracija SO_2 u hladnom dijelu godine bila čak manja nego izvan sezone grijanja.

4. MODELIRANJE DISPERZIJE SO_2

Model disperzije emisija SO_2 iz nove i stare toplane urađen za potrebe Studije uticaja na okoliš [13] pokazuje da toplana, s obzirom na visinu i brzinu izbacivanja zagađujućih materija, te temperaturu dimnih plinova, više zagađuje sjeverni dio zeničke kotline. Modeliranje disperzije urađeno je korištenjem softverskog paketa za modeliranje AermodView koji zasnovan na AMS/EPA regulatornom modelu i modelu disperzije AERMOD.

Rezultati modeliranja uticaja emisije SO_2 iz nove toplane na ambijentalne koncentracije SO_2 u zraku pokazuju da je doprinos emisije SO_2 za maksimalne satne prosjeke do 40 µg/m^3, a za godišnji prosjek do 1,5 µg/m^3. Na slikama 2 i 3 dat je uporedni prikaz disperzije polutanata iz stare i nove toplane korištenjem iste kolor skale.

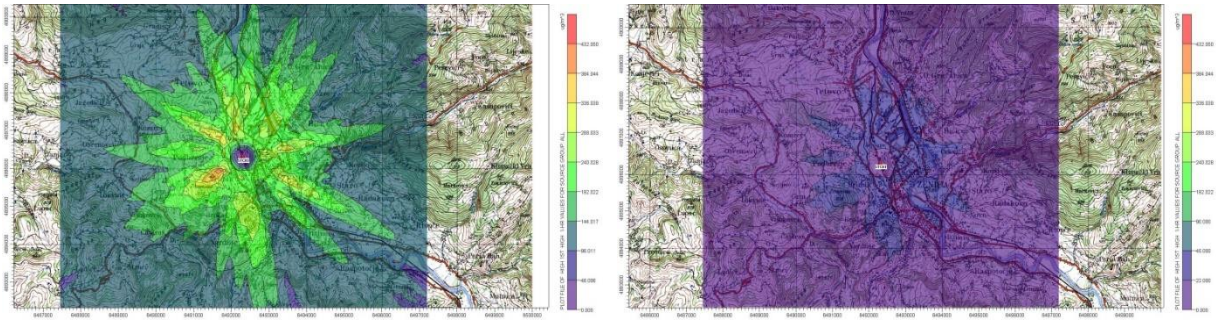

Sl. 2. Maksimalne satne koncentracije SO_2 od stare i nove toplane

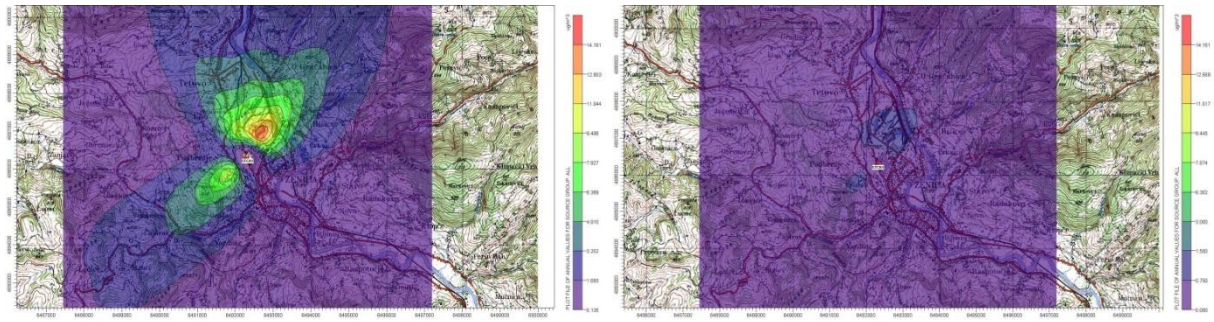

Sl. 3. Prosječna godišnja vrijednost koncentracije SO_2 od stare i nove toplane

Rezultati modeliranja su pokazali da se uticaj stare toplane na maksimalne satne koncentracije SO_2 kreće i preko 350 µg/m^3. Uzimajući u obzir da je granična vrijednost satnog prosjeka 350 µg/m^3, te prag uzbune 500 µg/m^3, može se zaključiti da samo postojeća toplana na određenim područjima zeničke kotline uzrokuje prekoračenje graničnih satnih vrijednosti. Uticaj na prosječnu godišnju vrijednost se kreće do 14 µg/m^3.

S obzirom na rezultate monitoringa kvaliteta zraka u periodu prije i poslije zatvaranja stare toplane može se zaključiti da, kada su u pitanju maksimalne satne vrijednosti, model nije dao zadovoljavajauće rezultate.

5. ZAKLJUČAK

Uklanjanjem dominantnog izvora emisija sumpor dioksida iz zeničke kotline nije došlo do značajnijeg poboljšanja kvaliteta ambijentalnog zraka u urbanom području grada Zenice. Zabilježena su samo određena poboljšanja kvaliteta zraka na mjernom mjestu koje se nalazi u blizni stare toplane.

Rezultati mjerenja kvaliteta zraka u periodu prije i poslije zatvaranja stare toplane pokazuju da korišteni modeli ne daju zadovoljavajuće rezultate rasprostiranja zagađujućih materija u zraku. U cilju sagledavanja uticaja na kvalitet zraka zeničke kotline potrebno je provesti istraživanje uticaja primarno nižih izvora zagađivanja zraka. Rezultati istraživanja pokazuju da postoji uticaj podignute i prizemne inverzije na kvalitet ambijentalnog zraka posebno u uslovima stabilnog stanja atmosfere, ali ovaj uticaj još uvijek nije adekvatno kvantificiran.

6. REFERENCE

[1] Duraković M, *Eksperimentalna verifikacija modela za simulaciju rasprostiranja polutanata iz industrijskih postrojenja i kućnih ložišta*, magistarski rad, Sarajevo, 2016.

[2] *Registar o postrojenjima i zagađivanjima ZDK*, Institut "Kemal Kapetanović", 2018

[3] RHZ Hrvatske, Studija utcaja glavnih izvora emisije SO_2 na kvalitet zraka u Zenici, Zagreb 1987

[4] Prcanovic H i dr., *Seasonal variations of sulfur dioxide in the air in Zenica City during 11 years period 2006 – 2016*, Int. J. Adv. Res. 6(3), 1133-1139, ISSN: 2320-5407.

[5] Trinh T T i dr., *Temperature Inversion and Air Pollution Relationship, and Its Effects on Human Health in Hanoi City*, Vietnam. Environmental Geochemistry and Health, 41, 929-937, 2018

[6] Johnson H R et al., PM2.5 *Pollution and Temperature Inversions: A Case Study in St. Louis, MO*, Senior Thesis, Iova State University Digital Repository, 2018;

[7] Nidzgorska-Lencewicz J, Czarnecka M, *Thermal Inversion and Particulate Matter Concentration in Wrocław in Winter Season*, Atmosphere, 2020

[8] Mašić A et al., *Drone Measurements of Temperature Inversion Characteristics and Particulate Matter Vertical Profiles in Urban Environments*, Proceedings of the 32nd DAAAM International Symposium, pp.0123-0126, B. Katalinic (Ed.), Published by DAAAM International, ISBN 978-3-902734-33-4, ISSN 1726-9679, Vienna, Austria DOI: 10.2507/32nd.daaam.proceedings.018, 2021

[9] Mašić A et al., *Experimental study of temperature inversions above urban area using unmanned aerial vehicle*; Thermal science: 2019, Vol. 23, No. 6A, pp. 3327-3338;

[10] Gutić S. *Fizičkogeografski faktori kvaliteta zraka u tuzlanskoj kotlini*, Baština sjeveroistočne Bosne 11, Tuzla 2019

[11] Tasić M et al., *Atmospheric aerosols and their influence on air quality in urban areas*, Physics, Chemistry and Technology Vol. 4, No 1, pp. 83 – 91, 2006

[12] Duraković M, Husika A, Metović S, *Investigation of the Concentration of Air Pollutants in the Vertical Profile in the Zenica Valley*. In: Ademović, N., Kevrić, J., Akšamija, Z. (eds) Advanced Technologies, Systems, and Applications VIII. IAT 2023. Lecture Notes in Networks and Systems, vol 644. Springer, 2023

[13] *Studija o procjeni utjecaja na okoliš za kogeneracijsko postrojenje za proizvodnju toplinske i električne energije i komprimiranog zraka* (toplana na plinovito gorivo), Zagrebinspekt d.o.o. Mostar, 2018

Autori: **mr.sc. Halim Prcanović, mr.sc. Mirnes Duraković, mr.sc. Sanela Beganović, prof.dr.sc. Samir Lemeš,** Univerzitet u Zenici, Fakultetska 3, 72000 Zenica, Bosna i Hercegovina.

E-mail: halim.prcanovic@unze.ba
mirnes.durakovic@unze.ba
sanela.beganovic@unze.ba
samir.lemes@unze.ba

ETIKUM 2023

INTERNATIONAL SCIENTIFIC CONFERENCE
NOVI SAD, SERBIA, DECEMBER 7-9, 2023

Rađenović, D., Tenodi, S., Pejin, Đ., Krčmar, D., Slijepčević, N., Bečelić Tomin, M., Tomašević Pilipović, D.

ASSESSING METAL CONCENTRATIONS IN SEDIMENT, PORE WATER AND SURFACE WATER: A COMPARATIVE STUDY

Abstract: *This study aimed to monitor and compare metal concentrations in sediment using conventional method and in pore water collected through passive sampling. Surface and pore water demonstrated good quality, while pseudo-total metal concentrations indicated sediment pollution (Class 3). Despite variations in concentrations, the sediment effectively retained metals, minimizing leaching into the water environment. Passive sampling exclusively targeted currently active water pollutants, enhancing the assessment of risks to the aquatic ecosystem. This method outperforms traditional sediment sampling, which can obscure risk evaluations by encompassing overall pollution.*
Key words: *monitoring, sediment, passive sampling, surface water*

1. INTRODUCTION

Sediment is a dynamic component of all aquatic systems and has a strong tendency to bind toxic and persistent compounds. Assessing sediment quality is pivotal in water quality protection and control programs [1]. Sediment dynamics are shaped by many processes occurring within the river basin, giving rise to the movement of contaminants bound to sediment particles. Due to different transport mechanisms, there is a potential resuspension of polluting substances, and their transport into different neighbouring biotic and abiotic media [2]. Conversely, the toxicity of these pollutants can undergo transformations as a consequence of desorption or chemical interactions with other compounds present in the aquatic environment. Understanding the complex interplay of these processes is crucial for effective environmental management and the preservation of water quality. The concentration of pollutants in the water-sediment system relies on the quantity of compounds introduced into the aquatic environment and the dynamic processes occurring within that environment [4].

The current approach to monitoring pollutants in sediment and surface water typically entails on-site sampling, which involves the use of bottles or grabs, followed by subsequent laboratory analysis [4, 5]. However, conventional sampling methods come with several drawbacks, including economic costs related to manpower and transportation, results that reflect the pollution level at the time of sampling, unrepresentativeness of the results (in cases where the level of pollution oscillates) and challenges in achieving the required sensitivity during the analytical process.

In response to the challenges mentioned, the development and implementation of alternative sampling methods have become imperative. Among these innovative techniques, passive sampling has emerged as one of the most contemporary and promising approaches [5]. Passive sampling stands out due to its fundamental attributes, which confer a range of advantages, both in terms of analytical capabilities and practical utility in research endeavours [6]. Key features of this sampling method include the simplicity of device construction, ease of technical operation, the ability to sustain continuous operation over extended periods, and the absence of an electricity requirement for sampler operation. Today, these passive samplers play a central role in the strategic pursuit of monitoring numerous priority and persistent substances.

The goal of this research was to monitor and compare metal concentrations in sediment, obtained by conventional sampling methods, with metal concentrations in pore water, collected through passive sampling. Also, the research included the analysis of the concentration of metals in the surface water, which was sampled during the research.

2. MATERIAL AND METHODS

Sediment from the Begej channel was gathered in accordance with the guidelines specified in SRPS ISO 5667-12 [7]. A "core sampler" (Eijkelkamp, The Netherlands) was employed to collect sediment samples without disturbing their structure. These samples were placed in glass jars and subsequently transported to the laboratory. Upon arrival at the laboratory, the samples were

thoroughly mixed to ensure homogeneity and then placed in glass containers. They were stored in a dark environment at a temperature of 4°C until they were ready for further analysis and use.

The SRPS EN 12880:2007 standard method [8] was employed to determine both the dry and organic matter content in the sediment. Additionally, the ISO 11277:2009 method [9] was used to assess the particle size distribution in the sediment.

For the analysis of pseudo-total metal content in a dried sediment sample, a microwave digestion method EPA 3051a [10] using Milestone, Star E, Italy, was utilized. This was followed by the application of the ICP-MS technique with a Perkin Elmer Sciex Elan 5000 instrument, in accordance with USEPA method 6020B [11].

The obtained pseudo-total metal concentrations in the sediment (measured in mg/kg dry sediment) were then compared to the values established by national regulations [12].

The SPeeper^{TM} system is employed to quantitatively assess the free dissolved concentration of metals and other dissolved inorganic species in various aqueous environments, including sediment pore water, surface water, and atmospheric water.

In the case of sediment pore water analysis SPeeper^{TM} passive sampler is used in situ. This passive sampler consists of a sampling vial filled with ultrapure water, separated from the surrounding environment by a semi-permeable membrane. The free dissolved metals and other constituents of the environmental water gradually pass through the membrane until the concentration of these substances inside the membrane reaches equilibrium with the concentration of the free dissolved metals in the surrounding water.

Fig. 1. Passive sampler

Subsequently, the sampling device (vial) can be removed from the sampling site, and the water enclosed within the membrane is collected for further analysis. A minimum sampling period of 28 days is recommended for this type of passive sampler to ensure accurate results.

Also, the concentration of metals in surface water, which was taken during sampling, was examined using the ICP-MS technique.

3. RESULTS AND DISCUSSION

Table 1 shows the pseudo total concentrations of metals in the sediment whose values were corrected for the content of organic matter and clay according to the national Regulation [12].

Table 1. Pseudo total metal content in sediment

Metals	Measured value	Corrected value	Classification
	mg/kg		
As	8.04	7.29	0
Cd	1.90	1.53	1
Cr	97.62	100.08	1
Cu	123.21	109.53	3
Pb	176.03	161.77	1
Ni	32.22	33.39	2
Zn	292.50	274.10	1

Class 0 - natural background of sediment, class 1 - slightly polluted sediment, class 2 - moderate pollution, class 3 - heavily polluted sediment; class 4 (4+) - extremely polluted sediment

According to the national Regulation [12], the limit values for evaluating sediment quality when washing sediment from watercourses refer to sediment containing 10% organic matter and 25% clay. When assessing sediment quality, limit values are corrected for a given sediment according to the measured content of organic matter and clay content. In the sediment, the organic matter content was 18.72%, and the clay content was 23.77%.

Based on the criteria for sediment quality assessment, copper is classified as class 3, which means that the sediment is polluted. According to the Regulation, it is not allowed to dispose of such sediment without special protection measures. For other metals, the classes are lower, but the sediment is characterized based on the highest class. However, the pseudo-total metal content does not provide a complete picture of the potential origin of the metals, as well as the way of their interaction with the sediment. In many cases, elevated concentrations of metals do not cause toxic effects if the metals are of natural geochemical origin.

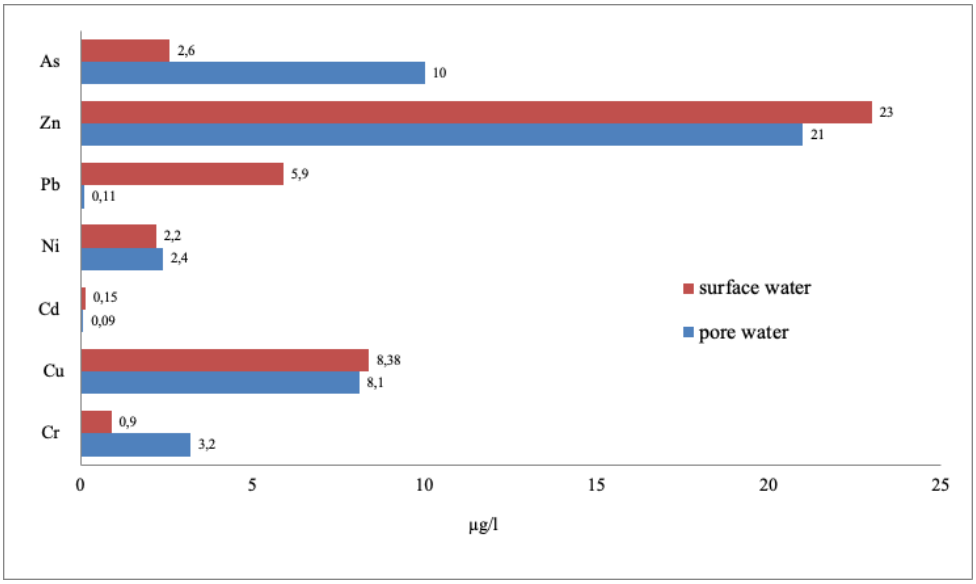

Fig. 2. Metal concentrations in surface water and sediment pore water

Figure 2 shows the metal concentrations detected in the water inside the membrane of the passive sampler (pore water), as well as the surface water collected during sampling. The lower concentrations of chromium, nickel, and arsenic in surface water relative to pore water suggest that these metals accumulate or adsorb to sediment at the bottom of the water body. The sediment may act as a reservoir for metals and prevent their leaching into the water, thus explaining the higher concentration of metals in the pore water that was in contact with the sediment. Also, metal concentrations in water can vary over time, especially depending on hydrological conditions and seasonal changes. Changes in water levels, water flow rates, temperature and precipitation can affect the balance of metals between sediment and water. In addition, differences in metal concentrations between surface and pore water may also indicate different sources of pollution.

Higher concentrations of copper, cadmium, lead and zinc were recorded in surface water compared to pore water, because surface water can transport metals from land and other surfaces in the water body. Surface water often comes into contact with urban areas and industrial zones where metal concentrations are usually higher due to industrial emissions, wastewater and urban pollution [13]. Soil erosion and particle movement can release metals into surface water, increasing metal concentrations in surface water.

The physicochemical properties of water and sediments exhibit significant variations along a waterway, primarily driven by the complex interplay of hydrodynamic processes and the characteristics of the stream geomorphology [14]. These dynamic factors influence the physical mixing of water and the transportation and deposition of particles with diverse physicochemical characteristics. Consequently, the geochemical behaviour of heavy metals, and subsequently, the associated toxicity risks, may differ depending on the specific type of aquatic ecosystem [13].

For pore water that was obtained as a result of passive sampling, there are no limit values with which to compare. We made a comparison with the national Regulation [12] and with the limit values of pollutants in surface waters for class 2. Water belonging to class 2 corresponds to an excellent ecological status according to the classification given in the regulation. By comparing the measured concentrations of metals in pore water and surface water with the limit values, it can be concluded that none of the measured concentrations exceeds the prescribed limit values for class 2. Based on this, it can be concluded that both surface and pore water has good quality, while pseudo total metal concentrations indicate that the sediment belongs to class 3, which characterizes it as a polluted sediment. Although the concentrations in surface and pore water are not comparable with the pseudo-total concentrations of metals in the sediment, it can be concluded that the sediment binds metals well, and their leaching into the water environment is very small.

By using passive sampling, the focus is exclusively on pollutants that are currently available and active in the water [5]. This allows us to better assess the actual risk to the aquatic ecosystem, as traditional sediment sampling methods capture overall pollution, which can confound risk assessment.

An example is precisely the results that were obtained and presented in this paper, where the analysis using the traditional method shows high

total concentrations of metals in the sediment, which suggests the need for remediation. However, passive sampling allows us to better understand the binding of pollutants to sediment, thereby reducing the likelihood that they will leach into surface water and pose a threat to the environment. This approach allows for a more precise assessment of the actual threat of pollution and enables more efficient management of the protection of aquatic ecosystems.

The current disadvantage of passive sampling is the high cost, however, there is great potential for cost reduction through mass production of the device. It is important to note that, although the initial investment is higher, this disadvantage can be overcome by numerous advantages such as reducing the need to use chemicals in the process of remediation of polluted areas [5, 6]. Also, passive sampling helps identify cases where remediation is not required, as there is no fear that pollutants will leach from the sediment and endanger wildlife.

4. CONCLUSION

Given these benefits, considering changes in the legislation for sediment quality assessment, to bring it more in line with passive sampling methods and the results they provide is a logical step. This would enable a more efficient and economical assessment and management of the pollution of water bodies, thus protecting the environment in a more adequate way and reducing financial costs.

5. ACKNOWLEDGEMENT

The research was financed by the Science Fund of the Republic of Serbia, #7753609, BEuSED.

6. REFERENCES

[1] Michalec B., Cupak A.: *Assessment of quality of water and sediments in small reservoirs in Southern Poland - A case study*, Environmental Engineering Research, 27(2), 200660, 2022.

[2] Dahlberg, A.K., Apler, A., Frogner-Kockum, P., Göransson, G., Snowball, I., Wiberg, K., Josefsson, S.: *Dispersal of persistent organic pollutants from fiber-contaminated sediments: biotic and abiotic pathways*, Sediments, Sec 2, Physical and Biogeochemical Processes, 21, p.p. 1852–1865, 2021.

[3]Akhtar N., Ishak M.I.S., Bhawani S.A., Umar K.: *Various Natural and Anthropogenic Factors Responsible for Water Quality Degradation: A Review*, Water, 13(19), 2660, 2021.

[4] Groten, J.T., Levin, S.B., Coenen, E.N., Lund, J.W., Johnson G.D.: *A Novel Suspended-Sediment Sampling Method: Depth-Integrated Grab (DIG)*, Applied Sciences, 13(13), 7844, 2023.

[5]Belháčová-Minaříková, M., Smedes, F., Rusina, T.P., Vrana, B.: *Application of equilibrium passive sampling to profile pore water and accessible concentrations of hydrophobic organic contaminants in Danube sediments*, Environmental Pollution, 267, 115470, 2020.

[6] Rusina, T.P., Smedes, F., Brborić, M., Vrana B.: *Investigating levels of organic contaminants in Danube River sediments in Serbia by multi–ratio equilibrium passive sampling*, Science of The Total Environment, 696, 133935, 2019.

[7] SRPS ISO 5667-12- Water quality - Sampling - Part 12: Guidance on sampling of sediment from riverbeds, lakes and estuaries.

[8] SRPS EN 12880:2007, Characterization of sludges - Determination of dry residue and water content.

[9] ISO 11277:2009, Soil quality-Determination of particle size distribution in mineral soil material.

[10] U.S. EPA. 2007. “Method 3051A (SW-846): Microwave Assisted Acid Digestion of Sediments, Sludges, and Oils,” Revision 1. Washington, DC.

[11] U.S. EPA. 2014. "Method 6020B (SW-846): Inductively Coupled Plasma-Mass Spectrometry," Revision 2. Washington, DC.

[12] Official Gazette of the Republic of Serbia, No. 50/2012. Regulation on limit values of pollutants in surface and ground waters and sediments and deadlines for their achievement.

[13] Hoang, H.G., Lin, C., Tran, H.T., Chiang, C.F., Bui, X.T., Cheruiyot, N. K., Shern, C.C., Lee, C.W.: *Heavy metal contamination trends in surface water and sediments of a river in a highly-industrialized region*, Environmental Technology & Innovation, 20, 101043, 2020.

[14] Li, M., Zhang, Q., Sun, X., Karki, K., Zeng, C., Pandey, A., Rawat, B., Zhang, F.: *Heavy metals in surface sediments in the trans-Himalayan Koshi River catchment: Distribution, source identification and pollution assessment*, Chemosphere, 244, 125410, 2020.

Authors: **Research assistant dr Dunja Rađenović, MSc Slaven Tenodi, MSc Đođre Pejin, dr Dejan Krčmar, dr Nataša Slijepčević, dr Milena Bečelić Tomin, Associate Professor dr Dragana Tomašević Pilipović,** University of Novi Sad, Faculty of Sciences, Department of Chemistry, Biochemistry and Environmental Protection, 21000 Novi Sad

E-mail: dunja.radjenovic@dh.uns.ac.rs
slaven.tenodi@dh.uns.ac.rs
djordje.pejin@dh.uns.ac.rs
dejan.krcmar@dh.uns.ac.rs
natasa.slijepcevic@dh.uns.ac.rs
milena.becelic-tomin@dh.uns.ac.rs
dragana.tomasevic@dh.uns.ac.rs

ETIKUM 2023 INTERNATIONAL SCIENTIFIC CONFERENCE
NOVI SAD, SERBIA, DECEMBER 7-9, 2023

Savković, M., Pušica, M., Caiazzo, C., Mijailović, N., Đapan, M.

INVESTIGATING MENTAL WORKLOAD IN ASSEMBLY WORKSTATIONS: AN INTEGRATED ANALYSIS OF EEG AND EYE TRACKING

Abstract: *This study presents an integrative multimodal framework for monitoring operator cognitive load through electroencephalography (EEG) and eye tracking analysis. During the experiment, which was carried out in two scenarios (ergonomic and non-ergonomic), 15 subjects participated and at the same time brain activity was monitored in real time with an EEG cap and eye movements by placing a frontal camera directly in front of the subjects. Through a multivariate analysis of the results of monitoring mental load and eye movements, it was shown that there is a significant correlation between specific eye movements and the level of mental load. The contribution of the work is reflected in the quantification of the mental load and determining when there is a drop in attention and concentration of the operator, and this has a largely positive effect on increasing productivity and reducing defects at assembly workstations.*
Key words: *assembly workstation, EEG, eye tracking, mental workload*

1. INTRODUCTION

In order to increase effectiveness and respond to market demands for timely delivery of high-quality products, modern manufacturing companies strive to achieve correct and consistent assembly of complex products. High cognitive load negatively affects the speed and time of execution of assembly tasks, the appearance of defects and the quality of final products [1]. Cognitive overload can lead to a drop in attention and a reduction in focus on the tasks being performed [2].

Therefore, monitoring the cognitive abilities and mental workload of workers who perform assembly activities is key to improving the efficiency of the production process and improving the safety and health of workers. This study combines the application of electroencephalography and eye movement monitoring via a frontal camera. Cognitive ergonomics as a new branch of ergonomics focuses on the study of human cognitive capacities (such as memory, perception, attention, etc.), during interaction with elements of the work environment (tools, machines, instructions and interfaces). EEG is the most commonly used method that allows monitoring the brain activity of subjects in real time in order to investigate when mental load occurs and how factors from the external environment affect brain activity during assembly work. Using the EEG method, Wang et al. found that delta waves and alpha waves can be used to detect sleepiness [3]. Some researchers used EEG signals to monitor brain activity and assess the alertness of subjects [4]. Fan et al. based on the monitoring of EEG signals, determined at which moment fatigue occurs while driving and proposed a method for fatigue detection [5]. Chen et al. applied EEG to monitor the mental load of subjects, with special attention paid to gamma bands [6].

According to research papers, various factors affect the cognitive load of the operator. The complexity of the product being assembled, the combination of complex activities with time pressure, work instructions, functionality and appropriateness of the tools used, distractions from the external environment, the operator's work experience, etc. are particularly highlighted. [7, 8, 9]. Scafà et al. [10] state the following as the most common reasons for the appearance of mental strain among operators: performing precise and fine movements over a long period of time, variety of tasks and operations, repetitiveness of activities, rhythm of work, lack of or complex work instructions.

Mental workload negatively affects operator performance [1; 11]. Also, mental fatigue and a drop in attention and concentration increase the duration of assembly activities [12]. As stated by the authors [13], due to a high level of cognitive load, defects occur, which further negatively affects the quality of the final product.

2. METHODS/METHODOLOGIES

In the case study, the brain activity of subjects who performed assembly activities at assembly workstations in two scenarios - a non-ergonomic (traditional) and an ergonomic scenario - was monitored via EEG. EEG is one of the most

frequently used methods in the literature for monitoring cognitive state and assessing mental workload. This method enables the measurement of brain activity in real time, provides objective results and thus overcomes the main drawback of subjective methods (such as interview and survey), which is subjectivity and bias.

Fifteen subjects between the ages of 19 and 30 participated in the experiment, and at the same time brain activity was monitored in real time via EEG and eye movements by placing a frontal camera directly in front of the subjects.

In both scenarios, the experiment was conducted in two 90-minute sessions. Before the start of the experiment, the subjects were given detailed instructions and given 15 minutes to practice performing these activities. After that, relaxing music was played for 5 minutes. Between the two sessions, the respondents had a 15-minute break.

In the non-ergonomic scenario, participants performed assembly activities at a traditional workstation analogous to a real industrial environment. In the ergonomic scenario, respondents performed activities on the proposed new ergonomic workstation that is aligned with lean principles [14].

The respondents assembled the final product in two variants - schemes and 3D images, whereby the 3D images were significantly more visually complex to assemble primarily because they were rotated at different angles. 60 seconds were provided for the assembly of easier schemes, and 90 seconds were available for more difficult schemes.

The participants were instructed not to consume alcoholic beverages the day before and on the day of participation in the research, as well as not to drink coffee at least three hours before the experiment. All participants voluntarily agreed to participate in the experiment, which they confirmed by signing the consent document after reading the summary of the experiment.

EEG data were recorded with a SMARTING wireless EEG system [14]. A small and lightweight EEG amplifier was firmly connected to a 24-channel electrode cap. Communication between SMARTING and the recording computer is established via a Bluetooth connection. Also, a frontal camera was installed, which had the role of monitoring the eye movements of the subjects in real time.

At the end of the experiment, the respondents orally answered questions related to the experience of working at a traditional and ergonomic workstation. They were asked whether they felt tired and mentally stressed while performing the activity and whether it happened during the entire duration of the experiment or only at certain moments, whether they were focused on performing the activity or if it came after a drop in attention at certain moments and how much it often happened. Also, they were asked a question in order to determine which factors, in their opinion, influenced the occurrence of fatigue and whether something hindered them during the performance of activities and whether they felt time pressure. A few days after the experiment, the respondents were sent a questionnaire by e-mail in order to collect data related to their experience during the experiment, where they were left with space to write their suggestions regarding the improvement of the performance of activities at the assembly workstations.

In this research paper, the quantification of the operator's mental load during the performance of mentally demanding, repetitive assembly activities in both scenarios was performed using the mental load index. The mental load index was calculated as the quotient of frontal theta and parietal alpha.

3. RESULTS

Figures 1. and 2. present the dependence of mental load index on time for one subject in both scenarios (non-ergonomic and ergonomic) for both sessions at the beginning, middle and end of each session. These are 6-minute segments at the beginning, middle and end of each session. In the first row is the first session and in the second row is the second session. The graphs show the dependence of the MWL index on time. Calculated mean values have been added to the graph titles.

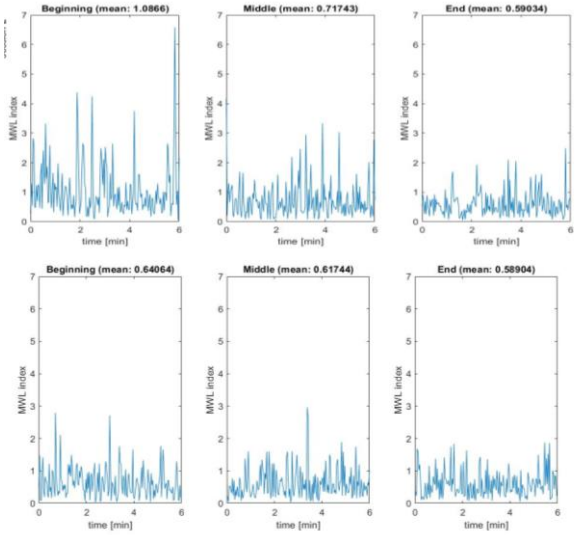

Fig. 1. EEG signals for one subject in both sessions in the non-ergonomic scenario

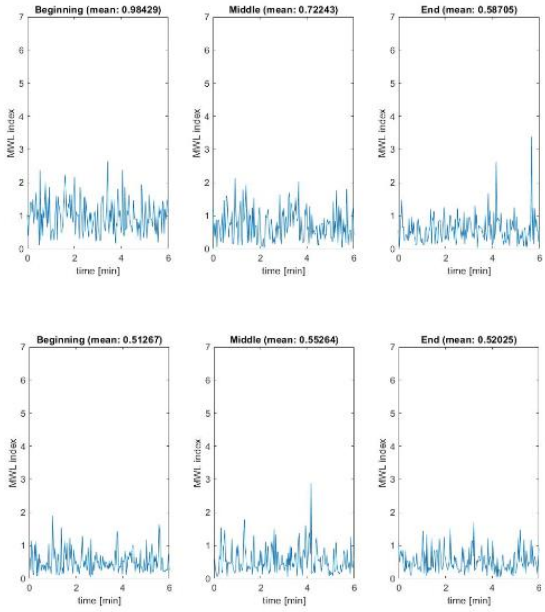

Fig. 2. EEG signals for one subject in both sessions in the ergonomic scenario

What can be concluded from the observation of the signal is that in the non-ergonomic scenario there is a greater difference between the maximum and minimum value of the signal in relation to the ergonomic position, which is in accordance with the assumption that the ergonomic scenario is more favorable for performing work activities and requires less mental load. A higher frequency of peaks in the signal was also observed in the non-ergonomic scenario, which actually means that we have a lower degree of continuity.

Another characteristic for both scenarios is that the menatal load index is lower during the second session when the subject has achieved some comfort and adaptation in performing the operation.

The results of monitoring the mental load of all 15 subjects via the mean values of mental load index (MWLi) are presented in Figure 3.

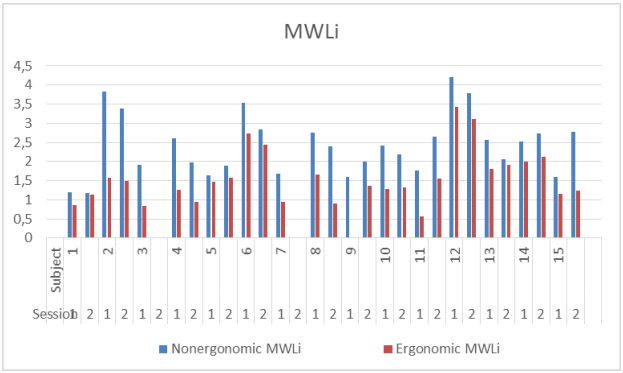

Fig. 3. Mental load index in non-ergonomic and ergonomic scenarios

The figure does not show values for subject no. 3 in the second session and subject no. 7 in the second session because the equipment did not work.

4. DISCUSSION

Based on the results of monitoring the mental load through the MWLi index, it can be concluded that all the respondents when performing assembly activities in the ergonomic scenario had a lower level of mental load compared to the traditional scenario. The results showed that the conditions of the working environment (temperature, air humidity, lighting, noise, etc.) greatly affect the mental workload of the operator. This can be seen from the results, considering that when the subjects were exposed to noise and when the lighting was inadequate in the non-ergonomic scenario, there was an increased strain and an increase in mental load in each subject compared to the ergonomic scenario.

Through a multivariate analysis of the results of monitoring brain activity, mental load and eye movements, it was shown that there is a significant correlation between specific eye movements and the level of mental load. According to the results of the EEG data analysis, changes were observed in the frontal and parietal regions, mainly in the theta and alpha bands, with increasing task difficulty. Also, according to the eye monitoring data, we can point out that blinking is reduced and pupil dilation is increased during the assembly of more cognitively demanding schemes. This can be justified by the fact that in those moments the respondent was maximally concentrated on the task and that his attention increased. Also, as the mental load during assembly activities increased, the eye movements accelerated.

Analyzing the results, it can be concluded that during the assembly phase of parts and components, there was an increase in the mental load of the respondents. This can be justified by the fact that at that stage the participant is focused on the scheme or 3D picture according to which he should connect the wires, he analyzes the schemes in detail, looks at the layout of the wires and thinks about how he should connect them. Also, the results show that the respondents were exposed to a lower level of mental load during the rest phase and the phase of retrieving parts from the box and wires from the container. Also, greater mental load was present when assembling more difficult schemes in the form of 3D images. Before the beginning of the first session of the experiment after listening to relaxing music and at the beginning of the second session after a break

of 15 minutes, no mental strain was observed in the subjects.

These results coincide with the results obtained from the survey and interviews. By filling out the survey and during the oral interview, the respondents stated that they felt a greater mental load and a drop in concentration while performing activities in a non-ergonomic scenario. Also according to their statements, they felt mental fatigue to the greatest extent from the middle to the end of the first session and at the end of the second session. At the beginning of the experiment, after listening to relaxing music, the subjects did not feel tired.

The contribution of the paper is reflected in the fact that the assembly tasks can be better organized in order to reduce mental fatigue, which will further contribute to increasing productivity and reducing errors and improving the operator's health.

5. CONCLUSION

In the paper, the quantification of mental load during the execution of assembly activities in ergonomic and non-ergonomic scenarios was performed. By analyzing the results of monitoring mental load and eye movements, it was determined that there is a significant correlation between specific eye movements and the level of mental load.

6. REFERENCES

[1] Falck, A.C.; Örtengren, R.; Rosenqvist, M. *Assembly failures and action cost in relation to complexity level and assembly ergonomics in manual assembly (part 2)*. Int. J. Ind. Ergon., 44, pp. 455-459, 2014.

[2] Young, M.S.; Brookhuis, K.A.; Wickens, C.D.; Hancock, P.A. *State of science: Mental workload in ergonomics*, Ergonomics, 58, pp. 1-17, 2015.

[3] Wang, C. et al. *Spectral Analysis of EEG During Microsleep Events Annotated via Driver Monitoring System to Characterize Drowsiness*. IEEE Trans. Aerosp. Electron. Syst. 56, pp. 1346-1356, 2020.

[4] Zheng, W. L., Lu, B. L. *A multimodal approach to estimating vigilance using EEG and forehead EOG*. J. Neural Eng., 14, 2017.

[5] Fan, C. et al. *Detection of Train Driver Fatigue and Distraction Based on Forehead EEG: A Time-Series Ensemble Learning Method*. IEEE Trans. Intell. Transp. Syst., 23, pp. 13559-13569, 2022.

[6] Chen, J., Taylor, J. E., Comu, S. *Assessing Task Mental Workload in Construction Projects: A Novel Electroencephalography Approach*. J. Constr. Eng. Manag. 143, 2017.

[7] Zaeh, M. F., Wiesbeck, M., Stork, S., Schubö, A. *A multi-dimensional measure for determining the complexity of manual assembly operations*. Prod. Eng. 3, pp. 489-496, 2009.

[8] Galy, E., Cariou, M., Mélan, C. *What is the relationship between mental workload factors and cognitive load types?*, Int. J. Psychophysiol, 83, pp. 269-275, 2012.

[9] Brolin, A., Thorvald, P., Case, K. *Experimental study of cognitive aspects affecting human performance in manual assembly*. Prod. Manuf. Res., 5, pp. 141-163, 2017

[10] Scafà, M., Papetti, A., Brunzini, A., Germani, M. *How to improve worker's well-being and company performance: A method to identify effective corrective actions*. Procedia CIRP 2019, 81, pp. 162-167, 2019.

[11] Thorvald, P., Lindblom, J. *Initial development of a cognitive load assessment tool*, in The 5th AHFE International Conference on Applied Human Factors and Ergonomics, Krakow, Poland, AHFE, 2014, pp. 223-232, 19-23 July 2014,

[12] Biondi, F. N., Cacanindin, A., Douglas, C., Cort, J. *Overloaded and at Work: Investigating the Effect of Cognitive Workload on Assembly Task Performance*. Hum. Factors, 63, pp. 813-820, 2021.

[13] Zare, M., Croq, M., Hossein-Arabi, F., Brunet, R., Roquelaure, Y. *Does ergonomics improve product quality and reduce costs? A review article.* Hum. Factors Ergon. Manuf. Serv. Ind. 26, pp. 205-223, 2016.

[14] Savković, M., Caiazzo, C., Djapan, M., Vukićević, A. M., Pušica, M., Mačužić, I. *Development of Modular and Adaptive Laboratory Set-Up for Neuroergonomic and Human-Robot Interaction Research*. Front Neurorobot., 16:863637, 2022 May 11.

Authors: **researcher Marija Savković, phd student Miloš Pušica, phd student Carlo Caiazzo, research associate dr Nikola Mijailović, Assoc. prof. dr Marko Đapan,** University of Kragujevac, Faculty of Engineering, Sestre Janjić 6, 34000 Kragujevac, Serbia, Phone.: +381 34 331 772, Fax: +381 34 331-772.

E-mail: marija.savkovic@kg.ac.rs
milos.pusica@mbraintrain.com
carlocaiazzo@fink.rs
nmijailovic3@gmail.com
djapan@kg.ac.rs

ETIKUM 2023

INTERNATIONAL SCIENTIFIC CONFERENCE
NOVI SAD, SERBIA, DECEMBER 7-9, 2023

Stepanov, A.V., Vasenev, I.I.

METROLOGICAL IOT SUPPORT FOR EVIDENCE OF HIGH AGROECOLOGICAL EFFICIENCY OF NEW AGROCHEMICALS USE ON DEGRADED PODZOLIC SOILS

Abstract: *The conducted research demonstrates the effectiveness of using IoT sensors in field experiments on application of agrochemicals obtained from waste to increase the metrological evidence of their direct positive effect on the conservation of organic matter of the formed soil horizons due to a detailed analysis of the daily and seasonal dynamics of the state of crops and agro-climatic conditions. The conducted studies have shown the statistically proven small environmental risks and high efficiency of compost from the quail dropping* application *for the restoration of erosionally disturbed sod-podzolic soils in the typical for Moscow region agrolandscape conditions.*

Key words: *Agrochemicals from waste, Conservation of organic matter, Degraded podzolic soils, Environmental monitoring, Metrological support.*

1. INTRODUCTION

Sod-podzolic soils dominating in the so called Non-Chernozem zone of the European and Western Siberian parts of Russia are characterized by a low thickness of their humus-accumulative horizon and low reserves of soil organic matter (SOM or humus), which quickly fall after intensive farming use and due to soil anthropogenic degradation [1, 2]. The accelerated development of their erosion is often accompanied by a sharp drop in soil fertility and the need for bioremediation, as in the case of man-made disturbance of these soils in the zone of impact of construction and transport projects [2, 3].

Peat-sand mixtures are often used to restore highly degraded and eroded sod-podzolic soils [4, 5], but their organic matter is characterized by low resistance to mineralization, and the soil absorbing complex is characterized by low capacity and unsaturation. Additional ameliorants need in this case [6, 7] for carbon balance stabilization in the regenerated topsoil of degraded sod-podzolic soils.

It is very expensive to use commercial fertilizers and in large quantities for their qualitative improvement, so in recent years there has been an increasing interest in using affordable and inexpensive industrial and agricultural waste and their derivatives for this purpose [7, 8]. One of them could be phosphogypsum – the industrial waste in the production of phosphorous fertilizers. The other ones are manure and bird droppings produced annually in large volumes at the large livestock complexes. They all are raw materials for agroecologically attractive, very valuable and potentially profitable ameliorants and fertilizers.

However, their use requires experimental substantiation of agroecological efficiency and environmental safety of application [2, 6, 7] in conditions of increased spatial heterogeneity of degraded lands and the initial state of waste, which can have a significant impact on local combinations of agro-climatic conditions, and they largely determine the intensity of the processes of transformation and mineralization of organic matter in the upper horizons of soils [9-12].

The use of IoT sensors [13] in experiments using agrochemicals obtained from waste could increase the evidence of their direct positive effect on the conservation of organic matter of the formed soil horizons due to a detailed analysis of the daily and seasonal dynamics of the state of crops and agro-climatic conditions.

Purpose of the paper is analysis the efficiency of using IoT sensors in field experiments on application of agrochemicals obtained from waste to increase the metrological evidence of their direct positive effect on the conservation of organic matter of the formed soil horizons due to a detailed analysis of the daily and seasonal dynamics of the state of crops and agro-climatic conditions in case of typical for Moscow region agrolandscape conditions with disturbed sod-podzolic soils.

2. MATERIALS AND METHODS

The research was carried out on the territory of the Agroecological Station of Field Experimental Station of the Russian State Agrarian University - Moscow Timiryazev Agricultural Academy (RSAU-MTAA – Fig. 1) in fall of 2022 and summer of 2023 with an abnormal for this location high precipitation (604 mm in May to August, that is 2 times more than the average long-term precipitation for this period – Table 1).

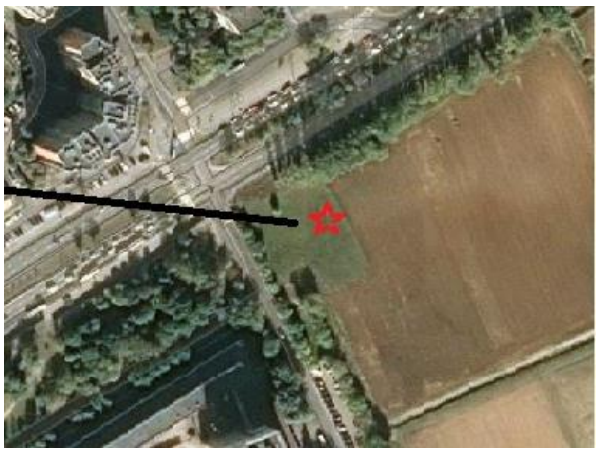

Fig. 1. The location of the Field demonstration experiment (55°50'24"N 37°33'02"E) at the Agroecological Station of the RSAU-MTAA.

Table 1. Weather conditions of the main growing season in 2023 in comparison with the average annual climatic data for 2011-2022.

Month	De-cade	Average air temperature, °C			Precipitation amount, mm		
		2011-2022		2023	2011-2022		2023
May	1	13,6	8,6	13,9	61,0	10,6	73,3
	2		16,4			4,2	
	3		16,5			58,5	
June	1	17,3	15,8	18,1	77,0	35,1	140
	2		19,8			1,2	
	3		18,6			104	
July	1	19,7	21,7	19,4	84,0	6,1	305
	2		17,1			143	
	3		19,3			156	
August	1	17,6	24,1	20,6	78,0	0,2	126
	2		21,5			117	
	3		16,6			8,8	
May-August		17,1		18,0	300		644

The micro-plot field experiment with 2 m x 2 m plots include variant without agrochemicals (as control), variants with 2.0 t/ha compost from quail droppings, variants with 1.5, 3.0, 4.5 and 6.0 t/ha doses of phosphogypsum, and variants with the use of phosphogypsum in combination with compost from quail droppings (in doses of 4.5 t/ha + 2.0 t/ha and 6.0 t/ha + 2.0 t/ha), which all were added to the peat-sand soil-ground (with a weight ratio 1 to 3) traditionally used in phytoremediation projects applied in a 15 cm layer to the surface of erosively degraded sod-podzolic soils.

As a model crop, a grass mixture was used with the following composition: pasture ryegrass (*Lolium perenne*) (40%), red Maxim 1 fescue (*Festuca rubra*) (40%), red Greenlight fescue (*Festuca rubra*) (10%), meadow bluegrass (*Poa pratensis*) (10%). Seeding rate: 200 g per plot.

Monitoring of soil organic carbon content, of the topsoil regimes and of the herbaceous biomass dynamics were carried out by traditional methods of agroecological monitoring [14]. Monitoring of air relative humidity and temperature, and of topsoil moisture and temperature – using IoT sensors and portable electronic devices (Checktemp 1 and Theratrobe HH2). Analysis of soil carbon dioxide emissions – using a portable gas analyzer LiCor-820 *in situ*. Accounting of aboveground biomass and its growth rate – by the sequential mowing and IoT sensors CropTalker.

The data were statistically processed using ANOVA and Microsoft Excel 2010.

3. RESULTS AND DISCUSSION

The conducted studies have shown the maximum similarity of not only seasonal, but also daily dynamics of the topsoil weight moisture (Fig. 2) and temperature (Fig. 3) of the studied variants of the field experiment.

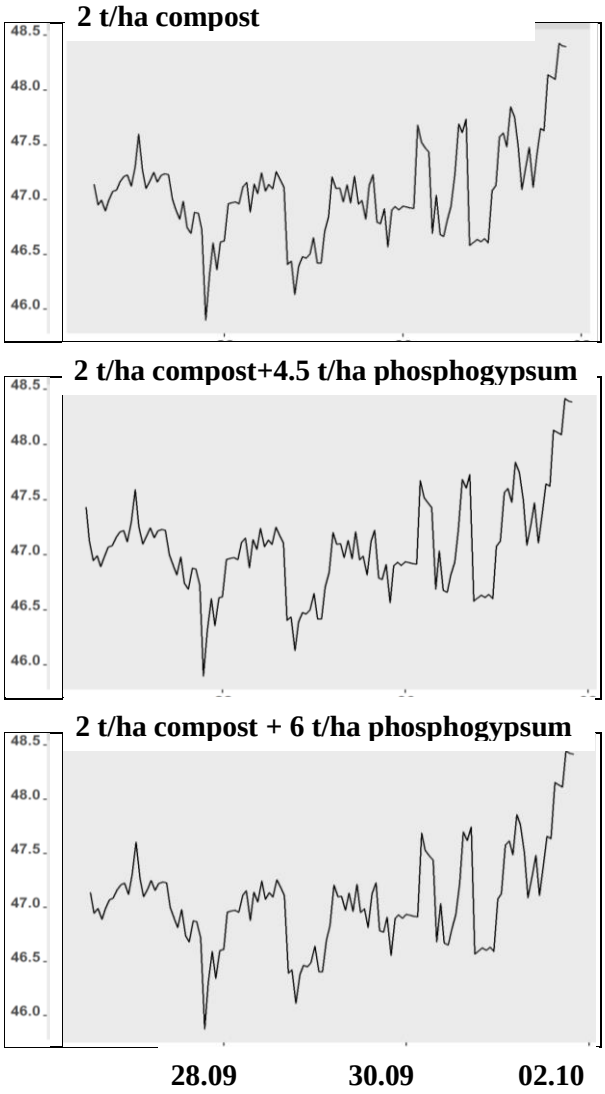

Fig. 2. Daily dynamics of the topsoil moisture of the studied variants with compost

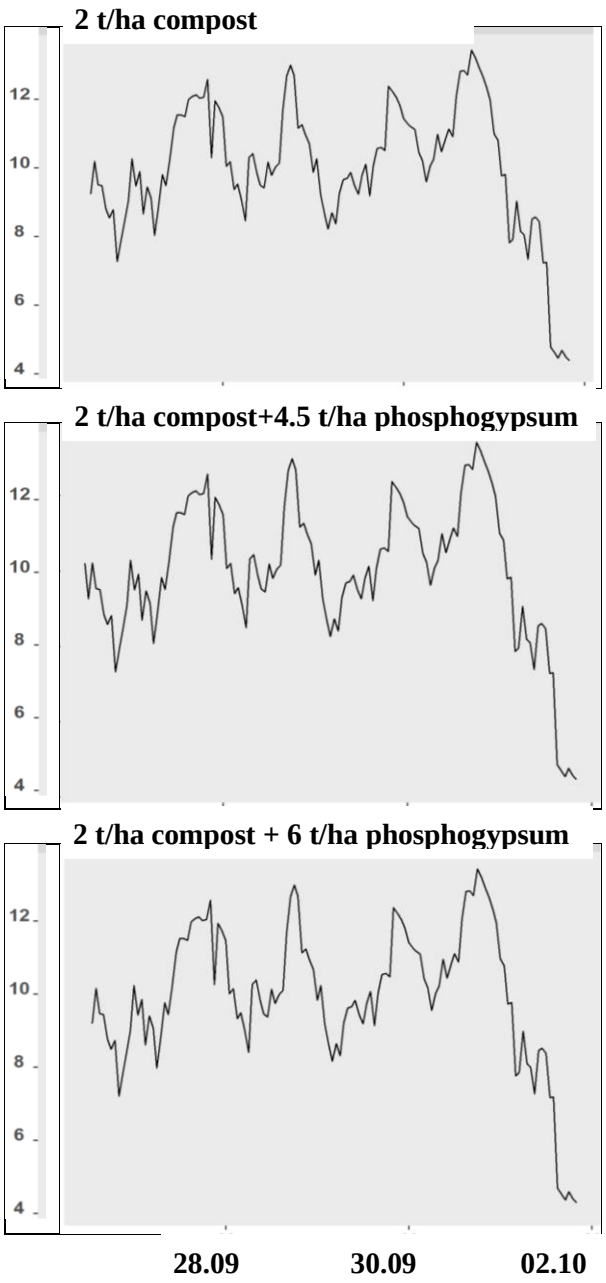

Fig. 3. Daily dynamics of the topsoil temperature of the studied variants with compost.

This makes it possible to exclude the possible influence of spatial heterogeneity of agro-climatic conditions when assessing the impact of applied agrochemicals on the state of the herbage and the upper horizons of the soils being restored.

In summer 2023 there are observed the highly pronounced differences between the control variant and variants with compost from quail droppings application without or with phosphogypsum in the rate of seasonal productivity of the above-ground grass (Fig. 4).

In case of compost application in dose only 2 t per ha in August 2022 total mass of the 2023 seasonally accumulated grassy biomass became in 5 times higher than in the control variant.

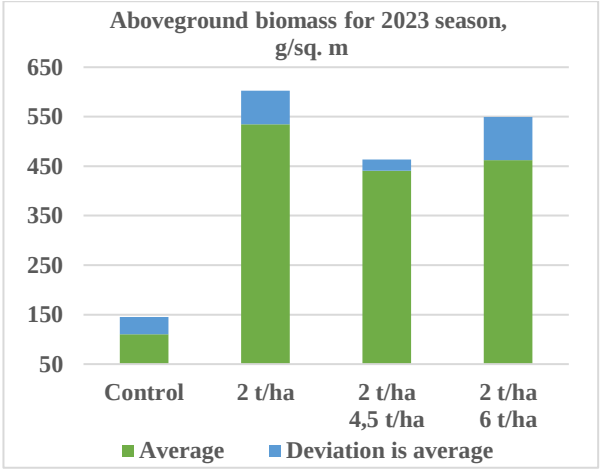

Fig. 4. Total for 2023 season average values of the aboveground grass biomass in the field experiment with compost (1st line) + phosphogypsum (2nd).

The only variant with quail droppings compost has minimum season dynamics and the minimum difference in its average value of soil CO_2 emission from the control variant (Fig. 5).

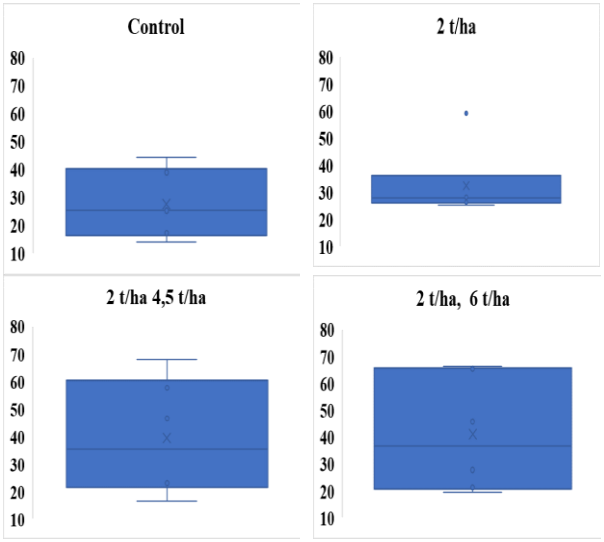

Fig. 5. Diagrams of the scope of seasonal dynamics of soil daily CO_2 emission (g CO_2 m^{-2} day^{-1}) by variants of experiment with compost (2 t/ha) + phosphogypsum (4,5 or 6 t/ha).

At the same time there are obvious differences in average value of topsoil CO_2 emission between the control and the variants with the quail compost application in combination with phosphogypsum. They are characterized by essential increasing the average value of soil CO_2 emission against the background of its pronounced seasonal dynamics.

Summing up the seasonal accumulation of organic carbon in the turf topsoil of the restored degraded sod-podzolic soils (ΔCorg-s), and in the grassy aboveground ($\sum$Corg-gr) plus root biomass ($\sum$Corg-r) minus the total seasonal carbon emission by the measured *in situ* soil CO_2 fluxes ($\sum$C-CO_2) allows one to quantify the integral carbon balance

between the soil-plant system and above layer of atmosphere (Table 2).

Table 2. Analysis of the integral carbon balance between the soil-plant system and above layer of atmosphere per May-August 2023 (in g per sq. m).

Variant	ΔC_{org-s}	$\sum C_{org-gr}$	$\sum C_{org-r}$	$\sum C\text{-}CO_2$	Total C sink
Control	12	55	17	903	-819
Compost 2 t/ha	1434	267	80	902	879
Compost 2 t/ha +P-G 4,5 t/ha	1733	220	66	1289	730
Compost 2 t/ha +P-G 6 t/ha	4	231	69	1499	-1195

4. CONCLUSIONS

The use of IoT sensors in experiments using agrochemicals obtained from waste increases the evidence of their direct positive effect on the conservation of organic matter of the formed soil horizons due to a detailed analysis of the daily and seasonal dynamics of the state of crops and agro-climatic conditions.

The conducted research allows consider the regeneration of the eroded disturbed sod-podzolic soils with use of compost from quail droppings as prospective prototype of the best available soil- and carbon-saving technology, taking into account the compost application aftereffect on the stabilization of carbon balance, the formation of large amount of herbaceous biomass plus environmentally safe and profitable disposal of organic waste from the highly concentrated animal production.

The research has been done with the support of project No. 075-15-2021-1030 of the Ministry of Science and Higher Education of Russia

5. REFERENCES

[1] Ivanov, I.V., Alexandrovsky, A.L., Makeev, A.O., etc.: *Evolution of soils and soil cover*, GEOS, Moscow, 925 p., 2015.

[2] Chernogorov, A.L., Chekmarev, P.A., Vasenev, I.I. Gogmachadze, G.D., *Agroecological land assessment and land use optimization*, Moscow University Press, Moscow, 2012.

[3] I.I. Vasenev, V.V. Chelnokov, V.V. Vershinin, T.N. Kovaleva, A.N. Glushko, A.S. Makarova, G.G. Priorov, V.M. Retivov, Yu E. Vasiliev, A.V. Matasov, *Development of a methodology for monitoring the environmental impact of waste of the year-round maintenance of highways* in *IOP Conference Series: Earth and Environmental Science*, 663, 1, 012053., 2021.

[4] Shchepeleva, A.S., Vasenev, I.V., Mazirov, I.M., Vasenev, I.I., Prokhorov, I.S., Gosse, D.D. Urban Ecosystems, 20, 2, 309-321, 2017.

[5] Shchepeleva, A.S., Vizirskaya, M.M., Vasenev, V.I., Vasenev, I.I. *Analysis of carbon stocks and fluxes of urban lawn ecosystems in Moscow megapolis*, Springer Geogr., 80–88, 2019.

[6] Griguletsky, V.G., Shiryaev, O.V., Ivakin, R.A. Ecological Bulletin of the North Caucasus, 17, 4, 20–28, 2021.

[7] Grabas, K., Pawełczyk, A., Stręk, W. [et al.], Waste and Biomass Valorization, 10, 10, 3143-3155, 2019.

[8] Yakovlev, A.S., Kaniskin, M.A., Terekhova, V.A. Eurasian Soil Science, 46, 6, 2013.

[9] Vizirskaya, M.M., Epikhina, A.S., Vasenev, V.I. [et al.], Bulletin of the Peoples' Friendship University of Russia. Series: Agronomy and Animal Husbandry, 5, 38–48, 2013.

[10] Vasenev, V.I., Stoorvogel, J.J., Ananyeva, N.D., Ivashchenko, K.V., Sarzhanov, D.A., Epikhina, A.S., Vasenev, I.I., and Valentini, R. *Quantifying spatial–temporal variability of carbon stocks and fluxes in urban soils from local monitoring to regional modeling* in The Carbon Footprint Handbook, 185–221, 2015.

[11] Tilaki, G.A.D., Rahmani, R., Hoseini, S.A., Vasenev, I. Acta Ecologica Sinica. 42, 1, 82-89, 2022.

[12] Hou, L., Kong, W., Qiu, Q., Yao, Y., Bao, K., Zhang, L., Jia, H., Vasenev, I., Wei, X., Agriculture, Ecosystems and Environment. 336, 108020, 2022.

[13] Digital technologies of agroecological monitoring and optimization of agriculture (edited by I.I. Vasenev). RSAU-MTAA, Moscow, 2022.

[14] Vasenev, I.I., Buzylev, A.V., Kurbatova, Yu.A. [et al.] Agroecological modeling and design. RSAU-MTAA, Moscow, 2010.

Authors: **Assisstent Andrey Stepanov, Prof. Dr Ivan Vasenev,** Russian State Agrarian University – Moscow Timiryazev Agricultural Academy, Ecology Department, Timiryazevskaya Ul., 49, 127434 Moscow, Russia, Phone.: +7 905 728 9421. E-mail: astepanov@rgau-msha.ru
vasenev@rgau-msha.ru

ETIKUM 2023 **INTERNATIONAL SCIENTIFIC CONFERENCE NOVI SAD, SERBIA, DECEMBER 7-9, 2023**

Taškov, T., Sokić, K., Bodroža D., Jevtić, S.

ADSORBENTI NA BAZI PRIRODNOG ZEOLITA ZA VEZIVANJE FARMACEUTSKI AKTIVNIH KOMPONENTI U TRETMANU KOMUNALNIH OTPADNIH VODA

Apstrakt: *Mogućnost primene prirodnog zeolita za uklanjanje toksičnih supstanci iz otpadnih voda predmet je velikog broja ispitivanja. Međutim, zbog negativno naelektrisane rešetke zeolit pokazuje afinitet isključivo za vezivanje katjona. Poslednjih godina sve češća je primena kompozita na bazi prirodnog zeolita sintetisanih u prisustvu neorganskih i organskih supstanci čime se postiže visoka efikasnost i prema anjonima i hidrofobnim organskim molekulima. U ovom radu sintetisana su dva kompozita za uklanjanje ciprofloksacina, jednog od najčešće korišćenih antibiotika. Dobijeni rezultati su pokazali da je moguće vezati više od 80% farmaceutski aktivne komponente što ukazuje na njihovu potencijalnu primenu u procesima prečišćavanja komunalnih otpadnih voda.*
Ključne reči: *prirodni zeolit, adsorpcija, ciprofloksacin, otpadne vode*

1. UVOD

Vode kontaminirane supstancama koje nastaju kao proizvodi metabolizma farmaceutski aktivnih komponenti predstavljaju opasnu vrstu zagađivača koji se ne mogu prečistiti uobičajenim postupcima [1]. Metode uklanjanja ovih supstanci iz komunalnih otpadnih voda danas su predmet intenzivnih istraživanja koja se baziraju na ispitivanju mogućnosti primene efikasnih, jeftinih, lako dostupnih i ekološki prihvatljivih adsorbenata. Postupak adsorpcije se izdvaja zbog jednostavnosti, fleksibilnosti i lakog izvođenja, kao i mogućnosti upotrebe alternativnih materijala čime se doprinosi sniženju cene celokupnog procesa prečišćavanja [2]. Prirodni zeoliti predstavljaju neorganske, mikroporozne, alumosilikatne polimere sa negativno naelektrisanom kristalnom rešetkom pogodnom za vezivanje katjona [3]. Pored toga, jednostavnim postupcima modifikacije njihovu površinu moguće je prilagoditi i za vezivanje anjona i hidrofobnih organskih molekula. Kompoziti na bazi zeolitne matrice pripremljeni sa neorganskim ili organskim modifikatorima pokazuju veću fizičko-hemijsku stabilnost, lakšu regeneraciju i veći kapacitet adsorpcije u poređenju sa netretiranim zeolitom [4]. Hidroksiapatit, $Ca_{10}(PO_4)_6(OH)_2$, usled prisustva anjonskih i katjonskih aktivnih mesta u strukturi, mogućnosti jonske izmene, biokompatibilnosti i niske cene predstavlja potencijalni adsorbent različitih tipova polutanata iz otpadnih voda [5]. Prisustvo hidroksiapatita može značajno uticati na adsorpciona svojstva prirodnog zeolita. Organski modifikatori, kao što su površinski aktivne supstance (surfaktanti), omogućavaju zeolitu vezivanje hidrofobnih polutanata sa negativnim naelektrisanjem. Monosloj molekula surfaktanta na površini zeolita kompozitu daje hidrofobni karakter, dok dvosloj negativno naelektrisanu površinu zeolita prevodi u pozitivnu čineći je dostupnom za vezivanje anjona. Na ovaj način omogućava se uspostavljanje interakcija i vezivanje lekova kao što su diklofen, ketoprofen i naproksen i njihovo efikasno uklanjanje iz vodenih rastvora [6,7]. Cilj ovog rada bio je priprema dva adsorbenta na bazi prirodnog zeolita za uklanjanje ciprofloksacina, jednog od najčešće korišćenih antibiotika širokog spektra. Kompoziti su dobijeni taloženjem hidroksiapatita na površini prirodnog zeolita u hidrotermalnim uslovima i tretmanom zeolita vodenim rastvorom ekološki prihvatljivog surfaktanta, benzalkonijum-hlorida.

2. EKSPERIMENTALNI DEO

U ovom istraživanju pripremljena su dva adsorbenta na bazi prirodnog zeolita-klinoptilolita ležišta Novakovići, Bosna i Hercegovina. Korišćena je frakcija zeolita veličine čestica između 63 μm i 125 μm.

Prvi adsorbent (ADS1) dobijen je sintezom kalcijum-hidroksiapatita (HAp) na površini prirodnog zeolita (NZ). U reakcionu suspenziju su dodati NZ i reaktanti za hidrotermalnu sintezu HAp: kalcijum-hlorid i amonijum-hidrogenfosfat. Pored toga, dodata je urea i natrijum-etilendiamintetraacetat. Molski odnos Ca/P u reakcionoj smeši iznosio je 1,67, dok je pH vrednost podešena na 9. Reakciona suspenzija je izložena sonifikaciji tokom 6 minuta u 3 ciklusa (Sonopuls, Bandelin mini20), kako bi se izbeglo formiranje zeolitnih agregata. Nakon toga

suspenzija je homogenizovana na magnetnoj mešalici i prebačena u autoklav od nerđajućeg čelika. HAp je kristalisao u hidrotermalnim uslovima na 160 °C i autogenom pritisku tokom 4 h. Nakon hidrotermalne sinteze, dobijeni uzorak je odvojen vakuum filtracijom, ispran destilovanom vodom i osušen preko noći na 105 °C.

Drugi adsorbent (ADS2) pripremljen je površinskom modifikacijom prirodnog zeolita vodenim rastvorom benzalkonijum-hlorida. Pre modifikacije, NZ je preveden u Na-oblik (NaNZ) mešanjem sa vodenim rastvorom natrijum-hlorida koncentracije 2 mol dm^{-3} tokom 24 h na 95 °C. Nakon toga, NaNZ je odvojen vakuum filtracijom, ispran do negativne reakcije na Cl^- jone i osušen preko noći na 105 °C. Surfaktant-modifikovani NaNZ dobijen je mešanjem vodenog rastvora benzalkonijum-hlorida, konc. 0,0125 mol dm^{-3}, sa suspenzijom NaNZ tokom 24 h na 25 °C. Odnos čvrste i tečne faze bio je 1:100. Dobijeni adsorbent je odvojen od suspenzije vakuum filtracijom i osušen preko noći na 60 °C. Adsorpciona svojstva kompozita ispitana su prema ciprofloksacinu (CF). Početna koncentracija CF u metanolu bila je 100 mg dm^{-3}, dok je odnos čvrste i tečne faze u suspenzijama iznosio 1:200. U suspenziji gde je korišćen ADS1, pH vrednost je podešena na 9, dok je u suspenziji gde je korišćen ADS2 pH vrednost podešena na 5. Suspenzije su mešane u vodenom kupatilu (Memmert, VNB 22) brzinom od 105 obrt min^{-1} na 20 °C tokom 3 sata. Nakon toga, adsorbent je odvojen od rastvora vakuum filtracijom. Koncentracija CF u rastvoru nakon adsorpcije određena je UV Vis spektrofotometrijom.

Za određivanje i praćenje faznog sastava adsorbenata korišćena je rendgenska difrakcija praha. Intenziteti difraktovanog rendgenskog zračenja mereni su na sobnoj temperaturi u opsegu od 2Θ 0,02° do 70° korišćenjem PHILIPS PV-1710 difraktometra. Termička svojstva su ispitivana termogravimetrijskom analizom zagrevanjem u struji sintetičkog vazduha pri protoku od 100 cm^3 min^{-1}, brzinom od 20 °C min^{-1} do temperature od 800 °C pomoću instrumenta SDT K600 (TA Instruments). Skenirajuća elektronska mikroskopija je korišćena za ispitivanje morfologije dobijenih uzoraka i veličine dobijenih kristala pomoću elektronskog mikroskopa TESCAN MIRA 3 KSMU. Koncentracije CF u rastvoru su određene korišćenjem Shimadzu UV-1800 UV/Vis spektrofotometra.

3. REZULTATI I DISKUSIJA

3.1 Strukturna analiza

Difraktogram praha NZ (slika 1) pokazao je da je dominantan mineral u uzorku klinoptilolit koji je prisutan sa udelom oko 82 mas.%. Pikovi na 2θ: 9,7; 12,8; 17,2; 19; 22,2 i 29,9 (°) potiču od klinoptilolita. Osim toga, u uzorku su prisutni i drugi minerali u vidu primesa pri čemu pikovi na: 20,9; 26,6 i 36,5 (°) ukazuju na prisustvo kvarca, dok pik na 29,1 (°) potiče od kalcita.

Na difraktogramu praha uzorka ADS1 prisutne su iste faze kao i u uzorku NZ čime je potvrđeno da kristaliničnost zeolita nije narušena. Pik na 2θ: 33,1 (°) potiče od HAp što potvrđuje da je hidrotermalnom sintezom na površini zeolita došlo do njegovog taloženja.

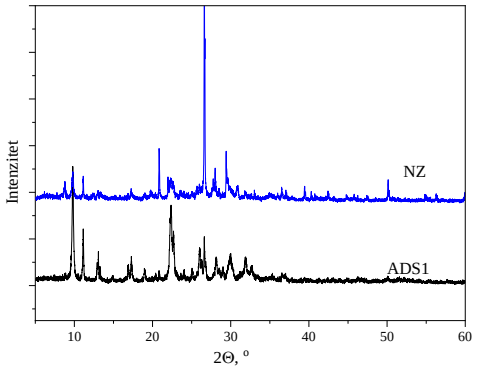

Sl. 1. Difraktogrami praha uzoraka NZ i ADS1

3.2 Infracrvena spektroskopija sa Furijeovom transformacijom

Na slici 2 prikazani su FTIR spektri prirodnog zeolita i oba pripremljena adsorbenta. Na sva tri sprektra uočava se nekoliko zajedničkih vibracionih traka koje su karakteristične za zeolit. Traka na oko 3600 cm^{-1} nastaje vibracijom hidroksilnih grupa prisutnih u zeolitnoj kristalnoj rešetki, dok je vibraciona traka na oko 1600 cm^{-1} posledica je prisustva slobodnih molekula vode. Trake na 400-1000 cm^{-1} nastaju vibracijom alumosilikatne rešetke.

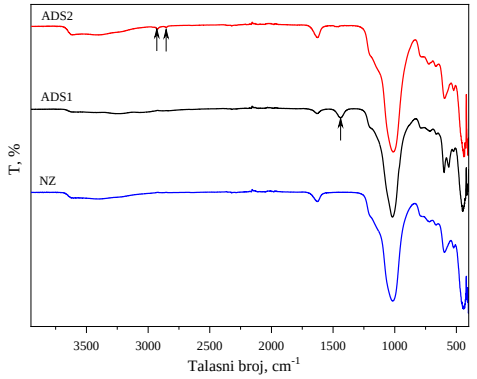

Sl. 2. FTIR spektri uzoraka NZ, ADS1 i ADS2

Na spektru uzorka ADS1 uočava se traka na oko 1400 cm^{-1} koja nastaje zbog vibracija hidroksilnih

grupa u strukturi kalcijum-hidroksiapatita koji je istaložen na površini zeolita.

Na spektru uzorka ADS2 uočava se prisustvo dve nove vibracione trake na oko 2920 cm^{-1} i 2850 cm^{-1} koje nastaju zbog vibracija C-H veza usled prisustva benzalkonijum-hlorida.

3.3 Termička analiza

Na slici 3 prikazane su TG krive uzoraka NZ, ADS1 i ADS1 nakon vezivanja farmaceutski aktivne komponente CF. Termička analiza NZ pokazala je da je ukupan gubitak mase 14,7 mas.% i da on potiče isključivo od dehidratacije. Ukupni gubitak mase uzorka ADS1 u istom temperaturnom intervalu je nešto manji i iznosi 14,1 mas.% što se može objasniti prekrivenošću površine zeolita kristalima HAp-a usled čega je dehidratacija otežana. Nakon adsorpcije CF, gubitak mase je veći u odnosu na ADS1 što ukazuje na vezivanje ciprofloksacina na površini adsorbenta.

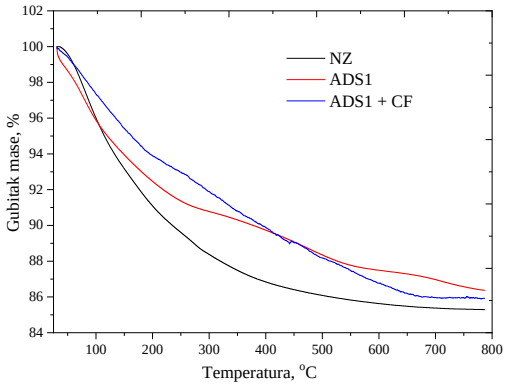

Sl. 3. TG krive uzoraka NZ, ADS1 i ADS1 nakon vezivanja CF

Zagrevanjem uzorka ADS2 do 800 °C ukupan gubitak mase potiče od dehidratacije i odlaska organske komponente (slika 4) i iznosi 15,2 mas.%.

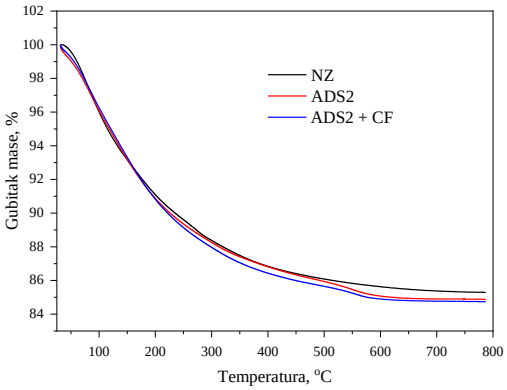

Sl. 4. TG krive uzoraka NZ i ADS2 pre i posle vezivanja CF

Rezultati termičke analize ADS2 nakon adsorpcije CF pokazali su veći ukupan gubitak mase, što ukazuje da je došlo do vezivanja ciprofloksacina.

3.4 Skenirajuća elektronska mikroskopija

Na slici 5 prikazana je morfologija uzorka NZ. Uočavaju se agregati nastali slepljivanjem kristala klinoptiloita u obliku listića veličine oko 5 μm.

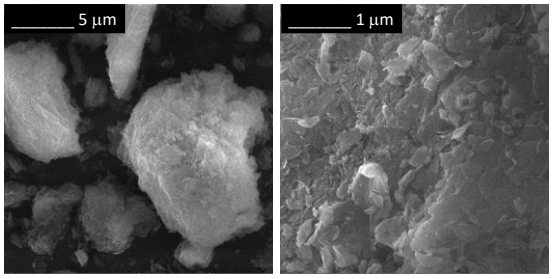

Sl. 5. SEM fotografije uzorka NZ

Mikrografija uzorka ADS1 (slika 6) pokazala je da je na površini zeolita došlo do taloženja kristala kalcijum-hidroksiapatita. Morfologija NZ je ostala nepromenjena nakon hidrotermalne sinteze HAp-a. Igličasti kristali HAp-a su neravnomerno raspoređeni na površini zeolita. Uočava se prisustvno sfetnih agregata, prečnika oko 5 μm koji odgovaraju HAp-u.

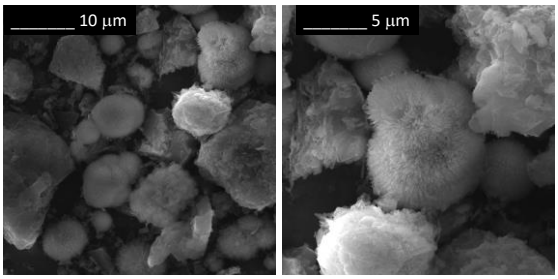

Sl. 6. SEM fotografije uzorka ADS1

3.5 Adsorpcija CF

Rezultati adsorpcije pokazuju da oba korišćena kompozita imaju veliku efikasnost uklanjanja ciprofloksacina iz vodenih rastvora.

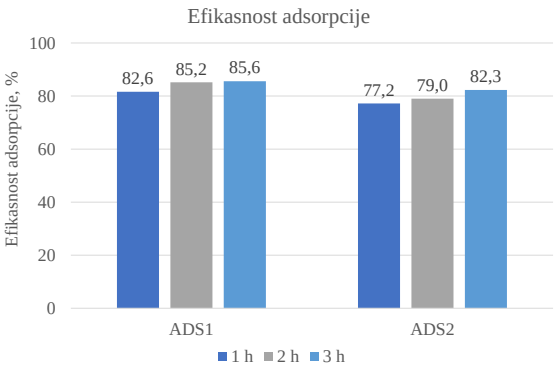

Sl. 7. Efikasnost adsorpcije CF

Najveća količina ciprofloksacina uklonjena je tokom prvog sata kontakta. Nakon 3 h ADS1 pokazuje efikasnost adsorpcije od 85,6 %, dok je

kod ADS2 82,3 % (slika 7). Takođe, kompozit ADS1 pokazuje veći adsorpcioni kapacitet u odnosu na ADS2 i oni redom iznose 4,28 i 4,12 mg CF g^{-1} adsorbenta (slika 8).

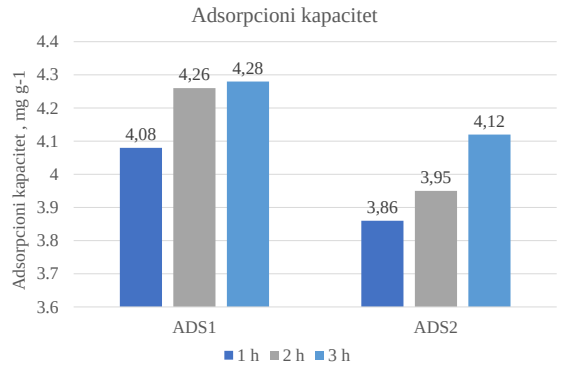

Sl. 8. Adsorpcioni kapacitet kompozita prema CF

4. ZAKLJUČAK

Cilj ovog rada bio je sinteza dva kompozita na bazi prirodnog zeolita/hidroksiapatita i surfaktant-modifikovanog prirodnog zeolita iz ležišta Novakovići, Republika Srpska za vezivanje farmaceutski aktivne komponente ciprofloksacina iz komunalnih otpadnih voda. Rendgenskom difrakcijom praha pokazano je da hidrotermalnom sintezom hidroksiapatita na površini zeolita nije došlo do narušavanja njegove kristaliničnosti. Skenirajuća elektronska mikroskopija potvrdila je prisustvo kalcijum-hidroksiapatita u obliku igličastih čestica u uzorku ADS1, dok su FTIR i termička analiza pokazali da je na površini ADS2 prisutan benzaloknijum-hlorid. Ispitivanje dobijenih adsorbenata za vezivanje ciprofloksacina iz vodenih rastvora pokazalo je da se tokom tri sata kontakta vezalo više od 80% aktivne komponente leka čime se potvrdilo da ovako pripremljeni materijali imaju dobru osnovu za primenu u postupcima prečišćavanja komunalnih otpadnih voda.

5. REFERENCE

[1] Jiang N., Shang R., Heijman S.G.J., Rietveld L.C.: *High-silica zeolites for adsorption of organic micro-pollutants in water treatment: a review*, Water Res. 144, p.p. 145 - 161, 2018.

[2] Burakov A.E., Galunin E.V., Burakova I.V., Kucherova A.E., Agarwal S., Tkachev A. G., Gupta V.K.: *Adsorption of heavy metals on conventional and nanostructured materials for wastewater treatment purposes: a review*, Ecotoxicol. Environ. Saf. 148, p.p. 702 - 712, 2018.

[3] Wen J., Dong H., ZengG.: *Application of zeolite in removing salinity/sodicity from wastewater: a review of mechanisms, challenges and opportunities*, J. Clean. Prod. 197, p.p. 1435 - 1446, 2018.

[4] Rad L.R., Anbia M.: *Zeolite-based composites for the adsorption of toxic matters from water: A review*, J. Environ. Chem. Eng., 9, p.p. 106088 - 106110, 2021.

[5] Pai S., Kini S. M., Selvaraj R., Pugazhendhi A.: *A review on the synthesis of hydroxyapatite, its composites and adsorptive removal of pollutants from wastewater*, J. Water Process Eng. 38 p.p. 101574, 2020.

[6] Smiljanić D., de Gennaro B., Izzo F., Langella A., Daković A., Germinario C., Rottinghaus G. E., Spasojević M., Mercurio M.: *Removal of emerging contaminants from water by zeolite-rich composites: a first approach aiming at diclofenac and ketoprofen*, Microporous Mesoporous Mater. 298, p.p. 110057, 2020.

[7] Smiljanić D., de Gennaro B., Daković A., Galzerano B., Germinario C., Izzo F., Rottinghaus G. E., Langella A.: *Removal of non-steroidal anti-inflammatory drugs from water by zeolite-rich composites: the interference of inorganic anions on the ibuprofen and naproxen adsorption*, J. Environ. Manag. 286, p.p. 112168, 2021.

Autori: **dipl. inž. Teodora Taškov[1], master inž. Katarina Sokić[1], doc. dr. Darko Bodroža[2], doc. dr Sanja Jevtić[1],** [1]Univerzitet u Beogradu, Tehnološko-metalurški fakultet, Karnedžijeva 4, 11000 Beograd, Srbija, telefon: +381 11 3370-425, Fax: +381 11 3370-387; [2]Univerzitet u Banjoj Luci, Tehnološki fakultet, Bulevar vojvode Stepe Stepanovića 73, 78000 Banja Luka, Bosna i Hercegovina, telefon: +387 51 434 357.

E-mail: teodora.taskov00@gmail.com
ksokic@tmf.bg.ac.rs
darko.bodroza@tf.unibl.org
sanja@tmf.bg.ac.rs

ETIKUM 2023

INTERNATIONAL SCIENTIFIC CONFERENCE
NOVI SAD, SERBIA, DECEMBER 7-9, 2023

Vasenev, I.I., Melese, S.M.

ASSESSMENT OF ENVIRONMENTAL MONITORING METROLOGICAL SUPPORT FOR PODZOLUVISOL PHYSICAL PROPERTIES IN DIFFERENT RELIEF FORMS

Abstract: *The seasonal dynamics of Podzoluvisol moisture and bulk density is investigated with especial attention on the metrological support of environmental monitoring with system analysis of the statistically evident regularities of these parameters spatial and temporal variability in the Forest Experimental Station which is considered as reference object of the urban environmental monitoring in Moscow megalopolis. The results were statistically processed using ANOVA in accordance with the GLM version 25 procedure. The conducted research revealed a pronounced seasonal dynamic of Podzoluvisols with a clear differentiation in the catena with different recreational load – already in case of triple repetition of soil samples.*

Key words: *Environmental monitoring, Metrological support, Podzoluvisol physical properties, Soil environmental functions, Spatial and temporal variability.*

1. INTRODUCTION

Topsoil moisture and bulk density are key variables in regulating the exchange of water and thermal energy between soil, plants and the atmosphere, largely determining the seasonal dynamics of the intensity of the production process, soil respiration, microbiological activity, reserves of productive moisture in the soil [1, 2, 3]. It is well known that the soil bulk density is influenced not only by its texture, the type of soil parent materials and soil-forming processes, the content and quality of humus, but also by the modern type and intensity of land use.

These are very dynamic, and at the same time, extremely informative indicators. It is well known that the soil bulk density of soil is influenced not only by its texture, the type of soil parent materials, the content and quality of humus, but also by the modern type and intensity of land use [4, 5, 6]. Seasonal dynamics of soil bulk density is largely determined by its natural moisture [7, 8]. The productive moisture reserve in the soil for the period of the main phenological phases of plant development is often used for functional and ecological assessment of land types, landscape design, yield forecasting and agroecological assessment of agricultural soils [9, 10].

In conditions of increased spatial heterogeneity of the sod-podzolic soil cover patterns of particular interest is the experimentally justified minimization of the repetitions of sampling the most ecologically significant and heterogeneous upper horizons of the soil profile analyzed in the process of environmental monitoring, while preserving the possibility of identifying statistically reliable patterns of their spatial variability and temporal dynamics.

Purpose of the paper is system analysis of the seasonal dynamics of Podzoluvisol moisture and bulk density with especial attention on the metrological support of their environmental monitoring with especial attention on the statistically evident regionally typological regularities of these parameters spatial and temporal variability in case of the Forest Experimental Station which is considered as reference object of the urban environmental monitoring in the Northern part of Moscow megalopolis.

2. MATERIALS AND METHODS

The Forest Experimental Station (FES) is a popular holiday destination for residents of several districts of Moscow. It is experiencing an increased level of recreational load and needs an ecologically balanced organization of the territory and recreational infrastructure to regulate the load. The FES natural conditions of the Forest experimental cottage are typical for the subzone of mixed coniferous-deciduous forests of the taiga-forest zone [10].

During the growing season (May – September) there are 366 mm precipitation – more than half of the annual value. The average annual air temperature is 3.7 °C. The number of days with positive temperatures reaches 206-216 per year. The relative humidity of the air averages 79% for the year, with the minimum in May (66%) and the maximum in November-December (87%).

The studies were conducted at 15 key

monitoring plots (KMS) located on 5 contrast elements of mesorelief: The summit of the flat moraine hill - The middle part of the north-eastern slope – The foot of the north-eastern slope / - The middle part of the south-western slope – The foot of the south-western slope. There are 3 plots on each relief element – with different levels of recreational load: minimal (control or conditional background) – medium – strong. The recreational load level was determined by the severity of the pathway network and the degree of disturbance of the ground vegetation cover (Table 1).

Table 1. The recreational load level assessment

Element of mesorelief	Level of recreational load	The area of the path network, %
summit of the flat moraine hill (SMH)	minimal	0.36
	medium	0.92
	strong	1.44
middle part of the north-eastern slope (NES)	minimal	1.40
	medium	2.98
	strong	3.36
foot of the north-eastern slope (F-NES)	minimal	1.12
	medium	2.85
	strong	3.16
middle part of the south-western slope (SWS)	minimal	1.76
	medium	3.14
	strong	3.76
foot of the south-western slope (F-SWS)	minimal	1.96
	medium	3.34
	strong	3.92

Morphogenetic and texture comparable sandy loam Podzoluvisols on the around 40-cm mantle loam underlain by red Moscow moraine are presented at all key monitoring sites.

At each key site, soil samples were taken monthly from April to October in triple repetition at three depths: 0-5 cm (mainly horizon A); 5-10 cm (horizon AEL); 10-15 cm (horizon ELA or EL).

The analysis of soil moisture was carried out by the thermal weight method, the soil bulk density – using mortise cylinders of 100 cm^3.

Soil moisture reserves are calculated for a layer of 0-15 cm – considering the values of soil moisture and bulk density differentiated for 5-cm layers.

The data were statistically processed using ANOVA in accordance with the GLM procedure (IBM SPSS) version 25 (with a difference of least significance (LSD) 0.01 and 0.05) and Microsoft Excel 2010.

3. RESULTS AND DISCUSSION

The investigations carried out in 2021 and 2022 showed a clearly expressed spatial differentiation of the seasonal dynamics of the topsoil horizons' moisture of the studied Podzoluvisols according to their location on the slope (Fig. 1) and the level of recreational load (Fig. 2).

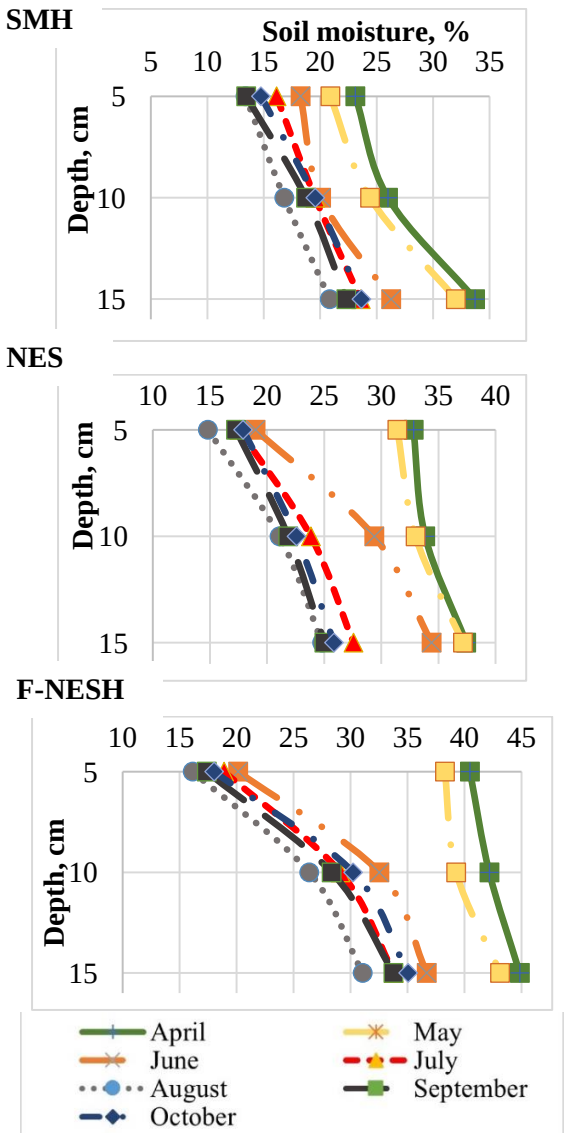

Fig. 1. Slope differentiation of seasonal dynamics of the topsoil moisture of the studied Podzoluvisols with minimal recreational load

In the spring months (April – May), the soil moisture of the humus-accumulative horizon in case of a minimum level of recreational load at the foot of the north-eastern slope (F-NES) was in 1.8 times higher than in the similar soil at the summit of the moraine hill (SMH).

Below the profile, the differences gradually smoothed out to 1.4 times in a layer of 10-15 cm – with minimal differences in 5% of the profile differentiation of soil moisture at the bottom of the slope.

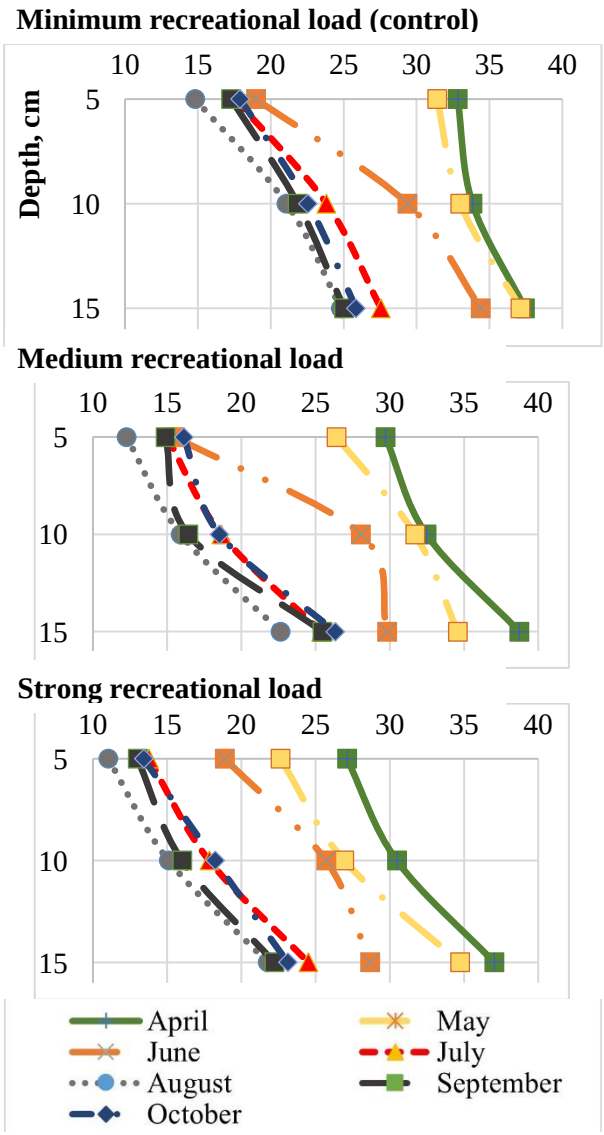

Fig. 2. Spatial differentiation of seasonal dynamics of the topsoil moisture of the studied Podzoluvisols with different recreational load at the middle part of the north-eastern slope

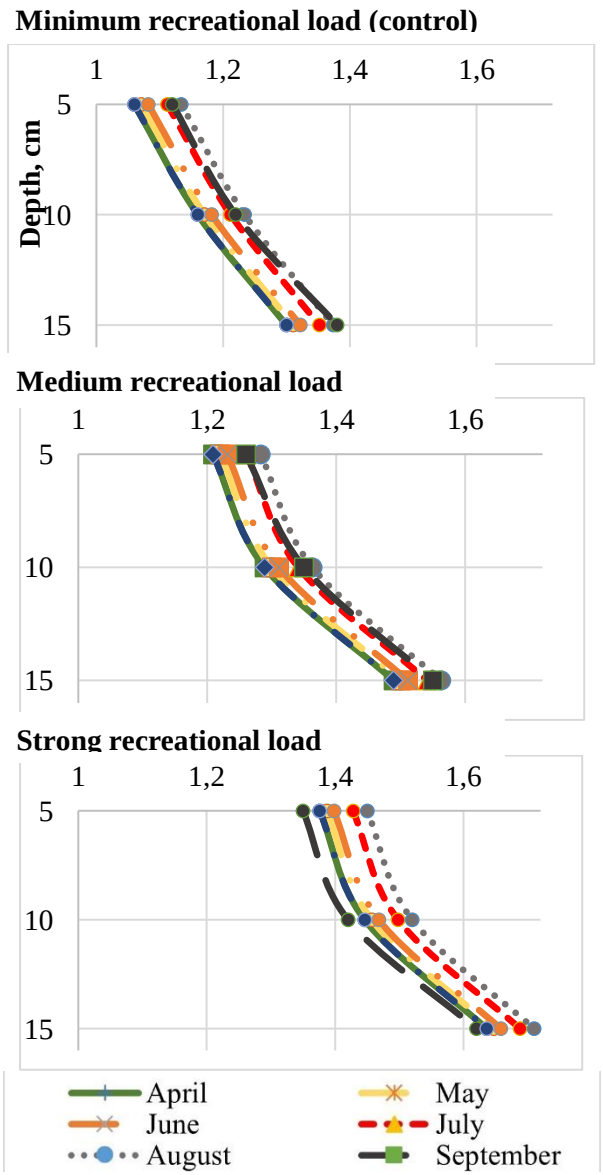

Fig. 3. Spatial differentiation of seasonal dynamics of the topsoil bulk density of the studied Podzoluvisols with different recreational load at the middle part of the north-eastern slope

The seasonal dynamics of the soil bulk density, as a rule, does not exceed 0.1 g / cm^3, following the well-known pattern of it decreasing during topsoil moistening-swelling and freezing-cracking. It is maximally expressed in the topsoil on a slope with a strong recreational load (Fig. 3), which are characterized by a strongly pronounced seasonal dynamics of moisture with strong drying in August (see Fig. 2).

Slope soils, at lower values of the topsoil bulk density with minimal recreational load, as a rule, are more compacted (by 0.25–0.3 g / cm^3) with increasing recreational load.

Differences in the topsoil horizons' moisture are statistically highly reliable when comparing all pairs of the considered elements of the slope catena with each other (Table 2). In the case of soil moisture, the differences are most pronounced between the relief elements.

In case of the topsoil bulk density (Table 3) differences are statistically highly reliable only between the plots of the slope (NES, F-NES) and the summit of the moraine hill (SMH). In case of topsoil bulk density, the differences are most pronounced between sites with different levels of recreational load.

Changes in topsoil moisture associated with different levels of recreational load are maximally expressed in Podzoluvisols at the bottom of the slope, changes in the density of addition – in Podzoluvisols at the summit of the hill.

Table 2. The significance of differences in topsoil moisture between Podzoluvisols at the contrast slope location with different recreational load

Recreational load	Topsoil moisture, % (M±δ)		
	SMH	NES	F-NES
minimal	21,3±2,0	26,1±2,2[a]	31,1±2,7[a]
medium	19,6±2,1*	23,5±2,1**	27,7±2,7**
strong	17,8±2,2*	22,0±2,8**	25,5±2,3**

a – significance of differences compared to the soil at the summit of the moraine hill at P<0.01.
Significance of differences compared to the control soil (with a minimum load level): * – significant at P<0.05; ** – significant at P<0.01.

Table 3. The significance of differences in topsoil bulk density between Podzoluvisols at the contrast slope location with different recreational load

Recreational load	Topsoil moisture, % (M±δ)		
	SMH	NES	F-NES
minimal	1,28±0,03	1,21±0,02[a]	1,20±0,03[a]
medium	1,44±0,01**	1,36±0,01**	1,31±0,02**
strong	1,57±0,03**	1,51±0,03**	1,40±0,02**

4. CONCLUSIONS

The conducted research revealed a pronounced seasonal dynamic of the studied properties of Podzoluvisols with a clear topsoil differentiation according to their location in the catena and the level of recreational load – already in case of triple repetition of analyzed soil samples in each elementary plot if they are sampled according to separate 5-cm horizons of topsoil taking into attention their differences as in relief form as in recreational load level.

The established dependences of seasonal dynamics of topsoil moisture and bulk density on the slope steepness and recreational load level will be useful for land-use planning and environmentally safe regulation of spatially differentiated recreational load in different parts of the urban slope landscape, even in case of a slight slope steepness (up to 3-4 °) and of the presence of vegetation cover close to natural conditions.

The research has been done with the support of project No. 075-15-2021-1030 of the Ministry of Science and Higher Education of Russia

5. REFERENCES

[1] Ivanov, I.V., Alexandrovsky, A.L., Makeev, A.O., etc.: *Evolution of soils and soil cover*, GEOS, Moscow, pp. 925, 2015.

[2] Zhuravsky, V.V., Mosina, L.V.: *Increase of soil bulk density in urban forest ecosystems under the influence of recreational loads as a leading factor of ecological distress*, AgroEcoInfo., Vol. 33, pp. 27, 2018.

[3] Vasenev, I.I., Vizerskaya, M.M., Vasenev, V.I.: *Comparative analysis of principal factors of spatial-temporal variability of CO2 emission from Moscow urban soils with various levels of anthropogenic impact*, Izvestiya TSKHA. Special Issue, pp. 102-112, 2012.

[4] Mosina, L.V., Zhukovsky, V.V.: *Microbiological diagnostics of problematic ecological situations at the object of recreational nature management over a 25-year period (on the example of Forest experimental station of the RSAU-MTAA)*, AgroEcoInfo, Vol. 30, pp.13, 2017.

[5] Vasenev, I.I.: *Soil functional-environmental evaluation and monitoring in urban ecosystems: principal functions, background objects and uniform algorithms of assessment*, Springer Geography, Vol. 4, pp. 161-171, 2018.

[6] Vasenev ,V.I., Yaroslavtsev, A.M., Vasenev, I.I., Demina, S.A., Dovltetyarova, E.A.: *Land-use change in new Moscow: first outcomes after five years of urbanization*, Geography, Environment, Sustainability, Vol. 12, pp. 24-34, 2019.

[7] Andreeva, I.V., Morev, D.V., Taller, E.B., Vasenev, I.I.: *Comparative assessment of the ecological state of Timiryazevsky forest park zones of the city of Moscow*, AgroEcoInfo, Vol. 48, pp. 21, 2021.

[8] Azovtseva, N.A., Smagin, A.V.: *Dynamics of physical and physico-chemical properties of urban soils when using salt deicing agents*, Soil science, Vol. 1, pp. 118-128, 2018.

[9] Yashin, I.M., Vasenev, I.I., Belopukhov, S.L.: *Guidebook of soil-ecological excursions in the forest and agricultural landscapes of the CFBGP and the megalopolis of Moscow*, RSAU-MTAA, Moscow, pp. 128, 2018.

[10] Vasenev, I.I., Avilova, A.A., Tikhonova, M.V., Ermakov, S.Yu.: *Assessment of within-forest variability in Albeluvisol quality in an urban forest ecosystem for the northern part of the Moscow megalopolis*, Springer Geography, pp. 133-144, 2020.

Authors: **Prof. Dr Ivan Vasenev, PHD-student Solomon Melese,** Russian State Agrarian University – Moscow Timiryazev Agricultural Academy, Ecology Department, Timiryazevskaya Ul., 49, 127434 Moscow, Russia, Phone.: +7 905 728 9421.

E-mail: vasenev@rgau-msha.ru
solyeme@gmail.com

ETIKUM 2023 INTERNATIONAL SCIENTIFIC CONFERENCE
NOVI SAD, SERBIA, DECEMBER 7-9, 2023

Yaroslavtsev, A. M., Seregin, I.A., Aleksandrov, N.A., Galić, Z., Vasenev, I.I.

ASSESSMENT OF IOT SHORT WAVE RADIATION SENSOR BASED ON AMS-AS7262 AND AS7263

Abstract: *The article presents approaches to estimation of the average hourly value of short-wave radiation under the data of measuring spectral characteristics of AMS sensors - AS 7263 and AS 7262 according to the results of monitoring of solar radiation at the ecological station of K.A. Timiryazev Russian Academy of Sciences of the Russian Academy of Sciences named after K.A. Timiryazev in 2022.*
Key words: *short-wave solar radiation, sky spectral characteristics, partial least squares method, IOT*

1. INTRODUCTION

Urbanization is a major contributor to changing land use patterns [1,2], contributing significantly to climate change [2].

Urban areas tend to experience higher temperatures compared to rural areas. This difference between temperatures is referred to as the Urban Heat Island (UHI) effect [3].

Studies have shown that this effect can occur at different scales and is mainly related to high density of buildings and urban structures that absorb solar radiation, use of materials with high absorption capacity, lack of green spaces, and production of anthropogenic heat factors [3].

As a result, the number and duration of heat waves increases, leading to heating of the air to extreme temperatures [4,5]. This phenomenon affects humans, leading to poor health and mortality, and increases the burden on infrastructure. In addition, there is an increase in the negative impact on the environment by increasing the frequency and intensity of forest fires, drought, etc. [5,6].

Plants in the process of photosynthesis actively convert solar energy to carry out their metabolism. The part of the solar spectrum, in the wavelength range of 400 to 700 nm, used by plants for photosynthesis is called photosynthetically active radiation (PAR) [7].

PAR is an important agrometeorological parameter with wide applications in fields such as agronomy, crop science and ecology. PAR is actively used in modeling gross or net primary production, used to estimate the productivity of individual plant varieties, and in models of ecosystem-atmosphere carbon exchange [7].

One of the factors influencing the occurrence of heat waves is solar radiation. The most commonly available measured solar radiation data are global horizontal irradiance (GHI), diffuse horizontal irradiance (DHI) and direct normal irradiance (DNI). However, measurements require expensive equipment.

2. OBJECTS AND METHODS

The research was conducted on the territory of the "Field Experimental Station" of the K.A. Timiryazev Russian State Academy of Agriculture named after K.A. Timiryazev during the period from July 22, 2022 to August 31, 2022.

The object of the study was the spectral characteristics of the sky, obtained from the TTR sensors and direct measurements of FAR by the Li190SB sensor.

Li190SB measures PAR as photon flux density in the wavelength range from 400 to 700 nm in units of micromol photons per meter square of surface per second. An important feature of the sensor is the ability to accurately measure incoming radiation at critical angles of incidence up to 85^{o} [8].

TTR is a device based on a microcontroller with an ATMega 328 chip. The spectral characteristics are measured using a spectrometer consisting of AMS sensors, AS 7263 and AS 7262 [9]. These are digital 6-channel multispectral sensors for spectral identification in the near infrared (NIR) and visible spectrum. In order to prevent the sensors from glare from direct sunlight and similarity of the measurements to the Li190SB Quantum Sensor, a PTFE Teflon filter measuring 50x25 mm and 5 mm thick was fitted. It is important to note that, unlike the Li190SB, the AS 7263 and AS 7262 spectrometers do not guarantee the accuracy of light intensity measurements at light incidence angles greater than 20^{o}.

For experimental purity, both devices were mounted at a height of 2 meters in close proximity to each other and were pointed at the zenith.

Table 1. Example of a summary table of raw data

Li190SB	TTR, digital values			
PPFD, μmol/s/m^2	610	680	450	500
36,161	5,736	5,456	8,665	11,064
107,147	3,441	3,294	4,848	6,300
124,780	3,441	3,294	4,848	6,300
141,182	2,513	2,448	3,338	4,478
145,798	3,441	3,294	4,848	6,300
159,602	15,527	15,328	20,956	28,000
171,254	2,076	1,993	2,990	3,870
172,712	1,783	1,706	2,669	3,421
172,712	1,783	1,706	2,669	3,421

Measurements were taken hourly with one minute exposure from 9 am to 3 pm, due to the fact that at other times of the day the TTR spectral sensors are not able to adequately estimate illuminance due to the critical angles of light incidence alone.

3. RESULTS

The regression analysis showed (Figure 1) a linear dependence of the measured values of PAR in the form of photon flux density (PPFD) and the decimal logarithm of the sums of digital values of the TTR spectrometer (TTSUM) in the wavelength range from 400 to 700 nm.

The coefficient of determination (R2) was 0.32 and standard error 0.19 with a number of degrees of freedom of 633, which is statistically significant for a sample size of n=500 (p-value <2.2e- 16).

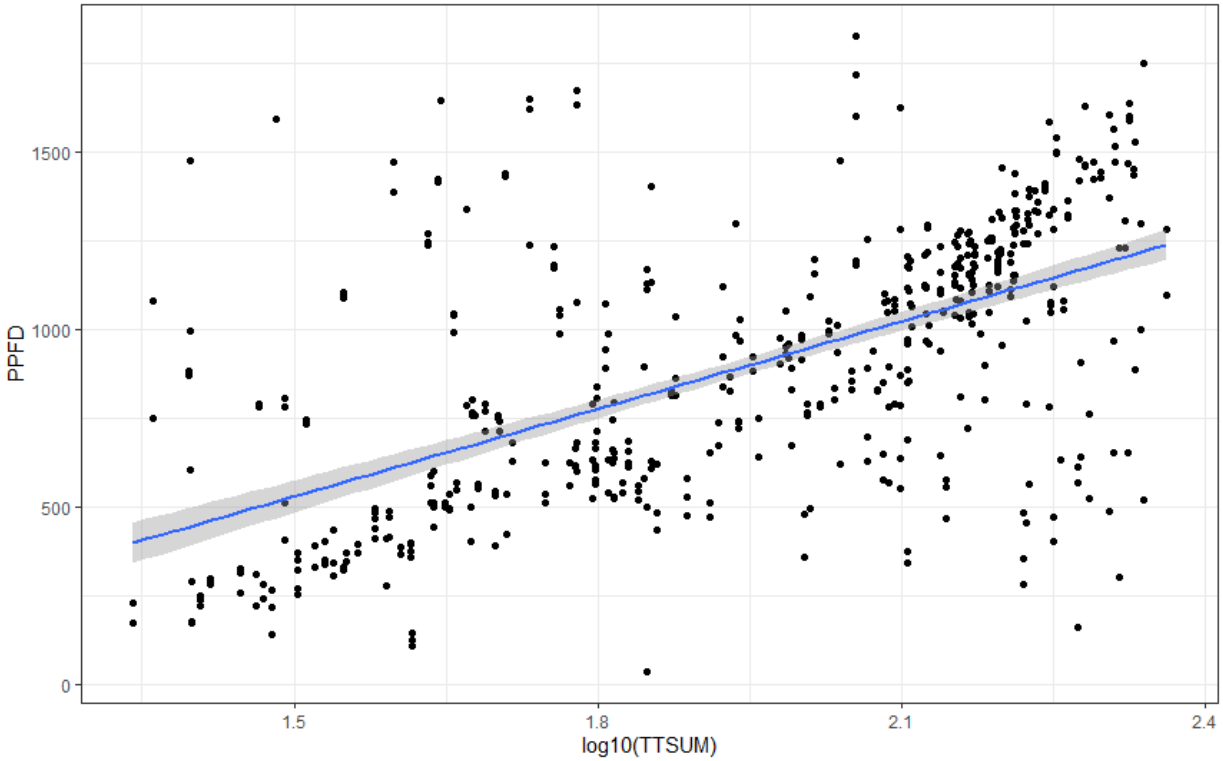

Fig. 1. Scatter plot of photon flux density values (μmol m-2 s-1) from the decimal logarithm of the sum of digital values of spectral characteristics of the visible part of the spectrum according to TTR data

At the next stage of analysis, in order to increase the accuracy of prediction, it was decided to use spectral components as separate variables rather than as a sum in model creation. In this case, the use of multiple regression methods is impossible due to multicollinearity, since all intensity values of individual wavelengths are often highly correlated with each other.

To circumvent this problem, we use the partial least squares (PLS) method, which is very close to the principal component method. This method is implemented in the R software environment in the form of the mdatools package [10].

The obtained model showed the highest prediction accuracy when 8 principal components were used (the accuracy increased insignificantly when more components were used, Fig. 2). The root mean square error (RMSE) was used as the

main indicator of accuracy, which, taking into account 50-fold cross-validation, amounted to 273 µmol m-2 s-1. At the same time, the new model also had a higher coefficient of determination compared to the linear model, 0.47.

Among the variables used in the model, not all were equally effective, so the largest contribution to the obtained model was made by the components numbered 1, 5, 6, 8, which correspond to the wavelengths: 610 nm, 810 nm, 860 nm and 500 nm, which leaves room for further optimization of both the model and the design of the TTR device itself.

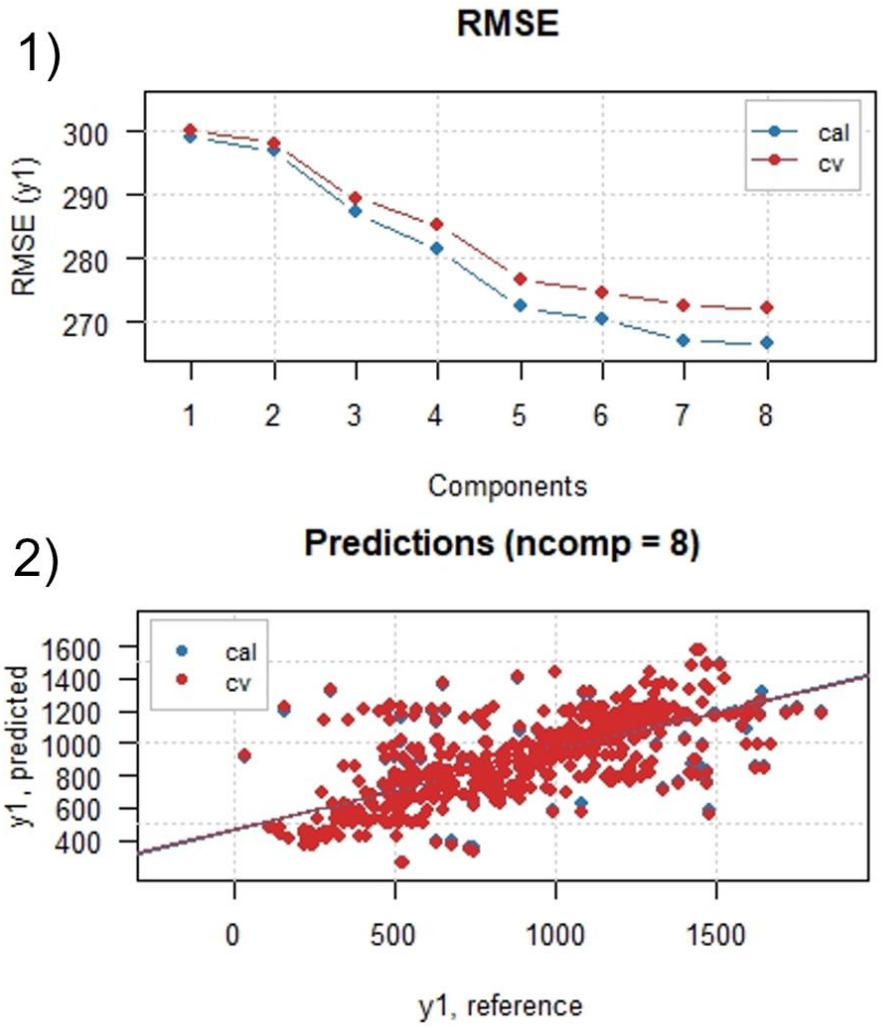

Fig. 2. 1) Variation of the mean-square error of the model predicting the FAR by spectral characteristics of visible light depending on the number of principal components used in the model, with and without taking into account crossvalidation 2) Scatter diagram of real FAR values depending on the values predicted by the model

4. CONCLUSIONS

The conducted studies showed the presence of statistically significant linear dependence between the logarithm of the sum of the spectral characteristics of the sky sensors AS 7263 and AS 7262 and the photon flux density of PAR measured by the quantum sensor Li190SB. The use of the partial least squares method allowed us to obtain a regression model for predicting the PAR values from the data of spectral sensors AS 7263 and AS 7262 with a mean square error of 273 µmol m-2 s-1.

The authors consider such accuracy sufficient for rough average daily estimation of PAR in field conditions.

5. REFERENCES

[1] Sahana M., Ahmed R., Sajjad H.: *Analyzing land surface temperature distribution in response to land use/land cover change using split window algorithm and spectral radiance model in Sundarban Biosphere Reserve, India*, Modeling Earth Systems and Environment, T. 2. – C, pp. 1-11, 2016.

[2] Yosef et al.: *Land Surface Temperature Regulation Ecosystem Service: A Case Study of Jaipur, India, and the Urban Island of Jhalana Reserve Forest*, Forests, Vol. 13, pp. 1101, 2022.
[3] Gago E. J. et al.: *The city and urban heat islands: A review of strategies to mitigate adverse effects*, Renewable and sustainable energy reviews, Vol. 25, pp. 749-758, 2013.
[4] Campbell S. et al.: *Heatwave and health impact research: A global review*, Health & place, Vol. 53, pp. 210-218, 2018.
[5] Perkins S. E., Alexander L. V., Nairn J. R.: *Increasing frequency, intensity and duration of observed global heatwaves and warm spells*, Geophysical Research Letters, Vol. 39, pp. 20, 2012.
[6] Coumou D., Rahmstorf S.: *A decade of weather extremes*, Nature climate change, Vol. 2, pp. 491-496, 2012.
[7] Wane, O., Ramírez Ceballos, J.A., Ferrera-Cobos, F., Navarro, A.A., Valenzuela, R.X., Zarzalejo, L.F.: *Comparative Analysis of Photosynthetically Active Radiation Models Based on Radiometric Attributes in Mainland Spain*, Land, Vol. 11, pp. 1868, 2022.
[8] Core L.: *190SB Quantum Sensor Manual*, 54, 2015.
[9] Alexandrov, N. A.: *Monitoring of spring wheat phenophases using wireless spectrometer networks*, in Proceedings of the International Scientific Conference of Young Scientists and Specialists devoted to the 135th anniversary of the birth of A. N. Kostyakov: collection of articles, Moscow, June 06-08, 2022. Volume 1. - Moscow: K.A. Timiryazev Russian State Agrarian University - MSHA, pp. 110-113, 2022.
[10] Kucheryavskiy, S.: *mdatools – R package for chemometrics*, Chemometrics and Intelligent Laboratory Systems, Vol. 198, 2020.

Authors: **Assoc. prof. dr Alexis Yaroslavtsev, Teaching assoc. Ivan Seregin, Ph.D. student Aleksandrov Nikita, Prof. dr Zoran Galić, Prof. dr Ivan Vasenev,** Russian State Agrarian University - Moscow Timiryazev Agricultural Academy, Timiryazevskaya st. 49, 127550 Moscow, Rissa, Phone.: +7 499 9772347

E-mail: yaroslavtsevam@rgau-msha.ru
iseregin@rgau-msha.ru
alexandrov_na@rgau-msha.ru
dr.zorangalic@gmail.com
vasenev@rgau-msha.ru

Conference SPONSORS

ETIKUM 2023

PROVINCIAL SECRETARIAT FOR HIGHER EDUCATION AND SCIENTIFIC RESEARCH

Bulevar Mihajla Pupina 16
21101 Novi Sad

Tel: (021) 487-4641
E-mail: psnauka@vojvodina.gov.rs
https://apv.visokoobrazovanje.vojvodina.gov.rs/

REPUBLIC SERBIA AUTONOMOUS PROVINCE OF VOJVODINA

UNIVERSITY OF NOVI SAD

Dr Zorana Đinđića 1
21102 Novi Sad
Republic of Serbia

Switchboard: +381 21 485 2000
E-mail: rektorat@uns.ac.rs
www.uns.ac.rs

FACULTY OF TECHNICAL SCIENCES

University of Novi Sad
Faculty of Technical Sciences
Trg Dositeja obradovića 6
21002 Novi Sad
Republic of Serbia

Tel.: (+381) 21 450 810
(+381) 21 6350 413
Fax: (+381) 21 458 133
E-mail: ftndean@uns.ac.rs
http://ftn.uns.ac.rs/691618389/fakultet-tehnickih-nauka

DEPARTMENT OF PRODUCTION ENGINEERING

University of Novi Sad
Faculty of Technical Sciences
Vladimira Perića- Valtera 2
21000 Novi Sad
Republic of Serbia

Secretariat of the Department:
Tel.: (+381) 21 450 366
(+381) 21 485 23 20
Fax: (+381) 21 454 495
E-mail: dpm@uns.ac.rs
www.dpm.ftn.uns.ac.rs

TOPOMATIKA D.O.O.

Industrijska ulica 3, Novaki
10431 Sveta Nedelja
Republic of Croatia

Tel.: +385 1 3496 010
Fax: +385 1 5999 722
E-mail: info@topomatika.hr
https://topomatika.hr/


ISBN 978-86-6022-617-6